Arun D. Singh
Bertil E. Damato
Editors

Clinical Ophthalmic Oncology

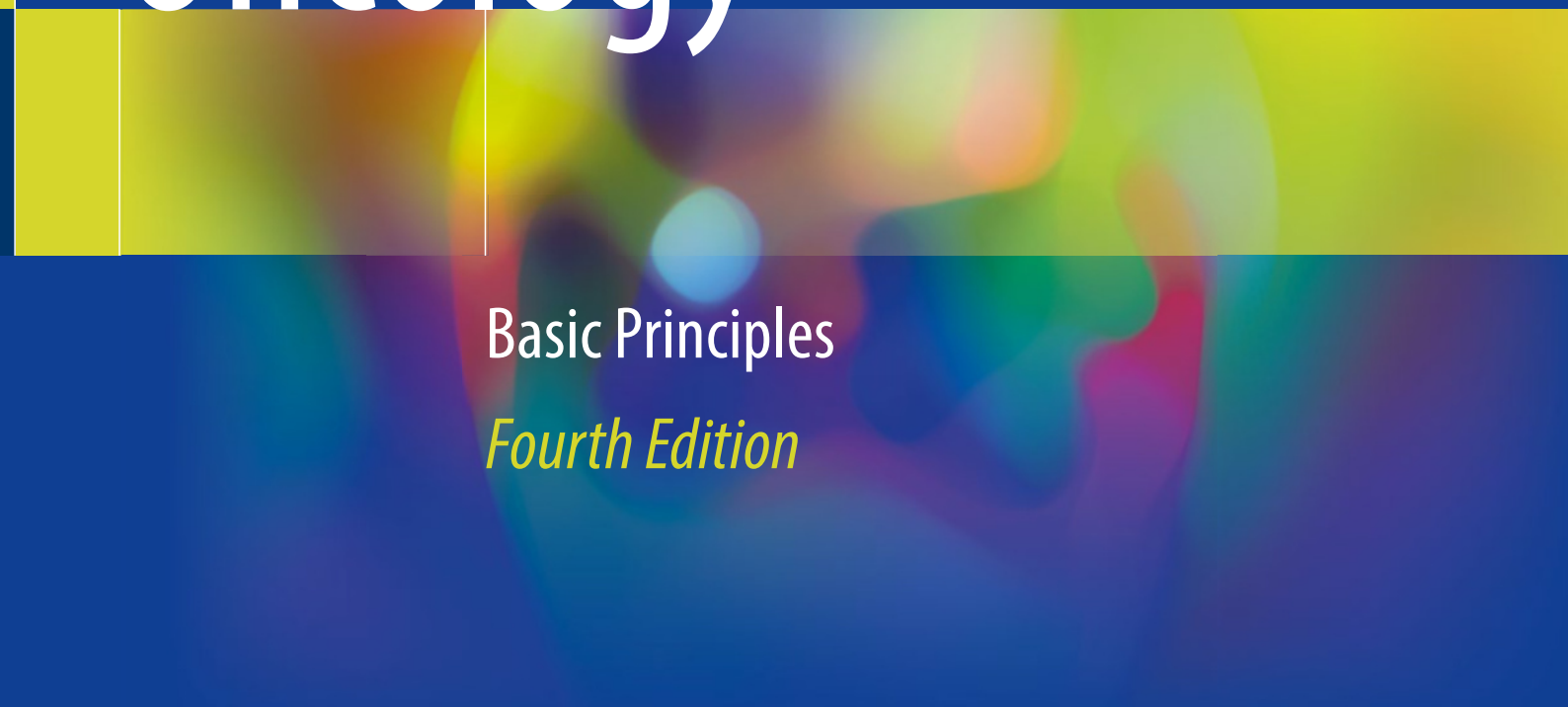

Basic Principles

Fourth Edition

Springer

Clinical Ophthalmic Oncology

Arun D. Singh • Bertil E. Damato
Editors

Clinical Ophthalmic Oncology

Basic Principles

Fourth Edition

Springer

Editors
Arun D. Singh
Department of Ophthalmic Oncology
Cole Eye Institute, Cleveland Clinic
Cleveland, OH, USA

Bertil E. Damato
Ocular Oncology Service
Moorfields Eye Hospital
London, UK

ISBN 978-3-031-75906-2 ISBN 978-3-031-75907-9 (eBook)
https://doi.org/10.1007/978-3-031-75907-9

© The Editor(s) (if applicable) and The Author(s), under exclusive license to Springer Nature Switzerland AG 2015, 2019, 2025

This work is subject to copyright. All rights are solely and exclusively licensed by the Publisher, whether the whole or part of the material is concerned, specifically the rights of translation, reprinting, reuse of illustrations, recitation, broadcasting, reproduction on microfilms or in any other physical way, and transmission or information storage and retrieval, electronic adaptation, computer software, or by similar or dissimilar methodology now known or hereafter developed.
The use of general descriptive names, registered names, trademarks, service marks, etc. in this publication does not imply, even in the absence of a specific statement, that such names are exempt from the relevant protective laws and regulations and therefore free for general use.
The publisher, the authors and the editors are safe to assume that the advice and information in this book are believed to be true and accurate at the date of publication. Neither the publisher nor the authors or the editors give a warranty, expressed or implied, with respect to the material contained herein or for any errors or omissions that may have been made. The publisher remains neutral with regard to jurisdictional claims in published maps and institutional affiliations.

This Springer imprint is published by the registered company Springer Nature Switzerland AG
The registered company address is: Gewerbestrasse 11, 6330 Cham, Switzerland

If disposing of this product, please recycle the paper.

Contents

1 **Principles of Cancer Epidemiology** 1
Annette C. Moll, Michiel R. de Boer, Lex M. Bouter, and Nakul Singh

2 **Cancer Survival: Analysis and Reporting** 11
Emily C. Zabor

3 **Etiology of Cancer** 17
Brian T. Hill, Haikoo Shah, and Allison Winter

4 **Cancer Pathology** 23
Gustav Stålhammar and Stefan Seregard

5 **Pathology Specimen: Handling Technique** 37
Hardeep Singh Mudhar

6 **Cancer Angiogenesis** 51
Julia H. Joo, Sujata Rao, and Arun D. Singh

7 **Immunology of Ocular Tumors** 73
Martine J. Jager, Sen Ma, Elisabet de Los Pinos, and Inge H. G. Bronkhorst

8 **Cancer Genetics** 81
Valeria Visconte and Arun D. Singh

9 **Cancer Staging** 87
Claudine Bellerive and Arun D. Singh

10 **Principles of Cryotherapy** 93
Dan S. Gombos and Kayla Walter

11 **Principles of Laser Therapy** 97
Hatem Krema

12 **Principles of Radiation Therapy** 103
Adannia Ufondu, Sheen Cherian, and Arun D. Singh

13 **Principles of Surgical Excision** 111
Bertil E. Damato

14 **Ocular Complications of Radiation Therapy** 121
Jose C. Puthussery and Arun D. Singh

15 **Principles and Complications of Chemotherapy** 137
Stacey Zahler, Nicola G. Ghazi, and Arun D. Singh

16 **Counseling Patients with Cancer** 151
Bertil E. Damato and Laura Hope-Stone

17 Tumor-Associated Cataract 161
Carlos A. Medina Mendez, Mary E. Aronow, Guillermo Amescua, Salomon Merikansky, and Arun D. Singh

18 Tumor-Associated Glaucoma 173
Zane Khademi, Annapurna Singh, and Arun D. Singh

19 Graft-Versus-Host Disease 185
Edgar M. Espana, Thomas A. Weppelmann, and Arun D. Singh

20 Diagnostic Techniques: Angiography 197
Ahmet Kaan Gündüz and Yağmur Seda Yeşiltaş

21 Diagnostic Techniques: OCT 229
Rubens N. Belfort, Aluisio Rosa Gameiro Filho, and Arun D. Singh

22 Diagnostic Techniques: Autofluorescence 253
R. Chris Bowen, Edoardo Midena, Raffaele Parrozzani, and Giulia Midena

23 Diagnostic Techniques: Ultrasonography 269
Brandy H. Lorek and Arun D. Singh

24 Diagnostic Techniques: FNAB 293
Hassan A. Aziz, David Pelayes, Charles V. Biscotti, and Arun D. Singh

25 Diagnostic Techniques: Other Biopsy Techniques 309
Bertil E. Damato, Armin Afshar, Rumana Hussain, Heinrich Heimann, Carl Groenewald, and Sarah E. Coupland

Index 319

Principles of Cancer Epidemiology

1

Annette C. Moll, Michiel R. de Boer, Lex M. Bouter, and Nakul Singh

1.1 Introduction

During the last decade, evidence-based medicine (EBM) has become a dominant approach in many medical fields, including ophthalmology [1, 2]. Clinical epidemiological studies provide evidence that can aid decision-making processes. An overwhelming amount of clinical epidemiological papers are being published every year, and critical appraisal of the findings can be challenging, especially for the busy clinician who is not formally trained in the field of clinical epidemiology. Therefore, the available evidence is increasingly bundled in clinical guidelines. The aim of this chapter is to provide readers with some basic knowledge to allow them to judge the value of clinical epidemiological papers and, thus, the pillars of evidence-based clinical guidelines. Examples from ocular oncology will be used to illustrate the methodological principles.

1.2 Research Question

A clinical epidemiological study should always start with a well-defined research question. Similarly, when reading a paper, one should always first identify the question(s) the authors wish to address (Fig. 1.1). Research questions can be aimed at explanation or description. Explanatory research examines causal relationships, while descriptive research is merely descriptive. In addition, research questions are also often categorized as etiological, diagnostic, or prognostic (Table 1.1). For example, an explanatory research question related to etiology in the field of ocular oncology is as follows: are children born after in vitro fertilization at higher risk of developing retinoblastoma as compared to children born after natural conception? [3] A correct explanatory research question should contain information on the patients, interventions, contrast, and outcomes (*PICO*) at issue.

A. C. Moll (✉)
Department of Ophthalmology, VU University Medical Center, Amsterdam, The Netherlands
e-mail: a.moll@vumc.nl

M. R. de Boer
Department of Health Sciences, VU Amsterdam, Amsterdam, The Netherlands

L. M. Bouter
Department of Epidemiology and Biostatistics, VU University Medical Centre, Amsterdam, The Netherlands

N. Singh
School of Medicine, Case Western University, Cleveland, OH, USA

© The Author(s), under exclusive license to Springer Nature Switzerland AG 2025

A. D. Singh, B. E. Damato (eds.), *Clinical Ophthalmic Oncology*, https://doi.org/10.1007/978-3-031-75907-9_1

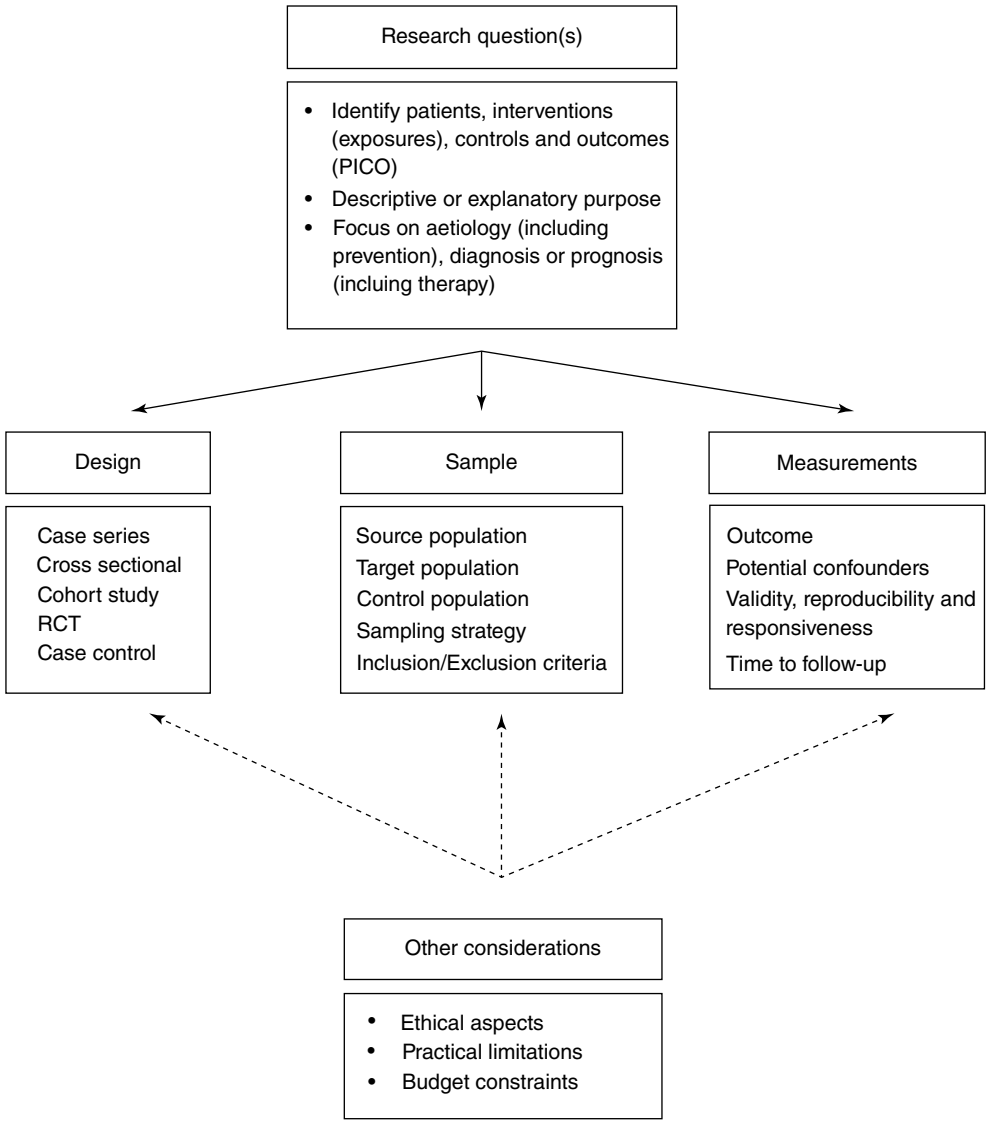

Fig. 1.1 Steps in designing a clinical epidemiological research

Table 1.1 Types of epidemiological research

Type of research	Purpose	Example
Etiology (including prevention)	To examine possible etiological factors for the occurrence of a disease	Association between ultraviolet radiation and uveal melanoma
Diagnosis	To examine the usefulness of diagnostic tests for the disease	Accuracy of magnetic resonance imaging in determining choroidal invasion of retinoblastoma
Prognosis (including interventions)	To examine possible prognostic factors for the disease	Association between external beam therapy for retinoblastoma and the incidence of second malignant neoplasms

1.3 Outcome Measures

Traditionally, prevalence, incidence, and mortality (survival) have been the outcome measures in clinical cancer epidemiology studies. More recently, quality-of-life measures have become increasingly popular. In ophthalmic oncology, visual acuity is also an important outcome measure.

1.3.1 Prevalence

Prevalence refers to the proportion of the study population with the condition of interest. Usually, prevalence is given for a specific moment in time (point prevalence), but sometimes it is estimated for a period of time (e.g., 1-year or lifetime prevalences). For example, the lifetime prevalence of

uveal melanoma in a Caucasian population with oculo (dermal) melanocytosis is estimated to be 0.26% [4].

1.3.2 Incidence

Whereas prevalence relates to existing cases, incidence relates to the proportion of new cases in the study population. It is important that the population under investigation is at risk of developing the condition. For example, persons with bilateral enucleation are no longer at risk of developing uveal melanoma. There are two different measures of incidence: cumulative incidence (CI) and incidence density (ID). CI is the proportion of new cases in a population at risk over a specified period of time. For example, the CI of second malignant neoplasms in hereditary retinoblastoma patients is 17% at the age of 35 years [5]. ID refers to the rate of developing the condition during follow-up, usually expressed as a proportion per person-year at risk.

1.3.3 Mortality

Cancer is among the leading causes of mortality. In order to understand processes that either hasten or delay this outcome, it is necessary to rigorously define the burden of disease. Clinical epidemiologists have created several concepts of mortality, all with their own definitions, interpretations, and uses. Unfortunately, many of these concepts use similar nomenclature, so it is important to always clarify the definition of mortality at hand. Broadly speaking, mortality rate refers to the incidence of death, and survival rate is its complement, i.e., survival rate = 100—mortality rate.

Population mortality is the chance that a person in the general population will die from a specific disease over a specified time frame. It is a useful concept for measuring the burden of disease in a population. For example, the population mortality for heart disease was 197.2 per 100,000 population per year in 2015. Therefore, it is a measure more important for public health policymakers as opposed to clinicians. This measure is calculated from death certificates, where the cause of death is known [6].

Overall mortality is the chance that a person with a disease will die within a time period after diagnosis. It is important to specify a time period for the mortality statistics—in the long run, mortality is 100% for any condition. Of note, this definition is indifferent to the cause of death. Overall mortality is the most common measure of mortality in the literature and is often used to guide prognosis. This measure is helpful in identifying risk factors for poor prognosis, as well as measuring disparities between populations. The interpretation of this measure is complicated by biases, including lead time, length, and overdiagnosis biases.

Cause-specific mortality is the chance that a person with a disease will die within a time period after diagnosis due to the disease. This is in contrast to overall survival, which does not distinguish between causes of death. Cause-specific mortality most closely measures the "deadliness" of a disease, but similar to overall mortality, it can be affected by lead time, length, and overdiagnosis bias.

Relative mortality is a proportion that compares the overall mortality of people with a disease to that of an unaffected but otherwise identical population. Relative mortality measures the excess mortality associated with a diagnosis compared to the general population. It is a convenient measure to calculate because it does not require the cause of death to be recorded. It is also a helpful measure for understanding the deadliness of a disease that affects the elderly, where patients are at risk of dying from other causes. To calculate relative survival, the overall survival of a cohort of patients is compared to life tables of the general population, matched by age, sex, race, and other important demographic features.

Conditional mortality is another clinically informative measure of mortality, which measures the chance that a person with a disease will die within a specified time period after having already lived with the disease for a certain amount of time. It is a helpful measure to assess how prognosis changes over time. Conditional survival requires a cohort of patients where long-term follow-up is close to complete.

1.3.4 Time-to-Event

Another class of outcomes that is of interest to clinical epidemiologists is time-to-event. Time to event measures the length of time that elapses from some start point to a defined endpoint, the most common time-to-event measure being survival, which is defined as the time from diagnosis to death (not to be confused with survival rate). Other events can be used as the endpoint, such as relapse or radiographic progression. Time-to-event data is typically graphically presented with a Kaplan–Meier plot, which displays a nonparametric estimation of the rate of survival in a population as a function of time [7].

1.3.5 Surrogate Endpoints

While overall mortality and cause-specific mortality are the two gold standard measures of mortality when evaluating the efficacy of interventions, other measures of efficacy are being proposed, such as surrogate endpoints, which are biomarkers that are intended to substitute for a clinical endpoint. Of note, these are not clinical quantities of interest but are correlated with them. Examples of surrogate endpoints include evidence of radiographic progression, biochemical

markers, and physical signs [8]. These are controversial measures and are not uniformly accepted within the scientific and regulatory community. Proponents of surrogate endpoints argue that they are preferable for reasons of feasibility, cost, length of study, and possible expediency of the drug approval process. Critics of surrogate endpoints point out that the evidence base for surrogate endpoints correlating closely with clinical outcomes is often tenuous.

1.3.6 Quality of Life

With increasing survival rates and severe side effects of some treatment modalities, quality-of-life measures have become increasingly important in ophthalmic oncology. These measures encompass symptoms and physical, social, and psychological functioning from a patient's perspective. Usually, quality of life is assessed with a structured questionnaire, and scores are summarized assuming an interval scale. Several questionnaires have recently been developed for patients with ocular diseases, such as the measure of outcome in ocular disease [MOOD]) [9].

1.4 Measures of Association

In epidemiological research, we are usually interested in how certain interventions or exposures are associated with outcomes; for example, is there an association between paternal age and retinoblastoma in the offspring? [10]. There are several statistical approaches that can be used to quantify associations, either as a ratio or as a difference, depending on the study design and statistical method used (Table 1.2).

1.4.1 Relative Risk

The ratio of cumulative incidences of exposed and unexposed individuals (or between treated and untreated patients) is the relative risk (RR). For example, in the Netherlands, the RR of retinoblastoma in children conceived by in vitro fertilization is between 4.9 and 7.2. This implies that the risk of getting retinoblastoma is between 4.9 and 7.2 times higher for children conceived after IVF than naturally conceived children.

1.4.2 Hazard Ratio

The ratio of incidence densities of unexposed and exposed patients (or between treated and untreated patients) is the hazard ratio (HR), which has a similar interpretation as the RR. This measure is often used in relation to mortality because we are generally interested not only in the proportion of patients that die but also in the time from baseline (diagnosis or start of treatment) until death. A special application of HR is the ratio of the observed to the expected number of cases (O/E ratio). In this case, the observed incidence density is calculated for the study population, and this is compared to the expected incidence density derived from a population registry (e.g. cancer registration). For example, in a study of lifetime risks of common cancers among 144

Table 1.2 The relation between outcome, measures of association, study designs, and statistical methods

Outcome	Measure of association	Computation	Study designs	Statistical methods
Prevalence	Prevalence rate	P_1/P_2	Cross-sectional	Chi-square test
				Logistic regression analysis
	Prevalence difference	$P_1 - P_2$	Cross-sectional	Chi-square test
Odds of exposure	Odds ratio	Odds of exposure group 1/odds of exposure group 2	Case-control study (cohort study, RCT)	Chi-square test
				Logistic regression
Cumulative incidence (CI)	Relative risk	CI_1/CI_2	Cohort study/RCT	Chi-square test
	Risk difference	$CI_1 - CI_2$	RCT	
Incidence density (ID)	Hazard ratio	ID_1/ID_2	Cohort study/RCT	Kaplan-Meier
				Cox regression
	Risk difference	$ID_1 - ID_2$	RCT	Kaplan-Meier
	O/E ratio	Observed ID/expected ID in general population	Cohort study/registry study	
Quality of life	Difference in mean score	$X_1 - X_2$	Cohort study/RCT	Independent *t*-test
				Linear regression analyses

P_1 prevalence group 1, *P_2* prevalence group 2, *CI* cumulative incidence, *CI_1* CI group 1, *CI_2* CI group 2, *ID* incidence density, *ID_1* ID group 1, *ID_2* ID group 2, *O/E ratio* observed to expected ratio, *RCT* randomized controlled trial X_1 = mean score group 1; X_2 = mean score group 2

hereditary retinoblastoma survivors, 41 cancer deaths were observed, whereas only 7.58 deaths due to cancer were expected. This data can be expressed as a standardized mortality ratio of 5.41 [11].

1.4.3 Odds Ratio

The odds ratio (OR) is the most commonly reported measure of association in the literature due to the fact that this is the statistic that can be derived from the popular logistic regression analysis. The OR is the ratio of the odds of outcome of interest between the exposed and the unexposed. Generally speaking, the OR is a good approximation of the RR or HR.

1.4.4 Differences in Risk

Differences in risks (RD) are preferably reported as outcomes in randomized controlled trials. The RD is easy to interpret and can be used to calculate the number of patients needed to treat (NNT) to prevent one extra event (e.g., death) compared to the standard treatment or placebo. The NNT can be calculated as the inverse of RD (1/RD). A related concept is that of the number needed to screen (NNS). This refers to the number of patients needed to be screened to prevent one extra event compared to the situation without a screening program. The NNS, thus, depends on the predictive probability of the screening test as well as on the efficacy of treatment for people that are diagnosed with that screening test. The value of routine neuroimaging screening of pineoblastoma in retinoblastoma patients is uncertain and a point of discussion [12].

1.4.5 Differences in Mean Score

For scores on interval scales, such as quality-of-life, differences in mean scores between exposed and unexposed participants are the most important measure of interest. These can be derived from independent samples *t*-test of general linear models (e.g., linear regression analysis).

1.5 Precision of the Estimate

When interpreting an outcome, we do not only want to know the numerical value of the point estimate but also the precision with which it has been assessed. In other words, can we be confident that the outcome is not just a chance finding? The usual standard for accepting an outcome as being beyond chance is p (probability) < 0.05. A more informative description is provided by the 95% confidence interval (CI). The rough interpretation of the 95% CI is that there is a 95% probability that the real value lies within the confidence interval.

Statistical significance and the width of confidence intervals are strongly dependent on the sample size of a study. This means that in very large samples, weak (and potentially unimportant) associations can be statistically significant. In contrast, in small samples, strong (and potentially important) associations are sometimes not statistically significant. Such findings should, of course, not be dismissed as being irrelevant. Instead, they should be replicated in larger study populations. Associations, although statistically significant, need not be clinically important. Therefore, interpretation of findings should never solely rely on statistical significance.

1.6 Bias

An estimate can be very precise but nevertheless inaccurate because of bias. Three main sources of bias exist: confounding, selection, and information bias.

1.6.1 Confounding

Confounding occurs when the association between exposure and outcome is influenced by a third variable that is related both to the exposure and the outcome (Fig. 1.2). A recent study found an association between cooking (as an occupation) and the incidence of ocular melanoma [13]. It could be argued that as many cooks work at night, it is possible that they could have relatively high exposure to sunlight due to daytime leisure activities compared to people working during the daytime. It is implied that the association between cooking and ocular melanoma could potentially (in part) be explained by a higher exposure to sunlight by cooks.

1.6.2 Selection Bias

Selection bias may occur when the chance of being included in the study population is not random for all members of the

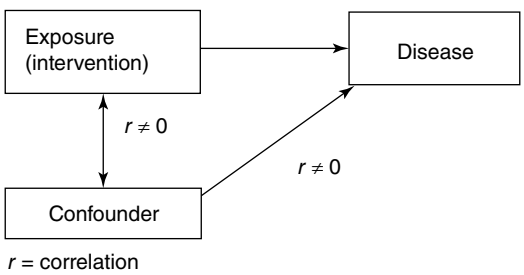

Fig. 1.2 Schematic representation of confounding

source population. For example, patients with an advanced tumor stage are more likely to be referred to a special cancer center than patients with a less advanced tumor stage. This form of selection bias is called referral bias. Selection bias could also be introduced in a study by choosing the wrong control group, especially if controls are selected from hospital patients.

1.6.3 Information Bias

Information bias occurs when outcome or exposure variables are not accurately assessed. This is especially problematic when this occurs differently for exposed versus nonexposed cases or for cases versus controls. A well-known type of information bias is recall bias. This refers to the phenomenon that patients tend to remember more details about exposures that are possibly related to their disease than controls. For example, patients with uveal melanoma are probably more aware of the fact that their disease could be related to sunlight exposure. In turn, they reflect upon their own past exposure to sunlight in much more detail than healthy controls. This can lead to a relative underestimation of exposure in controls and, hence, an overestimation of the association with sunlight exposure.

1.7 Study Designs

There are several research designs, such as case series, cross-sectional, cohort, randomized control trial, and case-control study, that can be adopted in order to address a research question. Each of the study designs has its advantages and disadvantages (Table 1.3).

1.7.1 Case Series

In the case series, the authors present the clinical data regarding a group of patients (e.g. tumor response to chemotherapy combined with diode laser in retinoblastoma patients). The major disadvantage is that this kind of study does not have a comparative design and does not permit an answer to a question such as "There is a good response, but compared to what, as there is no control group." [13].

1.7.2 Cross-Sectional Study

In a cross-sectional study, the outcome (and exposure) is assessed at one point in time. In prevalence studies, only the outcome is measured (e.g. prevalence of retinoblastoma in Denmark). In addition, the outcome between exposed and unexposed study participants can be compared in order to explore etiological questions. In a cross-sectional study on the association between iris color and posterior uveal melanoma, melanoma patients ($N = 65$) with light iris color were significantly more likely to have darker choroidal pigmentation than controls ($N = 218$) ($p = 0.005$). In addition, darker choroidal pigmentation was associated histologically with increased density of choroidal melanocytes ($p = 0.005$). The authors concluded that increased choroidal pigmentation, as a result of an increase in the density of pigmented choroidal melanocytes, is not protective but may actually be a risk factor for the development of posterior uveal melanoma in white patients [14].

The cross-sectional study design has the advantage that it is relatively easy to plan, that only one measurement is needed, and that it is inexpensive and quick to perform. From a methodological point of view, however, the design has

Table 1.3 Advantages and disadvantages of different study designs

Considerations		Type of study			
Methodological		Cross-sectional	Cohort	RCT	Case control
	Confounding	–	–	+	–
	Selection bias	–	±	±	–
	Information bias	±	±	±	–
	Prior exposure	–	+	+	–
	Incident cases	–	+	+	+
Practical	Length of study	+	–	±	+
	Organization	+	±	–	±
	Expenses	+	–	–	+

RCT randomized controlled trial
Negative score (–) indicates disadvantage compared to other study designs
Positive score (+) indicates advantage compared to other study designs
Equivocal score (±) indicates neither advantage nor disadvantage as compared to other study designs

some disadvantages. As both exposure and outcome are measured at the same time, we cannot be sure that the exposure preceded the outcome (the most important criterion for causality). Moreover, the outcome is always measured in terms of prevalent cases, and prevalent cases may have a relatively better prognosis (they are still alive) than the incident cases. Therefore, the associations found in a cross-sectional study can only rarely be interpreted as being causal.

1.7.3 Cohort Study

Some of the problems listed above can be overcome by conducting a (prospective) cohort study. At baseline, one starts with a cohort of people free from the outcome of interest. During or at the end of follow-up, incident cases in both the unexposed and the exposed groups are identified, and RRs or HRs can be calculated. Despite the theoretical advantages of a cohort design, there are some practical disadvantages. The cohort studies often need large sample sizes and/or long follow-ups to accumulate enough incident cases for meaningful analyses. These studies are often expensive. From a methodological point of view, the potential bias of (residual) confounding can never be totally excluded.

1.7.4 Randomized Controlled Trial

Randomized controlled trials are a specific type of cohort study. At the start of the study, participants are randomly assigned to the intervention group (treatment under investigation) or a control group (no treatment, placebo, or standard treatment). After the start of the treatment, patients often get better. This may be due to the treatment or other circumstances such as spontaneous resolution, effective co-interventions, and placebo effects. Only a sufficiently large, randomized, and blinded trial is useful to estimate the efficacy of drugs and other treatments. The best comparison is often between the new treatment and the best available one, not the sham treatment [15]. The randomization, if successful, ensures that confounding factors are evenly distributed between the intervention and control groups. As with the cohort studies, incident cases in both groups are determined during or at the end of follow-up, allowing for the risk estimates to be calculated.

For clinicians interested in evidence pertaining most directly to a particular class of patients, subgroup analyses can be very informative. The strength of evidence for subgroup effects depends on the question of whether hypotheses have been defined prior to analysis, whether potential problems regarding multiple comparisons have been considered, and whether there is biological plausibility of the effects found. Using these guidelines, the reader of a trial report should be able to decide if presented subgroup effects are of clinical importance or if the overall result is a better estimate of treatment effect [16].

1.7.5 Case-Control Study

In contrast to cohort studies, the starting point in case-control studies is not to assess the exposure status but the disease status. People with the disease of interest are selected, and a control group of people without the disease is subsequently recruited. The control group should include people from the same source population as the cases, implying that if any of the controls had developed the disease, they would have been eligible for inclusion in the study as a case.

The selection of a valid control group is important in case-control studies and has, therefore, generated a fair amount of discussion in the epidemiological literature. It is possible to select population controls, hospital controls, friends or relatives of patients, or any combination of these [17]. Case-control studies have the advantage of being relatively quick and inexpensive to conduct and are especially appealing in rare diseases. A disadvantage is the large potential for selection bias, especially in the recruitment of controls. In addition, there is also a real danger of information (recall) bias. Similar to cohort studies, bias by confounding can never be totally ruled out.

1.7.6 Pilot Study

A pilot study is often performed before the start of a large study. Its aim is to improve the methodological quality and evaluate the feasibility. The estimate of the effect of an intervention in a pilot study is determined to a large extent by chance and, therefore, cannot be considered conclusive. However, the inclusion of such results in a later cumulative meta-analysis may lead to sufficient power to assess the efficacy of an experimental intervention [18].

1.7.7 Systematic Review

In a systematic review, all available evidence (literature) on a certain topic is reviewed in a systematic, transparent, and reproducible manner. These studies can be especially useful when results from single studies are contradictory and/or have large confidence intervals due to a small sample size. When the studies in a systematic review are reasonably

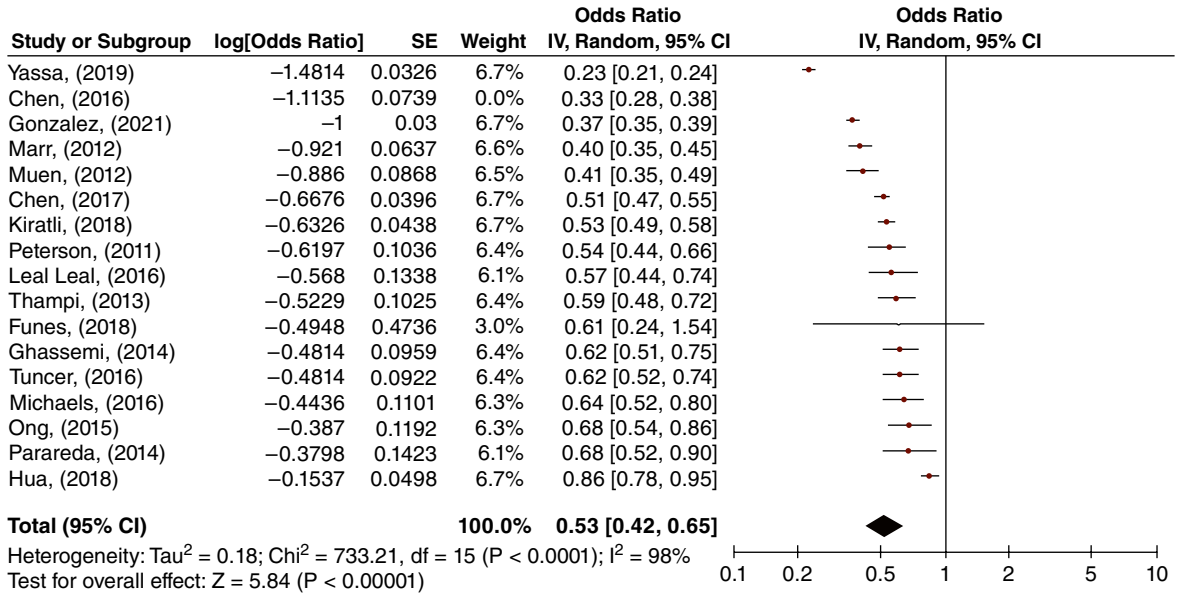

Fig. 1.3 Forest plot of the overall estimated effect sizes of enucleation rate. OR—odds ratio; 95% CI—95% confidence interval; SE—standard error; df—degrees of freedom. (Reproduced from: Yu G, Zhou X, Li J. A meta-analysis of the efficacy of intra-arterial chemotherapy for the management of retinoblastoma patients. Adv Clin Exp Med. 2023 Jul 24. doi: 10.17219/acem/166664)

homogenous, their results can be pooled in meta-analyses. This results in one effect size for all the studies together, with a much smaller confidence interval than the individual studies. An example is a systematic review of the survival of patients with uveal melanoma treated with brachytherapy. The result of this meta-analysis showed that the 5-year melanoma-related mortality rate was 6% for small and medium tumors and 26% for large tumors [19].

A recently published meta-analysis of intraarterial chemotherapy for retinoblastoma revealed a high level of heterogeneity ($I^2 = 98\%$) with an enucleation rate ranging from 0% to 44%. The estimated total pooled OR of enucleation rates was 0.53 (95% CI: 0.42–0.65, $p < 0.001$) (Fig. 1.3) [20].

1.8 Conclusions

In general, ophthalmic tumors are rare compared to other ophthalmic diseases. Therefore, it is difficult to conduct large studies with enough power to get statistically significant and clinically relevant results. A large number of studies are published each year, most of which are descriptive, concerning retrospective patient series. To conduct randomized clinical trials, international collaboration is necessary to include enough patients in the different treatment arms of the study. Furthermore, uniform definitions and study methodology are very important to compare the different studies in the literature and to be able to perform systematic reviews and meta-analyses.

References

1. Sackett DL. Clinical epidemiology. What, who, and whither. J Clin Epidemiol. 2002;55:1161–6.
2. Guyatt GH, Haynes RB, Jaeschke RZ, et al. Users' guides to the medical literature: XXV. Evidence-based medicine: principles for applying the users' guides to patient care. Evidence-based medicine working group. JAMA. 2000;284:1290–6.
3. Moll AC, Imhof SM, Cruysberg JR, et al. Incidence of retinoblastoma in children born after in-vitro fertilisation. Lancet. 2003;361:309–10.
4. Singh AD, De Potter P, Fijal BA, et al. Lifetime prevalence of uveal melanoma in white patients with oculo(dermal) melanocytosis. Ophthalmology. 1998;105:195–8.
5. Moll AC, Imhof SM, Bouter LM, et al. Second primary tumors in patients with hereditary retinoblastoma: a register-based follow-up study, 1945–1994. Int J Cancer. 1996;67:515–9.
6. U.S. Department of Health and Human Services. Principles of epidemiology in public health practice: An introduction to applied epidemiology and biostatistics. Atlanta, GA: Centers for Disease Control and Prevention (CDC). Office of Workforce and Career Development; 2006. p. 30333.
7. Kaplan EL, Meier P. Nonparametric estimation from incomplete observations. J Am Stat Assoc. 1958;53:457–81.
8. Cohn JN. Introduction to surrogate markers. Circulation. 2004;109(25):IV-20-IV-21.
9. Foss AJ, Lamping DL, Schroter S, et al. Development and validation of a patient based measure of outcome in ocular melanoma. Br J Ophthalmol. 2000;84:347–51.
10. Moll AC, Imhof SM, Kuik DJ, et al. High parental age is associated with sporadic hereditary retinoblastoma: the Dutch retinoblastoma register 1862–1994. Hum Genet. 1996;98:109–12.
11. Fletcher O, Easton D, Anderson K, et al. Lifetime risks of common cancers among retinoblastoma survivors. J Natl Cancer Inst. 2004;96:357–63.

12. Moll AC, Imhof SM, Schouten-van Meeteren AYN, et al. Screening for pineoblastoma in patients with retinoblastoma. Arch Ophthalmol. 2001;120:1774.
13. Harbour JW. What is the best treatment for retinoblastoma? Am J Ophthalmol. 2004;138:471–3.
14. Harbour JW, Brantley MA Jr, Hollingsworth H, et al. Association between choroidal pigmentation and posterior uveal melanoma in a white population. Br J Ophthalmol. 2004;88:39–43.
15. Abel U, Koch A. The role of randomization in clinical studies: myths and beliefs. J Clin Epidemiol. 1999;52:487–97.
16. Oxman AD, Guyatt GH. A consumer's guide to subgroup analyses. Ann Intern Med. 1992;116:78–84.
17. Lasky T, Stolley PD. Selection of cases and controls. Epidemiol Rev. 1994;16:6–17.
18. Friedman LM, Furberg CD, De Mets DL. Fundamentals of clinical trials. St Louis: Mosby; 1996.
19. Seregard S. Long-term survival after ruthenium plaque radiotherapy for uveal melanoma. A meta-analysis of studies including 1,066 patients. Acta Ophthalmol Scand. 1999;77:414–7.
20. Yu G, Zhou X, Li J. A meta-analysis of the efficacy of intra-arterial chemotherapy for the management of retinoblastoma patients. Adv Clin Exp Med. 2023;33:207. https://doi.org/10.17219/acem/166664.

Further Reading

Bouter LM, Zielhuis GA, Zeegers MP. Textbook of epidemiology. Houten: Bohn Stafleu van Loghum; 2018.
Fletcher RH, Fletcher SW, Wagner EH. Clinical epidemiology: the essentials. Baltimore: Williams & Wilkins; 1996.
Guyatt G, Rennie D, editors. Users' guide to the medical literature: a manual for evidence-based clinical practice. Chicago: AMA Press; 2002.
Rothman KJ. Epidemiology: an introduction. New York: Oxford University Press; 2002.
Sackett DL, Strauss SE, Richardson WS, Rosenberg W, Haynes RB. Evidence-based medicine. Edinburgh: Churchill Livingstone; 2000.
User's guide to evidence-based practice. Educative series of articles from the JAMA. www.cche.net/usersguides/main.asp.
Website of the centre for evidence-based medicine, Oxford, United Kingdom. www.cebm.net.

Cancer Survival: Analysis and Reporting

2

Emily C. Zabor

In clinical oncology research, survival endpoints, also known as time-to-event endpoints, are commonly of interest [1]. Examples of survival endpoints in oncology include time to progression, time to metastasis, and time to death. Survival data are unique among endpoints in oncology studies because their time-dependent nature means that the event of interest typically cannot be observed after the end of the study or after the point in time of data extraction. Therefore, instead of having a known, fixed value of the endpoint for every patient, censoring is introduced. Censoring occurs when a subject in a study has not experienced the event of interest by the end of data collection. Censoring can occur for a variety of reasons, including loss to follow-up, withdrawal from the study, or the end of a fixed study period. The occurrence of the event is dependent on how long a subject was observed in the study. A clear example of this is the endpoint of death. If a study continued long enough, every subject in the study would eventually die. Therefore, whether a subject is observed to be dead or alive depends entirely on when the follow-up time for the study ends. Consider a retrospective study where data will be extracted from electronic health records from January 1, 2015, through some time in 2019. A subject who died on August 6, 2019, would be treated as dead if the study extracted data through December 31, 2019, and the same subject would be considered alive if the study extracted data through June 30, 2019. The date of the subject's death did not change, but the subject's status with respect to the endpoint of death was different depending on the date of data extraction. This example illustrates why subjects who are not observed to have an event of interest in the study period cannot simply be considered event-free but rather must be considered censored, with consideration for how long they were followed in the study.

The ophthalmic oncology literature contains many examples of studies that analyze survival endpoints. In one study, investigators were interested in the association between disease- and treatment-related variables and recurrence-free survival and ocular survival in eyes treated with ophthalmic artery chemosurgery for retinoblastoma [2]. Recurrence-free survival was calculated from the end date of ophthalmic artery chemosurgery to the date of recurrence, defined as regrowth from regressed tumor and/or new subretinal or vitreous seeds. Ocular survival was calculated from the first visit date to the date of enucleation [2]. The study had a retrospective design, with data extracted for all patients having ophthalmic artery chemosurgery at a single center between May 2006 and February 2017. Therefore, all patients experiencing a recurrence or enucleation after February 28, 2017, were censored for this study. In another study, interest was in the association between age at presentation with iris melanoma and metastasis [3]. All patients with a clinical diagnosis of iris melanoma at a single center between August 25, 1970, and May 1, 2011, were included in the retrospective study [3]. Follow-up time began at the date of presentation and ended at the date of occurrence of iris melanoma–related metastasis. Therefore, any patient who experienced a metastasis after May 1, 2011, was considered censored for analysis of this study. A third study investigated the long-term survival of patients with uveal melanoma using the population-based Surveillance, Epidemiology, and End Results database [4]. All patients diagnosed between January 1, 1975, and December 31, 2016, were included in the study. Overall survival time was defined from the date of diagnosis with uveal melanoma to the date of death from any cause. Information on whether a patient had died was also available through December 31, 2016, so any patient who died after this date was censored for overall survival.

These examples from the ophthalmic oncology literature illustrate that there are always two components to survival endpoints: the observed time, defined from a start date of follow-up to the first of either the date of occurrence of the event of interest or the date of censoring, and an indicator of whether the event occurred during this time period. Both pieces of information must be considered in the analysis of

E. C. Zabor (✉)
Cleveland Clinic, Department of Quantitative Health Sciences & Taussig Cancer Institute, Cleveland, OH, USA
e-mail: zabore2@ccf.org

© The Author(s), under exclusive license to Springer Nature Switzerland AG 2025

A. D. Singh, B. E. Damato (eds.), *Clinical Ophthalmic Oncology*, https://doi.org/10.1007/978-3-031-75907-9_2

any censored survival endpoints, so special statistical analysis methods are required. This chapter will describe common statistical analysis methods for survival endpoints and will explain how to interpret and report the associated results.

2.1 Synthetic Data Example

A synthetic dataset will be used throughout this chapter to illustrate the statistical methods. The dataset and associated R code files to produce all results included in this chapter are available at https://github.com/zabore/manuscript-code-repository/Zabor_Clinical-Opthalmic-Oncology-Cancer-Survival. The synthetic data are based on a multi-institutional cohort of uveal melanoma patients who had undergone molecular prognostication. Variables in the dataset include the survival time in years, the survival status, an indicator of prognostic status based on molecular profiling results, age at diagnosis, and sex. Survival time was measured in years from the date of diagnosis to the date of death. Survival status is an indicator that is one if the patient died and zero if the patient was censored. The data include all patients diagnosed between January 1, 2005, and June 30, 2018, so that any patient still alive on June 30, 2018, was censored for survival status. Prognostic status is a binary variable indicating either a good or bad prognosis based on the molecular profiling results. The question of interest is whether prognostic status was associated with overall survival in uveal melanoma patients.

2.2 Methods for Survival Analysis

The most common statistical methods used to analyze survival data are the Kaplan–Meier method [5] and the Cox proportional hazards regression model [6]. The Kaplan–Meier method is a nonparametric approach to estimating the survival probability at a given time. The Kaplan–Meier estimator allows each patient to contribute information to the calculation of survival probability for as long as they are followed, either until event or censoring, and results in a step function where the value of the survival probability only changes at the time of each event [7]. The Kaplan–Meier survival curve is a plot of the survival probability on the y-axis by time on the x-axis and can be used to visualize the results. The Cox proportional hazards regression model describes the relationship between the hazard function and a set of one or more covariates [8]. The hazard is the probability that an individual who has already survived to a given time will have an event at that time [7]. Cox proportional hazards regression models can include a single covariate, deemed univariable models, or can include multiple covariates, deemed multivariable models. Note that a common reporting mistake is to refer to a multivariable model as a multivariate model. In statistics, a multivariate model refers to a model with multiple outcome variables, whereas a multivariable model refers to a model with multiple predictor variables, which is the model type being applied in most clinical oncology research. A key feature of the Cox proportional hazards regression model is that the hazard curves for the groups should be proportional and cannot cross, implying that the hazard in any one group is a constant multiple of the hazard in any other group [8].

2.3 Reporting Basics

One unique feature of survival data is that the power of a study is driven by the number of events, not the number of subjects. Therefore, it is essential to report the number of events in a study as well as the total number of subjects. It is important to note that while reporting the number of events is essential, it is not appropriate to report the percentage of events out of the total number of subjects. This is a common reporting mistake, but it is not an accurate summary measure due to the censored nature of the data. Another unique feature of time-to-event data is the time-dependent nature of the data, which makes it important to report the length of follow-up time in the study as a summary of how long patients were observed for the occurrence of the event of interest. Follow-up time is typically reported as a median. The most common approach to calculate the median is to estimate it directly among the event-free patients only and to also report the interquartile range. Only the event-free patients are used for this calculation because they are patients who had a more natural course of follow-up that was not interrupted by the occurrence of the event. It is a common reporting mistake to include all patients in the calculation of median follow-up time, but this estimate is not accurate as it represents a mixture of follow-up time among the event-free and time-to-event among those who had the event. Our synthetic dataset includes 1021 subjects. The median follow-up time among survivors was 4 years (IQR: 1.9–6 years). During this time, 357 subjects died from any cause.

2.4 Reporting Kaplan–Meier Results

The first step is to examine the full Kaplan–Meier survival curves plotted according to any covariate of interest. It is best practice to include a table indicating the number of patients at risk over time below the plot and to truncate the plot when the number at risk becomes low. What is considered low depends somewhat on the total sample size, but typically, curves would not be plotted beyond the point in time when there are less than five or ten patients still at risk in each

group. This is because estimates based on a small number of remaining patients are unstable. The x-axis should be labeled in a way that is descriptive, and simple default labeling such as "Time" should be avoided. For example, in the Kaplan–Meier plot of our synthetic data, shown in Fig. 2.1, the x-axis is clearly labeled "Years from diagnosis." The numbers at risk in each group over time are shown below the plot, and follow-up time was truncated at 12 years, which was the last time when at least ten patients remained at risk in both groups.

There are some additional measures that can be reported, depending on the data and the question of interest. The first is the median survival time. Median survival is the time corresponding to a survival probability of 0.5, or 50%, and represents the time to which half of the patients survive. Typically, the median survival time will be reported by group, along with a confidence interval (CI). For example, in Fig. 2.2, the median survival for patients with bad prognostic status is shown using a dotted line. The median survival for patients with bad prognostic status is 4 years (95% CI: 3.7–4.9), meaning that half of the patients with bad prognostic status survive to 4 years or beyond. The plot indicates that median survival time was not reached in this study for patients with good prognostic status, as the yellow curve has not fallen below the 0.5 point on the y-axis by the end of follow-up. Often, in this situation, the median survival would be reported as "NR" for not reached. A second measure that is common to report is x-year survival probability, where x represents a point in time where it is of interest to estimate the survival probability. It expresses the probability of surviving to or beyond x years. The x-year survival probability will usually be reported by group, along with a CI. For example, in Fig. 2.2, 5-year survival is shown using dashed lines for both patients with bad and good prognostic status. The 5-year survival probability for patients with bad prognostic status is 44% (95% CI: 39–49%), and the 5-year survival probability for patients with good prognostic status is 92% (95% CI: 89–96%). It is important to check that enough patients are still at risk at any point in time x when survival probability is reported to ensure the stability of the estimate. In the synthetic data example, there are still over 100 patients at risk in each group at 5 years, so there are plenty of data contributing to estimates at this point in time. The final measure that may be of interest to report is the log-rank P-value. The log-rank test for between-group differences equally weights observations over the entire follow-up time and is the most common way to compare survival curves between groups. Depending on the research question of interest, alternatives to the log-rank test are available that more heavily weight earlier or later portions of the follow-up period. At the bottom of Fig. 2.2, the log-rank P-value is reported as <0.001, indicating that there is a significant difference in survival probability over time between patients with bad and good prognostic status using the conventional 0.05 threshold for statistical significance.

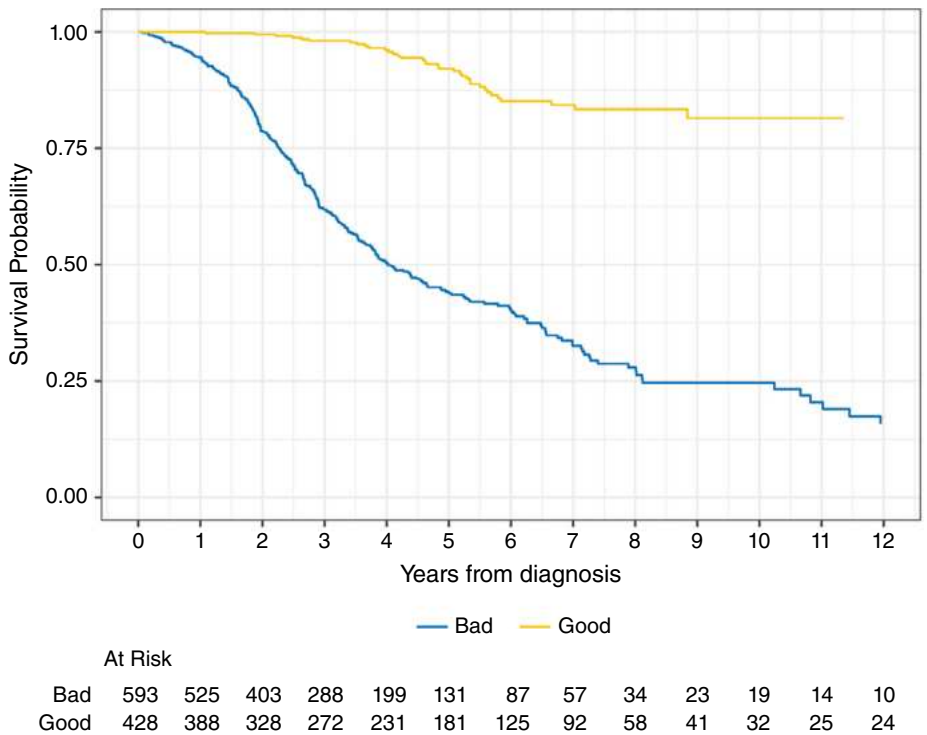

Fig. 2.1 Kaplan-Meier plot of survival probability according to prognostic group

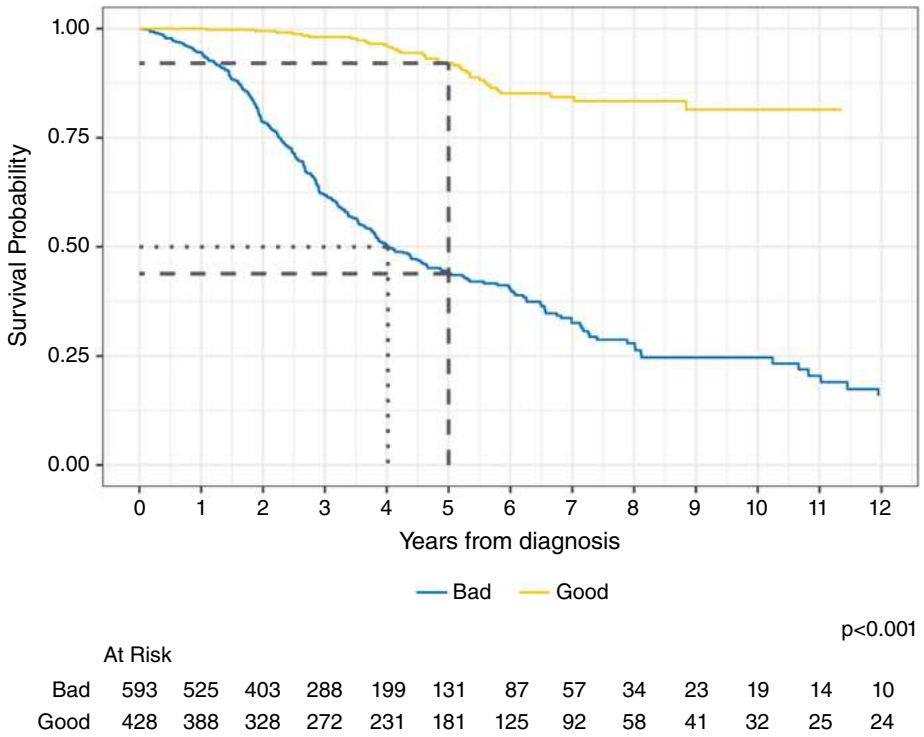

Fig. 2.2 Kaplan-Meier plot with median and 5-year survival, and long-rank *P*-value

2.5 Reporting Cox Regression Results

The results from a Cox proportional hazards regression model (referred to going forward simply as "Cox regression") are usually displayed in a table showing hazard ratios, confidence intervals, and often P-values. A hazard ratio (HR) represents the ratio of hazards between groups or for a particular unit change in a continuous variable at any point in time. The HR is interpreted as the instantaneous rate of occurrence of the event of interest in those who are still at risk for the event. A common reporting mistake is to interpret the hazard ratio as a risk, but a hazard is not the same as a risk, and therefore, this terminology should be avoided. A HR < 1 indicates a reduced hazard of the event of interest, whereas a HR > 1 indicates an increased hazard of the event of interest. Typically, multivariable Cox regression results would be reported, and any univariable Cox regression results would only be included if there was a strong rationale for why they were of interest [9]. The general rule of thumb is that there should be at least ten events per predictor level included in a multivariable Cox regression model though some suggest that there are scenarios where as few as five events per predictor level are adequate [10]. Hazard ratios are usually rounded to two decimal places. In Table 2.1, the multivariable Cox regression results are reported for a model in our synthetic data incorporating prognostic group, age at diagnosis, and sex. The model finds that good prognostic status was associated with a significantly reduced hazard of death (HR: 0.12, 95% CI: 0.08–0.16, and *P*-value<0.001) as compared to bad prognostic status when age at diagnosis and sex were held constant. This result implies that 0.12 times as many good prognostic status patients are dying as compared to bad prognostic status patients at any given time.

In this example, the main study question was related to the association of the prognostic group and death from any cause. The multivariable model included age at diagnosis and sex as adjustment factors, as they are known to be associated with the hazard of death in most populations and may also be associated with prognostic status. The HRs for these two factors are not of specific interest in this case, but it is best practice to show the full results for all variables included in a multivariable model when possible. Typically, adjustment variables should be selected a priori based on clinical importance or a hypothesis of association with both the outcome and the predictor of interest, as opposed to using variable selection procedures based on univariable P-values such as stepwise selection [9]. With a total of 357 events in the synthetic data, there is sufficient power to support three predictor levels, which requires a minimum of 30 events. It is of interest to note that age was presented as the hazard ratio for a 10-year increase. In this case, the hazard ratio for a one-year increase in age was 1.02, with a 95% CI of 1.01 to 1.03. Hazard ratios very close to 1 such as this can be difficult to interpret, and it can also happen that the value of one or both sides of the 95% CI takes the same value as the HR when rounded to two decimal places. Rescaling can produce a more interpretable result. To achieve the hazard ratio for a 10-year increase in age of 1.24 with a 95% CI of 1.14 to

Table 2.1 Multivariable Cox proportional hazards regression model results

Characteristic	HR[a]	95% CI[a]	*P*-value
Prognosis status			<0.001
Bad	–	–	
Good	0.12	0.08, 0.16	
Age at diagnosis (per 10 years)	1.24	1.14, 1.35	<0.001
Sex			0.001
Female	–	–	
Male	1.41	1.15, 1.74	

[a]HR = Hazard Ratio, CI = Confidence Interval

1.35, a new variable is created in the dataset that is simply the age at diagnosis divided by 10, and then it is included in the model.

2.6 Summary

This chapter introduced the need for special statistical methods to analyze survival data in the context of clinical ophthalmic oncology studies. Survival data are unique due to the inclusion of subjects who are censored, meaning the event of interest had not yet been observed by the end of the study or the time of data extraction. This leads to data consisting of two key components: the length of time each subject was followed and an indicator of whether the event of interest occurred. The Kaplan–Meier method and Cox proportional hazards regression models are the most common statistical methods to analyze survival data. Great care must be taken in creating databases related to survival analyses, as there are unique considerations surrounding dates of censoring and dates when follow-up should start depending on the event of interest. In addition, there are many more advanced topics in survival analysis that were beyond the scope of this chapter, including composite endpoints [11, 12], competing risks [13–15], and conditional survival [16, 17]. It is essential to consult with a biostatistician with expertise in survival analysis before undertaking any data collection related to an analysis of survival data to ensure not only that the appropriate statistical methods are applied but also that the correct data are collected to allow for a rigorous and accurate analysis.

References

1. Delgado A, Guddati AK. Clinical endpoints in oncology—a primer. Am J Cancer Res. 2021;11(4):1121–31.
2. Francis JH, Levin AM, Zabor EC, Gobin YP, Abramson DH. Ten-year experience with ophthalmic artery chemosurgery: ocular and recurrence-free survival. PLoS One. 2018;13(5):e0197081. https://doi.org/10.1371/journal.pone.0197081.
3. Shields CL, Kaliki S, Shah SU, Luo W, Furuta M, Shields JA. Iris melanoma: features and prognosis in 317 children and adults. J AAPOS. 2012;16(1):10–6. https://doi.org/10.1016/j.jaapos.2011.10.012.
4. Farquhar N, Thornton S, Coupland SE, Coulson JM, Sacco JJ, Krishna Y, et al. Patterns of BAP1 protein expression provide insights into prognostic significance and the biology of uveal melanoma. J Pathol Clin Res. 2018;4(1):26–38. https://doi.org/10.1002/cjp2.86.
5. Kaplan EL, Meier P. Nonparametric estimation from incomplete observations. J Am Stat Assoc. 1958;53(282):457–81. https://doi.org/10.1080/01621459.1958.10501452.
6. Cox DR. Regression models and life-tables. J R Stat Soc Ser B Methodol. 1972;34(2):187–220.
7. Clark TG, Bradburn MJ, Love SB, Altman DG. Survival analysis part I: basic concepts and first analyses. Br J Cancer. 2003;89(2):232–8. https://doi.org/10.1038/sj.bjc.6601118.
8. Bradburn MJ, Clark TG, Love SB, Altman DG. Survival analysis part II: multivariate data analysis--an introduction to concepts and methods. Br J Cancer. 2003;89(3):431–6. https://doi.org/10.1038/sj.bjc.6601119.
9. Assel M, Sjoberg D, Elders A, Wang X, Huo D, Botchway A, et al. Guidelines for reporting of statistics for clinical research in urology. J Urol. 2019;201(3):595–604. https://doi.org/10.1097/ju.0000000000000001.
10. Vittinghoff E, McCulloch CE. Relaxing the rule of ten events per variable in logistic and Cox regression. Am J Epidemiol. 2007;165(6):710–8. https://doi.org/10.1093/aje/kwk052.
11. Freemantle N, Calvert M, Wood J, Eastaugh J, Griffin C. Composite outcomes in randomized trials: greater precision but with greater uncertainty? JAMA. 2003;289(19):2554–9. https://doi.org/10.1001/jama.289.19.2554.
12. Montori VM, Permanyer-Miralda G, Ferreira-González I, Busse JW, Pacheco-Huergo V, Bryant D, et al. Validity of composite end points in clinical trials. BMJ. 2005;330(7491):594–6. https://doi.org/10.1136/bmj.330.7491.594.
13. Dignam JJ, Zhang Q, Kocherginsky M. The use and interpretation of competing risks regression models. Clin Cancer Res. 2012;18(8):2301–8. https://doi.org/10.1158/1078-0432.Ccr-11-2097.
14. Kim HT. Cumulative incidence in competing risks data and competing risks regression analysis. Clin Cancer Res. 2007;13(2 Pt 1):559–65. https://doi.org/10.1158/1078-0432.Ccr-06-1210.
15. Satagopan JM, Ben-Porat L, Berwick M, Robson M, Kutler D, Auerbach AD. A note on competing risks in survival data analysis. Br J Cancer. 2004;91(7):1229–35. https://doi.org/10.1038/sj.bjc.6602102.
16. Zabor EC, Gonen M, Chapman PB, Panageas KS. Dynamic prognostication using conditional survival estimates. Cancer. 2013;119(20):3589–92. https://doi.org/10.1002/cncr.28273.
17. Zabor EC, Radivoyevitch T, Singh AD, Kilic E, de Klein J, Kalirai H, et al. Conditional survival in uveal melanoma. Ophthalmol Retina. 2021;5(6):536–42. https://doi.org/10.1016/j.oret.2020.09.015.

Etiology of Cancer

3

Brian T. Hill, Haikoo Shah, and Allison Winter

3.1 Introduction

Cancer is a pathologic accumulation of clonal cells derived from a common precursor or cell of origin. The genesis of all neoplasms is genetic damage, which can be inherited or somatically acquired. In general, the genetic dysregulation that gives rise to uncontrolled cell proliferation results from activation of growth-promoting proto-oncogenes and/or deletion or inactivation of growth-inhibiting tumor suppressor genes. Additionally, mutations or dysregulation of genes that regulate programmed cell death (apoptosis) and genes involved in DNA repair also contribute to carcinogenesis. The most widely accepted theory of cancer development is the Knudson "2-hit" hypothesis, which posits that a mutation in one predisposing gene is necessary but not sufficient for malignancy and that only after the development of a second mutation will invasive cancer develop (Fig. 3.1) [1]. Cancer cells must also evade host immune surveillance and both innate and adaptive immune responses for continued proliferation. Exploiting this mechanism of carcinogenesis gave rise to a new era of antineoplastic immunomodulatory agents including immune checkpoint inhibitors, cellular therapy, and bispecific antibodies [2, 3]. In this chapter, we discuss the major categories of carcinogens and their role in the etiology of cancers, with an emphasis on common ophthalmic cancers.

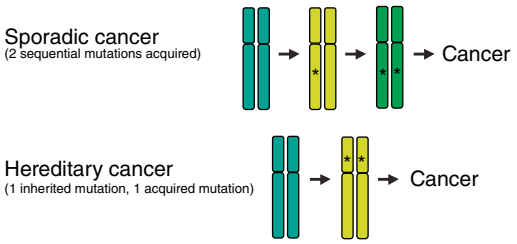

Fig. 3.1 Schematic representation of Knudson 2-hit hypothesis in which normal cells require two successive mutations to delete both functional copies of a given gene to develop cancer. In contrast, cells with germline mutations only require a single genetic event to develop malignancy

3.2 Carcinogenic Agents

While the precise etiology of most de novo malignancies remains unclear, extensive evidence suggests that various carcinogenic agents play a role in the development of numerous human cancers. These agents can be broadly classified into several groups, including infectious agents such as viruses, chemical substances encompassing occupational, environmental, and therapeutic agents, electromagnetic radiation (such as ultraviolet [UV], X-ray, gamma-ray), and immunosuppressive factors like HIV and immunosuppressive medications. These are shown in Table 3.1. Squamous

B. T. Hill · H. Shah · A. Winter (✉)
Department of Taussig Cancer Institute, Cleveland Clinic, Cleveland, OH, USA
e-mail: wintera2@ccf.org

© The Author(s), under exclusive license to Springer Nature Switzerland AG 2025

A. D. Singh, B. E. Damato (eds.), *Clinical Ophthalmic Oncology*, https://doi.org/10.1007/978-3-031-75907-9_3

Table 3.1 Various types of carcinogens

Chemicals	Radiation	Infectious	Dietary	Iatrogenic
Occupational	UV light	Virus	Fat	Radiation
Arsenic	*X-ray*	HPV	Calorie	Immunosuppression
Asbestos	*Gamma-ray*	EBV	Low fiber	Chemotherapy
Coal tars	*Nuclear radiation*	KSHV		
Soot		HTLV-1		
Benzene		HEP B/C		
Vinyl chloride				
Behavioral		Bacteria		
		H. pylori		
		C. psittaci		
Tobacco		Fungus		
		A. flavus		
Alcohol		Parasite		
		Schistosoma		
		Clonorchis		

cell carcinoma of the conjunctiva is associated with particular strains of HPV, while uveal melanoma's cause is multifactorial and remains largely unknown.

3.3 Chemical Carcinogens

Hundreds of chemicals have been shown to be carcinogenic in humans. Harm from these chemical carcinogens can be a result of occupational (asbestos, aniline dyes), environmental (alcohol, tobacco), or iatrogenic (chemotherapy, radiation) exposure. While many carcinogens are directly mutagenic to DNA, most carcinogens undergo activation after exposure to reactive metabolites that are responsible for genetic damage.

3.3.1 Environmental Exposure

Although it is difficult to assess the direct causality of certain environmental agents and carcinogenesis, perhaps the most well-documented agent known to cause cancer is asbestos. This is a naturally occurring mineral that historically has had a broad range of industrial and commercial applications; aerosolized fibers of asbestos are known to lodge in small airways, causing the production of reactive oxygen species and localized tissue damage and significantly predisposing exposed individuals to both lung cancer as well as mesothelioma [4, 5].

A number of other agents have been associated with elevated risks of various cancers through epidemiologic studies. Several agents have been implicated in lung cancer, including heavy metals (arsenic, cadmium, chromium, and nickel, as well as bischloromethl ether (BCME)) [6]. Aromatic amines such (4-AMP, 4-aminobiphenyl, naphthylamine, and benzidine) are associated with an increased risk of bladder cancer [6]. Aflatoxin and vinyl chloride are associated with liver cancers. An exhaustive list of known environmental carcinogens is beyond the scope of this text but should be considered when obtaining the occupational and social history of patients with newly diagnosed cancer.

3.3.2 Behavioral Exposure

3.3.2.1 Tobacco

Tobacco use is responsible for over 30% of cancer-related mortality in the United States and represents the single most common cause of preventable cancer. Cigarettes, as well as smokeless tobacco products, are associated with cancers of multiple organs, including the oral cavity, pharynx, larynx, lung, esophagus, stomach, pancreas, colon, rectum, kidney, bladder, ureter, and cervix. Over 70 carcinogens have been identified in tobacco, with the highest carcinogenic potency attributed to polycyclic aromatic hydrocarbons, nitrosamines, and aromatic amines [7, 8]. The risk of tobacco-associated cancer is proportional to total lifetime cigarette smoke exposure. The risk of lung cancer among long-term heavy smokers is approximately 20 times greater than non-smokers.

3.3.2.2 Alcohol

Excessive and repeated alcohol intake is associated with head and neck, esophageal, liver, rectal, and breast cancers. Interestingly, simultaneous exposure to alcohol and cigarette smoke results in a synergistic increase in the risk of oral cancer, with an increased relative risk of 35-fold when comparing heavy alcohol consumers to those who abstain from alcohol. Similar tobacco-alcohol interactions are also known for esophageal cancer.

3.4 Electromagnetic Radiation

3.4.1 Ultraviolet Light

Ultraviolet light B (UV-B) has a wavelength between 280 nm to 320 nm and is the primary oncogenic form of UV light, whereas ultraviolet A has a longer wavelength (UV-A, wavelength 320 nm to 400 nm) and insufficient energy to induce DNA damage. Ultraviolet light C (UV-C, 200 nm to 280 nm) is absorbed by the atmospheric ozone and, therefore, is not a significant environmental cause of cancer.

UV light induces the formation of pyrimidine dimers in affected DNA, which can result in inactivation of tumor suppressor genes such as p53. Patients diagnosed with Xeroderma pigmentosum (XP), an autosomal recessive disorder, have a defect in the nucleotide excision repair pathway (NER), leading to an inability to adequately repair DNA damage triggered by UV light. Consequently, they face a substantially heightened risk of developing skin cancer, which is at least 2000 times greater compared to individuals unaffected by this condition [9, 10]. This results in periocular and ocular surface cancers in affected patients [11].

Exposure to UV light from the sun has been linked to an increased occurrence of various types of skin cancer, notably squamous cell carcinoma, basal cell carcinoma, and melanoma [12].. In the eye, UV exposure increases the risk of ocular surface squamous neoplasia (OSSN), which includes dysplasia, carcinoma in situ, and squamous cell carcinoma of the conjunctiva or cornea. In the case of uveal melanoma, sunlight exposure has not been implicated as a cause of this condition, but known risk factors include Caucasian race, light skin color, blond hair, and blue eyes [13].

3.4.2 Ionizing Radiation (X-Rays and Gamma-Rays)

In the early twentieth century, it was recognized that radiation can cause tissue damage and various cancers, including acute leukemia and skin cancer. Ionizing radiation causes cell death by DNA damage, particularly by inducing double-stranded DNA breaks, leading to the induction of apoptosis and cell cycle arrest. In general, a dose-response relationship is well described, with both duration and intensity of radiation affecting the relative risk of developing cancer.

Sources of ionizing radiation include occupational exposure (e.g., X-rays) and exposure to nuclear power or atomic weapons. Iatrogenic sources of radiation for cancer treatment also cause secondary malignancies. The best-described data documenting radiation-induced cancers comes from the study of the survivors of the Chernobyl nuclear power plant disaster as well as the Hiroshima and Nagasaki atomic bomb events of World War II [14, 15]. In the latter case, the relative risk of all cancers was 1.53 and included multiple solid tumors arising in the breast, lung, esophagus, stomach, and genitourinary tract. All these solid tumors had a relative risk of between 1.2 and 2.4. In this population, a notable outlier was leukemia, which had a relative risk of 5.6 [14].

3.5 Infections Agents

A number of infectious agents are carcinogenic. The mechanisms by which each pathogen causes cancer are diverse and include causing genomic instability as a result of chronic inflammation, impairment of host immunity, and, in some cases, modulation of the balance between proliferation and antiproliferation signals.

3.5.1 Viruses

Several DNA and RNA viruses are carcinogenic. Human papillomavirus (HPV), Epstein-Barr virus (EBV), Hepatitis viruses B and C, and Kaposi sarcoma herpesvirus (KSHV) exemplify the best-described oncogenic viruses.

3.5.1.1 Human Papilloma Virus (HPV)

HPV was one of the first viruses to be identified as causing human cancer. Almost all of the 200+ genotypes of HPV infect epithelial cells and can cause benign papillomas (warts) or squamous cell carcinoma of the oral, laryngeal, cervical, and anogenital regions. The strongest associations with invasive cervical carcinoma are with HPV subtypes 16 and 18, which can be identified in approximately 85% of cases. HPV causes uncontrolled cellular proliferation by inactivating the tumor suppressor proteins p53 and pRb. HPV DNA with high oncogenic potential has been identified in dysplastic and malignant lesions of the conjunctiva and cornea, suggesting that HPV may contribute to the development of OSSN [16, 17].

3.5.1.2 Epstein-Barr Virus

Epstein-Barr virus (EBV) has been implicated in the pathogenesis of a number of cancers, including the endemic form of Burkitt lymphoma, B-cell lymphomas in immunosuppressed individuals (i.e., post-transplant lymphoproliferative disorder [PTLD]), and nasopharyngeal carcinoma. The mechanism by which EBV transforms B-lymphocytes into malignant cells is not clearly defined but most likely involves viral protein expression that leads to a viral latency program associated with cell survival and proliferation. This is particularly relevant to carcinogenesis in the absence of a host antiviral response due to immunosuppression, as with HIV-

associated lymphoma and/or PTLD. EBV infection is not clearly linked to ophthalmic cancer. Although DNA from viral EBV has been identified in primary intraocular and ocular adnexa lymphomas, this finding is of uncertain significance [18].

3.5.1.3 Kaposi Sarcoma Herpes Virus

Kaposi sarcoma herpes virus (KSHV), also known as human herpesvirus 8, is the causative agent of Kaposi sarcoma (KS). KS can affect the skin of any site and can also involve the eyelid and conjunctiva. This malignancy is rare in immunocompetent individuals. Its incidence increased significantly during the AIDS epidemic of the 1980s. Since the introduction of highly active antiretroviral therapy (HAART), the incidence of KS has decreased significantly.

3.5.1.4 Human T-Cell Lymphotropic Virus-1

Human T-cell lymphotropic virus type 1 (HTLV-1) infection is endemic in Asia, Africa, and much of Latin America. The most well-described cancer associated with HTLV-1 is T-cell leukemia/lymphoma. Known ophthalmic manifestations of HTLV-1 include ocular infiltrates in patients with adult T-cell leukemia/lymphoma as well as non-malignant ocular complications, such as retinal degeneration, neuro-ophthalmic disorders, uveitis, necrotizing retinal vasculitis, and keratoconjunctivitis sicca [19].

3.5.1.5 Hepatitis B and C Virus

Chronic infections by Hepatitis B or Hepatitis C viruses are well-defined risk factors for hepatocellular carcinoma. Extranodal marginal zone lymphoma is also associated with hepatitis C. Importantly, from the standpoint of ophthalmic cancers, there have been conflicting reports of an increased incidence of hepatitis C in patients with ocular adnexal lymphoma [20, 21].

3.5.2 Bacteria

3.5.2.1 Helicobacter Pylori

Helicobacter pylori (H. Pylori) infection is associated with peptic ulcer disease, gastric carcinoma, and mucosa-associated lymphoid tissue (MALT) lymphoma of the stomach [22, 23]. It is hypothesized that chronic inflammation from the infection leads to atrophic gastritis and consequent achlorhydria, gastrointestinal bacterial overgrowth, excess reduction of nitrates to nitrites, DNA damage, and, thus, carcinogenesis in the gastrointestinal epithelium and mucosa-associated lymphoid tissue. In the case of isolated gastric MALT lymphoma, *H. pylori* eradication can result in complete and often durable remission, thereby obviating the need for chemotherapy or radiation in many cases.

3.5.2.2 Chlamydia psittaci

A number of human diseases, including cancers, are strongly associated with infection by *Chlamydia*. *C. trachomatis* and *C. pneumoniae* have been shown to be associated with cervical carcinoma and lung cancer. In addition, *C. psittaci* has been associated with ocular adnexal lymphomas, although there appears to be geographic variation in the strength of this association [24].

3.5.3 Fungus

Aspergillus flavus is a fungus found in grains and peanuts. It produces aflatoxins that cause liver cancer, with the highest incidence occurring in the developing world, China, and South Africa.

3.5.4 Parasites

Schistosoma, *Clonorchis*, and *Opisthorchis* cause chronic inflammation, thereby leading to the development of cancer. The best-described association of cancer with parasitic infection is that of bladder cancer in individuals suffering from schistosomiasis.

3.6 Immune Evasion

It is well established that patients with compromised immunity have an increased susceptibility to cancer. This is particularly evident in patients with acquired immunodeficiency syndrome (AIDS), before the advent of highly active antiretroviral therapy (HAART) [25]. AIDS is associated with several subtypes of lymphoma, including Burkitt's lymphoma. AIDS can also cause Kaposi's sarcoma through HHV-8 infection. Furthermore, cancers arising in the context of chronic inflammation, as well as those with a high mutational burden, such as UV-associated malignancies (e.g., melanoma) and smoking-related lung cancer, evade T-cell surveillance by MHC downregulation or by upregulation of checkpoint inhibitors [26].

3.7 Dietary Factors

A considerable portion of cancer-related mortality can be linked, at least in part, to dietary choices. Diets that include an excess of calories from saturated fat are known to elevate the risk of hormone-dependent cancers, such as breast, ovarian, and endometrial cancers in females and prostate cancer in males. In contrast, a low-fiber diet is associated with an increased risk of colorectal cancer, whereas high dietary intake of red meat has been strongly associated with an increased risk [22].

3.8 Genetic Susceptibility

There are a number of well-defined inherited cancer syndromes, including Li-Fraumeni, Hereditary Nonpolyposis Colon Cancer and Polyposis Colon Cancer syndromes, mutations in the BRCA-1 and BRCA-2 oncogenes, and others. In the case of breast cancer, however, only approximately 10% of patients have an identifiable germline mutation. Many of the inherited cancer predisposition syndromes, such as BRCA-1 and 2, involve defects in DNA repair pathways.

In the case of ophthalmic cancers, inheritance of the retinoblastoma gene is particularly relevant because it shows an autosomal dominant inheritance pattern. In contrast, *Xeroderma pigmentosum* is autosomal recessive. A more comprehensive discussion of cancer genetic factors is discussed in Chap. 7.

3.9 Iatrogenic Cancers

3.9.1 Immunosuppression

Immunosuppression increases the risk of cancer, particularly lymphoma. After solid organ transplantation, lifelong immunosuppression with calcineurin inhibitors is well-known to increase the risk of PTLD, which is commonly EBV-positive. Inhibitors of tumor necrosis factor-alpha (TNF-α), such as infliximab, also increase the risk of lymphoma. In addition, solid organ transplant recipients have a three to five-fold increased lifetime risk of developing malignancy [27, 28].

3.9.2 Chemotherapy

Treatment-related myeloid malignancy is a well-known complication of conventional cytotoxic chemotherapy utilized in the treatment of lymphomas, leukemias, and breast cancer, among others. In patients who have received chemotherapy alone, the rate of secondary malignancy may be as high as 10%, especially in those who have received high-dose chemotherapy as part of an autologous hematopoietic stem cell transplant [29]. Hodgkin lymphoma testicular cancer and other cancers with higher cure rates are associated with higher rates of secondary malignancy because of longer survival. Two common culprits for treatment-related secondary malignancy include alkylating drugs such as cyclophosphamide and topoisomerase II inhibitors such as etoposide.

3.9.3 Radiation Therapy

Therapeutic radiation causes DNA damage and can result in a variety of cancers, including sarcoma, breast cancer, and hematologic malignancies such as myelodysplastic syndrome and acute leukemia. In patients with retinoblastoma, the increased risk of sarcomas after radiation is well-documented [30, 31].

3.10 Summary

The development of cancer can only rarely be attributed to a single cause. Genetic predisposition confers significant risks for developing cancer in a minority of patients. Risk can be increased by carcinogen exposure, immunosuppression, and environmental/iatrogenic causes. It can be difficult to quantify the individual contribution of several risk factors, but this is an area of active research and growth with the advent of advances in genetic testing and the identification of targetable mutations (Fig. 3.2).

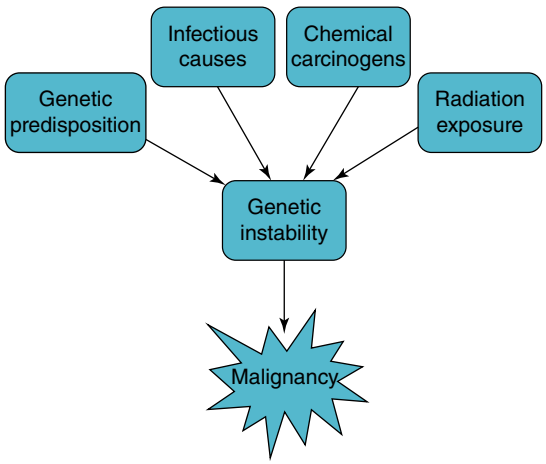

Fig. 3.2 Schematic representation of multiple factors potentially involved in malignant transformation

References

1. Nordling CO. A new theory on cancer-inducing mechanism. Br J Cancer. 1953;7(1):68–72.
2. Dunn GP, Bruce AT, Ikeda H, et al. Cancer immunoediting: from immunosurveillance to tumor escape. Nat Immunol. 2002;3(11):991–8.
3. Westin J, Sehn LH. CAR T cells as a second-line therapy for large B-cell lymphoma: a paradigm shift? Blood. 2022;139(18):2737–46.
4. Mossman BT, Gee JB. Asbestos-related diseases. N Engl J Med. 1989;320(26):1721–30.
5. Liu W, Ernst JD, Broaddus VC. Phagocytosis of crocidolite asbestos induces oxidative stress, DNA damage, and apoptosis in mesothelial cells. Am J Respir Cell Mol Biol. 2000;23(3):371–8.
6. International Agency for Research on Cancer. IARC monographs on the evaluation of carcinogenic risks to humans. Overall evaluation of carcinogencitic risks to humans. 1971-current; Monographs. p. 1–76.
7. Li Y, Hecht SS. Carcinogenic components of tobacco and tobacco smoke: a 2022 update. Food Chem Toxicol. 2022;165:113179.
8. Dept of Health and Human Services, Public Health Service, Office of Surgeon General How tobacco smoke causes disease: the biology and behavioral basis for smoking-attributable disease : a report of the Surgeon General. 2010.
9. Kraemer KH, Lee MM, Andrews AD, Lambert WC. The role of sunlight and DNA repair in melanoma and nonmelanoma skin cancer. The xeroderma pigmentosum paradigm. Arch Dermatol. 1994;130(8):1018–21.
10. Harris CC, Hollstein M. Clinical implications of the p53 tumor-suppressor gene. N Engl J Med. 1993;329(18):1318–27.
11. Lim R, Sethi M, Morley AMS. Ophthalmic manifestations of Xeroderma Pigmentosum: a perspective from the United Kingdom. Ophthalmology. 2017;124(11):1652–61.
12. Cleaver JE, Crowley E. UV damage, DNA repair and skin carcinogenesis. Front Biosci. 2002;7:d1024–43.
13. Singh AD, Rennie IG, Seregard S, et al. Sunlight exposure and pathogenesis of uveal melanoma. Surv Ophthalmol. 2004;49(4):419–28.
14. Pierce DA, Shimizu Y, Preston DL, et al. Studies of the mortality of atomic bomb survivors. Report 12, part I. Cancer: 1950-1990. Radiat Res. 1996;146(1):1–27.
15. Williams D. Cancer after nuclear fallout: lessons from Chernobyl accident. Nat Rev Cancer. 2002;2:543–9.
16. McDonnell JM, Mayr AJ, Martin WJ. DNA of human papillomavirus type 16 in dysplastic and malignant lesions of the conjunctiva and cornea. N Engl J Med. 1989;320(22):1442–6.
17. Nakamura Y, Mashima Y, Kameyama K, et al. Detection of human papillomavirus infection in squamous tumours of the conjunctiva and lacrimal sac by immunohistochemistry, in situ hybridisation, and polymerase chain reaction. Br J Ophthalmol. 1997;81(4):308–13.
18. Chan CC. Molecular pathology of primary intraocular lymphoma. Trans Am Ophthalmol Soc. 2003;101:275–92.
19. Buggage RR. Ocular manifestations of human T-cell lymphotropic virus type 1 infection. Curr Opin Ophthalmol. 2003;14(6):420–5.
20. Arnaud P, Escande MC, Lecuit M, et al. Hepatitis C virus infection and MALT-type ocular adnexal lymphoma. Ann Oncol. 2007;18(2):400–1. author reply 1-3
21. Ferreri AJ, Viale E, Guidoboni M, et al. Clinical implications of hepatitis C virus infection in MALT-type lymphoma of the ocular adnexa. Ann Oncol. 2006;17(5):769–72.
22. Parsonnet J, Friedman GD, Vandersteen DP, et al. Helicobacter pylori and the risk of gastric carcinoma. N Engl J Med. 1991;325:1127–31.
23. Parsonnet J, Hansen S, Rodriguez L, et al. Helicobacter pylori infection and gastric lymphoma. N Engl J Med. 1994;330(18):1267–71.
24. Ferreri AJM, Guidoboni M, Ponzoni M, et al. Evidence for an association between chlamydia psittaci and ocular adnexal lymphomas. J Natl Cancer Inst. 2004;96:586–94.
25. Boshoff C, Weiss R. AIDS-related malignancies. Nat Rev Cancer. 2002;2(5):373–82.
26. de Visser KE, Eichten A, Coussens LM. Paradoxical roles of the immune system during cancer development. Nat Rev Cancer. 2006;6(1):24–37.
27. Kinlen LJ, Sheil AG, Peto J, Doll R. Collaborative United Kingdom-Australasian study of cancer in patients treated with immunosuppressive drugs. Br Med J. 1979;2(6203):1461–6.
28. Adami J, Gabel H, Lindelof B, et al. Cancer risk following organ transplantation: a nationwide cohort study in Sweden. Br J Cancer. 2003;89(7):1221–7.
29. Bhatia S, Krailo MD, Chen Z, et al. Therapy-related myelodysplasia and acute myeloid leukemia after Ewing sarcoma and primitive neuroectodermal tumor of bone: a report from the Children's oncology group. Blood. 2007;109(1):46–51.
30. Wong FL, Boice JD Jr, Abramson DH, et al. Cancer incidence after retinoblastoma, Radiation dose and sarcoma risk. JAMA. 1997;278(15):1262–7.
31. Kleinerman RA, Schonfeld SJ, Sigel BS, et al. Bone and soft-tissue sarcoma risk in long-term survivors of hereditary retinoblastoma treated with radiation. J Clin Oncol. 2019;37(35):3436–45.

Cancer Pathology

4

Gustav Stålhammar and Stefan Seregard

4.1 Introduction

The earliest known descriptions of tumors (Latin for swelling. In Greek: *Onkos*) or tumorous growths as a disease appears on papyri from ancient Egypt. Hippocrates described several distinct types of such tumors, referring to them by the Greek word for cray or crayfish (*karkinos* or *carcinos*) by the appearance of their cut surface. Later, this was translated to its Latin equivalent (*cancer*). The term cancer now usually signifies a malignant neoplasm.

Currently, the field of oncology spans the research, prevention, diagnosis, and treatment of several hundreds of different types of tumors, including the ones originating from the eye and its immediate surroundings.

This text is intended as an overview of cancer pathology with particular reference to classification, tumorigenesis, microscopic features, sampling, and diagnostic techniques for ocular cancer.

4.2 Classification of Neoplasia

As noted above, tumors may be classified as benign or malignant depending on their potential for metastatic spread. Both types of neoplasms might, however, lead to morbidity and death, depending on factors such as cell of origin, immunological responses, nutritional conditions, extent, and location of the growth. Consequently, one should not confuse benign tumors for being uniformly harmless.

On the histological-morphological level, further characteristics separate malignant from benign lesions. However, other than the risk for metastatic spread, no single characteristic can reliably separate one from the other without exceptions. For example, basal cell carcinoma—the most frequently occurring human cancer, can display significant cellular dedifferentiation and pleomorphism and most certainly invades the stroma across the basement membrane but exceedingly rarely metastasizes. Typical differences between benign and malignant tumors are summarized (Table 4.11).

Table 4.11 Typical characteristic differences between benign and malignant tumors

Feature	Benign	Malignant
Cellular pleomorphism	None or mild	Mild to severe
Cellular dedifferentiation	None or mild	Mild to severe
Necrosis	Rare	Occasionally
Basement membrane invasion	Never	Frequent
Proliferation-and growth rate	Low	High
Metastatic spread	Never	Occasionally

G. Stålhammar (✉) · S. Seregard
St. Erik Eye Hospital, Solna, Sweden

Department of Clinical Neuroscience, Karolinska Institutet, Stockholm, Sweden
e-mail: gustav.stalhammar@ki.se; stefan.seregard@ki.se

© The Author(s), under exclusive license to Springer Nature Switzerland AG 2025

A. D. Singh, B. E. Damato (eds.), *Clinical Ophthalmic Oncology*, https://doi.org/10.1007/978-3-031-75907-9_4

4.2.1 Benign Tumors

Benign tumors are usually labeled by the suffix -oma. Some exceptions tend to cause confusion; lymphoma and melanoma are, by definition, malignant irrespective of the –oma suffix. To emphasize this, terms like malignant lymphoma and malignant melanoma are sometimes used.

- Adenomas are composed of cells originating from glandular epithelium.
- Hamartomas are composed of physiologic cells normally occurring at the affected site.
- Choristomas are composed of physiologic cells not normally occurring at the affected site.
- Teratomas are composed of pluripotent cells forming different types of tissue originating from one or more of the three germ cell layers. A teratoma may be either benign or malignant.

4.2.2 Malignant Tumors

- Carcinomas are malignant neoplasms of epithelial origin. For example, an adenocarcinoma of the lacrimal gland is a cancer derived from the glandular epithelium of the lacrimal gland.
- Sarcomas are derived from mesenchymal tissue.
- Blastomas are malignant tumors of embryonic origin. For example, retinoblastomas are derived from retinoblasts in the developing retina.
- Leukemias are malignancies of blood cells that arise from bone marrow precursor cells and are present in the peripheral blood.
- Lymphomas are malignancies derived from lymph nodes but may occasionally be present in other organs, such as the lacrimal gland or in peripheral blood.
- Melanomas are malignant tumors that originate from melanocytes, i.e., cells containing intracytoplasmic pigment lodged in melanosomes. These cells appear in the skin, uvea, conjunctiva, and a variety of other tissues.

4.3 Tumorigenesis and Hallmarks of Cancer

Advances in techniques for studying cancer genetics, gene expression, proteomics, metabolism, and tumor microenvironment have revolutionized our understanding of the tumorigenesis process, in which normal cells and tissues progressively evolve to a neoplastic state [1]. The rapidly accumulating information on the genetic and epigenetic constitution of malignancies has made it possible to tailor novel therapeutic agents, several of which are in clinical use. In 2000, Hanahan and Weinberg structured "hallmarks" of cancer, which mark the steps of tumorigenesis (i.e., the formation of a tumor or the gain of malignant properties by initially normal cells) [2]. This framework was updated in 2011 and then again in 2022 [1, 3]. The hallmarks include genomic instability and mutations, evading immune destruction, proliferative signaling and reprogramming energy metabolism, resisting growth suppressors, escaping cell death, replicative immortality, angiogenesis, invasion and metastasis, and the tumor microenvironment. Some of the hallmarks are outlined below. Genes involved in tumorigenesis are discussed in greater detail elsewhere (Chap. 6).

4.3.1 Genome Instability & Mutation

Believed to underlie many of the hallmark capabilities of neoplastic cells, genomic instability generates random mutations, including chromosomal rearrangements (Fig. 4.1). Conceptually and in a very broad sense, tumors progress by the stepwise accumulation of gain-of-function mutations of oncogenes that promotes cell survival and proliferation, or loss-of-function mutations of tumor suppressor genes. Genetic aberrations such as replication errors, deletions, DNA damage and methylation, histone modifications, and amplifications can occur randomly, be inherited, or be induced by external factors such as radiation, oxidative stress, viral infection, or a breakdown of the genomic maintenance machinery. Mutations that give a subclone of cells a selective advantage will accumulate throughout cell divisions and drive tumor evolution. Similarly, subclones of cells with increased genomic instability will more frequently generate events that either promote or impede expansion, further increasing both the genomic instability and the number of candidates for selective advantage. Non-tumorigenic regions may harbor "passenger" mutations that are not pathogenic but may serve as biomarkers [4]. Recurrent genetic aberrations and mutations across several different tumor types indicate that certain subsets of genetic regions are important drivers of tumorigenesis [5]. The advent of deep sequencing of entire cancer cell genomes has increased our knowledge of the tumorigenic potential and hierarchical arrangement of tumor subclones and the substantial plasticity in differentiation and dedifferentiation that follows genomic instability. The latter is one of the mechanisms proposed as an explanation for refractory treatment responses after an initial period of tumor regression [6]. Studies have shown that mutations of telomerase and telomeres are required to achieve endless replication and survival [7]. However, more recent evidence suggests that cells that survive the telomere erosion enter breakage-fusion-bridge cycles with resulting gross genetic aberrations. Tumor cells with these complex genetic alterations exemplify accelerated acquisition of mutations and rapidly progress to more malignant states [8].

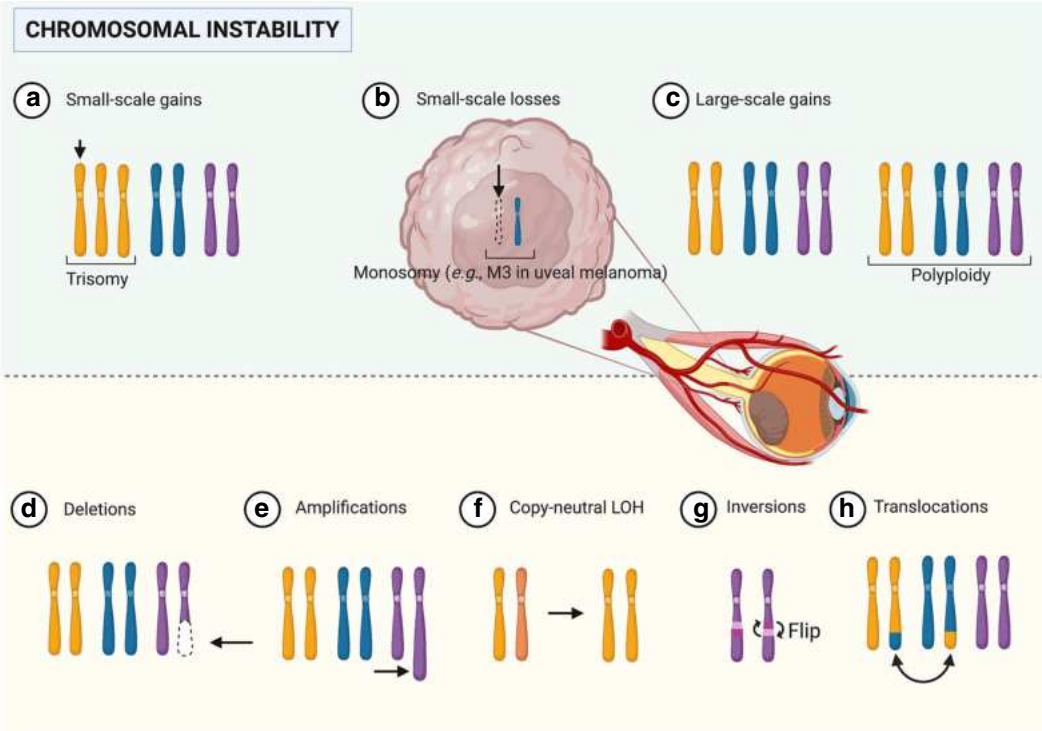

Fig. 4.1 Examples of chromosomal abnormalities in cancer. A multitude of different chromosomal aberrations underlie tumorigenesis, including numerical (left) and structural (right) instability. (**a**) Copy number gain can occur through, e.g., complete or partial trisomy, intrachromosomal, and extrachromosomal amplifications. (**b**) Small-scale losses include monosomy. In uveal melanoma, monosomy of chromosome 3 (M3) confers a poor prognosis. (**c**) Large-scale gains involve several chromosomes and are thereby typically associated with dramatic and complex alterations of the genome. (**d**) In deletions, a part of a chromosome is left out during replication. Some chromosomes have fragile spots in which breaks occur more easily. (**e**) Conversely, in amplification, a part of a chromosome is duplicated, which can lead to overexpression of oncogenes or other drivers. (**f**) In the copy-neutral loss of heterozygosity (LOH), there is no net change in the number of chromosomes. Rather, both copies in a chromosome pair may be flawed. In hereditary retinoblastoma, one parent's copy of the retinoblastoma 1 gene (RB1) has lost its function, and chance loss of heterozygosity in a retinal cell leads to tumor development. (**g**) Inversion: a 180° rotation of a segment. (**h**) Translocation: one chromosomal segment is translocated from one chromosome to another and vice versa

4.3.2 Avoiding Immune Destruction

The immune system plays an important role in eliminating both micrometastases and late-stage tumors [1]. Studies on patients with acquired immunodeficiency syndrome, as well as mouse models, have revealed that deficiencies of NK and T cells result in a higher risk of developing cancer, which suggests that both the adaptive and innate immune systems serve as barriers to tumor progression [9, 10]. Tumor cells must, therefore, be able to evade immunological killing in order to thrive. This can be achieved, e.g., by altering immunological reactions by secreting immunosuppressive factors such as TGF-β [11].

4.3.3 Sustaining Proliferative Signaling

Proliferative signaling has been recognized as one of the earliest and most important steps in tumorigenesis. It is mediated in large by growth factor ligands that bind to cell-surface receptors (frequently tyrosine kinase domains), which mediate proliferative signals, such as progression through the cell cycle, growth, survival, and energy metabolism [1]. By altering the proliferative signaling network, neoplastic cells become independent of their environment and are placed in a continuous proliferative state. Recently, new light has been shed on the adjustments of energy metabolism to suit the rapid growth of cancer cells [1]. The energy metabolism of cancer cells has been demonstrated to be different compared to normal cells; by using aerobic glycolysis, tumor cells can increase their uptake and utilization of glucose, which has been documented in many tumor types and is utilized to visualize tumor dissemination in PET scan examination [12].

4.3.4 Evading Growth Suppressors

Apart from activating proliferation, tumor cells must also be able to avoid signaling pathways that negatively regulate cell proliferation. The genes controlling progression in the cell cycle and inhibitory signaling are commonly referred to as tumor suppressor genes. Four of the classic suppressor genes are breast cancer gene 1 (BRCA1), BRCA2, retinoblastoma 1 gene (RB1), and BRCA1-associated protein 1 (BAP1). The activity of these is down-regulated in a wide range of tumors

[13]. Approximately 70% of women who inherit the BRCA1 mutation will develop breast cancer by the age of 80, and individuals with germline mutations of RB1 suffer a > 90% risk of developing retinoblastoma, as well as an increased risk for several other tumor types. In normal cells, cell-to-cell contact mediates the suppression of growth [1]. If normal cells lose cell-to-cell contact, they undergo programmed cell death. This inhibitory signal is often lost in tumor cells. A set of cell-surface adhesion molecules, most notably the cadherins (E-cadherin and N-cadherin), are commonly altered in tumor cells enabling the tumor cell to let go and then reattach, thus serving as an important step in metastatic spread [14, 15].

4.3.5 Resisting Cell Death

Apoptosis, the orderly conducted programmed cell death, can be triggered by environmental stress, elevated levels of oncogene signaling, telomere shortening, DNA damage, infection, and loss of attachment to other cells. It functions as a guardian against malignant genetic change [16]. By escaping programmed cell death, tumor cells manage to survive even though they harbor multiple genetic changes.

4.3.6 Enabling Replicative Immortality

Normal cells are only able to replicate a limited number of times before they enter either senescence or cell death. Telomeres protect the ends of chromosomes and are intimately involved in replicative immortality [1]. While telomerase, a protein that adds repeat sequences to the end of telomeres and thereby elongates them, is barely expressed in normal cells, its overexpression in malignancies allows the cells to escape destruction [6, 17].

4.3.7 Inducing or Accessing Vasculature

Tumors must acquire new vasculature by angiogenesis to be able to grow beyond a size of approximately 2 mm^3 (Chap. 4).

4.3.8 Activating Invasion & Metastasis

Tumor metastases account for approximately 90% of tumor-related deaths [18]. By pinpointing the processes underlying metastasis, a greater understanding and treatment options will emerge [19]. The metastatic process is thought to start with individual tumor cells dislodging from the primary tumor and spreading by blood or lymphatic vessels. The timing of tumor dissemination remains a subject of debate. There are two major models: the linear progression model, where a cell acquires a set of characteristics through stepwise alteration before dissemination, and the parallel progression model, where cells that are not yet fully neoplastic are circulating, suggesting that they are disseminated from an early malignant lesion [20, 21].

Tumor cells invade surrounding tissue by direct infiltration or by dissemination along blood or lymphatic vessels. In carcinoma, the breakdown of the basement membrane and stromal invasion signify the progression of an in situ carcinoma to invasive carcinoma. Note that this is not the case with tumors of non-epithelial origin, such as uveal melanomas, retinoblastomas, and sarcomas, whose relation to a basement membrane is more or less irrelevant for malignant classification. Carcinomas with minimally invasive features are sometimes referred to as microinvasive. Some malignant tumors show a particular affinity for spreading along peripheral nerves extending a considerable distance away from the primary site, e.g., perineural growth in squamous cell carcinoma or adenoid cystic carcinoma of the lacrimal gland. In some of these tumors, pain, tingling, or hypoesthesia due to invasion or compression of sensory nerve fibers may be the first clinical presentation.

The invasion-metastasis cascade is a complex, multistep process where tumor cells must be able to invade locally through the extracellular matrix and stromal cell layers. The precisely organized architecture of the surrounding normal epithelium serves as an effective barrier, which is overcome by invading tumor cells when the metastatic process starts [20]. The matrix metalloproteinases secreted by macrophages at the tumor periphery contribute to the loss of the basement membrane by proteolysis, which facilitates invasion of the stromal compartment [19, 20]. Invading cells must also become motile to escape the primary tumor; this is achieved by alterations in cell-surface proteins that promote migration. Alteration of the cytoskeleton allows for movement along the extracellular matrix and surface of other cells. Further, the Ras family of GTPases alters actin and myosin activity, which promotes movement [1]. After leaving the primary tumor and invading the stroma, the tumor cells must intravasate into blood or lymph vessels. Intravasation into blood vessels is facilitated by insufficient pericyte coverage and weak endothelial interaction of malignant blood vessels [19]. Acquiring an intrinsic vasculature, driven by secreted factors such as vascular endothelial growth factor (VEGF), is important for primary tumors in order to metastasize and for metastases to grow beyond a certain size. Indirect evidence for this has been obtained in uveal melanoma (and several other tumors), as tumor vessel counts have been associated with a poor prognosis [22]. Following intravasation, the tumor cells must survive the detachment from the supporting tumor matrix, the hemody-

namic forces in the circulation, as well as a hostile immune system. The process of extravasation begins when the cell attaches to the vessel wall in the target tissue. This is achieved either by a tumor forming in the vessel wall, which eventually ruptures the vessel wall or by penetrating the endothelial cells and pericyte layers, thereby establishing micrometastasis (Box 4.1) [23]. Tumors originating within the eye undergo hematogenous dissemination because there is no lymphatic drainage. Tumors originating in the orbit or eyelids may undergo either hematogenous or lymphatic spread, depending on the tumor type and specific relation to the respective vascular system.

It has been shown that breast cancer cells are more likely to leave the primary tumor and enter the systemic circulation during sleep [24]. This highlights the role of the circadian rhythm and associated hormones such as melatonin, testosterone, glucocorticoids, leptin, and insulin for the metastatic process. This is corroborated by recent findings in uveal melanoma, which demonstrate that factors related to metabolism and day-night-cycles modify prognosis: increasing body mass index (BMI) and birthplace latitude (i.e., distance from the equator) correlates with a more favorable prognosis, and melatonin is being investigated as a possible adjuvant treatment [25–28].

Little is known about the predilection for particular metastatic targets, but two major theories have emerged: the mechanistic theory, where tumor cells arrest within capillary beds due to size restrictions of the capillary vessels. The other theory describes receptor-ligand binding between tumor cells and capillaries, also known as the "seed and soil" theory: the provision of a fertile environment in which compatible tumor cells can grow. Most likely, the combination of both theories is true for the majority of metastatic malignancies. Some microenvironments seem to be more hospitable than others, exemplified by preferential dissemination by a wide range of different tumor types to the liver, bone marrow, and lung tissue [29]. Extravasation of tumor cells is more challenging than intravasation since intravasation occurs at the primary tumor site where the vasculature is already quite leaky and, therefore, easy to traverse [19]. After intravasation, the cancer cells must be able to adapt to a very different environment from that of the primary tumor. The process of metastasis is very inefficient. It has been suggested that only <0.01% of tumor cells that enter the circulation go through the metastatic process to establish clinical metastasis [29]. This is supported by the fact that tumor cells from primary breast, lung, and colon cancers, as well as skin- and uveal melanoma, have been found in the peripheral circulation long before any clinically detectable metastasis occurs [30]. By DNA sequencing of primary uveal melanomas and paired distant metastases, it has been shown that the latter have distinct genomic alterations, which indicates that there is a genetic evolution and selection process during disease progress [31].

Micrometastases of uveal melanoma have been found in the liver, lungs, bone marrow, myocardium, and other organs from five of six patients who had no signs of metastatic disease in clinical, radiological, or gross pathological examinations [32]. Even if the tumor cells initially survive in the new microenvironment, it is not certain that they will grow rapidly. On the contrary, most micrometastasis seems to go through a state of dormancy. This may be because of incompatibilities with the foreign environment or from failure to form sufficient vascular supply; it may also be that the cells proliferate, though a net increase does not occur because of the counteracting effects of a high apoptotic rate [19].

4.3.9 Emerging Hallmarks

In 2022, Hanahan summarized another decade of cancer research and concluded that phenotypic plasticity, disrupted differentiation, senescent cells, polymorphic microbiomes, and nonmutational epigenetic reprogramming could be added to the list of cancer hallmarks [3].

Unlocking cancer phenotypic plasticity is critical for tumor development. It involves dedifferentiation, blocked differentiation, and transdifferentiation. Dedifferentiation reverts cancer cells to progenitor-like states. Blocked differentiation prevents cells from reaching nonproliferative states. Transdifferentiation changes cell phenotypes. For instance, in colon cancer, loss of differentiation suppressors promotes dedifferentiation. In leukemia, fusion proteins block differentiation. Pancreatic cells can transdifferentiate in pancreatic cancer. Understanding these processes helps develop targeted therapies to restore normal differentiation and inhibit proliferation. Phenotypic plasticity is a complex aspect of cancer progression with potential for therapeutic interventions.

Cellular senescence is a state of irreversible growth arrest in cells, typically considered a defense against cancer. However, senescent cells can also promote tumor development and progression through the release of signaling molecules known as the senescence-associated secretory phenotype (SASP). The SASP can stimulate cancer cell growth, angiogenesis, invasion, metastasis, and immune suppression. Senescent cancer-associated fibroblasts (CAFs) and other stromal cells in the tumor microenvironment can also contribute to tumor progression. Understanding the role of senescent cells in cancer is crucial for developing targeted therapies to eliminate or modify their tumor-promoting effects.

The microbiota, the diverse collection of microorganisms residing in various body tissues, have a profound impact on

cancer development and progression. The gut microbiome, in particular, plays a crucial role in colon function and can either protect against or promote colon cancer. Dysbiosis in the gut microbiome can damage DNA, stimulate cell proliferation, and affect cellular metabolism. Microbiomes in other tissues, such as the lung, breast, and urogenital system, also influence cancer susceptibility and progression. Polymorphic microbiomes modulate the immune system, affecting immune responses, tumor-promoting inflammation, and the effectiveness of immunotherapies. Bacteria have been found within solid tumors, and variations in the tumor microbiome are associated with clinical features and immune phenotypes. While some bacteria directly stimulate proliferative signaling, their effects on other hallmark capabilities and their generalizability across different cancer types remain unclear. However, it is increasingly clear that polymorphic microbiomes, especially in the gut, are an enabling characteristic that intersects with other factors in cancer development and progression.

Nonmutational epigenetic reprogramming refers to changes in gene expression that occur without alterations in the DNA sequence. This phenomenon plays a role in cancer development and progression alongside genetic mutations. The tumor microenvironment, including factors like hypoxia and nutrient deprivation, can induce epigenetic modifications that contribute to the acquisition of hallmark cancer capabilities. Epigenetic heterogeneity within tumors, driven by factors such as physical properties of the microenvironment and paracrine signaling, leads to phenotypic diversity and the selection of cells with enhanced fitness for proliferation and invasion. Epigenetic regulation also affects stromal cells in the tumor microenvironment, which support tumor growth and progression. Understanding nonmutational epigenetic reprogramming is crucial for comprehending tumor evolution and identifying therapeutic targets.

4.3.10 The Tumor Microenvironment

Tumors are rarely isolated masses of homogenous proliferating cells but rather a makeup of different tumor subpopulations as well as tumor-associated stroma, normal tissue, vasculature, nerves, and infiltrating immune cells. A tumor can thereby be regarded as an organ of itself and not merely a bag of sick cells. Recent studies have shed light on the importance of the recruitment of normal cells, which play a distinct role in the development of neoplasms and also have been implicated in processes such as drug resistance [33]. The stroma surrounding the tumor is frequently reactive and shares similar upregulated pathways, e.g., chronic inflammation or wound healing tissue [34]. The tumor-associated stroma is induced by the neoplasm. In turn, the stromal cells may increase the aggressive behavior of the tumor by releasing growth-stimulating factors that enhance an epithelial-mesenchymal transition (EMT), in which malignant epithelium acquires characteristics necessary for dissemination [19, 35]. Other incidents in the symbiosis of the tumor and its microenvironment may increase the reactivity of the tumor surrounding stroma further. As an example, necrotic cell death releases pro-inflammatory signals into the surrounding microenvironment, which recruits inflammatory cells [34, 36]. These cells may promote angiogenesis, cancer cell proliferation, and invasiveness [36]. Necrosis may therefore act tumor promoting; indeed tumors with necrosis are associated with worse clinical prognosis.

Solid tumors constitute a mixture of different tumor clones at different stages of development, which lead to genetic heterogeneity [37]. The existence of cancer stem cells as an important composition of the proliferating neoplasm has been a source of ongoing discussion (Fig. 4.2). Cancer stem cells are defined by their ability to seed new tumors when inoculated in host mice [38]. They have been suggested as the culprits of acquired chemotherapy resistance as well as disease recurrence after successful debulking of primary disease where no residual disease can be detected [39].

Box 4.1 Steps in the Metastatic Process

- Tumor cell epithelial-mesenchymal transition and invasion of local vessels.
- Tumor cell survival in the circulation.
- Cellular extravasation and mesenchymal-epithelial transition.
- Adaption to the environment at a distant site and establishment of a micrometastasis.
- Acquirement of supportive microenvironment including nutrient, growth factor, and vascular supply for growth to macrometastasis.

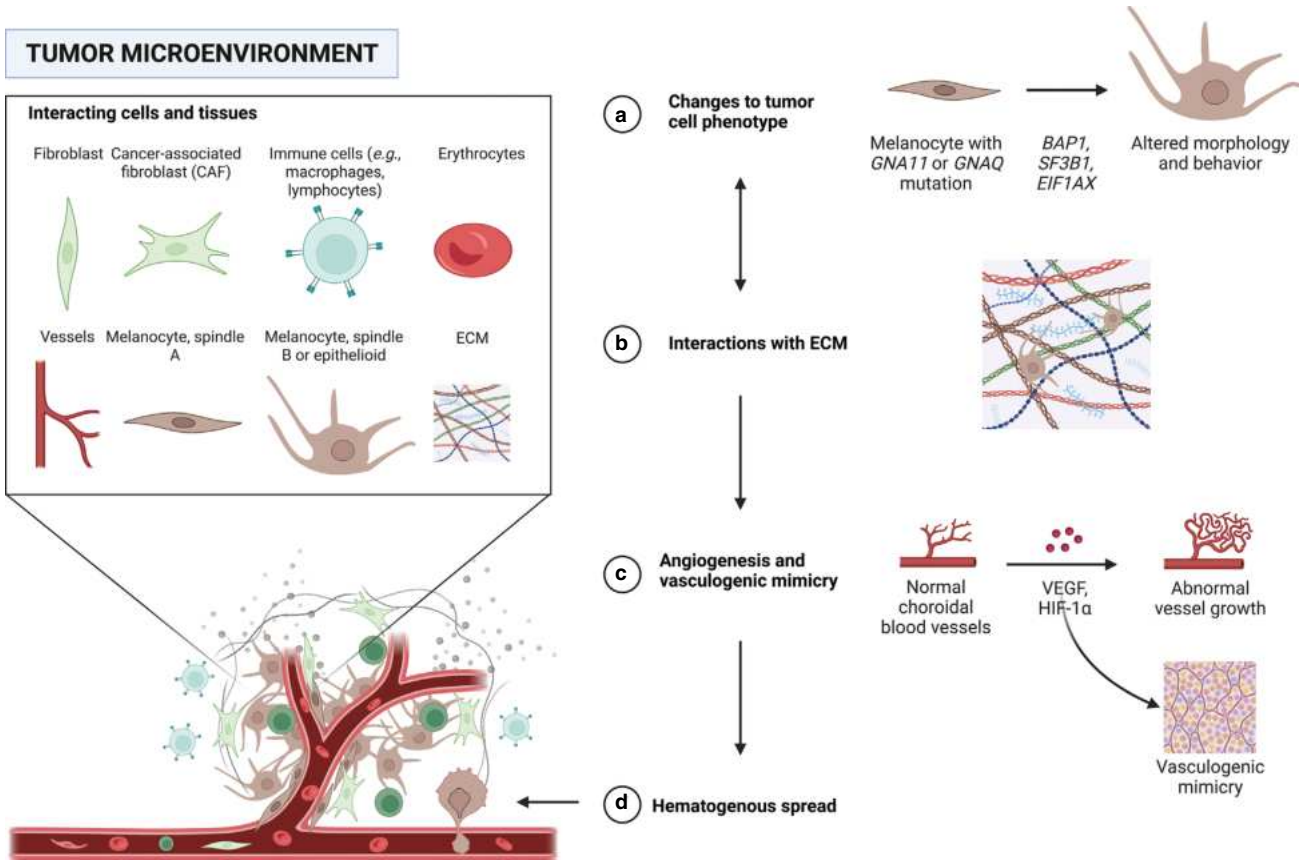

Fig. 4.2 Interacting cells and tissues of the tumor microenvironment. Simplified example of uveal melanoma dissemination. (**a**) *GNAQ* and *GNA11* encode protein members of the q class of G-protein alpha subunits involved in mediating signals between G-protein coupled receptors (GPCR) and downstream effectors. Constitutive activation of GPCR by activating mutations may, in turn increase the risk for further genetic events, including *BAP1*, *SF3B1*, and *EIF1AX* mutations, which correlates with metastatic risk and tumor cell interactions with the extracellular matrix (ECM). Changes to tumor cell phenotype may not necessarily precede tumor-ECM interactions, but ECM microenvironment factors, including hypoxia, may contribute to the changes in tumor cell phenotype. (**b**) By tumor-ECM interactions, ECM is remodeled, which may (**c**) increase vessel recruitment and formation of fluid-conducting patterned matrix channels without endothelial lining (vasculogenic mimicry). (**d**) Presence of vasculogenic mimicry is associated with a greatly increased risk for metastasis

4.4 Microscopic Features of Neoplasia

Certain histopathologic features differentiate benign and malignant tumors from surrounding normal tissues. In general, the differences from the normal tissue are more marked in malignant tumors than in benign tumors.

4.4.1 Cellular Proliferation

Many malignant tumors feature a large number of dividing cells with abnormal mitotic patterns. Cell proliferation markers like proliferating cell nucleolar antigen (PCNA), phosphohistone H3 (PHH3), Ki-67, and cyclins often reveal a larger proportion of proliferating cancer cells than detected by mitotic counts alone. A high mitotic index (mitotic count per unit of microscopic area) is often found in rapidly growing tumors, although this is usually balanced by the presence of many apoptotic cells. Not all cancers show high cell proliferation rates; typically, uveal melanoma features comparatively low counts but nonetheless may metastasize. However, in many cancers, including uveal melanoma, a high cell proliferation rate is associated with poor prognosis [40, 41].

4.4.2 Cellular Pleomorphism

When tissue and cellular architecture are distorted, the tissue is classified as dysplastic. Epithelial dysplasia may be divided into mild, moderate, and severe dysplasia. Severe dysplasia is characterized by full-thickness dysplasia with prominent cellular atypia and is synonymous with carcinoma in situ. It is debatable whether a slight or even moderate degree of dysplasia is precancerous, a condition inevitably leading to cancer. When tissue architecture is considerably distorted with individual cells showing a significant degree of variation in shape and size, including abnormal nuclei sometimes featuring binucleate or multinucleate forms, this is referred to as pleo-

morphism at the cellular level. Cellular pleomorphism, including the extreme state when the tissue of origin is no longer recognizable (anaplasia), is a hallmark of cancer.

4.4.3 Cellular Differentiation

Typically, cancers recapitulate the architecture of the tissue of their origin to some extent. For example, squamous cell carcinomas grow in sheets of keratin-producing cells attached to each other with an abundance of intercellular bridges, and skin melanomas can preserve a nest-building tendency with the physiological production of pigment. This recapitulation may closely resemble the original structure, and such cancers are highly differentiated, whereas others are poorly differentiated or even anaplastic. Usually, poorly differentiated cancers carry a worse prognosis than cancers more closely mimicking the original tissue appearance. In retinoblastoma, the rosettes appearing in moderately and highly differentiated retinoblastoma are believed to be an attempt to recapitulate the original retinal structure (Fig. 4.3).

In uveal melanoma, four basic cell types can be outlined in the progression from a benign precursor lesion to primary tumor and metastasis: normal melanocytes, spindle A and B, and epithelioid tumor cells. Differential expression of tumor suppressors, growth factors, and immune checkpoints could contribute to their relative over-and underrepresentation in benign, primary tumor, and metastatic samples. In normal choroidal tissue and nevi, only normal melanocytes and spindle A cells are represented. Epithelioid and spindle B cells are overrepresented in the base and apex, and spindle A cells are in the center of primary tumors. Liver metastases contain no normal melanocytes or spindle A cells (Fig. 4.4) [42].

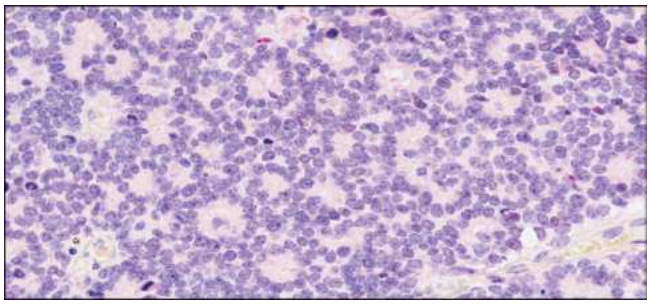

Fig. 4.3 Highly differentiated retinoblastoma with tumor cells arranged in a radiating, flowerlike pattern referred to as Flexner-Wintersteiner rosettes

4.4.4 Nuclear Cytoplasmic Ratio

Most neoplastic cells have a relatively large nucleus in relation to the amount of cytoplasm. However, this varies significantly with the type of neoplasia. Clear cell carcinoma of the kidney features large cells with abundant cytoplasm, whereas retinoblastoma typically is composed of cells with relatively large nuclei and small amounts of cytoplasm.

4.4.5 Tumor Infiltration by Normal Cells

In some malignant tumors, infiltration by macrophages or lymphocytes is a characteristic feature reflecting the recruitment of the immune system as well as physiologic cells by neoplastic tissue. Macrophage infiltration in uveal melanoma is associated with a poor prognosis [43].

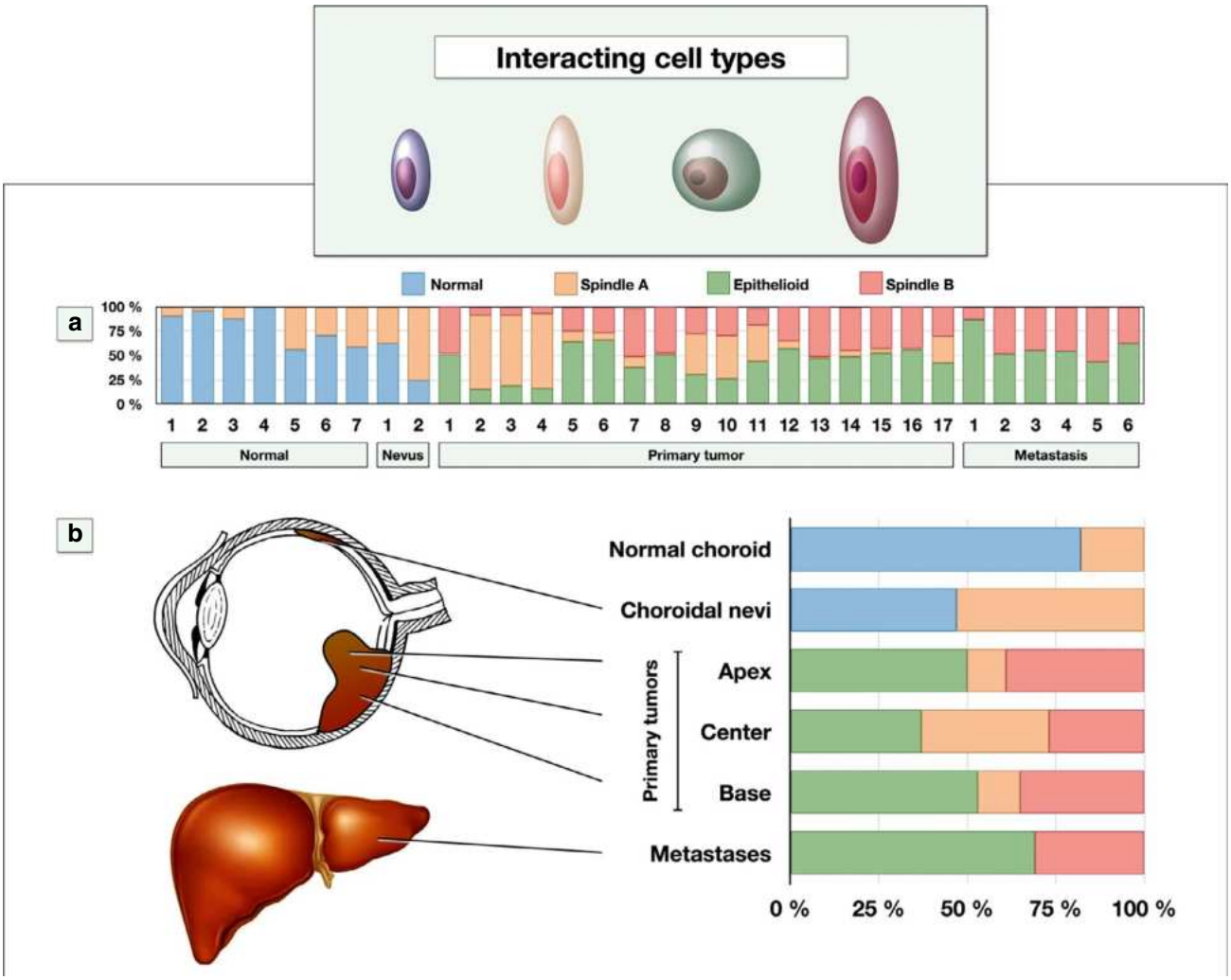

Fig. 4.4 Distribution of normal choroidal melanocytes, spindle A, spindle B, and epithelioid tumor cells in normal choroid, choroidal nevi, primary tumors, and metastases. (Reprinted from "Digital morphometry and cluster analysis identifies four types of melanocyte during uveal melanoma progression," Stålhammar & Gill. Page No. 6 (2023) [42]. Licensed under a Creative Commons Attribution 4.0 International License)

4.5 Tissue Sampling and Processing

4.5.1 Cytological Sampling

Sampling typically includes a number of individual cells disrupted from their original tissue. Diagnosis is, therefore, usually made on the morphological appearance of individual cells because the relationship to surrounding cells is lost. Cytological samples may be used for immunocytochemistry, which is conducted to characterize protein expression, and for auxiliary techniques such as flow cytometry. Two basic techniques are used for sampling.

4.5.1.1 Exfoliative Cytology

Exfoliative cytology involves the sampling of cells that are dispersed in fluids, e.g., cerebrospinal fluid sampled by lumbar puncture or forcibly removed by a spatula, brush, or some other instrument or filter paper. Cells may also be dislodged from a surface by a touch preparation, for example, imprint cytology for conjunctival tumors. The exfoliative sample is then spread on a glass slide and stained. Vitrectomy samples may be filtered through a membrane, e.g., a Millipore filter, centrifugated in a pellet (cytospin preparation), or paraffin-embedded as a cell block.

4.5.1.2 Aspiration Cytology

Aspiration cytology may be applied to palpable lesions, guided by ultrasound or computerized tomography imaging. Intraocular fine-needle aspiration biopsy (FNAB) is performed with needles between 21 and 25 gauges [44]. A pars plana approach guided by indirect ophthalmoscopy may be used, but clear cornea and transscleral routes have also been advocated [45–47]. The various techniques of intraocular biopsy are discussed in detail under uveal tumors. Local tumor spread using FNAB in loosely cohesive tumors is a

concern. For this reason, FNAB should only be used with extreme caution and almost never in suspected cases of retinoblastoma. The requirements for tissue handling vary between laboratories; therefore, it is advisable to contact the local cytopathologist before sampling.

4.5.2 Histopathologic Sampling and Processing

Tissue is obtained by incisional or excisional biopsy of the lesion. Caution not to coagulate or otherwise maltreat the tissue sample is recommended. Incisional biopsies or core needle biopsies with disruption of a tumor-surrounding capsule should be avoided in tumors prone to local recurrence, e.g., pleomorphic adenoma of the lacrimal gland. In such tumors, primary complete excision or possibly diagnostic FNAB followed by complete excision is recommended. Retinoblastomas should not be biopsied, considering the risk of extraocular spread. For other tumors, including uveal melanoma and choroidal metastases, biopsies are generally safe and provide important prognostic information (Fig. 4.5) [48]. The optimal fixative for the surgical biopsy varies depending on the local setting and the technique used for histopathologic examination, but for most cases formaldehyde is sufficient.

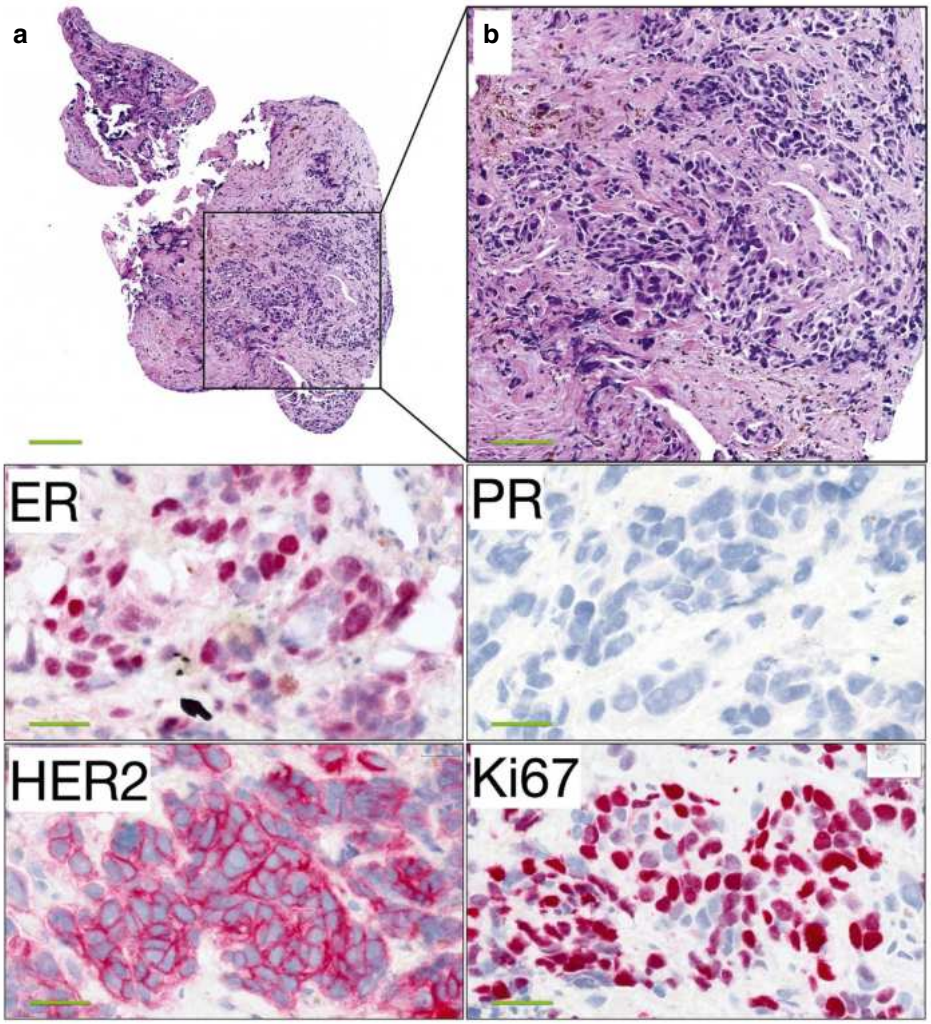

Fig. 4.5 Transvitreal incisional biopsy from a choroidal metastasis of breast cancer. A) Irregular clusters of enlarged epithelioid cells grow in choroidal tissue with severe fibrotic changes, which may be a reaction to tumor infiltration and inflammation. B) In larger magnification, the infiltrating tumor cells are seen with pleomorphism, hyperchromasia, and a tendency to form rounded gland-like structures. Most of the tumor cell nuclei were positive for ER (red, chromogen) but negative for PR (blue, hematoxylin). There was complete and intense membranous HER2 positivity in all tumor cells. The proliferation marker Ki67 was positive in a majority of tumor cell nuclei, in this area, about 140 of 180 tumor cells (78%), which suggests a very high rate of proliferation. Any visible staining above the background sufficed for the positive classification of a tumor cell in stains with ER, PR, and Ki67. ER: estrogen receptor. PR: progesterone receptor. HER2: human epidermal growth factor receptor 2. Scale bars: A 200 μm. B 100 μm. ER, PR, HER2, and Ki67 40 μm. (Reprinted from "Overrepresentation of human epidermal growth factor receptor 2 positive and Luminal B breast cancer metastases in the eyes and orbit," Stålhammar & Grossniklaus. Page No. 3 (2022) [52]. Licensed under a Creative Commons Attribution 4.0 International License)

When biopsying tissues like the conjunctiva or iris, care should be taken to orientate the specimen and to make sure the tissue is maintained flat and does not curl. This can be achieved by attaching the tissue to a piece of filter paper and annotating the specimen mount before immersion in the fixative. Assessment of the surgical margins is pivotal in any excisional tumor biopsy. To facilitate this, the surgical margins may be marked by the pathologist before gross sectioning and paraffin embedding. Also, special techniques like the Mohs technique using cryosectioning or modifications using vertical paraffin-embedded sections have been advocated for eyelid and skin tumors [49, 50]. Cryosectioning allows for a rapid assessment (within 30 mins) of margins or malignancy and can be used as a preoperative procedure; however, paraffin sections allow a more reliable microscopic assessment. Specific guidelines for histopathology reports on cancer specimens from the eye and adnexa have been discussed elsewhere [51].

4.6 Diagnostic Techniques

Traditionally, cancer diagnosis was made using light microscopic examination, but recent advances in molecular diagnostics have created a completely new set of tools with which tumors may be more accurately diagnosed and better characterized. Some of these techniques are outlined below.

4.6.1 Light Microscopy

When processed for routine light microscopy, samples are usually fixed in formaldehyde and then embedded in paraffin. This allows for the cutting of 3–4 μm thick sections. Paraffin sections are usually routinely stained with hematoxylin and eosin, although this may differ depending on the local routine. Other stains like the periodic acid-Schiff dye preferentially stain mucopolysaccharides and glycogen and are appropriate for the study of basement membrane material like the lens capsule.

4.6.2 Immunohistochemistry

The technique of staining specific cell surface, cytoplasmic, and nuclear antigens with color-labeled antibodies has revolutionized diagnostic pathology in the last couple of decades. Several commercially available antibodies may be used in combination with routine fixatives like formaldehyde, and staining may be enhanced by antigen retrieval techniques. Prolonged cold ischemia and fixation times may cause reduced staining, and the wary pathologist uses negative and positive controls. It should be noted that the interpretation of immunohistochemical stains is still somewhat subjective and that the markers cannot be relied on to detect disease with full sensitivity and specificity. For example, Ki67 will highlight proliferating tumor cells but also proliferating fully benign cells, including the lymphocytes that frequently infiltrate tumors. The reproducibility of immunohistochemical evaluations can be increased with digital image analysis and other automated procedures (Fig. 4.6). More recently,

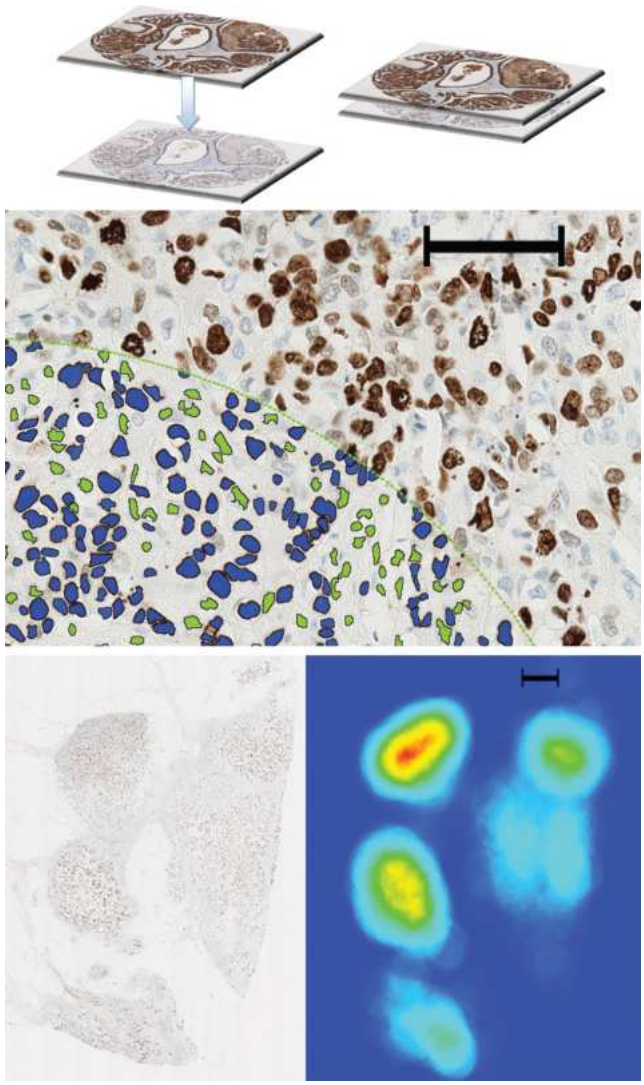

Fig. 4.6 Illustration of digital image analysis. Two adjacent tumor sections stained with a marker for the type of cell to be analyzed, e.g., an epithelial pancytokeratin marker such as CkMNF116 in breast cancer or Melan A/Mart-1 for melanoma and a biomarker of choice (such as estrogen receptors (ER), the proliferation marker Ki67 or BAP1) are aligned on top of each other. Thereby, the software can distinguish the fraction of Ki67/ER/BAP1-positive cells within the cell population of interest. Middle: Green dotted line marks part of a region of interest, automatically scored for Ki67 index. Blue polygons mark nuclei positive for both Ki67 and CkMNF116. Green polygons mark nuclei positive for CkMNF116 but negative for Ki67. The proportion of blue polygons to the sum of blue and green polygons constitutes the Ki67 proliferation index. Bottom: Illustration of heat map function where the digital image analysis system has analyzed the digitally scanned glass slide (left) for the tumor area with the highest concentration of cells stained by both the pancytokeratin marker and Ki67, marked in red (right). Scale bar, middle = 50 μm. Scale bar, lower = 500 μm (Reprinted from "Digital image analysis outperforms manual biomarker assessment in breast cancer", Stålhammar G et al. Page No. 321, Copyright (2016), with permission from Springer Nature [56])

artificial intelligence and its subsets have demonstrated great utility in the analysis of tissue sections, immunohistochemistry, and other complex tasks in clinical pathology [53–55].

Box 4.2 Artificial Intelligence Versus Machine Learning and Deep Learning

- **Artificial Intelligence** (**AI**): refers to a program that can sense, reason, act, and adapt.
- **Machine Learning (ML)**: subset of AI in which the performance of algorithms improves as they are exposed to more data over time.
- **Deep Learning (DL)**: subset of machine learning in which multilayered neural networks learn from vast amounts of data.

4.6.3 Additional Techniques

Recent advances in molecular pathology have generated numerous techniques for the genetic and epigenetic study of tumors. One of the mainstay laboratory techniques is the polymerase chain reaction (PCR). Several different types of PCR have been developed, including competitive or real-time PCR, which allows for sensitive assays of gene expression at the RNA level. Further, several experimental laboratory techniques have been translated into clinical use, e.g., flow cytometry in lymphoma and tissue imprints for gene rearrangements in rhabdomyosarcoma. In several cases, tissue needs to be submitted fresh, which requires close collaboration with the examining laboratory for optimal results. Microarrays, DNA, and RNA-sequencing have revolutionized our understanding of the tumor genome and transcriptome by making it possible to study all genes or a subset thereof in one experiment to the resolution of single nucleotides. Distinct cancer biomarkers and gene expression profiles have been identified through microarray studies. After vigorous evaluation, several assays have been developed and are now in clinical use. Three of the earliest assays developed include the MammaPrint®, Oncotype DX®, and PAM50 assays for breast cancer [57]. These assays predict prognosis and assess the likely benefit from treatment by analyzing signatures of multiple genes. This is crucial since, in most cancers, the probability of curative treatment and survival drops drastically once metastases appear. In uveal melanoma, genome-wide expression profiling has identified three distinct molecular subclasses of tumors: low-grade (class 1A) tumors with a 2% 5-year risk for metastasis, intermediate-grade (class 1B) tumors with a 21% 5-year risk for metastasis and high-grade (class 2) tumors with a 72% 5-year risk for metastasis [58]. From these results, a 15-gene assay under the trade name DecisionDx®-UM has been developed [14, 59]. Through fine-needle biopsies of uveal melanomas in vivo or a sample of archived formalin-fixed paraffin-embedded tissue, the assay can be used to determine each patient's metastatic potential. In turn, this enables accurate information to patients and relatives. Potentially, the identification of a high-risk group also enables the selection of patients to offer adjuvant therapy [60, 61]. This constitutes an important opportunity for randomized controlled trials of the effect of existing drugs and for the development of novel strategies. To this date, the absence of effective adjuvant treatment, even for patients with a near-certain likelihood for future metastasis, is, however, still a major obstacle to the improvement of survival in uveal melanoma. Several antibodies have been investigated in ocular tumors, including aflibercept (VEGF-Trap) and ipilimumab (anti-CTLA4) [62, 63]. Ipilimumab is applied in routine clinical treatment, and several drugs, including anaplastic lymphoma kinase (ALK), c-ros oncogene 1 (ROS1), VEGFR2, platelet-derived growth factor receptor b (PDGFRb) and c-kit -inhibitors are being investigated for their potential to prevent the development of clinically detectable metastases.

In line with the findings in microarray studies, proteomics holds a similar promise and generates vast amounts of data on protein expression. Next-generation sequencing of the whole genome has become a groundbreaking tool in the study of cancer cells. It is used for the characterization and identification of, e.g., DNA, RNA, exome, and transcriptome sequences of tumor cells. It enables the identification of, e.g., copy number variants, sequence variants, mutations, and structural changes such as chromosomal translocations and fusion genes. Various open-source projects aim at collecting sequence variants and mutations critical in the development of human cancers. Public sharing of data has enabled inclusion in larger data sets for reanalysis and construction of databases of cancer profiles.

Described here are only a handful of the techniques developed for research and clinical study of tumors. In the near future, many of the techniques used for experimental purposes will delineate central pathways in cancer cells with prognostic, diagnostic, and treatment implications in human cancer.

Acknowledgments Figures 4.1 and 4.2 were created with Biorender.com

References

1. Hanahan D, Weinberg RA. Hallmarks of cancer: the next generation. Cell. 2011;144:646–74. https://doi.org/10.1016/J.Cell.2011.02.013.
2. Hanahan D, Weinberg RA. The hallmarks of cancer. Cell. 2000;100:57–70. https://doi.org/10.1016/S0092-8674(00)81683-9.

3. Hanahan D. Hallmarks of cancer: new dimensions. Cancer Discov. 2022;12:31–46. https://doi.org/10.1158/2159-8290.Cd-21-1059.
4. Stratton MR. Exploring the genomes of cancer cells: progress and promise. Science. 2011;331:1553–8. https://doi.org/10.1126/Science.1204040.
5. Korkola J, Gray JW. Breast cancer genomes—form and function. Curr Opin Genet Dev. 2010;20:4–14. https://doi.org/10.1016/J.Gde.2009.11.005.
6. Meacham CE, Morrison SJ. Tumour heterogeneity and cancer cell plasticity. Nature. 2013;501:328–37. https://doi.org/10.1038/Nature12624.
7. Blasco MA. Telomeres and human disease: ageing, cancer And beyond. Nat Rev Genet. 2005;6:611–22. https://doi.org/10.1038/Nrg1656.
8. Artandi SE, Depinho RA. Telomeres and telomerase in cancer. Carcinogenesis. 2010;31:9–18. https://doi.org/10.1093/Carcin/Bgp268.
9. Teng MW, Swann JB, Koebel CM, Schreiber RD, Smyth MJ. Immune-mediated dormancy: an equilibrium with cancer. J Leukoc Biol. 2008;84:988–93. https://doi.org/10.1189/Jlb.1107774.
10. Kim MY, et al. Tumor self-seeding by circulating cancer cells. Cell. 2009;139:1315–26. https://doi.org/10.1016/J.Cell.2009.11.025.
11. Shields JD, Kourtis IC, Tomei AA, Roberts JM, Swartz MA. Induction of Lymphoidlike stroma and immune escape by tumors that express the chemokine Ccl21. Science. 2010;328:749–52. https://doi.org/10.1126/Science.1185837.
12. Jones RG, Thompson CB. Tumor suppressors and cell metabolism: a recipe for cancer growth. Genes Dev. 2009;23:537–48. https://doi.org/10.1101/Gad.1756509.
13. Burkhart DL, Sage J. Cellular mechanisms of tumour suppression by the retinoblastoma gene. Nat Rev Cancer. 2008;8:671–82. https://doi.org/10.1038/Nrc2399.
14. Onken MD, et al. Functional gene expression analysis uncovers phenotypic switch in aggressive uveal melanomas. Cancer Res. 2006;66:4602. https://doi.org/10.1158/0008-5472.Can-05-4196.
15. Berx G, Van Roy F. Involvement of members of the cadherin superfamily in cancer. Cold Spring Harb Perspect Biol. 2009;1:A003129. https://doi.org/10.1101/Cshperspect.A003129.
16. Adams JM, Cory S. The Bcl-2 apoptotic switch in cancer development and therapy. Oncogene. 2007;26:1324–37. https://doi.org/10.1038/Sj.Onc.1210220.
17. Shay JW, Wright WE. Hayflick, his limit, and cellular ageing. Nat Rev Mol Cell Biol. 2000;1:72–6. https://doi.org/10.1038/35036093.
18. Mehlen P, Puisieux A. Metastasis: a question of life or death. Nat Rev Cancer. 2006;6:449–58. https://doi.org/10.1038/Nrc1886.
19. Valastyan S, Weinberg RA. Tumor metastasis: molecular insights and evolving paradigms. Cell. 2011;147:275–92. https://doi.org/10.1016/J.Cell.2011.09.024.
20. Nagrath S, et al. Isolation of rare circulating tumour cells in cancer patients by microchip technology. Nature. 2007;450:1235–9. https://doi.org/10.1038/Nature06385.
21. Husemann Y, et al. Systemic spread is an early step in breast cancer. Cancer Cell. 2008;13:58–68. https://doi.org/10.1016/J.Ccr.2007.12.003.
22. Folberg R, et al. The morphologic characteristics of tumor blood vessels as a marker of tumor progression in primary human uveal melanoma: a matched case-control study. Hum Pathol. 1992;23:1298–305. https://doi.org/10.1016/0046-8177(92)90299-I.
23. Al-Mehdi AB, et al. Intravascular origin of metastasis from the proliferation of endothelium-attached tumor cells: a new model for metastasis. Nat Med. 2000;6:100–2. https://doi.org/10.1038/71429.
24. Diamantopoulou Z, et al. The metastatic spread of breast cancer accelerates during sleep. Nature. 2022;607:156–62. https://doi.org/10.1038/S41586-022-04875-Y.
25. Hagstrom A, Kal Omar R, Williams PA, Stalhammar G. The rationale for treating uveal melanoma with adjuvant melatonin: a review of the literature. BMC Cancer. 2022;22:398. https://doi.org/10.1186/S12885-022-09464-W.
26. Kal Omar R, Hagstrom A, Stalhammar G. Adjuvant melatonin for uveal melanoma (Amum): protocol for a randomized open-label phase iii study. Trials. 2023;24:230. https://doi.org/10.1186/S13063-023-07245-9.
27. Stalhammar G, Williams PA, Landelius T. The prognostic implication of latitude in uveal melanoma: a Nationwide observational cohort study of all patients born in Sweden between 1947 and 1989. Discov Oncol. 2022;13:116. https://doi.org/10.1007/S12672-022-00584-0.
28. Sabazade S, et al. Obesity paradox in uveal melanoma: high body mass index is associated with low metastatic risk. Br J Ophthalmol. 2023;108:bjo-2022-322877. https://doi.org/10.1136/Bjo-2022-322877.
29. Chambers AF, Groom AC, Macdonald IC. Dissemination and growth of cancer cells in metastatic sites. Nat Rev Cancer. 2002;2:563–72. https://doi.org/10.1038/Nrc865.
30. Bidard FC, et al. Detection rate and prognostic value of circulating tumor cells and circulating tumor Dna in metastatic uveal melanoma. Int J Cancer. 2014;134:1207–13. https://doi.org/10.1002/Ijc.28436.
31. Shain AH, et al. The genetic evolution of metastatic uveal melanoma. Nat Genet. 2019;51:1123–30. https://doi.org/10.1038/S41588-019-0440-9.
32. Gill VT, et al. Multiorgan involvement of dormant uveal melanoma micrometastases in postmortem tissue from patients without coexisting macrometastases. Am J Clin Pathol. 2023;160:164. https://doi.org/10.1093/Ajcp/Aqad029.
33. Straussman R, et al. Tumour micro-environment elicits innate resistance to Raf inhibitors through Hgf secretion. Nature. 2012;487:500–4. https://doi.org/10.1038/Nature11183.
34. Grivennikov SI, Greten FR, Karin M. Immunity, inflammation, and cancer. Cell. 2010;140:883–99. https://doi.org/10.1016/J.Cell.2010.01.025.
35. Dirat B, et al. Cancer-associated adipocytes exhibit an activated phenotype and contribute to breast cancer invasion. Cancer Res. 2011;71:2455–65. https://doi.org/10.1158/0008-5472.Can-10-3323.
36. Denardo DG, et al. Cd4(+) T cells regulate pulmonary metastasis of mammary carcinomas by enhancing Protumor properties of macrophages. Cancer Cell. 2009;16:91–102. https://doi.org/10.1016/J.Ccr.2009.06.018.
37. Navin N, et al. Tumour evolution inferred by single-cell sequencing. Nature. 2011;472:90–4. https://doi.org/10.1038/Nature09807.
38. Cho RW, Clarke MF. Recent advances in cancer stem cells. Curr Opin Genet Dev. 2008;18:48–53. https://doi.org/10.1016/J.Gde.2008.01.017.
39. Singh A, Settleman J. Emt, cancer stem cells and drug resistance: an emerging Axis of evil in the war on cancer. Oncogene. 2010;29:4741–51. https://doi.org/10.1038/Onc.2010.215.
40. Seregard S, Spångberg B, Juul C, Oskarsson M. Prognostic accuracy of the mean of the largest nucleoli, vascular patterns, and Pc-10 in posterior uveal melanoma. Ophthalmology. 1998;105:485–91. https://doi.org/10.1016/S0161-6420(98)93032-9.
41. Seregard S, Oskarsson M, Spangberg B. Pc-10 as a predictor of prognosis after antigen retrieval in posterior uveal melanoma. Invest Ophthalmol Vis Sci. 1996;37:1451–8.
42. Stalhammar G, Gill VT. Digital morphometry and cluster analysis identifies four types of melanocyte during uveal melanoma progression. Commun Med (Lond). 2023;3:60. https://doi.org/10.1038/S43856-023-00291-Z.
43. Mäkitie T, Summanen P, Tarkkanen A, Kivelä T. Tumor-infiltrating macrophages (Cd68(+) cells) and prognosis in malignant uveal melanoma. Invest Ophthalmol Vis Sci. 2001;42:1414.

44. Char DH, Kemlitz AE, Miller T. Intraocular biopsy. Ophthalmol Clin N Am. 2005;18:177–85. https://doi.org/10.1016/J.Ohc.2004.08.007.
45. Zorn KK, et al. Gene expression profiles of serous, Endometrioid, and clear cell subtypes of ovarian and endometrial cancer. Clin Cancer Res. 2005;11:6422–30. https://doi.org/10.1158/1078-0432.Ccr-05-0508.
46. Shields CL, et al. Fine-needle aspiration biopsy of iris tumors in 100 consecutive cases: technique and complications. Ophthalmology. 2006;113:2080–6. https://doi.org/10.1016/J.Ophtha.2006.05.042.
47. Bechrakis NE, Foerster MH, Bornfeld N. Biopsy in indeterminate intraocular tumors. Ophthalmology. 2002;109:235–42. https://doi.org/10.1016/S0161-6420(01)00931-9.
48. Herrspiegel C, et al. Nuclear expression of Bap-1 in Transvitreal incisional biopsies and subsequent enucleation of eyes with posterior choroidal melanoma. Br J Ophthalmol. 2021;105:582–6. https://doi.org/10.1136/Bjophthalmol-2020-316498.
49. Spencer JM, Nossa R, Tse DT, Sequeira M. Sebaceous carcinoma of the eyelid treated with Mohs micrographic surgery. J Am Acad Dermatol. 2001;44:1004–9. https://doi.org/10.1067/Mjd.2001.113692.
50. Malhotra R, Chen C, Huilgol SC, Hill DC, Selva D. Mapped serial excision for periocular lentigo maligna and lentigo maligna melanoma. Ophthalmology. 2003;110:2011–8. https://doi.org/10.1016/S0161-6420(03)00670-5.
51. Folberg R, et al. Recommendations for the reporting of tissues removed as part of the surgical treatment of common malignancies of the eye and its adnexa. Am J Surg Pathol. 2003;27:999–1004. https://doi.org/10.1097/00000478-200307000-00016.
52. Stalhammar G, Grossniklaus HE. Overrepresentation of human epidermal growth factor receptor 2 positive-and luminal B breast cancer metastases in the eyes and orbit. Eye (Lond). 2022;37:2499. https://doi.org/10.1038/S41433-022-02363-1.
53. Sun M, et al. Prediction of Bap1 expression in uveal melanoma using densely-connected deep classification networks. Cancers (Basel). 2019;11:1579. https://doi.org/10.3390/Cancers11101579.
54. Zhang H, et al. Piloting a deep learning model for predicting nuclear Bap1 Immunohistochemical expression of uveal melanoma from hematoxylin-and-eosin sections. Transl Vis Sci Technol. 2020;9:50. https://doi.org/10.1167/Tvst.9.2.50.
55. Wu S, et al. Artificial intelligence-based model for lymph node metastases detection on whole slide images in bladder cancer: a retrospective, multicentre, diagnostic study. Lancet Oncol. 2023;24:360–70. https://doi.org/10.1016/S1470-2045(23)00061-X.
56. Stalhammar G, et al. Digital image analysis outperforms manual biomarker assessment in breast cancer. Mod Pathol. 2016;29:318–29. https://doi.org/10.1038/Modpathol.2016.34.
57. Paik S, et al. A multigene assay to predict recurrence of tamoxifen-treated, node-negative breast cancer. N Engl J Med. 2004;351:2817–26. https://doi.org/10.1056/Nejmoa041588.
58. Onken MD, Worley LA, Ehlers JP, Harbour JW. Gene expression profiling in uveal melanoma reveals two molecular classes and predicts metastatic death. Cancer Res. 2004;64:7205–9. https://doi.org/10.1158/0008-5472.Can-04-1750.
59. Onken MD, et al. Collaborative ocular oncology group report number 1: prospective validation of a multi-gene prognostic assay in uveal melanoma. Ophthalmology. 2012;119:1596–603. https://doi.org/10.1016/J.Ophtha.2012.02.017.
60. Field MG, Harbour JW. Recent developments in prognostic and predictive testing in uveal melanoma. Curr Opin Ophthalmol. 2014;25:234–9. https://doi.org/10.1097/Icu.0000000000000051.
61. Shields CL, et al. Prognosis of uveal melanoma in 500 cases using genetic testing of fine-needle aspiration biopsy specimens. Ophthalmology. 2011;118:396–401. https://doi.org/10.1016/J.Ophtha.2010.05.023.
62. Danielli R, et al. Ipilimumab in pretreated patients with metastatic uveal melanoma: safety and clinical efficacy. Cancer Immunol Immunother. 2012;61:41–8. https://doi.org/10.1007/S00262-011-1089-0.
63. Tarhini AA, et al. Aflibercept (Vegf trap) in inoperable stage iii or stage iv melanoma of cutaneous or uveal origin. Clin Cancer Res. 2011;17:6574–81. https://doi.org/10.1158/1078-0432.Ccr-11-1463.

Pathology Specimen: Handling Technique

5

Hardeep Singh Mudhar

5.1 Introduction

Clear communication between the ocular oncologist and ocular pathologist is crucial to ensure that the patient's final histopathology report is intelligible, accurate, and contains as much relevant information as possible to ensure safe patient management.

The patient's histopathology report is a culmination of several key events in a pathological specimen's journey. This commences with the preparation and fixation of the specimen in theatre, the filling of the pathology request form, the delivery of the specimen to the histopathology laboratory, the handling of the specimen at the time of 'grossing/cut-up' followed by the microtomy and staining of the slides and finally the pathologist's interpretation of the slide followed by the creation of the pathology report. Errors can occur at any step of this process, so all accredited histopathology laboratories follow standard operating protocols that ensure a smooth running of the specimen's journey.

What follows is a simple guide to assist in the optimal handling of different types of pathological specimens generated by ocular oncologists in the histopathology laboratory.

5.2 Pathological Specimen Handling in Theatre Before Fixation

5.2.1 Multiple Biopsies from a Surgical Procedure

Biopsies from different ocular locations should be placed in separate formalin pots. If multiple biopsies from different sites are placed in the same formalin pot and one of the biopsies turns out to be malignant, it is impossible to say from where the biopsy originated, creating considerable anxiety for the clinician and patient.

5.2.2 Orientation of Specimens

This is an essential requirement to ensure the pathologist can report the clearance of tumour margins, and the surgeon can return to the contaminated margin and remove further tissue to achieve clearance if required. There are a variety of ways to do this, but the simplest and most effective way is to place marker sutures near particular margins and specify which margin has been marked on the pathology request form (Fig. 5.1a).

5.2.3 Conjunctival Mapping Biopsies

Conjunctival biopsies are prone to curling if placed straight into formalin. They should be attached to a firm material, such as a sponge (Fig. 5.1b), filter paper or card before placing into formalin. This will keep them flat, greatly facilitating orientation during embedding and allowing clear and safe assessment for the presence or absence of invasion by tumour. If multiple mapping biopsies are performed, the pathology request form must state the location of the biopsies (Fig. 5.1c).

5.2.4 Tissue Handling for Frozen Sections

Cases requiring frozen sections need to be booked with the pathology laboratory in advance to allow the availability of appropriately skilled pathology personnel. Frozen sections are usually required for the assessment of tumour clearance. Tissue destined for frozen sections should be orientated with marker sutures and a clear diagram drawn on the pathology request form. The tissue must not be fixed. It is useful to place the tissue on some cotton gauze or card to keep it as flat

H. S. Mudhar (✉)
National Specialist Ophthalmic Pathology Service (NSOPS), Department of Histopathology, E-Floor, Royal Hallamshire Hospital, Sheffield, UK
e-mail: hardeep.mudhar@nhs.net

© The Author(s), under exclusive license to Springer Nature Switzerland AG 2025

A. D. Singh, B. E. Damato (eds.), *Clinical Ophthalmic Oncology*, https://doi.org/10.1007/978-3-031-75907-9_5

as possible and then put it into a dry screw-top container. The surgeon's telephone number should be clearly written on the pathology request form so that the pathologist can contact the surgeon directly with the result of the frozen section assessment. It is always preferable for the pathologist to speak directly to the surgeon rather than another member of the theatre to avoid errors in the transfer of information (Figures 5.1d–h).

5.2.5 Sampling Fresh Tissue Prior to Fixation

Some tumours require fresh sampling for genetic/molecular investigations (diagnostic and prognostic testing) or research.

In the case of an enucleation, the optic nerve is sampled first and placed in a separate pot of formalin. This prevents fresh tumours from contaminating the optic nerve resection margin.

The globe is transilluminated, and using a scalpel, a sclera-choroidal flap is made beneath the tumour, with the scleral-choroidal flap hinged along one side. The fresh tumour is sampled carefully with scissors and forceps and placed in an appropriate medium and vessel (according to the pathology laboratory protocol). Some use a corneal trephine to cut a window into the sclera and choroid. After sampling the fresh tumour, the globe is fixed in formalin. An alternative strategy is to submit the intact specimen unfixed to the ocular pathology laboratory, where the pathologist can carry out the above steps.

Fig. 5.1 (**a**) A skin ellipse excision of a basal cell carcinoma from the lower lid, containing orientation sutures placed by the surgeon, to mark the superior and lateral margins. (**b**) A conjunctival mapping biopsy (tissue with brown hue) placed on a sponge to keep it as flat as possible by the surgeon in theatre. (**c**) Pathology request form that shows a clear diagram of the origin of the conjunctival mapping biopsies. (**d**) Fresh tissue sampled from the eyelid destined for frozen sectioning. (**e**) The surgeon placing marker sutures into the tissue in Fig 5.1d. (**f**) The surgeon marking the new margin with a marker pen. (**g**) The surgeon carefully sandwiching the fresh tissue between two pieces of sponge to keep it flat during transit to the pathology laboratory. (**h**) The tissue being placed in a vessel for transport to the pathology laboratory. (**i**) An enucleation specimen in a standard plastic pot containing 10% buffered formalin for fixation. (**j**) A short 25-gauge needle attached to short tubing is inserted through the scleral bed into the tumour, and aspiration is performed. (left). The contents of the needle, tubing and syringe are then rinsed into a tube of Cytolyt or other suitable transport medium (right). (**k**) Vitreous washings sent up to the pathology laboratory in the vitreous bag. The surgeon has fixed the specimen in the theatre with an equal volume of Cytolyt alcohol-based fixative. (**l**) A plastic impression cytology ring in a standard plastic pot containing 10% buffered formalin for fixation. (**m**) The surgeon has drawn a very helpful diagram on the pathology request form to aid orientation of the specimen. (**n**). A set up of the cut-up bench in a pathology laboratory for grossing ophthalmic pathology specimens. (**o**). A lower lid resection of a basal cell carcinoma, painted with yellow and blue tissue dyes in the pathology laboratory to facilitate margin assessment with sections are viewed at the microscope. (**p**). The specimen in Fig. O. sliced into 3 pieces. (**q**). Crystal violet dye used to stain a conjunctival mapping biopsy in the pathology laboratory. (r) The conjunctival mapping biopsy from Fig 5.1q being placed in the centre of some tracing paper, to be wrapped up and then placed in a tissue net for processing. (**s**) Fresh tissue destined for the frozen section being unwrapped in the pathology laboratory. (**t**) The fresh tissue from Fig 5.1s being measured. (**u**) The fresh tissue being placed in cryo-matrix prior to freezing. (**v**) The frozen tissue being sectioned on the cryostat. (**w**). The frozen sections stained with H&E ready for microscopic examination. (**x**). An iridectomy specimen containing a central brown melanoma. (**y**) An irido-cyclectomy sample for a brown, dome-shaped ciliary body melanoma. (**z**) The gross sampling of the specimen in Fig 5.1y. (**j**) [Reprinted from Singh AD, Pelayes DE, Brainard JA, Biscotti CV. History, indications, techniques and limitations. In: Biscotti CV, Singh AD (eds). FNA Cytology of Ophthalmic Tumors. Monogr Clin Cytol. Basel: Karger; 2012 (21):1–9. Copyright © 2011, Karger Publishers.] (**y,z**). (Reprinted from Ford AL, Mudhar HS, Farr R, et al. The ophthalmic pathology cut-up-Part 2. Current Diagnostic Pathology 2005; 11 (5): 340–348. With permission from Elsevier)

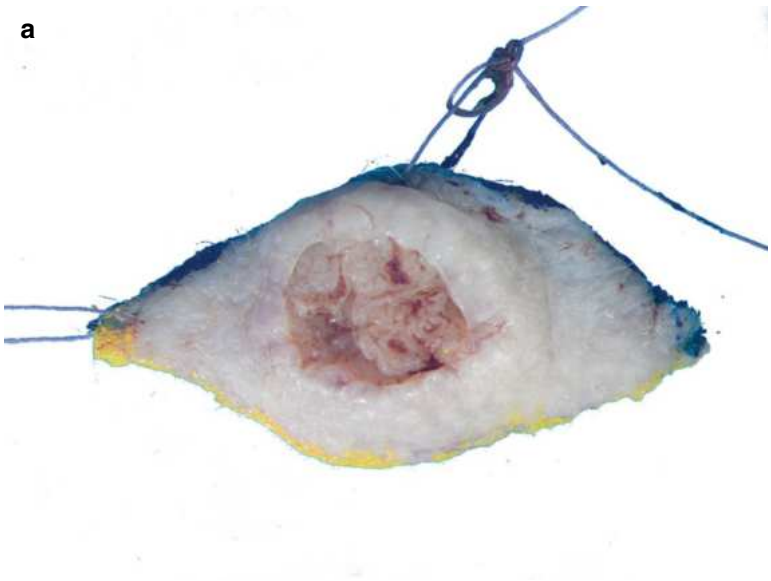
a

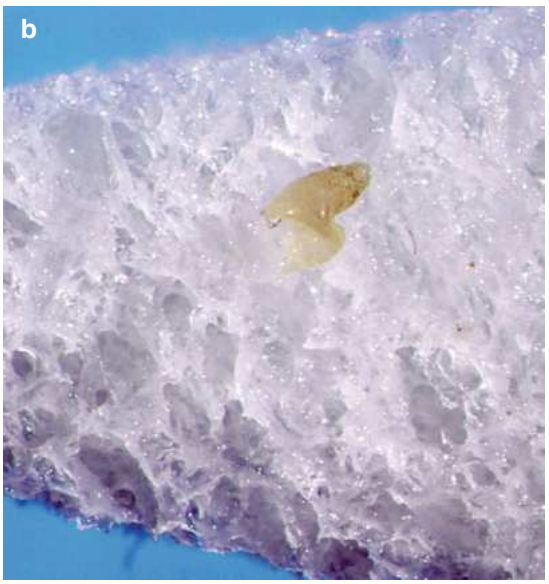
b

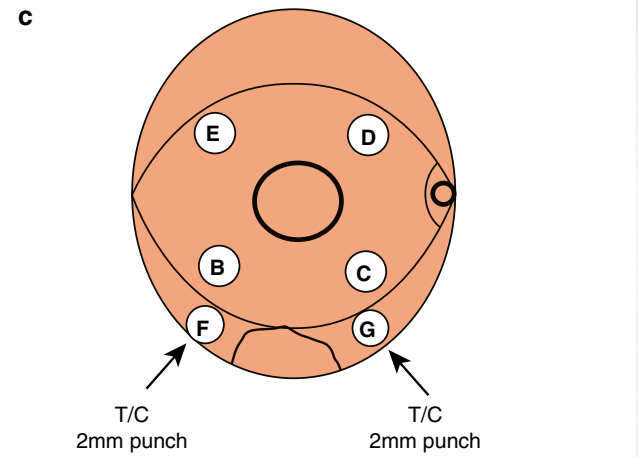
c
E
D
B
C
F
G
T/C
2mm punch
T/C
2mm punch

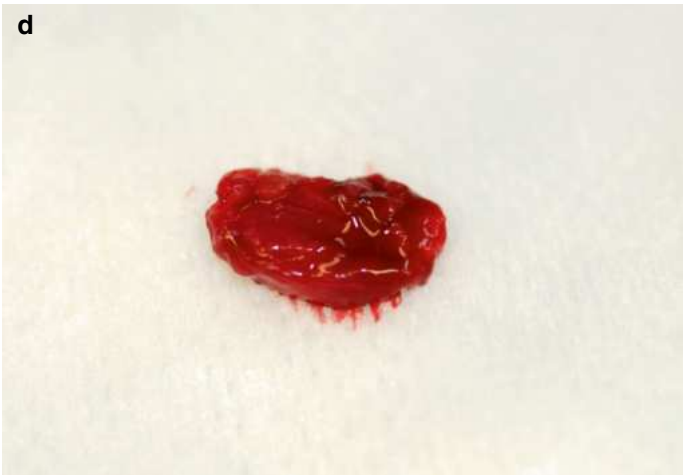
d

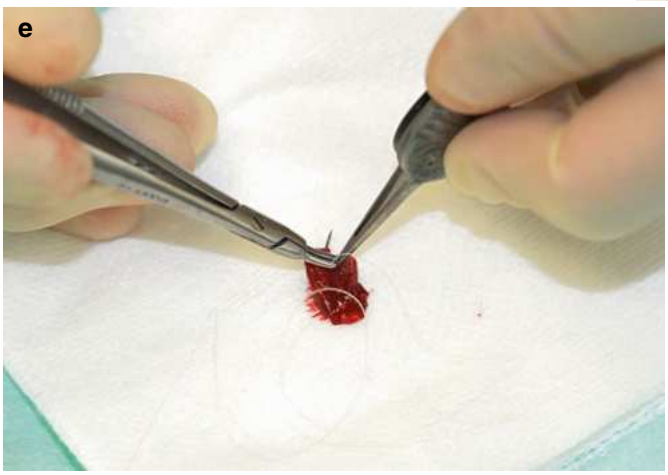
e

f

Fig. 5.1 (continued)

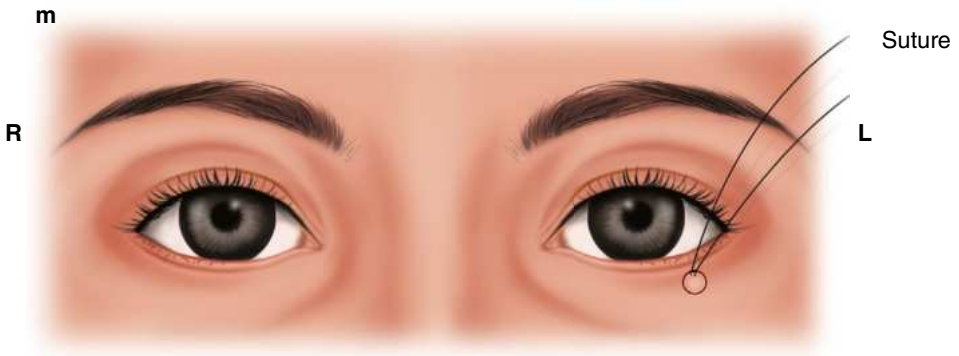

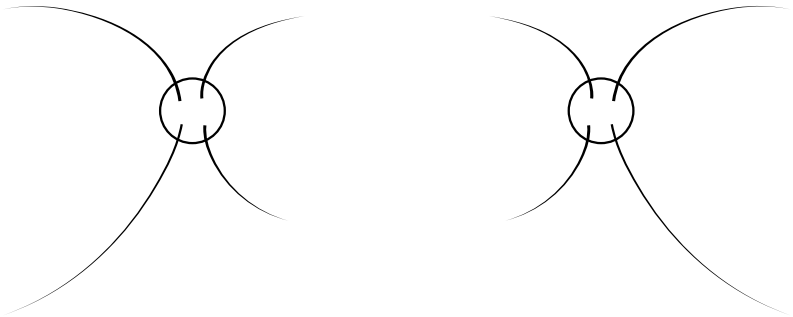

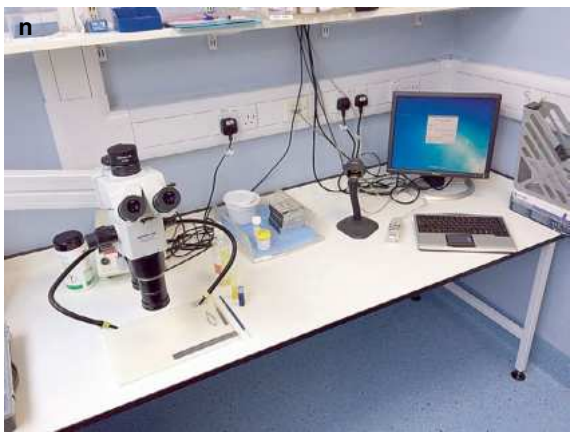

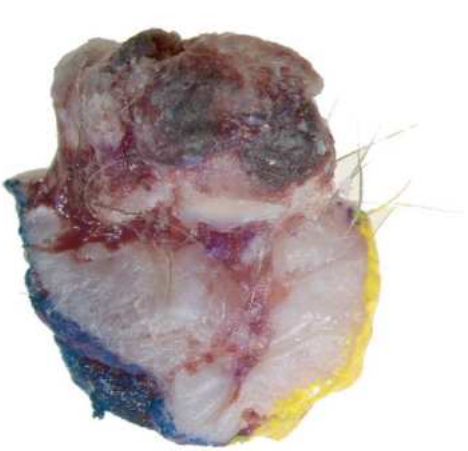

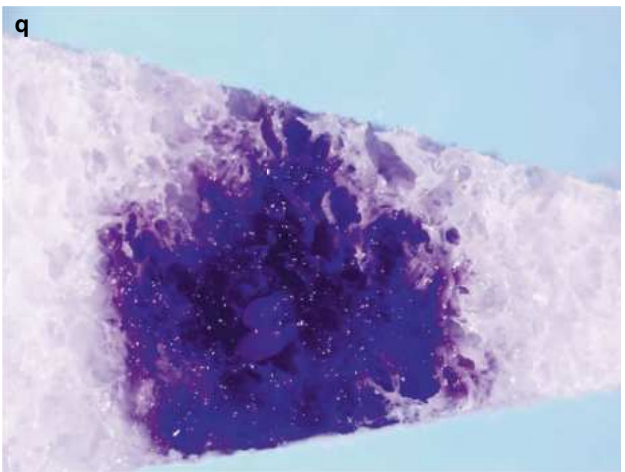

Fig. 5.1 (continued)

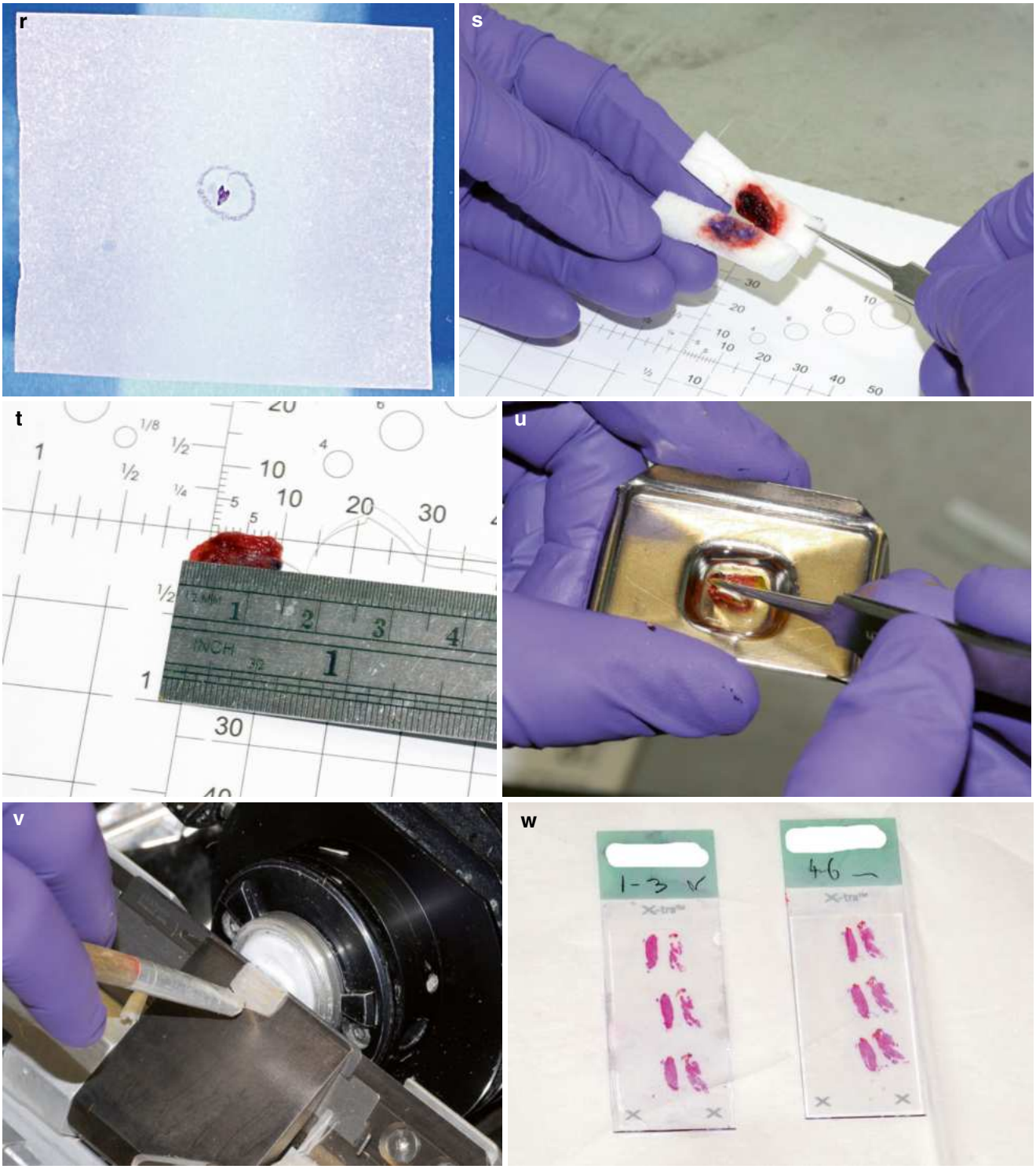

Fig. 5.1 (continued)

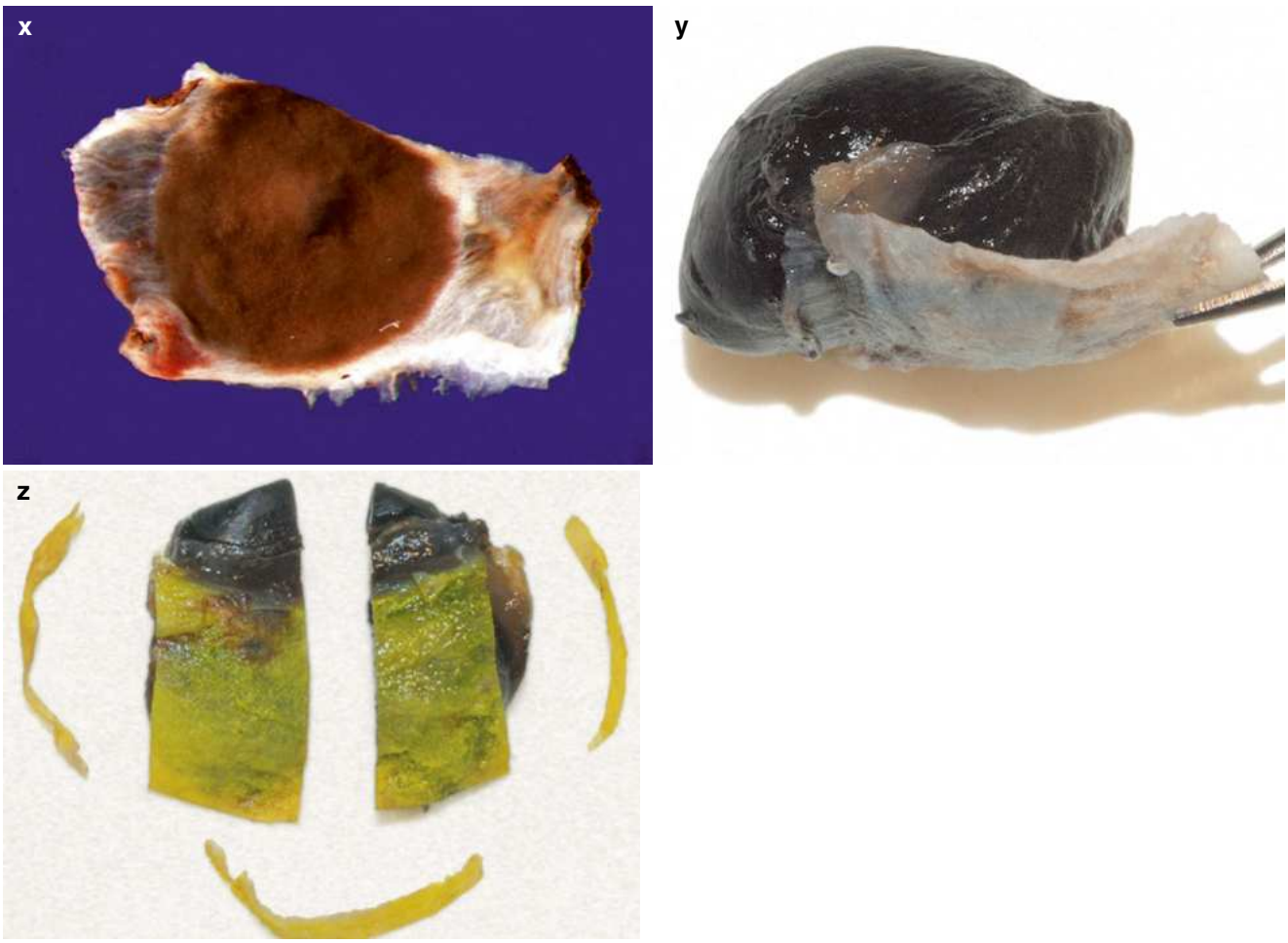

Fig. 5.1 (continued)

5.3 Fixation of Ocular Pathology Specimens [1–7]

The first question the ocular oncologist should address, preferably prior to the operation, is:

(a) ***Are there any circumstances when I should not fix the tissue?***

Below is a list of scenarios where tissue (all tissue or parts of the tissue) *should not be fixed*:

- Tissue for frozen sections (to assess margins of excision for eyelid, adnexal and orbital tumours).
- Tissue destined for research or tissue banking.
- Tissue needing molecular prognostic information may require special molecular studies on fresh tissue.
- Biopsies for flow cytometry (e.g. vitreous and fine needle aspiration specimens for assessment of lymphoma).

(b) ***Which fixative should I use to preserve the specimen(s)?***

This depends on the question that requires addressing, which ideally requires planning before the surgery. This allows the pathology laboratory to send appropriate fixatives to the theatre in time for the procedure to avoid fixation delay that could lead to artefacts. If the ocular oncologist is uncertain about the fixation of specimens, a simple phone call to the histopathologist will clarify which fixation protocol is required.

5.3.1 Surgical Tumour Specimens

Most routine ophthalmic specimens require fixation in standard 10% phosphate-buffered formalin in a leak-proof container (Fig. 5.1i). The formalin should ideally be 10× the volume of the specimen to allow timely penetration of the tissues at room temperature. To ensure this, an adequate-sized plastic container is required. If the specimen is very small, a small-volume container such as an Eppendorf tube is perfectly adequate and will reduce the time taken to find the specimen during handling in the pathology laboratory. It is important to place the specimen into the formalin rather than pour formalin onto the specimen in a dry pot. This is because the latter can eject the specimen from the pot with potential

loss of the specimen. Also, as good practice, it is much more preferable for the surgeon to place the specimen in the fixative so the surgeon is satisfied that it has been fixed. Enucleations require 24 h, and orbital exenterations may require up to 48 h.

5.3.2 Fine Needle Aspiration (FNA) Specimens [8–13]

Fine needle aspiration specimens (FNA) are preferably fixed in Cytolyt or Shandon Cytofixative (or equivalents), which are methanol/alcohol-based fixatives (Fig. 5.1j). These fixatives preserve the cytomorphology well and permit good-quality DNA to be extracted for molecular diagnostic tests. Cytolyt-preserved specimens can be used to make Thinprep slides as well. FNA samples are usually squirted into pre-filled tubes that contain the fixative. Sometimes, a capped syringe is submitted with a fixative in it. FNA of suspected lymphoma that requires flow cytometry should be preserved in RPMI medium.

5.3.3 Vitrectomy Specimens [8–13]

It is preferable to receive a pars plana vitrectomy specimen in a vitreous cassette or bag (Fig. 5.1k). If samples are required for microbiology, virology or PCR, these should have been sent from the initial core vitreous tap. Vitrectomy samples need to be preserved/fixed in an equal or excess volume of RPMI (if destined for flow cytometry) or Cytolyt/Shandon alcohol-based fixative. It is important to seal the bag or cassette to prevent leaks in transit.

5.3.4 Impression Cytology Samples

Impression cytology plastic rings can be dropped into a small pot of formalin for fixation (Fig. 5.1l).

5.3.5 Specimens Requiring Electron Microscopy

Buffered 2.5–3% glutaraldehyde is used to fix fresh specimens for transmission electron microscopy. This would be done for cases that are intended for research or in which the original interpretation of an initial tumour biopsy was equivocal, and clarification is sought from ultrastructure. It is best to place only part of the fresh tissue into buffered glutaraldehyde, as whilst it is an excellent fixative for ultrastructure, it adversely affects antigen retrieval for immunohistochemistry and extraction of DNA for molecular studies.

5.4 The Ophthalmic Pathology Request Form [14]

A pathology request form can be considered a referral letter and a primary source of communication between the surgeon and pathologist. A fully completed request form should accompany each specimen(s). Request forms are designed to provide: unique identification of the patient; destination of the report; clinician contact; date and time of specimen collection/removal and investigations required (e.g. histology/cytology); type of specimen and anatomical site of origin; clinical information so that the pathologist may handle the specimen appropriately and interpret microscopic findings in the proper context; an awareness of any health and safety issues with a given specimen.

Complete information must be supplied on the request form. Each specimen container should also be labelled with the patient identification data (minimum of three identifiers, e.g. first and last name, date of birth/age, gender and preferably patient's hospital number). The information must exactly match with the request form to prevent errors in the specimen and patient identification.

It is critical that there is no delay in filling out the request form, especially if multiple biopsies have been taken. Batch labelling of specimens should be avoided as this can lead to labelling errors. Again, it is best practice if the operating surgeon can fill out the request form rather than an assistant. A useful mindset to adopt is that the pathology request form is a medico-legal document and, therefore, requires care, thoroughness and clear communication when completing it.

Diagrams on the pathology request form are very helpful to indicate the orientation and location of specimens (Fig. 5.1m).

Stating a differential diagnosis on the request form is very helpful as the final report is a clinicopathological integrated synthesis.

Finally, it is not advisable to play mind games with your pathology colleagues. Some surgeons adopt an approach of 'Let's see if the pathologist can get the right answer' by withholding information or stating on the request form certain ancillary investigations the pathologist should do. Most pathologists would not advise their surgeon colleagues which scalpel to use in theatre. This kind of approach is guaranteed to sour the communication between the surgeon and pathologist and potentially compromise patient care. Patient care should always take primacy.

5.5 Transporting Specimens to the Pathology Laboratory

It is the surgeon's responsibility to indicate on the request form and specimen pot if the patient is known or suspected to be in a 'High Risk/Danger of Infection' category (e.g. HIV, TB, Hepatitis B, Hepatitis C), to facilitate appropriate handling in the laboratory. There are often hazard stickers available that facilitate this process. It is the surgeon's responsibility to ensure that all specimens are in suitable and approved containers. Approved containers have leak-proof lids and the appropriate hazard warning signs for the fixative, e.g. formalin.

Specimen containers should be closed securely and placed inside a sealed specimen bag.

Specimens received leaking or damaged are a danger to all those who come into contact with them, including theatre staff, porters and laboratory staff and can also compromise the diagnosis.

5.6 Handling Ophthalmic Surgical Specimens in the Pathology Laboratory [1–7]

Each accredited laboratory works to approve standard operating protocols designed to safely handle pathological tissue so that the most optimal outcome is obtained for patient management. A well-equipped arrangement for handling ophthalmic pathology specimens includes a high-quality dissecting microscope with a digital camera, the same instruments on the bench for dissecting/handling the tissue and a computer for dictating the gross/macroscopic findings (Fig. 5.1n).

The following sections outline how certain surgical specimens are handled in the pathology laboratory.

5.6.1 Eyelid Skin Tumour Resections

These specimens should arrive in the pathology laboratory with marker sutures placed by the surgeon, indicating the orientation of the specimen and with an annotated diagram on the pathology request form. They can comprise full-thickness or partial-thickness eyelid tissue and are commonly taken to remove basal cell carcinomas, which is the commonest malignant tumour of the eyelid. These are painted in tissue dyes by the pathologist or biomedical scientist and bread-sliced to create evenly sized pieces, some of which will contain the tumour (Fig. 5.1o–p).

5.6.2 Mapping Biopsies

These specimens are usually placed on a firm medium, such as a sponge or card in theatre, to flatten the specimen. The specimen is viewed under a dissecting microscope, and a few drops of tissue dye are placed on it (Fig. 5.1q). A particularly good dye is Crystal Violet, which dyes the mapping biopsy a deep purple colour. The dyed biopsy is placed in some tracing (Fig. 5.1r) paper, and then the paper is placed in a specimen net. This approach ensures delicate, small biopsies are not lost during their time in the processing machine. The dye withstands the processing chemicals and greatly facilitates edge-on orientation during paraffin wax embedding of the specimen, ensuring the correct orientation.

5.6.3 Frozen Tissue Handling

Fresh, unfixed tissue sent to the pathology laboratory is commonly sent for intraoperative diagnosis to achieve clear margins for tumour excision. Some surgeons sandwich the fresh tissue between pieces of sponge to keep the tissue flat during transit. This is a very helpful strategy to facilitate orientation at the time of embedding. In the pathology laboratory, the specimen is handled in a down draft hood, measured, any relevant margins painted with tissue dyes, embedded in cryo-matrix and frozen sections cut and stained with standard haematoxylin and eosin (H&E) (Fig. 5.1s–w).

5.6.4 Local Resection of Intraocular Tumours

Local resections of the iris, ciliary body and choroid are sight-sparing procedures for localised benign and malignant neoplasms. For iris tumour resections (Fig. 5.1x), the tumour size is measured, and its proximity to margins is noted. After taking the end margins, the specimen is usually sliced into consecutive parallel pieces around the iris circumference so that each piece contains the pupillary and peripheral margins. Local resections of ciliary body tumours comprise a ciliary body, possible anterior choroid and often some iris root, with partial-thickness sclera. Any obvious tumour is measured, and its position in relation to the margins is noted. The posterior and radial margins are sampled, and then the specimen is sliced in the anteroposterior plane, and the cut surface of the tumour is described (Fig. 5.1y, z).

5.6.5 Enucleation Specimens for Intraocular Tumours

The first thing when handling an enucleation for an intraocular tumour is to determine laterality. The long ciliary arteries are horizontal posteriorly. The superior oblique tendon is a broad, thin muscle insertion supero-temporally. The inferior oblique insertion is thicker and more muscular and is located postero-temporally. Once these landmarks have been identified (Fig. 5.2a, b), if the inferior oblique is to the left of the optic nerve, it is a left eyeball, and the converse is true for the right eyeball. The eyeball is trans-illuminated with a fibre-optic light source to indicate the position of the intraocular tumour (Fig. 5.2d). The position of the tumour is marked on the scleral surface with a marker pen (Fig. 5.2e). Tumour enucleations are sectioned to include the main site of the tumour, with the pupil and optic nerve included. This is called the block pupil-optic nerve block (PO block), with the plane of sectioning dependent on the position of the tumour, as determined by prior trans-illumination. The cut begins 2 mm from the external optic nerve edge and ends 2 mm inside the rim of the cornea (Fig. 5.2f). The cut should ideally travel from the posterior pole towards 2 mm inside the corneal rim; this prevents dislocation of the lens. However, it is equally effective to cut from side to side across the edge of the cornea (Fig. 5.2f). The intraocular tumour is then assessed with regards to its shape, colour, texture, size, location and position in relation to other structures (distance from optic nerve head and pars plana/plicata) are recorded (Fig. 5.2g). The effect on surrounding structures, such as retinal detachment, haemorrhages or areas of invasion, are noted.

5.6.6 Exenteration Specimens for Tumours

Various types of exenteration are performed, usually for uncontrolled intraocular malignancy that has spread beyond the globe or for primary orbital tissue malignancy. After usually 48 h of formalin fixation, the exenteration is painted with tissue dyes. If bone is included, this can be removed for decalcification. The lacrimal puncta are always medial, and the posterior aspect will include the optic nerve margin and orbital fat (Fig. 5.3a–c). The nasolacrimal duct margin is sampled to exclude the spread of tumours into the lacrimal drainage apparatus. This can happen with conjunctival pagetoid sebaceous and in situ melanoma. The basic approach is to bread-slice the specimen, producing a series of slices (Fig. 5.3d, e). The medial and lateral slices of the specimen can be further horizontally sliced to examine the distance of the tumour from the medial and lateral borders. The tumour's cut surface, size, shape, texture, location and relationship to surrounding anatomy is noted.

5.6.7 Cytology Handling [8–13]

5.6.7.1 Impression Cytology

The membrane on the surface of an impression cytology ring can be left in situ and stained with tectorial stains or by immunohistochemistry (by hand), after which the membrane

Fig. 5.2 (**a**) An enucleation viewed from behind. Arrowheads mark the location of the horizontal long ciliary arteries. Note the tendonous superior oblique muscle (so) and optic nerve (on). (**b**) Arrowheads mark the horizontal long ciliary arteries. Note the thicker muscular insertion of the inferior oblique muscle (io). This inserts to the left of the optic nerve (on), therefore, this is a left eye. (**c**) Arrowheads show the horizontal long ciliary arteries. The vortex veins (arrows) lie at approximately 45-degree angles from the optic nerve. (**d**) Transillumination of this eye with a fibre-optic light source (fo) reveals an anterior shadow in the ciliary-choroidal area. (**e**) The shadow in (**d**), marked out with a pen. (**f**) Penetration of the cornea 1–2 mm inside the limbus by the blade (arrow). This allows infiltration of the anterior chamber by wax, stabilising the anterior chamber and cornea during sectioning. Arrowheads point to tumour permeation of the drainage angle within the anterior chamber. (**g**) The shadow seen in (d) corresponds to a solitary ciliary-choroidal black tumour (arrow). Histology showed a uveal melanoma. L, lens. (**h**) Lateral (top left) and anterior (top right) views of the eye show the ideal parallel cuts (in this case, horizontal cuts). The resulting ring of tissue (bottom left) that includes the pupil and optic nerve is processed. In tumour cases (bottom right), the cuts may be oblique. In this case, the standard parallel cuts incorporate a ring of tissue comprising the tumour, optic nerve and pupil. (Reprinted from Ford AL, Mudhar HS, Farr R, et al. The ophthalmic pathology cut-up-Part 1: The enucleation and exenteration specimen. Current Diagnostic Pathology 2005; 11 (4): 284–290. With permission from Elsevier)

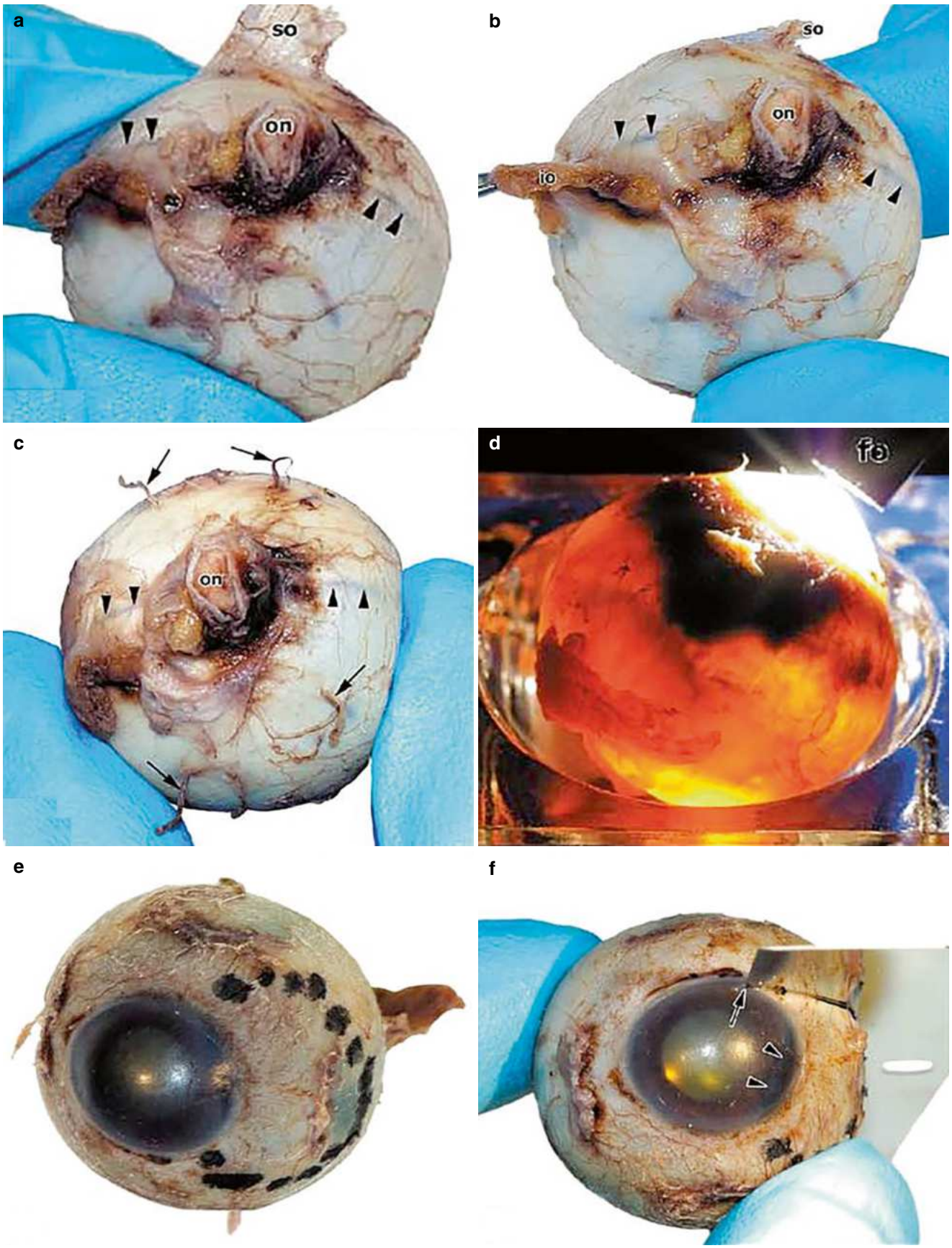
a
so
on
b
so
on
io
c
on
d
fo
e
f

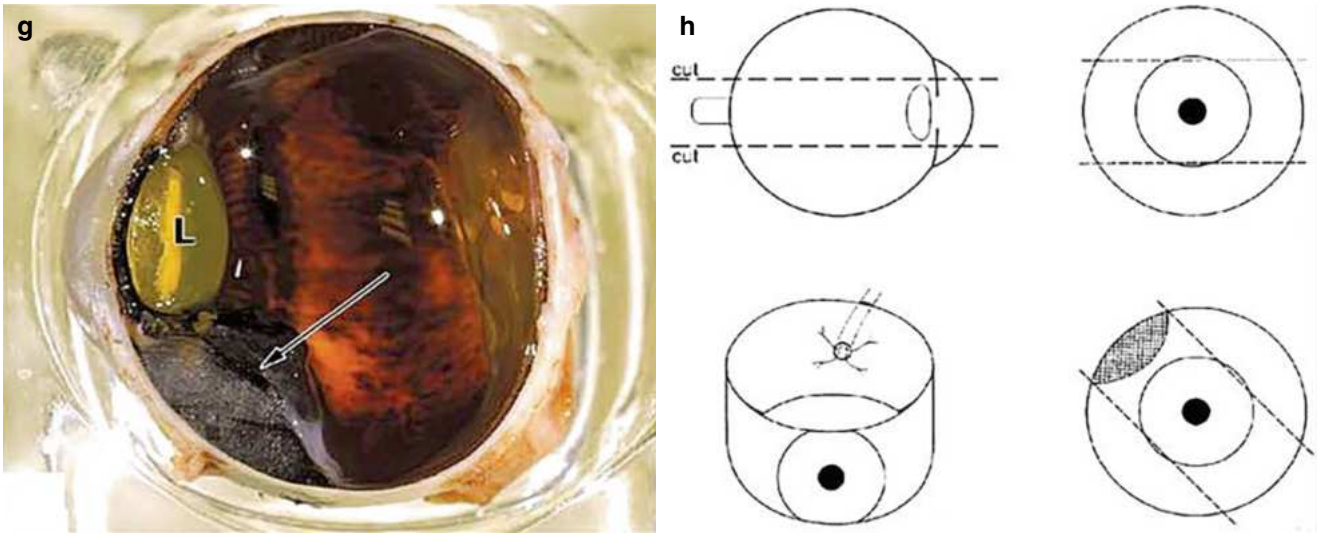

Fig. 5.2 (continued)

can be cut out gently and mounted on a glass slide with mountant and a coverslip.

5.6.7.2 FNAs

In our experience, FNAs of intraocular tumours are best handled by creating a cell block by centrifugation. After processing the cell block, between 10–20 serial sections are cut, and every tenth is stained with Haematoxylin and Eosin (H&E). This leaves many spares for ancillary investigations such as immunohistochemistry. Further serials can be cut if the initial sections reveal little material.

5.6.7.3 Vitreous Samples

Cases preserved in RPMI are exposed to flow cytometry in laboratories that have this modality. Alternatively, the vitreous washings that have been fixed with an equal volume of cytofixative (Cytolyt /Shandon alcohol-based fixative) can be centrifuged, and a cell block can be prepared. A serial ribbon of sections is cut, and every tenth section can be stained with Haematoxylin and Eosin (H&E). This leaves many spare sections in between for ancillary investigations such as immunohistochemistry and molecular analysis. Some laboratories save back at least a quarter to a third of the volume of the vitreous washings in case the sample requires DNA extraction for molecular investigations, e.g. for B cell or T cell clonality and MYD88 mutation testing in suspected cases of intraocular lymphoma. However, in our experience, molecular testing for B or T cell clonality and genetic testing for MYD88 mutation (commonly mutated in high grade B-cell lymphomas affecting the vitreous and retina) can be performed reliably on paraffin sections obtained from the vitreous cell block.

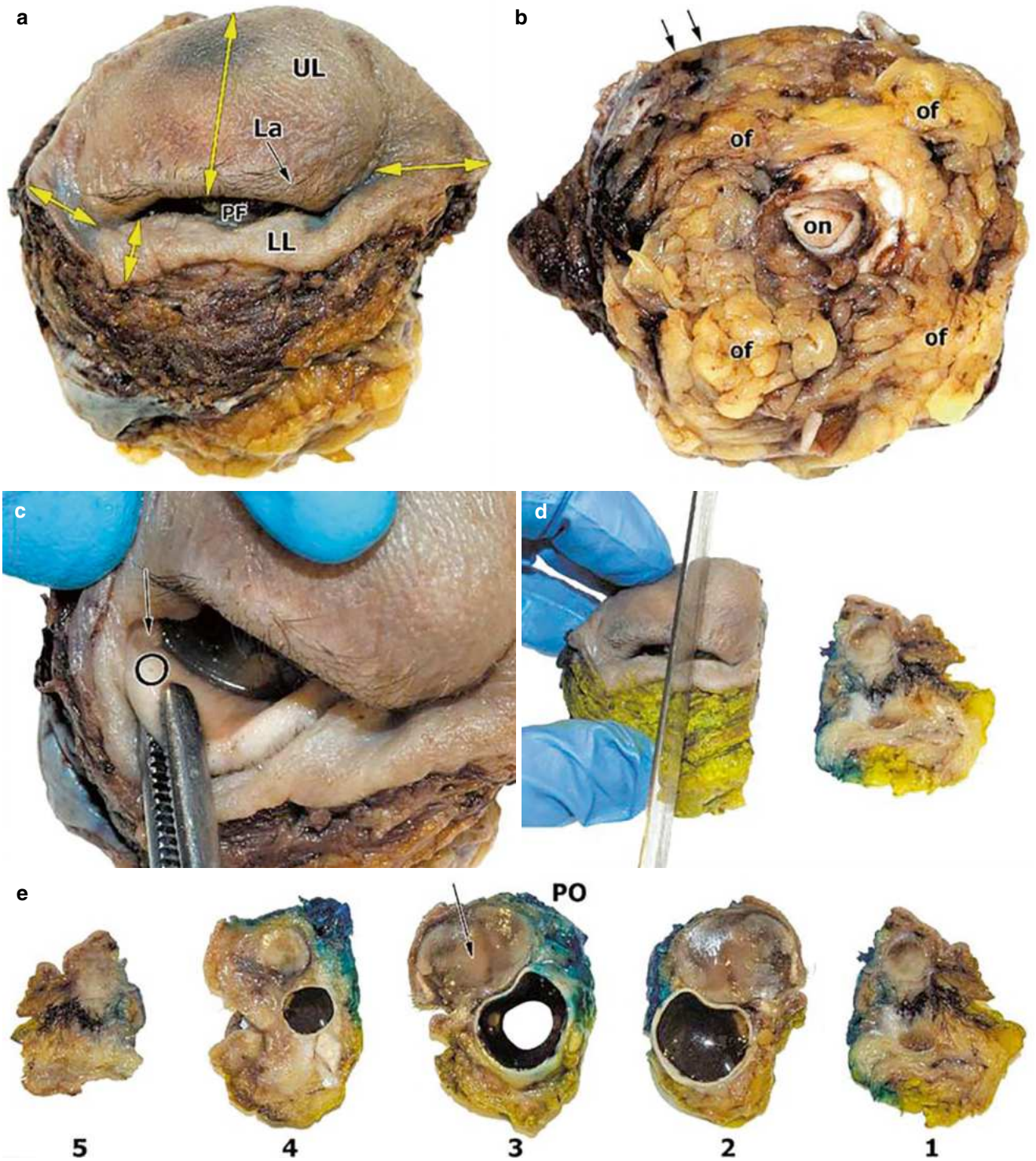

Fig. 5.3 (**a**) Anterior view of a complete left exenteration. Note the upper lid (UL) with prominent lashes (La), the palpebral fissure (PF) and the lower lid (LL) with fewer and shorter lashes. The yellow arrows denote how the measurement of the lid skin is made (**b**) Posterior view of (a). Note the optic nerve (on), location of the lacrimal gland (arrows) and orbital fat (of). (**c**) Eversion of the lower eyelid shows the lower punctum (circled) at the medial aspect of the lid margin and exposes the caruncle (arrow). Eversion of the upper eyelid will show the upper punctum in a similar location. (**d**) Bread-slicing the specimen in the vertical plane using a large skin graft blade. The first cut just avoids the globe. (**e**) A sliced exenteration with a tumour arising from the superior tarsal conjunctiva (arrow). PO, pupil—optic nerve block. Numbers indicate the order in which the slices were made: 1 = lateral, 5 = medial. (Reprinted from Ford AL, Mudhar HS, Farr R, et al. The ophthalmic pathology cut-up-Part 1: The enucleation and exenteration specimen. Current Diagnostic Pathology 2005; 11 (4): 284–290. With permission from Elsevier.)

References

1. Suvarna KS, Layton C, Bancroft JD. Bancroft's theory and practice of histological techniques. 7th ed. Churchill Livingstone; 2013.
2. Ford AL, Mudhar HS, Farr R, Parsons MA. The ophthalmic pathology cut-up part 1: the enucleation and exenterations specimen. Curr Diagn Pathol. 2005;11:284–90.
3. Ford AL, Mudhar HS, Farr R, Parsons MA. The ophthalmic pathology cut-up part 2: the enucleation and exenterations specimen. Curr Diagn Pathol. 2005;11:340–8.
4. Lee WR. Examination of the globe: technical aspects. In: Lee WR, editor. Ophthalmic histopathology. 2nd ed. London: Springer; 2002. p. 1–33.
5. Eagle RC. Specimen handling in the ophthalmic pathology laboratory. Ophthalmol Clin N Am. 1995;8:1–15.
6. Torczynski E. Preparation of ocular specimens for histopathologic examination. Ophthalmology. 1981;88:1367–71.
7. Eagle RC. Laboratory techniques and special stains. In: Eagle RC, editor. Eye pathology; an atlas and basic text. Philadelphia: WB Saunders Company; 1999. p. 283–90.
8. Augsburger JJ, Shields JA, Folberg R, Lang W, O'Hara BJ, Claricci JD. Fine needle aspiration biopsy in the diagnosis of intraocular cancer. Ophthalmology. 1985;92:39–49.
9. Grossniklaus HE. Fine-needle aspiration biopsy of the iris. Arch Ophthalmol. 1992;110:969–76.
10. Shields JA, Shields CL, Ehya H, Eagle RC, DePotter P. Fine-needle aspiration biopsy of suspected intraocular tumors. Ophthalmology. 1993;100:1677–83.
11. Engel H, de la Cruz ZC, Jimenez-Abalahin LD, Green WR, Michels RG. Cytopreparatory techniques for eye fluid specimens obtained by vitrectomy. Acta Cytol. 1982;26:551–60.
12. Green WR. Diagnostic cytopathology of ocular fluid specimens. Ophthalmology. 1984;91:726–49.
13. Singh AD, Pelayes DE, Brainard JA, Biscotti CV. History, indications, techniques and limitations. Monogr Clin Cytol. 2012;21:1–9.
14. Maudgil A, Salvi SM, Tan JH, Mudhar HS. Improving the interaction between the ophthalmology and histopathology departments. Eye (Lond). 2011;25(8):998–1004.

Cancer Angiogenesis

6

Julia H. Joo, Sujata Rao, and Arun D. Singh

6.1 Introduction

Angiogenesis, the growth of new blood vessels from pre-existing vasculature, is both a physiologic and pathologic process. The formation of new vessels is important during embryogenesis, wound healing, and in the uterus during the menstrual cycle and pregnancy. Interest in targeting angiogenesis for the treatment of cancer began in the early 1970s when it was postulated that the formation of new vessels in tumors is essential for tumor growth and metastasis [1]. Subsequently, our improved understanding of the regulation of angiogenesis has revealed an important role in other diseases, such as proliferative diabetic retinopathy and age-related macular degeneration, rheumatoid arthritis, and psoriasis [2]. In this chapter, we provide a brief review of the mechanism(s) of tumor development and the required angiogenesis, current applications in general and, more specifically, in ophthalmic oncology, and experimental drugs with potential for clinical applications. The final section of this review deals with the angiogenic aspects of a few specific ophthalmic tumors.

J. H. Joo
Cleveland Clinic Lerner College of Medicine,
Cleveland, OH, USA
e-mail: joo2@ccf.org

S. Rao
Ophthalmic Research, Cole Eye Institute, Cleveland Clinic,
Cleveland, OH, USA

Department of Molecular Medicine, Cleveland Clinic Lerner College of Medicine, School of Medicine, Case Western Reserve University, Cleveland, OH, USA
e-mail: raos7@ccf.org

A. D. Singh (✉)
Department of Ophthalmic Oncology, Cole Eye Institute,
Cleveland Clinic, Cleveland, OH, USA
e-mail: singha@ccf.org

6.2 Tumor Vascular Supply

Tumorigenesis is a multistep process partly enabled by the accumulation of mutations over time [3]. Small microscopic tumors, either primary or metastatic, can obtain their nutrients and oxygen by diffusion alone. However, with increasing distance from a capillary vessel, oxygen supply is insufficient for the proliferation of tumor cells (Fig. 6.1) [4]. Implantation of human tumor cells into mice revealed that only those tumors that could recruit a vascular supply could grow to a visible size [4]. The others were referred to as non-angiogenic tumors and remained microscopic in size, without any sign of growth, a phenomenon called "no take" [3]. Non-angiogenic tumors rely on the diffusion of oxygen and nutrients from their local microenvironment, thus limiting their growth and long-term survival. Some of these tumors use non-angiogenic processes, such as vessel co-option, vascular mimicry, and vascular splitting, to obtain oxygen and

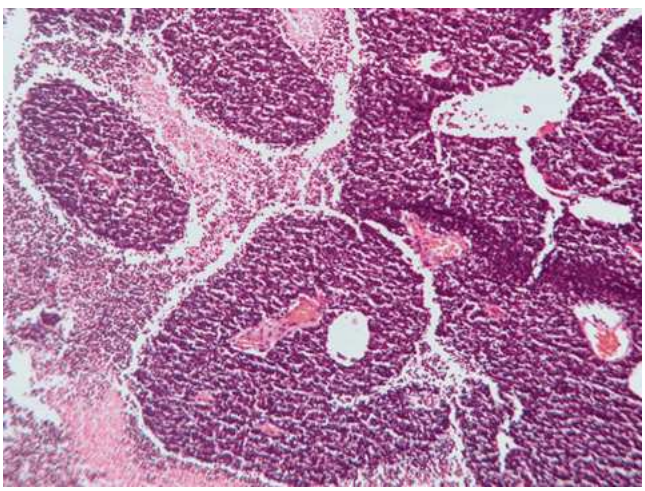

Fig. 6.1 With increasing distance from a capillary vessel, oxygen supply is insufficient for the proliferation of tumor cells. Note viable cells surrounding the central vessel. Areas of tumor necrosis are evident away from the vascular channels (untreated retinoblastoma). (Hematoxylin and eosin; original magnification 10×)

© The Author(s), under exclusive license to Springer Nature Switzerland AG 2025

A. D. Singh, B. E. Damato (eds.), *Clinical Ophthalmic Oncology*, https://doi.org/10.1007/978-3-031-75907-9_6

nutrients at a greater rate than diffusion alone. Moreover, some non-angiogenic tumors have been shown to undergo an "angiogenic switch" following an extended observation period, theorized to occur due to the increasing local hypoxia and associated accumulation of pro-angiogenic factors of a growing tumor without its own blood supply [5]. Altogether, these findings have contributed to the understanding that tumor growth is highly dependent on recruiting its own blood supply [5].

6.2.1 Angiogenic Switch

It is widely believed that all tumors rely on the growth of new blood vessels, the process known as angiogenesis, to grow to a clinically detectable size. The ability of a tumor to induce growth of its own vessels usually develops after malignant transformation in response to hypoxia and nutrient deprivation, called the angiogenic switch [6, 7] The necessity of a fecund blood supply in the exponentiation of malignant tumor growth was initially proposed by Judah Folkman in 1971 and has been supported by animal models, including those involving the eye, over the past several decades. For instance, tumor cells implanted in the corneal stroma of rabbits showed a low growth rate as long as the cornea remained avascular [8]. Placed centrally in the cornea, the tumors slowly grew peripherally until they reached the limbus, wherein blood vessels extended from the limbal plate toward the tumor. This neovascularization acutely accelerated tumor growth [8]. A similar phenomenon was observed for tumors placed in the anterior chamber of a rabbit eye. Whereas tumor cells placed on the iris were uniformly vascularized and experienced rapid and invasive growth, cells placed in the anterior chamber remained dormant [9]. Collectively, this demonstrated the necessity of tumor vascularization in malignant tumor growth. This realization raised further questions about how a dormant tumor can be triggered to actively proliferate upon the advent of neovascularization, a process now referred to as the "angiogenic switch."

The classic model of the angiogenic switch is characterized by the disruption of the balance of pro-angiogenic and anti-angiogenic factors toward the former [10]. Pro-angiogenic factors include those generated in response to hypoxia, which can accumulate due to the overpopulation of tumor cells in an increasingly oxygen-poor microenvironment. Arguably, the key regulator is vascular endothelial growth factor-A (VEGF-A), which is a major driver of physiological and pathological angiogenesis. Other positive regulators of angiogenesis include the fibroblast growth factor (FGF) and platelet-derived growth factor (PDGF) families, which can induce vascular endothelial cell proliferation. Proto-oncogene products such as KRAS, EGFR, and SRC also upregulate vascular growth and migration and are also considered pro-angiogenic factors [11]. On the other hand, endogenous anti-angiogenic factors keep vascular growth in check. These factors include components of the extracellular matrix or the basement membrane of blood vessels and will be discussed in greater detail later in this chapter [12]. The elucidation of pro-angiogenic factors inducing the angiogenic switch has led to the development of new therapies that target this step of tumor progression, termed anti-angiogenic therapy (AAT), several of which have now been tested in clinical trials.

6.2.2 Non-Angiogenic Tumor Vascularization

While angiogenesis has long been considered a hallmark of cancer [13], it is not the only process of tumor perfusion. The consideration of angiogenesis as a prerequisite to tumor progression and survival has also been called into question by some following the series of disappointing outcomes of clinical trials for AAT. Alternative processes of tumor vascularization, including vessel co-option (VCo) and vascular mimicry, have subsequently gained recognition as promising targets for certain cancers [14]. An emerging theory proposes that the ability of some tumors, including uveal melanomas, to use these alternative non-angiogenic mechanisms enables resistance to AAT [15] and predicts more aggressive diseases.

6.2.2.1 Vessel Co-Option

Of the alternative mechanisms of tumor vascularization, vessel co-option (VCo) has been the most studied and has been recognized in several human cancers [16]. VCo is characterized by the migration of tumor cells to the site of pre-existing blood vessels of healthy tissue, leading to the hijacking or "co-option" of the physiological vasculature for the growth of the tumor [17]. Initially identified in histological lung cancer specimens in 1997 by Pezzella and colleagues [18], VCo has now been linked to several cancers, particularly those of highly vascularized organs, such as the brain and liver [15, 16]. Evidence of VCo by histology has also been characterized in cutaneous and uveal melanomas, both in primary and metastatic tumors.[19] Tumors using VCo are often marked by a necrotic core from prolonged underperfusion, and co-opted vessels can appear dilated, leading to increased vessel permeability [20].

The hypothesized signaling pathways and mechanisms implicated in VCo are detailed in reviews elsewhere [16, 21], but the predominant themes among the pathways seem to be heightened cancer cell motility, invasiveness, metastatic propensity, and epithelial-to-mesenchymal (EMT) properties. These mechanisms have been proposed to confer resistance to anti-angiogenic therapy [16]. In patients with uveal melanoma liver metastases, those with evidence of VCo on liver biopsies experienced worse overall survival than those who did not, indicating the potential role of VCo as a prognostic

factor [22]. In the setting of cancers that have shown limited response to AAT, including uveal melanoma, adjuvant or monotherapies that inhibit VCo mechanisms could be a promising future direction.

6.2.2.2 Angiotropic Extravascular Migratory Metastasis & Pericytic Mimicry

While the hypermotility of cancer cells in VCo can explain the local movement and growth of tumors to nearby pre-existing vasculature, a similar process called angiotropic extravascular migratory metastasis (EVMM) relies on angiotropism and pericytic mimicry to enable non-hematogenous metastasis of tumor cells to adjacent organs [19]. The field emerged from the realization in the late 1990s that melanoma, among some other cancers, defied the theory proposed by Folkman that vascular density can predict tumor progression [23, 24]. Lugassy and Barnhill identified "angio-tumoral complexes" in malignant melanoma specimens wherein the vascular integrity of the tissues remained intact, but tumor cells seemed to have displaced and replaced the location of pericytic cells, which normally surround and support the vasculature [23]. Thus emerged the field of EVMM, which now postulates that tumor cells adhere to the abluminal surface of large vessels, mimicking pericytes, and migrate along the vessels to secondary sites as a mechanism of metastasis [25]. Intravasation of the tumor cells for hematogenous spread does not occur in EVMM. In patients with cutaneous melanomas, those with evidence of angiotropism on histopathology experienced greater rates of metastasis [22, 26].

The mechanisms of EVMM and VCo are highly similar, both characterized by highly mobile cancer cells, greater EMT phenotype, and AAT resistance. The two processes are increasingly considered to represent a continuum of cancer progression, with VCo representing local tumor migration and EVMM representing preliminary stages of metastasis [19].

6.3 Steps in Tumor Angiogenesis

The angiogenic response to a tumor is influenced significantly by the tumor microenvironment, which is comprised of multiple cell types [27, 28]. In addition to sprouting angiogenesis from pre-existing vessels, it is now apparent that new vessels can originate from cancer stem cells that have differentiated into endothelial cells as well as from endothelial progenitor cells recruited from the bone marrow [29]. Angiogenesis is induced by the secretion of VEGF from hypoxic cancer cells, which is bound to VEGF receptor 2 on endothelial cells. This induces vasodilation and an increase in vascular permeability because of the dissolution of adherens junctions and detachment of perivascular pericytes with consequent vascular leakage leading to extravasation of plasma [30]. Matrix metalloproteinases degrade the basement membrane and the surrounding extracellular matrix, facilitating vascular remodeling and amplifying the angiogenic stimulus by releasing additional angiogenic and inflammatory factors. Depending on the tumor microenvironment, MMPs can be pro- or anti-angiogenic [31–33].

Given a favorable tumor microenvironment for blood vessel growth, angiogenesis occurs by tip and stalk cell differentiation via the delta-like 4 (DLL4)-Notch signaling pathway [29]. Vascular endothelial cells exposed to high levels of VEGF show greater DLL4 expression and differentiate into tip cells, which leads to the growth of the new vascular branch. In turn, DLL4 binds Notch receptors on adjacent "stalk" cells, which will proliferate and grow to extend the vascular branch following the leading tip cells [34]. The new capillary then builds anastomoses with other capillaries, and the new vessel is stabilized by a new basal membrane and pericytes (Fig. 6.2). Concomitantly to this sprouting response, platelets are recruited to the site of basement membrane degradation and, upon activation, release angiogenic

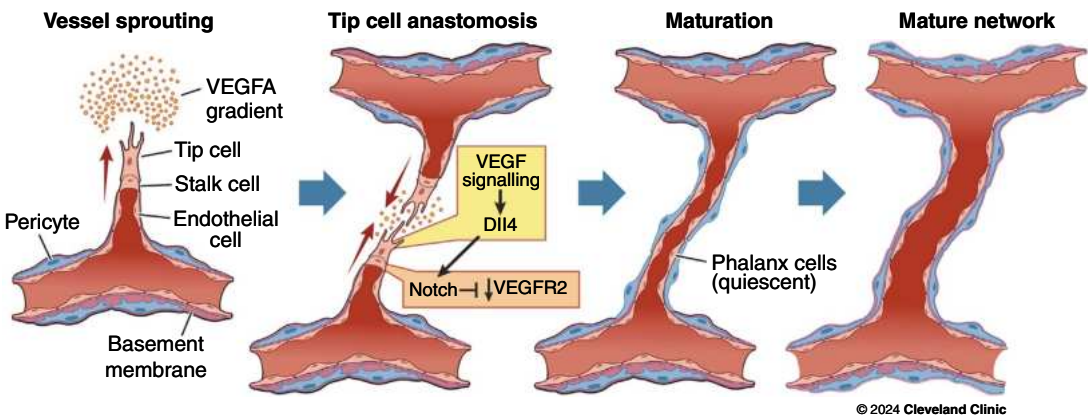

Fig. 6.2 Tip and stalk cell differentiation. Given a favorable tumor microenvironment for blood vessel growth, angiogenesis occurs by tip and stalk cell differentiation via the delta-like 4 (DLL4)-Notch signaling pathway. Vascular endothelial cells exposed to high levels of VEGF show greater DLL4 expression and differentiate into tip cells, which lead the growth of the new vascular branch. In turn, DLL4 binds Notch receptors on adjacent "stalk" cells, which will proliferate and grow to extend the vascular branch following the leading tip cells. The new capillary then builds anastomoses with other capillaries, and the new vessel is stabilized by a new basal membrane and pericytes

factors into the tumor microenvironment. Bone marrow-derived endothelial progenitor cells and myeloid cells are also recruited to this site and release additional factors [35].

6.4 Permeability of Tumor Vessels

While neovascularization can rapidly increase vessel density at the site of the tumor [36], the vessels generated tend to be leaky and highly permeable. The vessels are disorganized, tortuous, and show a chaotic blood flow, and thus, the tumor often remains hypoxic and nutrient-deprived [37, 38]. While VEGF has been presented thus far as a pro-angiogenic agent, high VEGF levels have paradoxically been associated with increased vascular permeability [39]. For example, VEGF has been shown to induce the formation of small pores in endothelial cell cytoplasm in a dose-dependent manner [40, 41]. The inflammatory markers and hypoxic signaling that promote angiogenesis also cause perivascular cells, which normally provide structural integrity to mature blood vessels, to detach from vessel walls. Platelets are recruited to the exposed basement membrane and, upon activation, release more VEGF, generating a positive feedback loop of increasing vessel permeability [42]. The leaky nature of these vessels leads to poor perfusion of the tumor, generating pockets of necrosis in the most hypoxic microenvironments. Moreover, the permeability enables tumor cells to more easily hijack the systemic vasculature, as inflammatory, pro-angiogenic, and oncogenic substrates, as well as tumor cells themselves, can readily enter and exit tumor vessels [40].

6.5 Metastatic Cascade

The metastatic cascade is a series of complex events that allow a tumor to disseminate and grow at a distant secondary site. Tumor cells must first grow locally and invade their local environment before they gain access to the bloodstream by invading local blood vessels (intravasation). The access to the circulation allows the tumor to disperse malignant cells into the bloodstream (Fig. 6.3). The capillaries in the tumor often lack a proper basement membrane and show a weak interaction of endothelial cells and only a few pericytes, making it easier for tumor cells to invade the lumen. The higher the density of vessels within a tumor, the more cells can escape to the circulation [43, 44]. For uveal melanoma, a correlation between tumor cell ingrowth into blood vessels and the development of distant metastasis has been established [45]. For breast carcinoma, intravasation was linked to cyclooxygenase-2 (COX-2) and its angiogenic property, stimulating the formation of unstable vessels that are easier to Invade [46]. Once in the systemic circulation, circulating tumor cells (CTCs) can reach distant organs. During that process, they have to survive without anchorage to their stratum and may soon become trapped in the capillaries as their diameter is usually larger than a capillary. Once the metastatic cells reach their target organ, they start to proliferate to form a secondary tumor under permissive conditions. It remains unclear whether the predilection of different tumor types to spread to specific organs is simply a passive process or if there is an active homing of CTCs, which is controlled by the expression of ligands on the cell surface [44]. However, without inducing the growth of new vessels, these secondary

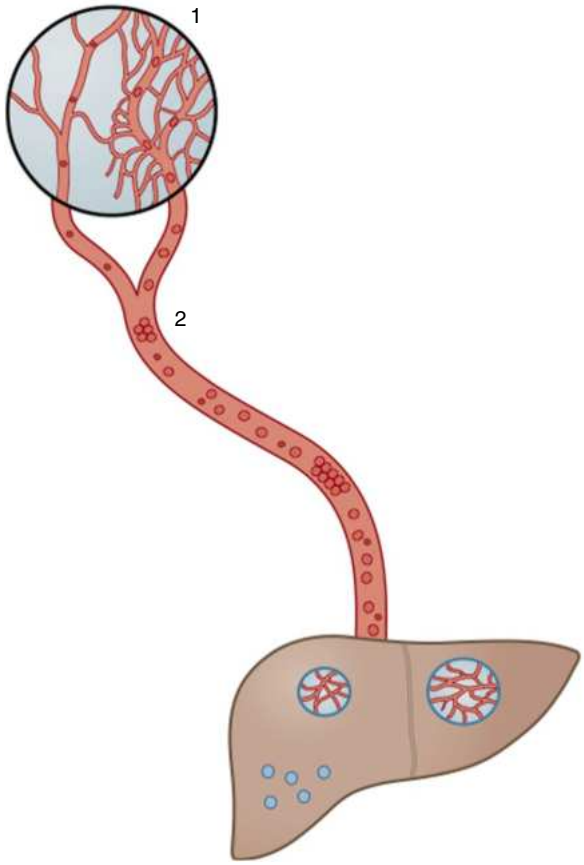

Fig. 6.3 Metastatic cascade. The metastatic cascade begins when tumor cells escape from the primary solid tumor and enter the general circulation. It seems that this shedding of tumor cells starts at an early stage, and uveal melanoma cells have been detected in the peripheral blood long before metastasis could be seen clinically. (1) Different parts of the tumor can show different vascular density, a fact that might contribute to the number of the cells that can give rise to metastasis. However, only a very few of those tumor cells can survive in the general circulation. (2) Formation of larger cell aggregates which also include platelets contributes to an increased survival of tumor cells. At their target site, they embolize a capillary or adhere to the vessel wall, pass it, and settle in the new organ. The mechanism behind the organotropism of metastasis is not fully understood. Besides hemodynamics, specific properties of the vessels, properties of the endothelium, and characteristics of the target organ, such as the expression of certain growth and chemotactic factors, might be important

tumors will grow slowly and might never reach a size that is clinically detectable. In fact, the proliferation rate does not differ significantly in such a dormant metastasis and in growing metastases, rather, the total number of cells is balanced by a high rate of apoptosis [47].

Matrix metalloproteinases (MMP), a family of proteases that cleave and degrade components of the extracellular matrix, are also known to play a crucial role in the metastatic cascade. The selective proteolytic activity of different MMPs can release pro- or anti-angiogenic substrates from the ECM or reveal binding sites that modulate interactions with endothelial cells to drive angiogenesis [48]. By degrading the basement membrane of the vessels, MMPs also compromise the integrity of the vessels, consequently enabling intravasation and extravasation of tumorigenic substrates [44]. Increased expression of MMPs has been shown in many types of tumors, including ocular melanoma and retinoblastoma, and has been linked to invasiveness and metastatic potential of the tumor [49–51]. In addition to the degradation of the extracellular matrix, MMP-9 (gelatinase B) also induces the expression of vascular endothelial growth factor (VEGF) and is an important trigger of angiogenesis in tumor metastasis [30, 52].

6.6 Promotors of Angiogenesis

Angiogenesis can be induced by a variety of factors and conditions. Inflammation, hypoxia, and mechanical factors can induce the production or the release of pro-angiogenic factors and cytokines. It has also been shown that the products of many oncogenes are pro-angiogenic and that this angiogenic activity might be one of their mechanisms of action [53].

6.6.1 Vascular Endothelial Growth Factor

The key molecular driver of angiogenesis, both physiologic and pathologic, is the vascular endothelial growth factor (VEGF). Initially discovered as a component of tumor ascitic fluid that caused increased vascular permeability in 1983, VEGF was isolated and characterized as an angiogenic agent in 1989 [54, 55]. The critical role of VEGF in development was also illustrated by a study in which knocking out a single VEGF allele resulted in abnormal blood vessel formation and early embryonic death [56]. Identifying the key signaling molecule for vascular growth enabled testing of the hypothesis presented by Folkman that angiogenesis is key for tumor growth and survival. Inhibiting VEGF using monoclonal antibodies has shown success in impeding tumor growth in some cancers [57, 58].

6.6.2 Functions of VEGF

In vitro and in vivo experiments have demonstrated that VEGF is a strong mitogen and survival factor for endothelial cells, promoting endothelial cell motility and the growth of new blood vessels and lymphatic vessels [59]. The VEGF-induced vasculature consists of a primitive vascular plexus that is highly fragile and hemorrhagic [60]. In vivo, it is physiologically expressed in areas of wound healing, bone growth, and the female reproductive organs [61]. VEGF plays a role in the pathogenesis of numerous ocular diseases, including retinopathy of prematurity (ROP), exudative and myopic choroidal neovascularization, diabetic macular edema (DME), neovascular age-related macular degeneration (nAMD), neovascularization of the iris and retinal vein occlusions. It has been shown that anti-VEGF treatment is beneficial in these diseases, with anti-VEGF intravitreal injections becoming a mainstay of treatment for nAMD and DME [62–64]. These therapies have not been shown to be as effective in treating ocular cancers, but studies combining their use with chemotherapeutic and anti-angiogenic agents are ongoing and will be discussed in greater detail later in this chapter.

6.6.3 Subtypes of VEGF

VEGF family of growth factors consists of six secreted glycoproteins (VEGF-A, -B, -C, -D, -E, and placenta growth factor [PlGF]) binding to different VEGF receptors (VEGFR) on the cell surface [65]. In general terms, when VEGF is mentioned, VEGF-A is the protein usually being referred to, as its interaction with VEGFR-2 induces the key signaling pathway that drives angiogenesis. VEGF-A is a secreted, freely-diffusible glycoprotein with a half-life time in the circulation of only 3 minutes. It forms homodimers and binds to VEGFR-1 and VEGFR-2 on the surface of endothelial cells. The gene for VEGF is located on the short arm of chromosome 6 (6p21) [66], and alternative splicing results in the different isoforms of the protein, which are named after the number of their amino acids [67]. VEGF isoforms 121, 145, 165, 189, and 206 differ in their affinities to the VEGF receptors and to structures of the extracellular matrix [68].

6.6.4 VEGF Receptors

The function of VEGF is mediated by different cell surface receptors, the VEGF receptors VEGFR-1 (Flt-1), VEGFR-2 (KDR/Flk-1), VEGFR-3 (Flt-4), and neuropilin (NRP-1 and NRP-2) receptors [69]. The VEGFRs are a family of transmembrane receptor tyrosine kinases. They all have an extra-

cellular immunoglobulin-like domain, a lipophilic transmembrane region, and an intracellular domain that includes the tyrosine kinase (TK) [70]. Of the VEGF receptors, VEGFR-2 is the best characterized for its critical role in angiogenesis. Similar to the lethality of the VEGF-A knockout, mice deficient in VEGFR-2 also failed to survive through development, signifying its necessity in vasculogenesis [39]. Several AATs also target VEGF receptors, particularly VEGFR-2, to inhibit angiogenesis more thoroughly.

6.6.5 Regulation of VEGF

An important factor for the upregulation of VEGF under physiologic and pathologic conditions is hypoxia. When tumors grow to a larger size, they usually show areas of necrosis, surrounded by underperfused regions, showing upregulation of VEGF [71]. Hypoxia in those regions with low oxygen concentration induces the expression of two hypoxia-inducible factors (HIF-1 and HIF-2) [72]. The α-subunits translocate to the nucleus and bind to subunit-β and hypoxia response elements. This induces the expression of VEGF and more than 60 other genes [73]. Under normoxic conditions, however, HIF undergoes rapid degradation. The von Hippel-Lindau (vHL) protein plays a key role in this process by forming a ubiquitination complex and labeling HIF for degradation by the proteasome [74]. If the vHL protein is missing, mutated, or not functional, HIF is not inactivated properly, and normoxic tissue behaves under hypoxic conditions.

6.6.6 Fibroblast Growth Factor

Fibroblast growth factor (FGF) belongs to a family of at least 22 proteins, of which only a few are related to angiogenesis. FGF was the first angiogenic protein to be purified. It has a strong affinity for heparin and heparin-sulfate and is stored in the extracellular matrix. Proteases can release FGF, which then can bind to their tyrosine kinase FGF receptors on the cell surface and lead to activation of the MAPK pathway by protein kinase C (PKC) dependent signaling.

The basic fibroblast growth factor (bFGF or FGF-2) and the acid fibroblast growth factor (aFGF or FGF-1) have been shown to induce angiogenesis [75]. FGF is elevated in the serum of cancer patients and also seems to play a role in Kaposi's sarcoma and hemangioma [76].

6.6.7 Angiopoietins

The four members of the angiopoietin family, ang-1, ang-2, ang-3, and ang-4, all bind to another group of receptor tyrosine kinases (RTK), the Tie (Tie-1 and Tie-2) receptors. All four angiopoietins are known to bind to the Tie-2 receptor. They do not induce proliferation but influence cell migration, sprouting tube formation, and cell survival. Additionally, Ang-1 reduces vascular leakage induced by VEGF [77]. Ligand for the Tie-1 receptor has not yet been identified. However, Tie-1 deficiency in mice results in severe vascular defects [78]. This suggests that Tie-1 is an important inhibitor of angiogenesis.

6.6.8 Matrix Metalloproteinases (MMPs)

Matrix metalloproteinases are a family of endopeptidases that can degrade the extracellular matrix (ECM) [79]. By this, they liberate angiogenic factors, e.g., FGF, which is stored within the ECM. Other factors are generated from components of the ECM, e.g., endostatin, which is a fragment of collagen XVIII. MMPs are divided into five subgroups: matrilysins, collagenases, stromelysins, gelatinases, and membrane-type MMPs (bound to the cell surface). They are generated in an inactive form and have to be activated to become functional, e.g., by plasmin, which activates MMP-1 and MMP-3, thus starting a cascade of reciprocal activation of MMPs [80, 81]. In tumors, MMPs play a decisive role in the angiogenic switch, in part by inducing the release of VEGF [52]. Inhibitors of MMPs, such as TIMP (tissue inhibitor of metalloproteinases), reduce angiogenic switching and/or slow down tumor growth [82]. However, as some MMPs also have anti-angiogenic effects, inhibitors of MMPs have to be used with caution, as the net effect of MMP inhibition is difficult to predict [81].

6.7 Inhibitors of Angiogenesis

Angiogenesis inhibitors can be classified in two ways based on their mechanism of action and whether they are endogenous or synthetic (pharmaceutical) [83]. Based on their mechanism of action, angiogenesis inhibitors can be classified as indirect or direct. Indirect inhibitors block endothelial cell stimulation by preventing the release of angiogenic factors by tumor cells, neutralizing the angiogenic factors, or blocking the receptors to which angiogenic factors bind. Direct inhibitors block the response of endothelial cells directly, inhibiting their response to any pro-angiogenic stimulus. As direct inhibition targets the genetically stable endothelial cells instead of the tumor cells, it is less prone to drug resistance and treatment failure [83].

6.7.1 Endogenous

6.7.1.1 Thrombospondin

Thrombospondin was the first naturally occurring inhibitor to be identified [84]. It acts indirectly by inhibiting matrix

metalloproteinase MMP-9 but also has a direct effect on endothelial cells. During tumorigenesis, it is downregulated by several oncogenes (ras, c-myc, v-src, c-jun), while tumor suppressor genes (p53, PTEN) induce thrombospondin.

6.7.1.2 Angiostatin

Angiostatin is a fragment of plasminogen that is generated from plasminogen by, among others, urokinase plasminogen activator (uPA) and matrix metalloproteinases (MMP) [85]. It can be found in the urine and serum only in the presence of a tumor, and its half-life time in the circulation is approximately 2.5 days, much longer than for VEGF. The effects of angiostatin are very selective for endothelial cells, including induction of cell arrest and apoptosis, and it can reduce the number of circulating precursor endothelial cells from the bone marrow. This makes angiostatin an interesting candidate for anti-angiogenic therapy. It has successfully been used in animal models [86] and has been transfected to uveal melanoma in dogs [87]. As angiostatin levels decrease in the serum after radiation therapy of the primary tumor, additional therapy with angiostatin could be used to prevent accelerated growth of metastatic tumors [88]. It also has been hypothesized that enucleation of an eye harboring an angiostatin-producing uveal melanoma could unwittingly exacerbate distant metastatic disease [89].

6.7.1.3 Endostatin

Like angiostatin, endostatin is a fragment of a larger molecule. Proteolytic enzymes, elastase, cathepsin L, and matrix metalloproteinases, cleave an internal fragment of collagen XVIII, generating endostatin. The gene for collagen XVIII is located on chromosome 21, and patients with Down's syndrome show higher levels of endostatin and, interestingly, have a lower overall incidence of solid tumors. Like angiostatin, its effects are very specific for endothelial cells, inhibiting many steps in angiogenesis. It inhibits VEGF matrix metalloproteinases, down-regulates c-myc, inhibits cyclin D-1, and promotes endothelial cell apoptosis. Another effect is the decrease of vascular permeability, and the reduction of edema could enhance the effect of chemotherapy (see further down). In animal models, it shows regression of tumors, sometimes to microscopic lesions, and until now, no toxicity and no drug resistance has been observed. In a mouse model of retinoblastoma, it has successfully been used in combination with oncolytic viruses to inhibit tumor growth [90]. Endostatin plays a critical role in the development of the retinal vessels. In Knobloch syndrome, a deficiency of endostatin, the hyaloid artery of the vitreous fails to regress [91], and endostatin levels are elevated in eyes with proliferative diabetic retinopathy [92]. Phase I clinical trial testing endostatin in advanced solid tumors demonstrated low toxicity and showed reduced blood flow and increased apoptosis of tumor and endothelial cells [93, 94].

6.8 Anti-Angiogenic Therapy in Clinical Practice

A detailed review of the clinical applications of several commercially available anti-angiogenic agents is beyond the scope of this chapter. Moreover, excellent reviews on this topic have been published [95, 96]. Nevertheless, it is important to point out that, despite the effects of anti-VEGF therapy on tumor vessels [97]. anti-VEGF monotherapy (i.e., without chemotherapy or radiation therapy) has failed to produce improvements in overall patient survival [95]. However, the beneficial effects of prolonging overall survival are apparent when bevacizumab (Avastin®) is added to standard chemotherapy for patients with colorectal and lung cancer and progression-free survival in breast cancer patients [95]. In contrast, the combination therapy bevacizumab and temozolomide failed to show any benefit [98]. Multitargeted tyrosine kinase inhibitors today are standard first-line and second-line treatments in patients with renal cell carcinoma [99, 100]. Anti-angiogenic therapy (anti-VEGF) has also been used in combination with checkpoint inhibitors (PD-1) in the treatment of renal cell carcinoma in von Hippel Lindau disease [101].

The relationship between anti-VEGF therapy and the usual methods of treatment, such as radiation therapy and chemotherapy, is complex and perhaps best explained by the concept of "vascular normalization"[102]. It is suggested that anti-VEGF therapy not only reduces vascular density but induces structural and functional changes in the tumor vasculature that improve cellular oxygenation and perfusion ("normalization") [102]. Improved oxygenation consequently increases the efficacy of radiation therapy and improves the delivery of chemotherapy. However, bevacizumab has also been shown to increase VEGF expression in vitro and animal models ("pseudohypoxic phenomenon"), presumably an adaptive tumor response [103]. Theoretical considerations of combining novel anti-VEGF therapies with standard forms of therapy are discussed in detail elsewhere [95].

6.8.1 Anti-Angiogenic Agents Tested in Clinical Trials

VEGF-A is the major positive regulator of angiogenesis and has consequently been the target of most AAT to prevent neovascularization. There are direct and indirect ways to inhibit VEGF. These include blocking the VEGF at the mRNA level with small interfering RNA (siRNA) [104], targeting the soluble VEGF ligand with antibodies, antibody fragments, or decoy receptors, blocking the extracellular domain of the VEGF receptors (VEGFR-2), and inhibition of the intracellular signaling pathway by blocking the receptor tyrosine kinase domain (Fig. 6.4) [105]. Other pro-angiogenic

targets have included PlGF, FGF, and PDGFR, which were discussed previously. Known anti-angiogenic agents have been combined with traditional chemotherapies for the treatment of uveal melanoma. The list of agents that have been tested in clinical trials or case series for melanomas of different subtypes [106, 107] is summarized in Table 6.1.

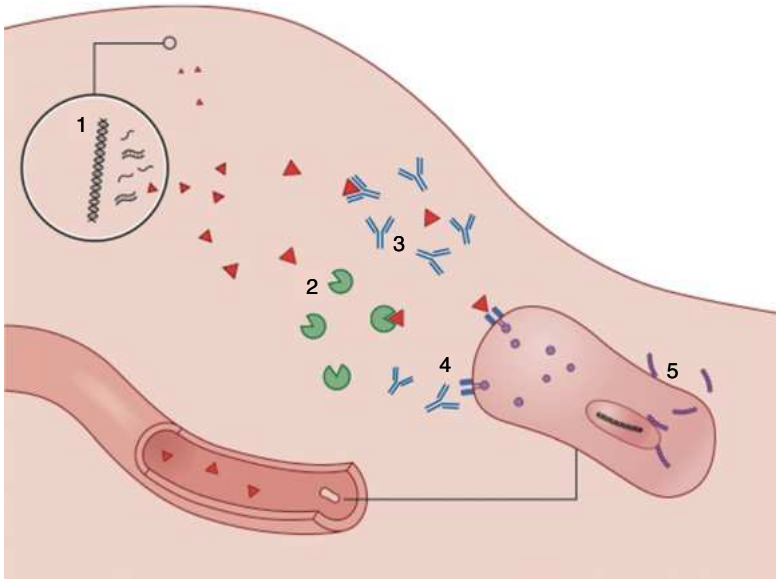

Fig. 6.4 Direct and indirect ways of inhibiting angiogenesis. Anti-angiogenic therapy can interfere with pro-angiogenic stimuli on different levels. (1) Antisense oligonucleotides bind to mRNA of pro-angiogenic factors, thus inhibiting translation by the ribosome and inducing degradation. (2) Small molecules, boligonucleotides, and (3) antibodies against diffusible circulating angiogenic factors bind and inactivate those factors, before they reach the endothelial cell. (4) Antibodies can also bind to the cell surface/transmembrane receptor and prevent stimulation by angiogenic factors. (5) Direct inhibitors bind to the cell surface or get internalized, exerting an inhibiting function on their target cells

Table 6.1 Prospective trials or case series with anti-angiogenic agents for melanoma

Agent	Target(s)	Author and year	Melanoma types included	Sample size (N)	Median age in years (range)	Key findings for OS
Bevacizumab	VEGF	Corrie 2018 [196]	Cutaneous	671	56 (range 18–88)	64% 5-year OS, HR = 0.98 (95% CI 0.82–1.16)
Bevacizumab+ IFN-α2b	VEGF, bFGF	Guenterberg 2011 [197]	Ocular	5	Mean 63.8 (range 53–71)	Median OS 43 weeks (range 7–91 weeks)
Bevacizumab+ paclitaxel+ carboplatin	VEGF	Kim 2012 [198]	Any	143	60 (range 27–85)	51.9% 1-year OS, median OS 12.3 months
Bevacizumab+ temozolomide	VEGF	Piperno-Neumann 2013 [199]	Ocular	35	55 (range 29–72)	Median OS 10 months (95% CI 8–15 months)
Aflibercept	VEGF-A, VEGF-B, PlGF	Tarhini 2011 [170]	Cutaneous and ocular	41	57 (range 23–84)	56.4% 1-year OS, median OS 16.3 months
Axitinib	VEGFR1–3	Fruehauf 2011 [200]	Any	32	65 (range 30–86)	28.1% 1-year OS, median OS 6.6 month (95% CI 5.2–9 months)
Axitinib+ carboplatin+ paclitaxel	VEGFR1–3	Algazi 2015 [201]	Any	38	Mean 65.4 +/− 10.6 years	Median OS 14.0 months (95% CI 10–17.9)
Cabozantinib	c-met, VEGFR2, c-kit, RET, FLT-3, TIE2, Axl	Daud 2017 [202]	Any	77	65 (range 30–90)	Median OS 9.4 months

(continued)

Table 6.1 (continued)

Agent	Target(s)	Author and year	Melanoma types included	Sample size (N)	Median age in years (range)	Key findings for OS
IFN-α2b	bFGF	Suarez-Kelly 2019 [203]	Cutaneous	34	52 (range 22–77)	Median OS 6.8 years (range 4.7 years-NR)
IFN-α2b	bFGF	Tarhini 2020 [204]	Cutaneous	636	54 (range 18–83)	67% 5-year OS (95% CI, 62–72%)
Thalidomide-IFNα2b	VEGF, bFGF, TNFα	Solti 2007 [205]	Cutaneous and ocular	15	Mean 56.7 (range 42–70)	Median OS 4.7 months (range 0.9–31.5)
Imatinib	ABL, c-kit, PDGFR	Hofmann 2009 [206]	Ocular	12	63 (range 47–82)	Median OS 6.8 months
Lenalidomide	VEGF	Zeldis 2009 [207]	Ocular	17	Not available	44% disease stabilization for a mean of 7 months (range 6–12 months)
Lenalidomide+ dacarbazine	VEGF	Hwu 2010 [208]	Cutaneous	28	61 (range 34–79)	Median OS 10.6 months (range 1.6–46 months)
Semaxanib+ thalidomide	VEGFR2, c-kit, PDGF, VEGF, bFGF, TNFα	Mita 2007 [209]	Any	12	58 (range 43–71)	1 complete response for 20 months, 1 partial response for 12 months, 4 patients with stable disease for 2–10 months
SU5416+ semaxanib	VEGFR1–3	Kuenen 2003 [210]	Cutaneous	20	53.5 (range 23–71)	Median OS 107.5 days (range 29–504 days)
Sorafenib	VEGFR1–3, PDGFR, c-kit, FLT-3, RET, Raf1, B-Raf	Scheulen 2017 [211]	Ocular	118	Not available	Median OS 14.8 months (3.7–38.3 months)
Carboplatin-paclitaxel + sorafenib	VEGFR1–3, PDGFR, c-kit, FLT-3, RET, Raf1, B-Raf	Bhatia 2012 [212]	Ocular	24	61 (range 48–73)	24% 1-year OS, median OS 11 months (95% CI 7–14 months)
Sunitinib	VEGFR1–3, PDGFR, c-kit, FLT-3, RET	Mahipal 2012 [213]	Ocular	20	69 (range 29–78)	44.4% 1-year OS, median OS 8.2 months

Trials and pilot studies testing AATs for melanoma of any subtype were included in this table. Any type of melanoma included indicates that ocular, cutaneous, mucosal, and acral melanomas were included. Ages of the patient at time of enrollment are the median age unless otherwise indicated. *OS* overall survival, *HR* hazard ratio, *NR* no relapse

6.9 Angiogenic Aspects of Specific Ophthalmic Tumors

6.9.1 Retinoblastoma

Histopathologic examination of retinoblastoma tumor shows a highly vascular tumor in which the vessels are cuffed by a layer of viable cells having a mean thickness of 90–100 microns and surrounded by necrotic debris. (Fig. 6.5) [108]. The extent of angiogenesis in retinoblastoma tumors may be a predictor of metastatic potential [109]. In a pilot study of patients with unilateral retinoblastoma treated solely by enucleation, it was observed that a tumor's relative vascular area was a better predictor of disease dissemination than either choroidal or optic nerve invasion [109]. Retinoblastomas express high amounts of VEGF [110]. Moreover, retinoblastoma cell lines, which express low levels of VEGF under normal culture conditions, show a strong increase in VEGF secretion under hypoxia, suggesting that focal hypoxia may act as a stimulus for VEGF production in retinoblastoma, which in turn contributes to tumor growth by stimulating angiogenesis [110].

6.9.2 Treatment

Specific anti-angiogenic treatment modalities have not been applied in the clinical routine until now for the treatment of the tumor. However, intravitreal ranibizumab has been used to treat the side effects of other treatment modalities, such as radiation therapy [111, 112]. In addition, several anti-angiogenic drugs have been evaluated for their effects on retinoblastoma in cell cultures and animal models. Combretastatin A-4 phosphate (CA-4P) induces a dose-dependent decrease in microvessel density and consequent tumor volume reduction in an animal model of hereditary retinoblastoma [113, 114]. Similarly, anecortave acetate (AA) could induce apoptosis and reduce tumor burden when used alone or in combination with glycolytic inhibitors [115, 116]. Bevacizumab has also shown an inhibitory effect on

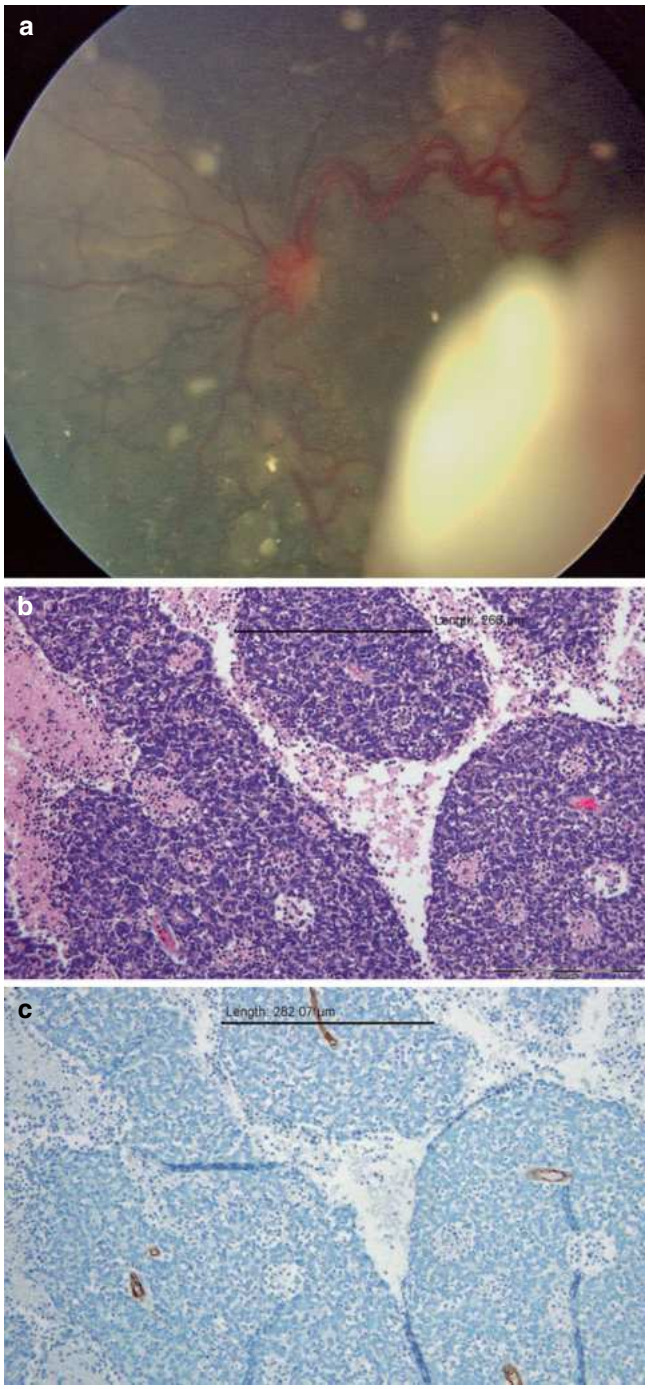

Fig. 6.5 Retinoblastoma. Prominent feeder vessel (**a**). Vitreous seeds are about 200 m diameter, which is maximum attainable size in the absence of intrinsic circulation. Islands of viable tumor cells surrounding a central blood vessel (**b**; Hematoxylin and eosin stain; original magnification 10×) and with endothelial stain (**c**; CD34 stain; original magnification 10x)

angiogenesis and growth of retinoblastoma [117]. However, the clinical challenge in the management of advanced retinoblastoma is the presence of vitreous seeding, which is not vasculature-dependent (Fig. 6.5). Effects on the differentiation of retinoblastoma cells have been demonstrated, however, without direct cell toxicity [118]. Therefore, solely on theoretical grounds, it is unlikely that anti-angiogenic therapies will play a major role in the management of advanced intraocular disease associated with vitreous seeding.

6.9.3 Uveal Melanoma

6.9.3.1 Pseudovascular Channels (Vasculogenic Mimicry)

The pseudovascular channels are identified as PAS-positive loops or networks in histological preparations (Fig. 6.6) as well as in vitro studies [119]. It is now believed that pseudovascular channels are laminin-rich extravascular matrix patterns that conduct plasma [120]. As these channels lack endothelial cells, are independent of angiogenesis, and do not conduct blood cells, the term "vasculogenic mimicry" is used to describe their origin. The angiogenesis-independent supply of the tumor with nutrients and oxygen via those channels might limit the effect of anti-angiogenic therapy in the treatment of primary uveal melanoma.

6.9.3.2 Tumor Ingrowth Into Blood Vessels

Getting access to the systemic circulation is a crucial step at the beginning of the metastatic cascade. Choroidal melanomas arise in a highly vascularized location and show a dense intrinsic vascularity. Intra-tumoral vessels can be seen in angiography ('double circulation') [121], and their presence has been used as a diagnostic factor [122].

6.9.3.3 Indocyanine Green Angiographic Patterns

In addition to the prominent intrinsic tumor vessels visible on angiography ('double circulation'), small microcirculatory patterns have been identified and shown to correlate with the risk for growth (malignant transformation) of a small choroidal melanocytic lesion [123, 124]. However, there are different interpretations of the nature of the microcirculatory patterns observed with ICG. One group believes that these represent pseudovascular channels [123, 125], whereas the other believes that they represent microcirculatory patterns derived from true vessels [124]. The latter view is compatible with the concept of "angiogenic switch" outlined above.

6.9.3.4 VEGF Expression

Despite an initial study indicating a lack of overexpression of VEGF in uveal melanoma [110], subsequent studies have indicated significant overexpression of not only VEGF [126–128] but also of bFGF in uveal melanoma [127]. However, there seems to be no correlation between the level

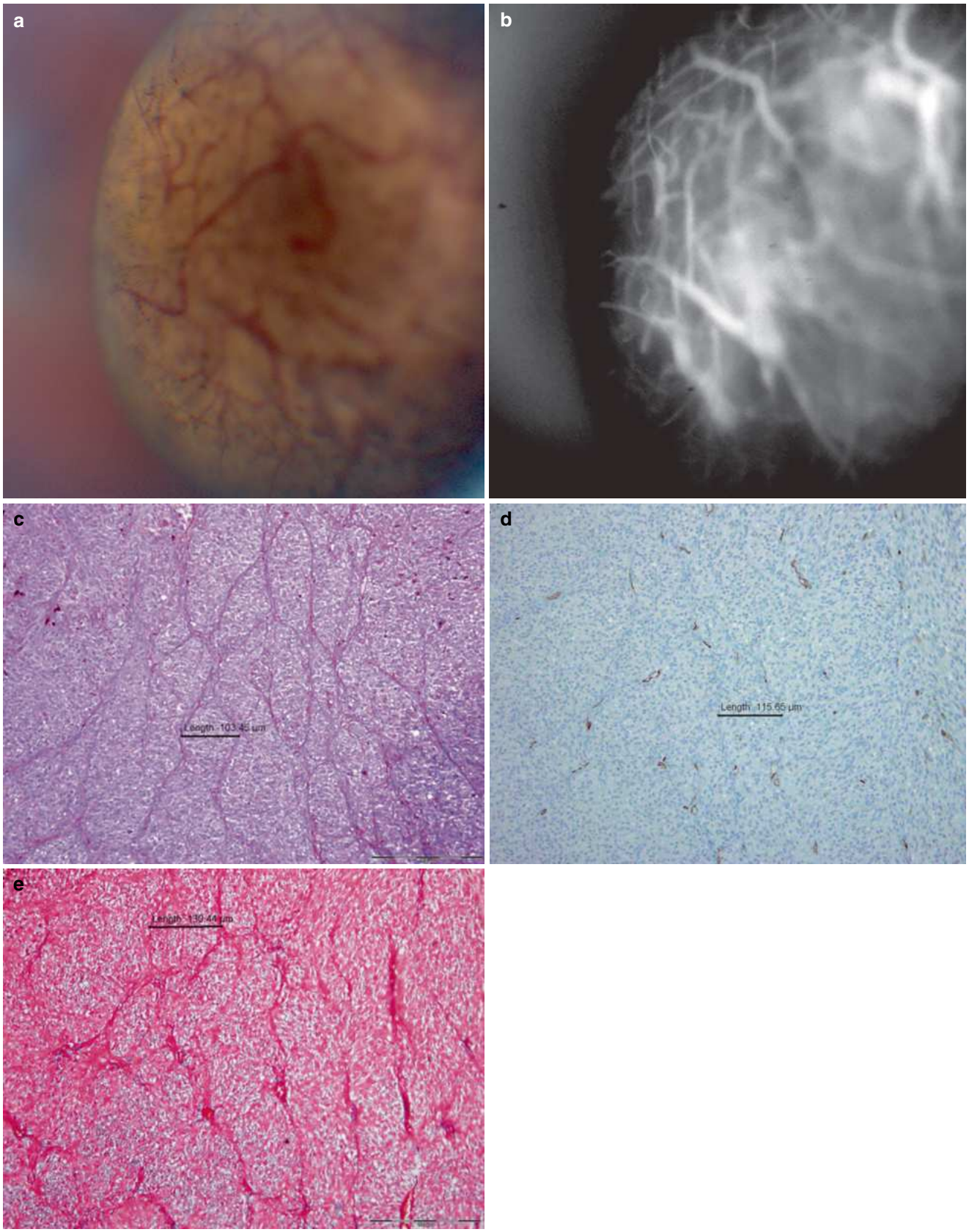

Fig. 6.6 Uveal melanoma. Intrinsic vessels within an amelanotic tumor (**a**). The abnormal choroidal vessels are best visualized with indocyanine angiography (**b**). Pseudovascular patterns are discernible (**c**; PAS stain; original magnification 20x). These "channels" are not lined by endothelium as shown by the absence of staining with CD34 (**d**; original magnification 20x). Note the presence of true tumor vessels that are stained brown. The exact nature and role of these "channels" are still investigational, but they do not contain collagen (**e**; Masson trichrome stain; original magnification 20)

of VEGF expression and tumor microvascular density [128], 6p21 region copy number (locus of the VEGF gene) [129], and metastasis [128]. Tumor necrosis [128] and previous radiotherapy [130] correlate with level of VEGF expression in uveal melanoma. A combination of radiotherapy and anti-VEGF treatment with bevacizumab has shown an additive effect in cell-cell cultures and animal models [131]. Increased expression of pro-angiogenic interleukin IL-8 seemed to induce resistance to anti-VEGF treatment [132]. However, overall, bFGF expression is more frequently observed than VEGF expression in uveal melanoma [127]. VEGF is also found in the vitreous and aqueous humor of eyes harboring choroidal melanoma [133], and vitreous level correlates with tumor size [134].

6.9.3.5 Metastatic Uveal Melanoma

Besides the growth of the primary tumor, angiogenesis also plays an important role in the growth of metastasis. Of the four clinical patterns of presentation of metastases (early metastasis, simultaneous metastasis, occult primary, long-term dormancy) [2], uveal melanomas seem typically to manifest a pattern of long-term dormancy [135]. Explanations for the different patterns have been given, including accumulating genetic mutations over time, changes in immunologic surveillance, and hormonal stimuli. However, with growing insight into the mechanisms of angiogenesis, an explanation based on a balance of pro-angiogenic and anti-angiogenic factors becomes persuasive [47]. The lack of an angiogenic switch can explain the long-term dormancy of micrometastasis. Production of anti-angiogenic factors such as thrombospondin, angiostatin, and endostatin by the primary tumor keeps metastatic tumors at a small size [136, 137]. Because these anti-angiogenic factors have a longer half-life time than the pro-angiogenic stimuli, their effects on metastases are stronger. With the removal of the primary tumor, the pro-angiogenic stimuli predominate, resulting in the growth of metastasis [138].

Although such a pattern of post-enucleation rise in mortality with uveal melanoma was attributed to the shedding of cells (Zimmerman-Mclean-Foster Hypothesis) [139], recent critical appraisal of the published evidence confirms such a trend in mortality but does not attribute it to mechanical shedding of the cells [140]. Rather, alternate explanations based on cell doubling models have been put forward [140–142]. As mentioned above, uveal melanoma produces angiostatin, and the drop in angiostatin levels after enucleation has been hypothesized to promote the growth of metastases [89]. Additional investigations are necessary to explain the clinically observed relationship between primary and metastatic uveal melanoma.

6.9.3.6 Treatment

In a murine model of uveal melanoma, topical application of 1% anecortave acetate (angiostatic agent) significantly slowed tumor growth [143]. However, accidental use of bevacizumab in three reported cases did not lead to growth arrest [144]. More so, an animal model even showed an acceleration of tumor growth after the addition of bevacizumab.[103] Such an apparently paradoxical growth of uveal melanoma has also been observed in two patients after intravitreous injection of bevacizumab [145]. Though bevacizumab has been proven effective in reducing subretinal fluid and vascular activity of choroidal nevi [146], there is—until now - no evidence for antitumoral effects justifying bevacizumab monotherapy. However, a combination of bevacizumab with radiotherapy has been suggested not only to reduce treatment-induced complications but also to achieve additive effects [131].

6.9.3.7 Radiation Retinopathy

The pathogenesis of radiation retinopathy includes the preferential loss of vascular endothelial cells and the relative sparing of pericytes [147]. Ultimately, the inner retinal ischemia leads to macular edema and neovascularization. Fluorescein angiography and OCT-angiography (OCT-A) are tools of utmost importance to evaluate radiation retinopathy. The earliest changes by angiography are of focal capillary closure with neighboring areas of irregular capillary dilation and microaneurysms (Fig. 6.7) [148, 149].

Among numerous treatment modalities available, intravitreal injections of bevacizumab are widely used (Fig. 6.8) [150]. Twenty-one patients with radiation retinopathy following palladium-103 brachytherapy were treated with intravitreal bevacizumab (1.25 mg/0.05 mL) every 6–12 weeks. After a mean follow-up of 7.8 months, 86% (18/21) had stable or improved visual acuity, with 14% (3/21) regaining two or more Snellen lines [151]. It is generally believed that the role of bevacizumab for radiation maculopathy is limited as the improvement is temporary, requiring multiple injections [152, 153]. Other anti-VEGF agents, such as ranibizumab and aflibercept, have also been used with similar effects [154–158]. However, other mechanisms (presumably inflammatory) also seem to be involved in the development of radiation retinopathy, as cases refractory to bevacizumab appear responsive to intravitreal dexamethasone [159–162].

6.9.3.8 Metastatic Uveal Melanoma

The chemotherapy regimens currently used in the treatment of metastatic cutaneous melanoma are ineffective against metastatic uveal melanoma [163, 164]. Sorafenib, a tyrosine kinase inhibitor targeting multiple receptors (VEGF and

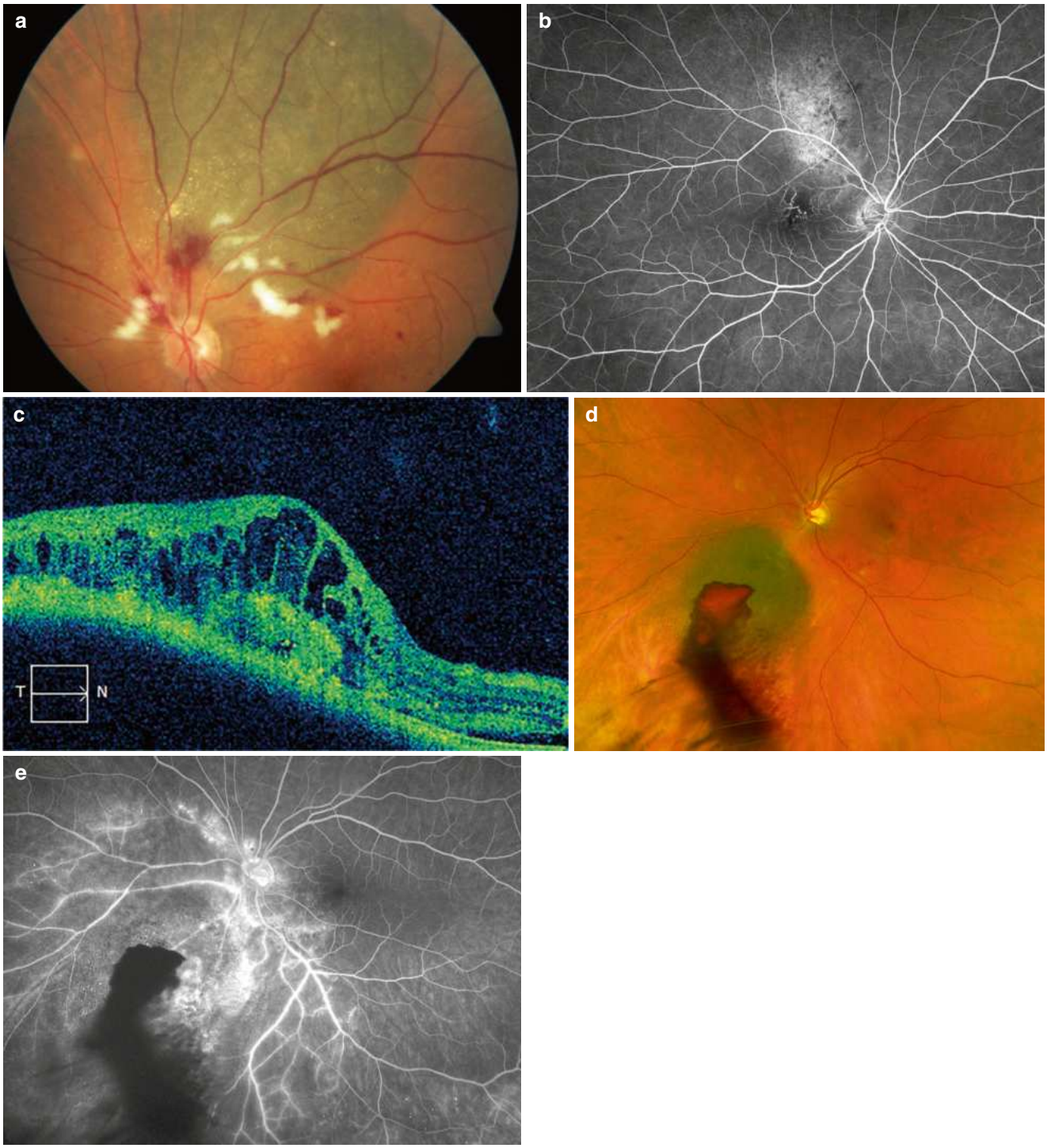

Fig. 6.7 Radiation retinopathy. Nonproliferative changes include cotton wool spots, telangiectasia, retinal hemorrhages, and macular edema (**a**). Retinal capillary nonperfusion in the macula and microaneurysms are most evident on the fluorescein angiography (**b**). Cystoid macular edema (**c**) and retinal neovascularization (**d**, proliferative radiation retinopathy) seen by fluorescein angiography causing vitreous hemorrhage (**e**)

PDGF receptors, c-Kit, and Flt-3), has been evaluated alone and in combination with fotemustine, carboplatin, and paclitaxel [165–167]. It appears to prolong progression-free survival; however, it has significant side effects. Sunitinib, another tyrosine kinase inhibitor, has also shown clinical benefit and is evaluated in clinical trials [168]. Intravenous

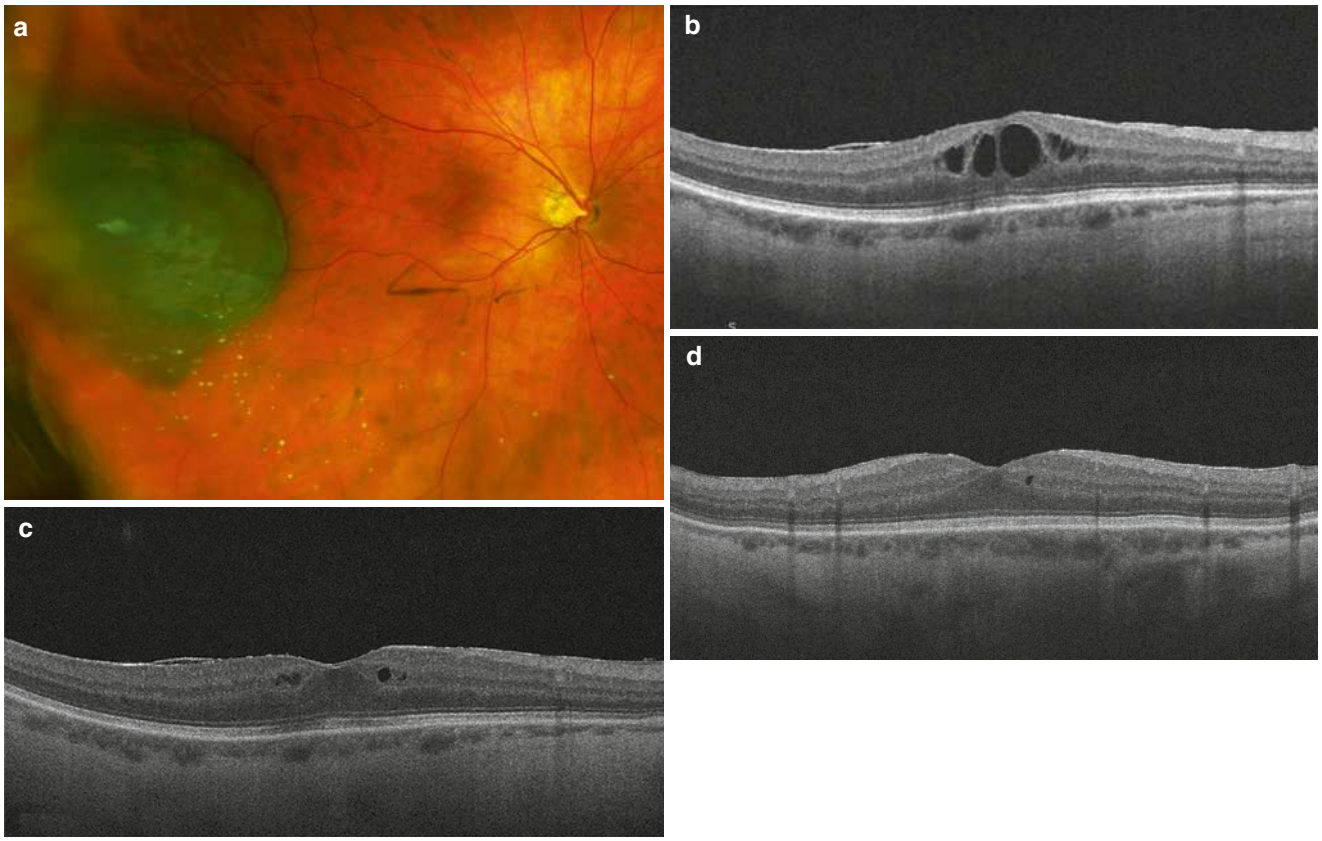

Fig. 6.8 A 70-year-old male patient who was treated for choroidal melanoma (right eye) by episcleral plaque brachytherapy (**a**, fundus photograph). Five months later, he developed cystoid macular edema (CME) due to radiation retinopathy with decrease in vision to 20/40 (initial: 20/20) (**b**, OCT). After intravitreal bevacizumab (second injection), the vision improved to 20/30 with reduction in CME (**c**, OCT). Normal foveal contour with trace intraretinal cysts and complete resolution of CME was achieved with a total of 13 injections (**d**, OCT)

aflibercept (VEGF-Trap) also improved survival in metastatic cutaneous and uveal melanoma; however, it showed significant toxicity [169]. Since GNAQ/GNA11/CYSLTR and PLCB4 are driver mutations in melanocytic uveal tumors and activate the RAS-ERK pathway, MEK inhibitors are currently in the focus of interest [170–172], as are immune checkpoint blockade and immunotherapy [173–179].

6.9.4 Von Hippel-Lindau Disease

The transcription factor HIF-2α plays an important role in oxygen sensing through the regulation of genes that promote adaptation during hypoxic conditions. In a normoxic environment, HIF-2α is degraded by von Hippel-Lindau (VHL) protein (Fig. 6.9) [180]. In the setting of VHL disease, there is a lack of functional protein and, therefore, stabilization and accumulation of HIF-2α. This results in HIF-2α translocation into the nucleus and subsequent interaction with the transcription factor HIF-1β, which then forms a complex that induces the expression of genes associated with cellular proliferation, angiogenesis, and tumor growth. The role of VEGF, as one of the upregulated genes, in retinal hemangioma, CNS hemangioblastoma, renal cell carcinoma, and pheochromocytoma in vHL syndrome is well established (Fig. 6.10) [181]. Belzutifan, a small molecule inhibitor of HIF-2α and an inducer of cytochrome P450 3A4, was approved by the FDA (2021) for the treatment of adult patients with VHL disease with CNS hemangioblastoma, pancreatic neuroendocrine tumor (pNET), and advanced RCC [182].

6.9.5 Treatment

Retinal capillary hemangioma is usually treated with laser photocoagulation and cryotherapy. In cases not amenable to usual therapies, systemic use of SU5416 (Semaxanib) and bevacizumab (Avastin®) has been described [183–185]. In the reported cases, there was stabilization of the lesion, reduction of retinal edema, and improved visual function. In a small series of three patients with VHL-associated retinal hemangioblastoma, belzutifan resulted in a reduction in tumor size, allowing subsequent consolidation with laser photocoagulation [186].

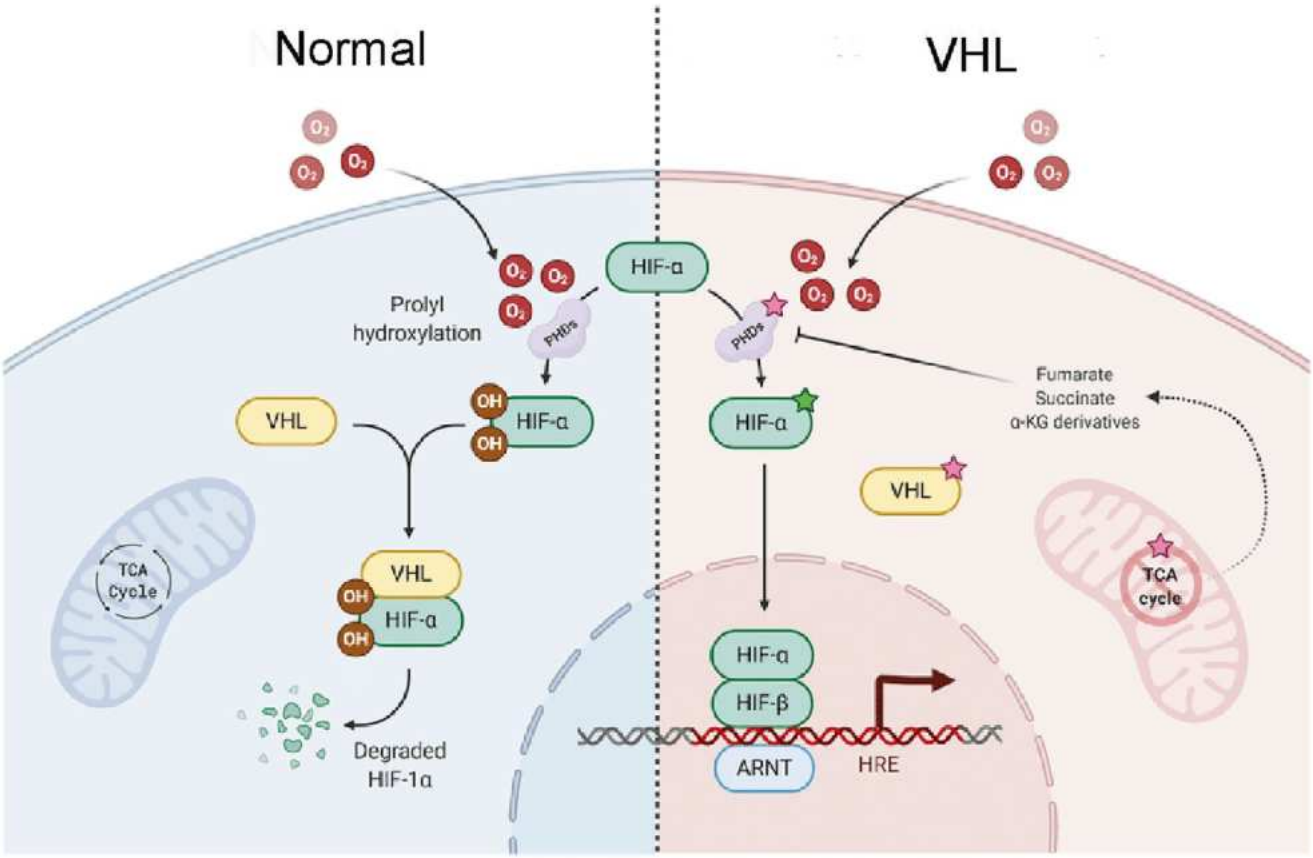

Fig. 6.9 Hypoxia-inducible factor (HIF) pathway regulation in normal states and in VHL. In the normal state (left), HIF signaling is impaired by the PHD enzyme class mediated hydroxylation of HIF-α, in turn marking the latter protein for proteolysis via the actions of the von Hippel Lindau (VHL) tumor suppressor protein. If oxygen levels are reduced, HIF-α escapes hydroxylation and degradation and initiates intra-nuclear target transcriptome programs, including those associated with angiogenesis. In RCH (right), activating EPAS1 (encoding HIF-2α) mutations (green star), inactivating VHL, PHD1/EGLN2, and PHD2/EGLN1 mutations (red stars) as well as aberrant TCA cycle regulation leading to inhibition of PHDs are main genetic events activating the HIF signaling cascade—even at normal oxygen levels. (Reproduced with permission from: Juhlin C. Challenges in Paragangliomas and Pheochromocytomas: from Histology to Molecular Immunohistochemistry. Endocrine Pathology 2021;32)

6.9.6 Conjunctival Squamous Cell Carcinoma (SSC)

Ultraviolet-B light exposure has consistently emerged as a major etiologic factor for SSC (Fig. 6.11) [187]. Human papillomavirus (subtypes 16 and 18) has been associated with SCC but is probably not an independent cause of conjunctival neoplasia. Systemic immunosuppression, as seen in acquired immune deficiency syndrome, is also a risk factor [188].

6.9.6.1 Treatment

Surgical excision with 2–3 mm margins has been the preferred approach for localized disease. Application of intraoperative supplemental cryotherapy (double freeze-thaw cycles) to conjunctival margins reduces the risk of tumor recurrence [189]. Topical chemotherapy has been advocated as an adjuvant for incomplete excision of large and diffuse primary or recurrent tumors [190]. While 5 fluorouracil and mitomycin-C are currently available chemotherapeutic agents, other topical agents such as interferon alpha-2b are no longer available [191, 192]. The antineoplastic effects of interferon-alpha 2b are due to a direct anti-proliferative effect, indirect anti-angiogenic effects, and immune-mediated effects [193]. In recurrent multifocal conjunctival carcinoma, repeated subconjunctival injections of ranibizumab induced (partial) regression in the majority of cases over a mean follow-up of 19 months [194].

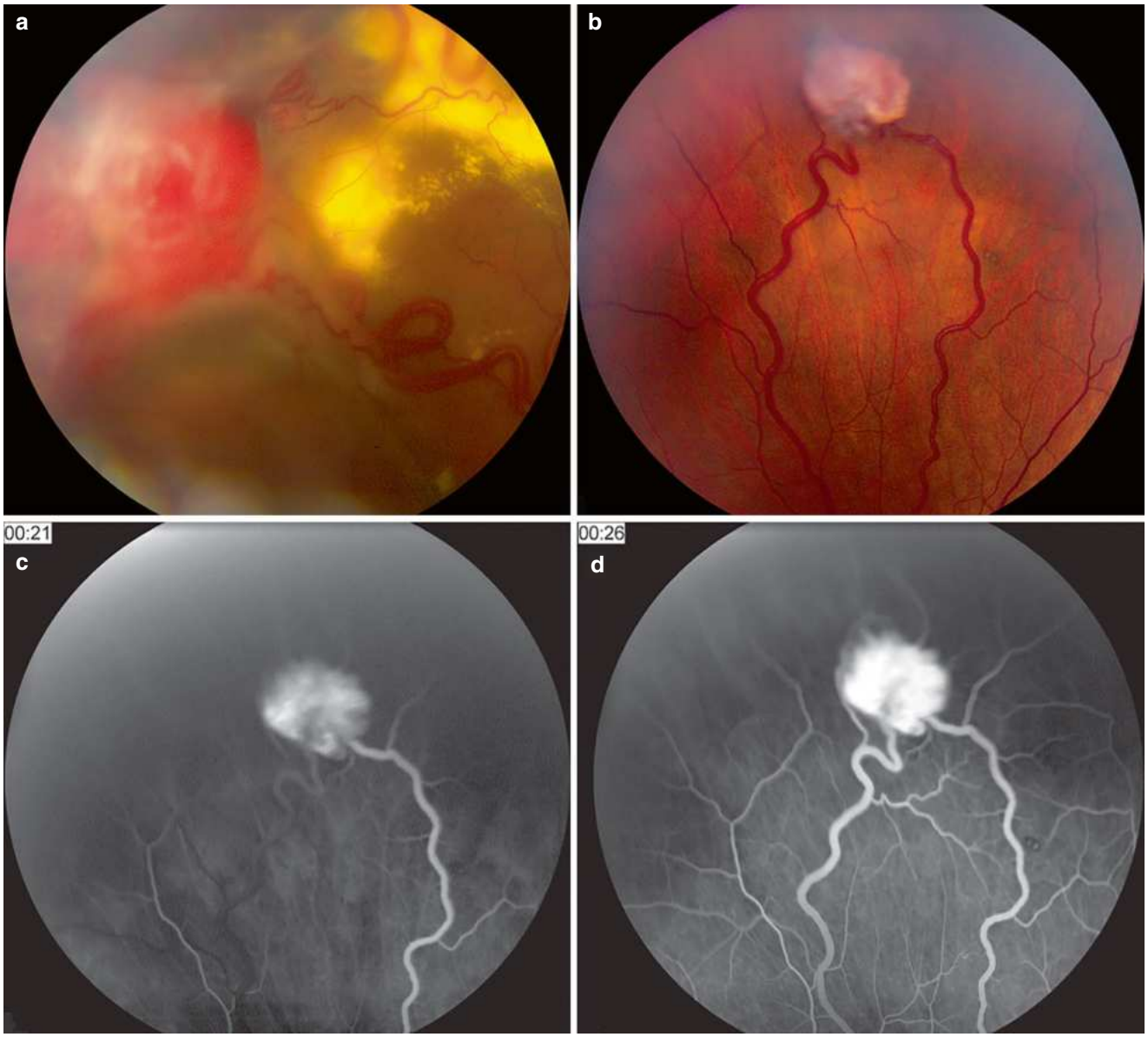

Fig. 6.10 Retinal capillary hemangioma. Ophthalmoscopic appearance of a large hemangioma with retinal exudation and detachment (**a**). Note prominent feeder vessels (**b**). Fluorescein angiogram initially fills the supplying artery (**c**) and the draining vein fluoresces few seconds later (**d**)

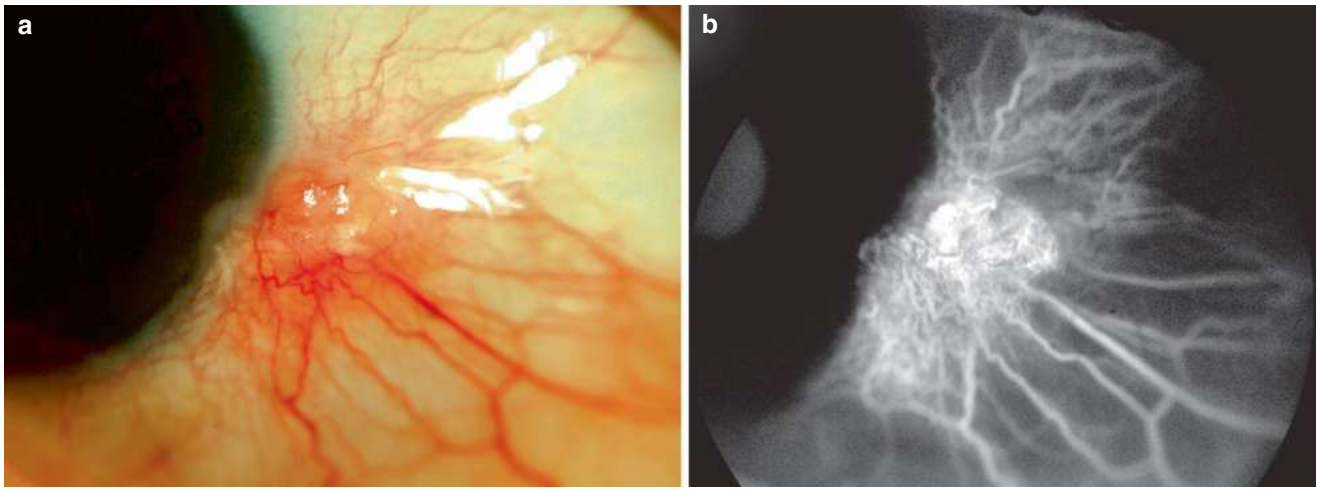

Fig. 6.11 Squamous cell carcinoma of the conjunctiva. Clinical appearance with prominent feeder and intrinsic vessels (**a**). The vessels are best visualized with fluorescein angiography (**b**)

6.10 Conclusions

Advances in technology offer possibilities for designing pharmaceutical agents that specifically target cellular pathways. Angiogenesis represents one such important pathway. Optimal clinical application and the efficacy of angiogenic inhibitors are currently under investigation. Treatments with angiogenic inhibitors already have a broad spectrum of applications in the management of intraocular and adnexal tumors that are expected to expand.

References

1. Folkman J. Tumor angiogenesis: therapeutic implications. N Engl J Med. 1971;285(21):1182–6.
2. Folkman J. Angiogenesis in cancer, vascular, rheumatoid and other disease. Nat Med. 1995;1(1):27–31.
3. Achilles EG, et al. Heterogeneity of angiogenic activity in a human liposarcoma: a proposed mechanism for "no take" of human tumors in mice. J Natl Cancer Inst. 2001;93(14):1075–81.
4. Tannock IF. Population kinetics of carcinoma cells, capillary endothelial cells, and fibroblasts in a transplanted mouse mammary tumor. Cancer Res. 1970;30(10):2470–6.
5. Naumov GN, Bender E, Zurakowski D, et al. A model of human tumor dormancy: an angiogenic switch from the nonangiogenic phenotype. J Natl Cancer Inst. 2006;98(5):316.
6. Hanahan D, et al. Transgenic mouse models of tumour angiogenesis: the angiogenic switch, its molecular controls, and prospects for preclinical therapeutic models. Eur J Cancer. 1996;32A(14):2386–93.
7. Folkman J, Hanahan D. Switch to the angiogenic phenotype during tumorigenesis, vol. 22. Princess Takamatsu Symp; 1991. p. 339–47.
8. Gimbrone MA Jr, et al. Tumor growth and neovascularization: an experimental model using the rabbit cornea. J Natl Cancer Inst. 1974;52(2):413–27.
9. Gimbrone MA Jr, et al. Tumor dormancy in vivo by prevention of neovascularization. J Exp Med. 1972;136(2):261–76.
10. Bergers G, et al. Tumorigenesis and the angiogenic switch. Nat Rev Cancer. 2003;3:6.
11. Kerbel R, et al. Clinical translation of angiogenesis inhibitors. Nat Rev Cancer. 2002;2:10.
12. Baeriswyl V, Christofori G. The angiogenic switch in carcinogenesis. Semin Cancer Biol. 2009;19(5):329.
13. Hanahan D, Weinberg RA. Hallmarks of cancer: the next generation. Cell. 2011;144(5):646.
14. Hanahan D. Hallmarks of cancer: new dimensions. Cancer Discov. 2022;12(1):31.
15. Donnem T, et al. Vessel co-option in primary human tumors and metastases: an obstacle to effective anti-angiogenic treatment? Cancer Med. 2013;2(4):427–36.
16. Kuczynski EA, et al. Vessel co-option in cancer. Nat Rev Clin Oncol. 2019;16:8.
17. Holash J, et al. Vessel cooption, regression, and growth in tumors mediated by angiopoietins and VEGF. Science. 1999;284(5422):1994–8.
18. Pezzella F, Pastorino U, Tagliabue E, et al. Non-small-cell lung carcinoma tumor growth without morphological evidence of neoangiogenesis. Am J Pathol. 1997;151(5):1417–23.
19. Lugassy C, Vermeulen PB, Ribatti D, et al. Vessel co-option and angiotropic extravascular migratory metastasis: a continuum of tumour growth and spread? Br J Cancer. 2022 Apr;126(7):973.
20. Küsters B, Leenders WP, Wesseling P, Smits D, Verrijp K, Ruiter DJ, Peters JP, van Der Kogel AJ, de Waal RM. Vascular endothelial growth factor-a(165) induces progression of melanoma brain metastases without induction of sprouting angiogenesis. Cancer Res. 2002;62(2):341–5.
21. Cuypers A, Truong A-CK, Becker LM, Saavedra-García P, Carmeliet P. Tumor vessel co-option: the past & the future. Front Oncol. 2022;12:12.

22. Barnhill R, Vermeulen P, Daelemans S, van Dam PJ, Roman-Roman S, Servois V, Hurbain I, Gardrat S, Raposa G, Nicolas A, Dendale R, Pierron G, Desjardins L, Cassoux N, Piperno-Neumann S, Mariani P, Lugassy C. Replacement and desmoplastic histopathological growth patterns: a pilot study of prediction of outcome in patients with uveal melanoma liver metastases. J Pathol Clin Res. 2018;4(4):227.
23. Lugassy C, Eyden BP, Christensen L, Escande JP. Angio-tumoral complex in human malignant melanoma characterised by free laminin: ultrastructural and immunohistochemical observations. J Submicrosc Cytol Pathol. 1997;29(1):19–28.
24. Barnhill RL, Busam KJ, Berwick M, Blessing K, Cochran AJ, Elder DE, Fandrey K, Karaoli T, White WL. Tumour vascularity is not a prognostic factor for cutaneous melanoma. Lancet. 1994;344(8931):1237–8.
25. Lugassy C, Bentolila LA, Wadehra M, Prakash R, Carmichael ST, Kleinman HK, Péault B, Larue L, Barnhill RL. Angiotropic malignant melanoma and extravascular migratory metastasis: description of 36 cases with emphasis on a new mechanism of tumour spread. Pathology. 2004;36(5):485.
26. Wilmott J, Haydu L, Bagot M, Zhang Y, Jakrot V, McCarthy S, Lugassy C, Thompson J, Scolyer R, Barnhill R. Angiotropism is an independent predictor of microscopic satellites in primary cutaneous melanoma. Histopathology. 2012;61(5):889.
27. Weis SM, Cheresh DA. Tumor angiogenesis: molecular pathways and therapeutic targets. Nat Med. 2011;17(11):1359–70.
28. De Palma M, Biziato D, Petrova TV. Microenvironmental regulation of tumour angiogenesis. Nat Rev Cancer. 2017;17(8):457–74.
29. Lugano R, Ramachandran M, Dimberg A. Tumor angiogenesis: causes, consequences, challenges and opportunities. Cell Mol Life Sci. 2020;77(9):1745.
30. Pepper MS. Role of the matrix metalloproteinase and plasminogen activator-plasmin systems in angiogenesis. Arterioscler Thromb Vasc Biol. 2001;21(7):1104–17.
31. Davis GE, et al. Regulation of tissue injury responses by the exposure of matricryptic sites within extracellular matrix molecules. Am J Pathol. 2000;156(5):1489.
32. Deryugina EI, Quigley JP. Pleiotropic roles of matrix metalloproteinases in tumor angiogenesis: contrasting, overlapping and compensatory functions. Biochim Biophys Acta. 2010;1803(1):103.
33. Sounni NE, Alexandra Paye LH, Noël A. MT-MMPS as regulators of vessel stability associated with angiogenesis. Front Pharmacol. 2011;2:2.
34. Milkiewicz M, et al. Regulators of angiogenesis and strategies for their therapeutic manipulation. Int J Biochem Cell Biol. 2006;38(3):333–57.
35. Folberg R, Maniotis AJ. Vasculogenic mimicry. APMIS. 2004;112(7–8):508–25.
36. Thompson WD, et al. Tumours acquire their vasculature by vessel incorporation, not vessel ingrowth. J Pathol. 1987;151(4):323–32.
37. Jain RK. Molecular regulation of vessel maturation. Nat Med. 2003;9(6):685–93.
38. Carmeliet P, Jain RK. Principles and mechanisms of vessel normalization for cancer and other angiogenic diseases. Nat Rev Drug Discov. 2011;10(6):417–27.
39. Shalaby F, et al. Failure of blood-Island formation and vasculogenesis in Flk-1-deficient mice. Nature. 1995;376(6535):62–6.
40. Roberts WG, Palade GE. Increased microvascular permeability and endothelial fenestration induced by vascular endothelial growth factor. J Cell Sci. 1995;108(6):2369.
41. Monsky WL, et al. Augmentation of transvascular transport of macromolecules and nanoparticles in tumors using vascular endothelial growth factor. Cancer Res. 1999;59(16):4129–35.
42. Weis SM, et al. Pathophysiological consequences of VEGF-induced vascular permeability. Nature. 2005;437:7058.
43. Gassmann P, Enns A, Haier J. Role of tumor cell adhesion and migration in organ-specific metastasis formation. Onkologie. 2004;27(6):577–82.
44. Valastyan S, Weinberg RA. Tumor metastasis: molecular insights and evolving paradigms. Cell. 2011;147(2):275–92.
45. Ly LV, et al. Intravascular presence of tumor cells as prognostic parameter in uveal melanoma: a 35-year survey. Invest Ophthalmol Vis Sci. 2010;51(2):658–65.
46. Gupta GP, et al. Mediators of vascular remodelling co-opted for sequential steps in lung metastasis. Nature. 2007;446(7137):765–70.
47. Holmgren L, O'Reilly MS, Folkman J. Dormancy of micrometastases: balanced proliferation and apoptosis in the presence of angiogenesis suppression. Nat Med. 1995;1(2):149–53.
48. Quintero-Fabián S, et al. Role of matrix metalloproteinases in angiogenesis and cancer. Front Oncol. 2019;9:9.
49. Grossniklaus HE, et al. Metastatic ocular melanoma to the liver exhibits infiltrative and nodular growth patterns. Hum Pathol. 2016;57:165–75.
50. Lai K, et al. Expression and distribution of MMPs and TIMPs in human uveal melanoma. Exp Eye Res. 2008;86(6):936–41.
51. Long H, Zhou B, Jiang FG. Expression of MMP-2 and MMP-9 in retinoblastoma and their significance. Int J Ophthalmol. 2011;4(5):489–91.
52. Bergers G, et al. Matrix metalloproteinase-9 triggers the angiogenic switch during carcinogenesis. Nat Cell Biol. 2000;2(10):737–44.
53. Kerbel RS, et al. Establishing a link between oncogenes and tumor angiogenesis. Mol Med. 1998;4(5):286–95.
54. Dvorak HF. Tumors: wounds that do not heal. Similarities between tumor stroma generation and wound healing. N Engl J Med. 1986;315(26):1650–9.
55. Ferrara N, Henzel WJ. Pituitary follicular cells secrete a novel heparin-binding growth factor specific for vascular endothelial cells. Biochem Biophys Res Commun. 1989;161(2):851.
56. Carmeliet P, et al. Abnormal blood vessel development and lethality in embryos lacking a single VEGF allele. Nature. 1996;380(6573):435–9.
57. Peak SJ, Levin VA. Role of bevacizumab therapy in the management of glioblastoma. Cancer management and research. Cancer Manag Res. 2010;2:97–104.
58. Ferrara N, et al. Angiogenesis as a therapeutic target. Nature. 2005;438(7070):967.
59. Ferrara N, et al. Molecular and biological properties of the vascular endothelial growth factor family of proteins. Endocr Rev. 1992;13(1):18–32.
60. Cao Y. Tumor angiogenesis and therapy. Biomed Pharmacother. 2005;59(Suppl 2):S340–3.
61. Ferrara N. Vascular endothelial growth factor: basic science and clinical progress. Endocr Rev. 2004;25(4):581–611.
62. Alon T, et al. Vascular endothelial growth factor acts as a survival factor for newly formed retinal vessels and has implications for retinopathy of prematurity. Nat Med. 1995;1(10):1024–8.
63. Young TL, et al. Histopathology and vascular endothelial growth factor in untreated and diode laser-treated retinopathy of prematurity. J AAPOS. 1997;1(2):105–10.
64. Adamis AP, Aiello LP, D'Amato RA. Angiogenesis and ophthalmic disease. Angiogenesis. 1999;3(1):9–14.
65. Neufeld G, et al. Vascular endothelial growth factor (VEGF) and its receptors. FASEB J. 1999;13(1):9–22.
66. Vincenti V, et al. Assignment of the vascular endothelial growth factor gene to human chromosome 6p21.3. Circulation. 1996;93(8):1493–5.
67. Houck KA, et al. The vascular endothelial growth factor family: identification of a fourth molecular species and characterization of alternative splicing of RNA. Mol Endocrinol. 1991;5(12):1806–14.

68. Shibuya M. Vascular endothelial growth factor (VEGF) and its receptor (VEGFR) signaling in angiogenesis: a crucial target for anti-and pro-Angiogenic therapies. Genes Cancer. 2011;2(12):1097.
69. Ferrara N, Gerber H-P, LeCouter J. The biology of VEGF and its receptors. Nat Med. 2003;9(6):669.
70. Matthews W, et al. A receptor tyrosine kinase cDNA isolated from a population of enriched primitive hematopoietic cells and exhibiting close genetic linkage to c-kit. Proc Natl Acad Sci USA. 1991;88(20):9026–30.
71. Verhoeff JJ, et al. Tumour control by whole brain irradiation of anti-VEGF-treated mice bearing intracerebral glioma. Eur J Cancer. 2009;45(17):3074–80.
72. Zagzag D, et al. Expression of hypoxia-inducible factor 1alpha in brain tumors: association with angiogenesis, invasion, and progression. Cancer. 2000;88(11):2606–18.
73. Harris AL. Hypoxia—a key regulatory factor in tumour growth. Nat Rev Cancer. 2002;2(1):38–47.
74. Iliopoulos O, et al. Negative regulation of hypoxia-inducible genes by the von Hippel-Lindau protein. Proc Natl Acad Sci USA. 1996;93(20):10595–9.
75. Javerzat S, Auguste P, Bikfalvi A. The role of fibroblast growth factors in vascular development. Trends Mol Med. 2002;8(10):483–9.
76. Ensoli B, et al. Synergy between basic fibroblast growth factor and HIV-1 tat protein in induction of Kaposi's sarcoma. Nature. 1994;371(6499):674–80.
77. Eklund L, Olsen BR. Tie receptors and their angiopoietin ligands are context-dependent regulators of vascular remodeling. Exp Cell Res. 2006;312(5):630–41.
78. Puri MC, et al. The receptor tyrosine kinase TIE is required for integrity and survival of vascular endothelial cells. EMBO J. 1995;14(23):5884–91.
79. Nagase H, Woessner JF Jr. Matrix metalloproteinases. J Biol Chem. 1999;274(31):21491–4.
80. Lee MH, Murphy G. Matrix metalloproteinases at a glance. J Cell Sci. 2004;117(Pt 18):4015–6.
81. Rundhaug JE. Matrix metalloproteinases and angiogenesis. J Cell Mol Med. 2005;9(2):267–85.
82. Brew K, Dinakarpandian D, Nagase H. Tissue inhibitors of metalloproteinases: evolution, structure and function. Biochim Biophys Acta. 2000;1477(1–2):267–83.
83. Cook KM, Figg WD. Angiogenesis inhibitors—current strategies and future prospects. CA Cancer J Clin. 2010;60(4):222.
84. Lawler J. Thrombospondin-1 as an endogenous inhibitor of angiogenesis and tumor growth. J Cell Mol Med. 2002;6(1):1.
85. Cao Y, Xue L. Angiostatin. Semin Thromb Hemost. 2004;30:1.
86. O'Reilly MS, et al. Angiostatin induces and sustains dormancy of human primary tumors in mice. Nat Med. 1996;2(6):689–92.
87. Andrawiss M, et al. Adenovirus-mediated gene transfer in canine eyes: a preclinical study for gene therapy of human uveal melanoma. J Gene Med. 2001;3(3):228–39.
88. Camphausen K, et al. Radiation therapy to a primary tumor accelerates metastatic growth in mice. Cancer Res. 2001;61(5):2207–11.
89. Apte RS, et al. Angiostatin produced by certain primary uveal melanoma cell lines impedes the development of liver metastases. Arch Ophthalmol. 2001;119(12):1805–9.
90. Wang H, et al. Combination of oncolytic adenovirus and endostatin inhibits human retinoblastoma in an in vivo mouse model. Int J Mol Med. 2013;31(2):377–85.
91. Sertie AL, et al. Collagen XVIII, containing an endogenous inhibitor of angiogenesis and tumor growth, plays a critical role in the maintenance of retinal structure and in neural tube closure (Knobloch syndrome). Hum Mol Genet. 2000;9(13):2051–8.
92. Noma H, et al. Regulation of angiogenesis in diabetic retinopathy: possible balance between vascular endothelial growth factor and endostatin. Arch Ophthalmol. 2002;120(8):1075–80.
93. Thomas JP, et al. Phase I pharmacokinetic and pharmacodynamic study of recombinant human endostatin in patients with advanced solid tumors. J Clin Oncol. 2003;21(2):223–31.
94. Herbst RS, et al. Phase I study of recombinant human endostatin in patients with advanced solid tumors. J Clin Oncol. 2002;20(18):3792–803.
95. Jain RK, et al. Lessons from phase III clinical trials on anti-VEGF therapy for cancer. Nat Clin Pract Oncol. 2006;3(1):24–40.
96. Jayson GC, et al. Antiangiogenic therapy in oncology: current status and future directions. Lancet. 2016;388(10043):518–29.
97. Willett CG, et al. Direct evidence that the VEGF-specific antibody bevacizumab has antivascular effects in human rectal cancer. Nat Med. 2004;10(2):145–7.
98. Piperno-Neumann S, et al. Phase II trial of bevacizumab in combination with Temozolomide as first-line treatment in patients with metastatic uveal melanoma. Oncologist. 2016;21(3):281–2.
99. Rini BI, Sosman JA, Motzer RJ. Therapy targeted at vascular endothelial growth factor in metastatic renal cell carcinoma: biology, clinical results and future development. BJU Int. 2005;96(3):286–90.
100. Pirrotta MT, Bernardeschi P, Fiorentini G. Targeted-therapy in advanced renal cell carcinoma. Curr Med Chem. 2011;18(11):1651–7.
101. Kuusk T, et al. Antiangiogenic therapy combined with immune checkpoint blockade in renal cancer. Angiogenesis. 2017;20(2):205–15.
102. Jain RK. Normalization of tumor vasculature: an emerging concept in antiangiogenic therapy. Science. 2005;307(5706):58–62.
103. El Filali M, et al. Bevacizumab and intraocular tumors: an intriguing paradox. Mol Vis. 2012;18:2454–67.
104. Reich SJ, et al. Small interfering RNA (siRNA) targeting VEGF effectively inhibits ocular neovascularization in a mouse model. Mol Vis. 2003;9:210–6.
105. Takeda A, et al. Suppression of experimental choroidal neovascularization utilizing KDR selective receptor tyrosine kinase inhibitor. Graefes Arch Clin Exp Ophthalmol. 2003;241(9):765–72.
106. Castet F, Garcia-Mulero S, Sanz-Pamplona R, et al. Uveal melanoma, angiogenesis and immunotherapy, is there any hope? Cancers. 2019;11(6):834.
107. Sabbah M, et al. RTK inhibitors in melanoma: from bench to bedside. Cancers. 2021;13(7):1685.
108. Burnier MN, et al. Retinoblastoma. The relationship of proliferating cells to blood vessels. Invest Ophthalmol Vis Sci. 1990;31(10):2037–40.
109. Marback EF, et al. Tumour angiogenesis as a prognostic factor for disease dissemination in retinoblastoma. Br J Ophthalmol. 2003;87(10):1224–8.
110. Kvanta A, Steen B, Seregard S. Expression of vascular endothelial growth factor (VEGF) in retinoblastoma but not in posterior uveal melanoma. Exp Eye Res. 1996;63(5):511–8.
111. Munier FL, et al. Intravitreal chemotherapy for vitreous disease in retinoblastoma revisited: from prohibition to conditional indications. Br J Ophthalmol. 2012;96(8):1078–83.
112. Munier FL, et al. Profiling safety of intravitreal injections for retinoblastoma using an anti-reflux procedure and sterilisation of the needle track. Br J Ophthalmol. 2012;96(8):1084–7.
113. Conway RM, et al. Retinoblastoma: animal models. Ophthalmol Clin N Am. 2005;18(1):25–39. vii
114. Escalona-Benz E, et al. Combretastatin A-4 prodrug in the treatment of a murine model of retinoblastoma. Invest Ophthalmol Vis Sci. 2005;46(1):8–11.
115. Jockovich ME, et al. Mechanism of retinoblastoma tumor cell death after focal chemotherapy, radiation, and vascular targeting therapy in a mouse model. Invest Ophthalmol Vis Sci. 2007;48(12):5371–6.

116. Houston SK, et al. Novel retinoblastoma treatment avoids chemotherapy: the effect of optimally timed combination therapy with angiogenic and glycolytic inhibitors on LH(BETA)T(AG) retinoblastoma tumors. Clin Ophthalmol. 2011;5:129–37.
117. Lee SY, et al. Inhibitory effect of bevacizumab on the angiogenesis and growth of retinoblastoma. Arch Ophthalmol. 2008;126(7):953–8.
118. Heo JW, et al. Inhibitory activity of bevacizumab to differentiation of retinoblastoma cells. PLoS One. 2012;7(3):e33456.
119. Folberg R, Hendrix MJ, Maniotis AJ. Vasculogenic mimicry and tumor angiogenesis. Am J Pathol. 2000;156(2):361–81.
120. Bajcsy P, et al. Three-dimensional volume reconstruction of extracellular matrix proteins in uveal melanoma from fluorescent confocal laser scanning microscope images. J Microsc. 2006;221(Pt 1):30–45.
121. Sallet G, et al. Indocyanine green angiography of choroidal tumors. Graefes Arch Clin Exp Ophthalmol. 1995;233(11):677–89.
122. Ossoinig KC. Standardized echography: basic principles, clinical applications, and results. Int Ophthalmol Clin. 1979;19(4):127–210.
123. Mueller AJ, et al. Complex microcirculation patterns detected by confocal indocyanine green angiography predict time to growth of small choroidal melanocytic tumors: MuSIC report II. Ophthalmology. 2002;109(12):2207–14.
124. Singh AD, et al. Small choroidal melanocytic lesions: features predictive of growth. Ophthalmology. 2006;113(6):1032–9.
125. Mueller AJ, et al. Imaging the microvasculature of choroidal melanomas with confocal indocyanine green scanning laser ophthalmoscopy. Arch Ophthalmol. 1998;116(1):31–9.
126. Abdel-Rahman MH, et al. Expression of vascular endothelial growth factor in uveal melanoma is independent of 6p21-region copy number. Clin Cancer Res. 2005;11(1):73–8.
127. Boyd SR, et al. Uveal melanomas express vascular endothelial growth factor and basic fibroblast growth factor and support endothelial cell growth. Br J Ophthalmol. 2002;86(4):440–7.
128. Sheidow TG, et al. Expression of vascular endothelial growth factor in uveal melanoma and its correlation with metastasis. Br J Ophthalmol. 2000;84(7):750–6.
129. Kariola R, et al. APC and beta-catenin protein expression patterns in HNPCC-related endometrial and colorectal cancers. Fam Cancer. 2005;4(2):187–90.
130. Boyd SR, et al. Vascular endothelial growth factor is elevated in ocular fluids of eyes harbouring uveal melanoma: identification of a potential therapeutic window. Br J Ophthalmol. 2002;86(4):448–52.
131. Sudaka A, et al. Combination of bevacizumab and irradiation on uveal melanoma: an in vitro and in vivo preclinical study. Investig New Drugs. 2013;31(1):59–65.
132. Lattanzio L, et al. Role of IL-8 induced angiogenesis in uveal melanoma. Investig New Drugs. 2013;31(5):1107–14.
133. Dunavoelgyi R, et al. Intraocular activation of angiogenic and inflammatory pathways in uveal melanoma. Retina. 2012;32(7):1373–84.
134. Nagarkatti-Gude N, et al. Cytokines and chemokines in the vitreous fluid of eyes with uveal melanoma. Invest Ophthalmol Vis Sci. 2012;53(11):6748–55.
135. Kujala E, Makitie T, Kivela T. Very long-term prognosis of patients with malignant uveal melanoma. Invest Ophthalmol Vis Sci. 2003;44(11):4651–9.
136. O'Reilly MS. Angiostatin: an endogenous inhibitor of angiogenesis and of tumor growth. EXS. 1997;79:273–94.
137. O'Reilly MS, et al. Endostatin: an endogenous inhibitor of angiogenesis and tumor growth. Cell. 1997;88(2):277–85.
138. O'Reilly MS, et al. Angiostatin: a novel angiogenesis inhibitor that mediates the suppression of metastases by a Lewis lung carcinoma. Cell. 1994;79(2):315–28.
139. Zimmerman LE, McLean IW, Foster WD. Does enucleation of the eye containing a malignant melanoma prevent or accelerate the dissemination of tumour cells. Br J Ophthalmol. 1978;62(6):420–5.
140. Singh AD, et al. The Zimmerman-McLean-Foster hypothesis: 25 years later. Br J Ophthalmol. 2004;88(7):962–7.
141. Eskelin S, et al. Tumor doubling times in metastatic malignant melanoma of the uvea: tumor progression before and after treatment. Ophthalmology. 2000;107(8):1443–9.
142. Singh AD. Uveal melanoma: implications of tumor doubling time. Ophthalmology. 2001;108(5):829–31.
143. Clark AF, et al. Inhibition of intraocular tumor growth by topical application of the angiostatic steroid anecortave acetate. Invest Ophthalmol Vis Sci. 1999;40(9):2158–62.
144. Lima BR, Schoenfield LR, Singh AD. The impact of intravitreal bevacizumab therapy on choroidal melanoma. Am J Ophthalmol. 2011;151(2):323–8 e2.
145. Francis JH, et al. Growth of uveal melanoma following intravitreal bevacizumab. Ocul Oncol Pathol. 2017;3(2):117–21.
146. Cavalcante ML, et al. Treatment of vascular activity secondary to atypical choroidal nevus using intravitreal bevacizumab. Clin Ophthalmol. 2014;8:1377–82.
147. Archer DB, Amoaku WM, Gardiner TA. Radiation retinopathy—clinical, histopathological, ultrastructural and experimental correlations. Eye (Lond). 1991;5(Pt 2):239–51.
148. Horgan N, et al. Classification and treatment of radiation maculopathy. Curr Opin Ophthalmol. 2010;21(3):233–8.
149. McCannel TA, et al. New ultra-wide-field angiographic grading scheme for radiation retinopathy after Iodine-125 brachytherapy for uveal melanoma. Retina. 2018;38(12):2415–21.
150. Monroe AT, et al. Preventing radiation retinopathy with hyperfractionation. Int J Radiat Oncol Biol Phys. 2005;61(3):856–64.
151. Gillies MC. Regulators of vascular permeability: potential sites for intervention in the treatment of macular edema. Doc Ophthalmol. 1999;97(3–4):251–60.
152. Bakri SJ, Larson TA. The variable efficacy of intravitreal bevacizumab and triamcinolone acetonide for cystoid macular edema due to radiation retinopathy. Semin Ophthalmol. 2015;30(4):276–80.
153. Finger PT. Radiation retinopathy is treatable with anti-vascular endothelial growth factor bevacizumab (Avastin). Int J Radiat Oncol Biol Phys. 2008;70(4):974–7.
154. Fallico M, et al. Intravitreal aflibercept for the treatment of radiation-induced macular edema after ruthenium 106 plaque radiotherapy for choroidal melanoma. Graefes Arch Clin Exp Ophthalmol. 2019;257(7):1547–54.
155. Finger PT, Chin KJ, Semenova EA. Intravitreal anti-VEGF therapy for macular radiation retinopathy: a 10-year study. Eur J Ophthalmol. 2016;26(1):60–6.
156. Jermak CM, et al. Triamcinolone acetonide in ocular therapeutics. Surv Ophthalmol. 2007;52(5):503–22.
157. Pooprasert P, Young-Zvandasara T, Al-Bermani A. Radiation retinopathy treated successfully with aflibercept. BMJ Case Rep. 2017;2017:bcr2017220744.
158. Seibel I, et al. Influence of Ranibizumab versus laser photocoagulation on radiation retinopathy (RadiRet)—a prospective randomized controlled trial. Graefes Arch Clin Exp Ophthalmol. 2020;258(4):869–78.
159. Bui KM, Chow CC, Mieler WF. Treatment of recalcitrant radiation maculopathy using intravitreal dexamethasone (Ozurdex) implant. Retin Cases Brief Rep. 2014;8(3):167–70.
160. Caminal JM, et al. Intravitreal dexamethasone implant for radiation maculopathy secondary to plaque brachytherapy in choroidal melanoma. Retina. 2015;35(9):1890–7.
161. Koc I, et al. Intravitreal dexamethasone (OZURDEX) implant for radiation maculopathy secondary to stereotactic radiotherapy for posterior uveal melanoma. Retin Cases Brief Rep. 2017;13:352.

162. Tarmann L, et al. Ozurdex((R)) reduces the retinal thickness in radiation maculopathy refractory to bevacizumab. Acta Ophthalmol. 2014;92(8):e694–6.
163. Singh AD, Borden EC. Metastatic uveal melanoma. Ophthalmol Clin N Am. 2005;18(1):143–50. ix.
164. Triozzi PL, Singh AD. Adjuvant therapy of uveal melanoma: current status. Ocul Oncol Pathol. 2014;1(1):54–62.
165. Bhatia S, et al. Phase II trial of sorafenib in combination with carboplatin and paclitaxel in patients with metastatic uveal melanoma: SWOG S0512. PLoS One. 2012;7(11):e48787.
166. Mouriaux F, et al. Sorafenib in metastatic uveal melanoma: efficacy, toxicity and health-related quality of life in a multicentre phase II study. Br J Cancer. 2016;115(1):20–4.
167. Niederkorn A, et al. Response of patients with metastatic uveal melanoma to combined treatment with fotemustine and sorafenib. Acta Ophthalmol. 2014;92(8):e696–7.
168. Mahipal A, et al. A pilot study of sunitinib malate in patients with metastatic uveal melanoma. Melanoma Res. 2012;22(6):440–6.
169. Tarhini AA, et al. Aflibercept (VEGF trap) in inoperable stage III or stage iv melanoma of cutaneous or uveal origin. Clin Cancer Res. 2011;17(20):6574–81.
170. Carvajal RD, et al. Selumetinib in combination with Dacarbazine in patients with metastatic uveal melanoma: a phase III, multicenter, randomized trial (SUMIT). J Clin Oncol. 2018;36(12):1232–9.
171. Carvajal RD, et al. Study design and rationale for a randomised, placebo-controlled, double-blind study to assess the efficacy of selumetinib (AZD6244; ARRY-142886) in combination with dacarbazine in patients with metastatic uveal melanoma (SUMIT). BMC Cancer. 2015;15:467.
172. Carvajal RD, et al. Effect of selumetinib vs chemotherapy on progression-free survival in uveal melanoma: a randomized clinical trial. JAMA. 2014;311(23):2397–405.
173. Afzal MZ, Mabaera R, Shirai K. Metastatic uveal melanoma showing durable response to anti-CTLA-4 and anti-PD-1 combination therapy after experiencing progression on anti-PD-1 therapy alone. J Immunother Cancer. 2018;6(1):13.
174. Algazi AP, et al. Clinical outcomes in metastatic uveal melanoma treated with PD-1 and PD-L1 antibodies. Cancer. 2016;122(21):3344–53.
175. Bender C, et al. Anti-PD-1 antibodies in metastatic uveal melanoma: a treatment option? Cancer Med. 2017;6(7):1581–6.
176. Heppt MV, et al. Prognostic factors and outcomes in metastatic uveal melanoma treated with programmed cell death-1 or combined PD-1/cytotoxic T-lymphocyte antigen-4 inhibition. Eur J Cancer. 2017;82:56–65.
177. Heppt MV, et al. Immune checkpoint blockade for unresectable or metastatic uveal melanoma: a systematic review. Cancer Treat Rev. 2017;60:44–52.
178. Jindal V. Role of immune checkpoint inhibitors and novel immunotherapies in uveal melanoma. Chin Clin Oncol. 2018;7(1):8.
179. Komatsubara KM, Carvajal RD. Immunotherapy for the treatment of uveal melanoma: current status and emerging therapies. Curr Oncol Rep. 2017;19(7):45.
180. Juhlin CC. Challenges in Paragangliomas and Pheochromocytomas: from histology to molecular immunohistochemistry. Endocr Pathol. 2021;32(2):228–44.
181. Chan CC, et al. VHL gene deletion and enhanced VEGF gene expression detected in the stromal cells of retinal angioma. Arch Ophthalmol. 1999;117(5):625–30.
182. Jonasch E, et al. Belzutifan for renal cell carcinoma in von Hippel-Lindau disease. N Engl J Med. 2021;385(22):2036–46.
183. Aiello LP, et al. Rapid and durable recovery of visual function in a patient with von hippel-Lindau syndrome after systemic therapy with vascular endothelial growth factor receptor inhibitor su5416. Ophthalmology. 2002;109(9):1745–51.
184. Wackernagel W, et al. von Hippel-Lindau disease: treatment of retinal haemangioblastomas by targeted therapy with systemic bevacizumab. Acta Ophthalmol. 2010;88(7):e271–2.
185. Girmens JF, et al. Treatment of von Hippel-Lindau retinal hemangioblastoma by the vascular endothelial growth factor receptor inhibitor SU5416 is more effective for associated macular edema than for hemangioblastomas. Am J Ophthalmol. 2003;136(1):194–6.
186. Ercanbrack CW, et al. Belzutifan-induced regression of retinal capillary hemangioblastoma: a case-series. Am J Ophthalmol Case Rep. 2024;33:102011.
187. Lee GA, Hirst LW. Ocular surface squamous neoplasia. Surv Ophthalmol. 1995;39(6):429–50.
188. Kestelyn P. Ocular problems in AIDS. Int Ophthalmol. 1990;14(3):165–72.
189. Fraunfelder FT, Wingfield D. Management of intraepithelial conjunctival tumors and squamous cell carcinomas. Am J Ophthalmol. 1983;95(3):359–63.
190. Frucht-Pery J, Rozenman Y, Pe'er J. Topical mitomycin-C for partially excised conjunctival squamous cell carcinoma. Ophthalmology. 2002;109(3):548–52.
191. Vann RR, Karp CL. Perilesional and topical interferon alfa-2b for conjunctival and corneal neoplasia. Ophthalmology. 1999;106(1):91–7.
192. Esquenazi S, Fry CL, Holley E. Treatment of biopsy proved conjunctival intraepithelial neoplasia with topical interferon alfa-2b. Br J Ophthalmol. 2005;89(9):1221.
193. Jonasch E, Haluska FG. Interferon in oncological practice: review of interferon biology, clinical applications, and toxicities. Oncologist. 2001;6(1):34–55.
194. Finger PT, Chin KJ. Refractory squamous cell carcinoma of the conjunctiva treated with subconjunctival ranibizumab (Lucentis): a two-year study. Ophthalmic Plast Reconstr Surg. 2012;28(2):85–9.

Immunology of Ocular Tumors

7

Martine J. Jager, Sen Ma, Elisabet de Los Pinos, and Inge H. G. Bronkhorst

7.1 Introduction

Understanding the fundamental immunological processes that play a role in tumor development should help us to better understand how to develop safe and efficient immune intervention strategies against ocular tumors and their metastases. Antitumor immune responses by T cells and antibodies may limit tumor growth, while on the other hand, the presence of tumor-infiltrating leukocytes may lead to the production of cytokines that stimulate tumor growth. In addition, environmental factors may have an influence on the tumor, as may aging, because aging is associated with a phenomenon known as para-inflammation, which is a local increase in infiltrating leukocytes and cytokines.

7.2 Innate and Specific Immune Responses

One can differentiate between basic general immune responses and induced specific ones. The most primitive and direct defense against microbes, trauma, or abnormal cells is the innate immune response. As soon as "danger" is encountered, granulocytes and macrophages are alerted and will try to inactivate this danger. If this response is inadequate, antigen-presenting cells will pick up parts of the microbes or abnormal cells and take them to the regional lymph node. Proteins of the microbe or the abnormal cells are degraded into peptides, which will be presented by the antigen-presenting cell to T lymphocytes. If the appropriate T cell encounters its own antigen, it will proliferate and become an activated T cell. There are different kinds of T cells, such as T cells that can kill (cytotoxic T cells, CTLs), those that can cause local inflammation (delayed-type hypersensitivity T cells), and regulatory T cells that are able to suppress other T cells.

Furthermore, T cells are needed to stimulate B cells to begin the production of specific antibodies. Finally, the different T and B cells will try to deal with the aggressor, and the end result is usually that the body takes care of the "danger." If not, the lack of an effective response may lead to the death of the host.

7.3 Immunological Escape

It appears that the immune responses that do exist are limited in their effectiveness inside the eye, which is known to be a relatively immunologically-privileged site. This implies that similar to the brain and the placenta, many immunological reactions are actively or passively downregulated, leading to the suppression of effective immunity. The development of effective antitumor antibodies or cytotoxic T lymphocytes (CTLs) is halted, as well as their activity. It is even possible that the presence of the tumor in the eye will induce systemic tolerance, thereby inhibiting effective immune responses against metastases. The presence of regulatory T cells may suppress an effective immune response. This is observed when antigens are injected into the anterior chamber of the eye of a mouse, which leads to the induction of systemic immune suppression known as anterior chamber-associated

M. J. Jager (✉)
Department of Ophthalmology, Leiden University Medical Center (LUMC), Leiden, The Netherlands

Department of Ophthalmology, University of Cologne, Cologne, Germany
e-mail: m.j.jager@lumc.nl

S. Ma
Department of Ophthalmology, Leiden University Medical Center (LUMC), Leiden, The Netherlands

E. de Los Pinos
Ura Biosciences, Cambridge, MA, USA

I. H. G. Bronkhorst
Department of Ophthalmology, Leiden University Medical Center (LUMC), Leiden, The Netherlands

Aura Biosciences, Cambridge, MA, USA

Department of Ophthalmology, Jeroen Bosch Hospital, 's-Hertogenbosch, The Netherlands

© The Author(s), under exclusive license to Springer Nature Switzerland AG 2025

A. D. Singh, B. E. Damato (eds.), *Clinical Ophthalmic Oncology*, https://doi.org/10.1007/978-3-031-75907-9_7

immune deviation (ACAID) [1]. ACAID is characterized by the presence of regulatory splenic T cells that prevent the development of delayed-type hypersensitivity and prevent the maturation and differentiation of precursor CTLs [2, 3]. In experimental animal models, it has been shown that tumor cells that are rejected when placed in the skin will grow when placed inside the eye.

7.4 Immunological Aspects of Uveal Melanoma

As much is known about the immunology of uveal melanoma (UM), this chapter will illustrate the role of immune responses specifically in that malignancy. For UM, an age-related influence can clearly be identified, as this malignancy is typically a disease of middle-aged people. One of the common early changes that lead to the development of UM is a mutation in either the GNAQ or GNA11 gene in a melanocyte. This stimulates cell proliferation [4]. In addition to the occurrence of a mutation in a melanocyte, the soil for growth should be fertile, and one of the important parameters may be the local inflammation that occurs in the eye and other parts of the body during aging [5]. An increase in pro-angiogenic macrophages may stimulate blood vessel formation. This increased blood vessel development may be the environmental factor that helps in the development of the intraocular tumor, leading to a clinically significant lesion [6]. Finally, a specific change is associated with metastasis formation, which is the loss of one chromosome 3. This genetic aberration together with a mutation in the BAP1 gene on the remaining chromosome 3 leads to a significant change in gene expression, which is associated with metastatic spread [7].

7.4.1 Immune Responses against UM in Humans

The eye is known as one of the immune-privileged organs. Even though intraocular tumors are partly shielded from immunological attack due to this immune-privileged environment, this does not prevent their detection by the immune system. Still, UM contains all kinds of tumor-infiltrating leukocytes (TIL), as demonstrated by immunohistochemical analysis (see below).

Clinical observations support the fact that an active immune system should be able to attack the intraocular tumor. Spontaneous eradication of UM has been described in some patients [8, 9]. Serum antibodies against melanoma-associated antigens were detected in 16 out of 22 patients [10]. Also, positive cutaneous delayed-type hypersensitivity reactions against melanoma-associated antigens occur in patients with UM, and the blood of UM patients often contains lymphocytes that are cytotoxic to uveal and skin melanoma cells [11]. Melanoma-specific $CD8^+$ T cells from patients with UM were able to recognize autologous and allogeneic uvea melanoma cells, indicating that tumor-associated antigens are shared between the various uvea melanoma cell lines [12, 13]. Unfortunately, these immune cells are unable to reject the intraocular tumor in vivo.

A variety of cutaneous melanoma antigens recognized by anti-melanoma CTL have been identified [14]. Similar to cutaneous melanomas, UMs have been shown to be antigenic: UM expresses tyrosinase, MART-1, and GP100 [15], while discussion exists regarding the expression of MAGE antigens in primary and metastatic UM [16]. UM patients have precursor lymphocytes that can recognize and kill target cells presenting peptides of these antigens [17]. Another interesting antigen is PRAME, which is especially expressed on high-risk UM as well as its metastases [18, 19]. It is a fine target for T cells.

7.4.2 HLA Antigen Expression

Tumor antigens can be recognized by CD8+ T cells in an MHC class I-restricted manner. In humans, the MHC complex is referred to as the human leukocyte antigen (HLA) system. Alterations in HLA expression levels will have serious consequences for the host defense against tumor growth. In many tumors, including cutaneous melanoma and UM, expression of HLA class I varies between tumors [20–22]. The absence of allele-specific HLA class I molecules may prevent recognition of the tumor cells by cytotoxic T cells. While HLA class I loss is associated with a worse patient survival in cutaneous melanoma, in contrast, in UM, a low HLA class I expression is correlated with better patient survival [20, 23, 24]. Similarly, the absence of HLA class II is correlated with a better survival of patients with UM [23, 24]. A lack of expression of HLA class I on UM causes the cells to become more susceptible to natural killer (NK) cell-mediated lysis in vitro [25]. TGFβ has been shown to decrease HLA expression [26]. Although NK cell-mediated lysis of UM is inhibited in the eye by macrophage migration inhibitory factor (MIF), it has been suggested that melanoma cells that disseminate from the eye into the liver are at risk of surveillance by NK cells [27, 28]. Progressive intraocular tumor growth and an increase in hepatic metastases were observed in experimental animal models deficient in NK cells [25, 29].

7.4.3 Leukocyte Infiltrate

Various tumor-infiltrating leukocytes, such as CD3+, CD8+, and CD4+ T cells, are present in UM [21, 30]. Previous studies did not always clearly reveal the relevance of these TIL in UM, as the presence of these cells was considered either favorable or unfavorable for the survival of patients [31, 32]. Recent studies analyzed the presence of different cell subtypes, including Foxp3+ regulatory T cells (Tregs); the majority of T cells were CD8 positive, but CD4+ and Foxp3+ cells were usually also present, and it was noticed that the presence of TILs was highly variable between tumors. A high number of Tregs was linked to a bad prognosis [33, 34]. The presence of any of the T cell types was increased in tumors with a prognostically bad loss of one chromosome 3 [35].

In addition to T cells, infiltrating leukocytes may be macrophages: the presence of high numbers of tumor-infiltrating macrophages within the primary ocular melanoma is associated with the loss of one chromosome 3 and increased mortality [35, 36]. Macrophages can belong to different subtypes: the M1 macrophages that play a role in antigen presentation and the M2 macrophages that have a pro-angiogenic function. The majority of intra-tumoral macrophages in UM are of the pro-angiogenic M2 type, which supports the prior finding of an association between the number of infiltrating macrophages and the presence of blood vessels in UM [37, 38]. T cell density correlated with the number of infiltrating

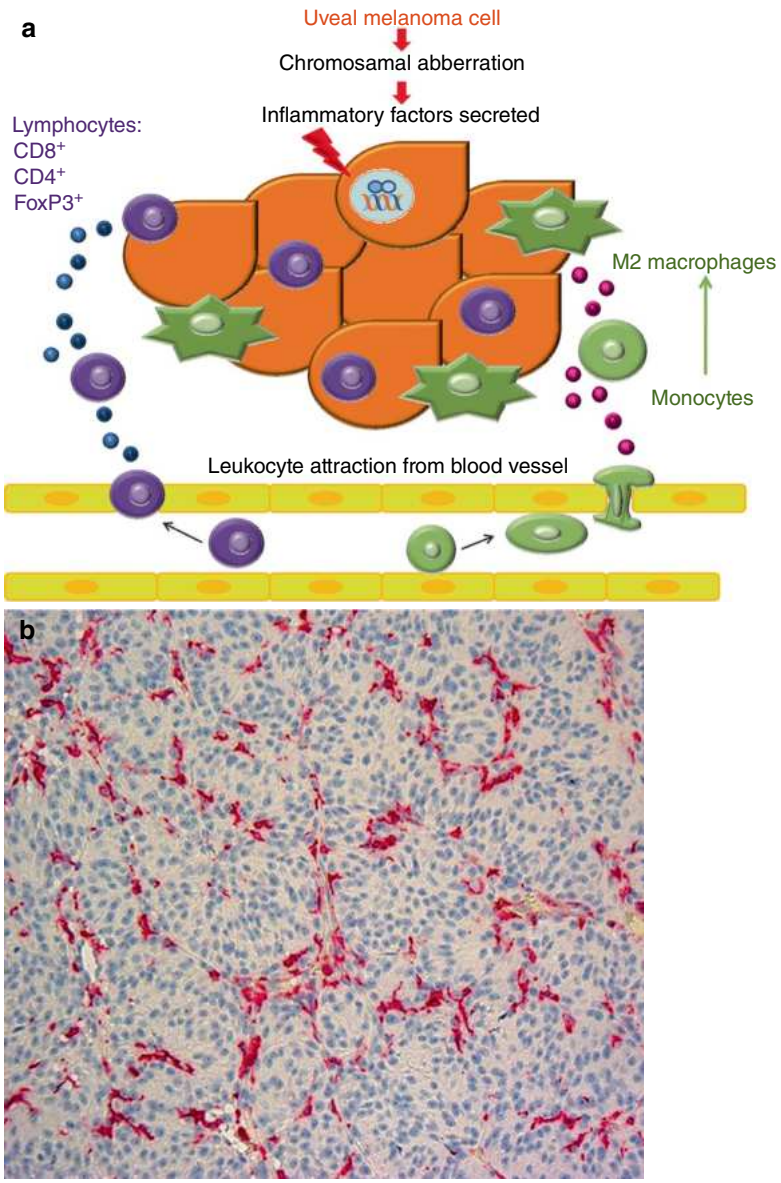

Fig. 7.1 Cancer-related inflammation in uveal melanoma. Inflammation is proposed to drive some cancers to more aggressive phenotypes. Studies show the presence of CD8+, CD4+, and FoxP3+ Treg cells in uveal melanoma, suggesting that they can induce a local immune response at the tumor site (**a**). Tumor-associated macrophages could also play an important role in inhibiting immune responses and angiogenesis, which has been linked to cancer development and progression (**b**)

macrophages, especially the number of M2 macrophages [33]. It has been suggested that Tregs may support the differentiation of monocytes to tumor-promoting M2 macrophages [39]. The strong correlation between tumor cell type and amount of infiltrate indicates that basic tumor characteristics must determine the influx of immune cells (Fig. 7.1) [40]. The amounts of different types of TIL were also correlated to the HLA class I and II expression levels, in keeping with the idea of a tumor-encompassing inflammatory phenotype [27]. A phenotype-genotype comparison showed that an early amplification of chromosome 8q was associated with an influx of macrophages, while loss of expression of chromosome 3/BAP1 resulted in a further increase in macrophages and an influx of T cells [41].

7.4.4 Previously Irradiated Tumors

As irradiation of a tumor may affect tumor characteristics and potentially induce an increased immune cell infiltration, immunohistochemistry to determine the amount of infiltrate was performed on a series of 46 UMs [42]. These UMs were enucleated after previous irradiation had taken place, and a complication that necessitated enucleation had occurred. This could be a lack of responsiveness, tumor recurrence, or, e.g., the development of untreatable glaucoma. Similar to previous studies on nonirradiated UM-containing eyes, a wide variation in the numbers of TIL was observed. Irradiated tumors did not contain more macrophages than nonirradiated UM, but the numbers of lymphocytes were significantly higher in previously irradiated eyes. This was true for CD3, CD4, CD8, as well as $Foxp3^+$ cells and independent of the reason for enucleation. Tumors containing epithelioid cells showed significantly more lymphoid infiltration.

These observations show an association between the presence of an infiltrate and a bad prognosis in irradiated and nonirradiated tumors. How the innate immune response is related to a worse prognosis is as yet poorly understood, but it may be that the influence of the intraocular environment is such that it leads to systemic immunosuppression instead of immune stimulation; this may have important implications for prospective immunotherapy, as discussed below.

7.4.5 Immunotherapy

Tumors that activate innate immune signals and recruit T cells also show high expression of selected immune suppressive pathways. This suggests that promoting better innate immune activation, facilitating T cell trafficking, and blocking specific negative regulatory pathways could improve immune-mediated rejection of UM. At present, no useful adjuvant or systemic treatment is available. Encouragingly, many drugs that target cancer-related inflammation are currently in clinical trials for other diseases. Obstacles to such studies include the rarity of UM, and clinical trials have only attracted limited numbers of patients with different characteristics (often unresectable or metastatic UM patients) in phase I or II trials [43]. Immune-based therapies have a long history in the treatment of cutaneous melanoma [44], and sometimes, UM patients are included. Some new immunotherapeutic approaches in (ongoing) trials in UM patients include fully human monoclonal anti-cytotoxic T lymphocyte antigen-4 (CTLA4) antibody (ipilimumab), anti-PD1 (nivolumab and pembrozilumab), anti-programmed death-ligand 1 (PD-L1) (atezolizumab), IFN-alpha 2b, and a dendritic cell vaccine therapy program. Gezgin et al. [45] tried to isolate and expand TIL from enucleated primary UM. TIL grew out when they were separated from their tumor environment. In 8 out of 17 tumors (47%), T cells were obtained that were responsive to their own UM cells. These results indicate that the tumor microenvironment contains cells or produces cytokines that inhibit T cells from responding. RNA-seq analysis showed that many of the tumors expressed immunomodulatory molecules, such as CTLA-4, galectin-3, PD-L1, lymphocyte activating 3 (LAG3), and indoleamine 2,3-dioxygenase 1.

7.4.5.1 Ipilimumab

The monoclonal antibody ipilimumab activates the body's immune system to fight cancer by blocking a protein known as fully human anti-CTLA-4. CTLA-4 is a molecule in T cells known to play a critical role in regulating immune responses. CTLA-4 suppresses the immune system's response to disease, so blocking its activity stimulates the immune system to fight melanoma. In 2010, Hodi et al. [46] reported the first study using ipilimumab with or without vaccination with anti-gp100 in 676 patients with unresectable stage III or IV cutaneous melanoma. Vaccination alone led to a median overall survival of 6.4 months, while the groups with ipilimumab alone or ipilimumab plus anti-gp100 had a median survival of 10.1 and 10.0 months, respectively. The assessment of the activity and safety of ipilimumab in a small group of 13 patients with UM showed overall no objective response [47]; the median survival was 36 weeks (1 year up to 172 weeks), with two patients developing stable disease, and with third patient achieving stable disease after initial progressive disease. Further studies have not shown any improvement in results [48].

7.4.5.2 Programmed Death-Ligand 1

Cell membrane-bound molecule PD-L1 is a component of the immune suppression by the tumor microenvironment. It may contribute to the tumor's capacity to evade immune elimination, induced by IFN-γ and by suppressing IL-2 production [49]. Interaction of PD-1 with PD-L1 downregulates T cell proliferation and cytokine production and induces T cell apoptosis, thereby promoting UM's escape from

T cell-mediated immune surveillance. The immunological approach by selective blockade of the immunological synapse using anti-PD-1 or anti-PD-L1 has been studied in UM, but similar to ipilimumab, hardly any successes have been achieved with other ICIs [48]. A great problem is the autoimmune diseases that are a side effect of de-blocking immune checkpoints. For the eye, orbital inflammation, tear gland disease leading to dry eye, conjunctivitis, keratitis, and uveitis are well-known complications.

7.4.5.3 Tebentafusp

A new phase in the treatment of UM arrived with the development of tebentafusp. Tebentafusp is a monoclonal T cell receptor that targets, on the one hand, glycoprotein 100, a melanocyte antigen, and on the other hand, anti-CD3. It needs to bind to an HLA-A2 molecule on the surface of a UM cell and then activates T cells to kill the UM cell. Compared to treatment with either pembrolizumab, ipilimumab, or dacarbazine, tebentafusp improved one-year overall and 6-month-progression-free survival [50]. While these early results have been confirmed, it is not a cure [51]. In addition, this treatment is only available for HLA-A2 positive patients, which constitute around 50% of Caucasians [52] .

7.4.5.4 Interferon-Alpha 2b

Another experience was reported with adjuvant IFN-alpha 2b [53]. Among 39 patients, serious side effects (e.g., leucopenia, thrombopenia) were seen, and the initial dose had to be reduced or therapy had to be withdrawn. Neither a univariate approach nor a multivariate approach could show a protective effect of interferon treatment on survival.

7.4.5.5 Dendritic Cell Therapy

Dendritic cell therapy (NCT00929019) may be used as an immunological adjuvant following local therapy (enucleation or irradiation). This immune vaccine trial has already shown promising results in cutaneous melanoma patients [54]. Based on tumor-specific genetic changes in the loss of chromosome 3, high-risk patients can easily be selected at an early stage in order to eliminate circulating tumor cells and micrometastatic lesions. Patients are immunized by their own dendritic cells, which stimulate T cells to detect remaining tumor cells and metastases. Tumor cell destruction is initiated by presenting tumor particles to cytotoxic T cells. In this way, one hopes to induce a specific and long-lasting immunity to prevent recurrent disease. One study showed stabilization of metastases in some UM patients [55] .

7.4.6 Immune-Related Response to Therapy

In those studies, besides survival, there is a particular focus on immune-related responses and adverse events, and sometimes, absolute lymphocyte counts are also evaluated. For example, a regressing lesion in one cutaneous melanoma patient revealed a significantly increased and selective $CD8^+$ T cell infiltrate and an acute decline in $CD3^+$ T cells following anti-PD-1 therapy [56]. In light of these observations, it is interesting to speculate that the therapy may cause redistribution of lymphocyte subsets from the blood into tumor and tissue sites (of course, validation has to be performed on larger numbers).

In other UM studies, which were initiated to inhibit tumor cell growth, not much is documented about the immunological effects. Contrary to primary UM, the immunological characteristics of its metastases are not well established. The presence of mononuclear inflammatory infiltrates in UM metastases has been reported [57]. One important consideration that should be made when designing clinical trials testing the effectiveness of various therapies of metastatic UM, is the fact that, in metastatic UM, monosomy 3 is associated with highly aggressive, rapidly progressive disease, while a prominent mononuclear inflammatory infiltrate in the metastases is associated with a better prognosis [58]. It is in contrast to what had been found in primary tumors. This study of exclusive metastasis material (and only studying 11 cases) indicates that host factors are relevant in the development and progression of metastatic disease and implies that immunological therapies to treat metastatic UM may have the potential to impact patient survival. In addition, one group found that hepatic metastases had significantly more intermediate and dendritic types of CD68-immunopositive macrophages than round ones [38]. The difference in the type of inflammatory cellular infiltrate between primary and metastatic tumors might have to be taken into account. In addition to a combination of anti-inflammatory approaches that target the tumor microenvironment with more knowledge-based selective tumoricidal drugs, future therapies should also take notice of the natural genetic variation (e.g., monosomy 3 or loss of BAP1 expression) that affects inflammation and immunity [58]. A still open question is whether leukocyte infiltration predicts the response to therapy, as suggested by a previous study in another malignancy [59]. As most immunotherapy studies have not been successful in UM, such studies are not very useful. For the treatment with tebentafusp, too little is currently known to predict which patients will respond.

7.4.7 Modulating Immune Responses Using Bel-Sar

While in UM, treatments with single or combined immune checkpoint inhibitors have not resulted in the same results as in cutaneous melanoma, there is hope. Combining checkpoint inhibitors with treatments that induce immunogenic cell death may offer an option to: (1) Stimulate the immune system and (2) Provide help for the immune checkpoint inhibitors. Huis In't Veld has combined treatment with a new virus-like drug conjugate, belzupacap sarotalocan (Bel-sar), with several immune checkpoint inhibitors to treat tumors in mice [60]. When cultured tumor cells were treated with Bel-sar and light-activated, a release of damage-associated patterns (DAMPs) was observed. In vivo treatment with Bel-sar and various immune checkpoint inhibitors was not only able to limit the growth of the treated tumors but also of untreated tumors (abscopal effect), with active T cells appearing in regional lymph nodes.

Another study showed that the Bel-sar treatment was able to change the type of tumor-infiltrating macrophages, with a shift occurring from pro-angiogenic M2 macrophages to more immunity-inducing M1 macrophages [61]. Bel-sar is currently under investigation in phase 2 (NCT04417530) and phase 3 (NCT06007690) clinical trials to investigate the effect of Bel-sar monotherapy on small choroidal melanoma and indeterminate lesions [62]. It would be of great interest to study the effect of Bel-sar on a patient's immune responses.

7.5 Conclusions

Immune cells often infiltrate in and around uveal melanoma, and it is suggested that the cancer cells can modulate and regulate these immune cells. The nature of the uveal melanoma microenvironment offers therapeutic opportunities. Preclinical studies have supported this premise, and clinical translation of many of these strategies is ongoing. Ultimately, by combining selective impairment of the neoplastic cell populations residing in the eye with immunotherapy and perhaps local immune response stimulating therapies—as this may be more effective than single therapy regimes—it may be possible to bring UM growth, invasion, and metastasis to a halt.

7.6 Industrial Relationship

Health Holland and Aura Biosciences have supported the research on belzupacap sarotolocan.

References

1. Streilein JW. Ocular immune privilege: therapeutic opportunities from an experiment of nature. Nat Rev Immunol. 2003;3(11):879–89.
2. Niederkorn JY, Streilein JW. Alloantigens placed into the anterior-chamber of the eye induce specific suppression of delayed-type hypersensitivity but Normal Cyto-toxic lymphocyte-T and helper lymphocyte-T responses. J Immunol. 1983;131(6):2670–4.
3. Wilbanks GA, Streilein JW. Characterization of suppressor cells in anterior chamber-associated immune deviation (Acaid) induced by soluble-antigen—evidence of 2 functionally and phenotypically distinct T-suppressor cell-populations. Immunology. 1990;71(3):383–9.
4. Van Raamsdonk CD, Bezrookove V, Green G, Bauer J, Gaugler L, O'Brien JM, et al. Frequent somatic mutations of GNAQ in uveal melanoma and blue naevi. Nature. 2009;457(7229):599–602.
5. Xu H, Chen M, Forrester JV. Para-inflammation in the aging retina. Prog Retin Eye Res. 2009;28(5):348–68.
6. Jager MJ, Shields CL, Cebulla CM, Abdel-Rahman MH, Grossniklaus HE, Stern M-H, et al. Uveal melanoma. Nat Rev Dis Primers. 2020;6(1):24.
7. Harbour JW, Onken MD, Roberson ED, Duan S, Cao L, Worley LA, et al. Frequent mutation of BAP1 in metastasizing uveal melanomas. Science. 2010;330(6009):1410–3.
8. Jensen O, Andersen SR. Spontaneous regression of a malignant melanoma of the choroid. Acta Ophthalmol. 1974;52(2):173–82.
9. Reese AB, Archila EA, Jones IS, Cooper WC. Necrosis of malignant melanoma of the choroid. Am J Ophthalmol. 1970;69(1):91–104.
10. Cochran AJ, Foulds WS, Damato BE, Trope GE, Morrison L, Lee WR. Assessment of immunological techniques in the diagnosis and prognosis of ocular malignant-melanoma. Brit J Ophthalmol. 1985;69(3):171–6.
11. Kan-Mitchell J, Liggett PE, Harel W, Steinman L, Nitta T, Oksenberg JR, et al. Lymphocytes cytotoxic to uveal and skin melanoma cells from peripheral blood of ocular melanoma patients. Cancer Immunol Immunother. 1991;33(5):333–40.
12. Huang XQ, Mitchell MS, Liggett PE, Murphree AL, Kan-Mitchell J. Non-fastidious, melanoma-specific CD8+ cytotoxic T lymphocytes from choroidal melanoma patients. Cancer Immunol Immunother. 1994;38(6):399–405.
13. Ksander BR, Geer DC, Chen PW, Salgaller ML, Rubsamen P, Murray TG. Uveal melanomas contain antigenically specific and non-specific infiltrating lymphocytes. Curr Eye Res. 1998;17(2):165–73.
14. Van Der Bruggen P, Zhang Y, Chaux P, Stroobant V, Panichelli C, Schultz ES, et al. Tumor-specific shared antigenic peptides recognized by human T cells. Immunol Rev. 2002;188:51–64.
15. Mulcahy KA, Rimoldi D, Brasseur F, Rodgers S, Lienard D, Marchand M, et al. Infrequent expression of the MAGE gene family in uveal melanomas. Int J Cancer. 1996;66(6):738–42.
16. Chen PW, Murray TG, Uno T, Salgaller ML, Reddy R, Ksander BR. Expression of MAGE genes in ocular melanoma during progression from primary to metastatic disease. Clin Exp Metastasis. 1997;15(5):509–18.
17. Saba J, McIntyre CA, Rees RC, Murray AK. Recognition of melanoma-associated peptides by peripheral blood mononuclear cells of ocular melanoma patients. Adv Exp Med Biol. 1998;451:241–4.
18. Field MG, Decatur CL, Kurtenbach S, Gezgin G, van der Velden PA, Jager MJ, et al. PRAME as an independent biomarker for metastasis in uveal melanoma. Clin Cancer Res. 2016;22(5):1234–42.

19. Gezgin G, Luk SJ, Cao JF, Dogrusöz M, van der Steen DM, Hagedoorn RS, et al. PRAME as a potential target for immunotherapy in metastatic uveal melanoma. Jama Ophthalmol. 2017;135(6):541–9.
20. Blom DJR, Luyten GPM, Mooy C, Kerkvliet S, Zwinderman AH, Jager MJ. Human leukocyte antigen class I expression—marker of poor prognosis in uveal melanoma. Invest Ophth Vis Sci. 1997;38(9):1865–72.
21. deWaardSiebinga I, Hilders CGJM, Hansen BE, vanDelft JL, Jager MJ. HLA expression and tumor-infiltrating immune cells in uveal melanoma. Graef Arch Clin Exp. 1996;234(1):34–42.
22. Hurks HMH, Metzelaar-Blok JAW, Mulder A, Claas FHJ, Jager MJ. High frequency of allele-specific down-regulation of HLA class I expression in uveal melanoma cell lines. Int J Cancer. 2000;85(5):697–702.
23. Ericsson C, Seregard S, Bartolazzi A, Levitskaya E, Ferrone S, Kiessling R, et al. Association of HLA class I and class II antigen expression and mortality in uveal melanoma. Invest Ophth Vis Sci. 2001;42(10):2153–6.
24. Krishnakumar S, Abhyankar D, Lakshmi SA, Shanmugam MP, Pushparaj V, Biswas J. HLA class II antigen expression in uveal melanoma: correlation with clinicopathological features. Exp Eye Res. 2003;77(2):175–80.
25. Ma D, Luyten GP, Luider TM, Niederkorn JY. Relationship between natural-killer-cell susceptibility and metastasis of human uveal melanoma-cells in a murine model. Invest Ophth Vis Sci. 1995;36(2):435–41.
26. Ma D, Niederkorn JY. Transforming growth-factor-Beta down-regulates major histocompatibility complex class-I antigen expression and increases the susceptibility of uveal melanoma-cells to natural-killer cell-mediated cytolysis. Immunology. 1995;86(2):263–9.
27. Jager MJ, Hurks HMH, Levitskaya J, Kiessling R. HLA expression in uveal melanoma: there is no rule without some exception. Hum Immunol. 2002;63(6):444–51.
28. Repp AC, Mayhew ES, Apte S, Niederkorn JY. Human uveal melanoma cells produce macrophage migration-inhibitory factor to prevent lysis by NK cells. J Immunol. 2000;165(2):710–5.
29. Apte RS, Sinha D, Mayhew E, Wistow GJ, Niederkorn JY. Cutting edge: role of macrophage migration inhibitory factor in inhibiting NK cell activity and preserving immune privilege. J Immunol. 1998;160(12):5693–6.
30. Durie FH, Campbell AM, Lee WR, Damato BE. Analysis of lymphocytic infiltration in uveal melanoma. Invest Ophth Vis Sci. 1990;31(10):2106–10.
31. Delacruz PO, Specht CS, Mclean IW. Lymphocytic infiltration in uveal malignant-melanoma. Cancer-Am Cancer Soc. 1990;65(1):112–5.
32. Whelchel JC, Farah SE, Mclean IW, Burnier MN. Immunohistochemistry of infiltrating lymphocytes in uveal malignant-melanoma. Invest Ophth Vis Sci. 1993;34(8):2603–6.
33. Bronkhorst IHG, Vu THK, Jordanova ES, Luyten GPM, van der Burg SH, Jager MJ. Different subsets of tumor-infiltrating lymphocytes correlate with macrophage influx and monosomy 3 in uveal melanoma. Invest Ophth Vis Sci. 2012;53(9):5370–8.
34. Mougiakakos D, Johansson CC, Trocme E, All-Ericsson C, Economou MA, Larsson O, et al. Intratumoral Forkhead box P3-positive regulatory T cells predict poor survival in Cyclooxygenase-2 positive uveal melanoma. Cancer-Am Cancer Soc. 2010;116(9):2224–33.
35. Maat W, Ly LV, Jordanova ES, de Wolff-Rouendaal D, Schalij-Delfos NE, Jager MJ. Monosomy of chromosome 3 and an inflammatory phenotype occur together in uveal melanoma. Invest Ophth Vis Sci. 2008;49(2):505–10.
36. Mäkitie T, Summanen P, Tarkkanen A, Kivelä T. Tumor-infiltrating macrophages (CD68 Cells) and Prognosis in malignant uveal melanoma. Invest Ophth Vis Sci. 2001;42(7):1414–21.
37. Bronkhorst IHG, Ly LV, Jordanova ES, Vrolijk J, Versluis M, Luyten GPM, et al. Detection of M2-macrophages in uveal melanoma and relation with survival. Invest Ophth Vis Sci. 2011;52(2):643–50.
38. Toivonen P, Makitie T, Kujala E, Kivela T. Microcirculation and tumor-infiltrating macrophages in choroidal and ciliary body melanoma and corresponding metastases. Invest Ophthalmol Vis Sci. 2004;45(1):1–6.
39. Biswas SK, Mantovani A. Macrophage plasticity and interaction with lymphocyte subsets: cancer as a paradigm. Nat Immunol. 2010;11(10):889–96.
40. Bronkhorst IHG, Jager MJ. Uveal melanoma: the inflammatory microenvironment. J Innate Immun. 2012;4(5–6):454–62.
41. Gezgin G, Dogrusöz M, van Essen TH, Kroes WGM, Luyten GPM, van der Velden PA, et al. Genetic evolution of uveal melanoma guides the development of an inflammatory microenvironment. Cancer Immunol Immun. 2017;66(7):903–12.
42. Vu THK, Bronkhorst IHG, Versluis M, Marinkovic M, van Duinen SG, Vrolijk J, et al. Analysis of inflammatory cells in uveal melanoma after prior irradiation. Invest Ophth Vis Sci. 2013;54(1):360–9.
43. Leyvraz S, Keilholz U. Ocular melanoma: what's new? Curr Opin Oncol. 2012;24(2):162–9.
44. Sapoznik S, Hammer O, Ortenberg R, Besser MJ, Ben-Moshe T, Schachter J, et al. Novel anti-melanoma immunotherapies: disarming tumor escape mechanisms. Clin Dev Immunol. 2012;2012:1.
45. Gezgin G, Visser M, Ruano D, Santegoets SJ, de Miranda NFCC, van der Velden PA, et al. Tumor-infiltrating T cells can be expanded successfully from primary uveal melanoma after separation from their tumor environment. Ophthalmol Sci. 2022;2(2):100132.
46. Hodi FS, O'Day SJ, McDermott DF, Weber RW, Sosman JA, Haanen JB, et al. Improved survival with Ipilimumab in patients with metastatic melanoma. New Engl J Med. 2010;363(8):711–23.
47. Danielli R, Ridolfi R, Chiarion-Sileni V, Queirolo P, Testori A, Plummer R, et al. Ipilimumab in pretreated patients with metastatic uveal melanoma: safety and clinical efficacy. Cancer Immunol Immun. 2012;61(1):41–8.
48. Carvajal RD, Sacco JJ, Jager MJ, Eschelman DJ, Bagge RO, Harbour JW, et al. Advances in the clinical management of uveal melanoma. Nat Rev Clin Oncol. 2023;20(2):99–115.
49. Yang WH, Chen PW, Li HC, Alizadeh H, Niederkorn JY. PD-L1: PD-1 interaction contributes to the functional suppression of T-cell responses to human uveal melanoma cells in vitro. Invest Ophth Vis Sci. 2008;49(6):2518–25.
50. Nathan P, Hassel JC, Rutkowski P, Baurain JF, Butler MO, Schlaak M, et al. Overall survival benefit with Tebentafusp in metastatic uveal melanoma. New Engl J Med. 2021;385(13):1196–206.
51. Piulats JM, Watkins C, Costa-García M, del Carpio L, Piperno-Neumann S, Rutkowski P, et al. Overall survival from tebentafusp versus nivolumab plus ipilimumab in first-line metastatic uveal melanoma: a propensity score-weighted analysis. Ann Oncol. 2024;35(3):317–26.
52. Maat W, Haasnoot GW, Claas FHJ, Schalij-Delfos NE, Schreuder GMT, Jager MJ. HLA class I and II genotype in uveal melanoma: relation to occurrence and prognosis. Invest Ophth Vis Sci. 2006;47(1):3–6.
53. Richtig E, Langmann G, Schlemmer G, Müllner K, Papaefthymiou G, Bergthaler P, et al. Safety and efficacy of interferon alfa-2b in the adjuvant treatment of uveal melanoma. Ophthalmologe. 2006;103(6):506–11.

54. de Vries IJM, Bernsen MR, Lesterhuis WJ, Scharenborg NM, Strijk SP, Gerritsen MJP, et al. Immunomonitoring tumor-specific T cells in delayed-type hypersensitivity skin biopsies after dendritic cell vaccination correlates with clinical outcome. J Clin Oncol. 2005;23(24):5779–87.
55. Bol KF, Mensink HW, Aarntzen EHJG, Schreibelt G, Keunen JEE, Coulie PG, et al. Long overall survival after dendritic cell vaccination in metastatic uveal melanoma patients. Am J Ophthalmol. 2014;158(5):939–47.
56. Brahmer JR, Drake CG, Wollner I, Powderly JD, Picus J, Sharfman WH, et al. Phase I study of single-agent anti-programmed Death-1 (MDX-1106) in refractory solid tumors: safety, clinical activity, pharmacodynamics, and immunologic correlates. J Clin Oncol. 2010;28(19):3167–75.
57. Krishna Y, McCarthy C, Kalirai H, Coupland SE. Inflammatory cell infiltrates in advanced metastatic uveal melanoma. Hum Pathol. 2017;66:159–66.
58. Abdel-Rahman MH, Cebulla CM, Verma V, Christopher BN, Carson WE, Olencki T, et al. Monosomy 3 status of uveal melanoma metastases is associated with rapidly progressive tumors and short survival. Exp Eye Res. 2012;100:26–31.
59. Halama N, Michel S, Kloor M, Zoernig I, Benner A, Spille A, et al. Localization and density of immune cells in the invasive margin of human colorectal cancer liver metastases are prognostic for response to chemotherapy. Cancer Res. 2011;71(17):5670–7.
60. Huis In't Veld RV, Ma S, Kines RC, Savinainen A, Rich C, Ossendorp F, et al. Immune checkpoint inhibition combined with targeted therapy using a novel virus-like drug conjugate induces complete responses in a murine model of local and distant tumors. Cancer Immunol Immunother. 2023;72:2405.
61. Ma S, Huis In't Veld RV, Houy A, Stern MH, Rich C, Ossendorp FA, et al. In vitro testing of the virus-like drug conjugate Belzupacap Sarotalocan (AU-011) on uveal melanoma suggests BAP1-related Immunostimulatory capacity. Invest Ophthalmol Vis Sci. 2023;64(7):10.
62. Kines RC, Varsavsky I, Choudhary S, Bhattacharya D, Spring S, McLaughlin R, et al. An infrared dye-conjugated virus-like particle for the treatment of primary uveal melanoma. Mol Cancer Ther. 2018;17(2):565–74.

Cancer Genetics

8

Valeria Visconte and Arun D. Singh

8.1 Introduction

Cancer genetics encompasses genetic and epigenetic aspects of multifaced malignant disorders. A large notion derives from the identification of chromosomal rearrangements or genomic alterations in malignant cells. The task of physicians and geneticists is to detect cancer as soon as possible by identifying individuals at high-risk caused by gene variants in oncogenes or tumor suppressors. Heritable gene variants can predict the risk of developing tumors and hematological malignancies. A plethora of genes and/or chromosomal anomalies are hallmarks of cancer initiation. Here, we will review key pathways and genes in cancer development.

8.2 Telomeres and Telomere Gene Mutations

Telomeres cap the ends of eukaryotic chromosomes. In humans, telomeres have a specific nucleotide repeat sequence, TTAGGG, that is double-stranded DNA but ends with a single-stranded DNA with a G-overhang. The G-rich telomeric repeats (G-strand) are located in the 5′ to 3′ strand, while the 3′ to 5′ strand is defined as the C-strand. The maintenance of telomere length depends on the telosome (telomerase, shelterin complex, CST complex). Per each division, about 50–200 bases are lost from the terminal sequence of the chromosomes. However, besides each replication, several other factors can trigger telomere shortening (e.g., oxidative stress, age, malignant diseases). Telomerase maintenance is crucial for human cells. The telomerase reverse transcriptase (*TERT*) encoding the catalytic subunit of the telomerase enzyme (an RNA-dependent DNA-polymerase) is located on chromosome 5p15.33 and is characterized by an atypical sequence in the promoter. It includes a transcription site, two E-boxes (5′-CACGTG-3′), and 5 GC boxes (5′-GGGCGG-3′). More than 80% of tumor cells express high telomerase activity. This activity correlates with TERT expression levels. TERT is crucial in malignant transformation (Fig. 8.1) [1].

Genetic mutations impacted telomerase maintenance, resulting in telomeropathies. Such mutations lead to short telomeres, often confined to hematologic cancers, triggering organ failure. The strong impact of telomere shortening is

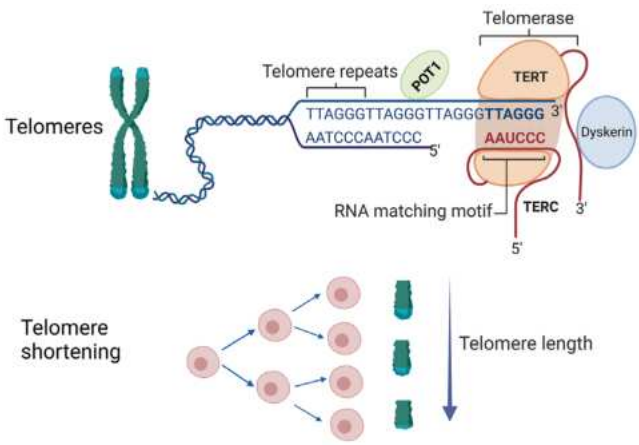

Fig. 8.1 The figure illustrates components of the telomere complex. Telomeres are regions containing repetitive sequences of DNA (TTAGGG) present at the end of chromosomes. The function of the telomeres is to allow a correct replication during cell division. *POT1* (protection of telomere 1) binds to the TTAGGG repeats and maintains telomere length. Telomerase is a ribonucleoprotein complex consisting of the telomerase reverse transcriptase (*TERT*), the telomerase RNA (*TERC*) gene, and the RNA-associated proteins, including Dyskerin. Telomeres shorten with each cell division and many diseases are characterized by telomere shortening. (The figure was created with BioRender.com)

V. Visconte (✉)
Department of Translational Hematology & Oncology Research, Taussig Cancer Institute, Cleveland Clinic, Cleveland, OH, USA
e-mail: visconv@ccf.org

A. D. Singh
Department of Ophthalmic Oncology, Cole Eye Institute, Cleveland Clinic, Cleveland, OH, USA
e-mail: singha@ccf.org

© The Author(s), under exclusive license to Springer Nature Switzerland AG 2025

A. D. Singh, B. E. Damato (eds.), *Clinical Ophthalmic Oncology*, https://doi.org/10.1007/978-3-031-75907-9_8

observed in age-related clonal diseases of the bone marrow [2]. Short telomeres are linked to cancer risk and span any age. Mutations in *TERT* promoter have been found in several cancers, including bone marrow failure disorders and conjunctival melanoma, and can activate telomerase, prolonging proliferation [2, 3]. Other mechanisms of TERT activation include promoter methylation, alterations of pre-mRNA, and increased copy number. In addition to *TERT* mutations, *TERT* polymorphisms responsible for the elongation of telomeres have also been reported in cancer. Variants in other genes important in the telomere machinery have been found in cancer. Pathogenic germline variants in the *POT1* gene produce an increase in telomere length and trigger a tumor predisposition syndrome (POT1-TPDS), which also includes cutaneous melanoma, among other cancers [4]. In the context of uveal melanoma (UM), a study investigated the expression profile and telomerase activity in 14 patients with UM using PCR-based telomeric repeat amplification protocol (TRAP) assay and found upregulation of telomerase activity [5]. A genome-wide association study in UM investigated the role of the TERT/CLPTM1L, a risk locus, and showed highly correlated risk alleles. A functional variant (rs452384) was identified in which the C risk allele correlated with a higher expression level and a longer telomere length [6]. *POT1* mutations have also been reported in families with glioma, [7] colorectal cancer, and lymphoid malignancies (Fig. 8.1) [8].

8.3 Candidate Genes

Alterations in expression and function of G-protein-coupled receptors are associated with tumorigenesis. Among them, *GNAS* mutations are detected by deep DNA sequencing in several cancers [9], while *GNAQ* or *GNA11* activating mutations are predominantly found in melanomas of the skin and eye [10]. Gain-of-function mutations in guanine nucleotide-binding protein *GNAQ* or *GNA11* (Q209L/P) and *BRAF* (V600E) are frequently observed in UM. Such mutations are present in almost all cells representing ancestral clones. These mutations alone are not able to develop into cancer unless other mutations cooperate in the process [11] [12]. In addition to the key role of Gαq signaling in the development of UM, recurrent mutations are found in *PLCB4* (p.D630), encoding phospholipase C β4, and *CYSLTR2* (p.L129Q), encoding Gαq-coupled receptor [13]. These mutations represent an alternative pathway to activate Gαq signaling in UM wild type for *GNAQ/11*. A recent study conducted a kinome-wide CRISPR-Cas9 sgRNA screen to discover synthetic lethal genes and their interactions to define vulnerability targets for treatments. The combined inhibition of MEK and FAK showed growth inhibition in UM cells and cytotoxicity in UM xenografts and metastatic UM [14]. This approach suggests that synergistic targeting of FAK and MEK/ERK can be used as precision therapy in UM triggered by this pathway. Along with this line of experiments, the axis CYSLTR2 → GNAQ/11 → PLCβ was demonstrated to be a signaling cascade activating the MAP kinase and FAK pathways via protein kinase C [15]. Similarly, ARF6 induces the trafficking of GNAQ and β-catenin from the plasma membrane to cytoplasm and small-molecule against ARF6 reduces UM cell proliferation [16].

Additional genetic events provide heterogeneity and are necessary for the tumor to progress. Besides *GNAQ/11*, mutations in *BAP1*, *SF3B1*, and *EIF1AX* are observed but less commonly [17–19]. *BRCA1*-associated protein-1 (*BAP1*) gene mapping on chromosome 3 is a tumor suppressor involved in cell proliferation. Germline *BAP1* pathogenic variants are associated with a predisposition to multiple cancers. Approximately 80% of metastatic UM carry *BAP1* mutations and are associated with decreased disease-free survival [20]. Such mutations produce a premature termination and alter the de-ubiquitinase activity of the BAP1 protein. Efforts in genetic testing using multi-panel genes (including six genes associated with hereditary melanoma) applied to peripheral blood DNA specimens have reported a germline *BAP1* mutation in 3.5% of unselected UM patients [21]. Alterations in BAP1 methylation have also been found in metastatic UM and correlate with copy number loss [22]. UM characterized by *BAP1* mutations and monosomy 3 has decreased disease-free survival rates [23]. Other common anomalies are found in the form of copy number alterations (especially the ones affecting chromosomes 1, 3, 6, 8, and 16), which are as common as mutations in *BAP1*, *SF3B1*, and *EIF1AX*. About 10–20% of UM patients harbor mutations in *SF3B1*, a gene located on chromosome 2 and encoding a component of the RNA-splicing machinery [24]. Studies have shown neoepitope targets associated with *SF3B1* mutations [25] and neoepitopes commonly shared by patients independently from the status of *SF3B1* [26]. *BAP1* loss and *SF3B1* mutation are more susceptible to chemotherapeutic drugs [27]. Other mutations mostly occur in *CDKN2A*, *EZH2*, *MED12*, *PBRM1*, *PIK3CA/R2*, and *PTEN* genes. *EIF1AX* mutations are detected more rarely and result in alternative selection of start sites impairing translation of transcripts.

8.4 Apoptosis and Cell Cycle

TP53 gene is located on chromosome 17p, a chromosome susceptible to loss in human cancer. It is mutated in half of the human cancers but rarely mutated in UM. However, the p53 protein is inhibited by overexpression of mouse double minute 2 (MDM2). MDM2 acts as a substrate-specific E3 ubiquitin ligase and as a negative regulator of p53. It func-

tions as maintenance feedback by sustaining the survival of UM cells. Targeting with small molecules induces apoptosis. MDM2 and p53 play a key role in regulating cell cycle and apoptosis. MDM2 overexpression impairs the control of cell proliferation, increases DNA damage, and promotes tumorigenesis by blocking E2F, ARF, and p53-dependent apoptosis [28]. In addition, deregulation of the cell cycle is a key feature of cancer. Loss of the retinoblastoma (Rb) gene can trigger p53 to induce apoptosis. Disruption of the p53 pathway can also increase the susceptibility to inactivate p53 by mutations directly on the p53 gene or on other regulators of p53.

UM cells also exhibit defects at several points of the BCL2 cascade. The BCL2 family of proteins includes the anti-apoptotic proteins (BCL2, BCLXL, BCLW, BFL1, MCL1), the BH3-only pro-apoptotic proteins (BAD, BIM, BMF, NOXA, PUMA) and multi-BCL2 homologous domain proteins (BAK, BAX, BOK). Results of the comparison of the BCL2 cascade between UM and CM showed low levels of BFL1 and high levels of PUMA proteins in UM compared to CM. These results support the use of BCL2 inhibitors [29].

8.5 Multi-Omics Analysis

Integrative genetics, an area built on the combination of several omics data types (genomic, proteomics, and metabolomics), has revolutionized the way how disease biology is explored (Fig. 8.2). The employment of machine learning tools has been implemented in the identification of prognostic biomarkers, analysis of digital pathology slides, target validation, and automation of cell count [30]. Deep learning tools have also been used to predict the mutational status of bone marrow smears [31]. Integrated multi-omics has been important for types of cancers that are difficult to study. Recent analyses using single-cell and whole-genome sequencing of frozen clinical specimens of UM have shown the applicability of integrative methods in UM [32]. Next-generation sequencing of spatially separated biopsies combined with digital PCR has detected diverse sub-populations within one tumor [33]. More recently, single-cell sequencing confirmed UM heterogeneity and showed that some chromosomal anomalies might reside in a subset of cells within the tumor rather than in all cells [34]. Genetic analysis of the characteristics of matched primary and metastatic UM has shown that metastatic lesions did not carry alterations originally present in the primary tumor, with the primary site of the tumor constituted by additional genetic changes [35]. Multi-omics analysis of datasets of UM in The Cancer Genome Atlas and immunohistochemistry of aurora kinase B (AURKB) showed an overexpression of AURKB in patients with UM and an association with poor prognosis. In vitro and in vivo studies demonstrated the efficacy of the AURKB-specific inhibitor, hesperidin, in decelerating UM by epigenetic silencing of the telomerase reverse transcriptase. Such an inhibitor influences the phosphorylation of the histone H3 at serine 10 at the promoter of the telomerase reverse transcriptase [36]. Along this line, bioinformatics methods are being tested to integrate several genetic and transcriptomic features of UM [37]. A combination of single-cell and bulk sequencing data of UM specimens was able to identify novel immune-related signatures associated with prognosis [38]. Using data from The Cancer Genome Atlas and gene set enrichment coupled with hierarchical clustering analysis, UM patients were classified into two immunity clusters. The prognostic immune signature included S100A13, MMP9, and SEMA3B genes with a lower expression of immune checkpoint genes in the low-risk group [38]. A recent study identified 130 prognostic immune genes, with six of them (*CL18*, *CXCL8*, *GTPBP1*, *JAG2*, *PRELID1*, *PTGER4*) constructing a prognostic signature in the UM dataset from The Cancer Genome Atlas [39]. Bioinformatics'

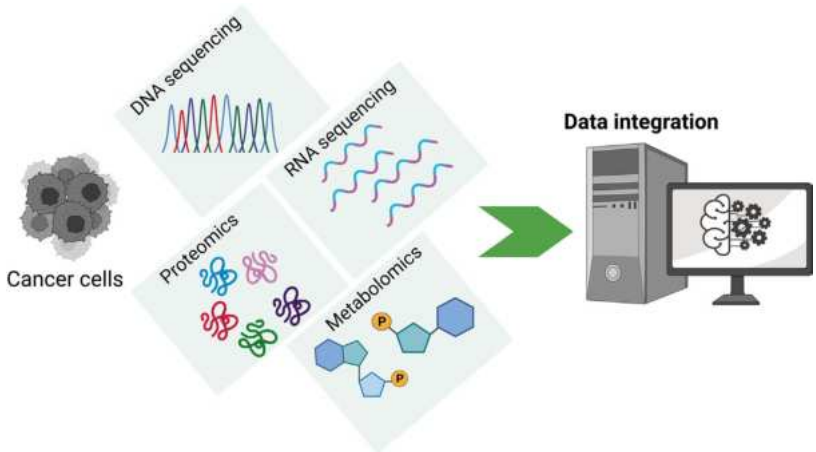

Fig. 8.2 Schematic representation of omics (data types) collected from cancer cells. The integration of results of DNA and RNA sequencing, interaction between proteins and protein structure (proteomics), and metabolites are combined through computer science. (The figure was created with BioRender.com)

methods also determined the correlation between TAP1 (immunomodulation-related protein) expression and UM prognosis [40]. Co-expression network analysis identified master regulatory genes (*SASH3*, *PLXNB1*, *FAM107A*, *VXS2*, *TNKS2*, *HM13*) [41].

References

1. Jafri MA, Ansari SA, Alqahtani MH, Shay JW. Roles of telomeres and telomerase in cancer, and advances in telomerase-targeted therapies. Genome Med. 2016;8(1):69.
2. Du HY, Pumbo E, Ivanovich J, An P, Maziarz RT, Reiss UM, et al. TERC and TERT gene mutations in patients with bone marrow failure and the significance of telomere length measurements. Blood. 2009;113(2):309–16.
3. Griewank KG, Murali R, Schilling B, Scholz S, Sucker A, Song M, et al. TERT promoter mutations in ocular melanoma distinguish between conjunctival and uveal tumours. Br J Cancer. 2013;109(2):497–501.
4. Nathan V, Palmer JM, Johansson PA, Hamilton HR, Warrier SK, Glasson W, et al. Loss-of-function variants in POT1 predispose to uveal melanoma. J Med Genet. 2021;58(4):234–6.
5. Heine B, Coupland SE, Kneiff S, Demel G, Bornfeld N, Hummel M, et al. Telomerase expression in uveal melanoma. Br J Ophthalmol. 2000;84(2):217–23.
6. Derrien AC, Houy A, Ganier O, Dingli F, Ningarhari M, Mobuchon L, et al. Functional characterization of 5p15.33 risk locus in uveal melanoma reveals rs452384 as a functional variant and NKX2.4 as an allele-specific interactor. Am J Hum Genet. 2022;109(12):2196–209.
7. Bainbridge MN, Armstrong GN, Gramatges MM, Bertuch AA, Jhangiani SN, Doddapaneni H, et al. Germline mutations in shelterin complex genes are associated with familial glioma. J Natl Cancer Inst. 2015;107(1):384.
8. McMaster ML, Sun C, Landi MT, Savage SA, Rotunno M, Yang XR, et al. Germline mutations in protection of telomeres 1 in two families with Hodgkin lymphoma. Br J Haematol. 2018;181(3):372–7.
9. Landis CA, Masters SB, Spada A, Pace AM, Bourne HR, Vallar L. GTPase inhibiting mutations activate the alpha chain of Gs and stimulate adenylyl cyclase in human pituitary tumours. Nature. 1989;340(6236):692–6.
10. Lietman CD, McKean M. Targeting GNAQ/11 through PKC inhibition in uveal melanoma. Cancer Gene Ther. 2022;29(12):1809–13.
11. Van Raamsdonk CD, Griewank KG, Crosby MB, Garrido MC, Vemula S, Wiesner T, et al. Mutations in GNA11 in uveal melanoma. N Engl J Med. 2010;363(23):2191–9.
12. Van Raamsdonk CD, Bezrookove V, Green G, Bauer J, Gaugler L, O'Brien JM, et al. Frequent somatic mutations of GNAQ in uveal melanoma and blue naevi. Nature. 2009;457(7229):599–602.
13. Moore AR, Ceraudo E, Sher JJ, Guan Y, Shoushtari AN, Chang MT, et al. Recurrent activating mutations of G-protein-coupled receptor CYSLTR2 in uveal melanoma. Nat Genet. 2016;48(6):675–80.
14. Paradis JS, Acosta M, Saddawi-Konefka R, Kishore A, Gomes F, Arang N, et al. Synthetic lethal screens reveal Cotargeting FAK and MEK as a multimodal precision therapy for GNAQ-driven uveal melanoma. Clin Cancer Res. 2021;27(11):3190–200.
15. Ma J, Weng L, Bastian BC, Chen X. Functional characterization of uveal melanoma oncogenes. Oncogene. 2021;40(4):806–20.
16. Yoo JH, Shi DS, Grossmann AH, Sorensen LK, Tong Z, Mleynek TM, et al. ARF6 is an actionable node that orchestrates oncogenic GNAQ signaling in uveal melanoma. Cancer Cell. 2016;29(6):889–904.
17. Harbour JW, Onken MD, Roberson EDO, Duan S, Cao L, Worley LA, et al. Frequent mutation of BAP1 in metastasizing uveal melanomas. Science. 2010;330(6009):1410–3.
18. Furney SJ, Pedersen M, Gentien D, Dumont AG, Rapinat A, Desjardins L, et al. SF3B1 mutations are associated with alternative splicing in uveal melanoma. Cancer Discov. 2013;3(10):1122–9.
19. Dono M, Angelini G, Cecconi M, Amaro A, Esposito AI, Mirisola V, et al. Mutation frequencies of GNAQ, GNA11, BAP1, SF3B1, EIF1AX and TERT in uveal melanoma: detection of an activating mutation in the TERT gene promoter in a single case of uveal melanoma. Br J Cancer. 2014;110(4):1058–65.
20. Koopmans AE, Verdijk RM, Brouwer RWW, van den Bosch TPP, van den Berg MMP, Vaarwater J, et al. Clinical significance of immunohistochemistry for detection of BAP1 mutations in uveal melanoma. Mod Pathol. 2014;27(10):1321–30.
21. Gillies B, Krema H, Chao A, Lando L, Farncombe KM, Butler M, et al. Oncologist-led germline genetic testing for uveal melanoma. Ophthalmic Genet. 2023;44(3):253–61.
22. Bakhoum MF, Curtis EJ, Goldbaum MH, Mischel PS. BAP1 methylation: a prognostic marker of uveal melanoma metastasis. NPJ Precis Oncol. 2021;5(1):89.
23. Karlsson J, Nilsson LM, Mitra S, Alsén S, Shelke GV, Sah VR, et al. Molecular profiling of driver events in metastatic uveal melanoma. Nat Commun. 2020;11(1):1894.
24. Harbour JW, Roberson EDO, Anbunathan H, Onken MD, Worley LA, Bowcock AM. Recurrent mutations at codon 625 of the splicing factor SF3B1 in uveal melanoma. Nat Genet. 2013;45(2):133–5.
25. Bigot J, Lalanne AI, Lucibello F, Gueguen P, Houy A, Dayot S, et al. Splicing patterns in SF3B1-mutated uveal melanoma generate shared immunogenic tumor-specific Neoepitopes. Cancer Discov. 2021;11(8):1938–51.
26. Yao T, Zhang Z, Li Q, Huang R, Hong Y, Li C, et al. Long-read sequencing reveals alternative splicing-driven, shared immunogenic neoepitopes regardless SF3B1 status in uveal melanoma. Cancer Immunol Res. 2023;11:1671.
27. Yu L, Zhou D, Zhang G, Ren Z, Luo X, Liu P, et al. Co-occurrence of BAP1 and SF3B1 mutations in uveal melanoma induces cellular senescence. Mol Oncol. 2022;16(3):607–29.
28. Jiang H, Luo J, Lei H. The roles of mouse double minute 2 (MDM2) oncoprotein in ocular diseases: a review. Exp Eye Res. 2022;217:108910.
29. Mukherjee N, Dart CR, Amato CM, Honig-Frand A, Lambert JR, Lambert KA, et al. Expression differences in BCL2 family members between uveal and cutaneous melanomas account for varying sensitivity to BH3 mimetics. J Invest Dermatol. 2022;142(7):1912–1922.e7.
30. Radakovich N, Nagy M, Nazha A. Artificial intelligence in hematology: current challenges and opportunities. Curr Hematol Malig Rep. 2020;15(3):203–10.
31. Diaz DJ, Kulikova AV, Ellington AD, Wilke CO. Using machine learning to predict the effects and consequences of mutations in proteins. Curr Opin Struct Biol. 2023;78:102518.
32. Wang Y, Fan JL, Melms JC, Amin AD, Georgis Y, Barrera I, et al. Multimodal single-cell and whole-genome sequencing of small, frozen clinical specimens. Nat Genet. 2023;55(1):19–25.

33. Versluis M, de Lange MJ, van Pelt SI, Ruivenkamp CAL, Kroes WGM, Cao J, et al. Digital PCR validates 8q dosage as prognostic tool in uveal melanoma. PLoS One. 2015;10(3):e0116371.
34. Gao G, Deng A, Liang S, Liu S, Fu X, Zhao X, et al. Integration of bulk RNA sequencing and single-cell RNA sequencing to reveal uveal melanoma tumor heterogeneity and cells related to survival. Front Immunol. 2022;13:898925.
35. Shain AH, Bagger MM, Yu R, Chang D, Liu S, Vemula S, et al. The genetic evolution of metastatic uveal melanoma. Nat Genet. 2019;51(7):1123–30.
36. Wang H, Pan H, Huang X. AURKB enhances chromosomal remodeling of Telomeric genes and accelerates tumorigenesis of uveal melanoma. Invest Ophthalmol Vis Sci. 2023;64(4):23.
37. Chalise P, Kwon D, Fridley BL, Mo Q. Statistical methods for integrative clustering of multi-omics data. Methods Mol Biol Clifton NJ. 2023;2629:73–93.
38. Wang W, Zhao H, Wang S. Identification of a novel immune-related gene signature for prognosis and the tumor microenvironment in patients with uveal melanoma combining single-cell and bulk sequencing data. Front Immunol. 2023;14:1099071.
39. Yang B, Fan Y, Liang R, Wu Y, Gu A. Identification of a prognostic six-immune-gene signature and a nomogram model for uveal melanoma. BMC Ophthalmol. 2023;23(1):2.
40. Zhu R, Chen YT, Wang BW, You YY, Wang XH, Xie HT, et al. TAP1, a potential immune-related prognosis biomarker with functional significance in uveal melanoma. BMC Cancer. 2023;23(1):146.
41. Diaz MJ, Tran JT, Montanez-Wiscovich M. Identification of three master regulatory genes with prognostic value for uveal melanoma by means of weighted co-expression network analysis. Skin Res Technol. 2023;29(7):e13358.

Cancer Staging

9

Claudine Bellerive and Arun D. Singh

9.1 Introduction

Several classification systems exist for tumor staging. To date, the universally accepted evidence-based standard for almost all types of eye cancer staging is the tumor, node, and metastasis (TNM) classification of the Union Internationale Contre le Cancer (UICC) and the American Joint Committee on Cancer (AJCC) [1].

The TNM classification is based on the local extent of the primary tumor (T), the regional lymph node involvement (N), and the presence of metastatic disease (M). Many different combinations of T, N, and M categories make it possible to determine the overall stage, which ranges from I to IV. Generally, a higher TNM stage category is associated with poor outcomes, increased risk of local tumor recurrence, or lower patient survival rates.

Once the diagnosis of eye cancer is made, staging is the critical step to determine the adequate management and surveillance strategy. To be consistent, a staging classification needs stability over time for comparison of protocol designs and treatment outcomes between different centers. Equally important, a staging classification requires the ability to evolve with the emergence of new diagnostic techniques and treatments to be valuable. Rapid advances in clinical, epidemiological, and experimental sciences represent a real challenge in ensuring the right balance between stability and adaptability.

It is also important to take into account the universal nature of a classification such as the AJCC/TNM classification. Given the high levels of inequality in access to adequate pathologists and laboratory services across the world, clinical cancer staging (cTNM) is still preferred.

9.2 History

TNM staging was initially developed by the French surgeon Pierre Denoix between 1943 and 1952 [2]. It was subsequently adopted 1 year later by the UICC. Founded by the American College of Surgeons in 1959, the AJCC introduced a simplified adaptation of the TNM staging used in the United States (US) [3]. In 1982, the two organizations agreed to embrace the unified version. The result of this work was the fourth edition of the *TNM Classification of Malignant Tumours*, published in 1987 [4]. As clinical cancer care keeps improving, periodic revisions and updates of the AJCC/TNM staging system have been required every 5–7 years. The existing seventh edition has been recently replaced by the eighth edition, published in 2016 and officially implemented on January first, 2018, in the US [5]. The AJCC version 9 TNM staging will be available electronically and will be released by chapters.

The AJCC/TNM staging classification is now widely used by eye cancer specialists, researchers, and registries. However, history shows that this was not always the case. The following are a few examples of previous classifications proposed during the past decades that failed to demonstrate significant prognostic value. Ocular adnexal lymphoma (OAL) has long been classified according to the Ann Arbor staging system, which was first designed for Hodgkin lymphoma in 1971 and then modified for non-Hodgkin lymphoma in 1977 [6]. Although OAL represents the most common primary orbital malignancy, encompassing more than 50% of all orbital tumors, it was not included in the AJCC/TNM classification before the seventh edition [7]. In response to some limitations related to the Ann Arbor classification, including the disproportionate staging distribution and the lack of sufficient information among specific anatomical locations and the bilaterality of tumors, Coupland

C. Bellerive (✉)
Ophtalmologiste Oncologue, CHU de Québec—Université Laval, Centre Universitaire D'ophtalmologie, Québec, QC, Canada
e-mail: claudine.bellerive.1@ulaval.ca

A. D. Singh
Department of Ophthalmic Oncology, Cole Eye Institute, Cleveland Clinic, Cleveland, OH, USA
e-mail: singha@ccf.org

© The Author(s), under exclusive license to Springer Nature Switzerland AG 2025

A. D. Singh, B. E. Damato (eds.), *Clinical Ophthalmic Oncology*, https://doi.org/10.1007/978-3-031-75907-9_9

and colleagues introduced the first TNM staging system for OAL in 2009 [8–10]. The seventh edition of the AJCC/TNM classification for OAL was then assessed, appearing to be predictive of disease-free survival [11, 12]. The subcategories of T1, T2, and T4 from the T stage have been removed in the eighth edition of the AJCC cancer staging system (Table 9.1). Pathological type of OAL remains an important indicator of clinical prognosis, diffuse large B cell lymphoma and mantle cell lymphoma showing significantly higher risk of mortality at 10 years [13, 14].

Table 9.1 Definition of primary tumor (T) for ocular adnexal lymphoma [5]

T Category	T Criteria
TX	Lymphoma extent not specified
T0	No evidence of lymphoma
T1	Lymphoma involving the conjunctiva alone without eyelid or orbital involvement
T2	Lymphoma with orbital involvement with or without conjunctival involvement
T3	Lymphoma with preseptal eyelid involvement with or without orbital involvement and with or without conjunctival involvement
T4	Orbital adnexal lymphoma and extraorbital lymphoma extending beyond the orbit to adjacent structures, such as bone, maxilofacial sinuses, and brain

[Used with permission of the American Joint Committee on Cancer (AJCC), Chicago, Illinois. The original and primary source for this information is the AJCC Cancer Staging Manual, Eight Edition (2017) published by Springer Science+Business Media]

Staging classification for intraocular retinoblastoma has also evolved over the last 60 years as the treatment strategies have improved. Before the mid-1990s, external beam radiation therapy (EBRT) was considered as the first-line treatment for retinoblastoma. The Reese-Ellsworth classification was proposed to predict response to the radiation [15]. With the advent of systemic chemotherapy combined with focal adjuvant treatments, this classification system has become quickly outdated and has been replaced by the International Intraocular Retinoblastoma Classification (IIRC), also known as the Children's Hospital of Los Angeles (CHLA) classification, created as a result of the International Symposium on Retinoblastoma held in Paris in May 2003 [16–18]. The International Classification for Retinoblastoma (ICRB) or Wills Eye Hospital (WEH) classification, has also been developed to estimate globe salvage after chemotherapy [19]. However, the discrepancies between those classifications in terms of group definitions emphasize the lack of standardization. Lastly, the eighth edition of AJCC/TNM classification has become an accurate tool for prognostication in cases of intraocular retinoblastoma, with the addition of heritability (group H; Hx, H0, H1) as an independent category [20–22], and significant changes have been made in the pathological classification system (Table 9.2). The ability of the eighth edition of the AJCC cancer staging system to

Table 9.2 Definition of primary tumor (T) for retinoblastoma

T Category	T Criteria
Clinical tumor (cT)	
TX	Unknown evidence of intraocular tumor
T0	No evidence of intraocular tumor
T1	Intraocular tumor(s) with subretinal fluid δ 5 mm from the base of any tumor
T1a	Tumors δ 3 mm and > 1.5 mm from the disc and fovea
T1b	Tumors >3 mm or closer than 1.5 mm to the disc and fovea
T2	Intraocular tumor(s) with retinal detachment, vitreous seeding, or subretinal seeding
T2a	Subretinal fluid >5 mm from the base of any tumor
T2b	Tumors with vitreous seeding or subretinal seeding
T3	Advanced intraocular tumor(s)
T3a	Phthisis or pre-phthisis bulbi
T3b	Tumor invasion of the pars plana, ciliary body, lens, zonules, iris, or anterior chamber
T3c	Increased intraocular pressure with neovascularization or buphthalmos
T3d	Hyphema or massive vitreous hemorrhage
T3e	Aseptic orbital cellulitis
T4	Extraocular tumor(s) involving the orbit, including optic nerve
T4a	Radiologic evidence of retrobulbar optic nerve involvement or thickening of the optic nerve or involvement of the orbital tissues
T4b	Extraocular tumor clinically evident with proptosis and orbital mass
Pathologic tumor (pT)	
T1	Intraocular tumor(s) without any local invasion, or with focal choroidal invasion, or pre- or intralaminar involvement of the optic nerve head
T2	Intraocular tumor(s) with local invasion
T2a	Concomitant focal choroidal invasion and pre- or intralaminar involvement of the optic nerve head
T2b	Tumor invasion of stroma of iris and/or trabecular meshwork and/or Schlemm's canal

(continued)

Table 9.2 (continued)

T Category	T Criteria
T3	Intraocular tumor(s) with significant local invasion
T3a	Massive choroidal invasion (> 3 mm in largest diameter, or multiple foci of focal choroidal involvement totaling >3 mm, or any full-thickness choroidal involvement)
T3b	Retrolaminar invasion of the optic nerve head, not involving the transected end of the optic nerve
T3c	Any partial-thickness involvement of the sclera within the inner two thirds
T3d	Full-thickness invasion into the outer third of the sclera and/or invasion into or around emissary channels
T4	Extraocular tumor(s) involving orbit, including optic nerve
T4a	Evidence of extraocular tumor: Tumor at the transected end of the optic nerve, tumor in the meningeal spaces around the optic nerve, full thickness invasion of the sclera with invasion of the episclera, adjacent adipose tissue, extraocular muscle, bone, conjunctiva, or eyelids.
Hereditary trait (H)	
HX	Unknown or insufficient evidence of a constitutional RB1 gene mutation
H0	Normal RB1 alleles in blood tested with demonstrated high-sensitivity assays
H1	Bilateral retinoblastoma, retinoblastoma with an intracranial primitive neuroectodermal tumor (i.e., trilateral retinoblastoma), patient with family history of retinoblastoma, or molecular definition of a constitutional RB1 gene mutation

[Used with permission of the American Joint Committee on Cancer (AJCC), Chicago, Illinois. The original and primary source for this information is the AJCC Cancer Staging Manual, Eight Edition (2017) published by Springer Science+Business Media]

predict both retinoblastoma metastasis-related mortality and globe salvage have been shown by the AJCC Ophthalmic Oncology Task Force (OOTF) in a multicenter, international, registry-based retrospective study [23, 24].

9.3 Purposes of Staging

9.3.1 Prognostic Relevance

For clinicians and patients, cancer staging is a useful clinical tool in determining the chances of survival. For example, Kujala et al. studied the mortality risk of uveal melanoma (UM) based on a TNM-based classification system and showed significant differences among anatomical subcategories of tumors. In an analysis of 7369 patients, they found a 10-year survival rate of 89% for T1 tumors, 77% for T2 tumors, 58% for T3 tumors, and 39% for T4 tumors, respectively [25]. Moreover, the AJCC-OOTF developed an international, multicentered database and validated for the first time the prognostic value of the seventh edition of the AJCC cancer staging system for uveal melanoma on a large cohort of patients [26]. The risk of metastasis at 10 years appears to increase by approximately twofold for each AJCC stage. The eighth edition of the AJCC cancer staging system is largely unchanged from the seventh edition for the T category of posterior uveal melanoma (Table 9.3). For conjunctival melanoma, the predictive value of the eighth edition of the AJCC cancer staging system has been confirmed by many studies, including a multicenter, international study of 288 cases of conjunctival melanomas [27, 28]. The relevance of this knowledge in clinical practice appears to be beneficial on multiple levels by improving the estimation of tumor control and life expectancy.

9.3.2 Therapeutic Relevance

Accurate clinical staging also allows for the identification of appropriate treatment strategies in patients newly diagnosed with primary eye cancer. Multimodality treatment should be considered for aggressive tumors or advanced local disease. Furthermore, patients with metastatic disease at the time of diagnosis should receive palliative therapy. The stage of cancer patients is recorded at initial presentation (pretherapy; cTNM—clinical or pTNM—pathological) as well as at certain times after treatment (posttherapy; yc/ypTNM). Restaging provides additional valuable information about response to treatment and tumor extension over the disease course (rTNM—retreatment classification). For example, routine staging for metastatic spread to the liver in patients with uveal melanoma is highly recommended. The use of a standardized cancer staging classification is critical to efficiently select optimal treatment options in curative, adjuvant, or palliative settings and to develop evidence-based cancer screening guidelines for national programs.

For ocular surface tumors, it has now been well demonstrated that histological examination is the most accurate staging method (Tables 9.4 and 9.5). The introduction of the term T is in the seventh edition of the AJCC classification for conjunctival squamous neoplasia and conjunctival melanoma, referring to a tumor “in situ,” emphasizing the role of pathologic factors such as tumor invasion as prognostic and therapeutic factors. Especially for conjunctival melanomas,

Table 9.3 Definition of primary tumor (T) for uveal melanoma

T Category	T Criteria
TX	Primary tumor cannot be assessed
T0	No evidence of primary tumor
T1	Tumor base δ9 mm with thickness δ6 mm Tumor base 9.1–12 mm with thickness δ3 mm
T1a	Tumor size category 1 without ciliary body involvement and extraocular extension
T1b	Tumor size category 1 with ciliary body involvement
T1c	Tumor size category 1 without ciliary body involvement but with extraocular extension δ5 mm in largest diameter
T1d	Tumor size category 1 with ciliary body and extraocular extension δ5 mm in largest diameter
T2	Tumor base δ 9 mm with thickness 6.1–9 mm Tumor base 9.1–12 mm with thickness 3.1–9 mm Tumor base 12.1–15 mm with thickness δ 6 mm Tumor base 15.1–18 mm with thickness δ 3 mm
T2a	Tumor size category 2 without ciliary body involvement and extraocular extension
T2b	Tumor size category 2 with ciliary body involvement
T2c	Tumor size category 2 without ciliary body involvement but with extraocular extension δ5 mm in largest diameter
T2d	Tumor size category 2 with ciliary body and extraocular extension δ5 mm in largest diameter
T3	Tumor base 3.1–9 mm with thickness 9.1–12 mm Tumor base 9.1–12 mm with thickness 9.1–15 mm Tumor base 12.1–15 mm with thickness 6.1–15 mm Tumor base 15.1–18 mm with thickness 3.1–12 mm
T3a	Tumor size category 3 without ciliary body involvement and extraocular extension
T3b	Tumor size category 3 with ciliary body involvement
T3c	Tumor size category 3 without ciliary body involvement but with extraocular extension δ5 mm in largest diameter
T3d	Tumor size category 3 with ciliary body and extraocular extension δ5 mm in largest diameter
T4	Tumor base 12.1–15 mm with thickness > 15 mm Tumor base 15.1–18 mm with thickness > 12 mm Tumor base >18 mm with any thickness
T4a	Tumor size category 4 without ciliary body involvement and extraocular extension
T4b	Tumor size category 4 with ciliary body involvement
T4c	Tumor size category 4 without ciliary body involvement but with extraocular extension δ5 mm in largest diameter
T4d	Tumor size category 4 with ciliary body and extraocular extension δ5 mm in largest diameter
T4e	Any tumor size category with extraocular extension >5 mm in largest diameter

[Used with permission of the American Joint Committee on Cancer (AJCC), Chicago, Illinois. The original and primary source for this information is the AJCC Cancer Staging Manual, Eight Edition (2017) published by Springer Science+Business Media]

Table 9.4 Definition of primary tumor (T) for conjunctival carcinoma [5]

T Category	T Criteria
TX	Primary tumor cannot be assessed
T0	No evidence of primary tumor
Tis	Carcinoma in situ
T1	Tumor (≤ 5 mm in greatest dimension) invades through the conjunctival basement membrane without invasion of adjacent structures
T2	Tumor (> 5 mm in greatest dimension) invades through the conjunctival basement membrane without invasion of adjacent structures
T3	Tumor invades adjacent structures (excluding the orbit)
T4	Tumor invades the orbit with or without further extension
T4a	Tumor invades orbital soft tissue without bone invasion
T4b	Tumor invades bone
T4c	Tumor invades adjacent paranasal sinuses
T4d	Tumor invades brain

[Used with permission of the American Joint Committee on Cancer (AJCC), Chicago, Illinois. The original and primary source for this information is the AJCC Cancer Staging Manual, Eight Edition (2017) published by Springer Science+Business Media]

tumor thickness, and histologic ulceration have been reported as independent risk factors for nodal metastasis, for distant metastasis, and for mortality but not caruncle or nonbulbar involvement [29, 30]. The depth of substantia propria invasion is also used to determine the indication of sentinel lymph node (SLN) biopsy, which assists in making a correct staging and therapeutic planning (e.g. adjuvant systemic therapy) [31].

9.3.3 Research Relevance

Eye cancers are quite uncommon. According to the American Cancer Society, the estimated number of new cases diagnosed for eye and orbit tumors in the US for 2024 is about 3320, with a stable incidence of approximately six new cases of ocular melanoma per million every year [32–34]. The US incidence is similar to that observed in studies conducted in Canada between 2011–2017 [35] By the harmonization of the cancer terminology, a uniform staging classification enables the international scientific community to collaborate and share data [36]. It helps to establish eligibility criteria for clinical trials and facilitate the comparison of study results from many different centers. Due to the high level of proto-

Table 9.5 Definition of primary tumor (T) for conjunctival melanoma

T Category	T Criteria
Clinical tumor (cT)	
TX	Primary tumor cannot be assessed
T0	No evidence of primary tumor
T1	Tumor of the bulbar conjunctiva
T1a	< 1 quadrant
T1b	ε 1 to <2 quadrants
T1c	ε 2 to <3 quadrants
T1d	ε 3 quadrants
T2	Tumor of the nonbulbar (forniceal, palpebral, and tarsal) conjunctiva and tumor involving caruncle
T2a	Noncaruncular and δ 1 quadrant of the nonbulbar conjunctiva involved
T2b	Noncaruncular and > 1 quadrant of the nonbulbar conjunctiva involved
T2c	Caruncular and δ 1 quadrant of the nonbulbar conjunctiva involved
T2d	Caruncular and > 1 quadrant of the nonbulbar conjunctiva involved
T3	Tumor of any size with local invasion
T3a	Globe
T3b	Eyelid
T3c	Orbit
T3d	Nasolacrimal duct and/or lacrimal sac and/or paranasal sinuses
T4	Tumor of any size with invasion of the central nervous system
Pathologic tumor (pT)	
TX	Primary tumor cannot be assessed
T0	No evidence of primary tumor
Tis	Melanoma confined to conjunctival epithelium
T1a	Tumor of the bulbar conjunctiva with invasion of the substantia propria, not >2.0 mm in thickness
T1b	Tumor of the bulbar conjunctiva with invasion of the substantia propria, > 2.0 mm in thickness
T2a	Tumor of the nonbulbar conjunctiva with invasion of the substantia propria not 2.0 mm in thickness
T2b	Tumor of the nonbulbar conjunctiva with invasion of the substantia propria 2.0 mm in thickness
T3a	Globe
T3b	Eyelid
T3c	Orbit
T3d	Nasolacrimal duct, lacrimal sac, and/or paranasal sinuses
T4	Tumor of any size with invasion of the central nervous system

[Used with permission of the American Joint Committee on Cancer (AJCC), Chicago, Illinois. The original and primary source for this information is the AJCC Cancer Staging Manual, Eight Edition (2017) published by Springer Science+Business Media]

col compliance and the large number of patients enrolled, the Collaborative Ocular Melanoma Study (COMS) has made important contributions to scientific peer-reviewed literature and healthcare management in conducting prospective multicenter randomized controlled trials [37–40].

9.4 Summary

The fundamental role of staging is to define tumor characteristics that reliably guide clinicians in estimation of prognosis, planning of initial treatments, and evaluation of outcomes. However, eye cancer is a heterogenous group of tumors, and their cancer staging is becoming complex as multiple new genetic factors and molecular biomarkers impact therapy and prognosis. These nonanatomic factors include among others gene expression profiling patterns, chromosomal alterations, and tumor biology. To enhance prognostic information and patient care, the challenge of the future staging system will be to integrate both anatomic and nonanatomic variables while remaining timely and accessible to developed and developing countries.

References

1. International Union against Cancer (UICC). TNM classification of malignant tumours. 2nd ed. Geneva: WHO; 1974.
2. Denoix PF. Nomenclature classification of cancer. Bull Inst Nat Hyg (Paris). 1952;7:743–8.
3. Fleming ID. AJCC/TNM cancer staging, present and future. J Surg Oncol. 2001;77(4):233–6.
4. Hermanek P, Sobin L. TNM classification of malignant tumors. 4th ed. New York: Springer; 1987.
5. Amin MB, Edge SB, Greene FL, Compton CC. AJCC cancer staging manual. 8th ed. New York: Springer; 2017.
6. Musshoff K. Clinical staging classification of non-Hodgkin's lymphomas. Strahlentherapie. 1977;153(4):218–21.
7. Margo CE, Mulla ZD. Malignant tumors of the orbit. Analysis of the Florida Cancer registry. Ophthalmology. 1998;105(1):185–90.
8. Coupland SE, White VA, Rootman J, Damato B, Finger PT. TNM staging of ocular adnexal lymphomas. In: SE LE, Byrd DR, Carducci MA, Compton CA, editors. AJCC cancer staging manual. 7th ed. New York: Springer; 2009.
9. Coupland SE, White VA, Rootman J, Damato B, Finger PT. A TNM-based clinical staging system of ocular adnexal lymphomas. Arch Pathol Lab Med. 2009;133(8):1262–7.
10. Rath S, Connors JM, Dolman PJ, Rootman J, Rootman DB, White VA. Comparison of American joint committee on cancer TNM-based staging system (7th edition) and Ann Arbor classification for predicting outcome in ocular adnexal lymphoma. Orbit. 2014;33(1):23–8.
11. Sniegowski MC, Roberts D, Bakhourn M, Mc Laughlin P, Yin VT. Ocular adnexal lymphoma: validation of American joint committee on cancer seventh edition staging guidelines. Br J Ophthalmol. 2014;98(9):1255–60.

12. Aronow ME, Portnell CA, Rybicki LA, Sweeenham JW, Singh AD. Ocular adnexal lympoma: assessment of a tumor-node-metastasis staging system. Ophthalmology. 2013;120(9):1915–9.
13. Kwon M, Lee JS, Lee C, et al. Prognostic factors for relapse and survival among patients with ocular adnexal lymphoma: validation of the eight edition of the American joint committee on cancer (AJCC) TNM classification. Br J Ophthalmol. 2021;105(2):279–84.
14. Olsen TG, Holm F, Mikkelsen LH, et al. Orbital lymphoma-an international multicenter retrospective study. Am J Ophthalmol. 2019;199:44–57.
15. Reese AB, Ellsworth RM. The evaluation and current concept of retinoblastoma therapy. Trans Am Acad Ophthalmol Otolaryngol. 1963;67:164–72.
16. Shields CL, Mashayekhi A, Au AK, et al. The international classification of retinoblastoma predicts chemoreduction success. Ophthalmology. 2006;113(12):2276–80.
17. Murphree AL. Intraocular retinoblastoma: the case for a new group classification. Ophthalmol Clin N Am. 2005;18(1):41–53.
18. Chantada G, Doz F, Antonelli CB, Grundy R, Clare Stannard FF, Dunkel IJ. A proposal for an international retinoblastoma staging system. Pediatr Blood Cancer. 2006;47(6):801–5.
19. Shields CL, Shields JA. Basic understanding of current classification and management of retinoblastoma. Curr Opin Ophthalmol. 2006;17:228.
20. Mallipatna A, Marino M, Singh AD. Genetics of retinoblastoma. Asia Pac J Ophthalmol (Phila). 2016;5:260–4.
21. Mallipatna A, Gallie BL, Chévez-Barrios P, Lumbroso-Le RL, Chantada G. Retinoblastoma. In: Amin M, Edge SM, Greene FL, et al., editors. The AJCC cancer manual. 8th ed. New York: Springer; 2016.
22. Yousef YA, Al-Hussaini M, Mehyar M, Sultan IY, Jaradat I. Predictive value of TNM classification, international classification, and Reese-Ellsworh staging of retinoblastoma for the likelihood of high-risk pathologic features. Retina. 2015;35(9):1883–9.
23. Tomar AS, Finger PT, Gallie Mallipatna A, et al. A multicenter, international collaborative study for American joint committee on cancer staging of retinoblastoma: part I: metastasis-associated mortality. Ophthalmology. 2020;127(12):1719–32.
24. Tomar AS, Finger PT, Gallie B, Mallipatna, et al. A multicenter, international collaborative study for american joint committee on cancer staging of retinoblastoma: part II: treatment success and globe salvage. Ophthalmology. 2020;127(12):1733–46.
25. Kujala E, Damato B, Coupland SE, Desjardins L, Bechrakis NE. Staging of ciliary body and choroidal melanomas based on anatomic extent. J Clin Oncol. 2013;31(22):2825–31.
26. The AJCC Ophthalmic Oncology Task Force. International validation of the American joint committee on cancer's 7th edition classification of uveal melanoma. JAMA Ophthalmol. 2015;133(4):376–83.
27. Jain P, Finger PT, Damato B, Coupland SE, et al. Multicenter, international assessment of the eighth edition of the American joint committee on cancer cancer staging manual for conjunctival melanoma. JAMA Ophthalmol. 2019;137:905–11.
28. Jia S, Zhu T, Shi H, et al. American joint committee on cancer tumor staging system predicts the outcome and metastasis pattern in conjunctival melanoma. Ophthalmology. 2022;129(7):P771–80.
29. Esmaeli B. Inclusion of histologic ulceration and tumor thickness in future American joint committee on cancer T category definitions for conjunctival melanoma. JAMA Ophthalmol. 2019;137:912–3.
30. Esmaeli B, Rubin ML, Xu S, et al. Greater tumor thickness, ulceration, and positive sentinel lymph node are associated with worse prognosis in patients with conjunctival melanoma: implications for future AJCC classifications. Am J Surg Pathol. 2019;43:1701–10.
31. Wong SL, Balch CM, Hurley P, Agarwala SS, et al. Sentinel lymph node biopsy for melanoma: American Society of Clinical Oncology and Society of Surgical Oncology joint clinical practice guideline. J Clin Oncol. 2012;30:2912–8.
32. American Cancer Society. Cancer Facts & Figures 2018. Atlanta: American Cancer Society; 2018.
33. Aronow ME, Topham AK, Singh AD. Uveal melanoma: 5-year update on incidence, treatment, and survival (SEER 1973-2013). Ocul Oncol Path. 2018;4:145–51.
34. Inskip PD, Devesa SS, Fraumeni JF Jr. Trends in the incidence of ocular melanoma in the United States, 1974-1998. Cancer Causes Control. 2003;14(3):251–7.
35. Conte S, Lagacé F, Ghazawi, et al. Uveal melanoma incidence trends in Canada: 1992-2919 vs. 2011-2017. Front Med (Lausanne). 2023;24(9):1001799.
36. Finger PT. The 7th edition AJCC staging system for eye cancer: an international language for ophthalmic oncology. Arch Pathol Lab Med. 2009;133(8):1197–8.
37. Hawkins BS. The collaborative ocular melanoma study (COMS) randomized trial of pre-enucleation radiation of large choroidal melanoma, IV: ten-year mortality findings and prognostic factors. COMS report number 24. Am J Ophthalmol. 2004;138(6):936–51.
38. Group COMS. The COMS randomized trial of iodone 125 brachytherapy for choroidal melanoma, V: twelve-year mortality rated and prognostic factors. COMS report no. 28. Arch Ophthalmol. 2006;124(12):1684–93.
39. Damato B. Legacy of the collaborative ocular melanoma study. Arch Ophthalmol. 2007;125(7):966–8.
40. Jampol LM, Moy CS, Murray TG. The COMS randomized trial of iodine 125 brachytherapy for choroidal melanoma: IV. Local treatment failure and enucleation in the first 5 years after brachytherapy. COMS report No. 19. Ophthalmology. 2002;109:2197–206.

Principles of Cryotherapy

10

Dan S. Gombos and Kayla Walter

10.1 Introduction

Cryotherapy (or cryosurgery) is the technique of precise freezing and thawing of undesirable tissue, resulting in cell death and regression. It is a highly effective technique available to the ophthalmologist for local control and eradication of various intra-and periocular tumors and can serve as an alternative or adjunct to other methods such as surgical excision or radiotherapy.

Arnott described using crushed ice and salt (NaCl) to freeze advanced breast and uterine malignancies in the mid-nineteenth century [1]. By the beginning of the twentieth century, solid CO_2 was being used to treat various skin and gynecologic cancers [1]. During this period, most freezing devices were crude and were only able to penetrate superficial layers of tissue, which limited their clinical application.

The commercial availability of liquid nitrogen and the introduction of the cryoprobe by Cooper and Lee in the 1960s heralded significant advancements in the field [1, 2]. For the ophthalmologist, modification of the cryoprobe led to significant surgical advances in cataract extraction, glaucoma management, and repair of retinal tears. Subsequent pioneering work by Lincoff [3], Fraunfelder [4], and Jackobeic [5] led to the application of cryotherapy in the management of various intra-and periocular tumors.

10.2 Mechanism of Tissue Injury

Initially, the cryoprobe begins cooling the tissues with the removal of heat. Over time, tissue in contact with the probe freezes. Subsequently, the freezing interface progresses in an outward direction, resulting in a temperature distribution that is coldest at the point of contact with the probe. Once freezing is complete, thawing is facilitated by heat from the adjacent tissues [1, 6].

10.2.1 Direct Effects

Microscopically, the initial decline in temperature in the extracellular space forms crystals, leading to a hyperosmotic environment that extracts water from the cells and causes them to shrink. As the temperature lowers, intracellular crystals form, leading to disruption of organelles and cell membranes. This affects the ability of membrane proteins to control intracellular ionic content. During the thawing phase, as the frozen water crystals dissolve, the extracellular space becomes hypotonic. Limited only by a defective cell membrane, extracellular water enters the cell and disrupts it [7]. In addition, the cold temperature physically disrupts the cellular cytoskeleton and denatures proteins [1, 6].

Cells at the center of the cryoablated tissue die from the disruptive process of extra-and intracellular ice formation after reaching a temperature below −40 °C [8]. However, for the peripheral cells that do not reach −40 °C, apoptosis and necrosis are the main pathways of cell death [9]. Both the intrinsic (mitochondrial) and extrinsic (membrane) pathways of apoptosis are activated in the peripheral cells following freezing at temperatures above −40 °C [9]. In tissue frozen to −30 °C, early onset apoptosis occurred within 90 minutes of thawing via membrane-mediated apoptosis [9]. In frozen tissue reaching −15 °C, apoptosis is delayed, occurring 6–24 h post-thaw via the mitochondrial apoptotic pathway. Post-thaw, there are elevated levels of the proapoptotic protein Bax in the cell, which releases cytochrome c from the mitochondria, a step in the mitochondrial pathway of apoptosis [10, 11].

D. S. Gombos (✉) · K. Walter
Department of Head and Neck, MD Anderson Cancer Center, Houston, TX, USA
e-mail: dgombos@mdanderson.org

© The Author(s), under exclusive license to Springer Nature Switzerland AG 2025

A. D. Singh, B. E. Damato (eds.), *Clinical Ophthalmic Oncology*, https://doi.org/10.1007/978-3-031-75907-9_10

10.2.2 Indirect Effects

Freezing temperatures are also associated with vascular stasis and cellular anoxia. Initially, the cold temperatures lead to vasoconstriction followed by vasodilation, increased vascular permeability, and edema during the thawing process. Endothelial damage leads to stagnation of blood and thrombus formation. The resultant hypoxia promotes tissue necrosis. Some experiments suggest that this mechanism is more important in the death of tumor cells than direct injury from freezing.

10.3 Technical Aspects

Certain technical factors such as tissue temperature, cooling rate, freeze-thaw cycle, and the number of repetitions influence the efficacy of cryotherapy [12, 13].

10.3.1 Tissue Temperature

Tissue temperature is the most important factor, with cell death occurring at temperatures between −20 and − 50 °C [14]. Reaching a temperature below −40 °C has been found to be effective when held at −40 °C for at least 1 min for two freeze-thaw cycles [8].

10.3.2 Cooling Rate

A rapid cooling rate is more effective in causing cell death. The cooling rate is dependent in part on the cryoprobe used.

10.3.3 Freeze-Thaw Cycle

Studies indicate that a slow thaw is among the most important variables contributing to cell death. A slow thaw is obtained by allowing the heat from the surrounding tissue to spread to the frozen tissue.

10.3.4 Number of Repetitions

Multiple freeze-thaw cycles further increase cell damage and death [15]. Some cancer cells may be able to avoid cell death even at temperatures of −40 °C, so a minimum of two freeze-thaw cycles is necessary to ensure the death of malignant cells [8].

10.4 Indications

Over the past 40 years, the indications for cryotherapy have expanded to a number of intra-and periocular tumors. In some instances, it serves as primary treatment, while in others, it functions in an adjuvant setting.

10.4.1 Eyelid Tumors

Eyelid lesions, including actinic and seborrheic keratosis, are generally amenable to cryotherapy, sometimes combined with surgical excision. Basal cell carcinoma, particularly lesions less than 1 cm in diameter, can be cured with this approach. Select cases of squamous cell and meibomian gland carcinoma of the lid have also been treated with cryotherapy as an alternative to surgical excision and/or radiotherapy [16–19].

10.4.2 Conjunctival Tumors

In the adjuvant setting, cryotherapy plays an important role in the management of conjunctival lesions. Conjunctival intraepithelial neoplasia and squamous cell carcinoma [20], conjunctival melanoma, and primary acquired melanosis with atypia [5] are amenable to adjuvant cryotherapy [21]. Treatment of ocular surface squamous neoplasia (OSSN) with excision and adjuvant cryotherapy has been shown to have a recurrence rate as low as 7.1% [22], and when compared to topical interferon alpha 2b therapy, there is no difference in recurrence rate [23]. It has also been described in the management of large bulky lesions where complete excision was challenging, including papillomas and lymphomas [24].

10.4.3 Intraocular Tumors

Certain intraocular tumors (particularly those anterior to the equator) are amenable to cryotherapy as the treatment of choice. Small peripheral retinal capillary hemangioblastomas [25], Coats's disease, and retinoblastoma foci (those less than 2 mm in thickness) respond well to cryotherapy [26, 27].

10.4.4 Orbital Tumors

The cryoprobe can be used intraoperatively to assist in the excision of orbital lesions such as cavernous hemangiomas and dermoid cysts. The probe is applied directly to the lesion,

allowing for traction and careful dissection from adjacent structures. The technique of freezing uveal melanoma prior to transection of the optic nerve ("no touch" enucleation) is rarely used today [28, 29]. It was proposed as a mechanism to reduce hematologic dissemination of intraocular cancer cells.

10.5 Techniques of Cryotherapy

Cryotherapy can be applied in various fashions depending upon the indication and location of the tumor.

10.5.1 Eyelid Tumors

Eyelid tumors can be treated with a liquid nitrogen spray. Following local anesthesia, the area is draped, and an ocular protector is placed over the eye to prevent freezing of the globe or adjacent structures. A thermocouple is inserted into the center of the lesion to monitor its temperature (recommended target temperature − 50 °C). Freezing is applied to the lesion and a margin of adjacent normal-appearing skin. A double freeze cycle is usually administered.

10.5.2 Conjunctival Tumors

Conjunctival tumors are generally treated with a hammerhead-shaped cryoprobe. In most instances, cryotherapy is performed as an adjunct to surgical excision. Following removal of the tumor, double or triple cryotherapy is administered to the underside of the conjunctiva (adjacent to the resection) and the scleral bed [21]. Cryotherapy as primary therapy can also be performed with newly designed cryoprobes [30].

10.5.3 Intraocular Tumors

Intraocular lesions (such as retinoblastoma and retinal capillary hemangioblastoma) are generally treated using a nitrous oxide retinal cryoprobe (Fig. 10.1). Local (retrobulbar) or general anesthesia (for children) is indicated. Using indirect ophthalmoscopy and scleral indentation, the lesion is isolated (Fig. 10.2). It is frozen under direct visualization such that the resulting ice ball completely encompasses the entire tumor (usually to a temperature of −70 °C). The lesion is allowed to slowly thaw, and the freeze-thaw cycle is repeated

Fig. 10.1 A retinal cryoprobe. Note the ice ball on the tip of the probe

Fig. 10.2 Technique for transcleral cryotherapy of an intraocular tumor under indirect ophthalmoscopic visualization

three times for retinoblastoma and Coats' disease [26, 27, 31]. The tumor is reexamined in 4–6 weeks and may require additional therapy. Most lesions can be treated transconjunctivally; however, those significantly posterior to the equator may require a conjunctival incision [26].

10.6 Complications

While cryotherapy is generally safe and effective, there are numerous complications that must be considered [32]. In most instances, transient edema and injection occur at the site of treatment. Lesions on the eyelid and close to the lash margin can develop ptosis, trichiasis, and ectropion. Hypertrophic scarring can occur, as can skin depigmentation in darker patients. Tissue cracking secondary to persistent probe adherence can occur if the probe is not allowed to fully thaw.

The conjunctiva generally tolerates freezing well. However, repeated application can lead to limbal stem cell failure, dry eye, and symblepharon formation. Periocular edema and pain are not uncommon following cryotherapy of intraocular lesions. Uveitis may develop, requiring the use of topical steroids. Cryotherapy can increase the risk of exudative and rhegmatogenous retinal detachments as well as vitreous hemorrhage. Muscle paresis and changes in pupillary response have also been described.

10.7 Conclusions

Cryotherapy is an excellent means of treating certain intra- and periocular tumors. In ophthalmic oncology, this generally translates to high cure rates and minimal ocular morbidity. Cryotherapy is effective in treating small and well-defined tumors. Good technique is critical, with a rapid freeze and slow thawing being most effective in causing cell death. Multiple freeze-thaw cycles further increase treatment effectiveness. When indicated, cryotherapy can serve as an alternative to more destructive treatment modalities such as surgical excision, chemotherapy, and radiation therapy.

References

1. Rubinsky B. Cryosurgery. Annu Rev Biomed Eng. 2000;21:157–87.
2. Cooper I, Lee A. Cryostatic congelation: a system for producing a limited controlled region of cooling or freezing of biological tissue. J Nerv Ment Dis. 1961;1961:259–63.
3. Lincoff H, McLean J, Long R. The cryosurgical treatment of intraocular tumors. Am J Ophthalmol. 1967;63:389–99.
4. Fraunfelder FT, Wallis TR, Farris HE, et al. The role of cryosurgery in external ocular and periocular disease. Trans Am Acad Ophthalmol Otolaryngol. 1977;83:713–24.
5. Jokobiec FA, Rini FJ, Fraunfelder FT, et al. Cryotherapy for conjunctival primary acquired melanosis and malignant melanoma. Experience with 62 cases. Ophthalmology. 1988;95:1058–70.
6. Gage AA, Baust J. Mechanisms of tissue injury in cryosurgery. Cryobiology. 1998;37:171–86.
7. Muldrew K, McGann LE. The osmotic rupture hypothesis of intracellular freezing injury. Biophys J. 1994;66:532–41.
8. Baust JG, Gage AA, Bjerklund Johansen TE, Baust JM. Mechanisms of cryoablation: Clincal consequences on malignant tumors. Cryobiology. 2014;68:1–11.
9. Robilotto AT, Baust JM, Van Buskirk RG, Gage AA, Baust JG. Temperature-dependent activation of differential apoptotic pathways during cryoablation in a human prostate cancer model. Prostate Cancer Prostatic Diseases. 2013;16:41–9.
10. Baust JG, Gage AA, Robilottto AT, Baust JM. The pathophysiology of thermoablation: optimizing cryoablation. Curr Opin Urology. 2009;19:127–32.
11. Elmore S. Apoptosis: a review of programmed cell death. Toxicol Pathol. 2007;35(4):495–516.
12. Gage AA, Baust JG. Cryosurgery for tumors—a clinical overview. Technol Cancer Res Treat. 2004;3:187–99.
13. Baust JG, Gage AA. Progress towards optimization of cryosurgery. Technol Cancer Res Treat. 2004;3:95–101.
14. Gage AA. What temperature is lethal for cells? J Dermatol Surg Oncol. 1979;5:459–60.
15. Gill W, Fraser J, Carter D. Repeated freeze-thaw cycles in cryosurgery. Nature. 1968;219:410–3.
16. Bullock JD, Beard C, Sullivan JH. Cryotherapy of basal cell carcinoma in oculoplastic surgery. Am J Ophthalmol. 1976;82:841–7.
17. Lubritz RR. Cryosurgery for benign and malignant skin lesions: treatment with a new instrument. South Med J. 1976;69:1401–5.
18. Fraunfelder FT, Zacarian SA, Wingfield DL, et al. Results of cryotherapy for eyelid malignancies. Am J Ophthalmol. 1984;97:184–8.
19. Kuflik EG. Cryosurgery updated. J Am Acad Dermatol. 1994;31:925–44.
20. Divine RD, Anderson RL. Nitrous oxide cryotherapy for intraepithelial epithelioma of the conjunctiva. Arch Ophthalmol. 1983;101:782–6.
21. Shields JA, Shields CL, De Potter P. Surgical approach to conjunctival tumors. The 1994 Lynn B. McMahan Lecture. Arch Ophthalmol. 1997;115:808–15.
22. Li AS, Shih CT, Rosen L, Steiner A, Milman T, Udell I. Recurrence of ocular surface squamous neoplasia treated with excisional biopsy and cryotherapy. Am J Ophthalmol. 2015;160(2):213–9.
23. Nanji AA, Moon CS, Galor A, Sein J, Oellers P, Karp CL. Surgical versus medical treatment of ocular surface squamous neoplasia: a comparison of recurrences and complications. Ophthalmology. 2014;121(5):994–1000.
24. Eichler MD, Fraunfelder FT. Cryotherapy for conjunctival lymphoid tumors. Am J Ophthalmol. 1994;118:463–7.
25. Singh AD, Nouri M, Shields CL, et al. Treatment of retinal capillary hemangioma. Ophthalmology. 2002;109:1799–806.
26. Shields JA, Parsons H, Shields CL, et al. The role of cryotherapy in the management of retinoblastoma. Am J Ophthalmol. 1989;108:260–4.
27. Sigler EJ, Randloph JC, Clazada JI, Wilson MW, Haik BG. Current management of coats disease. Surv Ophthalmol. 2012;59:30–46.
28. Fraunfelder FT, Boozman FW, Wilson RS, et al. No-touch technique for intraocular malignant tumors. Arch Ophthalmol. 1977;95:1616–20.
29. Wilson RS, Fraunfelder FT. "No-touch" cryosurgical enucleation: a minimal trauma technique for eyes harboring intraocular malignancy. Ophthalmology. 1978;85:1170–5.
30. Finger PT. "Finger-tip" cryotherapy probes: treatment of squamous and melanocytic conjunctival neoplasia. Br J Ophthalmol. 2005;89:942–5.
31. Mehta M, Sethi S, Pushker N, Kashyap S, Sen S, Bajaj MS, Ghose S. Retinoblastoma. Singapore Med J. 2012;53(2):128–36.
32. Wood JR, Anderson RL. Complications of cryosurgery. Arch Ophthalmol. 1981;99:460–3.

Principles of Laser Therapy

11

Hatem Krema

11.1 Introduction

The word LASER is an acronym for Light Amplification by Stimulated Emission of Radiation. In 1917, Albert Einstein postulated the basis of stimulated emission, which is the physical principle of laser generation [1].

Photon is the energy unit of the electromagnetic radiation spectrum that includes visible light. When a photon hits an electron revolving in its orbit around a nucleus, the electron absorbs the photon energy and bounces to revolve around the nucleus at a higher orbit. The atom is described then to be in an "excited state."

Stimulated emission is the process in which the electrons of atoms in the excited state are hit by passing photons known as "stimulating photons," causing these electrons to bounce back to their original orbit with the emission of their absorbed energy as photons, which propagate in the same direction, phase, and wavelength of the stimulating photons (Fig. 11.1).

In a state where more atoms are in an excited state than in a normal state, "population inversion" must be reached in a medium for stimulated emission to occur by the stimulating photons, which causes light amplification. This can be achieved by using an excitation source that can "pump" photons into the medium.

The medium is an optical cavity in which the emitted photons reflect back and forth between two mirrors at either end. This leads to the potentiation of the light rays as the trapped reflected light stimulates the emission of new photons. Eventually, amplified light can escape through one of the mirrors, which is made to be partially reflective, producing a laser beam.

The laser beam thus differs from ordinary light in being "unidirectional," "monochromatic," and spatially "coherent." Spatial coherence allows the laser beam to remain narrow over a great distance (collimation) to focus beam energy into a tight spot.

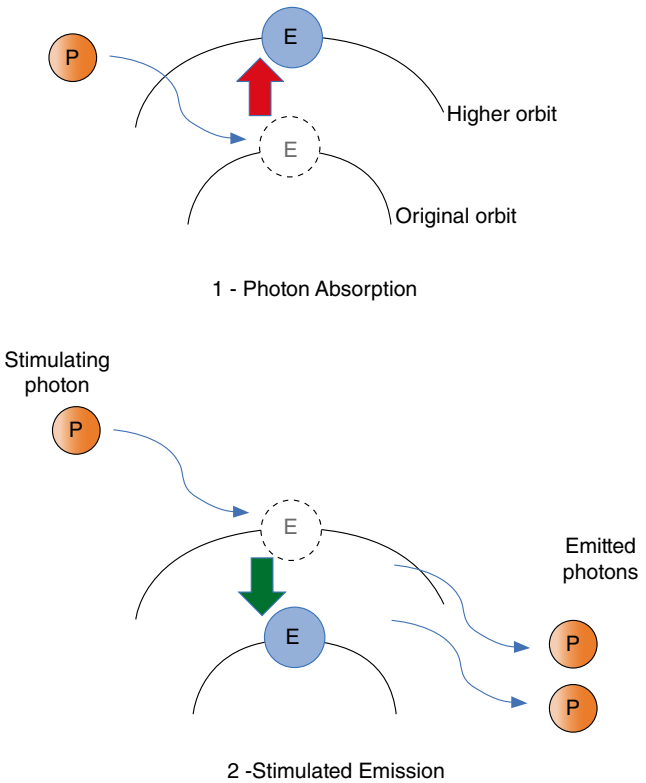

Fig. 11.1 Mechanism of stimulated emission. (**1**) Absorption of photon energy by an electron causes the bouncing of an electron to a higher orbit. (**2**) Stimulating photon hits the electron of an excited atom that causes electron to bounce to its original orbit with the release of a photon that moves with the stimulating photon in an identical phase, wavelength, and direction

The wavelength spectrum of ophthalmic lasers extends from 193 to 10,800 nm, including the visible light spectrum (390–700 nm). The shorter the wavelength of a laser, the higher its photon frequency and energy.

Emitted laser duration can vary from femtosecond pulses to infinity (continuous wave laser). Pulsed laser durations include pulses down to 1 ms produced by electronic shutters,

H. Krema (✉)
Ocular Oncology Service, Princess Margaret Cancer Center, University Health Network, Toronto, ON, Canada

© The Author(s), under exclusive license to Springer Nature Switzerland AG 2025

A. D. Singh, B. E. Damato (eds.), *Clinical Ophthalmic Oncology*, https://doi.org/10.1007/978-3-031-75907-9_11

a few microsecond pulses by pulsed flash lamps, nanosecond pulses (Q-switching), and femtosecond pulses (mode locking) [2].

11.2 Laser Effects on Tissues

11.2.1 Photothermal Effects

This effect depends upon the interaction between tissue chromophores (pigments) and laser wavelength, where absorbed laser energy by tissue chromophores is converted to thermal energy. Laser absorption by ocular tissue chromophores includes melanin, blood, and xanthophyll for visible light wavelengths, proteins for ultraviolet wavelength, and water for infrared wavelengths. The effect on tissue is a function of temperature degree and exposure duration. The effects may include vaporization, coagulation, and necrosis [3].

11.2.2 Photochemical Effects

Reactions such as isomerization of 11-cis retinal to all-trans retinal in photoreceptors upon light exposure are chemical and not associated with an appreciable thermal change. The photochemical effect is the principle of photodynamic therapy, in which a certain laser wavelength excites the molecules of a photosensitive dye injected through the blood. The excited photosensitizer transfers its energy to tissue oxygen, producing radicals that cause irreversible oxidation of cell structures in the areas where the dye accumulates, such as the walls of vascular tissue [4, 5].

11.2.3 Photomechanical Effects

Photodisruption occurs when laser absorption results in a rapid rise of tissue temperature beyond the vaporization threshold. In transparent ocular tissues, without pigment absorption, when high laser energy is delivered in the range of microseconds to nanoseconds, it could produce tissue ionization, plasma status, and vaporization temperatures above 100 °C producing explosive vapor bubbles, which could rupture nearby tissue or eject fragments of tissue from surfaces. This is the principle of excimer laser used for corneal surgeries [6, 7].

11.2.4 Types of Ophthalmic Lasers

Earlier types of lasers, such as xenon lamp, ruby laser, krypton, and dye laser, are currently not in common use for ophthalmic treatments [8, 9]. The commonly used ophthalmic lasers are summarized in Table 11.1.

11.2.5 Treatment Variables

Several variables influence the laser's impact on tissues. These include:

- Tissue absorption spectra:
  The amount of specific pigment in a tissue determines the degree of energy absorption by that tissue. The peak absorption spectrum varies for different pigments. For macular xanthophyll pigment within the neurosensory retina, the peak wavelength absorption is 420–500 nm, for melanin within the retinal pigment epithelial cells and choroidal melanocytes is 400–1000 nm, and for hemoglobin within red blood cells is 450–550 nm [10] (Fig. 11.2).
- Media clarity:
  Opacities in the path of the laser beam could interfere with efficient energy delivery because of light absorption and scattering. Longer wavelengths suffer less scattering and could penetrate deeper through blood or media opacity [11].
- Pulse duration:
  At shorter pulse durations, the width and axial extent of the retinal laser burns are smaller and less dependent on variations in laser power than at longer durations. Reduction of pulse duration is usually associated with more treatment tolerability [12].

Table 11.1 The currently used ophthalmic lasers

Laser type	Wavelength	Pulse duration	Effect on tissues
Excimer	193 nm	3–20 ns	Ablation
Argon	70% 488 + 30% 514 nm	[a]CW or ms pulses	Thermal
Diode	810 (635–1550) nm	CW to ns	Thermal + chemical
Nd:YAG	1064 (×2 frequency 532) nm	CW to 100 ps	Thermal + mechanical
Ho:YAG	2.12 μm	250 μs–100 ns	Thermal + mechanical
Er:YAG	2.94 μm	250 μs–100 ns	Thermal + mechanical
CO_2	9.2–10.8 μm	CW or ms pulses	Thermal

[a]*CW* continuous wave

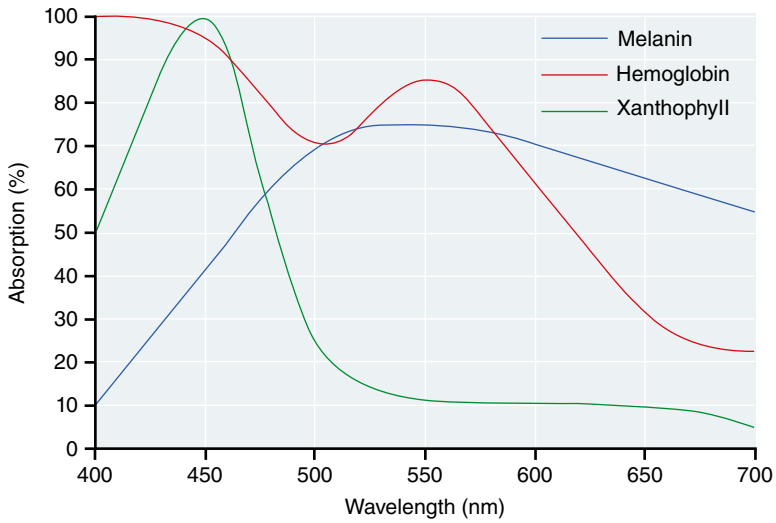

Fig. 11.2 Absorption spectra of visible wavelengths by three ocular pigments (melanin, hemoglobin, and xanthophyll). (Modified from Peyman et al. [10])

Table 11.2 The field of view and laser spot magnification of different auxiliary lenses

Lens type	Field of view	Spot magnification
Goldmann three-mirror	140°	1.08×
Mainster Wide Field	120°	1.5×
Mainster PRP 165	180°	1.96×
Mainster Standard	100°	1.05×
QuadrAspheric	140°	1.92×
Area Centralis	80°	0.92×

- Spot size:
  For a certain laser impact on tissues, the spot size is generally directly proportionate to the laser power. Thus, using a larger spot size requires a proportionate increase in laser power to maintain the same tissue impact. Reduction of spot size is usually associated with more treatment tolerability [13].
- Auxiliary lens magnification:
  The actual laser spot size on the retina can change from the emitted laser spot size by a magnification factor of the auxiliary lens used during laser delivery [13, 14] (Table 11.2).

11.2.6 Laser Delivery Systems

- Slit lamp mounted: It is the most frequent laser delivery method. Recently, Pattern Scan Laser allowed for the simultaneous delivery of multiple uniform laser burns by a single foot pedal press, thus reducing treatment session time. Advanced systems with retinal navigation and camera-based delivery allowed for fast customized laser applications monitored by the physician on a wide screen [15].
- Indirect ophthalmoscope attachment: Suitable for peripheral lesions and for pediatric patients under anesthesia.
- Fiber-optic probe: For endophotocoagulation, used during vitrectomy procedures and for transscleral laser treatment, e.g., cyclophotoablation, or treatment of small peripheral fundus tumors [9, 16, 17].

11.3 Techniques of Ophthalmic Laser Therapy

11.3.1 Laser Photocoagulation

It entails the use of high-intensity laser energy to raise the temperature of the target spot by several degrees above the body temperature to induce tissue coagulation. Currently, the commonly used lasers are frequency-doubled Nd:YAG 523 nm and argon laser. The laser energy is primarily absorbed by melanin in the RPE and choroid and by blood hemoglobin. The generated heat diffuses from RPE and melanocytes, resulting in coagulation of the adjacent photoreceptors and inner retina. This heat diffusion can be limited by using smaller spot sizes and shorter pulses to reduce injury to the neuroretina [3, 10, 18].

The advent of subthreshold laser delivery by "micropulse" technology ameliorated retinal side effects while still allowing for the full therapeutic effect [17, 19].

The thermal energy produced is directly proportionate to the density of absorbing pigment in the target tissue and inversely proportionate to the amount of subretinal fluid or the presence of high-flow blood vessels that could produce tissue cooling.

Clinical indications of laser photocoagulation include ablation of parts of the partially ischemic retina, e.g., in diabetic retinopathy or retinal vein occlusions, to reduce the formation of vascular endothelial growth factor (VEGF), which stimulates the growth of fragile new vessels, and increase vascular permeability leading to tissue edema.

The same concept is used in ophthalmic oncology to treat extensive ischemic radiation retinopathy. Pan or sectoral retinal photocoagulation is used as a second-line treatment for proliferative radiation retinopathy refractory to intraocular anti-VEGF injections [20].

Laser can also be applied directly to coagulate small fundus tumors, such as small retinoblastoma or retinal angioma. Multiple retinal burns can be applied at the base of a larger retinoblastoma to cut off its retinal blood supply and coagulate feeder vessels of a retinal hemangioblastoma. Confluent laser burns could create a barrage of chorioretinal scarring around a leaking vascular tumor, such as retinal capillary hemangioma or vasoproliferative tumor of the ocular fundus (VPTOF), to limit the extension of leaking subretinal fluid centrally [21–23].

Carbon dioxide laser depends also on the thermal effect. It is used to cut through tissues by flash-boiling extracellular or intracellular water molecules in contact with the beam. This vaporization sterilizes the tissue and seals capillaries. CO2 laser has been used for precise microsurgical excision of eyelid tumors and to vaporize periocular lymphangiomas and capillary hemangiomas [24].

Other indications of laser photocoagulation include laser trabeculoplasty, ablation of the extrafoveal choroidal neovascular membrane, and production of chorioretinal adhesions to surround a retinal break or degeneration.

11.3.2 Transpupillary Thermotherapy

Similar to laser photocoagulation, transpupillary thermotherapy (TTT) depends on the thermal effect of the laser. Nevertheless, tissue heating (~65 °C) develops gently and gradually and should not reach the level of photoreceptor coagulation. The system uses a large spot size (3 mm or larger) to deliver an 810 nm infrared diode laser over a long duration (>60 s), which can penetrate deeper to be absorbed by choroidal melanocytes and RPE.

Transpupillary thermotherapy has been initially used as a primary sole treatment for small choroidal melanomas at the postequatorial fundus [25]. Nonetheless, the long-term tumor control rates for small melanoma were disappointing, with 17% (8–56%) late recurrences at 3 years and reported cases of extraocular extension [26, 27].

The exact mechanism by which hyperthermia affects melanoma is unclear, though chemical and immunological theories were suggested [28].

Currently, TTT is used as an adjuvant treatment to radiotherapy for selected melanoma cases. TTT is applied for the treatment of small edge recurrence of melanoma post-radiotherapy, for ablation of small retinal or choroidal vascular tumors, and as a primary treatment for small retinoblastoma or post chemoreduction [29–31].

11.3.3 Photodynamic Therapy

Photodynamic therapy (PDT) depends upon the photochemical property of the laser. It utilizes a photosensitive intravenous drug, verteporfin, in combination with a low-power, long-duration infrared laser to treat vascular lesions of the retina and choroid [32].

Verteporfin is a benzoporphyrin derivative with a half-life of 5–6 h, which selectively collects in the abnormal blood vessels in the retina and choroid. Fifteen minutes after intravenous infusion of verteporfin (dose = 6 mg/m^2 dose), a low-power 690 nm laser is applied with a slit lamp delivery system (standard dose of 50 J/cm^2, intensity of 600 mW/cm^2) over 83 s. Laser activation of verteporfin causes the release of free radicals, which react with blood vessels' endothelium, inducing a local increase of immune modulation factors, such as histamines, thromboxane, and TNF-α. The anti-inflammatory response can lead to a series of events, including vasoconstriction, thrombosis, increased vascular permeability, blood stasis, and hypoxia [33, 34].

This selective vascular toxicity has been utilized to treat choroidal neovascular membranes (CNVM) of wet age-related macular degeneration (AMD), polypoidal choroidal vasculopathy, and central serous chorioretinopathy [35–37]. In ophthalmic oncology, PDT is the treatment of choice for small- and medium-sized circumscribed choroidal hemangioma and retinal capillary hemangioma, particularly those in juxtapapillary locations. Most of these vascular tumors are controlled by one treatment session, though few may require up to four sessions [38–40]. PDT also can reduce SRF in symptomatic choroidal nevi with serous detachment at the macula [41]. PDT has been tried as a primary treatment for small choroidal melanoma, but similar to TTT, the long-term local control rates were unsatisfactory [42, 43].

11.4 Summary

Laser has been progressively utilized in multiple medical applications since the middle of the twentieth century. Stimulated emission is the physical principle of laser beam generation. Laser energy varies according to its wavelength. There are several types of ophthalmic lasers that can produce thermal, chemical, or mechanical effects on the ocular tissues. Several factors determine the impact of laser such as the degree of absorption of tissue pigments of a specific laser wavelength, laser power, the size of laser spot on the target tissue, the duration of application, and media clarity.

Laser delivery systems can be attached to slit lamp and indirect ophthalmoscope, or laser can be delivered through a fiber-optic probe. Advanced delivery systems enabled for more tolerable, precise, and shorter treatment sessions.

Techniques of ophthalmic laser therapy include laser photocoagulation, transpupillary thermotherapy, and photodynamic therapy. These laser techniques are used in ophthalmic oncology as a primary or adjuvant tumor treatment and as a treatment for some radiation-induced toxicities.

References

1. Einstein A. On the quantum mechanics of radiation [in German]. Phys Z. 1917;18:121–8.
2. Schechter RJ. An introduction to basic laser physics. In: Tasman W, Jaeger EA, editors. Duane's clinical ophthalmology. 1992 Revised ed. Philadelphia: J.B. Lippincott Company; 1992. (1)69A:1–8.
3. Sramek C, Paulus Y, Nomoto H, et al. Dynamics of retinal photocoagulation and rupture. J Biomed Opt. 2009;14(3):034007.
4. LaMuraglia GM, Adili F, Karp SJ, et al. Photodynamic therapy inactivates extracellular matrix-basic fibroblast growth factor: insights to its effect on the vascular wall. J Vasc Surg. 1997;26(2):294–301.
5. Schmidt-Erfurth U, Miller J, Sickenberg M, et al. Photodynamic therapy of subfoveal choroidal neovascularization: clinical and angiographic examples. Graefes Arch Clin Exp Ophthalmol. 1998;236(5):365–74.
6. Vogel A, Venugopalan V. Mechanisms of pulsed laser ablation of biological tissues. Chem Rev. 2003;103(2):577–644.
7. Capon MR, Docchio F, Mellerio J. Nd:YAG laser photodisruption: an experimental investigation on shielding and multiple plasma formation. Graefes Arch Clin Exp Ophthalmol. 1988;226(4):362–6.
8. Fankhauser F, Kwasniewska S. Laser in ophthalmology. Basic, diagnostic and surgical aspects. The Hague: Kugler Publications; 2003.
9. Palanker DV, Blumenkranz MS, Marmor MF. Fifty years of ophthalmic laser therapy. Arch Ophthalmol. 2011;129(12):1613–9.
10. Peyman GA, Raichand M, Zeimer RC. Ocular effects of various laser wavelengths. Surv Ophthalmol. 1984;28(5):391–404.
11. Pomerantzeff O, Kaneko H, Donovan RH, et al. Effect of the ocular media on the main wavelengths of argon laser emission. Invest Ophthalmol Vis Sci. 1976;15:70–7.
12. Al-Hussainy S, Dodson PM, Gibson JM. Pain response and follow-up of patients undergoing panretinal laser photocoagulation with reduced exposure times. Eye (Lond). 2008;22:96–9.
13. Soleimani A, Rasta SH, Banaei T, et al. Effects of laser physical parameters on lesion size in retinal photocoagulation surgery: clinical OCT and experimental study. J Biomed Phys Eng. 2017;7(4):355–64.
14. Mainster MA, Crossman JL, Erickson PJ, et al. Retinal laser lenses: magnification, spot size, and field of view. Br J Ophthalmol. 1990;74(3):177–9.
15. Blumenkranz MS, Yellachich D, Andersen DE, et al. Semiautomated patterned scanning laser for retinal photocoagulation. Retina. 2006;26(3):370–6.
16. Verdaasdonk RM, van Swol CF. Laser light delivery systems for medical applications. Phys Med Biol. 1997;42(5):869–94.
17. Yadav NK, Jayadev C, Rajendran A, et al. Recent developments in retinal lasers and delivery systems. Indian J Ophthalmol. 2014;62(1):50–4.
18. L'Esperance FJ. Ophthalmic lasers. St. Louis: CV Mosby; 1983. p. 340–50.
19. Brader HS, Young LH. Subthreshold diode micropulse laser: a review. Semin Ophthalmol. 2016;31(1–2):30–9.
20. Finger PT, Kurli M. Laser photocoagulation for radiation retinopathy after ophthalmic plaque radiation therapy. Br J Ophthalmol. 2005;89(6):730–8.
21. Shields CL, Shields JA, Kiratli H, et al. Treatment of retinoblastoma with indirect ophthalmoscope laser photocoagulation. J Pediatr Ophthalmol Strabismus. 1995;2(5):317–22.
22. Schmidt D, Natt E, Neumann HP. Long-term results of laser treatment for retinal angiomatosis in von Hippel-Lindau disease. Eur J Med Res. 2000;5(2):47–58.
23. Singh AD. Ocular phototherapy. Eye. 2013;27(2):190–8.
24. Wesley RE, Bond JB. Carbon dioxide laser in ophthalmic plastic and orbital surgery. Ophthalmic Surg. 1985;16(10):631–3.
25. Oosterhuis JA, Journee-de Korver HG, Kakebeeke-Kemme HM, et al. Transpupillary thermotherapy in choroidal melanomas. Arch Ophthalmol. 1995;113(3):315–21.
26. Singh AD, Kivela T, Seregard S, et al. Primary transpupillary thermotherapy of "small" choroidal melanoma: is it safe? Br J Ophthalmol. 2008;92(6):727–8.
27. Singh AD, Rundle PA, Berry-Brincat A, et al. Extrascleral extension of choroidal malignant melanoma following transpupillary thermotherapy. Eye (Lond). 2004;18(1):91–3.
28. Dennaoui J, Bronkhorst IH, Ly LV, et al. Changes in immunological markers and influx of macrophages following trans-scleral thermotherapy of uveal melanoma. Acta Ophthalmol. 2011;89(3):268–73.
29. Shields CL, Cater J, Shields JA, et al. Combined plaque radiotherapy and transpupillary thermotherapy for choroidal melanoma: tumor control and treatment complications in 270 consecutive patients. Arch Ophthalmol. 2002;120(7):933–40.
30. Gunduz K. Transpupillary thermotherapy in the management of circumscribed choroidal hemangioma. Surv Ophthalmol. 2004;49(3):316–27.
31. Abramson DH, Schefler AC. Transpupillary thermotherapy as initial treatment for small intraocular retinoblastoma: technique and predictors of success. Ophthalmology. 2004;111(5):984–99.
32. Schmidt-Erfurth U, Hasan T, Gragoudas E, et al. Vascular targeting in photodynamic occlusion of subretinal vessels. Ophthalmology. 1994;101(12):1953–61.
33. Kramer M, Miller JW, Michaud N, et al. Liposomal benzoporphyrin derivative verteporfin photodynamic therapy. Selective treatment of choroidal neovascularization in monkeys. Ophthalmology. 1996;103(3):427–38.
34. Woodburn KW, Engelman CJ, Blumenkranz MS. Photodynamic therapy for choroidal neovascularization: a review. Retina. 2002;22(4):391–405.
35. Bressler NM, Treatment of Age-Related Macular Degeneration with Photodynamic Therapy (TAP) Study Group. Photodynamic therapy of subfoveal choroidal neovascularization in age-related macular degeneration with verteporfin: two-year results of 2 randomized clinical trials-tap report 2. Arch Ophthalmol. 2001;119(2):198–207.
36. Erikitola OC, Crosby-Nwaobi R, Lotery AJ, et al. Photodynamic therapy for central serous chorioretinopathy. Eye. 2014;28(8):944–57.
37. Wong CW, Cheung CM, Mathur R, et al. Three-year results of polypoidal choroidal vasculopathy treated with photodynamic therapy: retrospective study and systematic review. Retina. 2015;35(8):1577–93.
38. Boixadera A, Garcia-Arumi J, Martinez-Castillo V, et al. Prospective clinical trial evaluating the efficacy of photodynamic therapy for symptomatic circumscribed choroidal hemangioma. Ophthalmology. 2009;116:100–5.
39. Sachdeva R, Dadgostar H, Kaiser PK, et al. Verteporfin photodynamic therapy of six eyes with retinal capillary haemangioma. Acta Ophthalmol. 2010;88(8):e334–40.
40. Schmidt-Erfurth UM, Kusserow C, Barbazetto IA, et al. Benefits and complications of photodynamic therapy of papillary capillary hemangiomas. Ophthalmology. 2002;109(7):1256–66.
41. García-Arumí J, Amselem L, Gunduz K, et al. Photodynamic therapy for symptomatic subretinal fluid related to choroidal nevus. Retina. 2012;32(5):936–41.

42. Fabian ID, Stacey AW, Harby LA, et al. Primary photodynamic therapy with verteporfin for pigmented posterior pole cT1a choroidal melanoma: a 3-year retrospective analysis. Br J Ophthalmol. 2018;102(12):1705–10. https://doi.org/10.1136/bjophthalmol-2017-311747.

43. Turkoglu EB, Pointdujour-Lim R, Mashayekhi A, et al. Photodynamic therapy as a primary treatment for small choroidal melanoma. Retina. 2019;39(7):1319–25. https://doi.org/10.1097/IAE.0000000000002169.

Principles of Radiation Therapy

12

Adannia Ufondu, Sheen Cherian, and Arun D. Singh

12.1 Introduction

Radioactivity was first described by Henri Becquerel and Pierre and Marie Curie in the late 1890s. Wilhelm Roentgen discovered X-rays in 1895, and subsequent physics and biology research revealed the therapeutic properties of radiation. X-rays were first used to treat cancer in 1897. Soon after, the concept of brachytherapy was developed when radium was implanted into tumors for therapeutic effect. Low-voltage X-ray machines were built in the 1920s for the external treatment of superficial tumors. The first cyclotron (used to accelerate heavy particles such as protons, neutrons, and deuterons) was invented in 1932 in California. In 1951, the first clinical cobalt-60 unit was built in London, Ontario, Canada. It created a gamma-ray photon beam from the emissions of a cobalt-60 source as it underwent nuclear decay. External beam radiation therapy was further refined in 1953 with the development of linear accelerators (linacs) that could produce megavoltage electron and X-ray photon beams using pulsed microwaves and an electron gun. The first medical-use linear accelerator was installed in Hammersmith Hospital, London, in 1953.

With improvements in radiographic imaging techniques such as CT and MRI, conformal radiation therapy was developed. Three-dimensional conformal radiation therapy (3D-CRT), intensity-modulated radiation therapy (IMRT), stereotactic radiosurgery, and charged particle therapy focus on the accurate delivery of therapeutic doses while minimizing damage to surrounding normal structures. In this chapter, we review the basic principles of radiation therapy and its application in the definitive, adjuvant, salvage, and palliative management of a variety of ophthalmic cancers.

A. Ufondu · S. Cherian (✉)
Department of Radiation Oncology, Taussig Cancer Center, Cleveland Clinic Foundation, Cleveland, OH, USA
e-mail: cherias@ccf.org

A. D. Singh
Department of Ophthalmic Oncology, Cole Eye Institute, Cleveland Clinic, Cleveland, OH, USA

12.2 Basic Principles

The unique characteristics of an individual element are determined by its atomic structure—the number and configuration of electrons, protons, and neutrons. Radiation therapy takes advantage of the energy created by the interaction of these fundamental particles with each other. This energy can break chemical bonds and create ions, such as free radicals. These free radicals are key in damaging critical targets on the DNA, resulting in tumor cell death.

12.3 Dual Nature of Radiation

Radiation can be in the form of electromagnetic waves, particles, or both.

12.3.1 Electromagnetic Radiation

Electromagnetic or photon radiation has a broad spectrum of wavelengths ranging from 10^{7} m (radio waves) to 10^{-13} m (ultrahigh energy X-rays) (Fig. 12.1). Energy is propagated at the speed of light (c) with the frequency (ν) and wavelength (λ) being inversely related: $c = \nu\lambda$. Linear accelerators produce photon beams with wavelengths in the range of 10^{-11} to 10^{-13} m.

12.3.2 Particle Radiation

Particle radiation can be neutral (neutrons) or charged (protons, electrons). As the particles travel through space, they interact with matter and produce varying degrees of energy transfer to the medium. Linear accelerators and cyclotrons are used to produce this type of radiation.

© The Author(s), under exclusive license to Springer Nature Switzerland AG 2025

A. D. Singh, B. E. Damato (eds.), *Clinical Ophthalmic Oncology*, https://doi.org/10.1007/978-3-031-75907-9_12

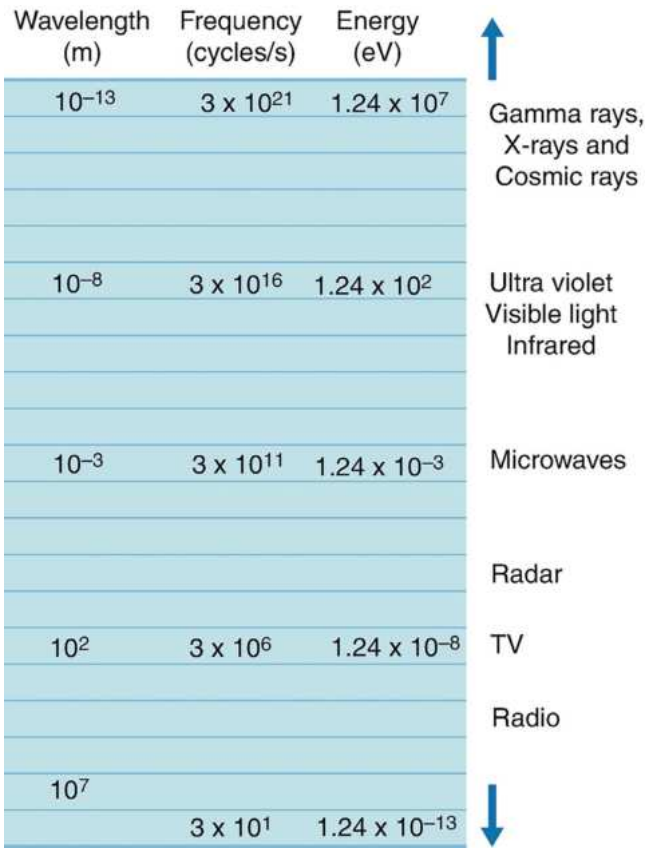

Fig. 12.1 The electromagnetic spectrum. Therapeutic X-rays and gamma rays are in the high-frequency, high-energy range. Ranges are approximate

12.4 Radioactive Decay

Radioactive elements are in an unstable, high-energy state and emit radiation to return to a stable, low-energy state. This process is called nuclear decay. Three different types of radiation can be emitted from the nucleus during this process: alpha particles with a positive electrical charge (helium nucleus), beta particles with a negative charge (electrons), and gamma rays with no electrical charge. Radioactive decay is the process utilized in cobalt-60 machines and Gamma Knife radiotherapy.

12.5 Ionizing and Nonionizing Radiation

Radiation has both ionizing and nonionizing effects on tissues. Ions are created when an atomic particle or photon with sufficient energy hits another atom, resulting in the loss of an electron, proton, or neutron. Both electromagnetic and particle radiation may directly damage the DNA molecule itself and impart single-strand breaks, double-strand breaks, or base-pair alterations. Much more common, however, is the indirect damage resulting from the ionization of surrounding atoms (free radicals) that go on to ionize and damage the DNA. Both direct and indirect DNA damage impair a cell's ability to regenerate and duplicate. Nonionizing effects mainly consist of the excitation of the outermost electrons of an atom and are of minimal clinical significance.

12.6 Teletherapy Sources

Teletherapy is the process of delivering radiation from a remote distance. In modern clinical practice, a cobalt-60 unit, linear accelerator, or cyclotron is used to generate and deliver external beam photon therapy and particle radiotherapy.

12.7 Cobalt-60 Unit

A cobalt-60 unit holds a radioactive cobalt source that is emitting gamma radiation as it decays to nickel-60. The average energy of the gamma photon beam is 1.25 million electron volts (MeV), with the maximum dose being delivered to a depth of 0.5–1 cm. With the advent of safer, faster, efficient, and precise medical use linear accelerators, Cobalt-60 teletherapy has fallen out of favor.

12.8 Linear Accelerator

A linear accelerator uses high-frequency electromagnetic waves to accelerate electrons to high energies through a linear vacuum tube. The monoenergetic electron beam can be used to treat superficial tumors. Typical energies used range from 6 to 18 (MeV), with 80% of the maximum dose delivered to a depth of 2–6 cm and a relatively steep dose drop-off beyond (Fig. 12.2).

When deeper tumors need to be treated or the skin needs to be spared, the linear accelerator electron beam is directed at a target (usually tungsten). The resultant atomic interactions produce a range of high-energy X-rays, also called photons. Photons are characteristically more penetrating than electrons. As an example, a 6 MeV electron beam creates a photon beam with a maximum energy of 6 megavolts (MV). Typical energies of photon beams range from 6 to 18 MV, with the depth of maximum dose deposition ranging from 1.5 to 3.5 cm and a more gradual dose drop-off beyond (Fig. 12.3).

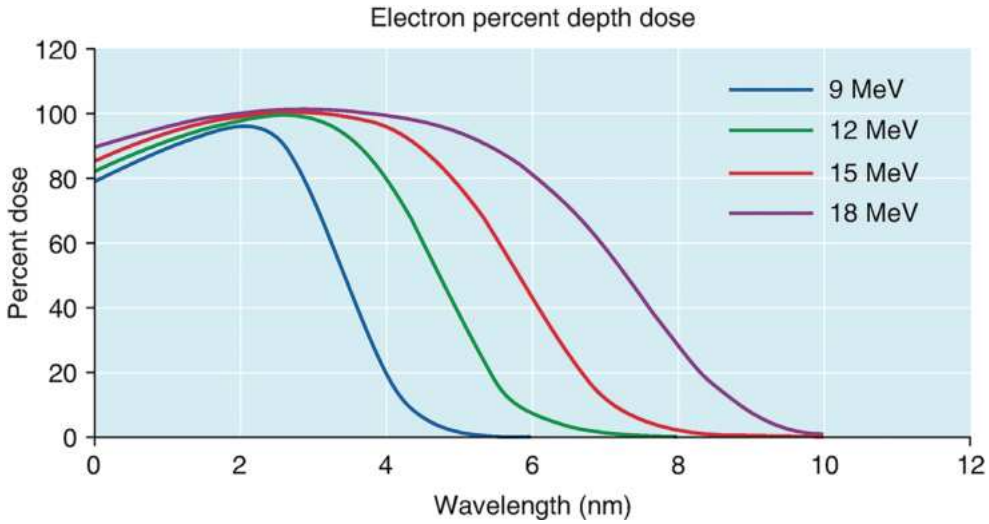

Fig. 12.2 Percent depth dose curves for commonly used electron beams. Divide the beam energy by 3 to estimate the depth in tissue of 80% of the maximum dose. Divide the beam energy by 2 to estimate the range of penetration

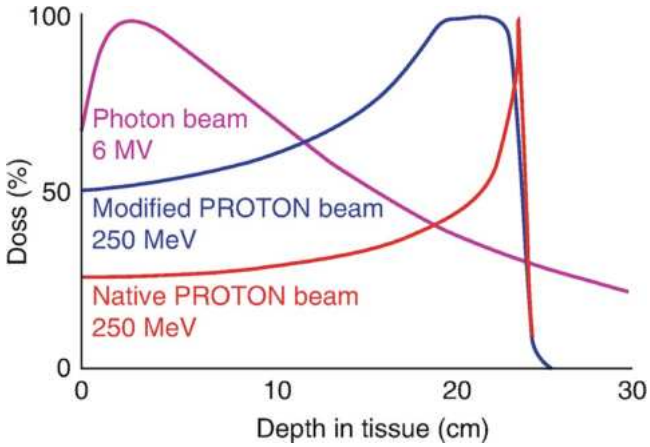

Fig. 12.3 The Bragg peak allows for low-energy deposition along the entrance pathway, very high-dose delivery over a narrow depth, with minimal exit dose. The spread-out Bragg peak allows for dose deposition over a greater distance for treatment of a larger volume of tissue. (Reprinted from https://commons.wikimedia.org/wiki/ File:BraggPeak.png. With permission from Creative Commons License 3.0: https://creativecommons.org/licenses/by-sa/3.0/deed.en)

12.9 Cyclotron

A cyclotron is a heavy particle accelerator capable of producing neutron and proton beams. Neutrons and protons have a higher linear energy transfer than photons, meaning they cause more damage as they pass through tissue. They cause direct damage to the DNA of a cell, making them potentially more effective at treating hypoxic tumor cells because there is no dependence on the production of oxygen radicals (free radicals).

Proton beams have a unique dose distribution characteristic called the Bragg peak. There is a steep peak of maximal dose deposit with sharp distal drop-off (Fig. 12.3). This Bragg peak can be directed accurately and precisely onto the tumor [1]. The sharp distal drop-off and minimal scatter from proton beams translate into a lower dose to surrounding normal tissues. Proton beam radiotherapy is used for the treatment of uveal melanoma and retinoblastoma [2, 3]. Proton beam radiotherapy of uveal melanoma is discussed under uveal tumors.

12.10 Radiation Parameters

12.10.1 Radiation Dose

Radiation-absorbed dose is defined in gray (Gy), which represents one joule of energy absorbed per kilogram of mass. Centigray (cGy) is also commonly used, and it is 1/100th of a gray. The previous dose convention used the rad, defined as 100 ergs absorbed per gram. As a centigray is equivalent to a rad, this allows comparisons between older published reports and current data.

12.10.2 Relative Biological Effectiveness

Relative biological effectiveness (RBE) is a measure of the efficiency of a specific radiation in producing a specific biological response. This can be expressed in the following equation, RBE = D_s/D_r, where D_s and D_r are the doses of

Table 12.1 Relative biological effectiveness (RBE) values of commonly used radiations

Radiation	RBE
Standard (250 kVp x-rays)	1.0
Linac (6–15 MeV)	~0.8
Cobalt-60	0.8–0.9
Protons	~1.1
Neutrons (19 MeV)	1–2

standard radiation (250 kVp X-rays) and test radiation (r) needed to produce an equivalent biological response (Table 12.1). Protons and neutrons have greater RBE than photons and electrons.

12.10.3 Cobalt Gray Equivalents

The amount of absorbed dose from neutron and proton beams is higher than with X-ray or gamma-ray beams. To facilitate comparisons to standard photon doses, the term cobalt gray equivalents (CGE) was developed: CGE = dose in proton or neutron gray x corresponding RBE value.

12.11 Treatment Parameters

12.11.1 Target Volume

Several target tissue volumes are considered when determining the prescription dose. Gross target volume (GTV) is the visible tumor extent. Clinical target volume (CTV) is the GTV plus margin to cover microscopic tumor extension or postoperative bed. Planning target volume (PTV), the volume ultimately treated, is CTV plus a safety margin accounting for setup variations and organ motion. An additional dosimetric margin is often added to the PTV to allow for physical dose buildup in tissue and, therefore, adequate dose delivery to the PTV. The treatment margin beyond the GTV typically ranges from 0.5 to 2 cm, depending on the accuracy of the treatment machine, the immobilization device, and the tumor type.

12.11.2 Total Dose

The total delivered dose depends on the tumor responsiveness, gross versus microscopic disease, and purpose of the radiation (curative or palliative).

12.11.3 Fractionation

In general, the total dose is broken into daily fractions delivered over many weeks. Fractionation is used to mitigate late radiation toxicity. Conventional fractionation schemes comprise 180–200 cGy fractions delivered once per day, 5 days per week. For a given therapeutic dose, fraction sizes >200 cGy are associated with a greater tendency for late side effects such as severe dry eye, cataracts, corneal ulceration, and optic neuropathy. Conversely, reducing the fraction size diminishes the therapeutic effects of radiation (tumor kill) when delivered in a conventional daily scheme. Recent data suggest that hyperfractionation (1.10–1.20 Gy/fraction; twice daily) may reduce the risk of radiation retinopathy in patients treated for head and neck cancer [4]. Palliative radiation therapy often utilizes larger fraction sizes given over a shorter period of time, with the assumption that the natural history of the disease precludes the development of late radiation effects. Some common dose/fractionation schedules are listed in Table 12.2.

12.11.4 Tissue Tolerance

In treating ophthalmic tumors with external beam radiation, radiation exposure to several critical structures such as the lens, optic nerve, opposite orbit, pituitary, and brain must be taken into account. Normal tissue tolerance to external beam radiation (180–200 cGy/fraction) and the total doses that result in 5% and 50% complication rates 5 years after treatment are listed in Table 12.3 [5]. Ophthalmic complications of radiation therapy are discussed in detail elsewhere [2].

Table 12.2 External beam radiation therapy dose/fractionation schedules for common ophthalmic cancers

Disease	Total dose	Dose per fraction	Number of fractions
Uveal melanoma	60–70 CGE (protons)	14–15 CGE	4–5
Retinoblastoma	40–50 Gy	2–2.5 Gy	20–25
Uveal/orbital metastasis	30 Gy	3 Gy	10
Orbital Adnexal lymphoma	24 Gy	2 Gy	12
Basal or squamous cell carcinoma of the eyelid	35–42.5 Gy	4.25–7 Gy	5–10
Palliation	30 Gy	3 Gy	10

CGE Cobalt gray equivalent

Table 12.3 Normal tissue tolerance dose to external beam radiation (cGy)

	Complication rate at 5 years		
Organ	5%	50%	Clinical endpoint
Brain	6000	7500	Necrosis, infarction
Optic nerve	5000	6500	Visual acuity <20/200
Optic chiasm	5000	6500	Visual acuity <20/200
Lens	1000	1800	Symptomatic cataract
Retina	4500	6500	Visual acuity <20/200

Based on data from Ref. [5]

12.12 Teletherapy Techniques

12.12.1 External Beam Therapy

When a patient is scheduled for external beam therapy, the first appointment is for simulation. During simulation, the patient is placed in the treatment position, including immobilization devices such as a customized thermoplastic mask. A high-resolution CT scanner ± MRI scanner is used to take images of the patient's anatomy in the treatment position. The tumor area and the surrounding normal structures are identified and contoured on the simulation images. The beam arrangement may be set at the time of simulation, or a dosimetrist may later create several plans to determine the best beam arrangement. Examples of beam arrangements include a simple technique of one en-face electron beam (Fig. 12.4), two-photon beams arranged in a perpendicular "wedged pair" (Fig. 12.5), opposing angles (Fig. 12.6), or other beam arrangements (Fig. 12.7). Several so-called lens-sparing techniques of beam design and arrangements have been developed in order to minimize radiation exposure to the lens and avoid radiation-induced cataracts [1, 6–12].

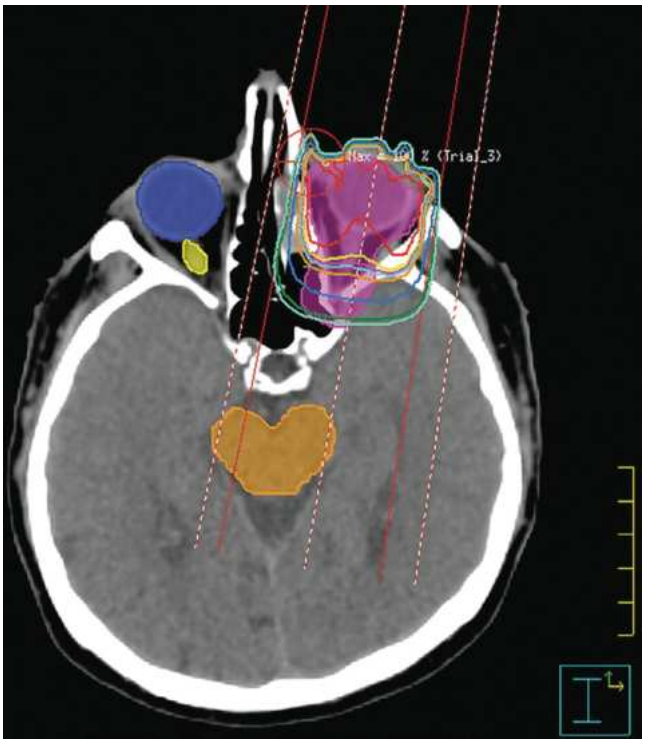

Fig. 12.4 Axial CT with en face photon beam demonstrating coverage of the planning target volume (PTV) covered by the 95% isodose line (aqua)

Fig. 12.5 Axial CT with "wedged pair" photon beam demonstrating coverage of the planning target volume (PTV) covered by the 95% isodose line

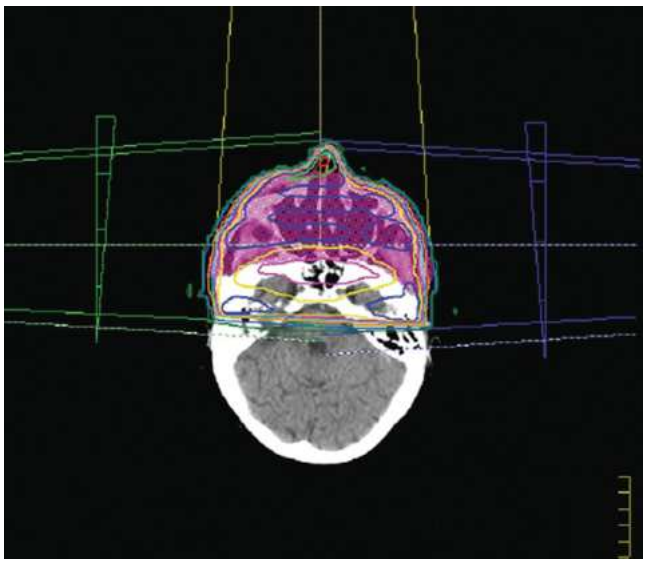

Fig. 12.6 Opposed lateral photon beams demonstrating coverage of the bilateral orbits (100% isodose line in yellow)

12.12.2 Conformal Radiation Therapy

Standard or conventional radiation therapy uses bony landmarks on fluoroscopy or external landmarks on physical examination to determine gross anatomical boundaries for field shapes and sizes. With simulation images from MRI and CT scanners, a radiation oncologist can precisely identify tumors and critical structures, calculate the dose they will receive, and design beam arrangements that will minimize long-term damage. This is termed conformal therapy.

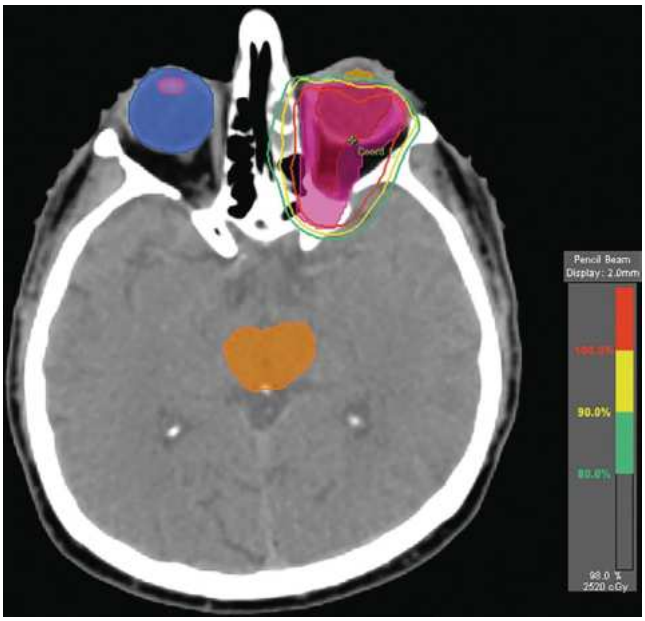

Fig. 12.7 Radiotherapy plan demonstrating isodose distributions with intensity-modulated radiotherapy (IMRT), which conform to the planning treatment volume (pink)

12.12.3 Three-Dimensional Conformal Therapy

Three-dimensional conformal therapy or 3D-CRT is the technique of using CT or MRI simulation images to create a three-dimensional target. Various beam arrangements are entered into the planning computer and altered until an acceptable dose distribution is reached for both the tumor and normal structures. This process of first entering the beam arrangements and then looking at the dosimetric outcomes is termed forward planning.

12.12.4 Intensity-Modulated Radiation Therapy

In intensity-modulated radiation therapy (IMRT), a process of inverse planning is often used, which means that the dose criteria are set before beam arrangements are designed. The computer generates a plan that best fits the specified criteria. During treatment, a multi-leaf collimator moves dynamically to create hot and cold spots within the volume of treated tissue. The intention is to deliver a tumoricidal dose to the

tumor volume while minimizing the delivery of high doses of radiation to nearby critical structures, including the lens.

12.13 Stereotactic Radiosurgery

Stereotactic radiosurgery uses highly conformal, precision-aimed radiation (usually within 0.5 mm of the specified isocenter) to treat small tumors (≤5 cm) at very high doses per fraction. A stereotactic frame fixed to the patient's skull is used for precise localization and positioning. Planning CT and MRI images are taken with the frame in place so that accurate coordinates can be established for the target. Two forms of stereotactic radiosurgery exist: linac-based and Gamma Knife.

12.13.1 Linac-Based Stereotactic Radiosurgery

In linac-based stereotactic radiosurgery, specialized cones or computer-controlled high-definition multi-leaf collimators with very fine-width leaves are used to target the tumor during multi-arc therapy [13]. Stereotactic radiosurgery for uveal melanoma is discussed under uveal tumors.

12.13.2 Treatment Delivery

Advances in technology have allowed for the development of highly conformal treatment plans through the ability to fuse MRI with CT for target delineation, the development of complex treatment machines, and progress in the capabilities of treatment planning systems. However, with increasing treatment complexity and smaller amounts of surrounding normal tissue included in treatment targets, the accuracy of reproducibility of the simulation setup becomes increasingly important. Historically, physical frames were applied to patients to ensure precise treatment delivery. Verification of treatment setup, or image guidance, for large treatment fields and simple fields is achieved with portal images. Patients treated with complex treatment plans, small setup margins, and small numbers of fractions undergo daily image guidance with more advanced systems, including low-resolution CT scans (cone-beam CT), orthogonal X-rays, fiducials, and motion-based gating systems being developed [14–19].

Patients treated with IMRT, fractionated stereotactic radiotherapy, or SRS may be treated with the Cyberknife® system [20–22]. This consists of a small, single-energy linear accelerator mounted on a robotic arm. Advantages of the Cyberknife® system include nearly unlimited treatment angles, whereas traditional linear accelerators rotate around a point in space, and the treatment table must be moved to accomplish similar treatment angles. However, image guidance is limited to orthogonal X-rays, whereas confirmation of patient positioning may be achieved with pretreatment cone-beam CT imaging prior to treatment with standard linear accelerators. Also, standard linear accelerators allow for treatment with either electrons or low-energy photons.

12.13.3 Gamma Knife Radiosurgery

With Gamma Knife, gamma-ray beams from 201 cobalt-60 sources are collimated to focus on a single point. The patient's head is positioned to place the tumor at that isocentric point [23]. Gamma Knife radiosurgery for uveal melanoma is discussed under uveal tumors.

12.13.4 Charged Particle Therapy

The use of charged particles for the treatment of ophthalmologic tumors is well-studied. Charged particles are well suited for the treatment of ophthalmologic tumors as the treatment target is often in proximity to several nearby critical structures, including the uninvolved orbital contents, optic nerves, and brain. The physical dose distribution characteristics of charged particle beams allow for the treatment of small structures to high doses while sparing nearby critical structures. Charged particles deliver a high concentration of energy over a discrete range, known as the Bragg peak, with a dramatic drop in dose deposition beyond the depth of maximum. The range of the Bragg peak may be widened, known as the "spread-out Bragg peak," to allow for treatment of tumors of any depth and diameter [14, 24].

The very sharp dose gradients offer a dosimetric advantage by delivering high radiation doses to the tumor target while minimizing dose exposure of nearby normal structures. To maximize the benefits of high-dose gradients, accuracy of delivery is paramount. Treatment frames, thermoplastic mesh masks molded to the anatomy of the individual, fiducial placement, video-based systems, orthogonal X-rays, and cone-beam CTs are used to ensure accurate setup prior to and, in some cases, during treatment delivery. This therapy offers dosimetric advantages but is not widely available. At the writing of this chapter, there are 44 centers offering proton radiotherapy in the United States, with ten more under construction or in development.

12.13.5 Brachytherapy

Brachytherapy is the process of placing a radioactive source next to or within a tumor. The dose characteristics of the isotopes used in brachytherapy are such that a very high dose of

radiation is given within millimeters of the source, and there is a steep dose drop-off outside of that range, thus protecting surrounding normal structures. Isotopes that have been employed include cobalt-60, iridium-192, ruthenium-106, gold-198, palladium-103, and iodine-125 [25]. Brachytherapy is used for the treatment of intraocular tumors such as choroidal metastasis [26], uveal melanoma [25, 27], and retinoblastoma [28]. Brachytherapy for uveal melanoma is discussed under uveal tumors.

12.14 Summary

Radiation therapy takes advantage of the energy created when electrons, protons, and neutrons interact with each other. Radiation can be in the form of particles and electromagnetic waves. Linear accelerators and cyclotrons are used to produce radiation. In addition, radioactive decay of an isotope can generate radiation. Radioactive decay is the process utilized in cobalt-60 machines and Gamma Knife radiotherapy. Radiation interacts with DNA, resulting in single-strand breaks, double-strand breaks, or base-pair alterations, impairing a cell's ability to regenerate and duplicate. Protons and neutrons have greater relative biological effectiveness than photons and electrons. Several treatment parameters, such as target volume, total dose, and fractionation, influence tissue effects. Larger doses per fraction (>200 cGy) are associated with a greater tendency for late side effects such as severe dry eye, cataract, radiation keratitis, and optic neuropathy. Normal tissues vary greatly in their tolerance to external beam radiation. Teletherapy techniques include conventional external beam therapy, three-dimensional conformal therapy, intensity-modulated radiation therapy, stereotactic radiosurgery, and Gamma Knife radiosurgery. Brachytherapy is the process of placing a radioactive source next to or within a tumor. Ruthenium-106, palladium-103, and iodine-125 are commonly used isotopes for the treatment of ophthalmic tumors. With continued improvements in radiographic imaging techniques and a better understanding of radiation tissue effects at the molecular level, it will be possible to precisely focus therapeutic dose while minimizing damage to surrounding normal structures.

References

1. Goitein M, Miller T. Planning proton therapy of the eye. Med Phys. 1983;10:275–83.
2. Gragoudas ES, Marie LA. Uveal melanoma: proton beam irradiation. Ophthalmol Clin N Am. 2005;18(111–8):ix.
3. Krengli M, Hug EB, Adams JA, et al. Proton radiation therapy for retinoblastoma: comparison of various intraocular tumor locations and beam arrangements. Int J Radiat Oncol Biol Phys. 2005;61:583–93.
4. Monroe AT, Bhandare N, Morris CG, et al. Preventing radiation retinopathy with hyperfractionation. Int J Radiat Oncol Biol Phys. 2005;61:856–64.
5. Emami B, Lyman J, Brown A, et al. Tolerance of normal tissue to therapeutic irradiation. Int J Radiat Oncol Biol Phys. 1991;21:109–22.
6. Chu FC, Huh SH, Nisce LZ, et al. Radiation therapy of choroid metastasis from breast cancer. Int J Radiat Oncol Biol Phys. 1977;2:273–9.
7. Maor M, Chan RC, Young SE. Radiotherapy of choroidal metastases: breast cancer as primary site. Cancer. 1977;40:2081–6.
8. Brady LW, Shields JA, Augsburger JJ, et al. Malignant intraocular tumors. Cancer. 1982;49:578–85.
9. Schipper J. An accurate and simple method for megavoltage radiation therapy of retinoblastoma. Radiother Oncol. 1983;1:31–41.
10. Nylén U, Kock E, Lax I, et al. Standardized precision radiotherapy in choroidal metastases. Acta Oncol. 1994;33:65–8.
11. Steenbakkers RJ, Altschuler MD, D'Angio GJ, et al. Optimized lens-sparing treatment of retinoblastoma with electron beams. Int J Radiat Oncol Biol Phys. 1997;39:589–94.
12. Bajcsay A, Kontra G, Récsán Z, et al. Lens-sparing external beam radiotherapy of intraocular metastases: our experiences with twenty four eyes. Neoplasma. 2003;50:459–64.
13. Zehetmayer M, Kitz K, Menapace R, et al. Local tumor control and morbidity after one to three fractions of stereotactic external beam irradiation for uveal melanoma. Radiother Oncol. 2000;55:135–44.
14. Zytkovicz A, Daftari I, Phillips TL, et al. Peripheral dose in ocular treatments with CyberKnife and Gamma Knife radiosurgery compared to proton radiotherapy. Phys Med Biol. 2007;52:5957–71.
15. Shin D, Yoo SH, Moon SH, et al. Eye tracking and gating system for proton therapy of orbital tumors. Med Phys. 2012;39:4265.
16. Riboldi M, Orecchia R, Baroni G. Real-time tumour tracking in particle therapy: technological developments and future perspectives. Lancet Oncol. 2012;13:e383–91.
17. Parkhurst JM, Price GJ, Sharrock PJ, et al. Next generation optical surface sensing for real-time measurement in radiotherapy. Annu Int Conf IEEE Eng Med Biol Soc. 2011;2011:6170–3. Available at: http://ieeexplore.ieee.org/lpdocs/epic03/wrapper.htm?arnumber=6091524. Accessed 1 Feb 2013.
18. Jaywant SM, Osei EK, Ladak S. Stereotactic radiotherapy in the treatment of ocular melanoma: a noninvasive eye fixation aid and tracking system. J Appl Clin Med Phys. 2003;4:156–61.
19. Amstutz CA, Bechrakis NE, Foerster MH, et al. Intraoperative localization of tantalum markers for proton beam radiation of choroidal melanoma by an opto-electronic navigation system: a novel technique. Int J Radiat Oncol Biol Phys. 2012;82:1361–6.
20. Bianciotto C, Shields CL, Lally SE, et al. CyberKnife radiosurgery for the treatment of intraocular and periocular lymphoma. Arch Ophthalmol. 2010;128:1561–7.
21. Zorlu F, Selek U, Kiratli H. Initial results of fractionated CyberKnife radiosurgery for uveal melanoma. J Neuro-Oncol. 2009;94:111–7.
22. Hirschbein MJ, Collins S, Jean WC, et al. Treatment of intraorbital lesions using the accuray CyberKnife system. Orbit. 2008;27:97–105.
23. Rennie I, Forster D, Kemeny A, et al. The use of single fraction Leksell stereotactic radiosurgery in the treatment of uveal melanoma. Acta Ophthalmol Scand. 1996;74:558–62.
24. Weber DC, Bogner J, Verwey J, et al. Proton beam radiotherapy versus fractionated stereotactic radiotherapy for uveal melanomas: a comparative study. Int J Radiat Oncol Biol Phys. 2005;63:373–84.
25. Finger PT. Radiation therapy for choroidal melanoma. Surv Ophthalmol. 1997;42:215–32.
26. Shields CL. Plaque radiotherapy for the management of uveal metastasis. Curr Opin Ophthalmol. 1998;9:31–7.
27. Diener-West M, Earle JD, Fine SL, et al. The COMS randomized trial of iodine 125 brachytherapy for choroidal melanoma, III: initial mortality findings. COMS Report No. 18. Arch Ophthalmol. 2001;119:969–82.
28. Shields CL, Shields JA, De Potter P, et al. Plaque radiotherapy for retinoblastoma. Int Ophthalmol Clin. 1993;33:107–18.

Principles of Surgical Excision

13

Bertil E. Damato

13.1 Introduction

Surgical tumor excision is by far the oldest form of treatment for cancer, having been practiced for thousands of years. Its scope and success depend on a wide variety of factors, such as anesthesia, infection control, imaging, pre- and post-operative care (at the ocular oncology center as well as the patient's local hospital), quality evaluation, safety measures, and standards of care, as well as multimodality therapy incorporating radiotherapy, chemotherapy, cryotherapy, and/or laser therapy. Surgical progress has also been enhanced by a better understanding of cancer, which has occurred thanks to advances in molecular pathology, computing, registries, statistics, and clinical trial methodology. Progress in surgical tumor excision will inevitably accelerate thanks to exponential advances in robotics, artificial intelligence, quantum computing, augmented reality, and other scientific advances we cannot begin to imagine. The aim of this chapter is to highlight the principles of surgical oncology as they pertain to ocular tumors.

13.2 Objectives of Surgical Tumor Excision

The objectives of surgical tumor excision include management planning (e.g., excision of conjunctival tumor to determine diagnosis and depth of invasion, if any), prevention of malignancy (e.g., excision of conjunctival nevus), conservation of a useful eye (e.g., iridocyclectomy for ciliary body melanoma), pain control (e.g., enucleation for neovascular glaucoma), prevention of metastatic disease (e.g., enucleation for retinoblastoma), and cosmetic improvement (e.g., excision of limbal dermoid).

These objectives must take account of the patients' needs, wishes, and fears, which must not be allowed to compromise their health and safety. For example, although a patient with uveal melanoma may be reluctant to undergo enucleation, this may be the best option if the tumor is very large so that the eye is most likely to become blind and painful after radiotherapy. The author has found that such patients usually change their minds and request enucleation once they are informed of the side effects of radiotherapy and reassured about the relatively good quality of life they will achieve after enucleation [1, 2].

The objectives of surgical excision should be based on any available scientific evidence, also taking any other therapeutic modalities into consideration. For example, when selecting treatment for an iris melanoma, the risks and benefits of iridectomy need to be weighed against those of brachytherapy and proton beam radiotherapy. It is important to ensure that the patient's choice of treatment is not based on any misconceptions. For example, some patients decline enucleation because they fear that this will overburden the fellow eye. Conversely, some patients with a small, peripheral melanoma select enucleation because they feel this would improve their chances of survival when radiotherapy is likely to be as effective (or ineffective) in achieving this aim.

13.3 Technical Aspects

13.3.1 Pre-operative Assessment

As with other forms of treatment, it is essential to define the tumor as accurately as possible with respect to dimensions, location, and extent, in addition to any concurrent ocular morbidity, such as exudative retinal detachment, cataract, and glaucoma. In addition to standard examinations, such as visual acuity, tonometry, slit lamp examination, and ophthalmoscopy, this involves color photography, ultrasonography, and, in selected cases, investigations such as optical coherence tomography, magnetic resonance imaging to detect the spread of retinoblastoma to optic nerve or orbit, and mag-

B. E. Damato (✉)
Ocular Oncology Service, Moorfields Eye Hospital, London, UK
e-mail: bertil.damato@nhs.net

© The Author(s), under exclusive license to Springer Nature Switzerland AG 2025

A. D. Singh, B. E. Damato (eds.), *Clinical Ophthalmic Oncology*, https://doi.org/10.1007/978-3-031-75907-9_13

netic resonance imaging or computed tomography to assess the depth of invasion of any advanced conjunctival malignancy.

Systemic investigations are aimed at assessing fitness for anesthesia and detecting any extraocular malignancy. These examinations depend on the tumor diagnosis. For example, detectable hepatic metastases from uveal melanoma are rare at the time of primary ocular treatment [3]; nevertheless, it is conventional practice to perform liver ultrasonography or magnetic resonance imaging, if only to have a baseline scan in case any abnormalities are found months or years later. Some would perform sentinel lymph node biopsy in patients with advanced conjunctival malignancy. In patients with retinoblastoma, brain magnetic resonance imaging is indicated to detect any pineoblastoma.

13.3.2 Prognostication

The chances of conserving the eye and vision after surgical excision are estimated according to tumor features. For example, local tumor control is less likely if an iris melanoma has diffuse margins. The risk of limbal stem cell deficiency is greater if a conjunctival malignancy shows extensive circumferential spread around the cornea. Similarly, the chances of hypotony and lens subluxation are greater after iridocyclectomy for ciliary body melanoma if the tumor shows extensive ciliary body involvement. With resection of choroidal melanomas, risk factors for enucleation include large basal diameter, diffuse margins, extraocular spread, optic disc involvement, and, with respect to exoresection, retinal perforation [4]. As with any form of treatment, the chances of conserving central vision depend mostly on tumor proximity to the fovea.

Conventionally, the risk of metastasis is estimated using the tumor, node, metastasis (TNM) staging system [5]. For patients with posterior uveal melanoma, the survival probability can be estimated using the Liverpool Uveal Melanoma Prognosticator Online (LUMPO), which, in addition to TNM predictors, also takes into account histologic and genetic factors as well as the patient's age and sex [6]. For situations where this is not available, the author and associates have also developed tables predicting metastatic death according to basal tumor diameter, age, and chromosome 3 status, if this is known [7].

13.3.3 Counseling

Counseling is aimed not only at obtaining informed consent but also at managing expectations and providing emotional support. The topics for discussion include ocular anatomy; diagnosis; natural history of the disease; risks and benefits of all therapeutic options; purpose of treatment (e.g., conservation of vision, prevention of metastatic disease, etc.), objectives of surgical excision (e.g., total excision, partial excision, etc.), details of the selected treatment, including any intraoperative and post-operative adjunctive therapy that is planned (e.g., cryotherapy, brachytherapy, topical chemotherapy); likely outcomes in terms of visual function, ocular preservation, local tumor control and survival; post-operative care and long-term management; sources of information; patient advocacy groups; condition's impact on work and other activities; financial implications; dealing with relatives and work colleagues; support available to meet psychological and any other needs; and name and contact details of the key worker (e.g., a specialist nurse) whom patients can communicate with if any questions or problems ever arise. This discussion should be held in a quiet room, without interruptions, with sympathy, and taking account of the emotional state of the patient and any accompanying persons. Patients should be given an opportunity to ask questions and express their feelings. It is difficult for them to remember all they are told. In addition to information leaflets, the author has for many years given them an audio recording of the conversation [8]. This recording is also uploaded into the patient's electronic medical records.

13.3.4 Pre-operative Medications

Pre-operative medications are the same as those administered before other ocular surgery. With posterior intraocular tumors, the pupil is dilated. If iridocyclectomy is to be performed for a ciliary body tumor that involves only the peripheral iris, then constriction of the pupil makes it easier to conserve the iris sphincter.

13.3.5 Anesthesia

The type of anesthesia is usually selected in consultation with an anesthetist and depends on the duration and complexity of the intended surgical procedure as well as the age, health, and preference of the patient. With conjunctival tumors, some surgeons routinely administer a subconjunctival injection of a local anesthetic with epinephrine, and others consider anesthetic drops to be sufficient for minor procedures. Conversely, trans-scleral "exoresection" of choroidal melanoma requires profound systemic hypotensive anesthesia lowering the systolic blood pressure for more than an hour with intra-arterial catheterization for blood pressure monitoring and intraoperative electroencephalogram (EEG) to ensure that the brain is well perfused throughout the operation [9].

13.3.6 Pre-operative Checks

As with any procedure, every precaution should be taken to ensure that the correct eye is operated on by confirming this with the patient, marking the forehead with a pen, and visualizing the tumor after taping the other eye shut or draping the patient. The surgeon should check the microscope (including the interpupillary distance of the oculars and the pedals). The planned steps of the operation should be discussed with the scrub nurse to ensure that the instrument set is complete and that all other necessary items are available (e.g., orbital implant for enucleation, correct plaque for adjunctive brachytherapy, transilluminator, laser, cryotherapy equipment, etc.). This discussion should also include the intended handling of the tumor specimen so that there is no uncertainty as to whether this will be transported to the laboratory fresh (e.g., to enhance genetic tumor analysis) or in a specified transport medium or fixative. A formal "time-out" is essential to ensure that all individuals in the operating room (including the patient) are identified, as well as highlighting any risk factors and confirming the procedure that is to be performed.

13.3.7 Sterilization of Operative Field

The operative field is sterilized as for any other surgical procedure, taking into account any allergies (e.g., iodine).

13.3.8 Exposure of Surgical Field

Exposure to the surgical field needs to be planned carefully to reduce the risk of complications. For example, a heavy eyelid speculum may increase the risk of vitreous loss when performing iridocyclectomy. Inexpert retraction by an assistant may complicate trans-scleral exoresection. Scleral traction sutures are invaluable in some procedures, but only if placed correctly in the right meridians and deep enough not to rip out at a critical point of the operation. Detachment of any rectus muscles overlying a choroidal melanoma makes it easier to define the tumor margins by transillumination and to position the plaque accurately over the tumor, thereby reducing the risk of local tumor recurrence and avoidable collateral damage to optic nerve and fovea; the risk of iatrogenic strabismus is reduced by measuring and documenting the knot-to-limbus distance before detaching the muscle and ensuring that this distance is the same when the muscle is re-attached [10]. Detachment of the inferior oblique muscle minimizes the tilting of the plaque away from the sclera, reducing the risk of local tumor recurrence.

13.3.9 Tumor Excision

Surgeons vary greatly in their attitude to surgical clearance margins. For example, with conjunctival tumors, some surgeons advocate wide safety margins, using an amniotic membrane graft to close the wound; the author prefers narrow safety margins so as to be able to close the wound by primary intention, avoiding the need for a graft and relying on adjunctive topical chemotherapy and/or radiotherapy to ensure local tumor control (Fig. 13.1) [11]. The author also follows a similar multimodality approach when excising uveal melanoma, administering adjunctive brachytherapy; however, with ciliary body tumors, such radiotherapy must be delayed for a month until healing has occurred to prevent cyclodialysis and hypotony [12].

Every effort should be taken to avoid seeding tumor cells to adjacent tissues. For example, conjunctival tumors are

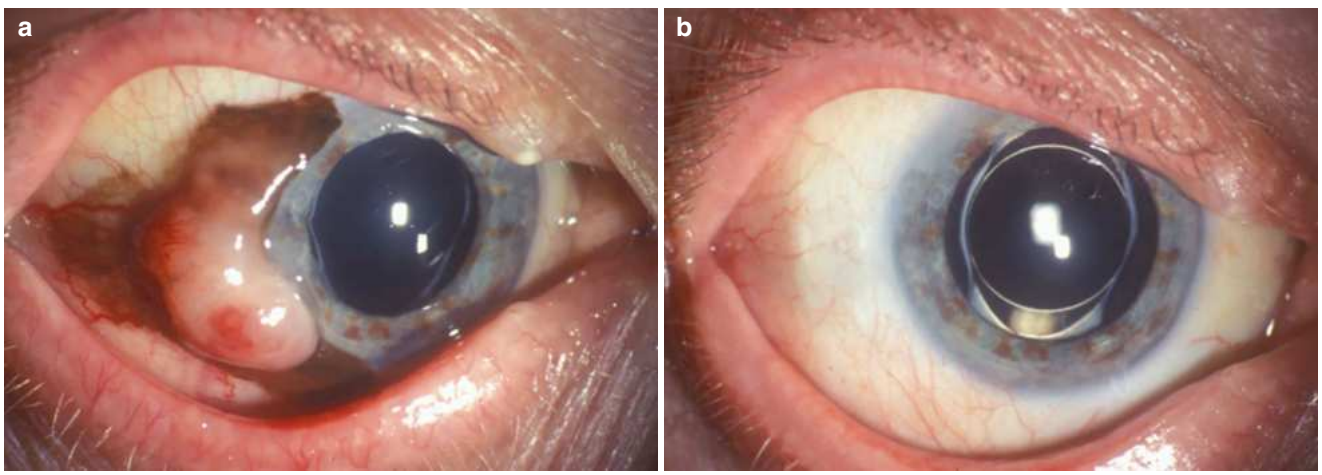

Fig. 13.1 Excision of a conjunctival melanoma from the right eye of a 58-year-old man. (**a**) Preoperative appearance. (**b**) Final result following excision, adjunctive ruthenium plaque brachytherapy and topical mitomycin-C chemotherapy

excised using a no-touch technique, with fresh instruments for closure and by applying meticulous hemostasis, with some authors also avoiding the instillation of lubricating drops until the tumor has been removed. With enucleation for retinoblastoma, scleral perforation is prevented by measures such as avoiding injection of local anesthetics until the globe has been removed, using a strabismus hook that protects the sclera when suturing muscles, or even detaching extraocular muscles without sutures, placing these sutures after insertion of the orbital implant.

Previously, proponents of the Zimmerman hypothesis believed that surgeons could cause metastatic disease by physically disseminating melanoma cells into the general circulation during enucleation, so they advocated preventative measures such as pre-enucleation radiotherapy. Concerns regarding iatrogenic metastatic spread have diminished as a result of a Collaborative Ocular Melanoma Study (COMS) reporting the failure of neoadjuvant radiotherapy to improve survival [13]. Nevertheless, some authors continue to perform neoadjuvant proton beam or stereotactic radiotherapy before the endoresection of choroidal melanoma to prevent disseminating viable tumor cells systemically [14].

Neoadjuvant chemotherapy has been recommended for patients with advanced retinoblastoma if the eye is buphthalmic and, therefore, at increased risk of globe rupture during enucleation [15]. Increasingly, systemic immune checkpoint inhibitors are being given to patients with advanced conjunctival malignancies in the hope of preventing exenteration, using agents such as ipilimumab with nivolumab for melanoma and cemiplimab with pembrolizumab for squamous carcinoma [16, 17]. Studies are currently in progress to assess systemic neoadjuvant treatment of large uveal melanomas with darovasertib, a protein kinase C inhibitor, to induce tumor regression so that radiotherapy can be performed instead of enucleation [18]. This approach, if successful, may also allow tumor resection in some cases.

As with any surgery, hemostasis is important. With conjunctival tumor excision, this is enhanced by including epinephrine in the subconjunctival anesthetic injection, placing a ring of diathermy burns around the tumor, and cauterizing the scleral bed as soon as any hemorrhage occurs. With tarsal conjunctival tumors, a large chalazion clamp is effective at preventing hemorrhage during tumor resection. With enucleation for uveal melanoma, a retrobulbar injection of bupivacaine with epinephrine is useful, as well as diathermy of the extraocular muscles before detachment, applying compression for several minutes after removing the eye, possibly using a test tube filled with ice and placing a pressure bandage on completing the operation. In addition to systemic hypotensive anesthesia during trans-scleral exoresection of choroidal melanoma, hemostasis is enhanced by applying diathermy to any vortex veins in the operative field as well as the short posterior ciliary arteries adjacent to the optic nerve in the quadrant of the tumor (Fig. 13.2) [4]. With the endoresection of choroidal melanoma, in addition to hypotensive anesthesia and elevation of the intraocular pressure, the tumor is removed with a vitreous cutter through an opening in the overlying retina (Fig. 13.3). To prevent accumulation of blood in the subretinal space, the lateral slopes of the melanoma are retained as long as possible while resecting the central part of the tumor so that any hemorrhage pools within the crater that is formed, from where the blood is easily aspirated [4].

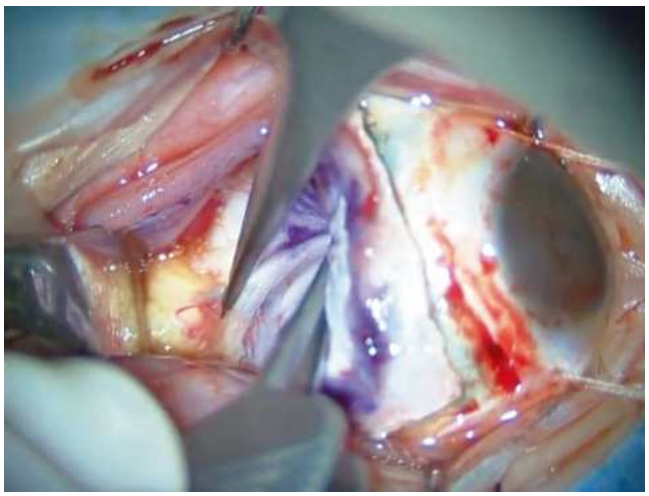

Fig. 13.2 Cauterization of posterior ciliary arteries during exoresection of a choroidal melanoma

Some surgical procedures are not widely performed because they require skills that can be gained only after extensive and regular experience with the technique. For example, with choroidal melanoma exoresection, the tumor is removed *en bloc* through a large scleral trapdoor. A serious complication of this procedure is the creation of a retinal break, which inevitably causes rhegmatogenous retinal detachment. To prevent this problem, core vitrectomy is performed to soften the eye so that the retina does not bulge through the scleral trapdoor and so that it falls away from the tumor when it is being excised. However, thick mushroom tumors tend to become adherent to the retina, and attempts to separate the two structures by blunt dissection often result in a retinal break. The author has found that a retinal tear can be prevented by scraping the tumor surface close to the retinal adhesion, using a sharp blade so that invisible bands are divided and so that the retina separates from the tumor intact (Fig. 13.4). If a retinal tear does occur, the chances of preventing rhegmatogenous retinal detachment with proliferative vitreoretinopathy are best if vitrectomy, removal of subretinal hemorrhage, endolaser retinopexy, and silicone oil tamponade are performed during the same operation, after

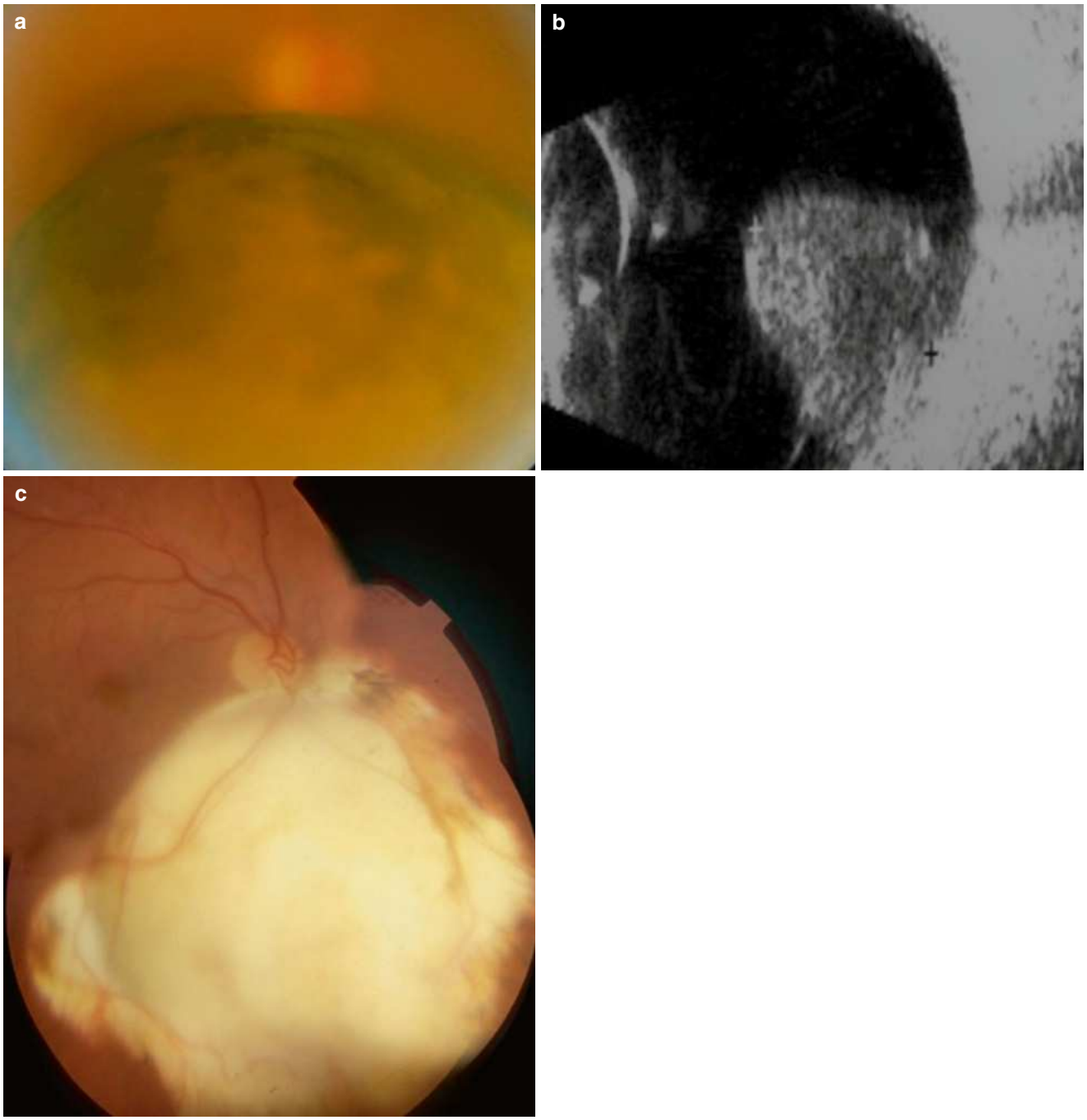

Fig. 13.3 Endoresection of choroidal melanoma in a 65-year-old man. (**a**) Pre-operative color photograph showing a thick choroidal melanoma inferior to the right optic disc, (**b**) b-scan ultrasound showing the tumor to have a basal diameter of 10.4 mm and a thickness of 9.6 mm, (**c**) post-operative photograph after cataract surgery. The patient retained 20/20 vision for many years with no local tumor recurrence

closing the lamellar scleral flap with sutures but before inserting a radioactive plaque, re-attaching any detached extraocular muscles, and closing the conjunctiva. The author was fortunate to have, as part of the oncology team, an "onco-VR surgeon" who was able to perform this vitreoretinal surgery at a few minutes´ notice. As with any surgery, successful outcomes are more likely when surgeons and their teams perform enough procedures regularly. For this reason, results published in journals by high-volume centers may not be reproduced by surgeons who undertake similar procedures less frequently.

All tumor specimens should be sent to the laboratory for histologic confirmation of diagnosis, assessment of grade of malignancy and surgical clearance margins, and, if possible,

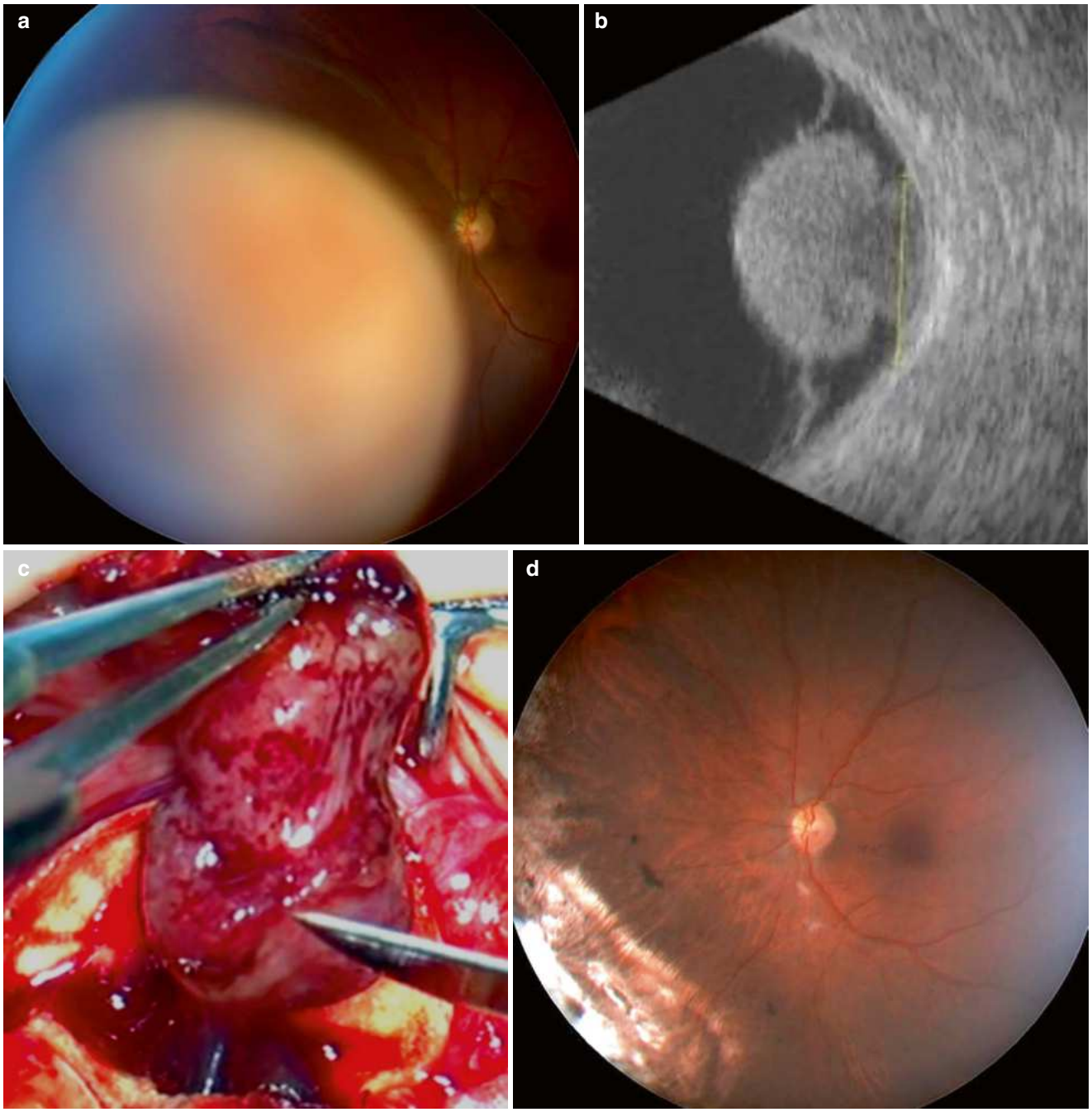

Fig. 13.4 Exoresection of a choroidal melanoma in a 45-year-old man. (**a**) Pre-operative fundus photograph showing the tumor to be located infero-nasally and anteriorly in the left eye, (**b**) B-scan ultrasound showing the tumor to have a mushroom shape with a basal diameter of 15.3 mm and a thickness of 11.0 mm, (**c**) Intra-operative photograph showing surgical incision of invisible bands attaching the retina to the tumor, (**d**) Fundus appearance 2 months post-operatively, when the visual acuity was 20/40, and (**e**) multiplex ligation-dependent probe amplification result showing chromosome 6p gain with no monosomy 3 and no chromosome 8q gain, indicating less than a 10% risk of metastatic death within 10 years

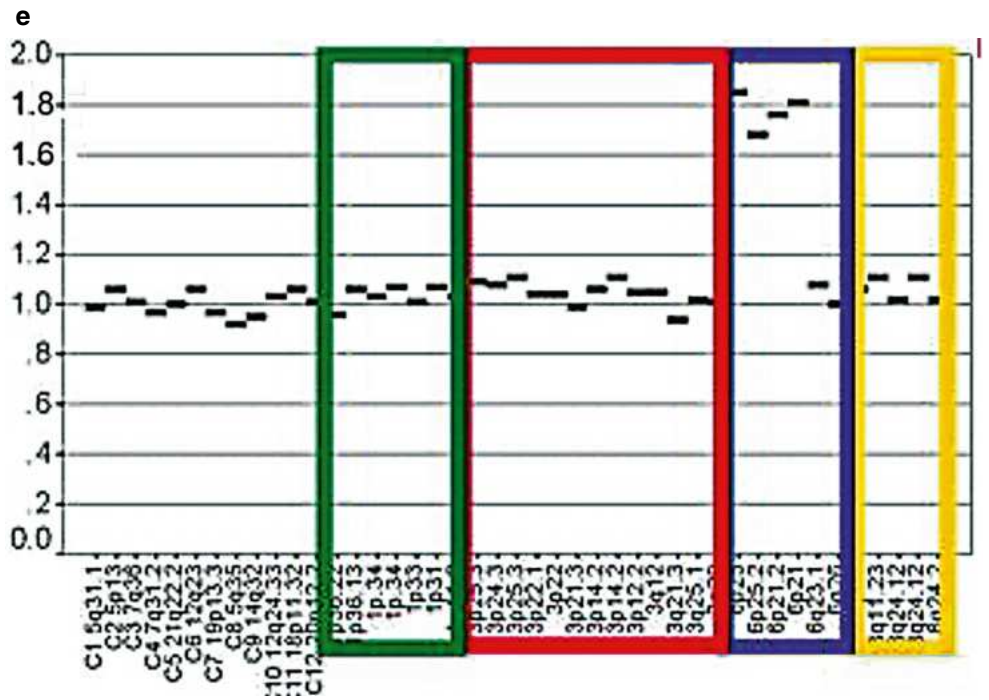

Fig. 13.4 (continued)

identification of any genetic predictors of metastasis specific to the tumor in question. After enucleation, genetic analysis of retinoblastoma tissue is indicated to identify the mutation, if this is not already known, so as to enhance the sensitivity of any blood tests and, hence, the probability of hereditary disease. Such analysis of retinoblastoma tissue or aqueous humor may also identify somatic mutations in the tumor that are of prognostic value with respect to ocular conservation and metastatic disease [19–21].

13.3.10 Wound Closure

Severe complications can occur if wound closure is inadequate. For example, conjunctival wound dehiscence may develop after adjunctive brachytherapy if the sutures dissolve before healing has occurred (Fig. 13.5). This may result in necrosis and perforation of any irradiated sclera that becomes exposed. After enucleation, the orbital implant may become exposed if Tenon's capsule is not adequately sutured without tension.

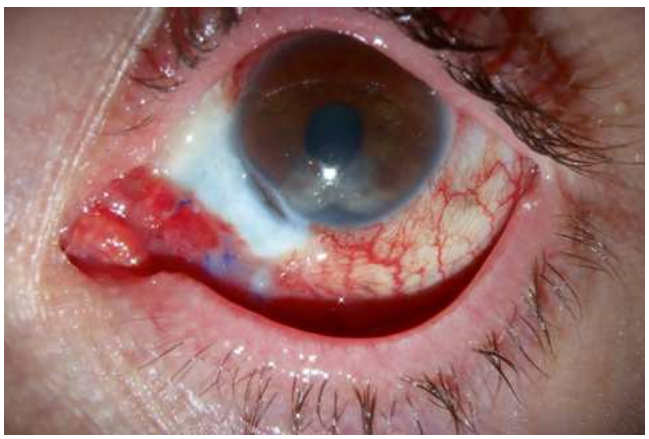

Fig. 13.5 Conjunctival dehiscence after ruthenium plaque brachytherapy for a cilio-choroidal melanoma in the left eye of a 36-year-old man. This patient subsequently developed scleral necrosis and perforation requiring enucleation

13.3.11 Infection Control

Measures to prevent nosocomial infection vary greatly between hospitals with respect to sterilization of the surgeon's hands, the wearing of shoes and surgical masks, sterilization of the operative field, and administration of antibiotics—topically, intracamerally, orally, or by intraoperative, intravenous injection.

13.3.12 Post-operative Care

In addition to the usual aspects of patient care, such as pain control, wound management, and suppression of excessive

inflammation, patients with ocular malignancy and their close relatives require additional measures, such as emotional support, because of concerns regarding mortality, visual handicap, and cosmesis. For example, patients tend to feel isolated and perhaps depressed the day after they return home from the hospital, so they find it helpful to receive a phone call from a member of the team at this time for emotional support and answers to any questions.

13.3.13 Long-term Follow-up

Long-term ophthalmic surveillance is aimed at detecting local tumor relapse as well as any ocular morbidity that may require treatment (e.g., uveitis, glaucoma, cataract, rhegmatogenous retinal detachment, orbital implant extrusion, eyelid problems, etc.).

Local tumor control is assessed by procedures such as slit lamp examination, gonioscopy, binocular indirect ophthalmoscopy, sequential color photography, autofluorescence imaging, optical coherence tomography, and/or ultrasonography—according to the site of the original tumor and type of treatment. With conjunctival malignancies, it is necessary to examine the entire conjunctiva, including the fornices, as well as palpating regional lymph nodes, bilaterally. After iridocyclectomy, ultrasound biomicroscopy is required unless the risk of relapse is low because of the time that has elapsed since the surgery or because of adjunctive radiotherapy. After choroidal melanoma excision, ultrasonography is useful for detecting any extraocular relapse. Further, if adequate ophthalmoscopic surveillance of the posterior segment is prevented by lens opacities, then cataract surgery is performed irrespective of the visual prognosis. Some surgeons also advocate enucleation if media opacities cannot be cleared.

Systemic surveillance is undertaken according to the risk of metastases in the regional lymph nodes, liver, and other organs, depending on the primary ocular malignancy. After excision of uveal melanoma, some authors advocate 6–12 monthly liver scans for at least 10 years in all patients, and others target such surveillance only at patients with a metastatic risk exceeding a particular level (e.g., 10% at 10 years) [22, 23]. After the excision of cutaneous melanoma, a team of experts has recommended a clinical exam; palpation or ultrasonography of regional lymph nodes; computed tomography of chest, abdomen, and pelvis; and/or brain MRI according to the estimated risk of metastatic disease [24]. A similar approach could be followed with conjunctival melanoma. After enucleation for retinoblastoma, systemic surveillance is directed by the risk of relapse in the orbit and brain as well as systemic metastatic disease and second malignant neoplasms [25].

13.4 Quality of Surgical Excision

Surgical outcomes have improved with the development of ocular oncology centers staffed by a highly specialized multidisciplinary team that includes surgical ocular oncologists and, increasingly, vitreoretinal surgeons with sub-specialty training in “oncoVR” enabling them to perform procedures such as tumor biopsy and endoresection more successfully.

As with other forms of surgery, measures to improve the quality of excision procedures include the availability of protocols and evidence of compliance with evidence-based standards; quality of documentation of surgical procedures in medical records; video recording of procedures for review of surgeons’ dexterity and skill in performing specific excisions, without omitting essential technical steps; and morbidity and mortality conferences. Quality is also enhanced by evaluations measuring outcomes such as ocular conservation, visual acuity, local tumor control, iatrogenic ocular morbidity, and, ideally, patient-reported outcomes such as pain control, emotional support, and satisfaction with information received about their condition and management. Such audits are more meaningful if they take into account all risk factors at baseline.

Results of surgical excision are also likely to improve if staff safety is protected by measures aimed at preventing fatigue and stress as well as improving ergonomics (e.g., preventing cervical problems in surgeons by educating them on safe posture when using an operating microscope). An important cause of stress in surgeons is failure, hence the importance of proper training, which, unfortunately, is often deficient. In addition, surgical trainees need to know that it is their responsibility to educate themselves about surgical instruments, suture materials, knots, and other essential knowledge. Through no fault of their own, some individuals lack the “3-D vision,” the dexterity, and/or the ability to improvise and innovate when performing surgery but are determined to become surgeons; the author has had to provide career advice to such trainees, gently redirecting them to a specialty that is more suited to their talents.

Finally, the success of surgical excision of ocular tumors is greatly influenced by ophthalmologists at the local hospital with respect to their ability to diagnose the tumor correctly, refer the patient efficiently, detect tumor recurrence and other ocular morbidity, and manage patients appropriately when problems arise. Ocular oncologists can improve the efficiency of care and clinical outcomes by providing guidance to such ophthalmologists at every opportunity (e.g., in reports after any follow-up assessment at the ocular oncology center). For example, it is helpful if advice is given on investigations that are likely to be useful, as well as those that would be unhelpful and wasteful of healthcare resources.

The local ophthalmologists would also welcome guidance on a reasonable follow-up schedule for a particular patient and on what to do if any concerns ever arise (e.g., sending images of the suspicious lesion to the ocular oncologist, who would either provide remote assistance or arrange to see the patient in person).

13.5 Conclusions

Tumor excision is only one step in the surgical oncological pathway, which includes pre-operative assessment, prognostication, patient counseling, anesthesia, infection control, post-operative care, long-term follow-up, quality assurance and, in selected cases, neoadjuvant and/or adjuvant chemotherapy, radiotherapy, or both. As with any surgery, outcomes are optimal if excision is performed by an ocular oncologist or oncoVR surgeon who is adequately trained and assessed, also practicing as part of a comprehensive multidisciplinary team in a high-volume oncology service having all the resources needed to provide the latest, evidence-based, holistic care.

References

1. Damato B, Hope-Stone L, Cooper B, Brown SL, Salmon P, Heimann H, Dunn LB. Patient-reported outcomes and quality of life after treatment of choroidal melanoma: a comparison of enucleation versus radiotherapy in 1596 patients. Am J Ophthalmol. 2018;193:230–51. https://doi.org/10.1016/j.ajo.2018.03.015.
2. Damato B, Hope-Stone L, Cooper B, Brown S, Heimann H, Dunn L. Patient-reported outcomes and quality of life after treatment for choroidal melanoma. Ocul Oncol Pathol. 2019;5(6):402–11.
3. Diener-West M, Reynolds SM, Agugliaro DJ, Caldwell R, Cumming K, Earle JD, Green DL, Hawkins BS, Hayman J, Jaiyesimi I, Kirkwood JM, Koh WJ, Robertson DM, Shaw JM, Thoma J, Collaborative Ocular Melanoma Study Group Report 23. Screening for metastasis from choroidal melanoma: the Collaborative Ocular Melanoma Study Group Report 23. J Clin Oncol. 2004;22(12):2438–44.
4. Damato BE, Afshar AR, Groenewald C, Heimann H. Surgical resection of choroidal melanoma. In: Schachat AP, editor. Ryan's retina. Philadelphia: Elsevier; 2023. p. 2746–55.
5. Kivela T, Kujala E. Prognostication in eye cancer: the latest tumor, node, metastasis classification and beyond. Eye (Lond). 2013;27(2):243–52.
6. Cunha Rola A, Taktak A, Eleuteri A, Kalirai H, Heimann H, Hussain R, Bonnett LJ, Hill CJ, Traynor M, Jager MJ, Marinkovic M, GPM L, Dogrusöz M, Kilic E, de Klein A, Smit K, van Poppelen NM, Damato BE, Afshar A, Guthoff RF, Scheef BO, Kakkassery V, Saakyan S, Tsygankov A, Mosci C, Ligorio P, Viaggi S, CHD LG, Bornfeld N, Bechrakis NE, Coupland SE. Multicenter external validation of the liverpool uveal melanoma prognosticator online: an OOG collaborative study. Cancers (Basel). 2020;12(2):477.
7. Damato B, Eleuteri A, Hussain R, Kalirai H, Thornton S, Taktak A, Heimann H, Coupland SE. Parsimonious models for predicting mortality from choroidal melanoma. Invest Ophthalmol Vis Sci. 2020;61(4):35.
8. Seider MI, Damato BE. Digital audio recording of initial patient visits to an ocular oncology clinic: a pilot study. Ophthalmic Surg Lasers Imaging Retina. 2015;46(5):597–9.
9. Damato B, Jones AG. Uveal melanoma: resection techniques. Ophthalmol Clin N Am. 2005;18(1):119–28. ix
10. Damato B, Patel I, Campbell IR, Mayles HM, Errington RD. Visual acuity after Ruthenium(106) brachytherapy of choroidal melanomas. Int J Radiat Oncol Biol Phys. 2005;63(2):392–400.
11. Damato B, Coupland SE. An audit of conjunctival melanoma treatment in Liverpool. Eye (Lond). 2009;23(4):801–9.
12. Damato B. Adjunctive plaque radiotherapy after local resection of uveal melanoma. Front Radiat Ther Oncol. 1997;30:123–32.
13. The Collaborative Ocular Melanoma Study (COMS) randomized trial of pre-enucleation radiation of large choroidal melanoma I: characteristics of patients enrolled and not enrolled. COMS report no. 9. Am J Ophthalmol. 1998;125(6):767–78.
14. Bechrakis NE, Foerster MH. Neoadjuvant proton beam radiotherapy combined with subsequent endoresection of choroidal melanomas. Int Ophthalmol Clin. 2006;46(1):95–107.
15. Luna-Fineman S, Chantada G, Alejos A, Amador G, Barnoya M, Castellanos ME, Fu L, Fuentes-Alabi S, Girón V, Goenz MA, Maldonado C, Méndez G, Morales RA, Ortiz R, Sanchez G, Wilson M, Rodríguez-Galindo C. Delayed enucleation with neoadjuvant chemotherapy in advanced intraocular unilateral retinoblastoma: AHOPCA II, a prospective, multi-institutional protocol in Central America. J Clin Oncol. 2019;37(31):2875–82.
16. Sa HS, Daniel C, Esmaeli B. Update on immune checkpoint inhibitors for conjunctival melanoma. J Ophthalmic Vis Res. 2022;17(3):405–12.
17. Ceylanoglu KS, Eisenberg A, Worden FP, Elner VM, Demirci H. Use of cemiplimab, an immune checkpoint inhibitor for conjunctival intraepithelial neoplasia. Cornea. 2024;43(4):528–30.
18. Hiong A, O'Day R, Fog LS, McKay D, McKenzie J, Ameratunga M, Joshua AM, Shackleton M. Globe salvage and vision preservation by neoadjuvant darovasertib and crizotinib in uveal melanoma. Ophthalmol Retina. 2024;8(4):325–30.
19. Berry JL, Xu L, Kooi I, Murphree AL, Prabakar RK, Reid M, Stachelek K, Le BHA WL, Reiser BJ, Chévez-Barrios P, Jubran R, Lee TC, Kim JW, Kuhn P, Cobrinik D, Hicks J. Genomic cfDNA analysis of aqueous humor in retinoblastoma predicts eye salvage: the surrogate tumor biopsy for retinoblastoma. Mol Cancer Res. 2018;16(11):1701–12.
20. Francis JH, Richards AL, Mandelker DL, Berger MF, Walsh MF, Dunkel IJ, Donoghue MTA, Abramson DH. Molecular changes in retinoblastoma beyond RB1: findings from next-generation sequencing. Cancers (Basel). 2021;13(1):149.
21. Afshar AR, Pekmezci M, Bloomer MM, Cadenas NJ, Stevers M, Banerjee A, Roy R, Olshen AB, Van Ziffle J, Onodera C, Devine WP, Grenert JP, Bastian BC, Solomon DA, Damato BE. Next-generation sequencing of retinoblastoma identifies pathogenic alterations beyond RB1 inactivation that correlate with aggressive histopathologic features. Ophthalmology. 2020;127(6):804–13.
22. Uveal Melanoma Guideline Development Group. Uveal melanoma. Melanoma Focus 2023 [cited 2024 25 Mar 2024]; Available from: https://melanomafocus.org/wp-content/uploads/2023/11/Uveal_Melanoma_EX_SUMMARY.pdf.
23. Weis E, Surgeoner B, Salopek TG, Cheng T, Hyrcza M, Kostaras X, Larocque M, McKinnon G, McWhae J, Menon G, Monzon J, Murtha AD, Walker J, Temple-Oberle C. Management of uveal melanoma: updated cancer care Alberta clinical practice guideline. Curr Oncol. 2023;31(1):24–41.
24. Garbe C, Amaral T, Peris K, Hauschild A, Arenberger P, Basset-Seguin N, Bastholt L, Bataille V, Del Marmol V, Dréno B, Fargnoli MC, Forsea AM, Grob JJ, Höller C, Kaufmann R, Kelleners-Smeets N, Lallas A, Lebbé C, Lytvynenko B, Malvehy J, Moreno-Ramirez D, Nathan P, Pellacani G, Saiag P, Stratigos AJ, ACJ VA, Vieira

R, Zalaudek I, Lorigan P, European Dermatology Forum (EDF), the European Association of Dermato-Oncology (EADO), and the European Organization for Research and Treatment of Cancer (EORTC), et al. European consensus-based interdisciplinary guideline for melanoma. Part 1: diagnostics: update 2022. Eur J Cancer. 2022;170:236–55.

25. Dimaras H, Corson TW, Cobrinik D, White A, Zhao J, Munier FL, Abramson DH, Shields CL, Chantada GL, Njuguna F, Gallie BL. Retinoblastoma. Nat Rev Dis Primers. 2015;1:15021.

Ocular Complications of Radiation Therapy

14

Jose C. Puthussery and Arun D. Singh

14.1 Introduction

Although radiation therapy is the standard treatment for most intraocular malignancies, various ocular complications may occur, including radiation-induced dry eye, cataracts, secondary glaucoma from neovascularization of the iris, scleral necrosis, retinopathy, and optic neuropathy. In this chapter, we review the ocular side effects of radiation administered from brachytherapy, proton beam radiation therapy, and external beam radiation therapy and their potential treatments. Emphasis is placed on radiation retinopathy and optic neuropathy, the two most visually significant complications of radiation therapy.

14.2 Periorbital Skin

14.2.1 Acute

Loss of eyelashes is one of the first and most common adverse effects to occur after radiation therapy, although they do usually grow back (Fig. 14.1). Erythema may occur within hours of radiation therapy, followed by desquamation and scaling of the skin taking about 2–4 weeks to resolve [1]. Severe dermatitis occurs with higher doses (40 Gy) [2].

14.2.2 Late

Loss of eyelashes and eyebrows may be permanent [2, 3]. Other late sequelae of regular and high-dose radiation therapy (40 Gy or higher) to the eyelids include trichiasis, telangiectasia, hyperpigmentation, hyperkeratosis, entropion, ectropion, and punctal occlusion. Eyelid atrophy, necrosis, and frank ulceration are uncommon.

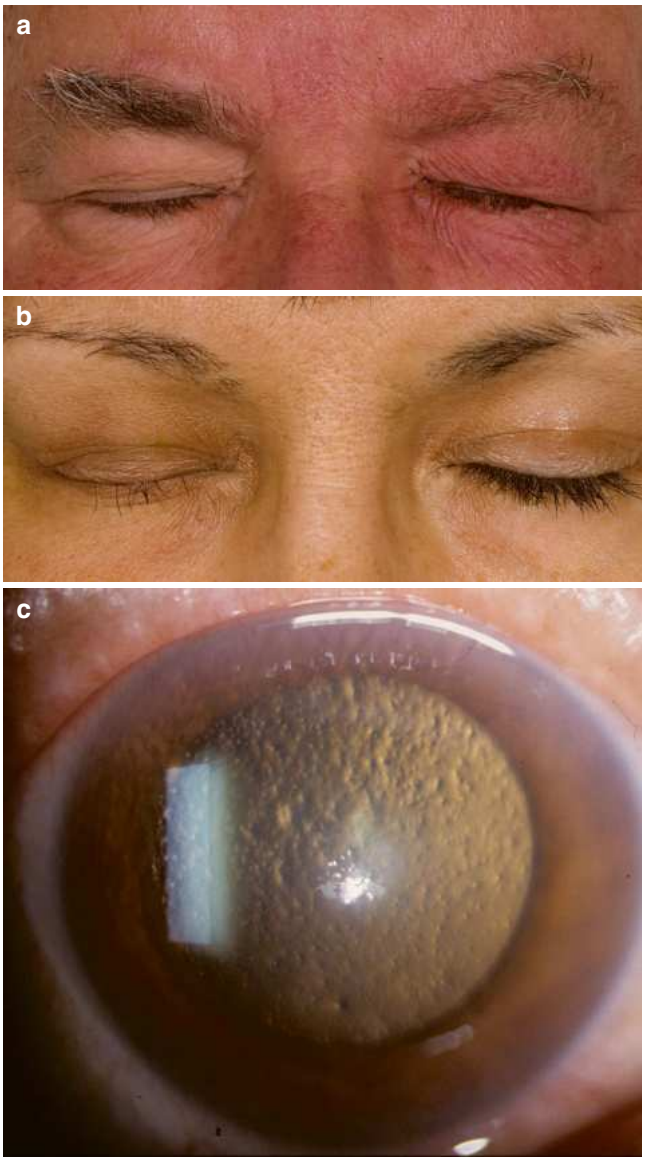

Fig. 14.1 Acute complications of radiotherapy. (**a**) Radiation dermatitis. (**b**) Loss of eyelashes. (**c**) Punctate keratitis

J. C. Puthussery · A. D. Singh (✉)
Department of Ophthalmic Oncology, Cole Eye Institute, Cleveland Clinic, Cleveland, OH, USA
e-mail: puthusj@ccf.org; singha@ccf.org

© The Author(s), under exclusive license to Springer Nature Switzerland AG 2025

A. D. Singh, B. E. Damato (eds.), *Clinical Ophthalmic Oncology*, https://doi.org/10.1007/978-3-031-75907-9_14

14.2.3 Treatment

Mild acute radiation effects can be relieved with the administration of topical corticosteroids, such as 1% hydrocortisone. Other options to treat acute radiation effects include trolamine-containing topical emulsions and hydrogel and hydrocolloid dressings [4]. Late effects may be remedied by wound debridement, antibiotic therapy, and reconstructive surgery.

14.3 Conjunctiva

14.3.1 Acute

Conjunctivitis, chemosis, and a clear or purulent discharge may occur when radiation therapy doses of >5 Gy are used [2, 3].

14.3.2 Late

Effects of radiation therapy on the conjunctiva include telangiectasia, symblepharon, and sequelae of loss of goblet cells (keratinization and scarring). Doses of approximately 50 Gy lead to conjunctival scarring, which in turn could lead to corneal damage if involving the palpebral conjunctiva, especially of the upper lid [5]. Severe contracture occurs with doses of more than 60 Gy, and symblepharon is frequent with doses above 80–100 Gy [6].

14.3.3 Treatment

Topical corticosteroids are indicated for early conjunctivitis and chemosis. Artificial tears and ointment help replace the moisture lost due to damage to goblet cells and keratinization.

14.4 Cornea

14.4.1 Radiation-Induced Dry Eye and Keratitis

Dry eye and keratitis are complications frequently seen after external beam radiation therapy for uveal metastases and proton beam radiation therapy for uveal melanoma but are infrequent following brachytherapy (Fig. 14.1). An increase in conjunctival epithelial stratification and reduction in goblet cells contribute to dry eye. Tear film instability and dysfunction may cause punctate epithelial erosions [7]. Radiation keratopathy also includes the development of limbal stem cell deficiency and chronic corneal inflammation associated with decreased corneal sensation [8]. Corneal nerve damage following radiation therapy could be an inciting factor for radiation keratopathy [9].

The effects of external beam radiation therapy on the lacrimal gland are well-studied. Exposure of the entire orbit to radiation for head and neck cancers can cause dry eye in 100% with doses ≥57 Gy, 20% with doses of 30–45 Gy, and 0% with <30 Gy [10]. The dose threshold for the lacrimal gland is different for fractionated stereotactic radiation, with a median dose of 10 Gy/fraction resulting in a 50% probability of dry eye syndrome [11]. Single fraction radiation to the lacrimal gland can also affect Schirmer test values at 24 months [12]. Radiation therapy causes near-total destruction of the histological architecture of the lacrimal gland, leading to aqueous deficient dry eye syndrome in 50% of patients at a mean radiation dose of 48 Gy (range, 40–66), with two-thirds developing it by the end of 5 years [13]. The radiation dose to the lacrimal gland is an important factor in the development of dry eye, and efforts should be made to respect its tolerance as much as possible without compromising tumor coverage.

Atrophy of the meibomian glands is another cause of radiation therapy-associated dry eye syndrome, with meibomian gland dysfunction occurring even with low-dose irradiation (<30 Gy) [14].

14.4.2 Treatment

Symptomatic treatment is recommended, including topical lubricants and lacrimal punctal occlusion.

14.5 Scleral Necrosis

Scleral necrosis following episcleral plaque brachytherapy has been reported, often in association with post-operative brachytherapy. Petrovich et al. described the histologic appearance of enucleated eyes with choroidal melanoma that had been treated with episcleral plaque brachytherapy, observing scleral atrophy in 33% of eyes (Fig. 14.2) [15]. However, in the clinical studies with iodine-125 brachytherapy, few reports mention scleral atrophy or necrosis as a complication. Stack et al. documented that none of their 84 patients developed scleral necrosis after iodine-125 brachytherapy [16]. Kaliki et al. reported a scleral necrosis rate of 1% following iodine-125 brachytherapy with ciliary body location being the strongest risk factor [17]. Correa et al. showed that thicker tumors (>6.5 mm, 24% at 45.4 months) were more likely to develop scleral necrosis than thinner tumors [18]. A large case-control study showed that radiation-induced scleral necrosis was seen in 3% of 3960 patients,

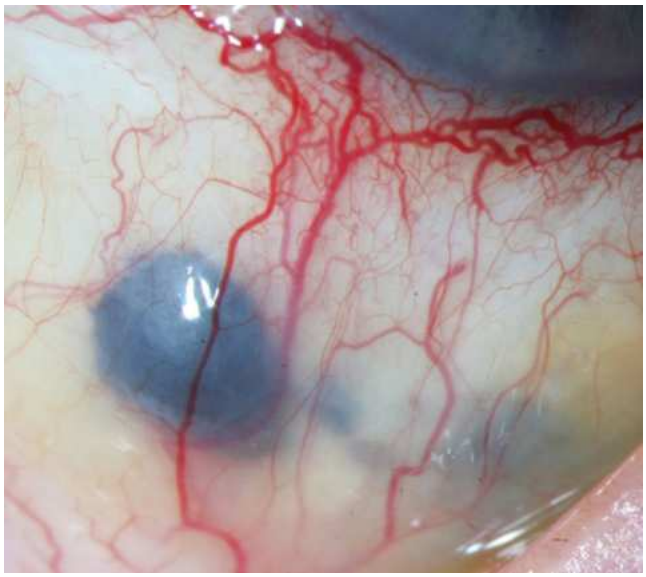

Fig. 14.2 Scleral atrophy 10 months following plaque radiotherapy for a large ciliochoroidal melanoma

with the mean time of occurrence being 30 months after brachytherapy [19]. Risk factors for scleral necrosis were noted to be scleral contact dose, posterior margin of tumor anterior to equator, extraocular extension, conjunctival dehiscence after therapy, superior rectus disinsertion, and the concomitant use of antiglaucoma medication [19]. Asymptomatic cases can be managed by observation [17], while cases with extensive scleral necrosis require scleral patch graft [18].

14.6 Extraocular Muscles

Extraocular muscles are theoretically shielded from most of the iodine-125 radiation as only 0.1% of radiation passes through a 0.5-mm-thick gold foil [20]. However, with the current episcleral plaque design, extraocular muscles may actually be exposed to a significant amount of laterally directed and uncollimated radiation. Kiratli et al. compared biopsy specimens from radiation-exposed extraocular muscles with non-irradiated extraocular muscles from enucleated controls and found that the radiation-exposed muscles had a focal decrease in muscular tissue with increased fibroblasts and collagen [21]. Furthermore, on electron microscopy, a loss of sarcoplasmic reticulum with mitochondrial swelling was noted. Another study by Alfreihi et al. showed that the radiation-exposed muscles appeared thicker on gross examination and revealed fibrosis, reactive enlargement, and vacuolization on microscopic examination. The function of radiation-exposed muscles seemed to be affected, with decreased versions, incomitant strabismus, and negative forced duction testing [22].

14.6.1 Dose Relationship

Sener et al. observed that 60% of their patients (12/20) had ocular alignment and motility problems following episcleral plaque brachytherapy [20]. However, only 10% (2/20) of patients complained of diplopia. Huang et al. showed similar findings, with only 2.5% of patients (11/438) developing strabismus post-episcleral plaque brachytherapy [23]. Perhaps these complications can be attributed to the combined effects of radiation and simply mechanical injury from muscle manipulation.

14.6.2 Treatment

Sener et al. suggest using either prism correction or botulinum toxin A injections in the early post-operative period and recommend waiting at least 6 months before pursuing surgical correction of strabismus, allowing for spontaneous recovery [20].

14.7 Iris

14.7.1 Iris Neovascularization and Neovascular Glaucoma

Though complications of the anterior segment occur frequently with external beam radiation, they can also occur following episcleral plaque brachytherapy [24]. Iris neovascularization is caused by angiogenic factors that are produced as a result of ischemia in the optic nerve, retina, and/or the irradiated tumor itself. This presents clinically as rubeosis iridis and neovascular glaucoma (Fig. 14.3). A careful

Fig. 14.3 Neovascular glaucoma following radiation therapy

examination of the iris and anterior chamber angle prior to pupillary dilation may detect early signs of neovascularization.

Rubeosis iridis following iodine-125 episcleral plaque brachytherapy is reported at rates of 4–23%, occurring at a mean of 26.7 months. Neovascular glaucoma rates ranged from 2% to 45%. Numerous factors may contribute to iris neovascularization. Studies using cobalt-60 and palladium-103 have associated increased neovascularization with an anterior tumor location [25, 26]. Increased tumor thickness is associated with higher rates as well as decreased time to the development of iris neovascularization and may be related to the elevated levels of tumor-related angiogenic factors [24, 27]. Recent data shows that preexisting diabetes acts synergistically with radiation to promote iris neovascularization and subsequent glaucoma [28]. Risk factors for the development of neovascular glaucoma following episcleral plaque brachytherapy include larger tumor size, smoking history (greater pack-years), pseudophakia, and higher grade of radiation retinopathy on fluorescein angiogram [29].

14.7.2 Treatment

Enucleation has traditionally been indicated for eyes with neovascular glaucoma in the setting of media opacity and poor vision. The rate of enucleation secondary to neovascular glaucoma after iodine-125 brachytherapy ranges from 1% to 12% and indicates the difficulty in managing this complication. Although controversial, tube-shunt procedures with vitrectomy and endolaser in eyes with good visual prognosis may also be considered. A report by Yeung et al. suggests that intravitreal bevacizumab may be used to treat neovascular glaucoma and salvage the eye following proton beam radiation therapy (Fig. 14.4) [30]. Another study showed that while intravitreal bevacizumab improved the IOP in neovascular glaucoma, it did not reduce the overall enucleation rate. Despite that, the authors concluded that intravitreal bevacizumab could be useful in the early phases or as a preventive modality [31, 32]. Panretinal photocoagulation (PRP) is effective for the treatment of neovascular glaucoma [31, 33]. Rates of neovascular glaucoma and enucleation in larger tumors could be reduced by adjuvant surgical procedures (endoresection or endodrainage-vitrectomy) [34] and existing rubeosis and neovascular glaucoma reversed by excising the irradiated tumor [35].

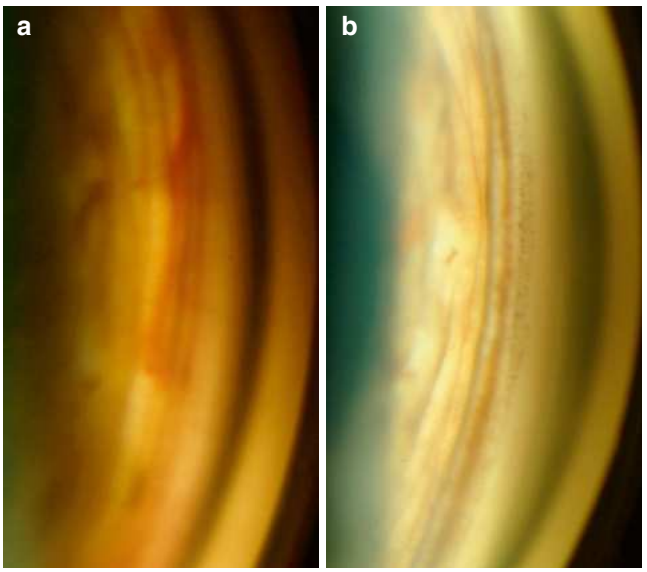

Fig. 14.4 Goniophotograph showing neovascularization and bleeding in the anterior chamber angle (**a**) Eight weeks after treatment with panretinal photocoagulation and intravitreal injection of bevacizumab (1.25 mg/0.05 ml). Note that the angle neovascularization and hyphema have resolved completely (**b**)

14.8 Lens

14.8.1 Clinical Features

Ionizing radiation is known to damage the lens equatorial lens fibers because of their high mitotic rate. The compensatory mitosis occurs with disrupted organization and leads to the deposition of Wedl cells at the posterior pole. The clinical appearance of a radiation cataract is of a small dot at the posterior pole of the lens and subsequently increases to a diameter of 1–2 mm [36]. The opaque region is comprised of scattered granules and vacuoles. As the cataract continues to develop, the center of the opacity clears, and the overall appearance is that of a doughnut with a total diameter of 3–4 mm. Radiation exposure may also lead to the development of cortical cataracts or exacerbate existing nuclear sclerotic cataracts (Fig. 14.5) [37].

14.8.2 Dose Relationship

The development of cataracts is associated with a dose-dependent increase in radiation to the lens. In the largest study to date, the Collaborative Ocular Melanoma Study fol-

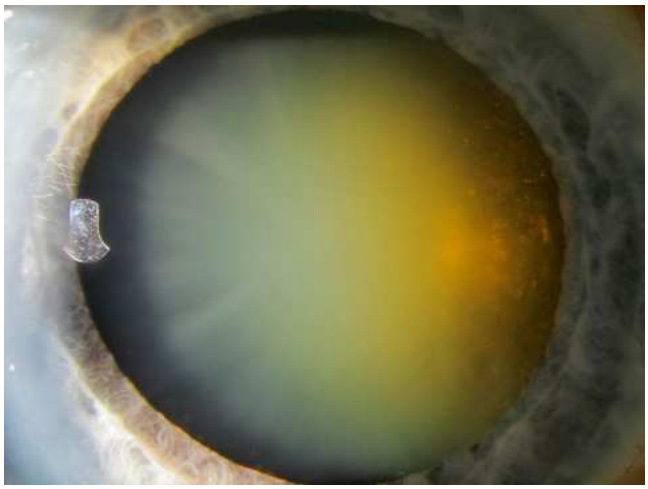

Fig. 14.5 Radiation exposure induced exacerbation of existing nuclear sclerotic cataract

lowed the incidence of cataract development in phakic patients over the first 5 years following iodine-125 brachytherapy [38]. In total, 68% (362/532) of eyes developed vision-limiting cataracts or underwent cataract surgery after iodine-125 brachytherapy, with a greater proportion developing cataracts following higher doses of the lens. With a cumulative dose to the lens of 24 Gy or more, the 5-year cumulative incidence of cataracts was 92% compared with 65% in those with less than 12 Gy. Studies examining the rate of cataract formation after proton beam therapy (PBT) have shown similar rates when compared to episcleral plaque brachytherapy [39].

The radiation dose to the lens is affected by both tumor size and location. Increasing tumor height has been shown to decrease the time to cataract development, and a greater tumor diameter increases the risk of cataracts [40]. The location of the tumor is also important, as treatment of an anterior tumor exposes the lens to more radiation. Fontanesi et al. found that cataracts developed earlier with anterior tumors (median 11 months post-treatment) compared with posterior tumors (median 26 months post-treatment) with a greater proportion of cataracts occurring in eyes with anterior tumors [41]. Data from patients treated with stereotactic radiation (10 Gy × 5 fractions) also suggests a dose-response relationship with cataract formation and dose to the lens and ciliary body with a median dose of 5 Gy/fraction causing a cataract in 50% of cases and an overall rate of CTCAE version 3 grade 3 cataracts of 10% [42]. Following proton beam therapy, no significant risk of vision-impairing cataracts below a dose of 10 GyRBE (photon-equivalent grays radiation biologically equivalent) has been reported [43]. Thus, a lens-sparing approach to radiation therapy could delay the rate of cataract formation.

14.8.3 Treatment

Radiation-induced cataracts may be successfully treated with standard surgical techniques with improvement in vision [38]. Patients whose vision may fail to improve frequently have comorbidities, including radiation retinopathy, vitreous hemorrhage, retinal detachment, or optic neuropathy. We have found that eyes developing cataracts following iodine-125 episcleral plaque brachytherapy tolerate standard phacoemulsification with lens implantation well, with outcomes comparable to that of the general population [44].

14.9 Radiation Retinopathy

14.9.1 Clinical Features

Radiation retinopathy was first described in 1933 and includes microaneurysms, telangiectases, hard exudates, cotton wool spots, macular edema, neovascularization, and vitreous hemorrhage (Fig. 14.6). The pathogenesis of radiation retinopathy has a significant inflammatory component and begins after radiation exposure with the preferential loss of vascular endothelial cells and relative sparing of pericytes [3]. It has been hypothesized that the differential sensitivity between retinal endothelial cells and pericytes may be related to the direct exposure of the endothelial cells to high ambient oxygen and iron from the blood that generates free radicals and damages cell membranes [45]. In acellular, poorly supported capillaries, microaneurysms emerge, and telangiectatic-like channels appear, straddling regions of nonperfusion. Ultimately, the inner retinal ischemia leads to neovascularization, vitreous hemorrhage, tractional retinal detachment, and macular edema. The Collaborative Ocular Melanoma Study (COMS) reported a visual acuity of 20/200 in 45% of patients at 3 years [46]. The onset of radiation retinopathy becomes obvious only after many months following episcleral plaque brachytherapy and can progress over many years.

Fluorescein angiography is a tool of the utmost importance to evaluate radiation retinopathy. On it, the earliest changes that appear are focal capillary closure with neighboring areas of irregular capillary dilation and microaneurysms (Fig. 14.6). Furthermore, radiation retinopathy can be classified in grades from 0 to 4, being grade 0, normal; grade 1, late foveal leakage; grade 2, late peripheral leakage; grade 3, presence of nonperfusion; and grade 4, retinal neovascularization (Fig. 14.7) [47, 48].

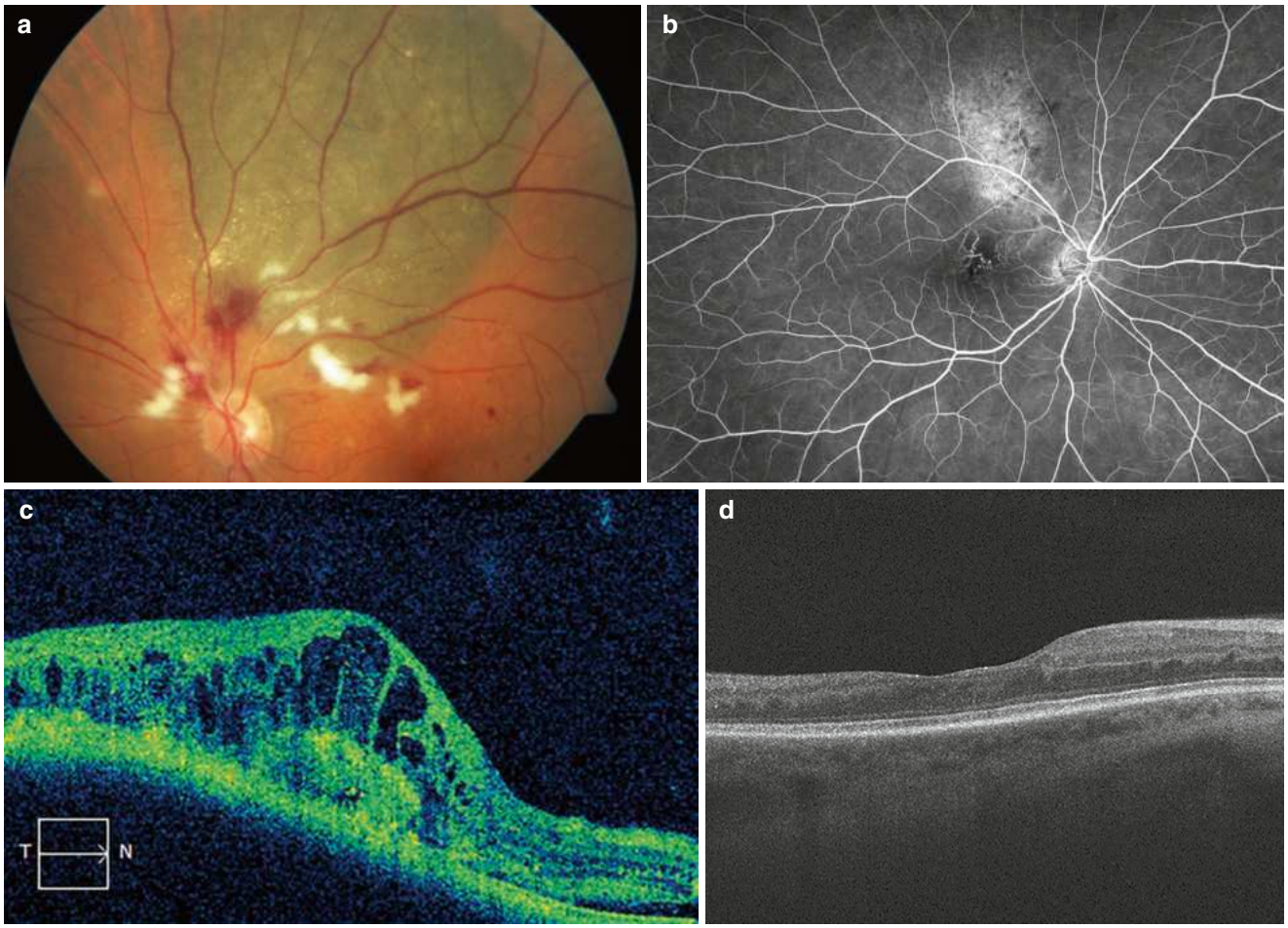

Fig. 14.6 Characteristic ophthalmoscopic features of non-proliferative radiation retinopathy, such as cotton wool spots, telangiectasia, retinal hemorrhages, and macular edema following brachytherapy for choroidal melanoma (**a**). Retinal capillary nonperfusion in the macula and microaneurysms are most evident on the fluorescein angiography (**b**). Cystoid macular edema (**c**) and foveal atrophy on optical coherent tomograph (**d**)

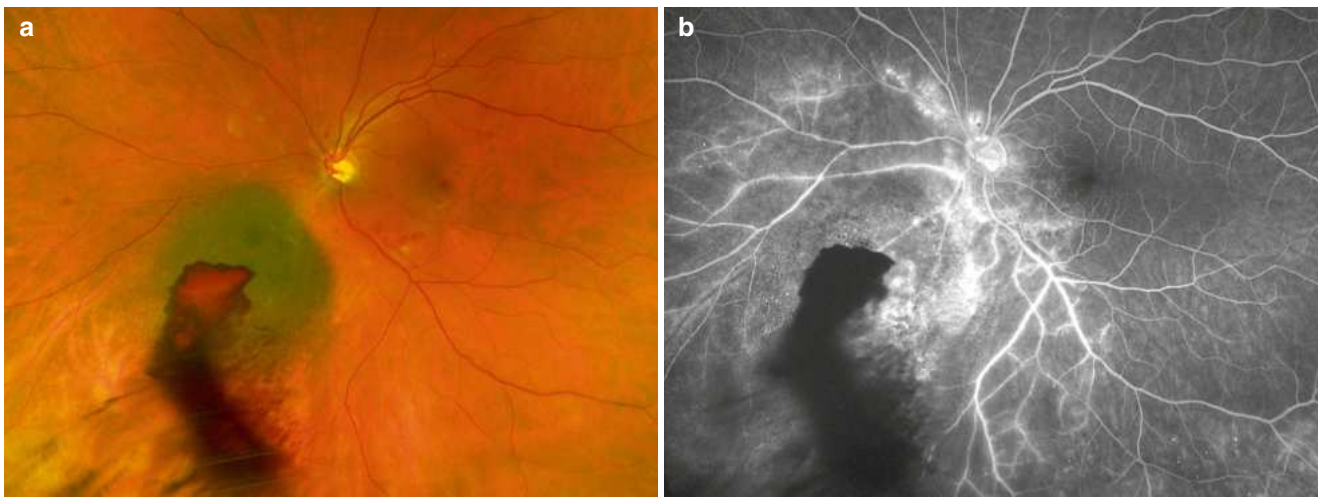

Fig. 14.7 Proliferative radiation retinopathy causing vitreous hemorrhage (**a**). Retinal neovascularization seen by fluorescein angiography (**b**)

14.9.2 Dose Relationship

The rate at which radiation-induced retinopathy and maculopathy develop ranges from 10% to 63% and 13% to 52%, respectively. The mean time to develop maculopathy was found to be 25.6 months after treatment [25, 47]. The risk of radiation retinopathy and maculopathy after episcleral plaque therapy is related to radiation dose and factors affecting radiation dose, such as the height and location of the tumor (Fig. 14.8) [49, 50]. Higher radiation dose and tumors with thickness greater than 4 mm increase the risk for radiation maculopathy. Stack et al. found a 63% risk for radiation maculopathy if the dose to the macula exceeded 90 Gy [16]. With the advent of ocular coherence tomography (OCT) to evaluate the macular anatomy and wide-field angiography, which detect preclinical features of altered retinal anatomy and function, radiation retinopathy is likely to occur in almost every patient treated with radiation over time. Tamplin et al. utilized OCT, OCT-angiography (OCT-A), visual fields, and dosimetry models to demonstrate differential thickness changes in two inner retinal layers suggestive of microvessel leakage and neurodegeneration. Additionally, there was decreased inner retinal capillary density indicative of microvascular pathology. The inner retinal thinning becomes dominant at later stages and correlates with vision loss and decreased vascularity [51]. Longitudinal OCT-A scans in a patient with radiation retinopathy following episcleral plaque brachytherapy showed focal capillary loss and enlargement of the foveal avascular zone along with vascular remodeling with these changes progressing over time despite improvement in clinical markers (cotton wool spots, retinal hemorrhages) (Fig. 14.9) [52].

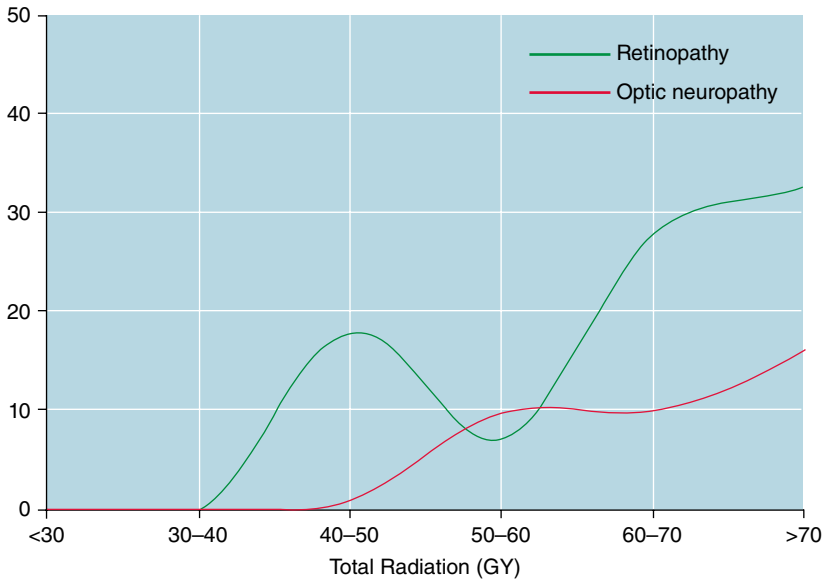

Fig. 14.8 Total dose of radiation and risk of radiation retinopathy and radiation optic neuropathy. (Based on data from: Monroe et al. [50] and Bhandare et al. [49])

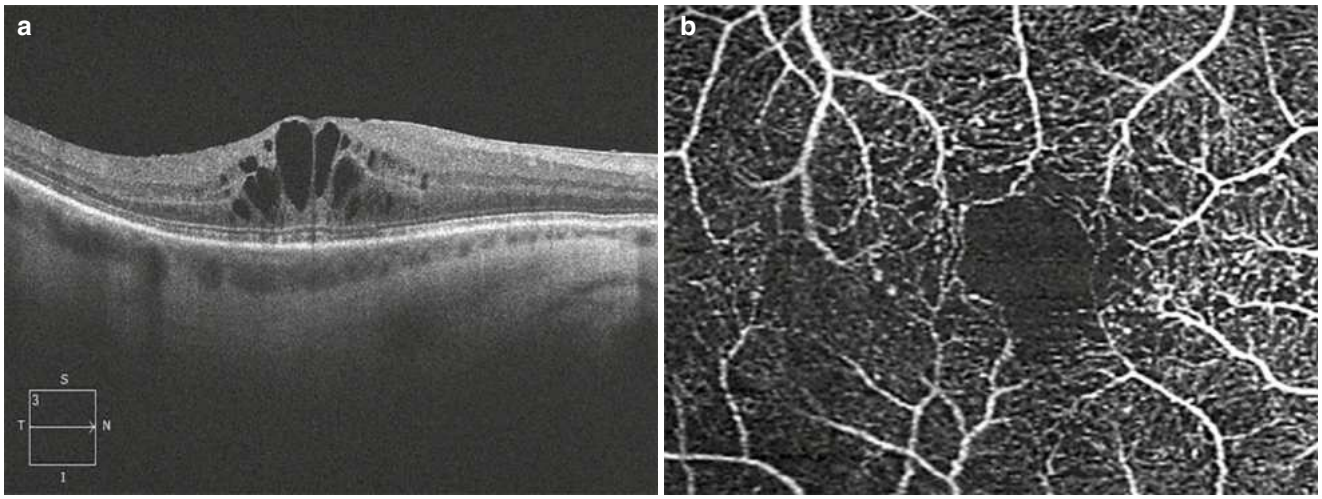

Fig. 14.9 Radiation induced cystoid macular edema (**a**, OCT) and associated retinal ischemia (**b**, OCTA)

14.9.3 Treatment

Numerous treatment modalities have been utilized in the management of radiation retinopathy and maculopathy. Recent studies and their results include intravitreal injections of triamcinolone and bevacizumab, intravitreal implants, laser photocoagulation, and hyperbaric oxygen treatment (Box 14.1) [50].

Box 14.1. Salient Features of Radiation Retinopathy

- Total dose and fraction size of radiation are the key determinants.
- The presence of diabetes and history of prior chemotherapy increases the risk and severity of radiation retinopathy.
- Doses of less than 45 Gy (fractions size ≤2.0 Gy) are unlikely to cause significant retinopathy in the absence of coexisting host risk factors.
- Insult to vascular endothelial cells is the underlying basis of radiation retinopathy.
- Telangiectasia and discrete foci of capillary nonperfusion, with retinal infarcts causing cotton wool spots, are the earliest features.
- The incidence peaks 2–3 years after radiation exposure.
- At present, there is no effective treatment of collateral damage to healthy ocular structures, but the "toxic tumor syndrome" can be treated by removing or ablating the irradiated tumor. Intravitreal steroids have been shown to be effective in selected cases.

Corticosteroids (periocular and intravitreal triamcinolone acetonide, intravitreal dexamethasone implant, fluocinolone acetonide implant) have been used to treat macular edema associated with radiation retinopathy. Although the mechanism is poorly understood, triamcinolone may help to restore a compromised inner blood-retinal barrier [49]. Triamcinolone acetonide is thought to modulate cytokines and regulate capillary permeability [53]. Kaplan et al. showed the utility of intravitreal triamcinolone in preserving vision in radiation maculopathy [54]. It can also be used in conjunction with anti-VEGF therapy with good results. A study utilizing a single 0.7 mg intravitreal dexamethasone implant demonstrated an initial reduction of central subfield thickness (CST) but showed progressive retinal thickening after 4 months of follow-up [55]. Zimmerman et al. used long-acting intraocular steroids (fluocinolone acetonide, Iluvien®) and showed a decrease in macular edema and improvement in visual acuity in 80% of patients [56]. The slow release of steroids allows for sustained control of macular edema, which correlated with stable visual acuity and decreased injection burden for patients (Fig. 14.10) [57]. However, steroid-induced glaucoma necessitating topical therapy and/or surgery may complicate corticosteroids as a treatment modality.

Bevacizumab has been used to treat exudative age-related macular degeneration, diabetic retinopathy, and vein occlusion (Fig. 14.11). Bevacizumab is a humanized monoclonal antibody to vascular endothelial growth factor (VEGF), and blocking VEGF is thought to decrease vascular permeability and inhibit abnormal neovascularization [58]. Twenty-one patients with radiation retinopathy following palladium-103 brachytherapy were treated with intravitreal bevacizumab (1.25 mg/0.05 ml) every 6–12 weeks. After a mean follow-up of 7.8 months, 86% (18/21) had stable or improved visual acuity, with 14% (3/21) regaining two or more Snellen lines [58].

However, some studies utilizing bevacizumab suggest that the improvement is likely temporary. Bakri et al. showed that while initial injections of bevacizumab reduced macular edema, multiple injections led to resistance [59]. It is our experience that intravitreal bevacizumab in patients with recent onset visual decrease secondary to radiation maculopathy has only a transient subjective response. It is generally believed that the role of bevacizumab for radiation maculopathy is limited, requiring multiple injections [60].

Other anti-VEGF agents, such as ranibizumab and aflibercept, have also been used with similar effects [61–65]. Seibel et al. compared monthly ranibizumab for 6 months to laser photocoagulation and noted that ranibizumab was superior in improving visual acuity and reducing central subfield thickness (CST) [65]. Another randomized study using either a fixed treatment interval of 6 weeks or a treat-and-adjust regimen of aflibercept showed significant improvement in CST with maintenance of visual acuity (20/50 or better) in nearly 50% of patients at 1-year follow-up and no difference in the number of injections between the cohorts [66]. A recent case series showed that patients with radiation retinopathy secondary to episcleral plaque brachytherapy who have failed monthly intravitreal bevacizumab may respond to aflibercept [67]. The use of brolucizumab has been very limited due to the potentially serious adverse effect of severe vision loss due to retinal vasculitis [68]. Thus, while anti-VEGF agents have been shown to improve outcomes in radiation retinopathy, the logistical and economic challenges associated with their long-term use should be an important consideration.

Panretinal laser photocoagulation has been shown to successfully treat proliferative radiation retinopathy, whereas focal photocoagulation may treat or prevent macular edema with a more variable degree of vision improvement (Fig. 14.12) [69, 70]. In 19 patients with radiation-induced macular edema, focal laser therapy led to the resolution of

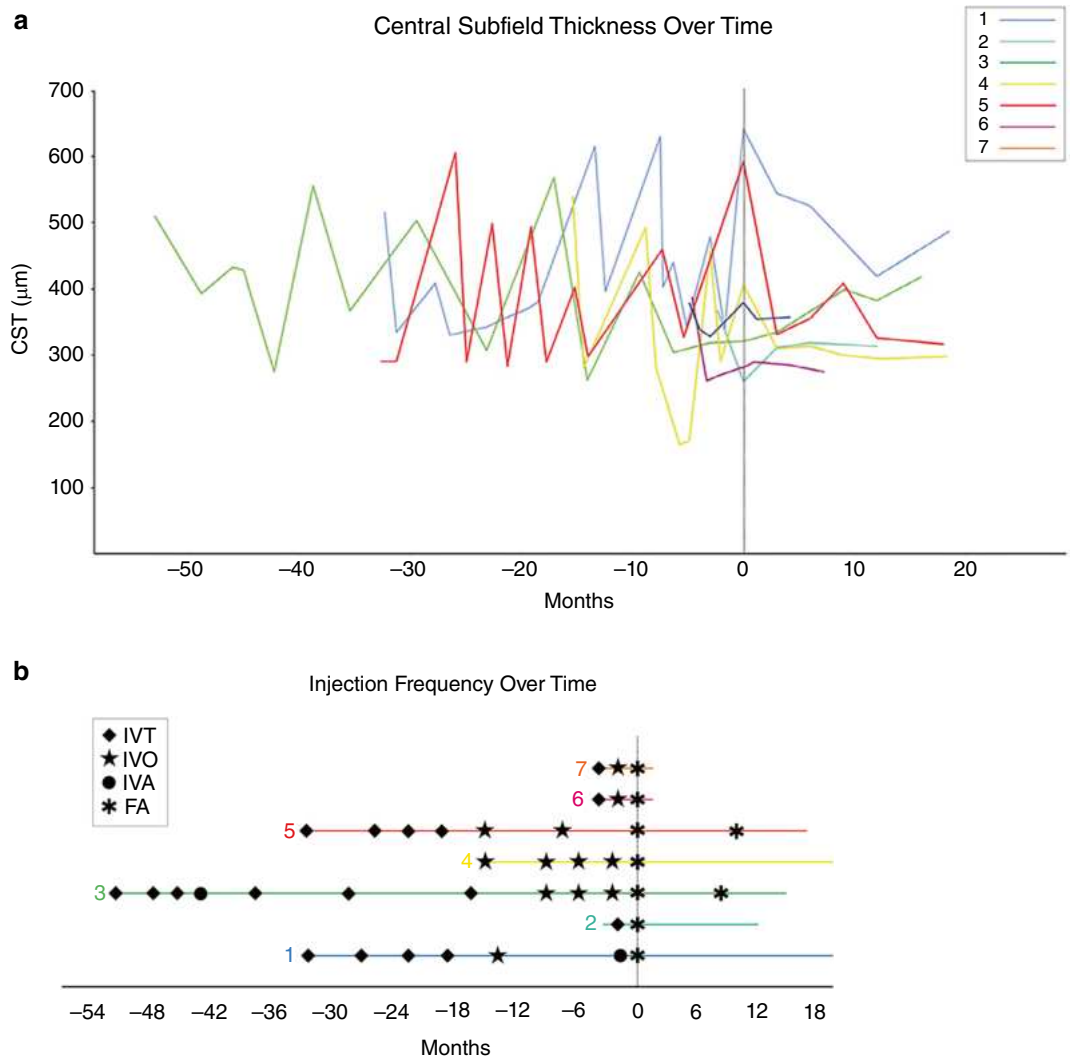

Fig. 14.10 Intravitreal Fluocinolone Acetonide implant for radiation retinopathy. Central Subfield Thickness (CST) over time (**a**). Each patient is assigned color. There is wide variance in thickness prior to FA implant insertion that is reduced afterwards. Time 0 indicates time when fluocinolone acetonide (FA) implant was inserted. Injection frequency over time (**b**). Medications including intravitreal triamcinolone (IVT), intravitreal Ozurdex (IVO), and intravitreal Avastin (IVA) are indicated by their respective symbols in the legend and matched in the injection timeline. (Reproduced with permission from: Singaravelu et al. [57])

edema in 26% (5/19) at 6 months compared with 4% (1/19) in the untreated group [70]. However, after 2 years, there was no significant difference in visual acuity between treated and untreated eyes. With the availability of anti-VEGF agents, the role of focal lasers for the treatment of radiation macular edema has become antiquated.

14.9.4 Preventive Strategies

As the current experience with treating radiation damage of the retina remains disappointing, recent efforts to attenuate iodine-125 with vitreous substitutes at the time of treatment have been reported.

Such preventive strategies will be particularly applicable in cases wherein a high risk of vision loss could be predicted [71]. Several approaches, including reduction of radiation dose [72–74], use of new brachytherapy implant designs [75], and use of periocular steroids [76] and anti-VEGF agents at the time of radiation exposure prior to the onset of radiation retinopathy, are under active investigation [77–80].

Oliver et al. were the first to demonstrate an attenuating effect of silicone oil 1000 centistokes, silicone oil 5000 centistokes, perfluorocarbon, and heavy liquid against iodine-125 in cadaver eyes, an in vitro model and with Monte Carlo modeling [81]. The effect of silicone oil 1000 centistokes was the most robust at approximately 55% when compared to vitreous [81]. Therefore, performing vitrectomy

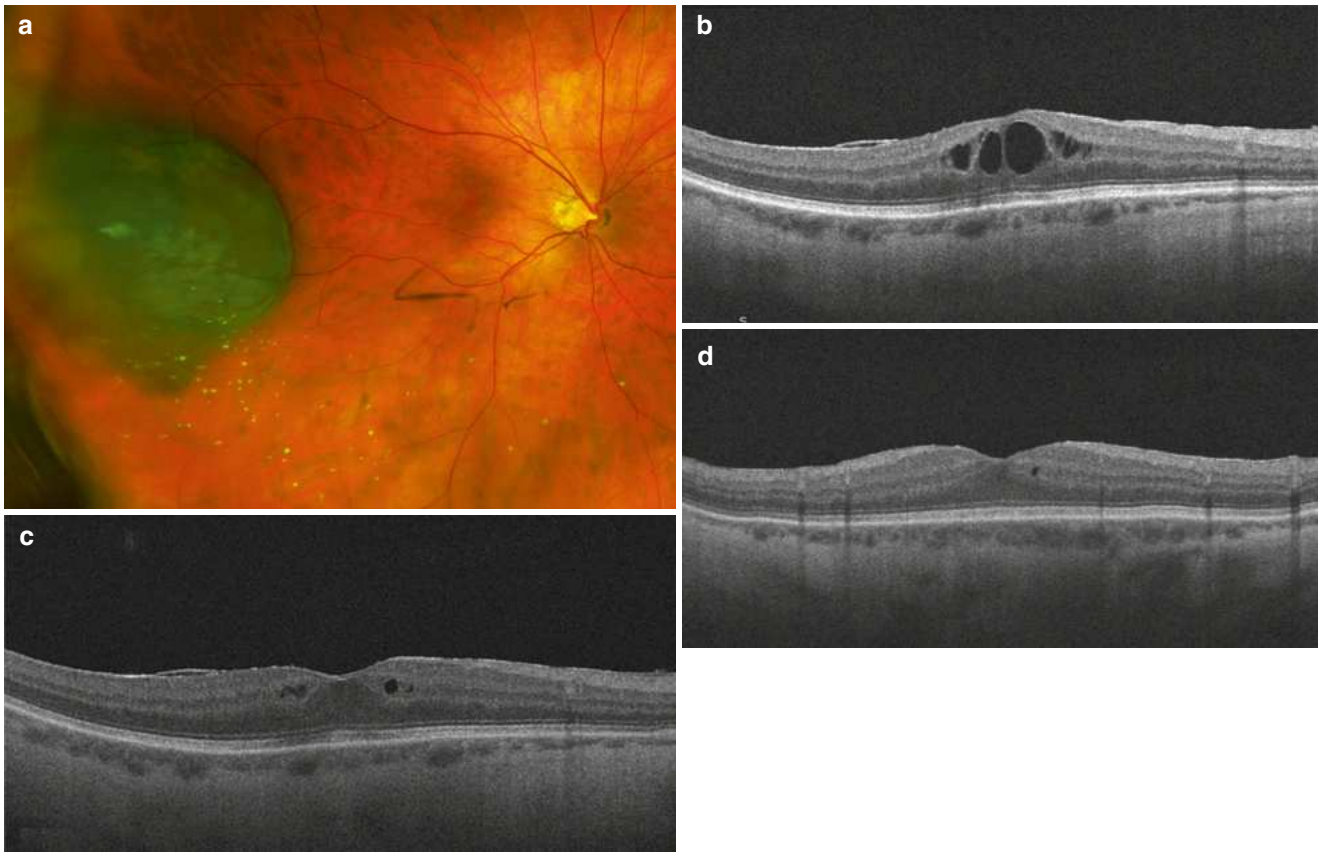

Fig. 14.11 A 70-year-old male patient who was treated for choroidal melanoma (right eye) by episcleral plaque brachytherapy (**a**, fundus photograph). 5 months later he developed cystoid macular edema (CME) due to radiation retinopathy with decrease in vision to 20/40 (Initial: 20/20) (**b**, OCT). After intravitreal Bevacizumab (second injection) the vision improved to 20/30 with reduction in CME (**c**, OCT). Normal foveal contour with trace intraretinal cysts and complete resolution of CME was achieved with a total of 13 injections (**d**, OCT)

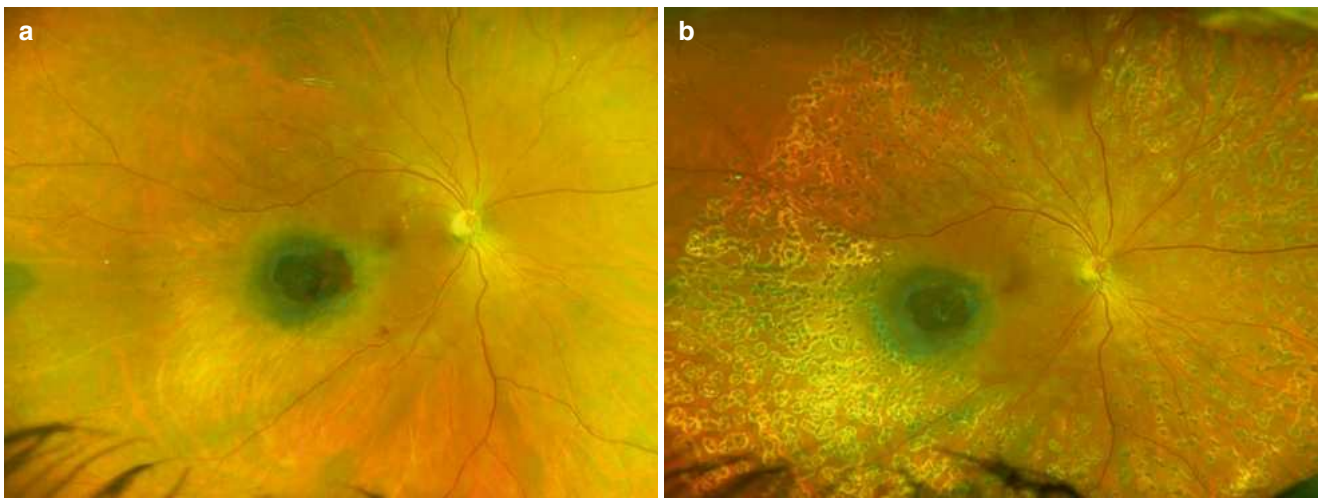

Fig. 14.12 Proliferative radiation retinopathy treated with pan retinal laser photocoagulation. Before (**a**) and after treatment (**b**)

with silicone oil 1000 centistokes at the time of iodine-125 episcleral plaque surgery may be a feasible method to reduce the exposure of healthy tissues to iodine-125 radiation and is currently being offered as a treatment option for uveal melanoma at some centers.

Anti-VEGF agents have been shown to have a role in preventing radiation retinopathy-related macular edema. Kim et al. studied 40 patients in whom intravitreal ranibizumab was initiated immediately after treatment completion prior to clinical evidence of radiation retinopathy. They showed high rates of visual acuity retention at 2 years compared to historical controls [79]. Another study suggested that early administration of intravitreal bevacizumab after episcleral plaque brachytherapy prevented or delayed vision-threatening radiation retinopathy and was well-tolerated [80].

As many of the studies have been limited by a small number of patients or retrospective design, a large prospective randomized controlled trial has been undertaken to develop well-validated preventive strategies for radiation retinopathy. The protocol AL (DRCR network) is underway to assess the role of intravitreal faricimab (Vabysmo®) or fluocinolone acetonide implant (Iluvien ®) in decreasing the risk of radiation retinopathy and subsequent vision loss [82]. The rationale for fluocinolone is the long-acting anti-inflammatory property, while that for faricimab is the dual mechanism of action (selective neutralization of VEGF and Ang-2) that may lead to better stabilization of the ocular vasculature. The study is expected to enroll 600 patients with the following objectives: (1) comparing long-term visual acuity outcomes in eyes treated with repeated anti-VEGF injections or sustained-release steroids with eyes initially observed and treated only if macular edema develops; (2) Determine if treatment with repeated anti-VEGF or sustained-release steroid versus initial observation can prevent or alter the course of radiation retinopathy and its consequences; and (3) Evaluate the natural history of radiation retinopathy with frequent multimodal imaging [82].

14.10 Toxic Tumor Syndrome

Severe radiation sequelae such as exudative retinal detachment, rubeosis, and neovascular glaucoma after proton beam irradiation and episcleral plaque brachytherapy may be due to the persistence of the irradiated necrotic tumor within the eye [83, 84]. Damato has proposed the concept of "toxic tumor syndrome," whereby radiation vasculopathy within the irradiated tumor results in exudation and release of angiogenic factors from the tumor that causes macular edema, hard exudates, serous retinal detachment, and neovascularization, all of which can resolve after laser ablation or resection of the offending tumor [85]. The pathogenesis is presumably due to the inflammatory response induced by the ischemic necrotic radiation-responsive larger/thicker tumor following radiation therapy [85]. The entity has also been described as retinopathy, with lipid exudates as the predominant feature [83, 86]. The treatment modalities have emphasized excision of the offending toxic tumor by endoresection, exoresection, or even enucleation for advanced cases [83–85, 87]. In our experience, intravitreal steroids have been useful in selected cases with lipid-predominant chorioretinopathy that could be considered a chronic variant of toxic tumor syndrome (Fig. 14.13).

Fig. 14.13 Toxic tumor syndrome. Lipid predominant chorioretinopathy that could be considered a chronic variant

14.11 Radiation Optic Neuropathy

14.11.1 Clinical Features

Although poorly understood, ionizing radiation is believed to damage the optic nerve through injury to both glial and endothelial cells. Over time, these injured cells accumulate and lead to demyelination and neuronal degeneration. Damage to the vascular endothelial cells leads to vascular occlusion and necrosis. Pathology specimens show a decreased number of endothelial cells and endothelial cell-lined vessels, as well as fibrosis of vessel walls, reactive gliosis, ischemic demyelination, and perivascular inflammation [88, 89]. The slow cellular turnover rate of endothelial and glial cells is consistent with the delayed onset of radiation-induced optic neuropathy [89].

Radiation-induced optic neuropathy may present with sudden, painless, monocular vision loss. Radiation therapy

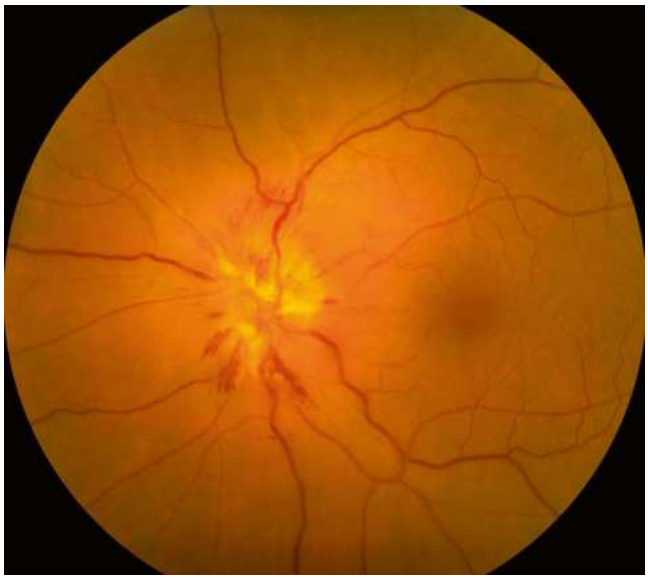

Fig. 14.14 Typical appearance of radiation optic neuropathy. Note optic disc swelling with surrounding exudates and hemorrhages

may lead to ischemic insult anterior to the lamina cribrosa, which causes swelling of the optic nerve head [88]. Other features of optic neuropathy may include disc swelling, peripapillary hard exudates, and hemorrhages (Fig. 14.14). Optic nerve head swelling eventually resolves, resulting in a pale and featureless nerve associated with limited vision [90].

14.11.2 Dose Relationship

Important risk factors for developing post-radiation optic neuropathy include close proximity of the tumor to the optic disc, greater dose to the optic disc, and large tumor size (Fig. 14.8) [91, 92]. Among patients undergoing episcleral plaque brachytherapy with adjunct silicone oil tamponade, the only patient who developed radiation optic neuropathy and light perception vision was the patient with the greatest tumor height of 11 mm [93]. A review of 158 patients with uveal melanoma treated with I-125 brachytherapy showed the highest risk (Hazard ratio: 2.33) of radiation optic neuropathy when the tumor was less than 6 mm from the disc [94]. A pooled analysis (103 studies and 21,263 patients) of episcleral plaque brachytherapy in uveal melanoma showed a 10% median incidence of radiation optic neuropathy at a median exposure dose of 42.8 Gy [95].

14.11.3 Treatment

There are some reports of spontaneous improvement of anterior radiation-induced optic neuropathy (Fig. 14.15) [96]. However, most cases progress to severe monocular vision loss and optic atrophy. Although there are studies examining treatment for optic neuropathy secondary to external beam radiation with bevacizumab, hyperbaric oxygen, corticosteroids, pentoxifylline, and vitamin E, few reports describe successful treatment for optic neuropathy after episcleral plaque brachytherapy [91, 97]. In a retrospective comparative case series, there were no differences related to visual acuity or optic atrophy development between patients treated with intravitreal therapy (triamcinolone, bevacizumab, and/or dexamethasone) and patients who were observed [98]. In a prospective study by Roelofs et al., patients who presented with decreased visual acuity due to radiation papillopathy improved to pre-papillopathy levels after treatment with bevacizumab (intravitreal) at the time of diagnosis and triamcinolone (intravitreal) 1 week later. The study, though, was limited by the small sample size ($n = 11$) and lack of a control group [99].

In a recently published meta-analysis of studies that relate to the treatment and prevention of RON, only studies ($n = 10$) reported results of hyperbaric oxygen therapy [100]. Early hyperbaric oxygen therapy (within 2 weeks) may be effective in improving or stabilizing vision (43%) patients compared with those (18%) who received hyperbaric oxygen therapy more than 2 weeks from the initial presentation. Additionally, meta-analysis suggests that systemic corticosteroids, systemic bevacizumab, and warfarin alone are likely ineffective treatments (Fig. 14.16) [100].

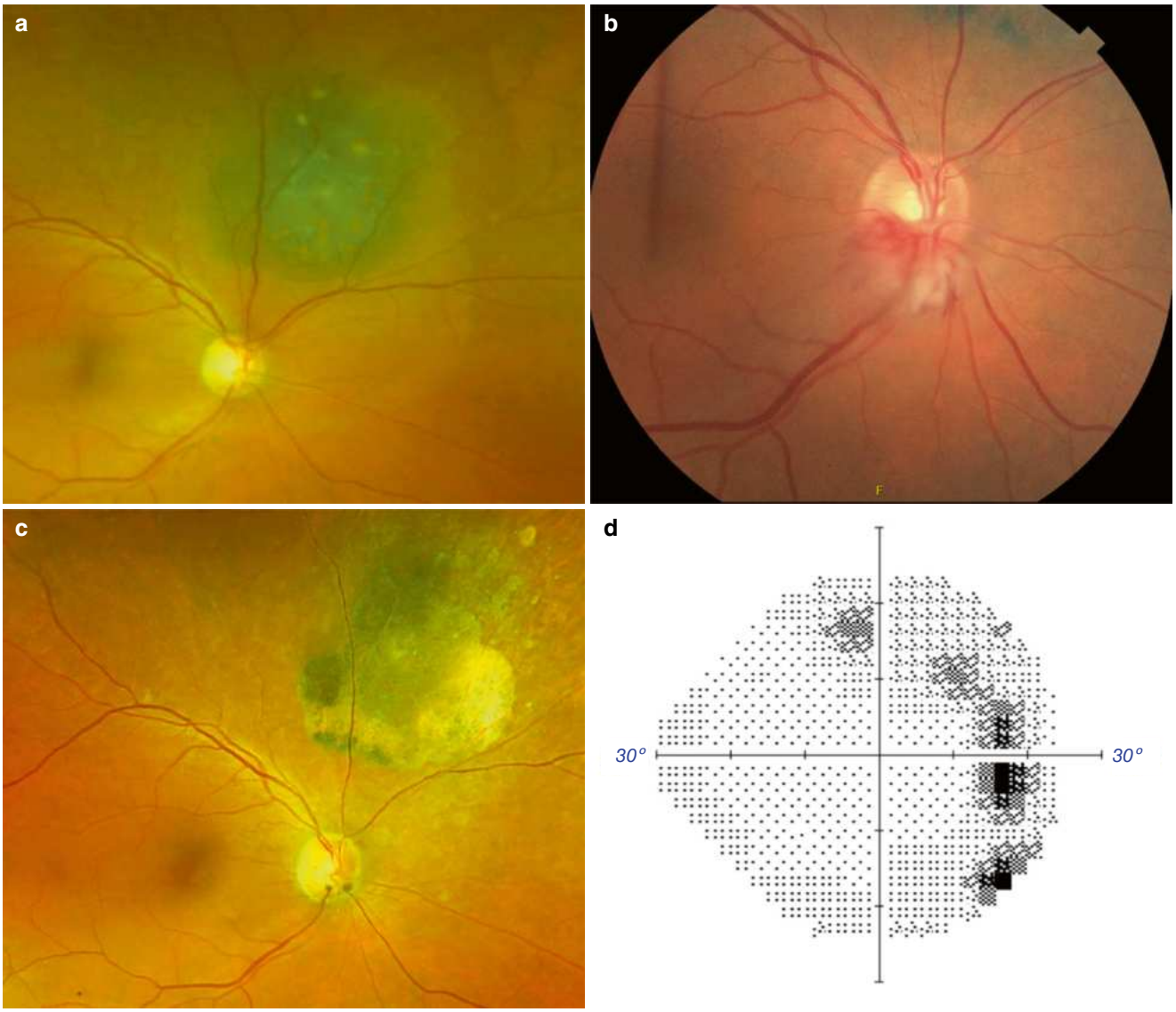

Fig. 14.15 A 65-year-old female with a choroidal melanoma (9 × 7.5 × 2.2) in the superonasal quadrant of the right eye that was treated with episcleral brachytherapy (85G delivered to the tumor apex over 72 h) (**a**). 37 months later the patient noted decreased visual acuity (20/60) and on fundus examination, disc was edematous with flame hemorrhages within primarily the inferior hemisphere of the nerve diagnostic of radiation optic neuropathy (**b**). 12 months after the decision to observe without any therapeutic intervention, the disc edema resolved and the visual acuity improved to 20/20 (**c**). Perimetry demonstrated an inferotemporal defect (tumor related) and a superior arcuate area of depression (RON related) (**d**). (Reproduced with permission from: Oakey et al. [96])

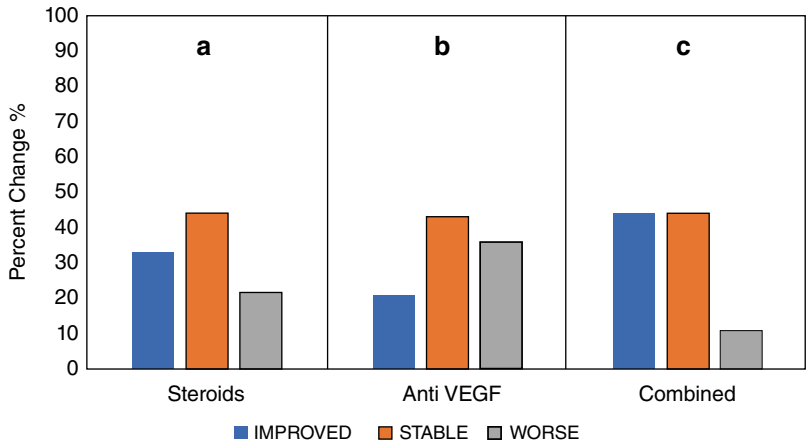

Fig. 14.16 Treatment of radiation optic neuropathy. The data is adapted from various sources to depict visual acuity among patients who received monotherapy anti-VEGF (bevacizumab), intraocular corticosteroid, or combination of both. Those patients who underwent combined therapy experienced less loss of acuity relative to monotherapy (corticosteroid anti-VEGF). (Reproduced with permission from: Oakey et al. [96])

14.12 Conclusions

While radiation complications are difficult to compare between brachytherapy, fractionated stereotactic therapy, and single fraction therapy because of differences in fraction size, total dose, dose rate, and treatment volumes, it is clear that the risk of many complications increases above certain dose thresholds. Future efforts may be directed toward limiting the exposure to healthy tissue at the time that the radiation is delivered, such as has been demonstrated with silicone oil 1000 centistokes placement at the time of brachytherapy and the use of preventive strategies such as anti-VEGF agents or long-acting steroid implants to decrease the rate of radiation complications.

References

1. Nuzzi R, Trossarello M, Bartoncini S, Marolo P, Franco P, Mantovani C, et al. Ocular complications after radiation therapy: an observational study. Clin Ophthalmol. 2020;14:3153–66.
2. Irvine AR, Wood IS. Radiation retinopathy as an experimental model for ischemic proliferative retinopathy and rubeosis iridis. Am J Ophthalmol. 1987;103(6):790–7.
3. Archer DB, Amoaku WM, Gardiner TA. Radiation retinopathy—clinical, histopathological, ultrastructural and experimental correlations. Eye (Lond). 1991;5(Pt 2):239–51.
4. Wei J, Meng L, Hou X, Qu C, Wang B, Xin Y, et al. Radiation-induced skin reactions: mechanism and treatment. Cancer Manag Res. 2019;11:167–77.
5. Jeganathan VS, Wirth A, MacManus MP. Ocular risks from orbital and periorbital radiation therapy: a critical review. Int J Radiat Oncol Biol Phys. 2011;79(3):650–9.
6. Durkin SR, Roos D, Higgs B, Casson RJ, Selva D. Ophthalmic and adnexal complications of radiotherapy. Acta Ophthalmol Scand. 2007;85(3):240–50.
7. Heimann H, Coupland SE, Gochman R, Hellmich M, Foerster MH. Alterations in expression of mucin, tenascin-c and syndecan-1 in the conjunctiva following retinal surgery and plaque radiotherapy. Graefes Arch Clin Exp Ophthalmol. 2001;239(7):488–95.
8. Le Q, Xu J, Deng SX. The diagnosis of limbal stem cell deficiency. Ocul Surf. 2018;16(1):58–69.
9. Harris DL, Yamaguchi T, Hamrah P. A novel murine model of radiation keratopathy. Invest Ophthalmol Vis Sci. 2018;59(10):3889–96.
10. Parsons JT, Bova FJ, Fitzgerald CR, Mendenhall WM, Million RR. Severe dry-eye syndrome following external beam irradiation. Int J Radiat Oncol Biol Phys. 1994;30(4):775–80.
11. Muller K, Nowak PJ, Naus N, de Pan C, van Santen CA, Levendag P, et al. Lacrimal gland radiosensitivity in uveal melanoma patients. Int J Radiat Oncol Biol Phys. 2009;74(2):497–502.
12. Horwath-Winter J, Schneider MR, Wackernagel W, Rabensteiner D, Boldin I, Haller-Schober EM, et al. Influence of single-fraction Gamma-Knife radiosurgery on ocular surface and tear function in choroidal melanoma patients. Br J Ophthalmol. 2013;97(4):466–70.
13. Tiwari S, Bhatt A, Nagamodi J, Ali MJ, Ali H, Naik MN, et al. Aqueous deficient dry eye syndrome post orbital radiotherapy: a 10-year retrospective study. Transl Vis Sci Technol. 2017;6(3):19.
14. Woo YJ, Ko J, Ji YW, Kim TI, Yoon JS. Meibomian gland dysfunction associated with periocular radiotherapy. Cornea. 2017;36(12):1486–91.
15. Petrovich Z, McDonnell JM, Palmer D, Langholz BM, Liggett PE. Histopathologic changes following irradiation for uveal tract melanoma. Am J Clin Oncol. 1994;17(4):298–306.
16. Stack R, Elder M, Abdelaal A, Hidajat R, Clemett R. New Zealand experience of I125 brachytherapy for choroidal melanoma. Clin Experiment Ophthalmol. 2005;33(5):490–4.
17. Kaliki S, Shields CL, Rojanaporn D, Badal J, Devisetty L, Emrich J, et al. Scleral necrosis after plaque radiotherapy of uveal melanoma: a case-control study. Ophthalmology. 2013;120(5):1004–11.
18. Correa ZM, Huth B, Augsburger JJ. Scleral necrosis in patients with posterior uveal melanomas evaluated by transcleral fine needle aspiration biopsy and treated by 125I plaque. Arq Bras Oftalmol. 2018;81(4):330–5.
19. Jabbarli L, Guberina M, Biewald E, Fluhs D, Guberina N, Le Guin CHD, et al. Scleral necrosis after brachytherapy for uveal melanoma: analysis of risk factors. Clin Experiment Ophthalmol. 2021;49(4):357–67.
20. Sener EC, Kiratli H, Gedik S, Sanac AS. Ocular motility disturbances after episcleral plaque brachytherapy for uveal melanoma. J AAPOS. 2004;8(1):38–45.
21. Kiratli H, Yilmaz PT, Sargon M. Ultrastructural alterations in extraocular muscles following iodine-125 brachytherapy for uveal melanoma. Strabismus. 2007;15(2):103–9.
22. Alfreihi SH, Pineles SL, McCannel TA, Prada AM, Velez FG. Surgical management of strabismus following choroidal melanoma plaque brachytherapy. J AAPOS. 2017;21(4):286–90 e2.
23. Huang JJ, Saleem A, Liao EX, Larocque M, Menon G, Murtha A, et al. Incidence of strabismus post-plaque brachytherapy in patients with uveal melanoma. Am J Ophthalmol. 2024;262:161–9.
24. Detorakis ET, Engstrom RE Jr, Wallace R, Straatsma BR. Iris and anterior chamber angle neovascularization after iodine 125 brachytherapy for uveal melanoma. Ophthalmology. 2005;112(3):505–10.
25. Char DH, Lonn LI, Margolis LW. Complications of cobalt plaque therapy of choroidal malanomas. Am J Ophthalmol. 1977;84(4):536–41.
26. Finger PT. Tumour location affects the incidence of cataract and retinopathy after ophthalmic plaque radiation therapy. Br J Ophthalmol. 2000;84(9):1068–70.
27. Fernandes BF, Weisbrod D, Yucel YH, Follwell M, Krema H, Heydarian M, et al. Neovascular glaucoma after stereotactic radiotherapy for juxtapapillary choroidal melanoma: histopathologic and dosimetric findings. Int J Radiat Oncol Biol Phys. 2011;80(2):377–84.
28. Peters V, Gurayah A, Jin W, Kwon D, Zhao W, Patel NV, et al. Clinical characteristics and postoperative complications as predictors of radiation toxicity after treatment with I125 eye plaque brachytherapy for uveal melanomas. Brachytherapy. 2022;21(6):896–903.
29. Kim EA, Salazar D, McCannel CA, Kamrava M, Demanes DJ, Lamb J, et al. Glaucoma after Iodine-125 brachytherapy for uveal melanoma: incidence and risk factors. J Glaucoma. 2020;29(1):1–10.
30. Yeung SN, Paton KE, Waite C, Maberley DA. Intravitreal bevacizumab for iris neovascularization following proton beam irradiation for choroidal melanoma. Can J Ophthalmol. 2010;45(3):269–73.
31. Mahdjoubi A, Najean M, Lemaitre S, Dureau S, Dendale R, Levy C, et al. Intravitreal bevacizumab for neovascular glaucoma in uveal melanoma treated by proton beam therapy. Graefes Arch Clin Exp Ophthalmol. 2018;256(2):411–20.

32. Hasegawa N, Teh BS, Tran K, Ivey F, Olek D, Pino R, et al. Retrospective analysis of radiation-induced complications of uveal melanoma patients treated with brachytherapy in the era of anti-VEGF. Am J Ophthalmol. 2024;260:49–59.
33. Mazzini C, Pieretti G, Vicini G, Nicolosi C, Scoccianti S, Pertici M, et al. Clinical outcomes and secondary glaucoma after gamma-knife radiosurgery and Ruthenium-106 brachytherapy for uveal melanoma: a single institution experience. Melanoma Res. 2021;31(1):38–48.
34. Seibel I, Riechardt AI, Heufelder J, Cordini D, Joussen AM. Adjuvant ab interno tumor treatment after proton beam irradiation. Am J Ophthalmol. 2017;178:94–100.
35. Gunduz AK, Mirzayev I. Surgical approach in intraocular tumors. Turk J Ophthalmol. 2022;52(2):125–38.
36. Cogan DG, Donaldson DD, Reese AB. Clinical and pathological characteristics of radiation cataract. AMA Arch Ophthalmol. 1952;47(1):55–70.
37. Ferrufino-Ponce ZK, Henderson BA. Radiotherapy and cataract formation. Semin Ophthalmol. 2006;21(3):171–80.
38. Collaborative Ocular Melanoma Study G. Incidence of cataract and outcomes after cataract surgery in the first 5 years after iodine 125 brachytherapy in the Collaborative Ocular Melanoma Study: COMS Report No. 27. Ophthalmology. 2007;114(7):1363–71.
39. Weber B, Paton K, Ma R, Pickles T. Outcomes of proton beam radiotherapy for large non-peripapillary choroidal and ciliary body melanoma at TRIUMF and the BC Cancer Agency. Ocul Oncol Pathol. 2015;2(1):29–35.
40. Lumbroso-Le Rouic L, Charif Chefchaouni M, Levy C, Plancher C, Dendale R, Asselain B, et al. 125I plaque brachytherapy for anterior uveal melanomas. Eye (Lond). 2004;18(9):911–6.
41. Fontanesi J, Meyer D, Xu S, Tai D. Treatment of choroidal melanoma with I-125 plaque. Int J Radiat Oncol Biol Phys. 1993;26(4):619–23.
42. Muller K, Naus N, Nowak PJ, Schmitz PI, de Pan C, van Santen CA, et al. Fractionated stereotactic radiotherapy for uveal melanoma, late clinical results. Radiother Oncol. 2012;102(2):219–24.
43. Thariat J, Jacob S, Caujolle JP, Maschi C, Baillif S, Angellier G, et al. Cataract avoidance with proton therapy in ocular melanomas. Invest Ophthalmol Vis Sci. 2017;58(12):5378–86.
44. Gill VT, Stalhammar G. Incidence, risk factors and outcomes of cataract surgery after plaque brachytherapy for posterior uveal melanoma. Heliyon. 2024;10(1):e23447.
45. Archer DB, Gardiner TA. Ionizing radiation and the retina. Curr Opin Ophthalmol. 1994;5(3):59–65.
46. Melia BM, Abramson DH, Albert DM, Boldt HC, Earle JD, Hanson WF, et al. Collaborative Ocular Melanoma Study (COMS) randomized trial of I-125 brachytherapy for medium choroidal melanoma. I. Visual acuity after 3 years COMS report no. 16. Ophthalmology. 2001;108(2):348–66.
47. Horgan N, Shields CL, Mashayekhi A, Shields JA. Classification and treatment of radiation maculopathy. Curr Opin Ophthalmol. 2010;21(3):233–8.
48. McCannel TA, Kim E, Kamrava M, Lamb J, Caprioli J, Yang D, et al. New ultra-wide-field angiographic grading scheme for radiation retinopathy after Iodine-125 brachytherapy for uveal melanoma. Retina. 2018;38(12):2415–21.
49. Bhandare N, Monroe AT, Morris CG, Bhatti MT, Mendenhall WM. Does altered fractionation influence the risk of radiation-induced optic neuropathy? Int J Radiat Oncol Biol Phys. 2005;62(4):1070–7.
50. Monroe AT, Bhandare N, Morris CG, Mendenhall WM. Preventing radiation retinopathy with hyperfractionation. Int J Radiat Oncol Biol Phys. 2005;61(3):856–64.
51. Tamplin MR, Wang JK, Binkley EM, Garvin MK, Hyer DE, Buatti JM, et al. Radiation effects on retinal layers revealed by OCT, OCT-A, and perimetry as a function of dose and time from treatment. Sci Rep. 2024;14(1):3380.
52. Binkley EM, Tamplin MR, Vitale AH, Boldt HC, Kardon RH, Grumbach IM. Longitudinal Optical Coherence Tomography Angiography (OCT-A) in a patient with radiation retinopathy following plaque brachytherapy for uveal melanoma. Am J Ophthalmol Case Rep. 2022;26:101508.
53. Aziz HA, Singh AD. Radiation chorioretinopathy: evidence for effective therapy. Int Ophthalmol Clin. 2015;55(1):53–61.
54. Kaplan RI, Chaugule SS, Finger PT. Intravitreal triamcinolone acetate for radiation maculopathy recalcitrant to high-dose intravitreal bevacizumab. Br J Ophthalmol. 2017;101(12):1694–8.
55. Frizziero L, Parrozzani R, Trainiti S, Pilotto E, Miglionico G, Pulze S, et al. Intravitreal dexamethasone implant in radiation-induced macular oedema. Br J Ophthalmol. 2017;101(12):1699–703.
56. Zimmermann L, Kneifel C, Grajewski L, Ciernik IF, Krause L. Treatment of radiation-induced maculopathy with fluocinolone acetonide. Graefes Arch Clin Exp Ophthalmol. 2020;258(11):2535–9.
57. Singaravelu J, Oakey ZB, Wrenn JM, Singh AD. Intravitreal fluocinolone acetonide implant for radiation retinopathy: report of preliminary findings. Retina. 2023;43(8):1364–9.
58. Gillies MC. Regulators of vascular permeability: potential sites for intervention in the treatment of macular edema. Doc Ophthalmol. 1999;97(3–4):251–60.
59. Bakri SJ, Larson TA. The variable efficacy of intravitreal bevacizumab and triamcinolone acetonide for cystoid macular edema due to radiation retinopathy. Semin Ophthalmol. 2015;30(4):276–80.
60. Finger PT. Radiation retinopathy is treatable with anti-vascular endothelial growth factor bevacizumab (Avastin). Int J Radiat Oncol Biol Phys. 2008;70(4):974–7.
61. Jermak CM, Dellacroce JT, Heffez J, Peyman GA. Triamcinolone acetonide in ocular therapeutics. Surv Ophthalmol. 2007;52(5):503–22.
62. Finger PT, Chin KJ, Semenova EA. Intravitreal anti-VEGF therapy for macular radiation retinopathy: a 10-year study. Eur J Ophthalmol. 2016;26(1):60–6.
63. Pooprasert P, Young-Zvandasara T, Al-Bermani A. Radiation retinopathy treated successfully with aflibercept. BMJ Case Rep. 2017;2017:bcr2017220744.
64. Fallico M, Reibaldi M, Avitabile T, Longo A, Bonfiglio V, Chronopoulos A, et al. Intravitreal aflibercept for the treatment of radiation-induced macular edema after ruthenium 106 plaque radiotherapy for choroidal melanoma. Graefes Arch Clin Exp Ophthalmol. 2019;257(7):1547–54.
65. Seibel I, Vollhardt D, Riechardt AI, Rehak M, Schmied S, Schiller P, et al. Influence of Ranibizumab versus laser photocoagulation on radiation retinopathy (RadiRet)—a prospective randomized controlled trial. Graefes Arch Clin Exp Ophthalmol. 2020 Apr;258(4):869–78.
66. Murray TG, Latiff A, Villegas VM, Gold AS. Aflibercept for radiation maculopathy study: a prospective, randomized clinical study. Ophthalmol Retina. 2019;3(7):561–6.
67. Srivastava O, Weis E. Outcomes of second-line intravitreal anti-VEGF switch therapy in radiation retinopathy secondary to uveal melanoma: moving from bevacizumab to aflibercept. Ocul Oncol Pathol. 2023;8(4–6):230–5.
68. Murray JE, Gold AS, Latiff A, Murray TG. Brolucizumab: evaluation of compassionate use of a complex anti-VEGF therapy. Clin Ophthalmol. 2021;15:4731–8.
69. Kinyoun JL, Zamber RW, Lawrence BS, Barlow WE, Arnold AM. Photocoagulation treatment for clinically significant radiation macular oedema. Br J Ophthalmol. 1995;79(2):144–9.
70. Hykin PG, Shields CL, Shields JA, Arevalo JF. The efficacy of focal laser therapy in radiation-induced macular edema. Ophthalmology. 1998;105(8):1425–9.

71. Aziz HA, Singh N, Bena J, Wilkinson A, Singh AD. Vision loss following episcleral brachytherapy for uveal melanoma: development of a vision prognostication tool. JAMA Ophthalmol. 2016;134(6):615–20.
72. Saconn PA, Gee CJ, Greven CM, McCoy TP, Ekstrand KE, Greven KM. Alternative dose for choroidal melanoma treated with an iodine-125 radioactive plaque: a single-institution retrospective study. Int J Radiat Oncol Biol Phys. 2010;78(3):844–8.
73. Murray TG, Markoe AM, Gold AS, Ehlies F, Bermudez E, Wildner A, et al. Long-term followup comparing two treatment dosing strategies of (125) I plaque radiotherapy in the management of small/medium posterior uveal melanoma. J Ophthalmol. 2013;2013:517032.
74. Echegaray JJ, Bechrakis NE, Singh N, Bellerive C, Singh AD. Iodine-125 brachytherapy for uveal melanoma: a systematic review of radiation dose. Ocul Oncol Pathol. 2017;3(3):193–8.
75. Marwaha G, Wilkinson A, Bena J, Macklis R, Singh AD. Dosimetric benefit of a new ophthalmic radiation plaque. Int J Radiat Oncol Biol Phys. 2012;84(5):1226–30.
76. Horgan N, Shields CL, Mashayekhi A, Salazar PF, Materin MA, O'Regan M, et al. Periocular triamcinolone for prevention of macular edema after plaque radiotherapy of uveal melanoma: a randomized controlled trial. Ophthalmology. 2009;116(7):1383–90.
77. Aiello LP, Avery RL, Arrigg PG, Keyt BA, Jampel HD, Shah ST, et al. Vascular endothelial growth factor in ocular fluid of patients with diabetic retinopathy and other retinal disorders. N Engl J Med. 1994;331(22):1480–7.
78. Shah SU, Shields CL, Bianciotto CG, Iturralde J, Al-Dahmash SA, Say EAT, et al. Intravitreal bevacizumab at 4-month intervals for prevention of macular edema after plaque radiotherapy of uveal melanoma. Ophthalmology. 2014;121(1):269–75.
79. Kim IK, Lane AM, Jain P, Awh C, Gragoudas ES. Ranibizumab for the prevention of radiation complications in patients treated with proton beam irradiation for choroidal melanoma. Trans Am Ophthalmol Soc. 2016;114:T2.
80. Powell BE, Finger PT. Anti-VEGF therapy immediately after plaque radiation therapy prevents or delays radiation maculopathy. Ophthalmol Retina. 2020;4(5):547–50.
81. Oliver SC, Leu MY, DeMarco JJ, Chow PE, Lee SP, McCannel TA. Attenuation of iodine 125 radiation with vitreous substitutes in the treatment of uveal melanoma. Arch Ophthalmol. 2010;128(7):888–93.
82. Loss DnARCTElFmIoFAmIIvOfPoVA. https://public.jaeb.org/drcrnet/view/UpcomeStudies.
83. McCannel TA. Post-brachytherapy tumor endoresection for treatment of toxic maculopathy in choroidal melanoma. Eye (Lond). 2013;27(8):984–8.
84. Konstantinidis L, Groenewald C, Coupland SE, Damato B. Transscleral local resection of toxic choroidal melanoma after proton beam radiotherapy. Br J Ophthalmol. 2014;98(6):775–9.
85. Damato B. Progress in the management of patients with uveal melanoma. The 2012 Ashton Lecture. Eye (Lond). 2012;26(9):1157–72.
86. Mills MD, Harbour JW. Lipid exudation following plaque radiotherapy for posterior uveal melanoma. Am J Ophthalmol. 2006;141(3):594–5.
87. Romano MR, Catania F, Confalonieri F, Zollet P, Allegrini D, Sergenti J, et al. Vitreoretinal surgery in the prevention and treatment of toxic tumour syndrome in uveal melanoma: a systematic review. Int J Mol Sci. 2021;22(18):10066.
88. Kline LB, Kim JY, Ceballos R. Radiation optic neuropathy. Ophthalmology. 1985;92(8):1118–26.
89. Levin LA, Gragoudas ES, Lessell S. Endothelial cell loss in irradiated optic nerves. Ophthalmology. 2000;107(2):370–4.
90. Miller NR. Radiation-induced optic neuropathy: still no treatment. Clin Experiment Ophthalmol. 2004;32(3):233–5.
91. Danesh-Meyer HV. Radiation-induced optic neuropathy. J Clin Neurosci. 2008;15(2):95–100.
92. Li PC, Liebsch NJ, Niemierko A, Giantsoudi D, Lessell S, Fullerton BC, et al. Radiation tolerance of the optic pathway in patients treated with proton and photon radiotherapy. Radiother Oncol. 2019;131:112–9.
93. Lyons LJ, Hinds ED, Chexal S, Berger B. Silicone oil and Iodine-125 brachytherapy for uveal melanoma in high-risk patients. Cureus. 2019;11(7):e5270.
94. King BA, Awh C, Gao BT, Wang J, Kocak M, Morales-Tirado VM, et al. Iodine-125 episcleral plaque brachytherapy for AJCC T4 posterior uveal melanoma: clinical outcomes in 158 patients. Ocul Oncol Pathol. 2019;5(5):340–9.
95. Buonanno F, Conson M, de Almeida RC, Oliviero C, Itta F, Liuzzi R, et al. Local tumor control and treatment related toxicity after plaque brachytherapy for uveal melanoma: a systematic review and a data pooled analysis. Radiother Oncol. 2022;166:15–25.
96. Oakey Z, Yeşiltaş YS, Singh AD. Radiation optic neuropathy: management options. Ocul Oncol Pathol. 2023;9(5–6):166–71.
97. Brown GC, Shields JA, Sanborn G, Augsburger JJ, Savino PJ, Schatz NJ. Radiation optic neuropathy. Ophthalmology. 1982;89(12):1489–93.
98. Eckstein D, Riechardt AI, Heufelder J, Zeitz O, Boker A, Brockmann C, et al. Radiation-induced optic neuropathy: observation versus intravitreal treatment: can visual acuity be maintained by intravitreal treatment? Am J Ophthalmol. 2019;208:289–94.
99. Roelofs K, Larocque MP, Murtha A, Weis E. The use of intravitreal anti-VEGF and triamcinolone in the treatment of radiation papillopathy. Ocul Oncol Pathol. 2018;4(6):395–400.
100. Yu CW, Joarder I, Micieli JA. Treatment and prophylaxis of radiation optic neuropathy: a systematic review and meta-analysis. Eur J Ophthalmol. 2022;32(6):3129–41.

Principles and Complications of Chemotherapy

15

Stacey Zahler, Nicola G. Ghazi, and Arun D. Singh

15.1 Introduction

The treatment of ocular cancer often requires a combination of both local control methods (i.e., surgery, local intra-ocular therapies, or radiation therapy) and systemic medical therapy. In the modern era of medicine, there has been quite an expansion of systemic anti-cancer therapy modalities, the most antiquated of which is cytotoxic chemotherapy. The overall survival rate of children and adolescents who are diagnosed with cancer has improved dramatically over the last more than half-century to more than 85% [1]. This can be attributed to the addition of chemotherapy to local control methods and to the tailoring of various chemotherapy regimens based on the molecular biology of specific types of cancer cells [2].

Numerous targeted therapies have been developed over the last two decades that work against various types of cancers. However, as these drugs continue to be studied and developed in attempts to improve efficacy and, thus, survival, chemotherapy remains the mainstay of cancer-directed therapy. This chapter will review the basic concepts of some common chemotherapeutic agents used in ocular cancers, as well as their common toxicities.

S. Zahler (✉)
Cleveland Clinic Children's, Cleveland, OH, USA
e-mail: ZAHLERS@ccf.org

N. G. Ghazi
Cleveland Clinic Abu Dhabi Eye Institute,
Abu Dhabi, United Arab Emirates

Cleveland Clinic Lerner College of Medicine,
Cleveland, OH, USA

A. D. Singh
Department of Ophthalmic Oncology, Cole Eye Institute,
Cleveland Clinic, Cleveland, OH, USA
e-mail: singha@ccf.org

15.2 Basic Principles of Chemotherapy

The discovery of chemotherapeutic agents in the 1940s stemmed from a "trial and error" screening approach in vitro, where both new and known compounds (such as antibiotics) were tested for anti-tumor cell activity [3]. It was only after the discovery of these compounds' cytotoxic effects that the mechanisms of action were recognized. Thus, most chemotherapeutic agents are non-selective in their mechanisms of action, rendering them harmful to not only tumor cells but also to normal, healthy cells. The effect of chemotherapy on healthy cells is the root cause of its untoward adverse reactions.

15.2.1 The Cell Cycle

Since many chemotherapeutic agents function by affecting various points within the cell cycle, it is prudent to review the normal cell cycle (Fig. 15.1). The cell cycle is divided into four phases: G1, S, G2, and M. G1 begins immediately after mitosis. It is a period when the cell carries on its usual non-mitotic functions, including cell growth and protein synthesis, and lasts until the beginning of the Synthesis (S) phase. The S phase is the period when the synthesis of DNA occurs and the genome is replicated. Once this is completed, the cell enters the G2 phase, which is the period of continued cell growth and preparation for mitosis prior to cell division. The Mitosis (or M) phase is the period where chromosome condensation occurs, the mitotic spindle appears, sister chromosomes separate, and the process of cell division occurs.

Knowledge of the normal cell cycle and how the various chemotherapeutic anticancer drugs disrupt this cycle is integral to developing effective chemotherapy regimens. Chemotherapy drugs with cell cycle-specific mechanisms of action will kill a fraction of tumor cells passing through that phase of the cell cycle at the time of drug administration. On the other hand, agents that are cell cycle non-specific produce a continuous exponential decrease in tumor cell sur-

© The Author(s), under exclusive license to Springer Nature Switzerland AG 2025

A. D. Singh, B. E. Damato (eds.), *Clinical Ophthalmic Oncology*, https://doi.org/10.1007/978-3-031-75907-9_15

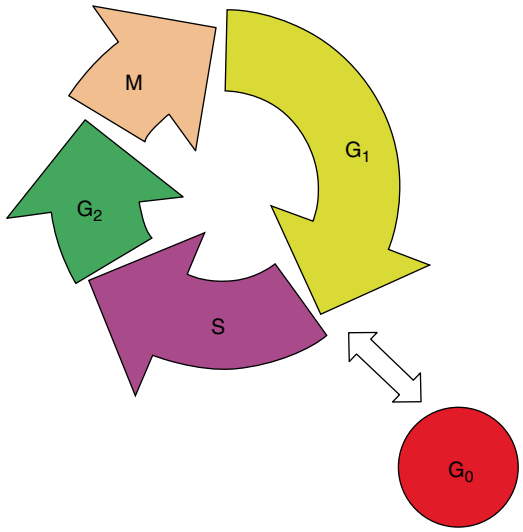

Fig. 15.1 The Cell Cycle. The cell generation cycle is divided into four phases: G1, S (synthesis), G2, and M (mitosis) phase. See text for complete description of each cell cycle phase. G0 cells are those that have left the cycling pool, either temporarily or permanently. Cells that are temporarily in G0 can be recruited back into the proliferative cycle by appropriate stimuli or growth factors. Some G0 cells may be terminally differentiated and cannot be recruited back into the proliferative cycle

vival because they affect all cells, regardless of their phase in the cell cycle. Chemotherapy itself is given in cycles of 14–42 days to allow for hematopoietic cell recovery of the bone marrow, as well as to achieve the goal of adequate tumor cell reduction.

15.2.2 Mechanisms of Action

Chemotherapeutic agents work in various ways via manipulating the DNA replication process, which results in apoptosis of the tumor cell or inhibition of tumor cell synthesis (Fig. 15.2). For instance, antimetabolites such as methotrexate inhibit the synthesis of purines (nucleotide precursors) or are incorporated directly into the DNA, and agents such as anthracyclines, epipodophyllotoxins, and camptothecins inhibit an important group of enzymes called topoisomerases. These enzymes are important in maintaining the structure of DNA and are critical to the processes of DNA replication, transcription, and repair as they cleave and ligate DNA; thus, inhibition of topoisomerases leads to DNA strand breaks [4]. Alkylating agents such as cyclophospha-

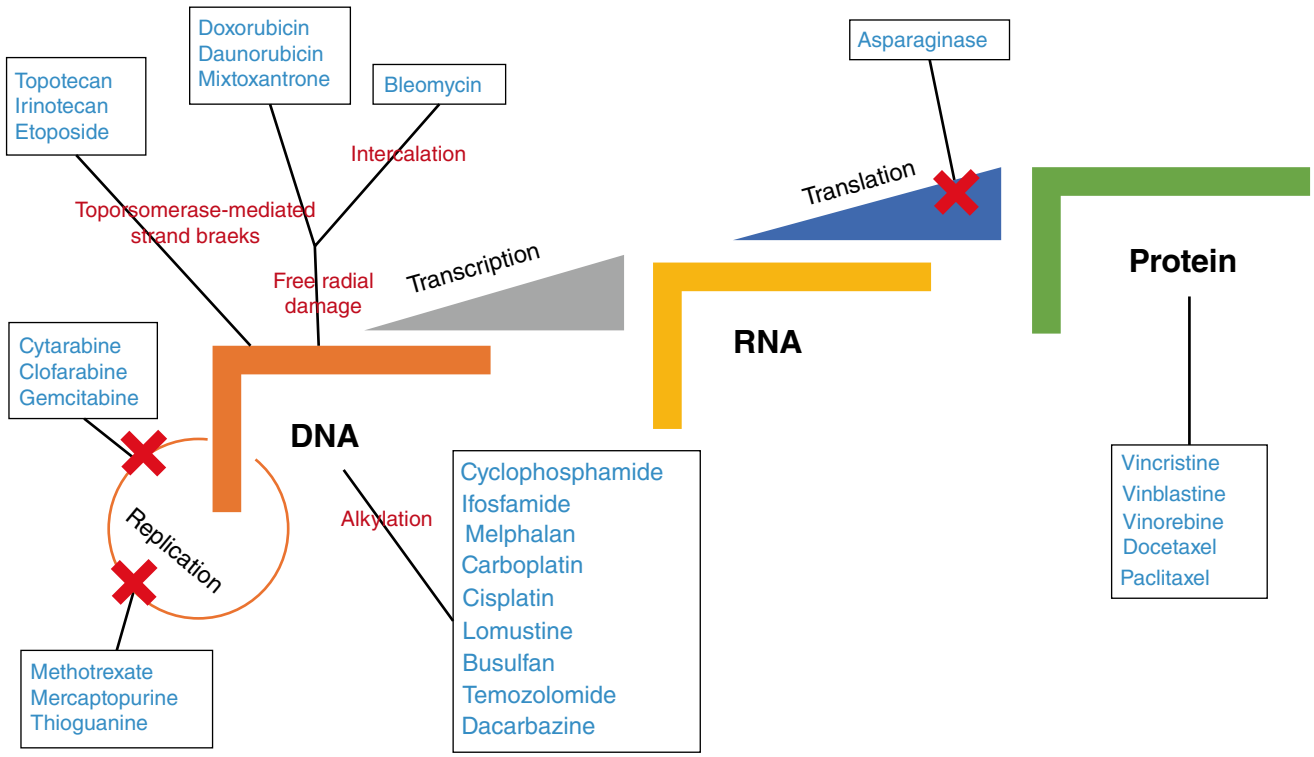

Fig. 15.2 Sites of action of commonly used chemotherapeutic agents on DNA, RNA, proteins, and the processes in between

Table 15.1 Commonly used chemotherapeutic agents and their mechanisms of action

Drug class	Drug name	Mechanism of action
Antimetabolites	Mercaptopurine	Arrests purine synthesis, interrupts DNA/RNA synthesis
	Methotrexate	Prevents thymidine synthesis, arrests conversion of folate to active form
	Cytarabine	Disrupts DNA by inhibiting DNA polymerase
	5-Fluorouracil	Disrupts DNA/RNA synthesis, inhibits thymidine synthesis
Alkaloids	Vinca alkaloids: Vincristine, vinblastine	Inhibits mitosis by binding tubulin
	Etoposide (VP-16)	Causes DNA strand breaks by inhibiting topoisomerase II
	Paclitaxel, docetaxel	Stabilize microtubules, leading to mitotic arrest
	Camptothecans: Topotecan, irinotecan	Causes DNA strand breaks by inhibiting topoisomerase I
Alkylating agents	Cyclophosphamide, melphalan, ifosfamide, dacarbazine, thiotepa	DNA disruption by intrastrand and interstrand cross-linking or methylation
	Cisplatin, carboplatin	Intra- and interstrand cross-linking of DNA by platination
Antibiotics	Anthracyclines: Doxorubicin, daunorubicin	DNA strand breaking, free radical formation, interference of DNA re-ligation (topoisomerase II-mediated)
Miscellaneous	Corticosteroids	Lympholysis
	L-asparaginase	Inhibition of protein synthesis by L-asparagine
	Rituximab	Anti-CD20 antibody
	Thalidomide, bevacizumab	Anti-angiogenesis
	Retinoic acid	Differentiating agent

mide, cisplatin, and carboplatin damage DNA by covalently binding to and inhibiting the cross-linking of base pairs within the tumor cell's DNA [5]. A summary of commonly used chemotherapeutic agents in ophthalmic cancers and their mechanisms of action are listed in Table 15.1.

An understanding of the mechanism of action of these drugs allows the oncologist to predict which tumors may respond to the drug based on their biochemical and cytokinetic profiles. Frequently, chemotherapeutic agents are used in combination with one another to produce additive or synergistic anti-tumor effects. One example of the success of combination chemotherapy is in a non-ophthalmic disease, childhood acute lymphoblastic leukemia (ALL). In the mid-twentieth century, patients were treated with single-agent aminopterin (a folate antagonist) and would attain a complete remission initially, only to relapse and die within a short time. However, once researchers began to use a combination of the most active chemotherapy drugs simultaneously, complete remissions would be sustained, and the survival rate of children with leukemia improved significantly [2]. Today, more than 90% of patients with standard-risk ALL can be cured of this disease.

The development of combination chemotherapy regimens requires thoughtful consideration of the tumor biochemical profile, potential toxicities that might overlap, and also how a drug combination might inhibit vital intracellular processes at specific time points during the tumor's cell cycle. For instance, antimetabolites such as 5-fluorouracil are inhibitory only during the S phase of the cell cycle and tend to be more cytotoxic with prolonged infusion times. The longer exposure time to the drug allows for a greater number of tumor cells that will be in the S phase and, hence, be sensitive to the antimetabolite agent [6].

15.2.3 Dose Intensification of Chemotherapy

Most chemotherapeutic agents have a steep dose-response curve—a small increase in the dose can significantly enhance the drug's therapeutic effect of tumor cell kill. For instance, in preclinical models of various cancer types, doubling the dose of cyclophosphamide allowed for up to a ten-fold increase in tumor cell death [7].

Relative dose intensity (RDI) is a mathematical equation defined as the ratio of the delivered dose intensity of chemotherapy to the standard dose intensity. RDI is most calculated using the Hryniuk model, where delivered intensity is calculated as the total dose delivered divided by the total time to complete chemotherapy [8]. Increasing dose intensity has been shown to improve clinical outcomes in various cancers, such as in localized Ewing sarcoma, where interval compression of a 5-drug regimen (chemotherapy given every 2 weeks instead of every 3 weeks) resulted in significantly improved 5-year event-free survival [9].

15.3 Clinical Pharmacology of Chemotherapeutic Agents

15.3.1 Pharmacokinetics

Pharmacokinetics is a particularly important concept in any type of medical therapy, but especially with cytotoxic chemotherapy. Pharmacokinetics specifies the quantitative aspects of drug disposition in the body, including drug absorption, distribution, metabolism, and excretion. Significant variability in anticancer drug disposition can occur, which can result from variations in patient age, excre-

tory organ function, rate of metabolism, extent of drug-protein binding, and interactions with other drugs the patient is taking. The pharmacokinetics of each anticancer drug are meticulously studied prior to its approval for use in humans. This occurs at first in vitro and in vivo in the laboratory setting, then is translated to clinical trials in humans.

In certain anticancer therapy regimens, the pharmacokinetics of a drug for a specific patient may be calculated prior to each dose administered. For instance, in hematopoietic stem cell transplantation, the alkylating agent busulfan, which is given at high doses in this scenario and can be quite nephrotoxic, hepatotoxic, and neurotoxic, is dosed based on the patient's specific pharmacokinetic area under the plasma drug concentration-time curve (AUC). Some clinicians follow a patient's plasma busulfan levels in case future doses require adjustments. This exemplifies the significant interpatient variability of a chemotherapy agent's systemic drug exposure.

15.3.2 Drug-Drug Interactions

Chemotherapeutic agents have a significant side effect profile, so they are given concomitantly with several other medications to abate adverse reactions. This introduces a risk of interactions between the various drugs given. It is imperative that clinicians are aware of these potential drug-drug interactions since not only may untoward side effects occur, but also the anti-tumor effect of the chemotherapeutic agent could be altered. For instance, multiple chemotherapeutic agents are metabolized by the CYP3A subfamily of drug-metabolizing enzymes [10]. Another drug that alters the activity of CYP3A (such as fluconazole—a commonly used prophylactic antifungal agent in immunocompromised patients) could alter the metabolism and clearance of the chemotherapeutic agent.

15.3.3 Chemotherapy Resistance

Resistance to anticancer drugs is the primary cause of treatment failure in cancer patients. Drug resistance can be present at diagnosis or develop over time by progressively increasing exposure to anticancer agents. Cancer cells undergo spontaneous generation of drug-resistant clones by mutation, deletion, gene amplification, translocation, or chromosomal rearrangement [11]. This occurs because of the inherent genetic instability that exists in cancer cells.

Tumor cells can be resistant to one drug or multiple drugs. The multi-drug resistance (MDR) phenomenon is where the tumor cells develop resistance to multiple functionally and structurally unrelated drugs. There are various biochemical pathways that comprise the mechanisms of MDR, including the activity of ATP-binding cassette (ABC) efflux transporters, which transport drug molecules out of the tumor cell. The P-glycoprotein, a cell surface protein found on both normal and tumor cells alike, is a building block of the ABC efflux transporters and has been found to be overexpressed in MDR tumors [12]. Other mechanisms of MDR include tumor cell DNA repair mechanisms, pathways that result in decreased influx of the chemotherapy drug into the tumor cell, the tumor cell sequestering the drug and inhibiting its function, and alterations in the tumor microenvironment that lead to decreased function of chemotherapy agents [12]. These mechanisms of MDR must be considered when choosing chemotherapy regimens, particularly in patients with relapsed or refractory disease.

15.4 Multimodal Therapy

Chemotherapy is often not the only form of treatment in orbital and ocular cancers, especially in solid cancers that are non-hematologic. In general, the best way to achieve complete remission and eventual cure of a solid tumor is to treat with effective local control therapy in addition to chemotherapy, such as radiation therapy, surgical resection, cryotherapy, or transpupillary thermotherapy.

15.4.1 Adjuvant Chemotherapy

Adjuvant chemotherapy is given in a setting where patients receive local control therapy to the primary tumor (surgery, radiation therapy, or intraocular therapies) at diagnosis or after neoadjuvant chemotherapy. The term "adjuvant" refers to systemic chemotherapy given after local control strategies are performed. The goal of adjuvant chemotherapy is to eradicate any residual tumor cells that may remain after local control therapy. This decreases the risk of relapse in many tumors. For example, in retinoblastoma, adjuvant chemotherapy is given after enucleation if there are certain high-risk features present in the enucleated eye [13].

15.4.2 Neoadjuvant Chemotherapy

Neoadjuvant chemotherapy is given to a patient prior to local control therapy (i.e., surgery or radiation therapy). This is most done in the setting of large, unresectable tumors, where there exists an increased risk for positive margins after a risky surgery or of significant toxicities/late effects from radiation therapy. The goal of giving systemic chemotherapy prior to local control therapy is to reduce tumor burden for local control therapy to be more successful. For instance, in retinoblastoma, neoadjuvant chemotherapy is useful in treating large tumors to achieve tumor size reduction so that sub-

sequent local cryotherapy or laser thermotherapy can be more efficacious if the tumor first shrinks with systemic chemotherapy [14]; hence the term "chemoreduction."

15.5 Commonly Used Chemotherapeutic Agents in Ophthalmic Cancers

Some of the most common primary ophthalmic cancers in adults are lymphoproliferative disorders (i.e., B cell non-Hodgkin lymphomas) and uveal melanoma, while the most common in children are retinoblastoma and orbital rhabdomyosarcoma. Here, we will review the standard systemic treatment regimens for each of these diseases (Table 15.2), keeping in mind that local control via radiation, plaque brachytherapy, cryotherapy, transpupillary thermotherapy, or surgery are crucial components of multimodal therapy to yield a sustained treatment response.

15.5.1 Orbital Lymphoma

Orbital lymphoproliferative disorders (i.e., lymphomas) are treated locally with radiation therapy, and the more aggressive B-cell NHL tumors (i.e., diffuse large B-cell lymphoma) are treated with a combination of chemotherapy and immunotherapy. The so-called R-CHOP regimen is used, which is a combination of the monoclonal anti-CD20 antibody, rituximab, with the conventional chemotherapy agent's cyclophosphamide, doxorubicin, and vincristine as well as prednisone [15]. In childhood NHL, the standard chemotherapeutic backbone is more intensive and includes additional agents, such as high-dose methotrexate and etoposide [16].

15.5.2 Metastatic Uveal Melanoma

The management of metastatic uveal melanoma has changed with the FDA approval of tebentafusp-tebn, a bispecific fusion protein that can redirect T-cells to target gp100 antigens in uveal melanoma cells. In a randomized controlled trial, patients treated with tebentafusp-tebn had an improved overall survival (OS) (median 21.7 months [95% CI, 18.6–23.6]) compared with the investigator's choice (median 16.0 months [95% CI, 9.7–19.4]) in previously untreated HLAA* 02:01–positive patients (HR:0.51, 95% CI: 0.37, 0.71 $p < 0.001$) [17]. The improvement in OS was predominantly observed in patients with smaller hepatic metastatic lesions (LDLM ≤3 cm [M1a]) (HR: 0.36, 95% CI: 0.21, 0.61) and not in those with larger lesions (LDLM >3 cm) (HR: 0.71, 95% CI: 0.44, 1.17 in M1b and HR: 0.76, 95% CI: 0.34, 1.82 in M1c) [18]. Similarly, in the multicenter, randomized, open-label, phase III (SCANDIUM Trial) trial wherein isolated hepatic perfusion with melphalan was superior to best alternative care (control group), the treatment benefit was evident only in smaller hepatic metastatic lesions

Table 15.2 Chemotherapy regimens of some common ophthalmic cancers

Tumor	Chemotherapy agents	Surgery	Radiation therapy	Local ophthalmic therapies
Orbital lymphoma	R-CHOP: Rituximab, cyclophosphamide, doxorubicin, vincristine, prednisone	+/–	+/–	–
Uveal melanoma (non-metastatic)	–	+	+	+/–
Uveal melanoma (metastatic)	Dacarbazine, temozolomide, cisplatin, bendamustine, fotemustine, treosulfan, targeted therapies (MEK or PD-1 inhibitors), tebentafusp-tebn	+	+	+/–
Conjunctival melanoma (metastatic)	Targeted therapies (i.e., PD-1 inhibition, MEK inhibition, BRAF inhibition)	+/–	+	+/–
Retinoblastoma (localized)	CEV: Carboplatin, etoposide, vincristine	+/–	+/–	+/–
Retinoblastoma (metastatic)	Induction: Vincristine, cyclophosphamide, cisplatin, etoposide Autologous SCT: Carboplatin, etoposide, thiotepa	+/–	+/–	+/–
Orbital rhabdomyosarcoma (localized)	VA: Vincristine + actinomycin-D, or VAC: Vincristine, actinomycin-D, cyclophosphamide	+/–	+	–
Orbital rhabdomyosarcoma (metastatic)	Age > 10 years, PAX/FOXO1 fusion negative: VDC/IE: Vincristine, doxorubicin, cyclophosphamide/ ifosfamide, etoposide VI: Vincristine + irinotecan during radiation therapy PAX-FOXO1 fusion positive: VAC, VAC/VI	+/–	+	–
Optic nerve glioma	Certain cases: Vincristine + carboplatin; vinblastine TPCV: Thioguanine, procarbazine, lomustine, vincristine MEK inhibitors (trametinib, selumetinib) BRAF inhibitors (dabrafenib) Pan-RAF inhibitors (tovorafenib) VEGFinhibitors (bevacizumab)	+/–	+/–	–

(LDLM ≤3 cm [M1a]) (HR: 0.46, 95% CI: 0.22, 0.95) and not in those with larger lesions (LDLM >3 cm) (HR:1.44, 95% CI: 0.57, 3.67 in M1b and HR:1.57, 95% CI: 0.22, 11.34 in M1c) [19, 20].

15.5.3 Retinoblastoma

Retinoblastoma is the most common intraocular cancer of childhood, though still quite rare, with 11.8 cases per million children per year in the United States [21]. Treatment depends on the stage and group of the tumor, but in general, systemic chemotherapy is used for bilateral or germline disease, trilateral or extraocular disease, for chemoreduction if a unilateral tumor is too large for local therapies, if a patient is too young/small for intra-arterial chemotherapy, and for patients in whom the enucleated eye has high-risk features [22–25]. Agents used in these settings include a 3-drug regimen of carboplatin, etoposide, and vincristine, which are typically given in six 28-day cycles. Patients with Group B disease can achieve adequate chemoreduction with the use of carboplatin and vincristine alone [26]. Patients with extraocular or metastatic retinoblastoma have a much worse prognosis than those with localized intraocular disease [27]. Thus, these patients are treated with an aggressive chemotherapy regimen that includes four induction cycles of vincristine, cisplatin, cyclophosphamide, and etoposide, followed by high-dose chemotherapy (carboplatin, etoposide, and thiotepa) and autologous stem cell rescue (or, autologous hematopoietic stem cell transplant) [28].

Additionally, patients with unilateral retinoblastoma may benefit from intra-arterial chemotherapy, where small doses of chemotherapy are introduced directly to the tumor via the ophthalmic artery during a femoral arterial catheterization procedure [29, 30]. The drugs used in this procedure are most commonly melphalan, topotecan, carboplatin, and sometimes a combination of these agents [29]. Intravitreal chemotherapy can also be given for those patients with vitreous seeding—melphalan is most commonly used in this setting [31]. These procedures have limited feasibility, however, and must be performed at an institution that has an established retinoblastoma program with an experienced ophthalmic oncologist, pediatric oncologist, and an interventional neuroradiologist.

15.5.4 Orbital Rhabdomyosarcoma

Rhabdomyosarcoma (RMS) is the most common sarcoma in children, and about 10% occur in the favorable site of the orbit [32]. The treatment of RMS is based on whether the patient has localized or metastatic disease. Patients with intermediate-risk disease are treated with 40 weeks of vincristine, actinomycin-D, and cyclophosphamide (VAC) and have an approximately 70% event-free survival at 3 years [33]. Patients with high-risk (metastatic) disease have a significantly worse prognosis [34]. Given the dismal prognosis of these patients, the standard of care remains the less intensive VAC or VAC/VI regimens (adding in vincristine + irinotecan cycles); some centers may choose a more aggressive approach utilizing combination dose-intense chemotherapy that includes 2-week cycles of vincristine, doxorubicin, and cyclophosphamide (VDC) alternating with ifosfamide and etoposide (IE) [35]. Irinotecan is also included in the treatment of patients with intermediate-risk RMS; this drug is known to be a sensitizer to radiation therapy, so it can be given during radiation. Of course, a critical component of RMS therapy is local control via radiation therapy and/or surgical resection [36].

15.6 Toxicities of Chemotherapy

Antineoplastic agents have the narrowest therapeutic window of all classes of drugs. This means that they can cause significant and potentially life-threatening toxicities fairly easily. The oncologist must balance the risk of toxicities against the risk of relapse, which might occur with inadequate treatment. Unfortunately, dose reductions or delays in therapy to mitigate toxicities can contribute to tumor recurrence or refractoriness and eventual death from disease. General toxicities caused by many chemotherapeutic agents include fatigue; nausea and vomiting; myelosuppression leading to leukopenia, anemia, and thrombocytopenia; alopecia; constipation and diarrhea; and mucositis. Less common but serious toxicities include neutropenic colitis (or typhlitis), sepsis/bacteremia or invasive fungal infections, sensorineural hearing loss, and peripheral neuropathy. A summary of commonly seen toxicities of specific chemotherapeutic agents is listed in Table 15.3.

Table 15.3 Systemic side effects of commonly used chemotherapy agents

Drug class	Drug name	Toxicity
Antimetabolites	Mercaptopurine	Hepatotoxicity
	Methotrexate	Hepatotoxicity, nephrotoxicity
	Cytosine arabinoside	Hepatotoxicity, nephrotoxicity, neurotoxicity
Alkaloids	Vinca alkaloids: Vincristine, vinblastine	Peripheral neuropathy, constipation, jaw pain
	Etoposide (VP-16)	Hepatotoxicity, nephrotoxicity, infusion-related hypotension/ hypertension or fever, secondary malignancy
Alkylating agents	Cyclophosphamide, ifosfamide	Hepatotoxicity, nephrotoxicity, hemorrhagic cystitis, infertility
	Cisplatin, carboplatin	Nephrotoxicity, ototoxicity, infusion-related reactions (rash, anaphylaxis)
Antitumor antibiotics	Anthracyclines: Doxorubicin, daunorubicin	Hepatotoxicity, cardiotoxicity
Camptothecin analogues (topoisomerase I inhibitors)	Irinotecan, topotecan	Diarrhea (acute or delayed)
Podophyllotoxin derivatives (topoisomerase II inhibitors)	Etoposide, teniposide, doxorubicin, mitoxantrone	Infusion-related reactions (hypotension, anaphylaxis) Secondary lymphoproliferative disorders (myelodysplastic syndrome, acute myelogenous leukemia) Cardiotoxicity
Miscellaneous	Corticosteroids	Cushing's syndrome, GI bleed, hyperglycemia, hypertension, hirsutism
	L-asparaginase	Pancreatitis, thrombosis, allergic reaction/anaphylaxis
	Interferon alpha	Fever, malaise, myalgias
	Thalidomide	Teratogenicity
	Retinoic acid	Hypervitaminosis A, hepatotoxicity

Systemic chemotherapy may also be associated with ocular side effects that may be acute or chronic. With the development of newer anticancer therapies and with the combination of more aggressive agents with these newer therapies, the risk of ocular and other adverse effects has increased. Moreover, as survival improves over time, patients live longer and have the potential for adverse late effects because of therapy.

Several commonly used chemotherapeutic agents have been reported to result in ocular morbidity [37–42]. Although a comprehensive review of the literature related to ocular side effects of chemotherapeutic agents is beyond the scope of this chapter, some of the commonly used agents and their ocular toxicities are summarized in Table 15.4. Some agents affect various ocular and periocular structures as well as the optic nerve, cranial nerves, and central nervous system components serving vision and oculomotor function. For some agents, the mechanism of a particular adverse reaction is known, but frequently, the exact etiology of many ocular side effects remains unknown.

It is important to realize, however, that while ocular side effects related to these agents are usually not preventable, many of them are reversible with either dose reduction or discontinuation of the drug (Fig. 15.3). Accordingly, the role of the ophthalmologist in performing baseline evaluation of patients receiving chemotherapy and following patients throughout and after their treatment course to screen for potential adverse reactions is critical. Some of these adverse reactions are a direct result of the chemotherapeutic agent (Table 15.4); however, other ocular adverse reactions are indirectly related to the drug. For example, an immunocompromised, myelosuppressed patient who has received cytotoxic chemotherapy has a risk of developing an opportunistic ocular infection such as CMV retinitis (Fig. 15.4) or retinopathy due to profound thrombocytopenia (Fig. 15.5). It may be difficult to discern whether an ocular adverse reaction is directly or indirectly related to the chemotherapeutic agents given; thus, it is important for the ophthalmologist and medical oncologist to maintain close collaboration to make the proper diagnosis and execute an appropriate treatment plan.

Table 15.4 Ocular side effects of commonly used chemotherapeutic agents

Chemotherapeutic agent/ class	Anatomic location	Specific ocular side effect
L-asparaginase, taxanes, and platinum salts	Ocular adnexal structures	Hyperpigmentation, sclerodermiform dermatitis, photosensitivity, and hypersensitivity reactions
Methotrexate	Ocular adnexal structures	Periocular edema, blepharitis
	Anterior segment	Conjunctivitis
	Posterior segment	Retinopathy with reduced b-wave amplitude on ERG, macular edema
	Optic nerve/ oculomotor nerves	Optic neuropathy and internuclear ophthalmoplegia
5-fluorouracil, capecitabine	Ocular adnexal structure	Blepharitis, eyelid dermatitis, cicatricial ectropion, punctual/canalicular/ductal stenosis, alopecia, phlebitis, chemical cellulitis, diffuse sclerosis, sterile folliculitis, and flushing reactions
	Anterior segment	Conjunctivitis, keratitis
Interferon	Ocular adnexal structures	Alopecia, trichomegaly, and hypertrichosis
	Anterior segment	Acute corneal graft rejection, glaucoma
	Posterior segment	Retinopathy with retinal hemorrhages, cotton wool spots, macular edema, & retinal ischemia
	Optic nerve	Anterior ischemic optic neuropathy
Mitomycin-C	Anterior segment	Conjunctivitis & keratitis, worse with topical application
Carmustine	Anterior segment	Conjunctivitis and keratitis
	Posterior segment	Retinal hard exudates, hemorrhages, infarcts, & retinal artery occlusion
	Optic nerve	Optic neuropathy
Tamoxifen	Anterior segment	Corneal subepithelial deposits, whorls & linear opacities, posterior subcapsular cataract
	Posterior segment	Pigmentary retinopathy, macular crystals & drusen, macular edema
	Optic nerve	Optic neuritis
Cytarabine	Anterior segment	Conjunctivitis & keratitis
Cisplatin and etoposide	Posterior segment	Retinopathy, reduced a-wave and absent b-waves on ERG, retinal ischemia, neovascularization
Cisplatin, vinblastine, and vincristine	Optic nerve and CNS	Optic neuritis with disc edema, transient cortical blindness or homonymous hemianopia, cranial nerve dysfunction
Intracarotid cisplatin	Ocular adnexal structures	Orbital myositis
	Posterior segment	Central retinal artery occlusion, uveal effusion
	Optic nerve	Optic neuritis
Chlorambucil	Anterior segment	Keratitis
	Posterior segment	Retinal hemorrhages
	Optic nerve	Papilledema
Cyclophosphamide	Ocular adnexal structures	Blepharitis, lacrimal duct stenosis
	Anterior segment	Kerato-conjunctivitis sicca
	Posterior segment	Retinal hemorrhages
Rituximab	Ocular adnexal structures	Transient periocular edema
	Anterior segment	Conjunctivitis
Paclitaxel	Posterior segment	Cystoid macular edema
Docetaxel	Anterior segment	Canalicular stenosis

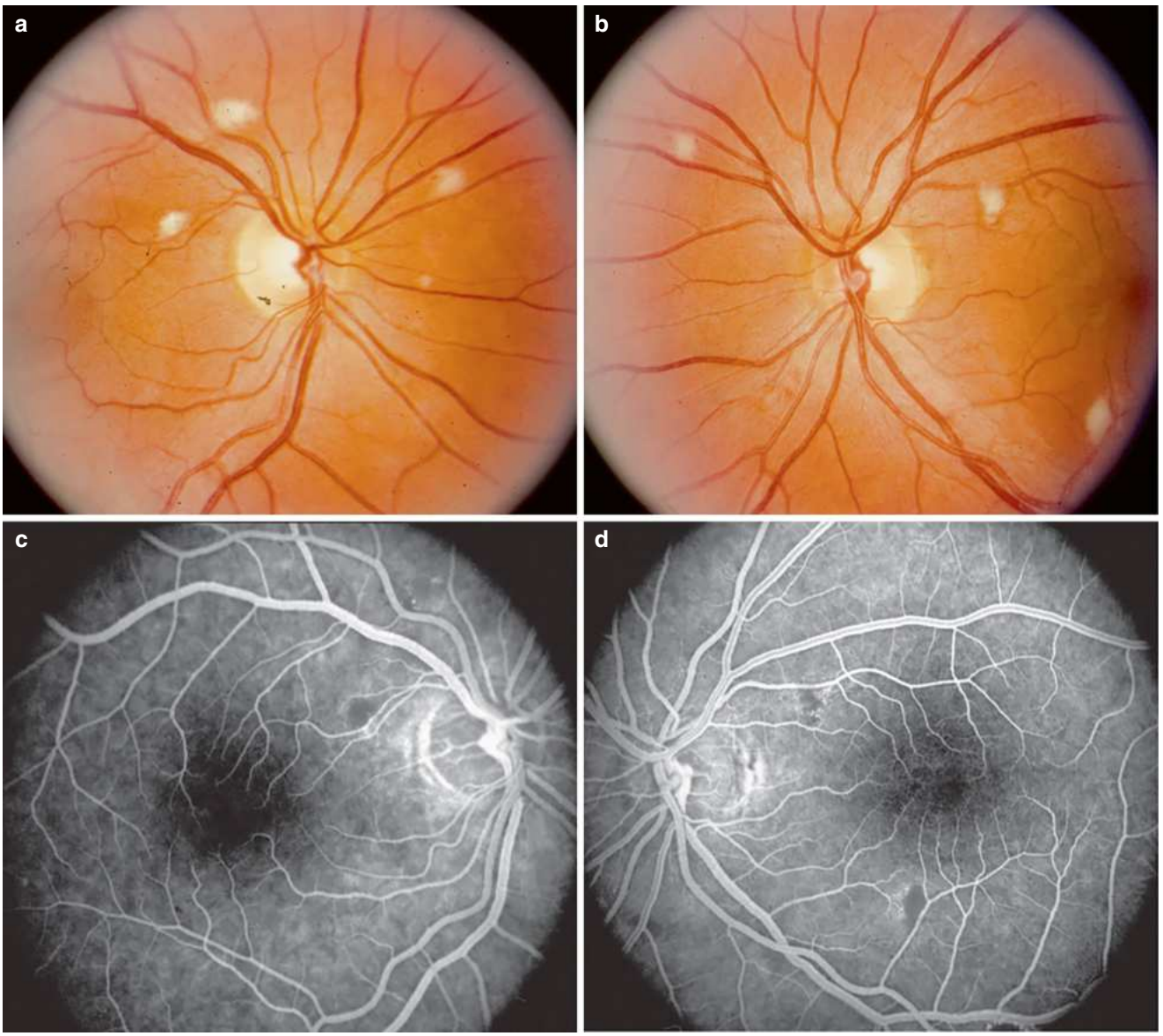

Fig. 15.3 A 30-year old male presented with complaints of mild visual distortion in both eyes of several weeks' duration. He had been in good health until 5 months prior, when he was diagnosed with a malignant cutaneous melanoma. The patient underwent surgical resection, and on histopathologic review, the primary tumor was graded T4bN2aM0. There was no evidence of metastatic disease. The patient received 20 days of high-dose IV interferon alpha 2b (30–36 million IU over 30 min) and was then switched to subcutaneous interferon injections. One week prior to presentation to the ophthalmologist, the patient was hospitalized for an acute stroke that presented with symptoms of right-sided facial droop, dysarthria, and right upper extremity weakness. MRI of the brain revealed an infarct involving the left caudate nucleus and a portion of the left posterior limb of the internal capsule. On examination, the patient's vision measured 20/20 without correction. Dilated fundus examination revealed scattered cotton wool spots throughout the posterior pole in both eyes (**a**, **b**). The rest of the ophthalmic examinations, including visual field testing, color vision and slit lamp exam, were normal. Fluorescein angiogram confirmed retinal capillary non-perfusion (ischemia) corresponding to the cotton wool spots (**c**, **d**). A recent history of stroke along with findings of focal micro-retinal infarctions prompted a complete review of coagulation and cardiovascular systems, which were all reported as normal except for an ejection fraction of 30%, suggestive of cardiomyopathy. Interferon treatment was discontinued promptly. Follow-up exam 10 months later showed complete resolution of retinopathy and full recovery from the stroke with no residual neurologic symptoms. A strong temporal relationship between the onset of symptoms and the initiation of interferon therapy and absence of any other probable cause of vasculopathy suggested that stroke, cardiomyopathy, and retinopathy observed in our patient had a shared underlying pathogenetic mechanism of interferon-induced ischemia

Fig. 15.4 A 58-year old man was referred for evaluation of floaters OD for the past couple of weeks. He had a history of colon cancer s/p resection and had received chemotherapy. Visual acuity was 20/50 OD and 20/25 OS. Anterior segment examination was normal. Fundus examination of the right eye revealed a hemorrhagic white retinal lesion of CMV retinitis

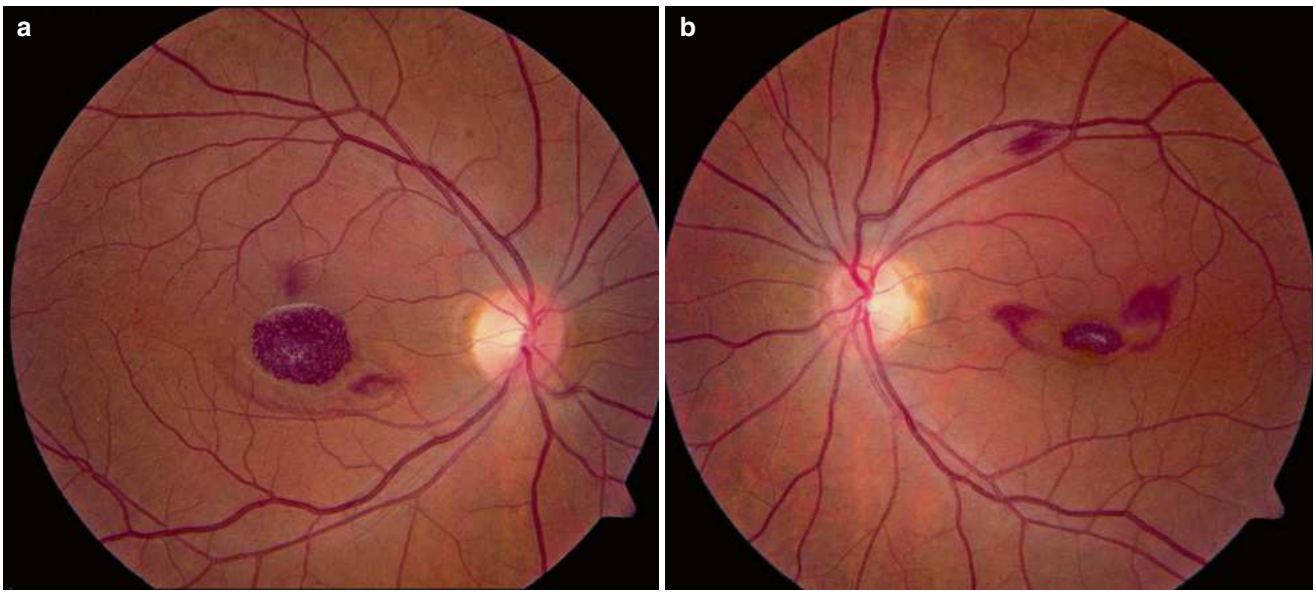

Fig. 15.5 A 30-year old female with diffuse large B-cell lymphoma, who had received 4 cycles of chemotherapy at the time of presentation, presented with blurred vision of 2 weeks' duration. Examination revealed visual acuity of 20/70 OD and 20/40 OS. Fundus examination showed bilateral localized retinal hemorrhages (**a**, **b**). Optical coherence tomography confirmed sub-ILM location of the hemorrhage (**c**, **d**). Eight weeks later, the hemorrhage had completed resolved with full visual recovery associated with normalization of blood counts (**e**, **f**)

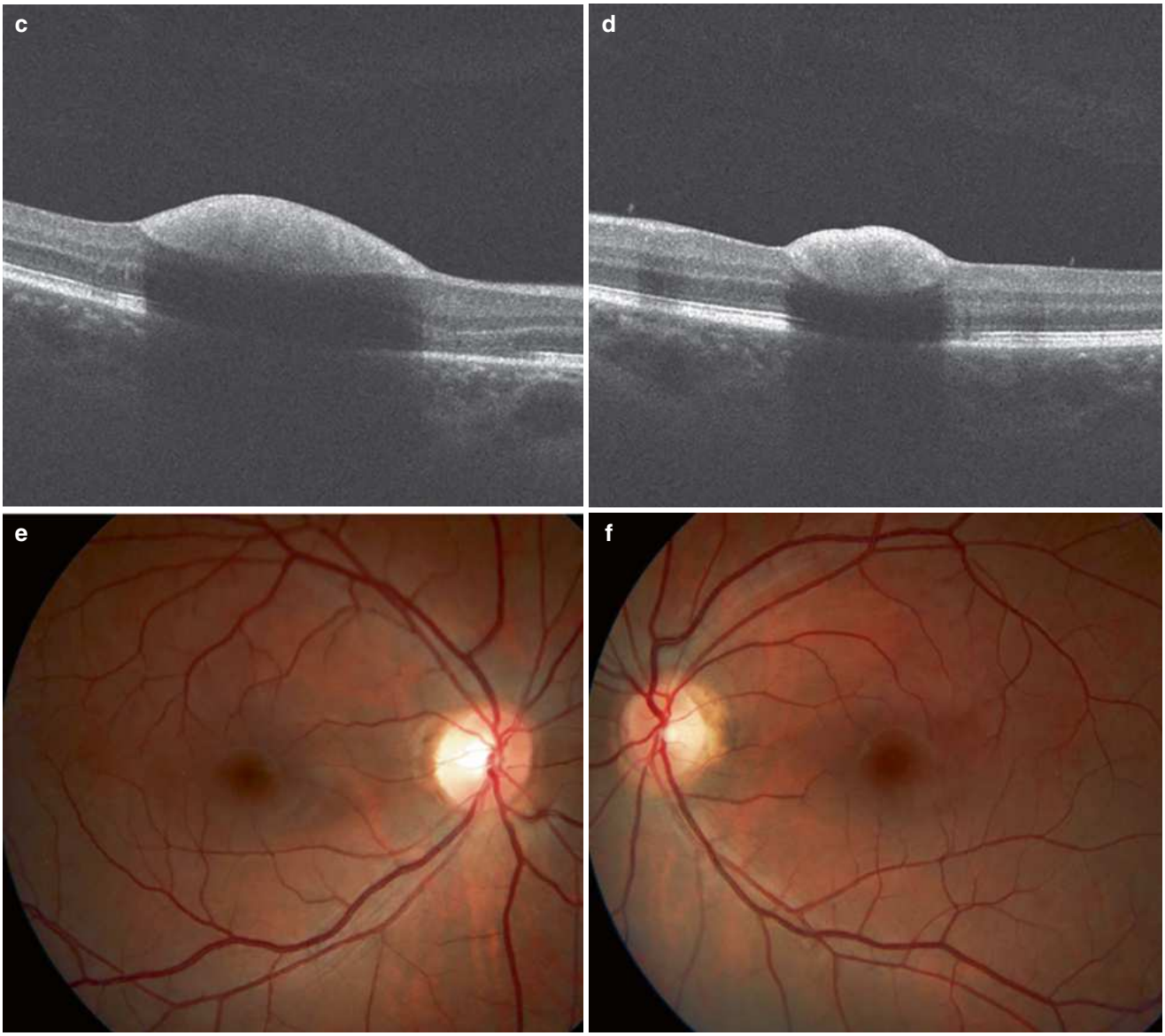

Fig. 15.5 (continued)

15.7 Summary

Several primary and secondary ophthalmic cancers exist that benefit from treatment with systemic chemotherapy. Most chemotherapy drugs have non-selective mechanisms of action against DNA, RNA, proteins, or metabolic pathways in tumor cells, but because of the non-selective properties of chemotherapy, normal cells are also affected. Chemotherapy is often given in combination with other agents to enhance cytotoxic effects, combat multi-drug resistance, and reduce the risk of relapse. Chemotherapy is given in repetitive cycles at maximum tolerated doses to allow for a constant fraction of tumor cell kill and to allow for recovery of affected normal cells. Chemotherapeutic regimens are often combined with local tumor control approaches to achieve the best outcomes in ophthalmic cancers. Antineoplastic drugs have the narrowest therapeutic window of any class of drugs, so the treating physician must balance the risk of toxicities against the risk of relapse in choosing chemotherapy regimens for patients with ophthalmic cancers. Newer targeted therapies have been studied over the last two decades and show promise in improving survival when given alone or in combination with conventional chemotherapy.

References

1. Poplack DG, Pizzo PA, editors. Principles and practice of pediatric oncology. 6th ed. Philadelphia, PA: Lippincott Williams & Wilkins; 2011.
2. Pui CH, Evans WE. A 50-year journey to cure childhood acute lymphoblastic leukemia. Semin Hematol. 2013;50(3):185–96.
3. Alley MC, Scudiero DA, Monks A, Hursey ML, Czerwinski MJ, Fine DL, et al. Feasibility of drug screening with panels of human tumor cell lines using a microculture tetrazolium assay. Cancer Res. 1988;48(3):589–601.
4. Pommier Y. DNA topoisomerase I and II in cancer chemotherapy: update and perspectives. Cancer Chemother Pharmacol. 1993;32(2):103–8.
5. Gerson SL, Bulgar AD, Weeks LD, Chabner BA. Alkylating agents. In: Chabner BA, Longo DL, editors. Cancer chemotherapy and biotherapy: principles and practice. Philadelphia, PA: Lippincott Williams & Wilkins, a Wolters Kluwer business; 2011. p. 267–92.
6. Harstrick A, Gonzales A, Schleucher N, Vanhoefer U, Lu K, Formento JL, et al. Comparison between short or long exposure to 5-fluorouracil in human gastric and colon cancer cell lines: biochemical mechanism of resistance. Anti-Cancer Drugs. 1998;9(7):625–34.
7. Frei E 3rd, Canellos GP. Dose: a critical factor in cancer chemotherapy. Am J Med. 1980;69(4):585–94.
8. Havrilesky LJ, Reiner M, Morrow PK, Watson H, Crawford J. A review of relative dose intensity and survival in patients with metastatic solid tumors. Crit Rev Oncol Hematol. 2015;93(3):203–10.
9. Womer RB, West DC, Krailo MD, Dickman PS, Pawel BR, Grier HE, et al. Randomized controlled trial of interval-compressed chemotherapy for the treatment of localized Ewing sarcoma: a report from the Children's Oncology Group. J Clin Oncol. 2012;30(33):4148–54.
10. Kivisto KT, Kroemer HK, Eichelbaum M. The role of human cytochrome P450 enzymes in the metabolism of anticancer agents: implications for drug interactions. Br J Clin Pharmacol. 1995;40(6):523–30.
11. Goldie JH, Coldman AJ. Drug resistance in cancer: models and mechanisms. New York: Cambridge University Press; 1998 (digital version 2009).
12. Vadlapatla RK, Vadlapudi AD, Pal D, Mitra AK. Mechanisms of drug resistance in cancer chemotherapy: coordinated role and regulation of efflux transporters and metabolizing enzymes. Curr Pharm Des. 2013;19(40):7126–40.
13. Chintagumpala M, Piao J, Gombos D, Chevez-Barrios P, Brock L, Dunkel IJ, et al. A multi-institutional feasibility study of intra-arterial chemotherapy in children with retinoblastoma. A Children's Oncology Group study (COG ARET12P1). Pediatr Blood Cancer. 2024;71(1):e30718.
14. Murphree AL, Villablanca JG, Deegan WF 3rd, Sato JK, Malogolowkin M, Fisher A, et al. Chemotherapy plus local treatment in the management of intraocular retinoblastoma. Arch Ophthalmol. 1996;114(11):1348–56.
15. Eckardt AM, Lemound J, Rana M, Gellrich NC. Orbital lymphoma: diagnostic approach and treatment outcome. World J Surg Oncol. 2013;11:73.
16. Minard-Colin V, Auperin A, Pillon M, Burke GAA, Barkauskas DA, Wheatley K, et al. Rituximab for high-risk, mature B-cell non-Hodgkin's lymphoma in children. N Engl J Med. 2020;382(23):2207–19.
17. Nathan P, Hassel JC, Rutkowski P, Baurain JF, Butler MO, Schlaak M, et al. Overall survival benefit with tebentafusp in metastatic uveal melanoma. N Engl J Med. 2021;385(13):1196–206.
18. Kivela T, Simpson E, Grossniklaus H, Jager M, Singh A, Caminal J. Uveal melanoma. In: Amin M, Edge S, Greene F, Byrd D, Brookland R, Washington M, editors. AJCC cancer staging manual. Chicago: Springer; 2017. p. 813–26.
19. Olofsson Bagge R, Nelson A, Shafazand A, All-Eriksson C, Cahlin C, Elander N, et al. Isolated hepatic perfusion with melphalan for patients with isolated uveal melanoma liver metastases: a multicenter, randomized, open-label, phase III trial (the SCANDIUM trial). J Clin Oncol. 2023;41(16):3042–50.
20. Olofsson Bagge R, Nelson A, Shafazand A, All-Eriksson C, Cahlin C, Elander N, et al. Survival after isolated hepatic perfusion as a treatment for uveal melanoma liver metastases: results from a randomized controlled trial (the SCANDIUM trial). ASCO Annual Meeting 2023.
21. Broaddus E, Topham A, Singh AD. Incidence of retinoblastoma in the USA: 1975–2004. Br J Ophthalmol. 2009;93(1):21–3.
22. Chung CY, Medina CA, Aziz HA, Singh AD. Retinoblastoma: evidence for stage-based chemotherapy. Int Ophthalmol Clin. 2015;55(1):63–75.
23. Brennan RC, Qaddoumi I, Billups CA, Free TL, Haik BG, Rodriguez-Galindo C, et al. Comparison of high-risk histopathological features in eyes with primary or secondary enucleation for retinoblastoma. Br J Ophthalmol. 2015;99(10):1366–71.
24. Chantada GL, Dunkel IJ, de Davila MT, Abramson DH. Retinoblastoma patients with high risk ocular pathological features: who needs adjuvant therapy? Br J Ophthalmol. 2004;88(8):1069–73.
25. Gobin YP, Dunkel IJ, Marr BP, Francis JH, Brodie SE, Abramson DH. Combined, sequential intravenous and intra-arterial chemotherapy (bridge chemotherapy) for young infants with retinoblastoma. PLoS One. 2012;7(9):e44322.
26. Friedman DL, Krailo M, Villaluna D, Gombos D, Langholz B, Jubran R, et al. Systemic neoadjuvant chemotherapy for gGroup B intraocular retinoblastoma (ARET0331): a report from the Children's Oncology Group. Pediatr Blood Cancer. 2017;64(7):e26394.
27. Hu HM, Zhang WL, Wang YZ, Shi JT, Li B, Zhang Y, et al. [Clinical features, treatment and prognosis of retinoblastoma in distant metastasis stage]. Zhonghua Yan Ke Za Zhi [Chin J Ophthalmol]. 2017;53(2):121–27.
28. Dunkel IJ, Chan HS, Jubran R, Chantada GL, Goldman S, Chintagumpala M, et al. High-dose chemotherapy with autologous hematopoietic stem cell rescue for stage 4B retinoblastoma. Pediatr Blood Cancer. 2010;55(1):149–52.
29. Abramson DH, Marr BP, Dunkel IJ, Brodie S, Zabor EC, Driscoll SJ, et al. Intra-arterial chemotherapy for retinoblastoma in eyes with vitreous and/or subretinal seeding: 2-year results. Br J Ophthalmol. 2012;96(4):499–502.
30. Jabbour P, Chalouhi N, Tjoumakaris S, Gonzalez LF, Dumont AS, Chitale R, et al. Pearls and pitfalls of intraarterial chemotherapy for retinoblastoma. J Neurosurg Pediatr. 2012;10(3):175–81.
31. Munier FL, Gaillard MC, Balmer A, Soliman S, Podilsky G, Moulin AP, et al. Intravitreal chemotherapy for vitreous disease in retinoblastoma revisited: from prohibition to conditional indications. Br J Ophthalmol. 2012;96(8):1078–83.
32. Joshi D, Anderson JR, Paidas C, Breneman J, Parham DM, Crist W. Age is an independent prognostic factor in rhabdomyosarcoma: a report from the Soft Tissue Sarcoma Committee of the Children's Oncology Group. Pediatr Blood Cancer. 2004;42(1):64–73.
33. Meza JL, Anderson J, Pappo AS, Meyer WH. Analysis of prognostic factors in patients with nonmetastatic rhabdomyosarcoma treated on intergroup rhabdomyosarcoma studies III and IV: the Children's Oncology Group. J Clin Oncol. 2006;24(24):3844–51.
34. Oberlin O, Rey A, Lyden E, Bisogno G, Stevens MC, Meyer WH, et al. Prognostic factors in metastatic rhabdomyosarcomas: results of a pooled analysis from United States and European cooperative groups. J Clin Oncol. 2008;26(14):2384–9.

35. Weigel BJ, Lyden E, Anderson JR, Meyer WH, Parham DM, Rodeberg DA, et al. Intensive multiagent therapy, including dose-compressed cycles of ifosfamide/etoposide and vincristine/doxorubicin/cyclophosphamide, irinotecan, and radiation, in patients with high-risk rhabdomyosarcoma: a report from the Children's Oncology Group. J Clin Oncol. 2016;34(2):117–22.
36. Borinstein SC, Steppan D, Hayashi M, Loeb DM, Isakoff MS, Binitie O, et al. Consensus and controversies regarding the treatment of rhabdomyosarcoma. Pediatr Blood Cancer. 2018;65(2).
37. al-Tweigeri T, Nabholtz JM, Mackey JR. Ocular toxicity and cancer chemotherapy. A review. Cancer. 1996;78(7):1359–73.
38. Kawano T, Shigehira M, Uto H, Nakama T, Kato J, Hayashi K, et al. Retinal complications during interferon therapy for chronic hepatitis C. Am J Gastroenterol. 1996;91(2):309–13.
39. Esmaeli B, Amin S, Valero V, Adinin R, Arbuckle R, Banay R, et al. Prospective study of incidence and severity of epiphora and canalicular stenosis in patients with metastatic breast cancer receiving docetaxel. J Clin Oncol. 2006;24(22):3619–22.
40. Schmid KE, Kornek GV, Scheithauer W, Binder S. Update on ocular complications of systemic cancer chemotherapy. Surv Ophthalmol. 2006;51(1):19–40.
41. Zinchuk O, Watanabe M, Hayashi N, Fukushima A, Ueno H. A case of tamoxifen keratopathy. Arch Ophthalmol. 2006;124(7):1046–8.
42. Hazin R, Abuzetun JY, Daoud YJ, Abu-Khalaf MM. Ocular complications of cancer therapy: a primer for the ophthalmologist treating cancer patients. Curr Opin Ophthalmol. 2009;20(4):308–17.

Counseling Patients with Cancer

16

Bertil E. Damato and Laura Hope-Stone

16.1 Introduction

A wide variety of primary and metastatic cancers can involve the eye. In addition to threatening patients with visual impediment, ocular discomfort, and loss of the eye, most cancers are also highly lethal, so that patients are faced with the possibility of systemic illness, incapacity, and death.

Ophthalmologists, nurses, and any others involved in cancer care need to understand their patients' needs and fears. They must also be able to recognize and respond to patients' psychological concerns appropriately. Every oncology service should have systems for providing appropriate psychological support to patients and their relatives.

The aims of this chapter are to describe the ocular morbidity that can be caused by cancer, the psychological problems that can arise, and the measures that can be taken to address these problems.

16.2 Challenges Faced by Patients with Eye Cancer

Care providers need to be aware of the challenges that are faced by patients with cancer affecting the eye.

16.2.1 Uveal Melanoma

Patients with uveal melanoma experience visual loss when the tumor or any associated retinal detachment involves the fovea. The eye can become painful if the tumor is allowed to reach an advanced stage. There are concerns about metastatic disease, which tends to develop months or years after apparent good health in about 50% of patients, especially if the tumor shows chromosome 3 loss or a class 2 gene expression profile. Patients experience uncertainty as to whether a small tumor of unknown malignancy should be observed, treated, or biopsied. This is because it is not known whether ocular treatment ever influences survival and, if so, in whom. When choosing between enucleation and eye-conserving therapy, the expectation is that quality of life is better if enucleation is avoided; however, eye-conserving therapy requires more intensive and more prolonged treatment, with regular follow-up visits to the hospital and, in some cases, salvage treatment and even secondary enucleation. For these reasons, there has been a long debate as to whether well-being after radiotherapy is better than that after enucleation. The authors have performed an audit of the quality of life in 1596 patients with choroidal melanoma, measuring visual function, comfort, concerns, moods, and well-being according to type of treatment, age, sex, general health, social support, and other factors [1, 2]. Compared to patients who had received radiotherapy, those who had undergone enucleation were more likely to experience ocular discomfort, visual difficulties, worries about future health, and reduced wellbeing; however, they also tended to be older, with more advanced tumors, increased risk of metastatic disease and poorer general health [1]. After adjusting for these adverse factors, levels of well-being after enucleation and radiotherapy were similar to each other and to that of the general population [1].

16.2.2 Ocular Metastasis

Ocular secondaries are distressing, especially if they are the first sign of metastatic disease after the apparent cure of the primary tumor. The situation is even worse when the metastases are the first sign of any malignancy, as often happens in patients with lung cancer. In patients already suffering from systemic metastases, the development of ocular disease

B. E. Damato (✉)
Ocular Oncology Service, Moorfields Eye Hospital, London, UK
e-mail: bertil.damato@nhs.net

L. Hope-Stone
Liverpool Ocular Oncology Centre and Clinical Health Psychology Service, Liverpool University Hospitals NHS Trust, Liverpool, UK

University of Liverpool, Liverpool, UK
e-mail: l.hope-stone@liverpool.ac.uk

© The Author(s), under exclusive license to Springer Nature Switzerland AG 2025

A. D. Singh, B. E. Damato (eds.), *Clinical Ophthalmic Oncology*, https://doi.org/10.1007/978-3-031-75907-9_16

places an added burden, especially if the general health is poor. Further, there are concerns about visual impairment, especially when metastases are present in both eyes.

16.2.3 Vitreoretinal Lymphoma

Vitreoretinal lymphoma usually affects both eyes, causing floaters and blurred vision. All too often, the disease is misdiagnosed as uveitis so that proper treatment is delayed by months or years, and this can be upsetting to some patients. This type of lymphoma is highly aggressive and usually affects the brain, causing mental illness, epilepsy, and/or a wide variety of functional defects, usually with a fatal outcome.

16.2.4 Retinoblastoma

Retinoblastoma presents in the first few years of life, causing loss of central vision if the macula is involved, and loss of the eye if the tumor is advanced, as is often the case with unilateral disease. Patients with germline retinoblastoma tend to develop multiple tumors, usually affecting both eyes. These patients are also at risk of developing pineoblastomas and about 30% develop second malignant neoplasms in other parts of the body, especially in bone, skin, and lungs. Further, each of their children will have a 50% chance of inheriting the mutation. The management of patients with retinoblastoma places onerous demands on the family, as patients need general anesthesia for magnetic resonance imaging, intra-arterial chemotherapy, and other procedures, in addition to ocular examinations, which are required every 3–4 weeks for at least 2 years. Some parents blame themselves for the disease in their child. They may also feel guilty if treatment was delayed because they did not immediately act when they first noticed leukocoria. Healthy siblings of patients with retinoblastoma can also develop psychological problems.

16.3 Emotions and Fears

It is common for people with cancer to experience psychological distress, which is an understandable response to a traumatic and threatening life event (Box 16.1). On receiving a diagnosis of cancer, many patients experience a range of strong emotions, such as fear, anger, sadness, and many others, which may be overwhelming in their intensity. For the majority, this distress will be a short-lived experience, not causing lasting problems [3]. In such cases, it can be understood as part of the patients' normal adjustment to their diagnosis However, for some, the diagnosis and treatment of cancer increase the risk of developing persistent depression, anxiety, and other forms of psychological morbidity, such as adjustment disorder.

Uncertainty can be very unsettling, so it is only natural for patients to be afraid of "the unknown" and to worry about what side effects might occur as a result of their treatment, whether their tumor will recur, and how long they might live. These valid concerns make many individuals feel "like a walking time-bomb" or "in limbo" as if their life is "put on hold." In patients with uveal melanoma, survival prognostication has improved greatly with the discovery that metastatic disease develops almost exclusively in patients whose tumor shows loss of chromosome 3 (i.e., "monosomy 3") and/or a class 2 gene expression profile, especially with genetic aberrations such as chromosome 8q gain and BAP1 loss. However, not all patients are offered genetic tumor analysis by their ophthalmologist, so they then must cope with uncertainty [4]. In patients with vitreoretinal lymphoma, there are concerns about the high risk of brain involvement by the cancer. Patients with germline retinoblastoma have an uncertain future because of the risk of second malignancies, such as osteosarcoma, lung cancer, and so on.

Not surprisingly, the diagnosis of eye cancer comes as a shock to most patients. Many want to know why this has happened to them "out of the blue." They wonder whether they have done anything to deserve their illness and can feel angry, especially if they feel they have led a healthy life so that they perceive their situation as being "unfair." In fact, ocular malignancies are not related to harmful activities, such as smoking, except in some patients with ocular metastases from lung cancer. Some individuals can learn to live with uncertainty. For many, however, this is not possible without help and support. Professionals, therefore, need to be alert to the distress that can develop because of uncertainty at different times during the cancer trajectory.

In addition to worries about their general health and mortality, patients with ocular malignancy are concerned about visual loss and all its implications. Some fear that they will lose their ability to work and their independence, becoming a burden to others. Their self-esteem and identity are therefore threatened. In patients with uveal melanoma, serious visual impediment is rare, even with the tumor or its treatment causes significant loss of vision, and this is because the fellow eye is usually healthy. However, many patients tend to curtail activities such as driving, especially at night. Many conditions, such as metastases, retinoblastoma, vitreoretinal lymphoma, and paraneoplastic syndromes, affect both eyes, often causing significant visual impairment.

Quite reasonably, patients are also afraid that they might lose their eye and that this may cause disfigurement, which might disrupt social relationships, work, and other important aspects of life. Although loss of the eye is indeed traumatic, most patients adapt well to monocularity so that their quality of life is not as poor as they might have expected. The well-

being of these patients is better than it would have been had they developed ocular complications after receiving radiotherapy or some other form of eye-conserving therapy, which is why the eye was removed in the first instance.

Many patients are concerned about the potential for ocular tumor recurrence, which is a serious problem, requiring patients to endure further therapy and, in many cases, loss of vision or the eye. Recurrent disease is worrying also because of its possible impact on survival. Surprisingly, some patients with uveal melanoma are anxious about local recurrence even after the eye has been removed; it is therefore important to reassure patients repeatedly about the rarity of orbital recurrence after enucleation [1]. Understandably, fears about terminal illness and death are amplified in patients with a poor survival probability, such as those with monosomy-3 uveal melanoma [5]. Schuermeyer et al. report decision regret after genetic prognostic testing in patients with this tumor [6]; however, others have found such regret to be rare [4]. Feelings of uncertainty have fertile ground in which to develop, so that fears of local recurrence and metastases are highly relevant in these patients. These fears can cause significant psychological morbidity [7].

Worries about local tumor recurrence and metastasis may be allayed temporarily when patients receive good news after ocular examination or systemic investigations. Such reassurance is often the main benefit of follow-up visits. In patients with uveal melanoma, for example, liver scans are performed regularly even though it is recognized that treatment for metastatic disease only rarely prolongs life, although recent clinical trials are encouraging. This is mostly because of the positive impact on the patient's wellbeing, although there are always hopes that early diagnosis and treatment might be beneficial. Worries about recurrence and metastasis often re-emerge after a few weeks or months, so repeated reassurance is required.

Giving information can help reduce uncertainty, but it needs to be sensitive to patients' changing needs and to consider individuals' contextual factors, such as stage of disease, prior life experience, age, gender, and degree of social support. It is important to explore patients' reasons for selecting prognostication to ensure that they understand the implications of their decision and to consider the possibility of a poor prognosis being given to them [8]. Recognizing the critically important role of caring professionals whom patients can trust, it is not just the security of the relationship with the clinician that is important; it is the hope that if the disease is found, there will be the medical expertise and technology available to treat it [9]. Furthermore, while it may be a relief when an intensive course of treatment ends, patients may feel insecure because they receive less attention from the clinician [10].

Box 16.1 Patients' Emotions and Fears When Informed of Their Diagnosis and Treatment

- Uncertainty about local tumor control and survival
- Sense of "unfairness"
- Concerns about possible loss of independence
- Fears about facial deformity

16.4 Coping Mechanisms

Patients develop their own individual coping mechanisms, with varying degrees of success, which depend on their personality, background, previous and concurrent challenges, illness perceptions, and perceived support from family and friends. Crying and other manifestations of distress sometimes make patients feel that they are not coping, which is not the case. It is often helpful to remind people that their emotions are quite understandable, given the circumstances. In the early stages of their disease, some people reduce their distress by retreating into a form of temporary denial or avoidance of their illness. Such responses represent normal psychological defenses that can be adaptive in the short term. However, a complication for patients with ocular malignancy is that some common distraction strategies, such as watching TV or reading, might be difficult if vision is impaired. The ability to cope can be diminished by poor general health, and especially by mental illness, for example, in patients with cerebral metastases or lymphoma. The benefits of support from close relatives and friends cannot be underestimated.

16.5 Patients' Needs

Understandably, patients desperately want to survive and resume normal life as quickly and painlessly as possible (Box 16.2). They are anxious to do everything possible to achieve these ends. They, therefore, want to know that they are receiving the best possible treatment and what they can do to improve their prospects. Most want to be informed about their condition and its treatment and are usually keen to be involved in decisions about their treatment and care. However, it should be noted that patients vary in the amount of information they want to receive, and this need may change over time [11]. Most (but not all) patients wish to feel involved in decision-making, and the authors' impression is that they are more likely to accept any side effects of their therapy if they have had some say in their treatment selection. This does not necessarily mean they want to take responsibility for medical decisions [12]; for this reason,

Damato immediately and repeatedly reassures patients that they have made the correct decision (if this is indeed the case), thereby assuming responsibility for any adverse outcomes that might arise. Above all, patients want to be treated as individuals with dignity and respect. They wish to have their say and need to feel understood. Different patients have different needs at different stages of their illness, and psychological management needs to be responsive to this variability [13]. A survey by the Ocular Melanoma Foundation in the US revealed severe shortcomings in the way patients' needs were addressed, the main problems including poor communication, lack of compassion, and inadequate emotional support [4].

Box 16.2 Patients' Emotional Needs

- Reassurance that they are receiving the best possible treatment
- Involvement in decision-making
- To be treated with dignity as individuals
- To feel they are heard and understood

16.6 Eliciting and Addressing Patients' Emotional Needs

Although the potential for psychological distress among cancer patients is recognized, in many cases, such distress remains undetected and untreated [14]. Eliciting and addressing patients' emotional needs should not be considered as something separate from medical care. Instead, it should be recognized as an indispensable component of routine clinical practice [13].

Many barriers inhibit this process, some attributable to patients' attitudes, beliefs, and behavior and some to clinicians [15]. It is often the case that patients normalize or somatize their feelings, and this may reduce their chances of detection. Furthermore, many feel that their concerns are unreasonable or consider it inappropriate to raise them with the ophthalmologist [15]. Damato has addressed this problem by having a list of questions, all of which are asked of every patient. These elicit responses about visual difficulties, various forms of discomfort, and concerns about appearance, local tumor control, future health, and survival. Some ophthalmologists feel that it is not their role to address patients' psychological needs [15]. They may feel uncomfortable about doing so or may consider themselves inadequately trained to respond to patients' emotional distress. As a result, they might employ techniques such as changing the subject, ignoring the cues, minimizing the distress, or offering false or premature reassurance, which inhibit patients from disclosing their fears and feelings [15]. Some patients misconstrue such behavior as indicating a lack of care [4]. Practitioners may also be concerned that by responding to patients' distress, they may lengthen the consultation, whereas research indicates the opposite is often the case [16].

Even when ophthalmologists feel that it is their role to address patients' psychological concerns, they sometimes lack the necessary skills to elicit symptoms and provide appropriate support. It is, therefore, important that they are trained in techniques that increase their confidence and encourage rather than discourage emotional disclosure by patients. Such techniques might include demonstrating empathy through active listening, the use of open questions, responding to emotional cues (verbal and non-verbal), acknowledging patients' distress, and the use of a patient-centered consulting style [15]. We have shown that anxiety and depression can be predicted by the severity of symptoms, functional problems, and worries about recurrent disease soon after treatment [17].

16.7 Communication

Effective communication is key to eliciting and addressing patients' psychological needs (Box 16.3). It also fosters good relationships between the patients and their carers. Patients' psychological well-being is greatly influenced by the way in which they are informed about their diagnosis and treatment. The way healthcare staff respond to patients' concerns is also important [18, 19]. If information is poorly communicated and patients' concerns are left undisclosed and unresolved, patients can become confused and resentful and have a high risk of developing clinical anxiety or depression [18, 20]. If done well, communication can lessen distress and assist understanding and adaptation [19, 20].

Consequently, it is important to ensure that patients receive as much information as they want and that this information is provided honestly and compassionately in simple and unambiguous language [21]. When counseling patients about their condition, it is useful to describe the ocular anatomy and the tumor briefly, using a model eye and pictures of the tumor. Next, the patient is informed of how the tumor is likely to behave and what might happen to the eye, vision, and general health if treatment is withheld or delayed. This is a good lead-in to a discussion on the objectives of treatment, explaining what is and what is not achievable. Patients appreciate the candor, so ophthalmologists must avoid any temptation to give an unduly optimistic prognosis for fear of causing distress. The preferred treatment is introduced, together with the logistics involved (i.e., anesthesia and days in hospital). Alternative treatments are discussed, with reasons why they are less suitable than the preferred approach. Patients must

be informed about all therapeutic modalities and tests (e.g., uveal melanoma biopsy) and not only those that are available at the center they happen to be attending. Estimates of the chances of achieving the main objectives and of developing complications are given in terms that the patient can understand. It is important to ensure that a particular treatment is selected for the right reasons. For example, patients with uveal melanoma tend to select enucleation because they believe this gives them a better chance of survival than radiotherapy, which is not the case. Similarly, such patients (i.e., those with uveal melanoma) may decline tumor biopsy because they are concerned that the surgical procedure might disseminate the tumor to distant organs; there is no evidence that such iatrogenic metastatic disease ever occurs. The patient is then informed of plans for early aftercare and long-term follow-up. The impact of the patient's condition on driving and other activities is considered. Finally, any family implications are discussed, whether or not the disease is hereditary.

The information given to the patient can be summarized in the charts. Damato has prepared a list of outcomes, side effects, and complications so that any estimates given to patients are recorded. It is preferable if these discussions are conducted by a senior clinician and /or specialist oncology nurse having specialist skills in counseling cancer patients. Ideally, these discussions should be held in surroundings that are quiet, private, and comfortable. Enough time for proper discussion should be allowed, and precautions should be taken to prevent interruption by non-urgent phone calls and distractions. If possible, and if the patient agrees, a close relative or friend should be present. The physician should try to find out how much the patient wishes to know about prognosis and other sensitive issues and should respect the patient's wishes. The patient and any accompanying persons should be given plenty of opportunity to ask questions and to express their views. The physician should confirm that the patient has understood what has been said. It is often difficult for patients to remember what they were told at times of high emotions [21]. Therefore, for several years, the senior author has given each new patient an audio recording of the actual consultation [22]. Feedback has been positive, although a few patients have preferred not to listen to the recording [22]. Other useful aids to communication could include guidebooks and information leaflets specific to the selected treatment and planned aftercare.

Immediately after the consultation, it is helpful if the patient and any accompanying persons can spend some time with a specialist nurse in a quiet room. There are usually many questions that patients consider too trivial to trouble a doctor with. It is often necessary for the nurse to provide consolation, reassurance, and other psychological support. Some patients find it helpful to speak to someone who has been through a similar experience, and it is useful to have a "bank" of volunteer patients who are available on the telephone. During their stay in the hospital, patients find it reassuring when they are kept informed of how their treatment is progressing. It is well known that many patients feel particularly "low" soon after their return home from the hospital. It is, therefore, comforting for them to receive a telephone call from a specialist nurse at this difficult time.

Because of the rarity of ophthalmic tumors, patients find it difficult to get appropriate information and advice from their family doctor and from general ophthalmologists at their own hospital. It is, therefore, useful for them to be able to contact the ocular oncology service at any time if they ever have any questions or concerns. Appropriate contact information, such as a telephone number or e-mail address, should be provided. Patients and their families should also be informed of any organizations and websites that they might find helpful.

Increasingly in Britain, correspondence to the family doctor and general ophthalmologist is also sent to the patient. The senior author has followed this practice for several years, with positive feedback. However, if the results of pathological or genetic investigations might cause distress, they should first be communicated in person, ideally at a hospital clinic or, if this is not possible, by means of a prearranged telephone call.

Follow-up assessments provide a good opportunity for psychological support, and the ocular oncologist can be particularly effective in this regard, for example, reminding the patient of a good prognosis that was originally given or emphasizing that the chances of local tumor recurrence become very small once the tumor has responded well to conservative therapy. In patients who were initially given a guarded prognosis, there might be scope for encouraging optimism once the "danger period" has passed without incident.

At all times, the clinician should use every opportunity to encourage hope and optimism, albeit in an honest and realistic manner.

Box 16.3 Requirements for Effective Communication

- Quiet surroundings, free of interruptions and distractions
- Compassion and empathy
- Close friend or relative accompanying the patient
- Respect for how much they wish to know
- Opportunity to ask questions and express opinions
- Help remembering what was said
- Chance to speak to previously treated patients

16.8 Decision-Making

In many countries, "paternalistic" selection of treatment and other aspects of care has largely been replaced by the Shared-Decision Making (SDM) model, and a "matched leadership approach" to SDM has been advocated in cancer care [23, 24]. Although most patients want to have a say in their care, it is often difficult for them to decide what is best for them, especially if they are overwhelmed by the information provided to them and distraught as a result of their illness. Furthermore, many patients do not wish to take responsibility for major life-changing decisions.

The senior author approaches decision-making by first determining the patient's priorities, needs, and fears, then explaining how these are met by the various options, and finally encouraging the patient to indicate the preferable course of action. Almost always, the patient spontaneously selects what the senior author considers to be the optimal treatment or action, whereupon the author immediately reassures the patient that the correct decision has been made. In this way, patients benefit by "having a say" in the decision-making without being burdened by the responsibility for their decision [25]. When the patient selects what the author considers to be an inappropriate course of action, gentle probing usually reveals a misconception or misunderstanding so that the problem is resolved with further explanation. This approach is most successful when patients trust their clinician [26]. To merit such trust, the senior author continuously performs a wide range of quality control studies evaluating not only objective outcomes, such as local tumor control, but also subjective measures, such as the patients' long-term quality of life and satisfaction with the decision-making process.

Cancer psychologists are trained to support patients in the decision-making process by helping them explore potential outcomes. Referral to an appropriate psychologically trained practitioner would therefore be recommended.

16.9 Psychological Support

As they begin to adjust to their diagnosis and its implications, patients will each face a unique set of challenges shaped by their own personal circumstances, prior experience, and beliefs [18]. Consequently, different patients are likely to require individualized psychological support, which may change at different stages of their illness [13]. Because of this variability, no single approach will meet the needs of all patients, and it is, therefore, best to view the patient as an "expert" in his or her own emotional adjustment [13]. Further, a crucial component in assessing psychological support needs in relation to adjustment is recognizing whether patients have coping resources that allow them to adjust and recover over time, and it is imperative not to undermine this natural process [27, 28].

Table 16.1 Patients requiring additional psychological support

- Failing to adjust over time
- Experiencing an intense emotional reaction that compromises their mechanisms for family and social support
- "Stuck" in a way that is likely to inhibit future adjustment
- Help with decision-making around treatment and prognostication
- Experiencing emotional problems that are unlikely to resolve over time in a supportive environment

The build-up of a patient's unresolved concerns has been shown to predict later distress [19]. Careful assessment by interview is therefore recommended to identify and explore (1) the specific challenges faced by each patient, (2) the availability of emotional support, and (3) the patient's ability to use different ways of coping. It may be helpful at this time to engage with patients in problem-solving, including identifying and accessing sources of practical and emotional support and considering alternative coping responses that may reduce the emotional impact of their illness, also promoting adaptation. Eventually, in a supportive environment, most patients will adjust to their condition and its implications in their own time [11]. However, some patients may require more specialized help from appropriately trained cancer psychologists (Table 16.1).

16.10 Patient-Reported Outcome Measures (PROMs)

It is not only the length of survival that is important to patients but also the quality of that survival. There are many ways in which the quality-of-life (QoL) and mood of patients with uveal melanoma might be impaired. Firstly, many of these patients must come to terms with a high chance of early death, even if their ocular tumor has been successfully eradicated. Secondly, most patients need to cope with some degree of visual loss, which may restrict their activities. Some may also be concerned about cosmetic deficits caused by treatment such as iridectomy or enucleation. Assessment of patient-reported outcomes using self-report questionnaires to measure quality-of-life and mood can provide a better understanding of the effects of treatment over time. Ophthalmologists can then advise patients about the functional difficulties they may experience and how they are likely to respond emotionally to their condition. Further, predictors of distress have been identified from these studies, providing further insights into those vulnerable to persistent distress [29]. Such understanding can enable clinicians to anticipate problems and adjust behavior and care accordingly and can inform future tailored psychological interven-

tion and support. Additionally, by means of a simple tick box on the questionnaire, patients can be asked at regular intervals whether they would like any psychological support.

Unfortunately, studies investigating PROMs after treatment for uveal melanoma have produced conflicting results [30–35], possibly because of small sample sizes, and few have made comparisons with normative data. Therefore, units need to monitor these outcomes routinely so as to audit their own practice and to build up large data sets that would provide more definitive information about PROMs after uveal melanoma. As mentioned, the authors have performed a long-term audit of more than 1500 patients with choroidal melanoma, many of whom completed multiple questionnaires. This has provided valuable insights, for example, revealing how, in most patients, quality of life is determined most strongly by conditions and events that are unrelated to their ocular disease [15].

16.11 Self-Help

Every opportunity should be taken to encourage and facilitate self-help. There are many ways in which patients can improve their own well-being, and most are successful in discovering their individual ways of coping. Some patients may find it helpful to write down their experiences when newly diagnosed with cancer, so this idea could be suggested [36]. All patients should also be signposted to self-help materials and informed of any self-help groups that are available, both in their community and online. Indeed, self-help strategies are often preferred by cancer survivors rather than formal support, and supported self-management can increase an individual's capacity to adjust and cope with the biopsychosocial sequalae of cancer treatment [37, 38]. Considerations for organizing effective psychological care to be available to patients with eye cancer are summarized in Table 16.2.

Table 16.2 Considerations for providing effective psychological care

• Appropriate training of all staff coming into contact with patients so that distress can be recognized
• Mechanisms to empower patients to recognize and manage their own psychological needs
• Protocols for assessing all patients psychologically at key points in their care pathway
• Protocols for providing psychological support that is appropriate to the severity of any distress, with mechanisms for organizing specialist care if needed
• Information on how to contact emergency psychiatric services is readily available wherever patients are at risk of self-harm
• Systems enabling patients and caregivers to participate in their own care, self-help activities, and peer support
• Mechanisms for ensuring that the psychological needs of staff caring for patients and caregivers are adequately met

16.12 Posttraumatic Growth and Positive Change

Much of the research on psychological sequalae to a cancer diagnosis focuses on negative outcomes and adverse effects on people's lives [39, 40]. However, cancer survivors can also benefit from adversity, have positive outcomes, and experience posttraumatic growth (PTG) following a cancer diagnosis.

Posttraumatic growth (PTG) refers to a positive change in response to a highly challenging, stressful life event that threatens an individual's fundamental assumptions and expectations of their life and can give rise to distress [41, 42].

Patients seem to do particularly well if they feel that some good has come out of their crisis, for example, discovering what is and what is not important in their life, helping others, fundraising, and getting closer to their friends and family. Further, there is evidence that cancer patients experience posttraumatic growth (PTG) in the following domains: appreciation of life, revaluation of priorities, increased personal strength, and feeling closer to loved ones [43]. Therefore, opportunities to acknowledge and foster PTG positive change should be encouraged.

16.13 Family Support

Living with the biopsychosocial sequalae of a potentially life-threatening disease and vision-related difficulties places a significant burden and strain on patients. They may require high levels of support from informal family carers. Patients' well-being is greatly enhanced by any support they receive from relatives and friends [1]. Such carers may themselves need support as they also must adapt to the changes that a patient faces while also serving as a primary source of emotional, psychological, and physical support [44]. Being a carer has been shown to have had negative outcomes on quality-of-life, mental and physical health, but their needs are often neglected [45, 46]. It is, therefore, helpful for the clinician to acknowledge all carers who are present in any consultation and to provide them with recognition and encouragement.

Some patients faced with a diagnosis of cancer gain reassurance from still feeling physically well. That is, because their bodies feel normal, they can regard the cancer as less threatening. Their carers, however, do not have access to this way of coping [47]. Carers also often feel that they cannot share their concerns and fears with the patient for fear of upsetting the patient. Clinicians, therefore, often have the role of promoting open communication between patients and their carers, thereby circumventing the "conspiracy of silence" that can add to the burden for each party [18].

Carers may benefit from speaking with a member of the clinical team when the patient is absent, for example, if the patient is admitted to the hospital or in the operating room. It is, therefore, helpful to prepare for such an eventuality in advance by proactively obtaining and documenting the patient's consent for such communication.

Oncology services should also be ready to provide support to close friends and relatives at a time of bereavement. Carers will avail themselves of this support only if they know in advance that this service is provided.

16.14 Support from Patient Organizations

Patients and carers should be informed of any organizations that can provide them with support. Examples of such organizations include Cure OM, the Ocular Melanoma Foundation (OMF), and A Cure in Sight (ACIS) in the United States and Ocumel UK in the United Kingdom.

16.15 Children with Cancer: What Should They Be Told?

It is difficult to speak to a child about cancer and its implications. However, even very young children can sense fear and anxiety among family members [18]. If children are deprived of information about what is happening, they may generate their own ideas, causing them to fantasize or worry. Consequently, it is generally recommended that parents are as honest as possible with their child, allowing the patient to openly express fears and ask questions [35].

Parents know their children better than anyone else; therefore, their judgment of what is the right thing to do for their child and how much they should tell him or her should be supported and encouraged [18]. In a recent study of parents who had lost a child to cancer, it was observed that parents who talked to their dying child about death had no regrets about having done so [48]. Some parents who did not talk to their child about death subsequently wished they had done so. Clearly, the clinician's aim in such circumstances should be to help parents make the best decision for their family [49].

When providing any information to a child (as with adults), it is clearly important to use language that can be understood [13]. It should be noted that children are developing all the time. Consequently, information considered appropriate at one age may no longer be sufficient as the child gets older [18]. Therefore, it is important to establish the child's intellectual capacity as well as the level of understanding of the illness or treatment in question. Explanation and reassurance can then be provided in ways that make sense to the child [13].

16.16 Conclusions

Treatment of the cancer forms only a small part of patient care. Psychological support is extremely important. Such support should be provided not only to the patients themselves but also to their close relatives. Any support should be tailored to each individual case.

References

1. Damato B, Hope-Stone L, Cooper B, Brown SL, Salmon P, Heimann H, et al. Patient-reported outcomes and quality of life after treatment of choroidal melanoma: a comparison of enucleation versus radiotherapy in 1596 patients. Am J Ophthalmol. 2018;193:230–51.
2. Damato B, Hope-Stone L, Cooper B, Brown S, Heimann H, Dunn L. Patient-reported outcomes and quality of life after treatment for choroidal melanoma. Ocul Oncol Pathol. 2019;5(6):402–11.
3. White CA. Cognitive behaviour therapy for chronic medical problems: a guide to assessment and treatment in practice. Wiley; 2001.
4. Afshar AR, Deiner M, Allen G, Damato BE. The patient's experience of ocular melanoma in the US: a survey of the Ocular Melanoma Foundation. Ocul Oncol Pathol. 2018;4(5):280–90.
5. Brown SL, Hope-Stone L, van der Voort N, Hussain R, Heimann H, Coventry WL, et al. Associations between empirically proportionate and disproportionate fears of cancer recurrence and anxiety and depression in uveal melanoma survivors: five-year prospective study. Br J Health Psychol. 2024;29(3):662–75.
6. Schuermeyer I, Maican A, Sharp R, Bena J, Triozzi PL, Singh AD. Depression, anxiety, and regret before and after testing to estimate uveal melanoma prognosis. JAMA Ophthalmol. 2016;134(1):51–6.
7. Humphris GM, Rogers S, McNally D, Lee-Jones C, Brown J, Vaughan D. Fear of recurrence and possible cases of anxiety and depression in orofacial cancer patients. Int J Oral Maxillofac Surg. 2003;32(5):486–91.
8. Brown SL, Fisher PL, Morgan A, Davies C, Olabi Y, Hope-Stone L, et al. 'I don't like uncertainty, I like to know': how and why uveal melanoma patients consent to life expectancy prognostication. Health Expect. 2022;25(4):1498–507.
9. Portmann J. Like marriage, without the romance. J Med Ethics. 2000;26(3):194–7.
10. Back AL, Arnold RM, Baile WF, Tulsky JA, Fryer-Edwards K. Approaching difficult communication tasks in oncology. CA Cancer J Clin. 2005;55(3):164–77.
11. Leydon GM, Boulton M, Moynihan C, Jones A, Mossman J, Boudioni M, et al. Cancer patients' information needs and information seeking behaviour: in depth interview study. BMJ. 2000;320(7239):909–13.
12. Wright EB, Holcombe C, Salmon P. Doctors' communication of trust, care, and respect in breast cancer: qualitative study. BMJ. 2004;328(7444):864.
13. Salmon P. The psychology of medicine and surgery: a guide for psychologists, doctors, nurses and counsellors. Chichester: Wiley; 2000.
14. Maguire P. Improving the detection of psychiatric problems in cancer patients. Soc Sci Med. 1985;20(8):819–23.
15. Ryan H, Schofield P, Cockburn J, Butow P, Tattersall M, Turner J, et al. How to recognize and manage psychological distress in cancer patients. Eur J Cancer Care (Engl). 2005;14(1):7–15.

16. Butow PN, Brown RF, Cogar S, Tattersall MH, Dunn SM. Oncologists' reactions to cancer patients' verbal cues. Psychooncology. 2002;11(1):47–58.
17. Brown SL, Hope-Stone L, Heimann H, Damato B, Salmon P. Predictors of anxiety and depression 2 years following treatment in uveal melanoma survivors. Psychooncology. 2018;27(7):1727–34.
18. Maguire P. Breaking bad news. Eur J Surg Oncol. 1998;24(3):188–91.
19. Brennan J. Cancer in context. Oxford: Oxford University Press; 2004.
20. Fallowfield L, Jenkins V. Communicating sad, bad, and difficult news in medicine. Lancet. 2004;363(9405):312–9.
21. Kim MK, Alvi A. Breaking the bad news of cancer: the patient's perspective. Laryngoscope. 1999;109(7 Pt 1):1064–7.
22. Ah-Fat FG, Sharma MC, Damato BE. Taping outpatient consultations: a survey of attitudes and responses of adult patients with ocular malignancy. Eye (Lond). 1998;12(Pt 5):789–91.
23. Barry MJ, Edgman-Levitan S. Shared decision making—pinnacle of patient-centered care. N Engl J Med. 2012;366(9):780–1.
24. Brown SL, Salmon P. Reconciling the theory and reality of shared decision-making: a "matching" approach to practitioner leadership. Health Expect. 2019;22(3):275–83.
25. Mendick N, Young B, Holcombe C, Salmon P. The ethics of responsibility and ownership in decision-making about treatment for breast cancer: triangulation of consultation with patient and surgeon perspectives. Soc Sci Med. 2010;70(12):1904–11.
26. Cook SA, Damato B, Marshall E, Salmon P. Reconciling the principle of patient autonomy with the practice of informed consent: decision-making about prognostication in uveal melanoma. Health Expect. 2011;14(4):383–96.
27. Hope-Stone L, Ablett J, Salmon P. Reflections on a health psychology service for patients with uveal melanoma: the challenge of psychological screening and intervention when distress is 'normal'. J Clin Psychol Med Settings. 2019;26(4):421–9.
28. Hope-Stone L. Delivering an NHS health psychology service for patients with eye cancer. In: Health psychology in clinical practice. Routledge; 2021. p. 42–59.
29. Davies C, Brown SL, Fisher P, Hope-Stone L, Fisher D, Morgan A, et al. Predictors of emotional distress in uveal melanoma survivors: a systematic review. Eye (Lond). 2023;37(5):907–24.
30. Brandberg Y, Kock E, Oskar K, af Trampe E, Seregard S. Psychological reactions and quality of life in patients with posterior uveal melanoma treated with ruthenium plaque therapy or enucleation: a one year follow-up study. Eye (Lond). 2000;14(Pt 6):839–46.
31. Chabert S, Velikay-Parel M, Zehetmayer M. Influence of uveal melanoma therapy on patients' quality of life: a psychological study. Acta Ophthalmol Scand. 2004;82(1):25–31.
32. Melia M, Moy CS, Reynolds SM, Hayman JA, Murray TG, Hovland KR, et al. Quality of life after iodine 125 brachytherapy vs enucleation for choroidal melanoma: 5-year results from the Collaborative Ocular Melanoma Study: COMS QOLS Report No. 3. Arch Ophthalmol. 2006;124(2):226–38.
33. Cruickshanks KJ, Fryback DG, Nondahl DM, Robinson N, Keesey U, Dalton DS, et al. Treatment choice and quality of life in patients with choroidal melanoma. Arch Ophthalmol. 1999;117(4):461–7.
34. Reimer J, Esser J, Fleiss A, Hessel A, Anastassiou G, Krausz M, et al. Quality of life in patients with malignant choroidal melanoma after radiotherapy. Graefes Arch Clin Exp Ophthalmol. 2003;241(5):371–7.
35. Reimer J, Voigtlaender-Fleiss A, Karow A, Bornfeld N, Esser J, Helga Franke G. The impact of diagnosis and plaque radiotherapy treatment of malignant choroidal melanoma on patients' quality of life. Psychooncology. 2006;15(12):1077–85.
36. Willig C. 'Unlike a rock, a tree, a horse or an angel ...': reflections on the struggle for meaning through writing during the process of cancer diagnosis. J Health Psychol. 2009;14(2):181–9.
37. Clover KA, Mitchell AJ, Britton B, Carter G. Why do oncology outpatients who report emotional distress decline help? Psychooncology. 2015;24(7):812–8.
38. Jefford M, Howell D, Li Q, Lisy K, Maher J, Alfano CM, et al. Improved models of care for cancer survivors. Lancet. 2022;399(10334):1551–60.
39. Balfe M, O'Brien K, Timmons A, Butow P, O'Sullivan E, Gooberman-Hill R, et al. What factors are associated with posttraumatic growth in head and neck cancer carers? Eur J Oncol Nurs. 2016;21:31–7.
40. Menger F, Mohammed Halim NA, Rimmer B, Sharp L. Posttraumatic growth after cancer: a scoping review of qualitative research. Support Care Cancer. 2021;29(11):7013–27.
41. Tedeschi RG, Shakespeare-Finch J, Taku K, Calhoun LG. Posttraumatic growth: theory, research, and applications. New York: Routledge; 2018.
42. Tedeschi RG, Calhoun LG. Posttraumatic growth: conceptual foundations and empirical evidence. Psychol Inq. 2004;15(1):1–18.
43. Tanyi Z, Mirnics Z, Ferenczi A, Smohai M, Meszaros V, Kovacs D, et al. Cancer as a source of posttraumatic growth: a brief review. Psychiatr Danub. 2020;32(Suppl 4):401–11.
44. Harvey J, Berndt M. Cancer caregiver reports of post-traumatic growth following spousal hematopoietic stem cell transplant. Anxiety Stress Coping. 2021;34(4):397–410.
45. Leonidou C, Giannousi Z. Experiences of caregivers of patients with metastatic cancer: what can we learn from them to better support them? Eur J Oncol Nurs. 2018;32:25–32.
46. Harrison JD, Young JM, Price MA, Butow PN, Solomon MJ. What are the unmet supportive care needs of people with cancer? A systematic review. Support Care Cancer. 2009;17(8):1117–28.
47. Salander P, Bergenheim T, Henriksson R. The creation of protection and hope in patients with malignant brain tumours. Soc Sci Med. 1996;42(7):985–96.
48. Wolfe L. Discussing death with a dying child. CA Cancer J Clin. 2005;55:2–3.
49. Kreicbergs U, Valdimarsdottir U, Onelov E, Henter JI, Steineck G. Talking about death with children who have severe malignant disease. N Engl J Med. 2004;351(12):1175–86.

Tumor-Associated Cataract

17

Carlos A. Medina Mendez, Mary E. Aronow, Guillermo Amescua, Salomon Merikansky, and Arun D. Singh

17.1 Introduction

Cataracts are opaque areas in the lens, which should otherwise be clear. Cataract can be secondary to age or due to mechanical, chemical, or radiation trauma. They are the single largest cause of blindness in the world, accounting for over 47% of blindness worldwide [1, 2]. Intraocular tumors are a rare but important cause of cataract, and the presence of intraocular tumor as an underlying cause should be excluded when the cataract is unilateral, total, sectoral, or posterior subcapsular without obvious cause such as trauma, inflammation, or steroid use (Fig. 17.1). The cataract may be caused by the tumor itself or by previous interventions to diagnose (biopsy) or treat (steroids, excision, radiation, chemotherapy) the intraocular tumor. In the case of a poor view of fundoscopy, the clinician must rely on thorough examination techniques and ancillary tests such as ultrasonography and ultrasound biomicroscopy to determine the presence and extent of an intraocular tumor [3]. It is important to remember that the management of patients with intraocular tumors is complex and sometimes controversial, and in some instances, the tumor may have been treated with unfamiliar techniques. In this chapter, we will discuss the various treatment-related causes of cataracts, specific tumor entities associated with cataracts, and special considerations for the management of cataracts in patients with intraocular tumors.

C. A. Medina Mendez (✉)
Retinal Consultants, Sacramento, CA, USA

M. E. Aronow
Genentech, South San Francisco, CA, USA

G. Amescua
Department of Cornea and External Diseases, Bascom Palmer Eye Institute, University of Miami, Miami, FL, USA

S. Merikansky
Bascom Palmer Eye Institute, University of Miami, Miami, FL, USA

A. D. Singh
Department of Ophthalmic Oncology, Cole Eye Institute, Cleveland Clinic, Cleveland, OH, USA

© The Author(s), under exclusive license to Springer Nature Switzerland AG 2025

A. D. Singh, B. E. Damato (eds.), *Clinical Ophthalmic Oncology*, https://doi.org/10.1007/978-3-031-75907-9_17

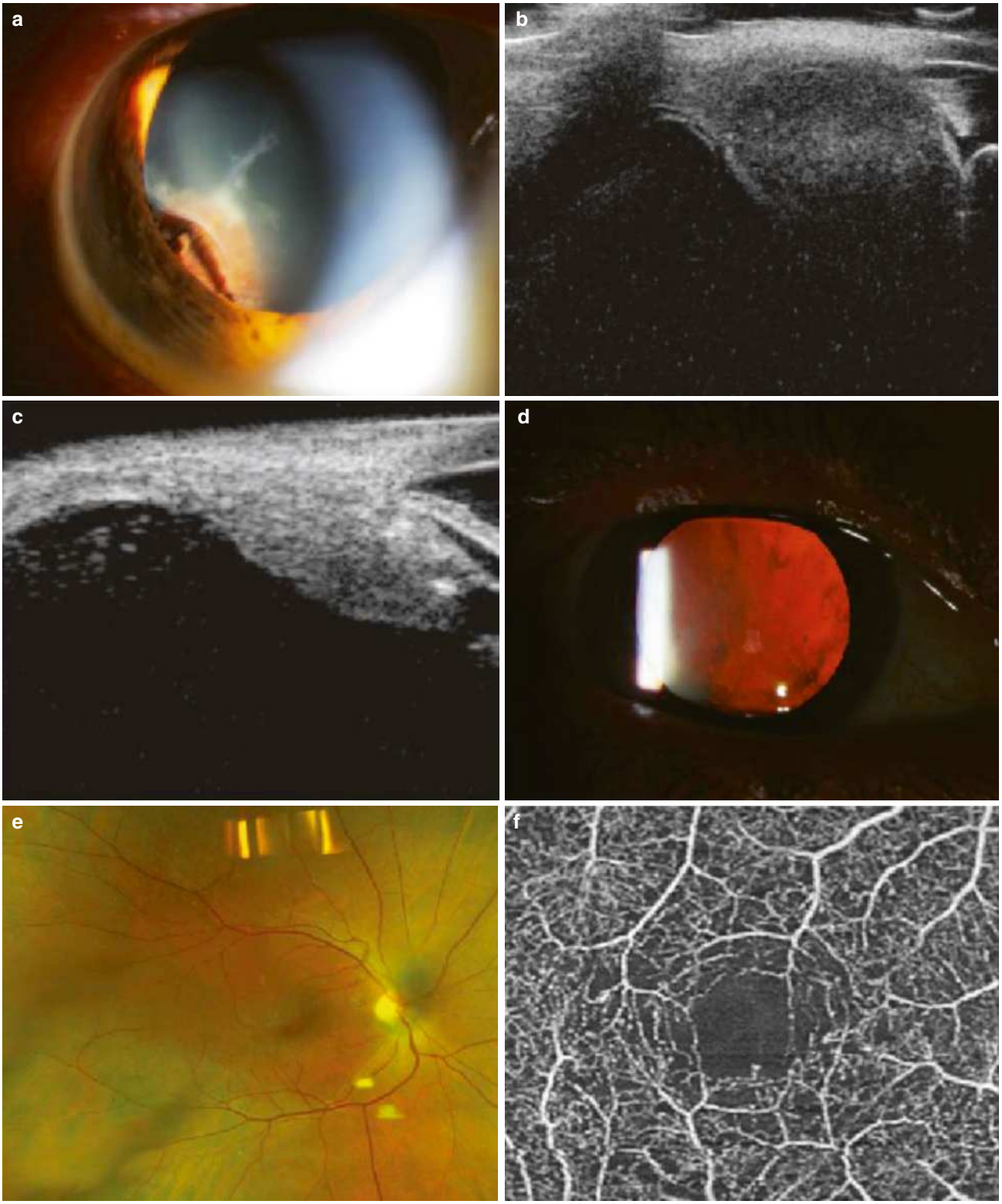

Fig. 17.1 A 54-year-old man presented with visual acuity of 20/60 in the right eye attributable to cataract (**a**) secondary to ciliochoroidal melanoma (**b**, 9.0 × 7.0 mm in base and height 7.5 mm). Following episcleral brachytherapy (85 Gy delivered to tumor apex over 72 h), the tumor regressed to the height of 2.4 mm over 36 months (**c**). Six months following brachytherapy, with documented regression of the tumor, he underwent uncomplicated cataract surgery with clear corneal temporal incision phacoemulsification with insertion of a posterior chamber intraocular lens (PCIOL) for the worsening cataract (**d**, visual acuity 20/100). The visual acuity improved to 20/20 with normal fundus appearance (**e**) and normal macular capillary network (**f**). Four weeks after surgery, visual acuity was reduced to 20/30 with the onset of cystoid macular edema (CME) (**g**). The CME persisted despite 4 months of topical therapy (nonsteroidal and steroid eye drops), eventually requiring intravitreal triamcinolone (4 mg in 0.1 mL) (**h**). Over the period of 30 months since cataract surgery, he received five intravitreal triamcinolone injections for recurrent CME. (Cataract surgery performed by Annapurna Singh, MD, Cleveland, Ohio)

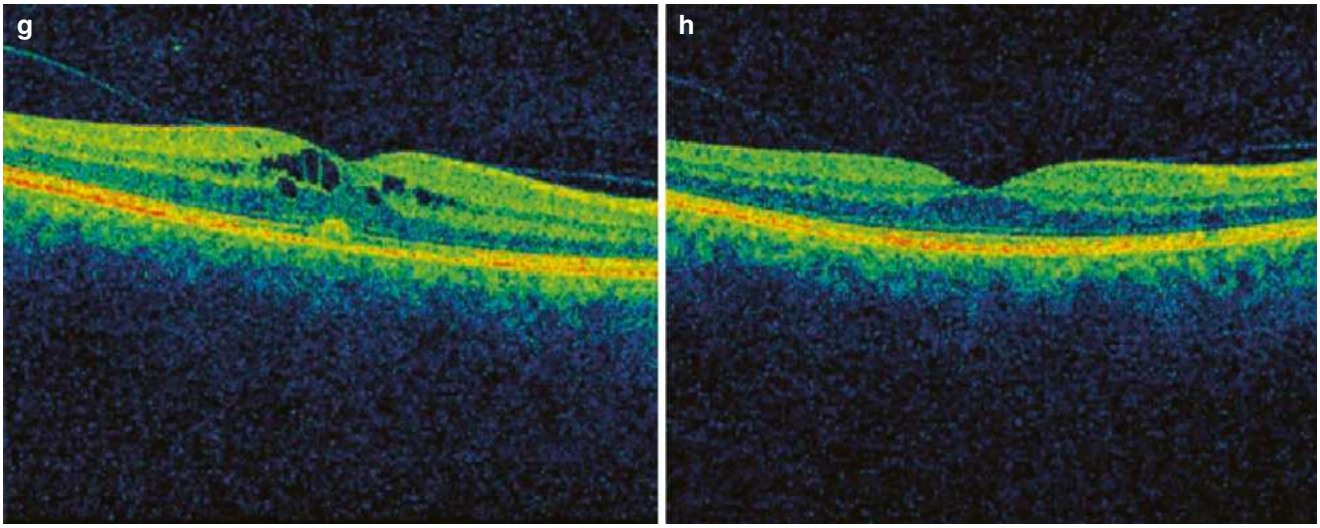

Fig. 17.1 (continued)

17.2 Surgical Treatment-Induced Cataract

Fine-needle aspiration biopsy, performed for diagnostic or prognostic purposes, may rarely (less than 1%) be complicated by the development of cataract [4, 5]. Transpupillary thermotherapy is also known to cause heat-induced focal cataracts in approximately 24% of patients, and these may become visually significant [6]. Iridectomy, iridocyclectomy, choroidectomy, vitrectomy, and virtually any intraocular procedure can lead to cataract formation either due to surgical manipulation, postoperative inflammation, or the use of steroids (Fig. 17.2).

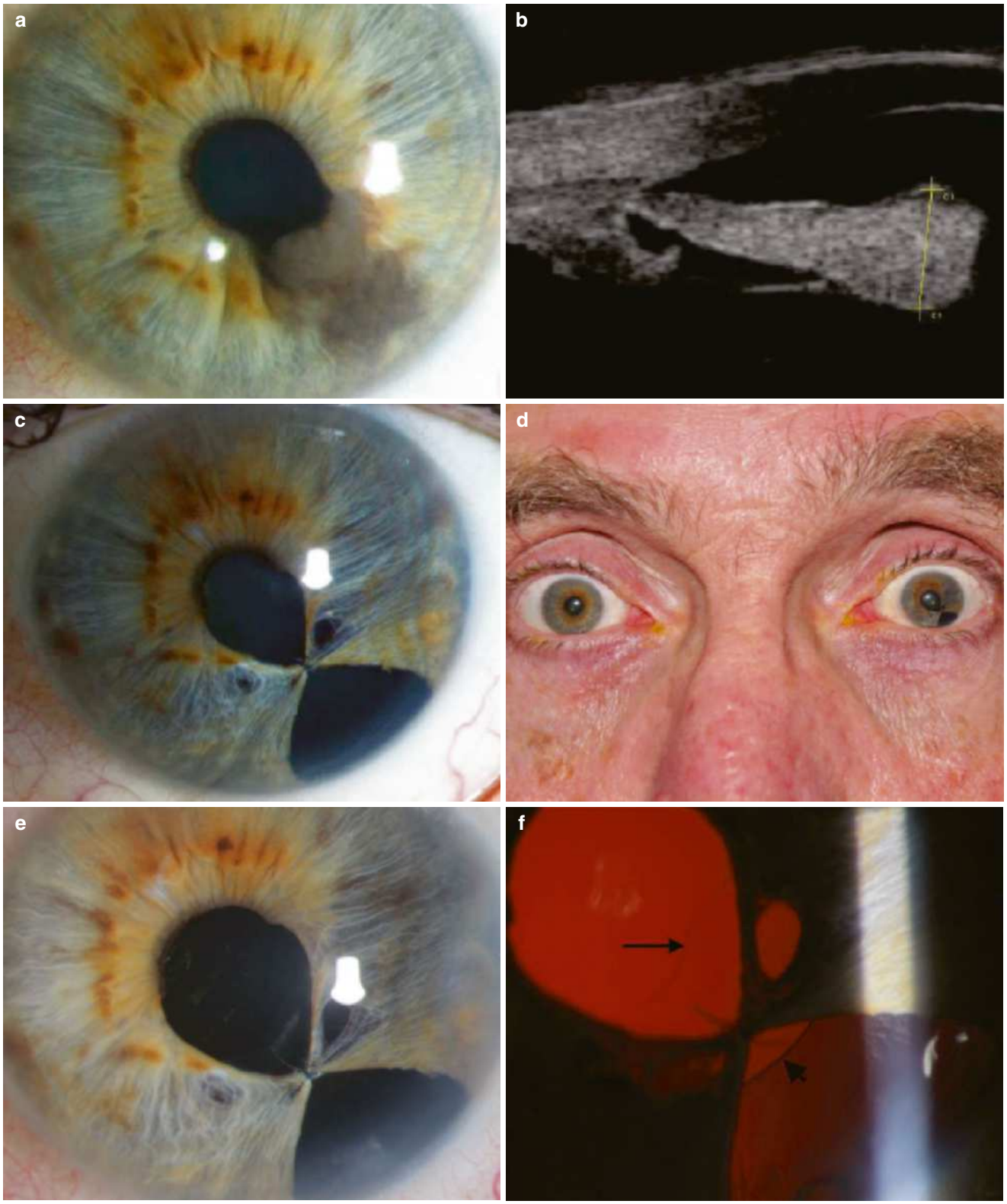

Fig. 17.2 A 61-year-old male was evaluated for an enlarging pigmented multinodular iris mass located in the inferotemporal quadrant (3.5 × 1.6 mm) (**a**). Gonioscopic examination excluded angle pigmentation and seeding. UBM confirmed nodular thickening of the iris (**b**). The tumor was excised by a small incision approach, which included pupilloplasty (**c**). Histopathology confirmed spindle cell melanoma. Surgical margins were clear. At 6-month follow-up visit, local recurrence and metastases were absent, and the pupils were almost symmetric in ambient light (**d**). 4.5 years later, he developed visually significant cataract (VA 20/50). He underwent uncomplicated cataract surgery (clear corneal temporal incision phacoemulsification with insertion of PC IOL) (**e**). The capsulorrhexis was modified to avoid release of the pupilloplasty suture (**f**, arrow, edge of capsulorrhexis; arrowhead, edge of the IOL in the capsular bag). (Cataract surgery performed by Annapurna Singh, MD, Cleveland, Ohio)

17.3 Radiation-Induced Cataract

Radiation is often used for the treatment of intraocular and periocular tumors. It is administered externally in the form of external beam radiation, proton beam radiotherapy, or stereotactic radiotherapy or internally in the form of brachytherapy. The crystalline lens is exquisitely sensitive to radiation. Doses of less than 2 Gy have been reported to cause cataracts [7]. Lensectomy is the only curative treatment for a radiation-induced cataract.

The incidence of cataracts after radiation exposure is high, with a reported range between 45% and 100% [8]. As part of the Collaborative Ocular Melanoma Study (COMS), phakic patients who were treated with iodine-125 brachytherapy and had no history of cataract were observed for the development of vision-limiting lenticular opacities or cataract surgery. During the first 5 years of follow-up, cataract developed in 362 (68%) of the eyes, and of these, 49 (9%) of the eyes underwent cataract surgery. The 5-year rate of reported cataract in the eyes receiving a dose to the lens of ≥16 Gy was 92%. After cataract surgery, visual acuity improved by two lines or more in 32 (66%) of patients and remained stable in 12 (26%) of patients.

Cataracts may develop as early as 1 month following treatment and as late as 7 years, depending on several factors, including the type of radiation, total dose, and delivery portals [9]. Ionizing radiation has been primarily associated with posterior subcapsular cataracts, although cortical and nuclear changes have also been reported (Fig. 17.3).

In the COMS, the most common cause of lack of visual improvement after cataract surgery was the presence of radiation retinopathy. Cataract surgery did not affect the mortality or metastasis adversely [10].

Aside from cataract formation, radiation therapy can also result in ocular surface damage, leading to decreased tear production and keratitis, both of which can have a profound effect on vision and comfort. Furthermore, these factors can impact the surgeon's view during subsequently planned surgeries. Corneal anesthesia may lead to neurotrophic ulcers. The ocular surface should, therefore, be optimized prior to performing cataract surgery. Special considerations must be taken by the surgeon as these patients might have other radiation-induced changes in their anterior chamber that can make cataract removal more challenging. Iris neovascularization and neovascular glaucoma are not infrequent, and the surgeon should closely monitor the patient for any changes in the iris and intraocular pressure. Radiation retinopathy and neuropathy may limit visual recovery following cataract surgery. The use of lead shields and fractionation of the radiation dose have been shown to decrease the total dose of radiation to the lens [11, 12].

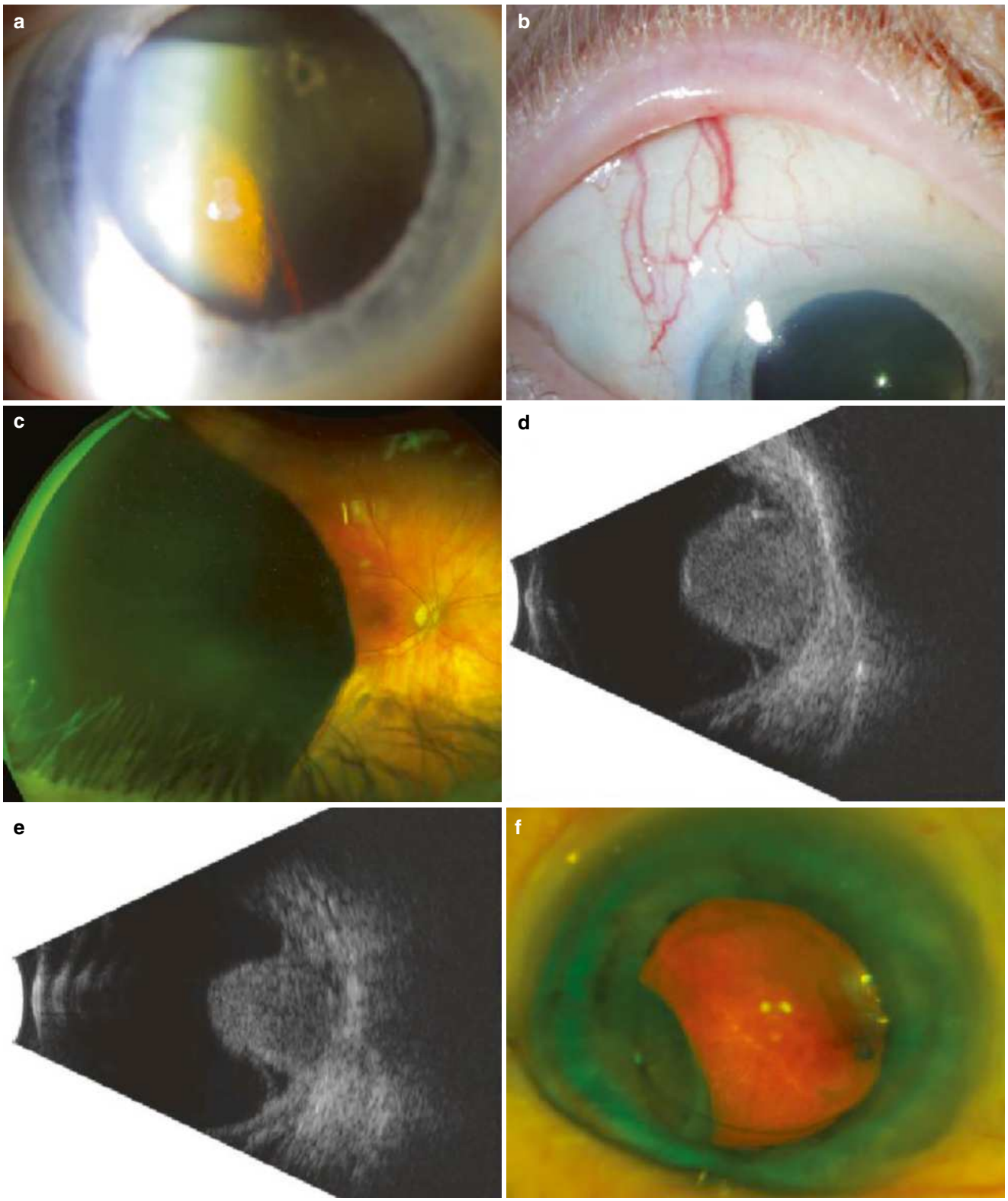

Fig. 17.3 A 71-year-old woman presented with visual acuity of 20/40 in the right eye attributable to cataract (**a**). Note sentinel vessels that suggest the presence of a ciliary body tumor (**b**). Fundus examination (**c**) and ultrasonography revealed a ciliochoroidal melanoma (**d**, 15.0 × 12.0 mm in base and height 10.0 mm). Following episcleral brachytherapy (85 Gy delivered to tumor apex over 72 h), the tumor regressed minimally to the stable height of 9.0 mm over 24 months (**e**). Eighteen months following brachytherapy, with documented regression of the tumor, she underwent cataract surgery. Although fundus examination was now possible (**f**), the visual acuity improved only to 20/400 because of radiation retinopathy (noted even prior to cataract surgery) manifesting predominantly as CME (**g**). Therefore, no additional therapy was advised. As the cataract was mature with posterior synechiae (**h**), the surgery was challenging requiring ancillary maneuvers. (Cataract surgery performed by Annapurna Singh, MD, Cleveland, Ohio)

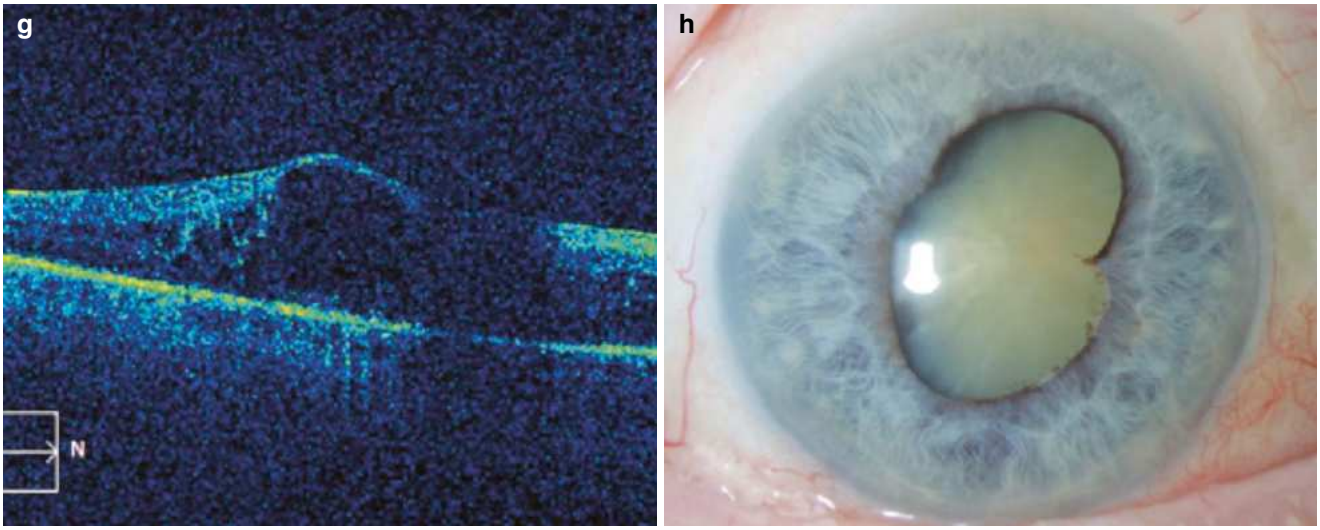

Fig. 17.3 (continued)

17.4 Chemotherapy and Hormonal Therapy-Induced Cataract

A number of chemotherapeutic agents and hormones used in the treatment of cancer patients have been shown to cause cataracts. It is well known that corticosteroids (such as dexamethasone and prednisone) administered either locally or systemically can cause cataracts. Anastrozole and busulfan are commonly used in the management of cancer patients and are also known to cause cataracts [13, 14]. In one clinical trial, 6.8% of postmenopausal women treated with tamoxifen developed cataract [15]. Cataract is the most common complication observed in patients receiving intravitreal methotrexate for intraocular lymphoma [16].

17.5 Specific Entities

17.5.1 Medulloepithelioma

Medulloepithelioma is a rare tumor of the ciliary pigment epithelium. It usually becomes apparent during the first decade of life and presents as an irregular, variably sized, white, or gray translucent mass. Cysts are present in some tumors. Medulloepithelioma is divided into teratoid and nonteratoid types and may either have benign or malignant cytologic features. Because the tumor arises from the ciliary body, it is often hidden by the iris and difficult to diagnose until the tumor is significant in size. For this reason, thorough evaluation, including a fully dilated funduscopic examination, transpupillary and transocular transillumination, as well as ancillary testing such as ultrasonography and ultrasound biomicroscopy, is helpful in determining the presence and extent of the tumor. Because most of these tumors are cytologically malignant, enucleation is usually advisable. A subset of these tumors may be managed by local resection or brachytherapy [3]. Medulloepithelioma should be suspected as an underlying cause of a nontraumatic cataract in a child. The presence of a lens coloboma or iris/angle neovascularization should increase suspicion.

Prior to cataract removal, stable tumor regression and absence of recurrence must be established in consultation with the treating oncologist. Any comorbidities, such as tractional retinal detachment, radiation optic neuropathy, and radiation retinopathy, may not favor cataract removal because of limited visual potential. Published reports of cataract removal in cases of treated medulloepithelioma are not available due to the rarity of the disease.

17.5.2 Retinal Lymphoma

Vitreoretinal lymphoma is a variant of primary central nervous system non-Hodgkin's lymphoma, which usually presents in elderly patients. Intraocular involvement may occur prior to, after, or at the time of central nervous system (CNS) disease.

Diagnosis can be challenging, especially in cases where intraocular involvement precedes systemic symptoms, and these patients are sometimes mistakenly treated for uveitis. Once the diagnosis is made, treatment with ocular radiation is implemented and is adequate in controlling ocular involvement in most cases [17]. Because of the high incidence of bilateral disease, irradiation of both eyes is frequently performed. Despite a high rate of ocular disease control, many patients ultimately develop CNS disease. Combinations of

intravitreal, intrathecal, and systemic chemotherapeutic agents, including methotrexate have been used; however, mortality remains high, and most patients die within 2 years of diagnosis of CNS involvement [18, 19].

Cataract is the most common complication observed in patients receiving intravitreal methotrexate; furthermore, most of these patients have also undergone a diagnostic vitrectomy prior to starting treatment [16]. A major goal of ocular treatment in patients diagnosed with retinal lymphoma is to maximize quality of life. Currently, there are no data to support an increase in morbidity or mortality in patients with vitreoretinal lymphoma following cataract surgery. Cataract surgery in these patients may be appropriate and should be considered on a case-by-case basis.

One study reported the progression of cataracts in 73% of the eyes receiving intravitreal methotrexate. Cataract surgery was successful in seven of eight eyes that underwent cataract extraction with intraocular lens implantation [16]. In one case an expulsive suprachoroidal hemorrhage occurred intraoperatively, and subsequently, the eye became phthisical [16].

17.5.3 Retinoblastoma

Retinoblastoma is a malignant tumor arising from the retina. A typical clinical presentation is that of a young child with leukocoria, strabismus, "red eye," heterochromia, hyphema, or pseudohypopyon. The average age of diagnosis is 24 months for unilateral and 12 months for bilateral cases [3]. Although cataract is not commonly observed in patients with retinoblastoma, the clinician should rule out intraocular malignancy in all pediatric cataracts. Ancillary testing such as ultrasonography is helpful in cases where the view of the fundus using ophthalmoscopy is inadequate.

Improvements in early detection and treatment have made globe-conserving therapy for retinoblastoma increasingly common. Although chemotherapy with or without cryotherapy and thermotherapy is frequently selected, plaque radiotherapy or external beam radiation continues to be used as salvage therapy, albeit rarely, as a last resort because of the risk of inducing malignancy. In cases where salvage therapy is used, doses more than 40 Gy are delivered, and cataract is expected to develop 1–3 years following treatment [7]. Cataract impairs vision as well as the ability of the ophthalmologist to examine the retina, and amblyopia is of particular concern in the young. As previously mentioned, radiation is associated with posterior subcapsular cataract, and this occurs in 22–87% of the eyes after external beam radiation and 9.7–31% of the eyes after brachytherapy [20].

Of particular concern in retinoblastoma is the possibility of tumor dissemination when intraocular surgery is performed. Although no association with systemic metastasis has been observed, there are reports of local tumor recurrence after cataract surgery [21, 22]. Several studies have shown that cataract extraction with or without intraocular lens placement is safe in patients who have previously received radiation treatment for retinoblastoma [7, 20, 21, 23]. Adequate treatment of the tumor, as well as an appropriate quiescent interval of 12–18 months, appears to be key in preventing recurrence and metastasis [22–25]. Although both clear corneal and pars plana approaches have been successfully used, a pars plana approach may be preferable as this is more likely to prevent postoperative wound leak in the child who is prone to eye rubbing. Subconjunctival spread of the tumor via the scleral tunnel has, however, been observed [21].

Pediatric cataract surgery is associated with a high likelihood of developing posterior capsular opacities. The decision to perform a primary posterior capsulotomy and anterior vitrectomy at the time of cataract surgery should be based on the patient's age, quiescent interval, location and stage of the tumor, and clarity of the visual axis once the cataract has been removed. It has been postulated that leaving the posterior capsule intact may potentially function as a barrier to tumor spread as well as reducing the risk of retinal detachment. Therefore, it may be prudent to leave the capsule intact initially and to consider capsulotomy as a second procedure only if necessary.

17.5.4 Uveal Melanoma

Uveal melanoma is the most common primary intraocular malignancy in adults. Iris melanoma is the least aggressive of the three types of uveal melanoma and is usually not associated with severe cataract. The presence of a sectoral cataract could imply ciliary body involvement and may be the presenting feature of ciliary body melanoma, which is the most lethal of all uveal melanomas [3]. Management of uveal melanoma depends on the tumor size and location, as well as the visual potential of the eye. Brachytherapy, proton beam radiotherapy, thermotherapy, stereotactic radiotherapy, resection, and enucleation are the most common methods of treatment. Resection of the tumor may include iridectomy, iridocyclectomy, and transscleral or transretinal choroidectomy.

Uveal melanoma should be suspected with any cataract having an atypical presentation, as several cases have been reported of unsuspected uveal melanoma diagnosed after cataract extraction [26–29]. In these cases, a complete investigation, including ultrasonography and ultrasound biomicroscopy, should be performed. Some authors advocate the use of ultrasonography in all eyes with opaque media regardless of history and even in the case of bilateral senile cataracts. The eye should be examined for episcleral sentinel vessels, which are usually present. Transillumination can also be used to detect a ciliary body melanoma in the setting of a dense cataract.

Two hypotheses have been proposed regarding the safety of performing cataract surgery in patients treated for uveal melanoma. The first is that the tumor has received adequate irradiation/ treatment and is, therefore, incapable of metastasis. The second is that many patients who present with uveal melanoma already have hepatic micrometastases at the time of diagnosis [30].

Outcomes after cataract extraction in the setting of treated melanoma are well documented. The Collaborative Ocular Melanoma Study demonstrated that 83% of the study eyes (532) developed cataract 5 years after treatment [10]. Of these, only 12% underwent cataract surgery. Such surgery did not affect the mortality or metastasis adversely [10]. After cataract surgery, visual acuity increased by two lines or more in two-thirds of the patients (66%). Vision-limiting complications were reported in 33 of 49 eyes. This included radiation retinopathy, which was present in 67% of eyes and was the most common cause of lack of visual improvement after cataract surgery. CME was reported in 13 eyes, and neovascular glaucoma in 6 eyes. Other less common comorbidities included diabetic retinopathy [1], vitreous hemorrhage [1], radiation optic neuropathy [1], and retinal detachment [1, 10]. Other authors have reported similar postoperative issues [31, 32]. In a large retrospective study including 72 eyes, rubeosis iridis, secondary glaucoma, and posterior synechia were present in about one-third of cases. Intraoperatively, defects of the posterior capsule occurred in 12.5% of the eyes. Visual acuity equal to or better than preoperative vision was achieved in 95.8% of the patients. Treatment of radiation retinopathy and tumor metastasis was described in 13.8% and 8.3% of patients, respectively.

Another more recent retrospective cohort study by Sepulveda-Beltran et al. included 47 eyes with a diagnosis of uveal melanoma and underwent post-radiation cataract surgery with at least 6 months of follow-up. This study reported that cataract surgery was safe and effective in improving visual acuity in individuals with post-radiation cataracts, showing a significant improvement of two lines of best-corrected visual acuity during the first year of follow-up (66%). The authors have advocated for following using a multi-disciplinary approach with proper surgical planning and a focus on early postoperative aggressive anti-inflammatory and anti-VEGF therapies when needed.

Recently, combined micro incisional vitrectomy and phacoemulsification with intravitreal triamcinolone acetonide injection and direct endolaser tumor ablation have been reported to be safe and effective in patients treated for uveal melanoma with complications from I-125 brachytherapy [33]. The results of these studies show a relatively low complication rate and unchanged metastatic rates, suggesting that cataract surgery in adequately treated patients is a safe procedure that improves visual acuity in most patients.

17.5.5 Uveal Metastases

Metastatic disease is the most common intraocular malignancy. Metastatic breast cancer is the most commonly diagnosed metastasis, constituting about half of all the patients diagnosed with metastatic disease to the uvea. This is followed by lung cancer, which is present in about one-quarter of all patients with uveal metastatic disease. Other less common primary sites include prostate carcinoma, gastrointestinal carcinoma, renal cell carcinoma, and cutaneous melanoma. Up to one-quarter of the patients are found to have bilateral metastases at the time of presentation, and multifocal infiltrates are common. Ocular treatment is aimed at improving quality-of-life, and the main goal of treatment is to preserve or improve vision.

Cataract is common in patients with uveal metastasis, as external beam radiation is the most commonly used modality for treatment [34]. Cataract surgery should be considered in patients with significant visual impairment due to a cataract. Potential benefits, current quality-of-life, associated comorbidities, and life expectancy are important considerations (Fig. 17.4).

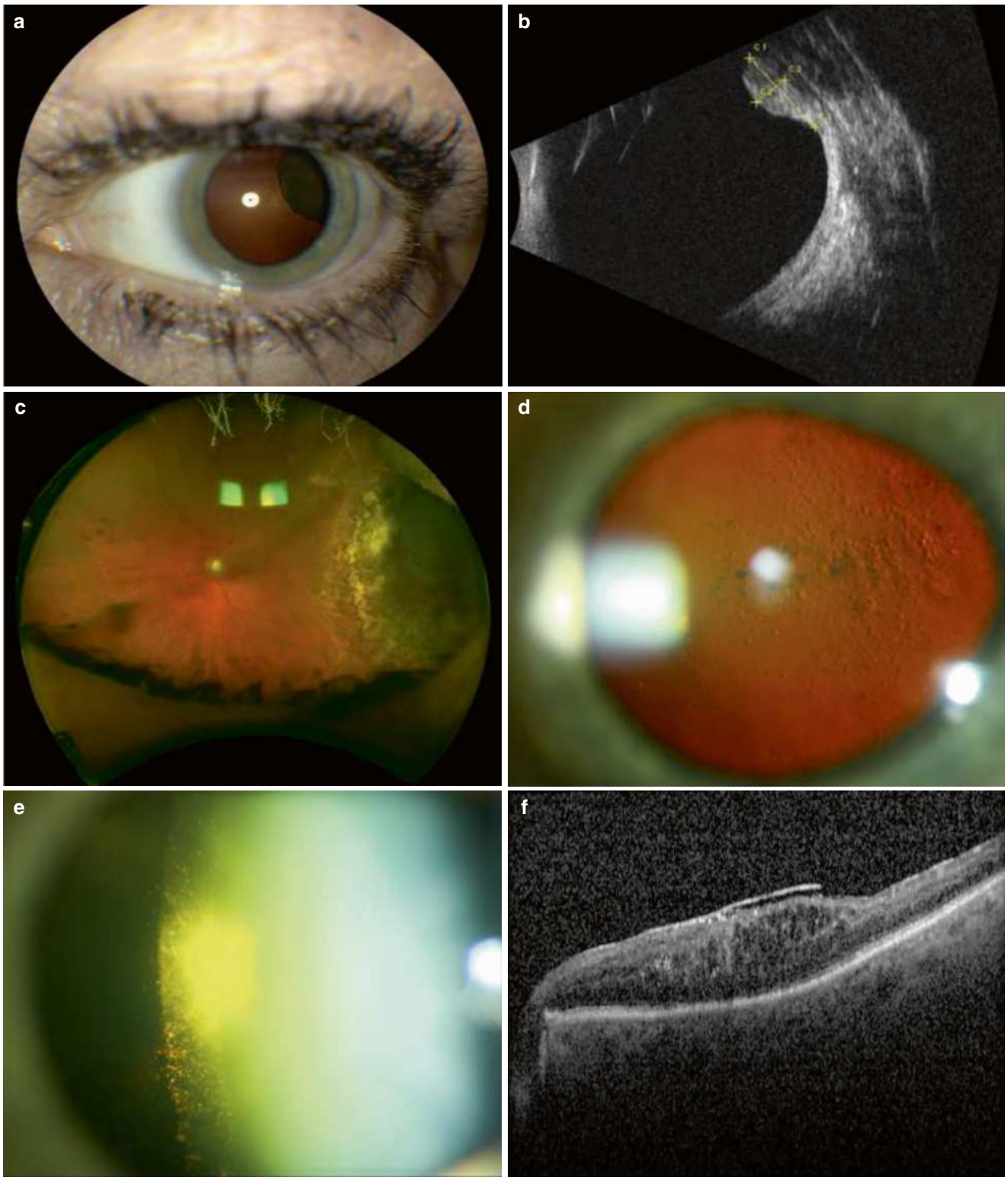

Fig. 17.4 A 60-year-old female referred after noticing flashes and floaters on left eye (**a**), a mushroom-shaped ciliochoroidal mass was found with dimensions of 14.9 x 14.5 mm and height of 10 cm (**b**, **c**). Biopsy confirmed ciliochoroidal melanoma. The patient received episcleral brachytherapy (I-125 plaque 85 Gy delivered to tumor apex over 72 h). After radiation, the patient had severe inflammation and vitreous seeding was present, also a visual significant cataract developed, with the presence of pigmented cells suggestive of melanocytic cells on the lens capsule (**d**, **e**). The patient underwent uncomplicated cataract surgery with clear corneal incision and insertion of PC IOL (**g**). The patient also developed epiretinal membranes and macular edema (**f**), The visual acuity after the surgery was 20/800. After 4 months of aggressive anti-inflammatory and anti-VEFG therapy, the visual acuity improved to 20/150. Melanocytic pigment was noticeable on the posterior capsule (**h**). (Cataract surgery performed by Guillermo Amescua, MD, Miami, Fl. Ophthalmic oncological management by J. William Harbour MD)

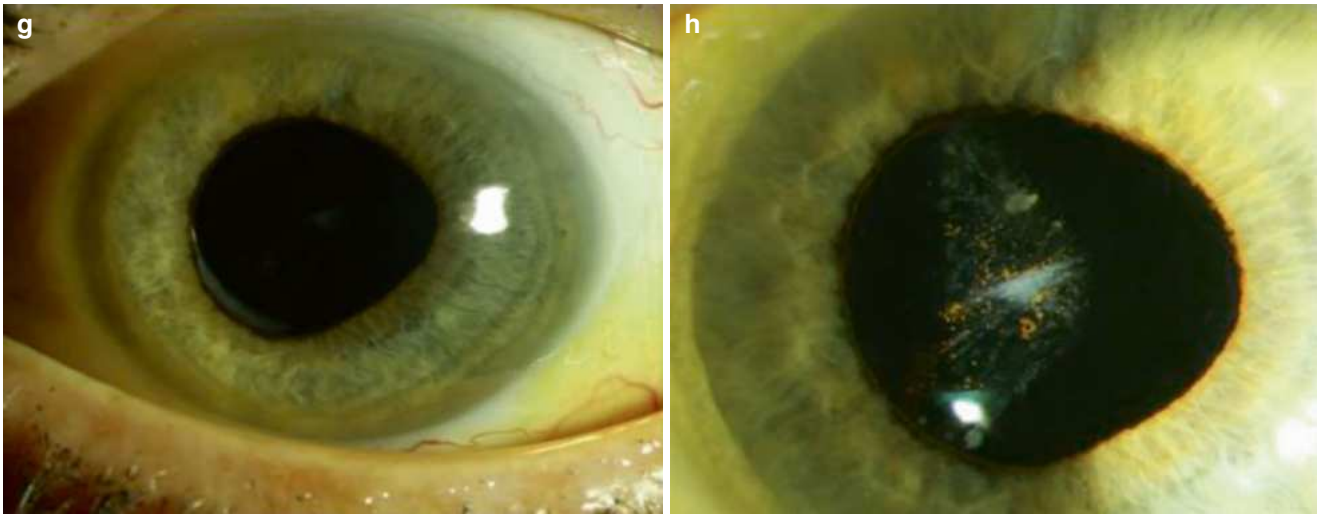

Fig. 17.4 (continued)

17.6 Perioperative and Intraoperative Considerations

Special consideration should be taken in the perioperative and intraoperative management of tumor-associated cataract. Ancillary intraoperative maneuvers such as the use of trypan blue, synechiolysis, and the use of Malyugin ring or iris retractors may be necessary to reduce the risk of posterior capsular rupture. Despite uncomplicated phacoemulsification with placement of the intraocular lens within the capsular bag and lack of capsular bag rupture, postoperative CME is a frequent occurrence (18%) [35]. Intravitreal steroids and anti-VEGF are strongly recommended to adequately treat postoperative CME in a high percentage of patients undergoing tumor-associated cataract surgery (7%) [35–37].

17.7 Summary

Cataracts are commonly found in patients with intraocular tumors. There are several special considerations, such as monocular status, associated comorbidities, and potential benefit of surgical intervention in a setting of shortened life expectancy, that must be assessed when managing a patient with a tumor-related cataract (Table 17.1). The risk factors, management, and visual outcome of tumor-associated cataract depend on the location, size, type of intraocular tumor, and previous interventions. Management of tumor-related cataracts should be undertaken in conjunction with an ocular oncologist or an ophthalmologist who is experienced in dealing with intraocular tumors.

Table 17.1 Special considerations for management of tumor-associated cataract

Factor	Comment
Dry eyes	Surface issues, lubrication, punctal plugs
Astigmatism	Irregular or regular, suboptimal visual outcome
Iridectomy	Photophobia, pupilloplasty, iris prosthesis
Zonular support	Gentle manipulations, capsular rings
Associated glaucoma	Combined surgery
Radiation retinopathy	Combined PRP and intravitreal anti-VEGF
Radiation optic neuropathy	Poor visual outcome
Monocular status	Choice of anesthesia
Risk of tumor dissemination	Document tumor stability
Immunocompromised status	Risk of infection
Shortened life expectancy	Careful assessment of benefit

PRP pan-retinal photocoagulation, *VEGF* vascular endothelial growth factor

References

1. Resnikoff S, Pascolini D, Etya'ale D, et al. Global data on visual impairment in the year 2002. Bull World Health Organ. 2004;82(11):844–51.
2. Allen D. Cataract. Clin Evid (Online). 2011;2011. PMID 21718561.
3. Taban M, Taban M, Bolling J, et al. Ocular complications of radiotherapy. In: Singh AD, Damato BE, Pe'er J, et al., editors. Clinical ophthalmic oncology. 1st ed. Philadelphia: Saunders-Elsevier; 2007. p. 45–9.
4. Shields CL, Manquez ME, Ehya H, et al. Fine-needle aspiration biopsy of iris tumors in 100 consecutive cases: technique and complications. Ophthalmology. 2006;113(11):2080–6.

5. Singh AD, Medina CA, Singh N, et al. Fine-needle aspiration biopsy of uveal melanoma: outcomes and complications. Br J Ophthalmol. 2016;100(4):456–62. https://doi.org/10.1136/bjophthalmol-2015-306921. PMID: 26231747.
6. Shields CL, Santos MC, Diniz W, et al. Thermotherapy for retinoblastoma. Arch Ophthalmol. 1999;117(7):885–93.
7. Hoehn ME, Irshad F, Kerr NC, et al. Outcomes after cataract extraction in young children with radiation-induced cataracts and retinoblastoma. J AAPOS. 2010;14(3):232–4.
8. Ferrufino-Ponce ZK, Henderson BA. Radiotherapy and cataract formation. Semin Ophthalmol. 2006;21(3):171–80.
9. Cogan DG, Donaldson DD, Reese AB. Clinical and pathological characteristics of radiation cataract. Arch Ophthalmol. 1952;47(1):55–70.
10. Collaborative Ocular Melanoma Study Group. Incidence of cataract and outcomes after cataract surgery in the first 5 years after iodine 125 brachytherapy in the Collaborative Ocular Melanoma Study: COMS Report No 27. Ophthalmology. 2007;114(7):1363–71.
11. Esik O, Ikeda H, Mukai K, et al. A retrospective analysis of different modalities for treatment of primary orbital non-Hodgkin's lymphomas. Radiother Oncol. 1996;38(1):13–8.
12. Servodidio CA, Abramson DH. Acute and long-term effects of radiation therapy to the eye in children. Cancer Nurs. 1993;16(5):371–81.
13. Hazin R, Abuzetun JY, Daoud YJ, et al. Ocular complications of cancer therapy: a primer for the ophthalmologist treating cancer patients. Curr Opin Ophthalmol. 2009;20(4):308–17.
14. Kaida T, Ogawa T, Amemiya T. Cataract induced by short-term administration of large doses of busulfan: a case report. Ophthalmologica. 1999;213(6):397–9.
15. Howell A, Cuzick J, Baum M, et al. Results of the ATAC (Arimidex, tamoxifen, alone or in combination) trial after completion of 5 years' adjuvant treatment for breast cancer. Lancet. 2005;365(9453):60–2.
16. Smith JR, Rosenbaum JT, Wilson DJ, et al. Role of intravitreal methotrexate in the management of primary central nervous system lymphoma with ocular involvement. Ophthalmology. 2002;109(9):1709–16.
17. Berenbom A, Davila RM, Lin HS, et al. Treatment outcomes for primary intraocular lymphoma: implications for external beam radiotherapy. Eye (Lond). 2007;21(9):1198–201.
18. Singh AD, Lewis H, Schachat AP, et al. Lymphoma of the retina and central nervous system. 1st ed. Philadelphia: Saunders-Elsevier; 2007.
19. Deangelis LM, Hormigo A. Treatment of primary central nervous system lymphoma. Semin Oncol. 2004;31(5):684–92.
20. Osman IM, Abouzeid H, Balmer A, et al. Modern cataract surgery for radiation-induced cataracts in retinoblastoma. Br J Ophthalmol. 2011;95(2):227–30.
21. Brooks HL Jr, Meyer D, Shields JA, et al. Removal of radiation-induced cataracts in patients treated for retinoblastoma. Arch Ophthalmol. 1990;108(12):1701–8.
22. Honavar SG, Shields CL, Shields JA, et al. Intraocular surgery after treatment of retinoblastoma. Arch Ophthalmol. 2001;119(11):1613–21.
23. Payne JF, Hutchinson AK, Hubbard GB 3rd, et al. Outcomes of cataract surgery following radiation treatment for retinoblastoma. J AAPOS. 2009;13(5):454–8.e3.
24. Portellos M, Buckley EG. Cataract surgery and intraocular lens implantation in patients with retinoblastoma. Arch Ophthalmol. 1998;116(4):449–52.
25. Chodick G, Kleinerman RA, Stovall M, et al. Risk of cataract extraction among adult retinoblastoma survivors. Arch Ophthalmol. 2009;127(11):1500–4.
26. Verbeek AM, Brink HM. Uveal melanomas diagnosed in the 6 months after lens-implant surgery. Doc Ophthalmol. 1991;78(3–4):211–8.
27. O'Leary SW, Ramsey MS. Unsuspected uveal melanoma diagnosed after cataract extraction. Can J Ophthalmol. 1990;25(7):333–5.
28. Shields JA, Augsburger JJ. Cataract surgery and intraocular lenses in patients with unsuspected malignant melanoma of the ciliary body and choroid. Ophthalmology. 1985;92(6):823–6.
29. Chess J, Henkind P, Albert DM, et al. Uveal melanoma presenting after cataract extraction with intraocular lens implantation. Ophthalmology. 1985;92(6):827–30.
30. Shields JA. Cataract surgery after radiotherapy for uveal melanoma. Arch Ophthalmol. 1992;110(4):473–4.
31. Wachtlin J, Bechrakis NE, Schueler AO, et al. Phacoemulsification following treatment of choroidal melanoma. Graefes Arch Clin Exp Ophthalmol. 2000;238(12):942–8.
32. Gragoudas ES, Egan KM, Arrigg PG, et al. Cataract extraction after proton beam irradiation for malignant melanoma of the eye. Arch Ophthalmol. 1992;110(4):475–9.
33. Lonngi M, Murray TG, Sisk RA, et al. Combined microincisional vitrectomy and phacoemulsification in the management of complications associated with 125-I brachytherapy treated patients and uveal malignant melanoma. In: ARVO 2012. Fort Lauderdale Florida.
34. Tsina EK, Lane AM, Zacks DN, et al. Treatment of metastatic tumors of the choroid with proton beam irradiation. Ophthalmology. 2005;112(2):337–43.
35. Singh A, Davanzo J, Echegaray J, et al. Radiation induced cataracts: surgical outcomes. In: ARVO 2018. Hawaii; 2018.
36. Choi D, Amescua G. Radiation induced cataract surgical outcomes. In: ARVO 2018. Hawaii; 2018.
37. Sepulveda-Beltran PA, Levine H, Gibbons AG, et al. Post-radiation cataract management: outcomes in individuals with uveal melanoma. Curr Ophthalmol Rep. 2022;10:218–27.

Tumor-Associated Glaucoma

18

Zane Khademi, Annapurna Singh, and Arun D. Singh

18.1 Introduction

Glaucoma secondary to intraocular tumors is not uncommon. The risk of this problem developing depends on the tumor type and location. A review of 2597 patients with intraocular tumors found elevated intraocular pressure in 5% of tumor-containing eyes at the time of diagnosis [1]. Of those eyes, 2111 had uveal melanoma, and secondary IOP elevation was present in 3% of these eyes. Seventeen percent of the melanoma eyes involved the ciliary body, and there were 7% with iris involvement and 2% with choroidal involvement. Two hundred and fifty-six of the 2597 eyes had uveal metastases, and glaucoma occurred in 5% of these patients [1]. Another survey of 227 cases of metastatic carcinoma to the eye and orbit found that glaucoma was present in 7.5% of patients [2]. In a retrospective case series of 144 eyes presenting with iris melanoma, 40% had concurrent glaucoma, which was related to angle infiltration by melanoma, angle neovascularization, and hyphema [3].

Direct invasion of the angle and ciliary body as well as pigment dispersion from uveal melanomas commonly leads to elevated IOP. Tumors that are metastatic to the eye can infiltrate the angle or close the angle by mass effect and are associated with higher rates of glaucoma. Angle neovascularization associated with retinoblastomas can lead to secondary glaucoma. A clinical review of 149 eyes with retinoblastoma found increased IOP in 23% of these eyes, and histopathologic evidence of glaucoma was present in 50% of enucleated eyes in this series [4]. Tumors such as lymphoma, leukemia, benign reactive hyperplasia, medulloepithelioma, iris adenoma, and iris melanocytoma account for a small percentage of intraocular tumors and are infrequently associated with secondary glaucoma. These tumors rarely present with elevated IOP as the initial manifestation.

18.2 Pathogenesis

Intraocular tumors can present with both open-angle and angle-closure glaucoma through various mechanisms.

18.2.1 Open-Angle Glaucoma

There are three principal mechanisms by which intraocular tumors can cause open-angle glaucoma: direct closure of the anterior chamber angle by the tumor mass, tumor cells seeding the anterior chamber angle, and necrotic tumor cells engulfed by macrophages that obstruct the outflow pathways in the trabecular meshwork.

Closure of the anterior chamber angle by mass effect can be caused by many types of tumors, including melanoma, nevus, metastasis, and medulloepithelioma. Extension of melanoma and nevus across the trabecular meshwork can result in increased IOP [1]. In cases of ciliary body or iris melanoma, patients may present with heavy pigmentation in the angle, anterior synechiae, and elevated IOP—mimicking iridocorneal endothelial syndrome [5].

Tumor cells can seed the anterior chamber angle and lead to open-angle glaucoma. Metastatic tumors typically infiltrate the trabecular meshwork to increase IOP and cause glaucoma (Fig. 18.1) [1, 6]. Metastases of systemic melanoma can also cause pigmentary dispersion in the angle, resulting in glaucoma. In cases of intraocular melanoma, pigmented cells are dispersed into the anterior chamber and can become lodged in the spaces of the trabecular meshwork, hindering the outflow of aqueous humor (Fig. 18.2) [7]. Leukemias and lymphomas can result in a pseudohypopyon in the anterior chamber composed of layered tumor cells

Z. Khademi · A. Singh (✉)
Glaucoma Service, Cole Eye Institute, Cleveland, OH, USA
e-mail: khademz@ccf.org; singha2@ccf.org

A. D. Singh
Department of Ophthalmic Oncology, Cole Eye Institute, Cleveland Clinic, Cleveland, OH, USA
e-mail: singha@ccf.org

© The Author(s), under exclusive license to Springer Nature Switzerland AG 2025

A. D. Singh, B. E. Damato (eds.), *Clinical Ophthalmic Oncology*, https://doi.org/10.1007/978-3-031-75907-9_18

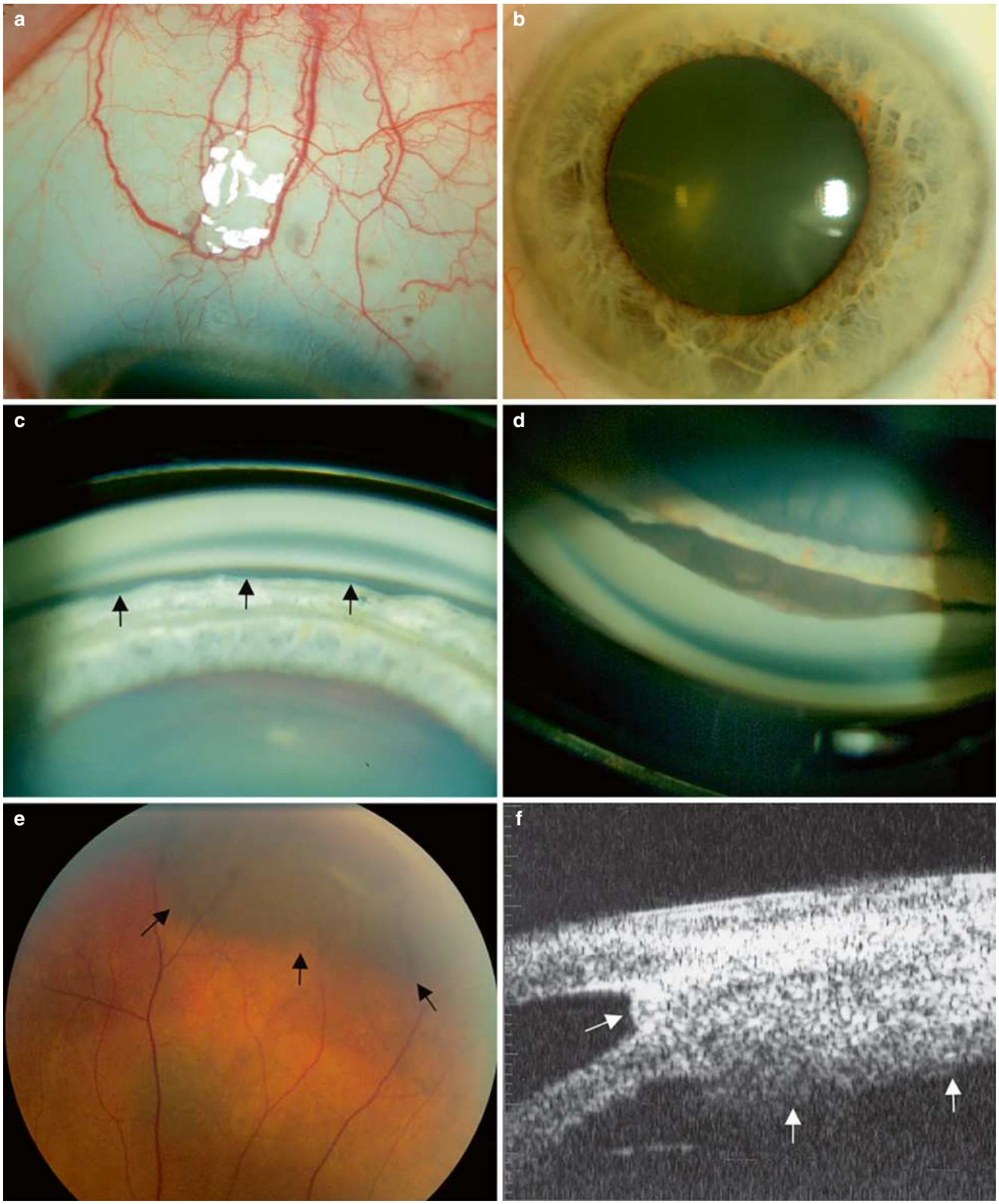

Fig. 18.1 A 64-year-old woman was diagnosed with ocular hypertension OS. The IOP was 35 mmHg. On external examination prominent sentinel vessels and episcleral pigmentation were noted superiorly (**a**). The anterior segment appeared normal (**b**). On gonioscopy, there was diffuse pigment seeding in the angle (**c**, arrows) with an area of tumor extension from 12 to 1 o'clock at the meridian (**d**). Ophthalmoscopy revealed peripheral choroidal melanoma (**e**, arrows). Ciliary body and angle extension were confirmed by ultrasound biomicroscopy (**f**, arrows)

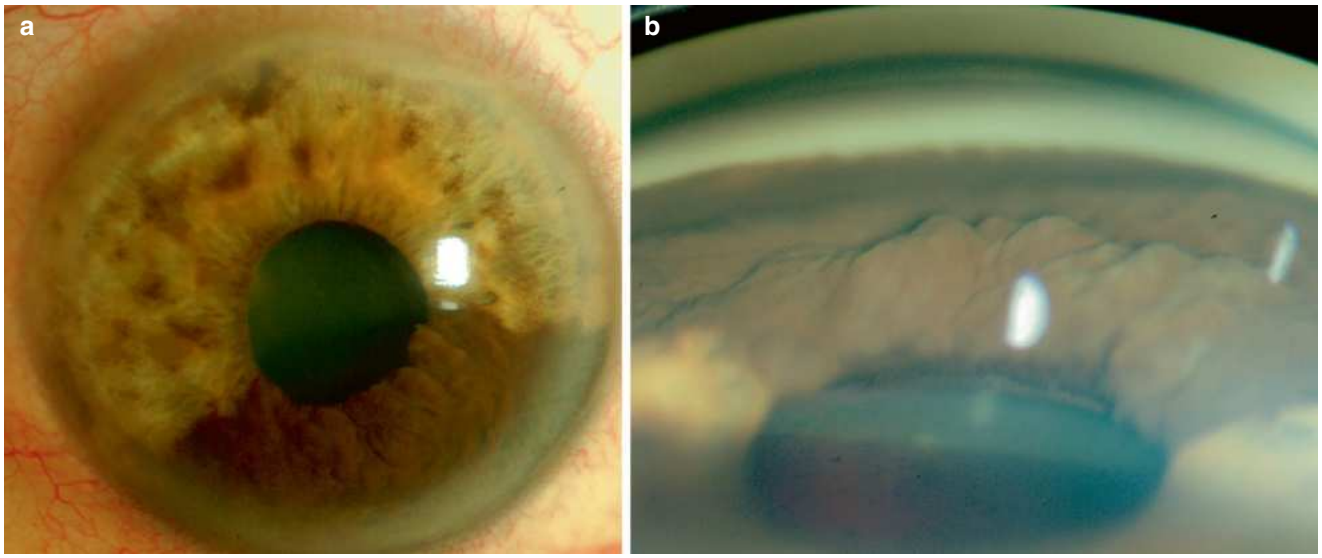

Fig. 18.2 Diffuse iris melanoma of the lower half of the iris causing secondary glaucoma (IOP = 26 mmHg) (**a**). Gonioscopy confirmed pigment seeding in the angle (**b**)

deposited within the angle resulting in open-angle glaucoma.

The third mechanism is specific to melanotic tumors. Necrotic tumor cells are engulfed by macrophages, which accumulate in the angle to occlude the spaces within the trabecular meshwork and raise intraocular pressure, causing melanomalytic glaucoma (Fig. 18.3) [7–9].

18.2.2 Angle-Closure Glaucoma

Angle-closure is commonly seen in patients with intraocular tumors. This occurs through three main mechanisms: forward movement of the lens-iris diaphragm, peripheral anterior synechiae formation, and neovascular glaucoma.

Tumor-mass effect can cause forward rotation of the lens-iris diaphragm, leading to the closure of the anterior chamber angle. Patients can present with manifestations of acute or chronic angle-closure glaucoma. This is more commonly seen with posterior segment tumors and is frequently accompanied by retinal detachment. Therefore, any patient with unilateral serous retinal detachment and glaucoma should raise suspicion for underlying malignancy.

Forward movement of the iris by anterior uveal tumors such as ciliary body melanoma can result in occlusion of the trabecular meshwork and PAS formation. Often, these tumors are misdiagnosed as primary angle closure glaucoma, resulting in delayed detection of the ciliary body mass and a worse prognosis [10]. These anterior chamber tumors may also present with a sectoral cataract, which in conjunction with the glaucomatous findings should raise suspicion for a potential mass [11]. Massive subretinal hemorrhage can also result in forward movement of the iris and PAS formation and is seen in patients with leukemia or myelodysplastic syndrome [12, 13].

Iris neovascularization (rubeosis iridis) is a common cause of angle-closure glaucoma in intraocular melanomas [1, 7]. Intraocular metastasis, retinoblastoma, and medulloepithelioma can also be associated with neovascularization and secondary glaucoma. Radiation-induced retinal ischemia can lead to neovascularization and is an important cause of glaucoma, as this is a common treatment modality for intraocular tumors (Fig. 18.4).

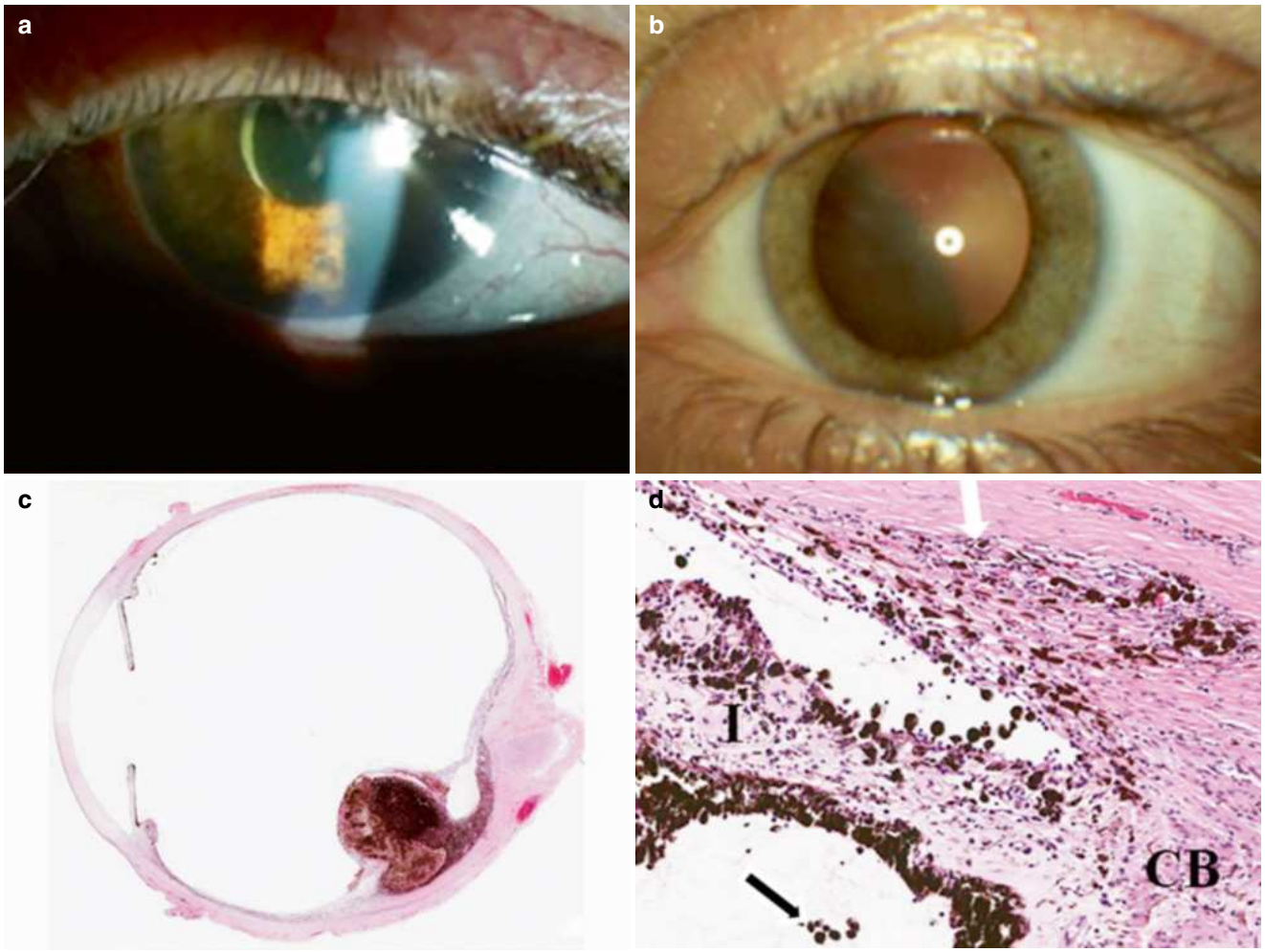

Fig. 18.3 A 46-year-old woman presented with pain and an intraocular pressure of 63 mmHg in the left eye 2 years after plaque brachytherapy for uveal melanoma. Examination revealed pigmented material in the anterior chamber (**a**), a choroidal mass (**b**), and marked pigmentation in an open trabecular meshwork with gonioscopy. Histopathology of this blind, painful eye confirmed the diagnosis of spindle type uveal melanoma (**c**), with foci of necrosis and pigment laden macrophages (melanophages). Melanophages (black arrow) were deposited on the ciliary body (**d**) (CB), iris (I) and in the trabecular meshwork (white arrow, C indicates cornea). (Reproduced with permission from: Burris CK, Rodriguez ME, Raven ML. Melanomalytic Glaucoma. Ophthalmology 2015;122(12):2422)

Fig. 18.4 Neovascular glaucoma 13 months following Iodine-125 plaque radiotherapy for a medium-sized choroidal melanoma

18.3 Clinical Features

Patients with glaucoma are typically asymptomatic; however, glaucoma-related to intraocular tumors is frequently associated with presenting ocular symptoms. Iris heterochromia, poor response to IOP-lowering therapy, serous retinal detachment, and sectoral cataract in a patient with unilateral or very asymmetric glaucoma should alert the clinician to the possibility of an intraocular tumor [6, 14].

18.4 Diagnostic Evaluation

A thorough ophthalmic examination, including slit lamp biomicroscopy, gonioscopy, transpupillary transillumination, and posterior segment examination is critical. On slit lamp

examination, the iris may reveal a melanotic or nonmelanotic lesion, and pigmented cells may be present in the anterior chamber, indicative of an anterior or posterior melanoma [7, 8]. The iris may be displaced and may show neovascularization or the lens can be subluxed or focally opacified.

Direct tumor invasion of the anterior chamber angle may be seen on gonioscopy, as well as angle seeding by pigmented or non-pigmented tumor cells or neovascularization of the angle [1, 4, 15].

Malignant melanomas can often show transillumination defects, as shown in a report of 23-ring melanomas, in which 100% of patients had transillumination defects [16]. Dilated fundus examination may reveal a choroidal tumor, retinal detachment, or vitreous seeding with tumor cells. In cases of angle closure or occludable angles, dilation should be postponed until after peripheral iridotomy or iridectomy.

Clinical examination alone may not be adequate to provide a definitive diagnosis of the tumor. For example, iris nevi and melanomas can be clinically indistinguishable. Fluorescein angiography of the iris, ultrasound biomicroscopy, and anterior segment OCT can be helpful in identifying malignant lesions [17]. Ultrasound biomicroscopy is useful in detecting ciliary body and choroidal tumors but cannot reliably distinguish between a benign and a malignant lesion [18, 19]. This type of scan can detect tumor growth and extension and is therefore useful for monitoring suspicious lesions and when considering surgical tumor resection [18, 20]. When these modalities are inconclusive, a fine-needle aspiration biopsy of the tumor can provide a definitive diagnosis [21, 22]. In cases of suspected vitreoretinal lymphoma, vitrectomy can confirm the diagnosis [23].

18.5 Specific Entities

18.5.1 Childhood Glaucoma

Glaucoma in childhood is typically associated with congenital and developmental anomalies, which can usually be easily distinguished from glaucoma secondary to intraocular tumors. In cases of neovascular angle closure, one must consider retinoblastoma, as this is the most common cause of glaucoma in these patients (Fig. 18.5). Retinoblastoma-associated glaucoma with iris neovascularization as the initial presenting sign has been reported in 7% of cases [24]. Any child with neovascular glaucoma should be evaluated for retinoblastoma. Other conditions that present with neovascular glaucoma include retinopathy of prematurity, persistent hyperplastic primary vitreous, retinal dysplasia, Coats' disease, toxocariasis, and infantile retinal detachment [25]. Additionally, some rare childhood conditions associated with glaucoma include phakomatoses, juvenile xanthogranuloma, and medulloepithelioma.

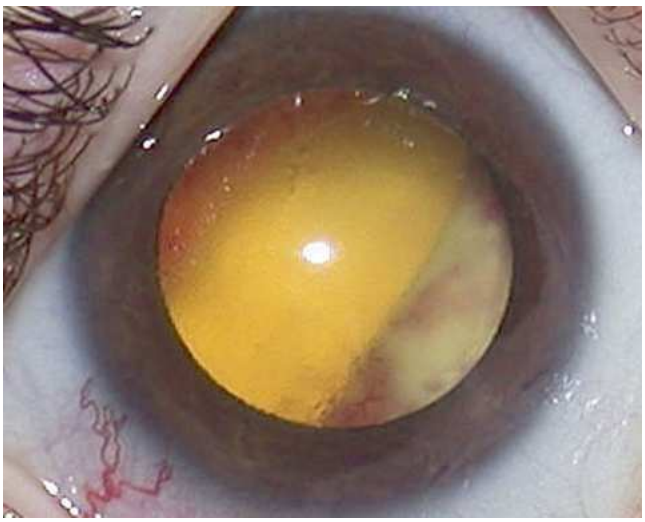

Fig. 18.5 Neovascular glaucoma associated with Stage E retinoblastoma (as per international retinoblastoma classification). Note ectropion uveae

18.5.1.1 Sturge-Weber Syndrome

Cutaneous vascular hamartomas or hemangiomas along the distribution of the fifth cranial nerve are the hallmarks of Sturge-Weber syndrome, and most patients present with a cutaneous hemangioma, especially of the upper eyelid. Central nervous system involvement can include leptomeningeal angioma and cortical calcifications. Dilated and tortuous episcleral veins and telangiectatic conjunctival vessels are commonly seen on ophthalmic examination [26]. Approximately half of these patients are affected by glaucoma, which is usually secondary to elevated episcleral venous pressure but can also be the result of anomalous development of the anterior chamber angle, fluid hypersecretion from the ciliary body, and abnormal hemodynamics of the episcleral vasculature (late-onset glaucoma) [27]. These patients can also present with congenital glaucoma, which can cause corneal edema, megalocornea, and buphthalmos [28]. Though a majority of cases have unilateral involvement of glaucoma, it is important to recognize that the fellow eye may develop glaucoma, as well. In one cohort of 47 Sturge-Weber patients with initially unilateral glaucoma with a median of 8.4 years of follow-up, the fellow eye was diagnosed with glaucoma in 14.9% of patients—more commonly in girls within 4 years of initial SWS diagnosis, and in cases with choroidal hemangioma [29]. Therefore, it is important to monitor both eyes closely in these patients.

18.5.1.2 Neurofibromatosis Type 1

Hyperpigmented lesions, or café-au-lait spots and neurofibromas within the peripheral nervous system, are characteristic of neurofibromatosis type 1. Lisch nodules can be seen on anterior segment examination, and elevated IOP can result from iris neovascularization secondary to retinal vaso-

proliferative tumor or developmental angle anomalies [30]. Neurofibromas of the upper eyelid have been associated with higher rates of glaucoma. Glaucoma occurs more commonly when there is orbitofacial involvement, as revealed by a retrospective chart review of 95 patients diagnosed with NF1 over a 15-year period. Of these patients with facial involvement, glaucoma occurred only ipsilaterally, with a prevalence of 23%, always with globe enlargement, and required glaucoma surgery, albeit with a poor prognosis [31].

18.5.1.3 Von Hippel-Lindau Disease

Neovascular glaucoma can be seen in these patients with neglected or advanced cases of retinal capillary hemangioma.

18.5.1.4 Juvenile Xanthogranuloma

Ocular manifestations of juvenile xanthogranuloma include lightly pigmented iris lesions, histologically composed of foamy histiocytes, and Touton giant cells. These tumors can cause spontaneous hyphema, resulting in secondary glaucoma. Direct invasion of the anterior chamber angle by histiocytes can also lead to elevated IOP and glaucoma. Patients with this condition also have yellow papular skin lesions on the head and neck [32].

18.5.1.5 Medulloepithelioma

Medulloepitheliomas arise from the non-pigmented epithelium of the ciliary body. They can be benign or malignant and appear as a whitish-gray mass of the ciliary body or iris. Neovascularization of the anterior chamber angle, forward displacement of the iris, and PAS formation are common causes of glaucoma in these patients (Fig. 18.6) [33, 34].

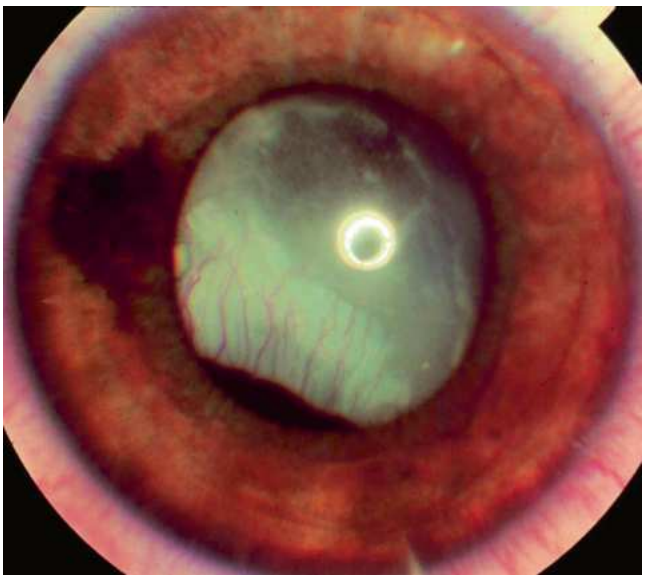

Fig. 18.6 A 38-month-old girl presented with leukocoria of 2 months duration. On examination, lens coloboma and a vascularized retrolental sheet (cyclitic membrane) were noted. A pigmented mass was seen in the ciliary body region from the 6 to 8 o'clock position. Tumor recurred after excision necessitating enucleation. Histopathologically, the lesion was confirmed to be a malignant teratoid medulloepithelioma. (Reprinted from Singh A, Singh AD, Shields CL, Shields JA. Iris neovascularization in children as a manifestation of underlying medulloepithelioma. J Pediatr Ophthalmol Strabismus 2001;38(4):224–8. With permission from Slack Incorporated)

18.5.2 Adult Glaucoma

18.5.2.1 Iris Stromal Cysts

Both angle-closure and open-angle glaucoma can be caused by iris stromal cysts, whether these cysts occur spontaneously or following surgery or trauma to the eye. Ultrasound biomicroscopy can differentiate iris cysts from malignant lesions [35]. In addition to iris cysts, ciliary body cysts may also occur and present as angle-closure glaucoma from a mixed mechanism of both lens abnormalities and anterior displacement of the iris by the cysts, potentially leading to peripheral anterior synechiae [36, 37].

18.5.2.2 Melanocytoma

Melanocytomas are benign pigmented tumors that usually affect the optic nerve but which can occur within the iris or ciliary body. These tumors can cause glaucoma by extension into the trabecular meshwork or by dispersion of pigment or necrotic melanocytoma cells (Fig. 18.7) [38].

18.5.2.3 Fuchs Adenoma

Fuchs adenoma is a benign tumor of the ciliary body that can involve the iris. Glaucoma can occur as a result of pigment dispersion [39].

18.5.2.4 Uveal Melanoma

Very advanced choroidal melanomas can cause glaucoma by pushing the lens/iris diaphragm forward to close the angle. Large tumors with severe retinal detachment can also induce iris neovascularization and neovascular glaucoma. Iris and ciliary body melanomas can cause glaucoma by annular spread around the angle [15]. Tapioca melanomas of the iris are associated with glaucoma, which has been reported in a third of these patients [40, 41]. Iris melanomas with secondary glaucoma tend to be diffuse and are therefore associated with increased risks for local tumor recurrence, enucleation, and metastasis [3]. These risks do not occur when glaucoma is coincidental and unrelated to the tumor. Not only can uveal melanomas themselves lead to secondary glaucoma while the tumor is present, but glaucoma can also be present

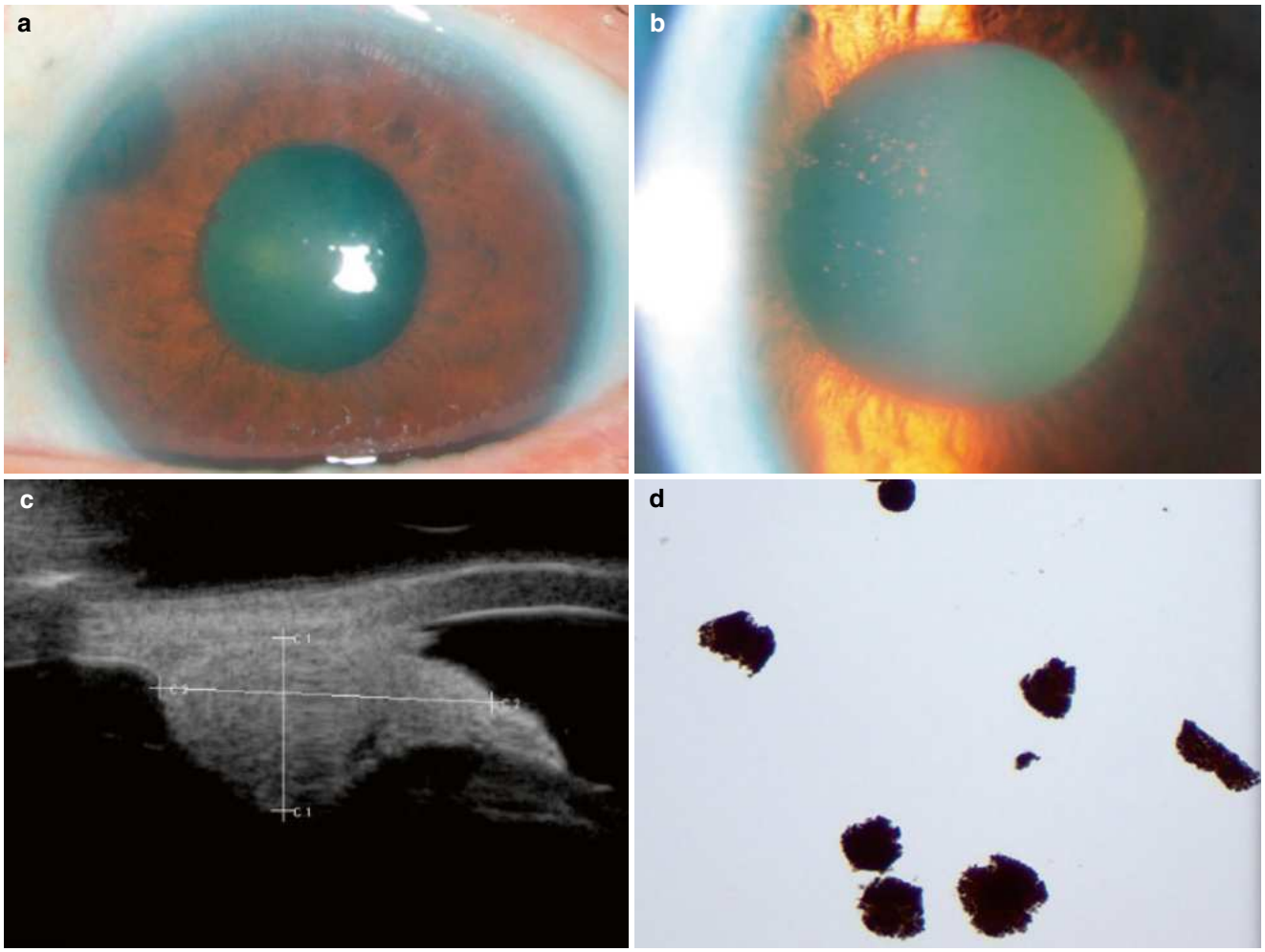

Fig. 18.7 A 54-year-old female with a pigmented iris lesion and uncontrolled glaucoma in the left eye. The intraocular pressure (IOP) was 54 mmHg despite anti-glaucoma medications. Slit lamp examination showed corneal edema and a darkly pigmented small iridociliary lesion (**a**) with diffuse pigment shedding onto anterior iris and lens surface (**b**) and diffuse circumferential pigmentation of the trabecular meshwork. UBM showed a ciliary body mass (**c**, 4 × 3 × 2 mm). Diagnostic fine needle aspiration biopsy of the main tumor and anterior chamber lavage were performed. Cytology revealed polygonal cells with dense intracytoplasmic pigment obscuring nuclear details diagnostic of a melanocytoma (**d**). During follow-up as the tumor continued to cause new pigment shedding with high IOP excision of the primary tumor via iridocyclectomy was performed. At postoperative 1 month the IOP was 13 mmHg with maximal medical therapy for glaucoma requiring glaucoma shunt surgery. At 6 months the IOP remained below 13 mmHg and the VA was 20/50 without recurrence of pigment shedding

in the post-management period. In a retrospective chart review of 271 patients over 46 years, increased intraocular pressure on presentation, more advanced AJCC clinical T subcategory, increased mean tumor basal diameter, and plaque radiotherapy treatment were the characteristics of these patients with specifically iris melanoma that predicted post-management glaucoma [42]. Another study of 374 eyes with uveal melanoma and iodine-125 brachytherapy over a 10-year period identified risk factors for both secondary open-angle and neovascular glaucoma after therapy. The risk factors for secondary open-angle glaucoma were older age, greater tumor size, iris melanomas, higher baseline intraocular pressure, involvement of the ciliary body, and prior combined brachytherapy with vitrectomy and silicone oil placement. The risk factors for neovascular glaucoma included larger tumor size, greater smoking history, pseudophakia, and higher grade of radiation retinopathy severity on fluorescein angiogram [43].

18.5.2.5 Metastatic Tumors

Intraocular metastases most commonly arise from carcinomas of the lung and breast. These metastases are usually

located in the posterior choroid, although they can develop in the iris or ciliary body [44]. Glaucoma is more commonly associated with anterior segment metastases, which tend to cause iris neovascularization and hyphema (Fig. 18.8) [6].

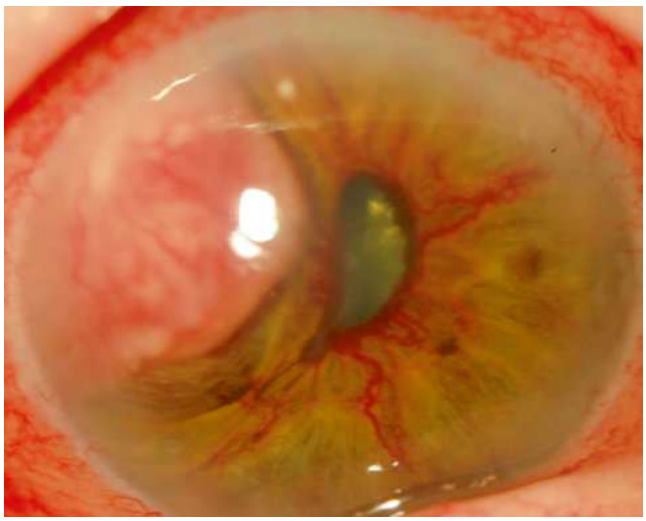

Fig. 18.8 Iris metastasis from endometrial carcinoma causing neovascular glaucoma

18.5.2.6 Leukemia/Lymphoma

Choroidal infiltration by leukemia can cause massive subretinal hemorrhage and acute angle-closure glaucoma [10]. Anterior segment exam may reveal pseudohypopyon or hyphema with resultant open-angle glaucoma (Fig. 18.9) [45, 46]. Lymphoma can affect the anterior segment to present as iritis with elevated IOP, although this is rare [47]. Investigation for recurrence of leukemia or lymphoma is essential in these patients presenting with iritis.

18.5.2.7 Myelodysplastic Syndrome/Multiple Myeloma

A few cases of myelodysplastic syndrome presenting with serous retinal detachment and angle-closure glaucoma have been reported [13]. A case of multiple myeloma presenting as iritis has been reported, with cytologic analysis of the aqueous sample revealing neoplastic plasmacytoma cells [48]. Another case of extramedullary plasmacytoma presenting as unilateral anterior and intermediate uveitis that was preceded by ipsilateral open-angle glaucoma has been reported with vitreous biopsy showing numerous atypical plasma cells despite a negative systemic workup for multiple myeloma [49].

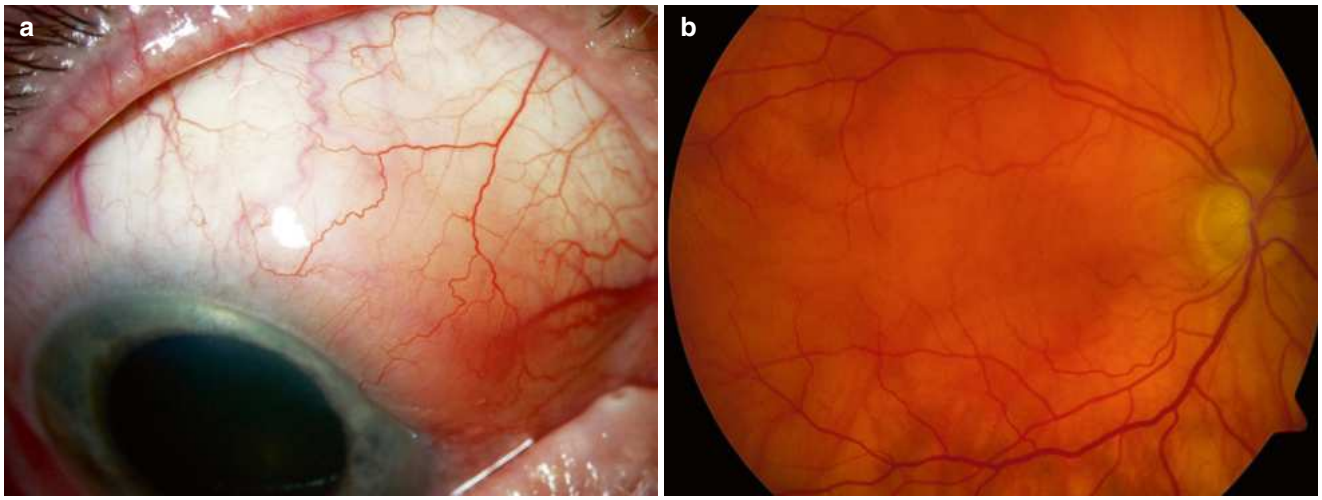

Fig. 18.9 A 68-year-old otherwise healthy gentleman with history of refractory, unilateral open-angle glaucoma in his right eye was referred for evaluation before a glaucoma filtering procedure. External examination of the right eye demonstrates episcleral venous dilation in the right eye associated with faintly demarcated, slightly raised, pink subconjunctival infiltrates restricted to the superior nasal quadrant with subtle inferior perilimbal extension (**a**). Fundus photography: fundus photographs demonstrate flat, yellow, choroidal infiltrates in both eyes, which extend into the periphery as discrete lesions (**b**). Indocyanine green angiography: Indocyanine angiography confirms the presence of infiltrative lesions in the choroid as demonstrated by persistent hypofluorescence in both eyes (**c**). B-scan ultrasonography: representative selections illustrate the presence of hyperechoic choroidal lesions with orbital extension in both eyes, more prominent in the right than in the left (**d**). Given his bilateral eye involvement he was started on Rituximab infusion at a dose of 750 mg weekly for 4 weeks as an upfront systemic therapy followed by radiation therapy consisting of 2520 cGy in 14 fractions to both eyes due to limited response to Rituximab. At 5-year follow-up, the patient was in complete remission. Visual acuity is 20/40 right eye and 20/20 left eye with symmetric IOP off medical therapy. (Reproduced with permission from: Sears NC, Singh A, Singh AD. Ocular Adnexal Lymphoma Presenting as Refractory Unilateral Open-angle Glaucoma. Journal of Glaucoma 2016;25:e741–e4)

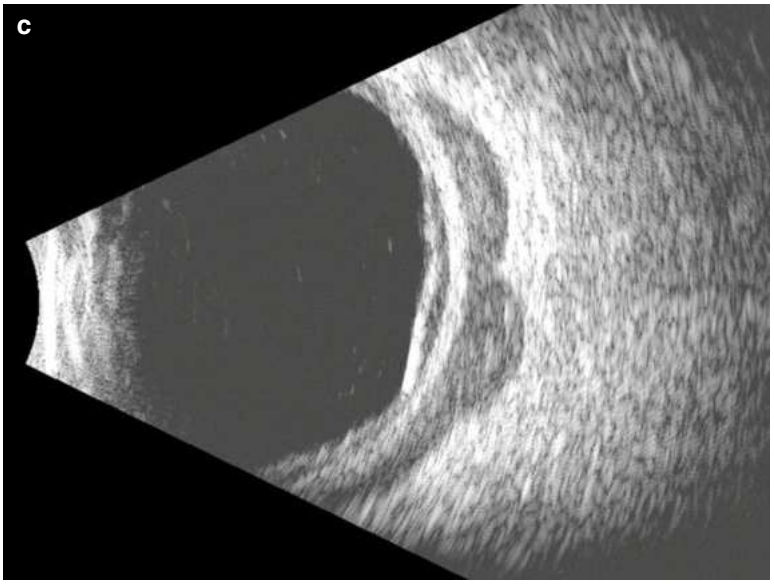

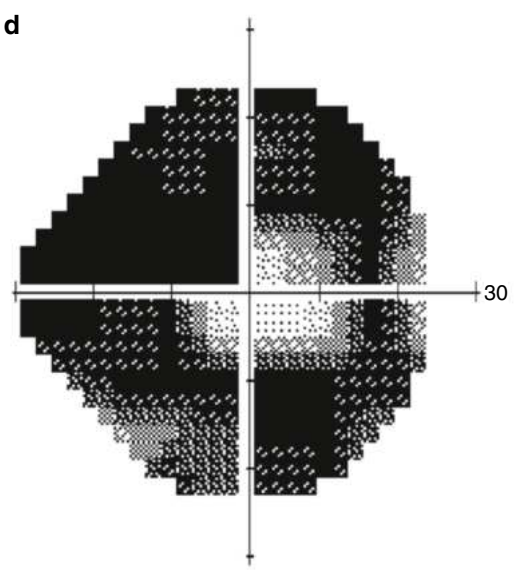

Fig. 18.9 (continued)

18.6 Treatment

Treatment of the tumor results in an improvement in intraocular pressure in most cases. In patients whose glaucoma does not respond to tumor ablation, management can be difficult [44, 45]. Filtering surgery should be safe in patients with uveal melanoma if the tumor has been successfully treated by radiotherapy or local resection (Fig. 18.10) [50]. In cases of retinoblastoma, however, filtering surgery carries the risk of iatrogenic dissemination of the tumor and should be avoided [51]. Laser trabeculoplasty can be considered in these patients, taking care to avoid areas of the anterior chamber angle that involve the tumor. Tumors that are associated with pigment dispersion and secondary glaucoma may respond well to laser trabeculoplasty [52]. A cyclodestructive procedure can also be considered, as the integrity of the anterior chamber is preserved, and the procedure can be titrated to some degree. One retrospective review of 27 eyes with secondary glaucoma following radiotherapy for uveal melanoma that underwent cyclophotocoagulation showed sustained intraocular pressure lowering at 24 months, with 6 of these eyes developing hypotony [53]. Additionally, cyclophotocoagulation can be helpful in patients with significant recalcitrant acute intraocular pressure elevation due to active neovascular glaucoma. These cases are at higher risk of postoperative hyphema when active with urgent glaucoma tube shunt placement, which can clog the filtering device, causing an initial pressure spike in the early postoperative period and potentially requiring an anterior chamber washout. The cyclodestructive procedure can temporize pressure without invasive surgery, potentially delaying the need for a filtering procedure and allowing this to be performed when hyphema risk is lower. Techniques that do not penetrate the anterior chamber, including canaloplasty and deep sclerotomy, have shown promising results in these patients, as well [54]. Neovascular glaucoma developing after radiotherapy (i.e., "toxic tumor syndrome") can resolve if the offending tumor is excised [55, 56]. In many cases of ciliary body or choroidal melanoma and retinoblastoma associated with glaucoma, patient comfort can be achieved only by enucleation.

When non-penetrating surgery is unsuccessful, penetrating surgery can be considered. Radiotherapy can result in local conjunctival inflammation and scarring, which can compromise trabeculectomy. Minimally invasive techniques such as goniotomy, trabeculotomy, supraciliary stenting, and others can be considered in these patients [57]. With the growing surgical advances in the glaucoma space, depending on the severity of intraocular elevation and glaucoma, the degree of angle-based surgery can now even be titrated as needed with ab-interno techniques: traditional nasal goniotomy or 360-degree trabeculotomy in addition to 180° goniotomy with or without canaloplasty. Given the aggressive nature of glaucoma in these eyes, however, tube shunting may be more appropriate. In a case series of 31 patients with elevated IOP, following proton beam radiotherapy for anterior uveal melanoma with documented tumor regression, that were treated with Baerveldt shunt implantation, 86% of patients treated with glaucoma medications achieved adequate IOP control [58]. On follow-up exam, none of these patients had local or systemic dissemination of their tumors. Of note, newer filtering procedures, such as the XEN gel stent implant, may be more challenging and prone to failure in childhood glaucomas due to the thicker tenon layer and more robust post-operative inflammatory response in these patients [59].

Patients with Sturge-Weber syndrome-associated glaucoma require special consideration. With the advent of newer glaucoma drops, topical netarsudil—which works by relaxing the trabecular meshwork smooth muscle to improve outflow and

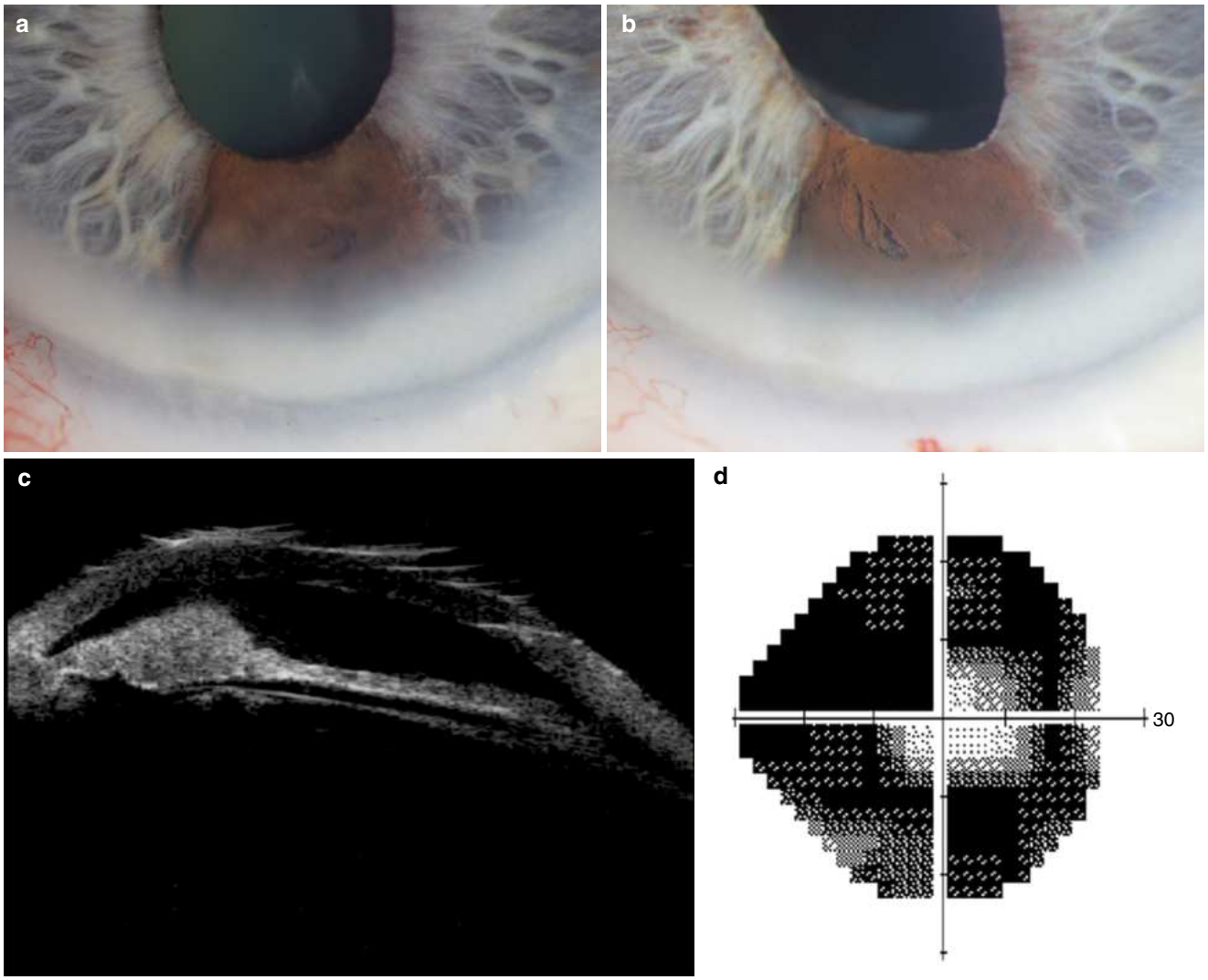

Fig. 18.10 Iris melanoma that was confirmed by a diagnostic biopsy and treated with plaque brachytherapy. Slit lamp appearance (**a**) and UBM (**b**). Over subsequent follow up the tumor appeared regressed (**c**). 30 months later he required trabeculectomy for secondary glaucoma (non-neovascular) that could not controlled by maximal medical therapy. Note pigment deposit noted within the bleb (**d**) which has remained stable for 24 months without evidence of extraocular extension of melanoma

may reduce episcleral venous pressure—may be effective in lowering intraocular pressure in these patients [60]. In patients with high IOP caused by elevated episcleral venous pressure, surgical therapy is frequently required, although these patients have an increased risk of intraoperative choroidal effusion and expulsive hemorrhage [61]. Angle-based glaucoma surgery carries a decreased risk of complications and has been performed in these patients. Though it can achieve early intraocular pressure reduction, many patients ultimately fail and subsequently require another form of glaucoma surgery [62, 63]. However, trabeculotomy performed in conjunction with a traditional filtering surgery such as trabeculectomy has shown some success [64]. As far as filtration surgery is concerned, both valved Ahmed glaucoma implants and trabeculectomies have been performed and both appear to be safe and efficacious in controlling glaucoma in these patients [65, 66]. Transscleral cyclophotocoagulation has also shown a mild reduction in intraocular pressure [67]. If filtration surgery must be undertaken, appropriate steps to reduce the chance of expulsive hemorrhage, including the use of viscoelastic devices, pre-placement of scleral sutures, and prophylactic sclerotomy, should be considered. Oral propranolol as an adjunct to glaucoma surgery—used 1 week prior and for 6 weeks after—may be considered an effective method for minimizing sight-threatening choroidal effusion postoperatively in these patients based on a prospective cohort study of 12 patients [68].

18.7 Summary

Open-angle and angle-closure mechanisms can be associated with glaucoma in intraocular tumors. Patients presenting with unilateral glaucoma should be evaluated for associated intraocular tumors. The management of glaucoma associated

Table 18.1 Special considerations for management of tumor-associated glaucoma

Factor	Comment
Dry eyes	Surface issues, lubrication, punctal plugs
Conjunctival scarring	Choice of surgery
Iris abnormalities	Synechiae, iridectomy
Associated cataract	Combined surgery
Radiation retinopathy	Combined PRP and intravitreal anti-VEGF
Radiation optic neuropathy	Poor visual outcome
Risk of tumor dissemination	Document tumor stability
Immunocompromised status	Risk of infection
Shortened life expectancy	Careful assessment of benefit

PRP pan retinal photocoagulation, *VEGF* vascular endothelial growth factor

with intraocular tumors should be individualized and adjusted according to the mechanism of elevated intraocular pressure and comorbidities (Table 18.1).

References

1. Shields CL, Shields JA, Shields MB, Augsburger JJ. Prevalence and mechanisms of secondary intraocular pressure elevation in eyes with intraocular tumors. Ophthalmology. 1987;94(7):839–46.
2. Ferry AP. Carcinoma metastatic to the eye and orbit: I. A clinicopathologic study of 227 cases. Arch Ophthalmol. 1974;92(4):276.
3. Shields CL, Shah SU, Bianciotto CG, et al. Iris melanoma management with iodine-125 plaque radiotherapy in 144 patients: impact of melanoma-related glaucoma on outcomes. Ophthalmology. 2013;120(1):55–61.
4. Yoshizumi MO, Thomas JV, Smith TR. Glaucoma-inducing mechanisms in eyes with retinoblastoma. Arch Ophthalmol. 1978;96(1):105–10.
5. Lee V, Cree IA, Hungerford JL. Ring melanoma—a rare cause of refractory glaucoma. Br J Ophthalmol. 1999;83(2):194–8.
6. Ferry AP. Carcinoma metastatic to the eye and orbit: II. A clinicopathological study of 26 patients with carcinoma metastatic to the anterior segment of the eye. Arch Ophthalmol. 1975;93(7):472.
7. Yanoff M. Glaucoma mechanisms in ocular malignant melanomas. Am J Ophthalmol. 1970;70(6):898–904.
8. Yanoff M. Melanoma lytic glaucoma: report of a case. Arch Ophthalmol. 1970;84(4):471.
9. Burris CK, Rodriguez ME, Raven ML. Melanomalytic glaucoma. Ophthalmology. 2015;122(12):2422.
10. Escalona-Benz E, Benz MS, Briggs JW, et al. Uveal melanoma presenting as acute angle-closure glaucoma: report of two cases. Am J Ophthalmol. 2003;136(4):756–8.
11. Stalhammar G, Damato BE, Fili M. Adenoma of the nonpigmented ciliary epithelium presenting as glaucoma. Am J Ophthalmol Case Rep. 2023;32:101871.
12. Kozlowski IMD, Hirose T, Jalkh AE. Massive subretinal hemorrhage with acute angle-closure glaucoma in chronic myelocytic leukemia. Am J Ophthalmol. 1987;103(6):837–8.
13. Wohlrab T-M, Pleyer U, Rohrbach JM, et al. Sudden increase in intraocular pressure as an initial manifestation of myelodysplastic syndrome. Am J Ophthalmol. 1995;119(3):370–2.
14. Harbour JW, Augsburger JJ, Eagle RC. Initial management and follow-up of melanocytic iris tumors. Ophthalmology. 1995;102(12):1987–93.
15. Demirci H, Shields CL, Shields JA, et al. Ring melanoma of the anterior chamber angle: a report of fourteen cases. Am J Ophthalmol. 2001;132(3):336–42.
16. Demirci H, Shields CL, Shields JA, et al. CME ring melanoma of the ciliary body: report on twenty-three patients. Retina. 2002;22(6):698–706.
17. Jakobiec FA, Depot MJ, Henkind P, Spencer WH. Fluorescein angiographic patterns of iris melanocytic tumors. Arch Ophthalmol. 1982;100(8):1288–99.
18. Pavlin CJ, McWhae JA, McGowan HD, Foster FS. Ultrasound biomicroscopy of anterior segment tumors. Ophthalmology. 1992;99(8):1220–8.
19. Maberly DAL, Pavlin CJ, McGowan HD, et al. Ultrasound biomicroscopic imaging of the anterior aspect of peripheral choroidal melanomas. Am J Ophthalmol. 1997;123(4):506–14.
20. Katz NR. Ultrasound biomicroscopy in the management of malignant melanoma of the iris. Arch Ophthalmol. 1995;113(11):1462.
21. Midena E, Segato T, Piermarocchi S, Boccato P. Fine needle aspiration biopsy in ophthalmology. Surv Ophthalmol. 1985;29(6):410–22.
22. Char D, Kemlitz A, Miller T. Intraocular Biopsy. Ophthalmol Clin N Am. 2005;18(1):177–85.
23. Chan C-C, Wallace DJ. Intraocular lymphoma: update on diagnosis and management. Cancer Control. 2004;11(5):285–95.
24. Ellsworth RM. The practical management of retinoblastoma. Trans Am Ophthalmol Soc. 1969;67:462–534.
25. Moazed K, Albert D, Smith TR. Rubeosis iridis in "pseudogliomas". Surv Ophthalmol. 1980;25(2):85–90.
26. Sullivan TJ, Clarke MP, Morin JD. The ocular manifestations of the Sturge-Weber syndrome. J Pediatr Ophthalmol Strabismus. 1992;29(6):349–56.
27. Cibis GW, Tripathi RC, Tripathi BJ. Glaucoma in Sturge-Weber syndrome. Ophthalmology. 1984;91(9):1061–71.
28. Javaid U, Ali MH, Jamal S, Butt NH. Pathophysiology, diagnosis, and management of glaucoma associated with Sturge–Weber syndrome. Int Ophthalmol. 2017;38(1):409–16.
29. Shin YI, Ha A, Jeong Y, et al. Incidence of and risk factors for fellow-eye involvement in Sturge-Weber syndrome children with unilateral glaucoma. J Glaucoma. 2024;33(1):40–6.
30. Grant WM, Walton DS. Distinctive gonioscopic findings in glaucoma due to neurofibromatosis. Arch Ophthalmol. 1968;79(2):127–34.
31. Morales J, Chaudhry IA, Bosley TM. Glaucoma and globe enlargement associated with neurofibromatosis type 1. Ophthalmology. 2009;116(9):1725–30.
32. Zimmerman LE. Ocular lesions of juvenile xanthogranuloma*. Am J Ophthalmol. 1965;60(6):1011–35.
33. Singh A, Singh AD, Shields CL, Shields JA. Iris neovascularization in children as a manifestation of underlying medulloepithelioma. J Pediatr Ophthalmol Strabismus. 2001;38(4):224–8.
34. Broughton WL, Zimmerman LE. A clinicopathologic study of 56 cases of intraocular medulloepitheliomas. Am J Ophthalmol. 1978;85(3):407–18.
35. Marigo FA, Esaki K, Finger PT, et al. Differential diagnosis of anterior segment cysts by ultrasound biomicroscopy. Ophthalmology. 1999;106(11):2131–5.
36. Almulhim A, Alsirhy E, Al-Obeidan SA. Bilateral multiple ciliary body cysts with angle-closure glaucoma in an 18-year-old patient. Middle East Afr J Ophthalmol. 2022;29(2):100–2.
37. Turner ML, de Alba Campomanes AG, Stewart JM, Oatts JT. Congenital ciliary body cysts causing lens abnormalities and secondary angle closure glaucoma in a child. Am J Ophthalmol Case Rep. 2022;28:101723.

38. Nakazawa M, Tamai M. Iris melanocytoma with secondary glaucoma. Am J Ophthalmol. 1984;97(6):797–9.
39. Shields JA, Augsburger JJ, Sanborn GE, Klein RM. Adenoma of the iris-pigment epithelium. Ophthalmology. 1983;90(6):735–9.
40. Reese AB, Mund ML, Iwamoto T. Tapioca melanoma of the iris. Am J Ophthalmol. 1972;74(5):840–50.
41. Zakka KA, Foos RY, Sulit H. Metastatic tapioca iris melanoma. Br J Ophthalmol. 1979;63(11):744–9.
42. Shukla AG, Vaidya S, Yaghy A, et al. Iris melanoma: factors predictive of post-management secondary glaucoma in 271 cases at a Single Ocular Oncology Centre. Eye (Lond). 2023;37(5):938–46.
43. Kim EA, Salazar D, McCannel CA, et al. Glaucoma after iodine-125 brachytherapy for uveal melanoma: incidence and risk factors. J Glaucoma. 2020;29(1):1–10.
44. Bloch RS, Gartner S. The incidence of ocular metastatic carcinoma. Arch Ophthalmol. 1971;85(6):673–5.
45. Rosenthal AR. Ocular manifestations of leukemia. A review. Ophthalmology. 1983;90(8):899–905.
46. Sears NC, Singh A, Singh AD. Ocular adnexal lymphoma presenting as refractory unilateral open-angle glaucoma. J Glaucoma. 2016;25:e741–4.
47. Saga T, Ohno S, Matsuda H, et al. Ocular involvement by a peripheral T-cell lymphoma. Arch Ophthalmol. 1984;102(3):399–402.
48. Shakin EP, Augsburger JJ, Eagle RC, et al. Multiple myeloma involving the iris. Arch Ophthalmol. 1988;106(4):524–6.
49. Ayton T, Cherepanoff S, Gottlieb D, et al. Intraocular solitary extramedullary plasmacytoma presenting as unilateral anterior and intermediate uveitis preceded by refractory glaucoma. BMC Ophthalmol. 2021;21(1):66.
50. Grossniklaus HE. Iris melanoma seeding through a trabeculectomy site. Arch Ophthalmol. 1990;108(9):1287.
51. Honavar SG, Shields CL, Shields JA, et al. Intraocular surgery after treatment of retinoblastoma. Arch Ophthalmol. 2001;119(11):1613–21.
52. Girkin CA, Goldberg I, Mansberger SL, et al. Management of iris melanoma with secondary glaucoma. J Glaucoma. 2002;11(1):71–4.
53. Piirtola A, Puska P, Kivelä T. Red laser cyclophotocoagulation in the treatment of secondary glaucoma in eyes with uveal melanoma. J Glaucoma. 2014;23(1):50–5.
54. Hondur A, Onol M, Hasanreisoglu B. Nonpenetrating glaucoma surgery: meta-analysis of recent results. J Glaucoma. 2008;17(2):139–46.
55. Konstantinidis L, Groenewald C, Coupland SE, Damato B. Transscleral local resection of toxic choroidal melanoma after proton beam radiotherapy. Br J Ophthalmol. 2014;98(6):775–9.
56. Romano MR, Catania F, Confalonieri F, et al. Vitreoretinal surgery in the prevention and treatment of toxic tumour syndrome in uveal melanoma: a systematic review. Int J Mol Sci. 2021;22(18):10066.
57. Sharkawi E, Oleszczuk JD, Bergin C, Zografos L. Baerveldt shunts in the treatment of glaucoma secondary to anterior uveal melanoma and proton beam radiotherapy. Br J Ophthalmol. 2012;96(8):1104–7.
58. Iwach AG, Hoskins HD, Hetherington J, Shaffer RN. Analysis of surgical and medical management of glaucoma in Sturge-Weber syndrome. Ophthalmology. 1990;97(7):904–9.
59. Schellhase H, Fuest M, Kuerten D, et al. Failure of XEN gel stent implantation as a stand-alone procedure in congenital glaucoma: case report of secondary congenital glaucoma in neurofibromatosis type 1. Case Rep Ophthalmol Med. 2021;2021:9947167.
60. Kaufman AR, Elhusseiny AM, Edward DP, et al. Topical netarsudil for treatment of glaucoma with elevated episcleral venous pressure: a pilot investigation in Sturge-Weber syndrome. Eur J Ophthalmol. 2023;33(5):1969–76.
61. Christensen GR, Records RE. Glaucoma and expulsive hemorrhage mechanisms in the Sturge-Weber syndrome. Ophthalmology. 1979;86(7):1360–6.
62. Hu M, Liang T, Leng F, et al. Outcomes of microcatheter-assisted trabeculotomy for glaucoma associated with Sturge-Weber syndrome and phakomatosis pigmentovascularis. Am J Ophthalmol. 2023;248:51–9.
63. Yeung HH, Kane SA, Turlapati N, et al. Failure of goniosurgery for glaucoma associated with Sturge-Weber syndrome. J Pediatr Ophthalmol Strabismus. 2020;57(6):384–7.
64. Sood D, Rathore A, Sood I, et al. Long-term intraocular pressure after combined trabeculotomy-trabeculectomy in glaucoma associated with Sturge-Weber syndrome. Eur J Ophthalmol. 2018;28(2):210–5.
65. Kaushik J, Parihar JKS, Jain VK, Mathur V. Ahmed valve implantation in childhood glaucoma associated with Sturge-Weber syndrome: our experience. Eye (Lond). 2019;33(3):464–8.
66. Sarker BK, Malek MA, Mannaf SMA, et al. Outcome of trabeculectomy versus Ahmed glaucoma valve implantation in the surgical management of glaucoma in patients with Sturge-Weber syndrome. Br J Ophthalmol. 2021;105(11):1561–5.
67. Al Owaifeer AM, Almutairi AT, Schargel K. The outcomes of transscleral cyclophotocoagulation in pediatric glaucoma secondary to Sturge-Weber syndrome. J AAPOS. 2022;26(2):78.e1–5.
68. Kaushik S, Kataria P, Joshi G, et al. Perioperative propranolol: a useful adjunct for glaucoma surgery in Sturge-Weber syndrome. Ophthalmol Glaucoma. 2019;2(4):267–74.

Graft-Versus-Host Disease

19

Edgar M. Espana, Thomas A. Weppelmann, and Arun D. Singh

19.1 Introduction

Allogeneic (genetically different, same species) hematopoietic stem cell transplantation (HSCT) is a well-established therapy for a variety of hematological malignancies, inherited disorders of metabolism, histiocytic and granulomatous disorders, adjuvant therapy in kidney transplant, and recently, multiple sclerosis [1–5]. The indications for HSCT and the number of procedures continue to increase, with an estimated 1.5 million performed worldwide between the years 1957 and 2019 [6]. Syngeneic transplantation (between identical twins) or autologous (from the patient's own cells) represents the optimal form of HSCT and, unlike other allogeneic donors, does not carry a risk of GVHD [2, 7]. Even with sibling donors, who are more likely than unrelated donors to be HLA-matched, 25–35% of recipients develop GVHD [7]. Despite HLA matching between receptor and donor (sibling or unrelated), substantial numbers of patients will develop GVHD because of differences in minor histocompatibility antigens outside the major HLA loci [2, 7].

Dr. Edward Thomas was a pioneer in applying the results of early bone marrow transplantation in animal studies to the treatment of human leukemia. In 1959, Thomas et al. reported on a patient with end-stage leukemia who was treated with total-body irradiation, followed by an infusion of her identical twin's marrow [8]. In 1990, the Nobel Prize in Medicine was awarded to Dr. Thomas in recognition of his pioneering work in the field of marrow transplantation.

GVHD remains the most frequent and serious complication limiting the broader application of HSCT. Unfortunately, transplant recipients with GVHD have a reduced quality-of-life and increased risks for long-term morbidity and mortality in comparison to recipients who do not develop this disease.

19.2 Etiology

In 1966, Billingham formulated three requirements for the development of GVHD: the graft must contain immunologically competent cells; the recipient must express tissue antigens that are not present in the transplant donor; and the recipient must be incapable of mounting an effective response to eliminate the transplanted cells [9]. It is now recognized that T lymphocytes are immunologically competent cells that, when transferred from donor to host, promote the development of GVHD [10].

In an allogeneic HSCT, recipients receive immunoablative chemotherapy or radiation prior to a hematopoietic cell infusion containing mature donor T-cells from either marrow or more commonly peripheral blood stem cells (PBSCs). Donor T-cells promote hematopoietic engraftment, reconstitute T-cell immunity, and mediate a potent beneficial antitumor effect [9, 10]. GVHD develops when donor T cells respond to recipient tissue antigens secondary to mismatches between major and minor histocompatibility antigens [11, 12]. Risk factors for the development of chronic GVHD include a prior episode of acute GVHD, receipt of peripheral blood stem cell grafts, transplantation of grafts from female donors in male recipients, HLA disparity between recipient and donor, older age of the recipient or donor, and a diagnosis of chronic myeloid leukemia [12].

E. M. Espana (✉) · T. A. Weppelmann
Department of Ophthalmology, University of South Florida, Tampa, FL, USA

A. D. Singh
Department of Ophthalmic Oncology, Cole Eye Institute, Cleveland Clinic, Cleveland, OH, USA
e-mail: singha@ccf.org

© The Author(s), under exclusive license to Springer Nature Switzerland AG 2025

A. D. Singh, B. E. Damato (eds.), *Clinical Ophthalmic Oncology*, https://doi.org/10.1007/978-3-031-75907-9_19

19.3 Pathogenesis

Four definite factors influence the pathogenesis of GVHD:

1. *Sources of Hematopoietic Stem Cells*

   HSCs are normally present in the peripheral blood at very low numbers. A number of different stimuli, including hematopoietic growth factors and inhibitors of certain chemokine receptors, result in the mobilization of HSC from the marrow to the peripheral blood. PBSCs have largely replaced the marrow for autologous and most allogeneic transplantations; unfortunately, peripheral blood stem cells also contain T cells that increase the incidence and prolong the course of GVHD. PBSCs are associated with an increased risk of GVHD [13]. Another source of hematopoietic stem cells is blood from the umbilical cord [2, 14]. Because these cells are immunologically quiescent, it is feasible to cross major histocompatibility barriers and improve rejection rates. Cord blood as a source of stem cells has several advantages: its transplantation requires less stringent HLA matching than is required for that of the peripheral blood or marrow, and mismatched cord blood cells are less likely to cause GVHD [14, 15].
2. *Preparation of Donor*

   For 4 or 5 days before apheresis, granulocyte colony-stimulating factor (GCSF) is used to mobilize stem cells to the peripheral circulation. Stem cells are isolated from the circulatory system based on the cell membrane expression of CD34+, a hematopoietic progenitor cell marker [16]. These peripheral blood CD34+ stem cells are capable of forming colonies of granulocytes/macrophages, erythrocytes, and other multipotential or immature progenitors. The CD34+ stem cells are frozen until they are infused into the recipient.
3. *Preparation of Recipient*

   The recipient receives a conditioning regimen consisting of chemotherapy, which is often combined with radiotherapy and T-cell-depleting antibodies designed to immunosuppress the host to decrease graft rejection. This is followed by the infusion of prepared donor cells [2].
4. *Basis for Tissue Damage*

   Whereas bone marrow cells and GCSF-mobilized PBSCs are both enriched with hematopoietic progenitors, they also contain mature T-cells that are responsible for graft rejection [2, 9, 10]. Reduced incidence of severe GVHD is offset by high rates of graft failure, relapse of malignant disease, and infections. Chronic GVHD is often characterized by fibrosis with little inflammation and involves one or multiple organs in the integumentary, musculoskeletal, cardiovascular, respiratory, gastrointestinal, reproductive, and central and peripheral nervous systems. A proposed conceptual model divides the pathophysiology of chronic GVHD into three phases: early inflammation caused by tissue injury (phase 1), followed by chronic inflammation and dysregulated B-cell and T-cell immunity (phase 2), and culminating in tissue repair with fibrosis (phase 3) [12, 17].

19.4 Classification of GVHD

Graft-versus-host disease clinically presents in an acute or chronic form. Historically, these two forms were arbitrarily defined according to the time of onset after transplantation (less than or more than 100 days, respectively) [2]. A clear distinction between acute and chronic forms of GVHD as originally described can no longer be delineated. In 2005, the National Institutes of Health working group sought to standardize the definitions of acute and chronic GVHD [18]. The diagnosis of chronic GVHD (cGVHD) moved toward specific signs, degree of organ involvement (mild, moderate, severe), laboratory data, and histopathological confirmation rather than time of onset after transplantation. Additionally, cGVHD was subcategorized into classic chronic GVHD without acute GVHD features and chronic GVHD with overlapping acute GVHD characteristics. The 2014 National Institutes of Health report further clarified the overlap subcategory to address the different clinical presentations that may occur within this group [19]. It has recommended documentation of all acute and chronic GVHD manifestations that may assist in prognosis, treatment guidance, clinical trial eligibility, and identification of biomarkers. The diagnostic criteria and severity scoring for each organ system, including the eyes, were also refined [19].

19.5 Acute GVHD

Despite prophylactic measures, the incidence of acute GVHD (aGVHD) in patients receiving transplants from an HLA-identical sibling is estimated to be 40–60% and is 75% in patients receiving transplants from HLA-matched unrelated donors [20]. The sine qua non of aGVHD is selective epithelial damage to target *organs*: the skin, mucosas, liver, and gastrointestinal tract, within 14–42 days of infusion [21]. A hyperacute presentation of GVHD may occur within 14 days of infusion in patients with severe HLA mismatched donors or in those who received inadequate GVHD prophylaxis [22]. Hyperacute GVHD is manifested by high fever and severe cutaneous involvement (generalized erythema with desquamation) (Fig. 19.1), in addition to hepatitis and intestinal symptoms.

In acute ocular graft-versus-host disease, the histopathological changes are mainly seen in the conjunctiva and lacrimal gland tissue [23]. As mentioned previously, aGVHD is

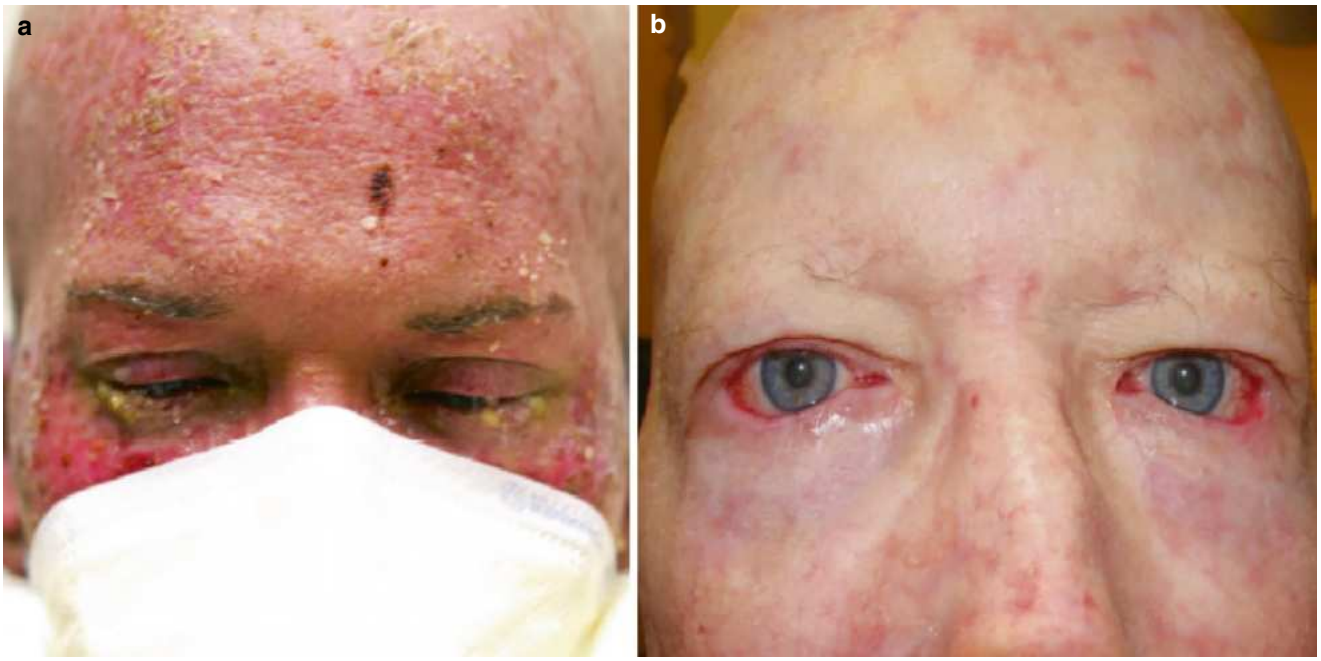

Fig. 19.1 External photos demonstrating differences in clinical presentation between acute and chronic GVHD. Skin blistering and desquamation of mucosas are typical of acute GVHD (**a**). Loss of eyelashes, skin thinning, ocular redness, ectropion, or entropion is commonly seen in cGVHD (**b**)

primarily a T-cell-mediated immune process. The conjunctival tissue of patients with aGVHD presents with pseudomembranous conjunctivitis. Donor-derived mononuclear T lymphocytes have been detected by immunohistochemistry [23, 24].

19.6 Chronic GVHD

The incidence of cGVHD ranges widely from 6% to 80% and is fatal in approximately 10% of the cases; it is one of the main causes of post-HSCT morbidity and mortality. The chronic presentation of GVHD has features resembling autoimmune disorders such as scleroderma, Sjögren's syndrome, primary biliary cirrhosis, wasting syndrome, bronchiolitis obliterans, immune cytopenias, and chronic immunodeficiency. Other factors that increase the risk of cGVHD include older recipients and those who have already experienced aGVHD [2].

Symptoms usually present within 3 years of allogeneic HSCT and are often preceded by a history of aGVHD [2, 7]. Manifestations of cGVHD may be restricted to a single organ or tissue or may be widespread. These can lead to debilitating sequelae such as joint contractures, decreased sight, end-stage lung disease, or mortality from profound chronic immune suppression-induced life-threatening infections [2, 7, 12, 19]. The NIH working group recommends that the diagnosis of cGVHD is made after one diagnostic manifestation of cGVHD or at least one distinctive manifestation plus a pertinent biopsy, laboratory or other tests, evaluation by a specialist, or radiographic imaging showing cGVHD in the same or another organ. After a diagnosis of GVHD is made, the NIH global scoring system (Table 19.1)

Table 19.1 NIH global severity of chronic GVHD

NIH global severity of chronic GVHD	Criteria
Mild chronic GVHD	One or two organs involved with no more than score 1 *plus* lung score 0
Moderate chronic GVHD	Three or more organs involved with no more than score 1
	OR
	At least one organ (not lung) with a score of 2
	OR
	Lung score 1
Severe chronic GVHD	At least one organ with a score of 3
	OR
	Lung score 2 or 3

Adapted from Jagasia et al. [19]. With permission from Elsevier
Key points:
In skin: higher of the two scores to be used for calculating global severity
In lung: FEV1 is used instead of clinical score for calculating global severity
If the entire abnormality in an organ is noted to be unequivocally explained by a non-GVHS documented cause, that organ is not included for calculation of the global severity
If the abnormality in an organ is attributed to multifactorial causes (GVHD plus other causes), the scored organ will be used for calculation of the global severity regardless of the contributing causes (no downgrading of organ severity score)

Table 19.2 Organ scoring of chronic GVHD, ocular

	Score 0	Score 1	Score 2	Score 3
Keratoconjunctivitis sicca (KCS) confirmed by ophthalmologist	No symptoms	Mild dry eye symptoms not affecting ADL (requirement of lubricating eye drops ≤3× per day)	Moderate dry eye symptoms partially affecting ADL (requiring lubricating eye drops >3× per day or punctual plugs), *WITHOUT* new vision impairment due to KCS	Severe dry eye symptoms significantly affecting ADL (special eyewear to relieve pain *OR* unable to work because of ocular symptoms *OR* loss of vision due to KCS)

Adapted from Jagasia et al. [19]

can be applied, which scores the eight major organ systems (skin, mouth, eyes, gastrointestinal tract, liver, lungs, genital tract, and fasciae/ joints) on a scale from 0 to 3. Table 19.2 outlines the scoring criteria for ocular involvement in cGHVD.

19.7 Clinical Ophthalmic Features

19.7.1 Ocular Surface Manifestations

Dry eye is the most frequent ocular symptom, usually occurring approximately 6 months post-transplantation [25]. In chronic ocular GVHD, inflammatory destruction of the conjunctiva and lacrimal gland with fibrosis occurs, resulting in aqueous tear deficiency and frequently a damaged ocular surface [26]. Extensive destruction, tissue atrophy, and fibrosis of the tubuloalveolar glands and ducts in the lacrimal gland have been shown in histology [21].

19.7.2 Symptoms and Signs

Ocular cGVHD mimics other immunologically mediated inflammatory diseases of the ocular surface, and there are no specific symptoms or clinical signs. Ocular manifestations, present in 60–90% of patients with cGVHD, primarily affect structures of the anterior segment, mainly the lacrimal glands, meibomian glands, and conjunctiva [27, 28] (Table 19.3). Typical symptoms of cGVHD are dry eye, photophobia, foreign body sensation, irritation, burning, epiphora, redness, and blurriness [28–30].

Table 19.3 Targeted ocular tissues in GVHD and their potential findings

Lacrimal gland	Decreased tear secretion
Meibomian gland	Meibomian gland inflammation or atrophy
Conjunctiva	Edema, chemosis
	Pseudomembranes
	Conjunctiva erosions
	Palpebral and subtarsal conjunctiva scarring
Cornea	Punctate keratopathy
	Mucus filaments
	Epithelial defects
	Secondary corneal infections
	Melt or necrosis
	Scarring
	Anesthesia

19.8 Target Tissues

19.8.1 Lacrimal Glands

The lacrimal glands are an important ocular target for the pathogenesis of GVHD, with cytotoxic effects mediated by both CD4+ and CD8+ T cells against the periductal epithelial cells of the lacrimal gland, resulting in ductal stenosis and aqueous tear deficiency. Fibrotic processes often affect both lacrimal glands, reducing their secretory capacity or causing complete stasis with distended ductules and obliteration of duct lumen, similar to bile duct damage seen in liver cGVHD [17]. Histological studies also show extensive destruction, tissue atrophy, and fibrosis of the tubuloalveolar glands and ducts in the lacrimal glands, with an increase in CD34+ stromal fibroblasts accompanied by mild lymphocytic infiltration [26].

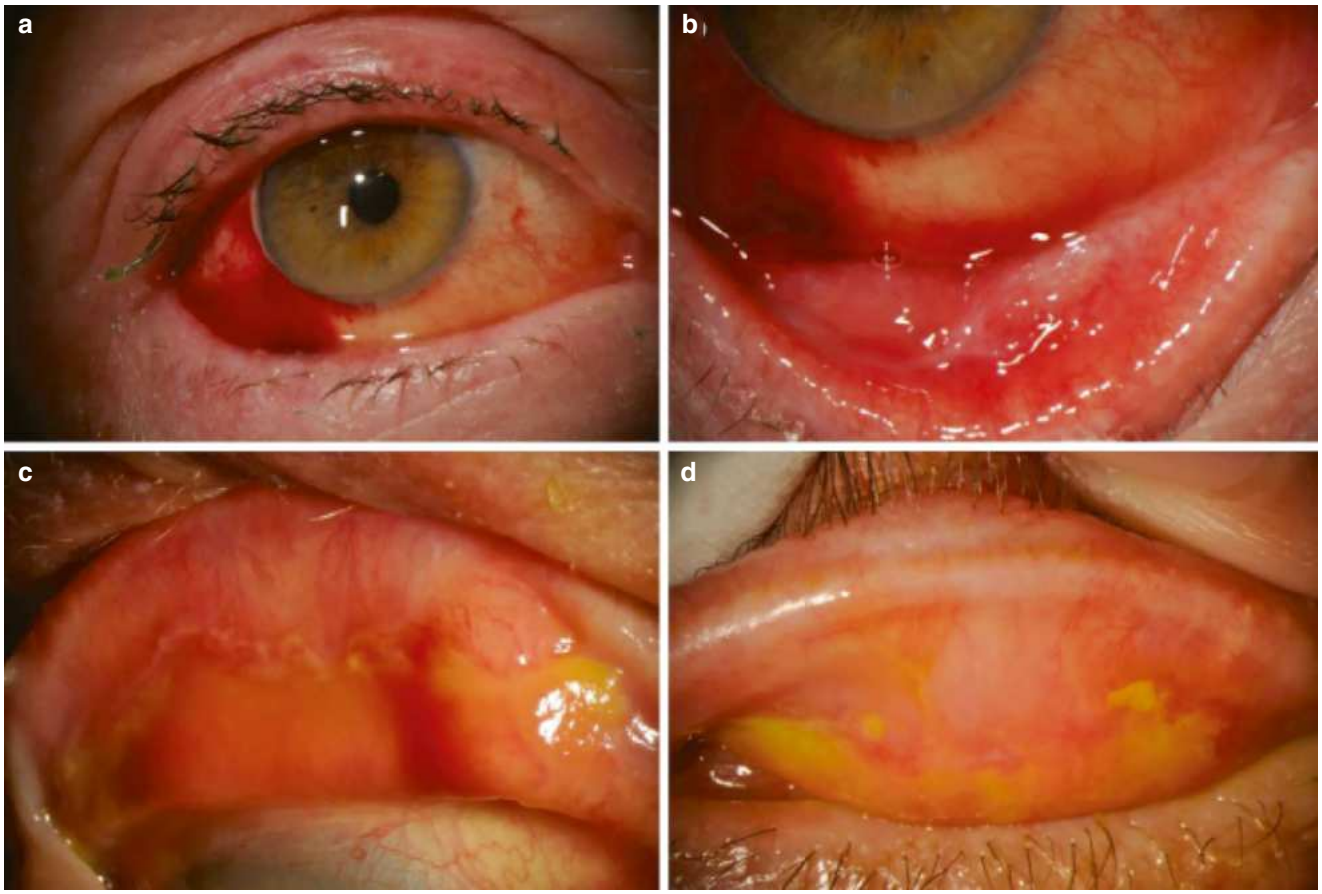

Fig. 19.2 Slit-lamp photos in a case of aGVHD demonstrating bilateral membrane formation in the bulbar (**a**, **b**) and tarsal conjunctiva (**c**, **d**) a few weeks posttransplantation

19.8.2 Meibomian Glands

Besides aqueous tear deficiency, a progressive decline of conjunctival goblet cells and the dysfunction of meibomian glands contribute to the overall breakdown of the ocular tear film, causing severe keratoconjunctivitis sicca [27, 31]. In vivo confocal microscopy shows destruction of the ductal epithelia due to lymphocyte infiltration, sloughing of epithelial cells, pseudomembrane formation, and subsequent excessive fibrosis around the orifices, ducts, ductules, and acini of the meibomian glands. Together, all these findings explain the development of meibomian gland disease [32].

19.8.3 Conjunctiva

Pseudomembranous conjunctivitis can rarely occur in cGVHD and is partly considered an acute variant of GVHD [31]. Sterile inflammatory conjunctival involvement is a common finding, which can be accompanied by subconjunctival hemorrhage, formation of pseudomembranes, loss of lashes, and punctal stenosis or closure (Fig. 19.2). Palpebral and subtarsal conjunctival scarring is seen in a number of patients, sometimes resulting in the formation of cicatricial lagophthalmos (Fig. 19.3a) [31, 33].

19.8.4 Cornea

Corneal findings include punctate keratopathy, formation of mucus filaments, painful erosions, secondary corneal infections, and eventually, scarring and neovascularization (Fig. 19.3b) [28, 31, 33]. Less frequently, sterile corneal stromal necrosis and perforations may occur [34]. Decreased innervation and increased dendritic cells are noted with confocal microsmicroscopy [35]. Superior limbic keratoconjunctivitis in the setting of ocular chronic GVHD is believed to be more common in peripheral stem cell transplantation patients compared with bone marrow copy recipients [27].

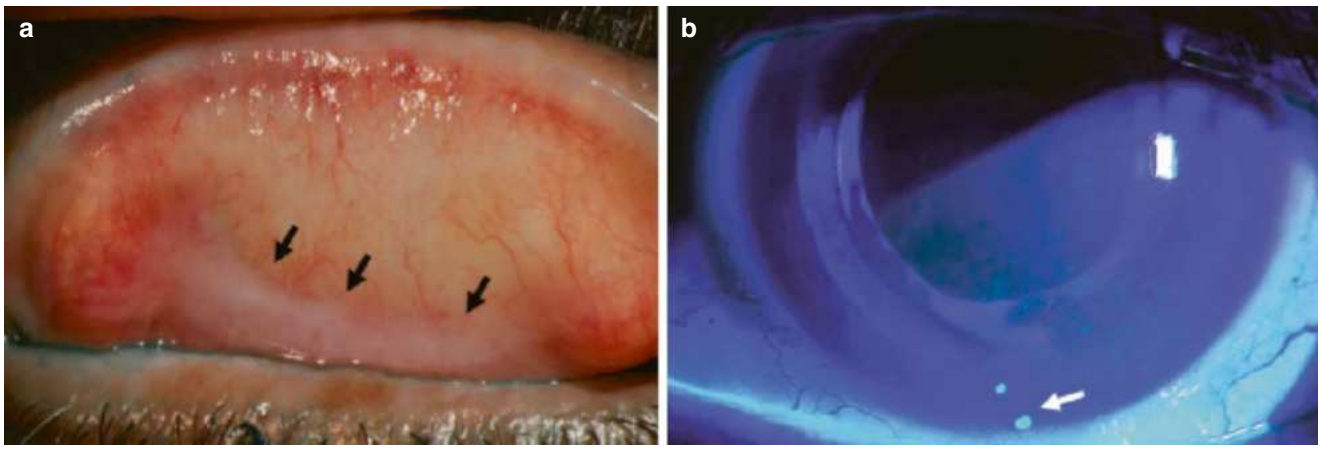

Fig. 19.3 Slit lamp photos show typical findings in cases of chronic ocular GVHD in this 47-year-old male 2 years posttransplantation. Subtarsal fibrosis is a common finding in these patients and is easily noted with lid eversion, shown by black arrows (**a**). Fluorescein staining demonstrates punctate erosion localized mostly in the exposure area of the cornea and filaments, shown by white arrow (**b**)

19.8.5 Diagnostic Evaluation

A full ophthalmological exam, including best-corrected visual acuity and slit lamp examination using vital dyes such as lissamine green, rose bengal stain, or fluorescein dyes is needed to evaluate punctate keratopathy, corneal erosions, or ulcers. Additionally, a thorough subtarsal and meibomian gland inspection, evaluation of tear film break-up time, and a Schirmer test are essential in patients suspected of having ocular GVHD [27, 28]. According to Filipovich et al. [18], a diagnosis of chronic GVHD can be made by low Schirmer test values (without topical anesthesia) with a mean value of <5 mm at 5 min in both eyes. This is considered sufficient for ocular GVHD trials, but a positive Schirmer test accompanied by distinctive manifestations in at least one other organ is required for the diagnosis of chronic systemic GVHD and potential inclusion in general chronic GVHD trials [19].

While the Schirmer test is useful for diagnosis, serial values poorly correlate to patient-reported symptoms during follow-up [36]. Follow-up should focus more on evaluating the frequency of lubricating eye drops, the ability to conduct activities of daily living, and decreased vision due to dry eye [19]. Special diagnostics such as tear film osmolarity, corneal sensitivity testing, in vivo confocal microscopy for inflammatory cells, and photo documentation can also assist in therapeutic decisions and follow-up. It may also be beneficial to use quality-of-life questionnaires such as the Ocular Surface Disease Index to evaluate the extent of the disease and the response to treatment.

Slit-lamp examination of the lens should also be performed to assess for posterior subcapsular cataract, which commonly occurs secondary to steroid and radiation treatment [37]. Systemic steroid therapy and topical steroid therapy also necessitate assessment for glaucoma, including intraocular pressure measurements and visual field testing. Posterior scleritis, choroidal thickening, and serous detachments have rarely been observed in the acute or hyperacute GVHD setting and are also thought to be related to sequela of total body radiation or frequent, high-dose, systemic steroid use [27].

19.8.6 Differential Diagnosis

The most common ocular manifestation of GVHD is keratoconjunctivitis sicca, which usually develops in conjunction with inflammatory signs of the conjunctiva (conjunctival edema, chemosis, pseudomembrane formation) and chronic blepharitis [27, 31]. Keratoconjunctivitis sicca primarily results from either aqueous tear deficiency or abnormal tear composition. Other less common causes include decreased nerve sensitivity, eyelid disorders, and decreased tear production, which may occur in certain systemic disease processes and aging. The differential diagnosis of aqueous tear deficiency consists of autoimmune diseases such as Sjögren's syndrome, a multitude of medications (i.e., antihistamines or antidepressants), and any disease process that results in infiltration of the lacrimal gland, including sarcoidosis, tumors, or post-radiation fibrosis.

Profound atrophy of the eyelid margin, keratinization of the palpebral conjunctiva, development of entropion or ectropion, atrophy of the meibomian glands, loss of lashes, and stenosis, or closure of the lacrimal punctum can all occur consequently from cGVHD [38].

19.9 Treatment of Systemic GVHD

19.9.1 Biomarkers in Serum and Tears

Currently, no specific serum biomarkers have been established for the diagnosis of systemic GVHD; however, there are multiple proteins and gene polymorphisms that have

been associated with cGVHD. Additionally, the ratio of tolerogenic to pro-inflammatory cells is being studied as a potential indicator and target for therapy [12]. Tears have been examined for possible biomarkers as well. Studies have identified numerous pro-inflammatory cytokines that are elevated in patients with cGVHD, including IL-1, IL-2, IL-6, IL-8, IL-10, IL-17, IP-10/CXL-10, ICAM-1, TNF-alpha, EGF, lymphotoxin-alpha (LT-alpha), E-selectin, B-cell activation factor, and neuropilin-1 [39]. One study compared 22 patients with chronic GVHD to 21 healthy subjects and concluded that elevated levels of both IL-8/CXCL8 and IP-10/CXCL10 could be predictive of ocular cGVHD when combined with age and sex to yield a sensitivity of 86% and specificity of 95% [39].

19.9.2 Prevention of Systemic GVHD

Prevention of acute GVHD by the use of pharmacologic prophylaxis is an integral component of the management of patients undergoing allogeneic HSCT [7, 20, 22, 31]. A regimen based on methotrexate with a calcineurin inhibitor, a cytoplasmic enzyme important for the activation of T-cells, is a standard practice and is recommended in different studies [20, 22, 31]. For higher-risk groups (such as mismatched donors and older patients), more intensive immunosuppression is often required [7, 31].

19.9.3 Treatment of Established Systemic GVHD

Although many therapeutic options have been used in the management of systemic GVHD, adequate treatment remains a challenge. The management is guided by a multidisciplinary approach, including adjustment of immunosuppression and aggressive supportive care. The treatment approach should include multiple strategies (topical and oral medications, surgery, environmental control, and systemic immunosuppression). Communication with the transplantation team is crucial for optimal management of GVHD patients. However, in patients with cGVHD that involves three or more organs or severe damage in any single organ, systemic immunosuppressive therapy may be considered [19].

Use of steroids, with or without the concomitant use of a calcineurin inhibitor, remains the standard of care. Second-line options include immunomodulatory therapies (extracorporeal photopheresis, mechanistic target of rapamycin inhibitors, thalidomide, hydroxychloroquine, vitamin A analogues, and clofazimine) and cytotoxic agents (mycophenolate, methotrexate, cyclophosphamide, pentostatin) [40]. cGVHD has been associated with increased B-cell activation, and further therapies have targeted B-cell receptor signaling [12]. Recently ibrutinib, a treatment for B-cell cancers that targets Bruton's tyrosine kinase and interleukin-2inducible T-cell kinase, became the first FDA-approved drug for glucocorticoid-resistant chronic GVHD [12].

19.9.4 Treatment of Ocular GVHD

Patients with ocular symptoms need close ocular supportive care focused on improving ocular surface lubrication, eyelid anatomy and function, and decreasing ocular surface inflammation. See Table 19.4.

19.9.4.1 Topical Lubricants

The traditional treatment for dry eye symptoms consists of topical lubricants [28, 41]. Many brands are available, and there is a large individual variability in symptom relief efficiency and tolerance. No data is available on the efficacy of specific artificial tear brands in ocular GVHD, and often, they are not adequate to control severe symptoms. Ocular cGVHD is a complex problem of the ocular surface with multiple dysfunctional tear components.

19.9.4.2 Topical Corticosteroids

Corticosteroids remain essential for controlling active chronic graft-versus-host disease. Systemic steroids represent the mainstay in the treatment of exacerbations of cGVHD, but not enough data are available on the efficacy of topical steroids in ocular GVHD. In a small study of seven patients with conjunctival GVHD, resolution or improvement of the conjunctival signs was achieved using topical 1% prednisolone, but the signs of sicca remained unchanged [42]. In contrast, Yin et al. argued against the efficacy of low-dose steroids in the treatment of sicca symptoms in cGVHD [43]. Patients receiving topical corticosteroids should be monitored for adverse effects. In the presence of corneal epithelial defects, stromal thinning, or infiltrates, topical corticosteroids are contraindicated.

Table 19.4 Treatment options for ocular GVHD

Ocular treatments	Systemic treatments
Artificial tears	Oral corticosteroids
Lubricating ointment	Mycophenolate Mofetil
Punctual occlusion/cautery	Doxycyclycine
Topical corticosteroids	Sirolimus
Tacrolimus	Tacrolimus
Mucolytic (10% *N*-acetylcysteine) therapy	Extracorporeal Photopheresis
Cyclosporine A	
Autologous serum drops	
Bandage contact lens	
Scleral contact lens	
Tarsorrhaphy	

19.9.4.3 Topical Cyclosporine A

Cyclosporine A is a cyclic polypeptide produced by the fungus *Tolypocladium inflatum* Gams. Cyclosporine 0.05% ophthalmic emulsion (Restasis; Allergan, Inc., Irvine, CA) has been FDA-approved for the treatment of dry eye disease since 2003. Cyclosporine A emulsion has been shown to decrease the number of activated T-cells in the ocular surface, increase the goblet cell density of the conjunctiva, decrease epithelial cell apoptosis, and reduce pro-inflammatory cytokines [44]. In patients with moderate to severe dry eye not related to GVHD, treatment with cyclosporine 0.05% or 0.1% gave significantly greater improvement than vehicle in two objective signs of dry eye disease: corneal staining and categorized Schirmer values [44]. In a small study of eight cGVHD patients treated with cyclosporine 0.05%, ophthalmic suspension was administered twice a day for at least 3 months. Researchers noted increased mean Schirmer scores, longer tear breakup time, and improved subjective symptoms [44]. In another study of only 16 patients (32 eyes) with ocular GVHD, dry eye symptoms improved in 62.5% of patients, and corneal fluorescein staining improved in all eyes after a mean follow-up of 90 days [45]. Baptista Malta reported a retrospective study with 105 patients, of whom 43 patients developed ocular cGVHD. All patients were initially started on topical cyclosporine before the HSCT. They concluded that cyclosporine is helpful in decreasing the incidence and severity of dry eyes in patients if started before the transplant [46].

19.9.4.4 Topical Tacrolimus

FK506 (tacrolimus) is a macrolide antibiotic extracted from the soil fungus *Streptomyces tsukubaensis*, and its mechanisms of action and pharmacokinetics are similar to CsA [47], although the immunosuppressive potency of tacrolimus in vitro is 50–200 times greater. Although the beneficial effect of systemic tacrolimus on ocular GVHD has been observed [20, 47], topical administration might seem a better treatment option because of the adverse effects associated with its long-term systemic administration. Topical tacrolimus was found to be safe, well-tolerated, and effective for the treatment of ocular GVHD [48–50]. Results from a randomized control trial (40 patients and 80 eyes, compared to topical methylprednisolone) demonstrated that tacrolimus was more effective than methylprednisolone at reducing the corneal fluorescein staining score (CFS) and ocular surface disease index (OSDI). Both methylprednisolone and tacrolimus decreased intercellular adhesion molecule-1 (ICAM-1) expression; however, only tacrolimus decreased HLA-DR expression. Neither drug affected the Schirmer test scores, and methylprednisolone was associated with a significant increase in intraocular pressure [50].

19.9.5 Novel Drug Therapies

Multiple clinical trials in various phases are currently recruiting or ongoing to test novel therapies for ocular GVHD and repurpose established medications used to treat other diseases. Existing therapies include brimonidine, vigamox, intravenous immune globulin, and lifitigrast [51]. Of these, lifitegrast was well tolerated and led to a significant reduction in the NIH ocular GVHD severity scores among 44% of patients; however, this was a small, retrospective cohort study (18 patients) [51]. New biologic therapies include umbilical mesenchymal stem cell-derived exosomes, DNAse eye drops, allogeneic platelet lysate eye drops, amniotic fluid eye drops, and cellular adhesion molecule-101.

19.9.6 Autologous Serum Eye Drops

Fox et al. described serum drops as a tear substitute free of preservatives in 1984. Autologous serum contains vitamin A, epidermal growth factor, fibronectin, and transforming growth factor beta, which are all needed for a healthy ocular surface epithelium [52]. The efficacy and safety of autologous serum drops were investigated in a small study of 14 patients with ocular GVHD and severe cGVHD not responsive to conventional therapy using artificial tears. After 4 weeks of treatment, significant improvement was observed in dryness symptoms and fluorescein scores and also in rose bengal staining and tear breakup time [53]. This improvement was noted in all patients at the 4-week follow-up [53]. The risk of contamination and subsequent infection is a possible complication of autologous serum drops. Administration of serum eye drops is one of the most effective therapies for symptom relief in our own experience.

19.9.7 Contact Lenses

In patients with cGVHD affecting the ocular surface, two different types of lenses can be used: the bandage soft lens [54] and the scleral rigid lens. The fluid-ventilated, gas-permeable scleral lens has been effective in mitigating symptoms and in the treatment of moderate and severe ocular surface disorders of multiple etiologies. The fluid-filled reservoir shields the cornea from blink trauma, noxious environmental stimuli, and inflammatory mediators in the tears. The body-temperature saline reservoir also prevents corneal cooling and nerve firing that occurs during the inter-blink intervals.

One of the scleral lenses used (Boston Scleral Lens Prosthetic Device) was approved for the management of corneal disorders by the Food and Drug Administration in 1994. Takahide published a retrospective review on nine patients fitted for refractory ocular surface disease secondary to cGVHD with this type of device [55], and a more recent publication with their experience is available [56]. Contact lens fitting was prompted by debilitating ocular discomfort, visual impairment, or keratopathy. Some of the patients evaluated were using artificial tears, cyclosporine eye drops, punctal plugs, autologous serum tears, and moisture cham-

ber eyewear. All patients reported improvement of ocular symptoms, reduced use of topical lubricants after fitting, and improvement in the Ocular Surface Disease Index [53].

The same group published results of 33 consecutive patients with severe dry eye from cGVHD, unresponsive to conventional therapy. Ninety-four percent of patients reported improvement in photophobia in the worse eye. Ninety-seven percent of patients reported improvement in life quality with no complications noted during the follow-up period [57]. Schornack reported the successful use of the Jupiter scleral contact lens (Medlens Innovations, Front Royal, VA or Essilor Contact Lens, Inc., Dallas, TX) in the management of ten eyes of five patients with cGVHD. All patients had improvement in symptoms and some improved visual acuity. Jupiter lenses are commercially available in the USA and may therefore be more accessible and affordable to patients who could potentially benefit from this treatment [58]. Similar results from Europe have been published [59].

Although scleral lenses are an essential tool in the armamentarium, their use is not widespread. Published data suggests that scleral rigid gas-permeable lenses are an important therapeutic option for patients with recalcitrant ocular surface compromise and debilitating symptoms. High cost, inadequate fitting, poor tolerance, and discomfort with blinking in the presence of severe meibomian gland disease and keratinization discourage their widespread use. To our knowledge, no comparative prospective study has evaluated differences between available scleral lenses.

19.9.8 Cataract Surgery in cGVHD

Posterior subscapular cataracts are more prevalent in patients with cGVHD due to radiation exposure and systemic corticosteroid use [60, 61]. Cataracts are considered the most common cause of decreased vision in patients with cGVHD [62]. cGVHD causes significant surface disease, and it is thought that the nerve and tissue damage induced by cataract surgery and toxicity from postoperative drops may exacerbate corneal pathology [61]. Retrospective reviews have shown that patients with even severe cGVHD can achieve good visual acuity after cataract surgery with aggressive pre- and postoperative treatment of surface disease [37, 60–65]. However, despite meticulous preoperative management, complications can still occur (Fig. 19.4). de Melo Franco et al. reviewed 72 eyes of 41 patients with cGVHD who underwent phacoemulsification cataract surgery and noted corneal ulceration with perforation in two eyes and band keratopathy in one eye [66]. These patients did not show worsening dry eye disease but had a worsening trend on the Ocular Surface Disease Index. Shah et al. reviewed ten eyes of six patients with severe cGVHD and found two patients who developed corneal melt months after surgery [37]. Saboo et al. reviewed 62 eyes with cGVHD who underwent surgery and found that 8% developed corneal epithelial defects, which resolved within a week

Fig. 19.4 Slit lamp photo shows an area of corneal melting in the right eye of this 37-year-old male with cGVHD and severe ocular involvement. Melting occurred 5 days after uneventful cataract surgery

of treatment. Additionally, 6% developed filamentary keratitis, and 16% developed corneal punctate keratitis in the acute postoperative period. Corneal punctate keratitis resolved within a month in a trend that matched the general population [63]. Given these potential issues, preoperative assessment should include a thorough review of systems to determine if the patient's systemic immunosuppression is adequate [37]. Preoperative treatment of surface disease includes, but is not limited to, artificial tears, lubricating ointment, punctual occlusion, cyclosporine, topical steroids, contact lenses, and serum tears. Preoperative measurements and imaging should show consistency on surface treatment in order to improve refractive accuracy. Considerations for the surgeon include a superior incision protected by the upper lid and less exposed to dryness, suturing the wound, and patching the eye after surgery.

19.9.9 Follow-Up

According to the participants in the German/ Austrian/ Swiss Consensus Conference on clinical practice in chronic GVHD, recommendations for monitoring patients include (1) a baseline ophthalmological workup including the Schirmer test before HSCT, (2) a screening examination at day 100–200 after HSCT, and (3) an ophthalmological assessment in case of ocular symptoms or any other manifestations of GVHD. An ophthalmologist should complete these examinations. This protocol allows for (1) a baseline examination to detect progressive KCS earlier, (2) a diagnosis of ocular cGVHD earlier, and (3) an early start with treatment to prevent excessive scarring and inflammation processes that may lead to serious complications.

19.10 Prognosis of GVHD

19.10.1 Systemic GVHD

Severe aGVHD has a poor prognosis, with 25% long-term survival (5 years) for grade III disease and 5% for grade IV [2]. In chronic GVHD, mild disease tends to have a good prognosis, whereas severe disease correlates with higher no-relapse mortality and survival [67]. Using the 2005 NIH global severity scoring, the 2-year overall survival was found to be 62%, 86%, and 97% in severe, moderate, and mild disease, respectively [67].

19.10.2 Ocular GVHD

Few authors have studied the long-term prognosis in patients affected by ocular cGVHD. In a case series of 49 patients, Sales et al. report that in the long term, dry eye symptoms diminish in many patients with cGVHD as a result of effective treatment. Although only nine patients completed this 3-year prospective case series, stable visual acuity, tear production, and lissamine green staining and a statistically insignificant improvement in dry eye symptoms were reported [21].

Another retrospective cohort study reported that 39% of 56 patients with cGVHD developed symptoms of photophobia, irritation, and foreign body sensation [68]. Over time, patients required fewer topical medications to control their symptoms; only 5% of patients required more than two medications for dry eye disease management at the end of follow-up [68].

In contrast, Ogawa et al. study on a series of 53 patients suggested that the symptoms of dry eye, including ocular fatigue, foreign body sensation, pain, blurring, photophobia, and epiphora, were almost universally worse among 22 participants at 30 months after HSCT in comparison to their status preceding HSCT [69] (Fig. 19.5).

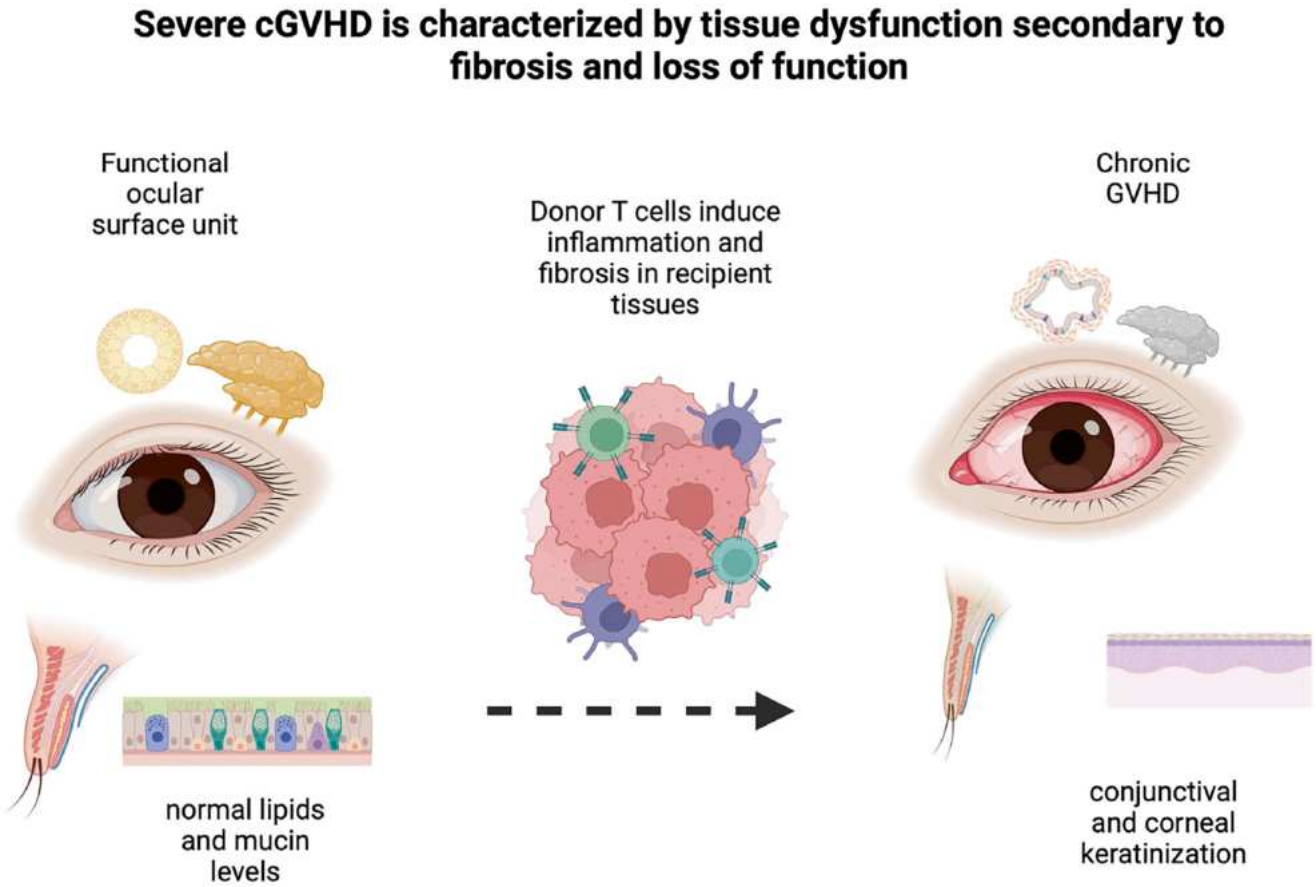
Severe cGVHD is characterized by tissue dysfunction secondary to fibrosis and loss of function
Functional ocular surface unit
Donor T cells induce inflammation and fibrosis in recipient tissues
Chronic GVHD
normal lipids and mucin levels
conjunctival and corneal keratinization

Fig. 19.5 Illustration summarizes the pathophysiology of cGVHD and the role of fibrosis induced by inflammation compromising tissue function. Characteristically, tissue fibrosis occurs in lids, conjunctiva, lacrimal glands, and meibomian glands. Antifibrotic treatments are needed in the future

References

1. Copelan EA. Hematopoietic stem-cell transplantation. N Engl J Med. 2006;354(17):1813–26.
2. Ferrara JL, Levine JE, Reddy P, et al. Graft-versus-host disease. Lancet. 2009;373(9674):1550–61.
3. de la Morena MT, Gatti RA. A history of bone marrow transplantation. Immunol Allergy Clin N Am. 2010;30(1):1–15.
4. Chen YB, Kawai T, Spitzer TR. Combined bone marrow and kidney transplantation for the induction of specific tolerance. Adv Hematol. 2016;2016:6471901.
5. Mancardi G, Sormani MP, Muraro PA, et al. Intense immunosuppression followed by autologous haematopoietic stem cell transplantation as a therapeutic strategy in aggressive forms of multiple sclerosis. Mult Scler. 2018;24(3):245–55.
6. Niederwieser D, Baldomero H, Szer J, et al. Hematopoietic stem cell transplantation activity worldwide in 2012 and a SWOT analysis of the Worldwide Network for Blood and Marrow Transplantation Group including the global survey. Bone Marrow Transplant. 2016;51(6):778–85.
7. Choi SW, Levine JE, Ferrara JL. Pathogenesis and management of graft-versus-host disease. Immunol Allergy Clin N Am. 2010;30(1):75–101.
8. Thomas ED, Lochte HL Jr, Lu WC, et al. Intravenous infusion of bone marrow in patients receiving radiation and chemotherapy. N Engl J Med. 1957;257(11):491–6.
9. Billingham RE. The biology of graft-versus-host reactions. Harvey Lect. 1966;62:21–78.
10. Kernan NA, Collins NH, Juliano L, et al. Clonable T lymphocytes in T cell-depleted bone marrow transplants correlate with development of graft-v-host disease. Blood. 1986;68(3):770–3.
11. Loiseau P, Busson M, Balere ML, et al. HLA association with hematopoietic stem cell transplantation outcome: the number of mismatches at HLA-A, -B, -C, -DRB1, or -DQB1 is strongly associated with overall survival. Biol Blood Marrow Transplant. 2007;13(8):965–74.
12. Zeiser R, Blazar BR. Pathophysiology of chronic graft-versus-host disease and therapeutic targets. N Engl J Med. 2017;377(26):2565–79.
13. Pidala J, Anasetti C, Kharfan-Dabaja MA, et al. Decision analysis of peripheral blood versus bone marrow hematopoietic stem cells for allogeneic hematopoietic cell transplantation. Biol Blood Marrow Transplant. 2009;15(11):1415–21.
14. Barker JN, Krepski TP, DeFor TE, et al. Searching for unrelated donor hematopoietic stem cells: availability and speed of umbilical cord blood versus bone marrow. Biol Blood Marrow Transplant. 2002;8(5):257–60.
15. Wagner JE, Barker JN, DeFor TE, et al. Transplantation of unrelated donor umbilical cord blood in 102 patients with malignant and nonmalignant diseases: influence of CD34 cell dose and HLA disparity on treatment-related mortality and survival. Blood. 2002;100(5):1611–8.
16. Platzbecker U, Ehninger G, Bornhauser M. Allogeneic transplantation of CD34+ selected hematopoietic cells—clinical problems and current challenges. Leuk Lymphoma. 2004;45(3):447–53.
17. Cooke KR, Luznik L, Sarantopoulos S, et al. The biology of chronic graft-versus-host disease: a task force report from the national institutes of health consensus development project on criteria for clinical trials in chronic graft-versus-host disease. Biol Blood Marrow Transplant. 2017;23(2):211–34.
18. Filipovich AH, Weisdorf D, Pavletic S, et al. National Institutes of Health consensus development project on criteria for clinical trials in chronic graft-versus-host disease: I. Diagnosis and staging working group report. Biol Blood Marrow Transplant. 2005;11(12):945–56.
19. Jagasia MH, Greinix HT, Arora M, et al. National Institutes of Health Consensus development project on criteria for clinical trials in chronic graft-versus-host disease: I. The 2014 Diagnosis and Staging Working Group report. Biol Blood Marrow Transplant. 2015;21(3):389–401.e1.
20. Ram R, Gafter-Gvili A, Yeshurun M, et al. Prophylaxis regimens for GVHD: systematic review and meta-analysis. Bone Marrow Transplant. 2009;43(8):643–53.
21. Sale GE. Does graft-versus-host disease attack epithelial stem cells? Mol Med Today. 1996;2(3):114–9.
22. Socie G, Blazar BR. Acute graft-versus-host disease: from the bench to the bedside. Blood. 2009;114(20):4327–36.
23. Jabs DA, Hirst LW, Green WR, et al. The eye in bone marrow transplantation. II. Histopathology. Arch Ophthalmol. 1983;101(4):585–90.
24. Hirst LW, Jabs DA, Tutschka PJ, et al. The eye in bone marrow transplantation. I. Clinical study. Arch Ophthalmol. 1983;101(4):580–4.
25. Ogawa Y, Kuwana M. Dry eye as a major complication associated with chronic graft-versus-host disease after hematopoietic stem cell transplantation. Cornea. 2003;22(7 Suppl):S19–27.
26. Ogawa Y, Kodama H, Kameyama K, et al. Donor fibroblast chimerism in the pathogenic fibrotic lesion of human chronic graft-versus-host disease. Invest Ophthalmol Vis Sci. 2005;46(12):4519–27.
27. Kim SK. Ocular graft vs. host disease. Ocul Surf. 2005;3(4 Suppl):S177–9.
28. Espana EM, Shah S, Santhiago MR, et al. Graft versus host disease: clinical evaluation, diagnosis and management. Graefes Arch Clin Exp Ophthalmol. 2013;251(5):1257–66.
29. Westeneng AC, Hettinga Y, Lokhorst H, et al. Ocular graft-versus-host disease after allogeneic stem cell transplantation. Cornea. 2010;29(7):758–63.
30. Blecha C, Wolff D, Holler B, et al. Verification of the new grading scale for ocular chronic graft-versus-host disease developed by the German-Austrian-Swiss consensus conference on chronic GVHD. Ann Hematol. 2016;95(3):493–9.
31. Riemens A, te Boome L, Imhof S, et al. Current insights into ocular graft-versus-host disease. Curr Opin Ophthalmol. 2010;21(6):485–94.
32. Ban Y, Ogawa Y, Ibrahim OM, et al. Morphologic evaluation of meibomian glands in chronic graft-versus-host disease using in vivo laser confocal microscopy. Mol Vis. 2011;17:2533–43.
33. Tabbara KF, Al-Ghamdi A, Al-Mohareb F, et al. Ocular findings after allogeneic hematopoietic stem cell transplantation. Ophthalmology. 2009;116(9):1624–9.
34. Koch KR, Joussen AM, Huber KK. Ocular involvement in chronic graft-versus-host disease: therapeutic approaches to complicated courses. Cornea. 2011;30(1):107–13.
35. He J, Ogawa Y, Mukai S, et al. In vivo confocal microscopy evaluation of ocular surface with graft-versus-host disease-related dry eye disease. Sci Rep. 2017;7(1):10720.
36. Inamoto Y, Chai X, Kurland BF, et al. Validation of measurement scales in ocular graft-versus-host disease. Ophthalmology. 2012;119(3):487–93.
37. Shah A, Santhiago MR, Espana EM. Cataract surgery in patients with chronic severe graft-versus-host disease. J Cataract Refract Surg. 2016;42(6):833–9.
38. Tung CI. Graft versus host disease: what should the oculoplastic surgeon know? Curr Opin Ophthalmol. 2017;28(5):499–504.
39. Cocho L, Fernandez I, Calonge M, et al. Biomarkers in ocular chronic graft versus host disease: tear cytokine- and chemokine-based predictive model. Invest Ophthalmol Vis Sci. 2016;57(2):746–58.
40. Wolff D, Schleuning M, von Harsdorf S, et al. Consensus conference on clinical practice in chronic GVHD: second-line treatment of chronic graft-versus-host disease. Biol Blood Marrow Transplant. 2011;17(1):1–17.

41. Savini G, Prabhawasat P, Kojima T, et al. The challenge of dry eye diagnosis. Clin Ophthalmol. 2008;2(1):31–55.
42. Robinson MR, Lee SS, Rubin BI, et al. Topical corticosteroid therapy for cicatricial conjunctivitis associated with chronic graft-versus-host disease. Bone Marrow Transplant. 2004;33(10):1031–5.
43. Yin J, Kheirkhah A, Dohlman T, et al. Reduced efficacy of low-dose topical steroids in dry eye disease associated with graft-versus-host disease. Am J Ophthalmol. 2018;190:17–23. pii: S0002-9394(18)30125-9.
44. Donnenfeld E, Pflugfelder SC. Topical ophthalmic cyclosporine: pharmacology and clinical uses. Surv Ophthalmol. 2009;54(3):321–38.
45. Lelli GJ Jr, Musch DC, Gupta A, et al. Ophthalmic cyclosporine use in ocular GVHD. Cornea. 2006;25(6):635–8.
46. Malta JB, Soong HK, Shtein RM, et al. Treatment of ocular graft-versus-host disease with topical cyclosporine 0.05%. Cornea. 2010;29(12):1392–6.
47. Simpson D. Drug therapy for acute graft-versus-host disease prophylaxis. J Hematother Stem Cell Res. 2000;9(3):317–25.
48. Ogawa Y, Okamoto S, Kuwana M, et al. Successful treatment of dry eye in two patients with chronic graft-versus-host disease with systemic administration of FK506 and corticosteroids. Cornea. 2001;20(4):430–4.
49. Tam PM, Young AL, Cheng LL, et al. Topical 0.03% tacrolimus ointment in the management of ocular surface inflammation in chronic GVHD. Bone Marrow Transplant. 2010;45(5):957–8.
50. Abud TB, Amparo F, Saboo US, et al. A clinical trial comparing the safety and efficacy of topical tacrolimus versus methylprednisolone in ocular graft-versus-host disease. Ophthalmology. 2016;123(7):1449–57.
51. Cheng X, Huang R, Huang S, et al. Recent advances in ocular graft-versus-host disease. Front Immunol. 2023;14:1092108.
52. Rocha EM, Pelegrino FS, de Paiva CS, et al. GVHD dry eyes treated with autologous serum tears. Bone Marrow Transplant. 2000;25(10):1101–3.
53. Ogawa Y, Okamoto S, Mori T, et al. Autologous serum eye drops for the treatment of severe dry eye in patients with chronic graft-versus-host disease. Bone Marrow Transplant. 2003;31(7):579–83.
54. Inamoto Y, Sun YC, Flowers ME, et al. Bandage soft contact lenses for ocular graft-versus-host disease. Biol Blood Marrow Transplant. 2015;21(11):2002–7.
55. Takahide K, Parker PM, Wu M, et al. Use of fluid-ventilated, gas-permeable scleral lens for management of severe keratoconjunctivitis sicca secondary to chronic graft-versus-host disease. Biol Blood Marrow Transplant. 2007;13(9):1016–21.
56. DeLoss KS, Le HG, Gire A, et al. PROSE treatment for ocular chronic graft-versus-host disease as a clinical network expands. Eye Contact Lens. 2016;42(4):262–6.
57. Jacobs DS, Rosenthal P. Boston scleral lens prosthetic device for treatment of severe dry eye in chronic graft-versus-host disease. Cornea. 2007;26(10):1195–9.
58. Schornack MM, Baratz KH, Patel SV, et al. Jupiter scleral lenses in the management of chronic graft versus host disease. Eye Contact Lens. 2008;34(6):302–5.
59. Magro L, Gauthier J, Richet M, et al. Scleral lenses for severe chronic GvHD-related keratoconjunctivitis sicca: a retrospective study by the SFGM-TC. Bone Marrow Transplant. 2017;52(6):878–82.
60. Benyunes MC, Sullivan KM, Deeg HJ, et al. Cataracts after bone marrow transplantation: long-term follow-up of adults treated with fractionated total body irradiation. Int J Radiat Oncol Biol Phys. 1995;32(3):661–70.
61. Dunn JP, Jabs DA, Wingard J, et al. Bone marrow transplantation and cataract development. Arch Ophthalmol. 1993;111(10):1367–73.
62. Allan EJ, Flowers ME, Lin MP, et al. Visual acuity and anterior segment findings in chronic graft-versus-host disease. Cornea. 2011;30(12):1392–7.
63. Saboo US, Amparo F, Shikari H, et al. Outcomes of phacoemulsification in patients with chronic ocular graft-versus-host disease. Graefes Arch Clin Exp Ophthalmol. 2015;253(6):901–7.
64. Balaram M, Dana MR. Phacoemulsification in patients after allogeneic bone marrow transplantation. Ophthalmology. 2001;108(9):1682–7.
65. Penn EA, Soong HK. Cataract surgery in allogeneic bone marrow transplant recipients with graft-versus-host disease(1). J Cataract Refract Surg. 2002;28(3):417–20.
66. de Melo FR, Kron-Gray MM, De la Parra-Colin P, et al. Outcomes of cataract surgery in graft-versus-host disease. Cornea. 2015;34(5):506–11.
67. Arai S, Jagasia M, Storer B, et al. Global and organ-specific chronic graft-versus-host disease severity according to the 2005 NIH Consensus Criteria. Blood. 2011;118(15):4242–9.
68. de la Parra-Colin P, Agahan AL, Perez-Simon JA, et al. Dry eye disease in chronic graft-versus-host disease: results from a Spanish retrospective cohort study. Transplant Proc. 2011;43(5):1934–8.
69. Ogawa Y, Okamoto S, Wakui M, et al. Dry eye after haematopoietic stem cell transplantation. Br J Ophthalmol. 1999;83(10):1125–30.

Diagnostic Techniques: Angiography

20

Ahmet Kaan Gündüz and Yağmur Seda Yeşiltaş

20.1 Introduction

Intraocular tumors are usually diagnosed clinically. Fluorescein angiography (FA) and indocyanine green angiography (ICGA) are usually not needed to diagnose the majority of intraocular tumors. However, these diagnostic techniques are still widely used in the evaluation of retinal and choroidal tumors as ancillary tests. Fluorescein angiography provides visualization of the retinal tumors while ICGA reveals vascular patterns of the choroidal tumors. Fluorescein angiography can still provide important information in certain choroidal tumors and in demonstrating choroidal folds. Among choroidal tumors, ICGA is particularly useful in establishing the diagnosis of choroidal hemangioma, both circumscribed and diffuse types. Indocyanine green angiography also plays an important role in differentiating neoplastic conditions from non-neoplastic lesions, including central serous chorioretinopathy and polypoidal choroidal vasculopathy (Table 20.1). In addition, over the past few decades, these dye-based invasive diagnostic procedures have played a pivotal role in expanding our understanding of retinal and choroidal anatomy, pathology, and physiology. Ocular angiography techniques are also used to assess disease progression and treatment side effects (e.g., radiation retinopathy). Composite image technology and wide-angle angiography systems have made it possible to see multiple or extensive areas of interest in one photograph, improving diagnostic accuracy.

Fluorescein angiography has recently been supplemented by optical coherence tomography angiography (OCTA) in the evaluation of tumors at the posterior pole as well as radiation retinopathy. OCTA is a non-invasive, dye-less procedure that provides information concerning both the superficial and deep capillary plexuses as well as the choroidal vasculature, whereas FA gives information about only the superficial capillary plexus. OCTA does not require an injection of dye and,

Table 20.1 Fluorescein (FA) and indocyanine green angiographic (ICGA) findings of some common retinal and choroidal tumors

Lesion	FA (early)	FA (mid)	FA (late)	ICGA (early)	ICGA (late)
Retinoblastoma	Hyper	Hyper	Hyper, leakage	NA	NA
Retinal hemangioblastoma	Hyper	Hyper	Hyper, leakage	Hyper	Hyper, leakage
Retinal vasoproliferative tumor	Hyper	Hyper	Hyper, leakage	Hyper	Hyper, leakage
RPE adenoma	Hypo	Hyper	Hyper, leakage	Hyper	Hyper, leakage
Choroidal nevus	Hypo	Hypo	Hypo	Hypo	Hypo
Choroidal melanoma	Hypo, hyper	Hyper	Hyper, leakage	Hypo, iso	Hypo, iso
Choroidal hemangioma	Hyper	Hyper	Hyper, leakage	Hyper	Hypo
Choroidal metastasis	Hypo	Hyper	Hyper	Hypo	Hypo
Choroidal lymphoma	Hypo	Hypo	Hypo	Hypo	Hyper, hypo
Vitreoretinal lymphoma	Hypo	Hyper	Hyper	Hypo	Hyper, hypo

Hypo hypofluorescence, *iso* isofluorescence, *hyper* hyperfluorescence, *NA* enough data not available, *RPE* retinal pigment epithelium

A. K. Gündüz (✉)
Department of Ophthalmology, Ankara University Faculty of Medicine, Ankara, Turkey

Y. S. Yeşiltaş
Department of Ophthalmology, University of Health Sciences, Gülhane Training and Research Hospital, Ankara, Turkey

© The Author(s), under exclusive license to Springer Nature Switzerland AG 2025

A. D. Singh, B. E. Damato (eds.), *Clinical Ophthalmic Oncology*, https://doi.org/10.1007/978-3-031-75907-9_20

therefore, avoids the adverse effects arising from the dyes used in angiography. Many OCTA platforms can only image the posterior segment of the eye. Intraocular tumors can manifest around the optic disc and in the macula but also anywhere in the fundus; therefore, FA and ICGA are still useful in evaluating more peripheral tumors and simulating conditions.

20.2 Basic Principles

Both FA and ICGA are based upon fluorescence, whereby light of shorter wavelengths (higher frequency and thus higher energy) is absorbed by molecules of the dye, which are excited to a higher energy state. As these molecules return to a lower energy state, they release energy in the form of light with a higher wavelength (lower energy). Fluorescein angiography uses fluorescein sodium, which absorbs light around 490 nm (blue wavelength) and emits at 514 nm (green). Indocyanine green (ICG) absorbs light at around 790 nm (near-infrared) and emits around 810 nm. The camera uses a filter that only allows the lower wavelengths to enter the eye and another filter that only allows the higher wavelengths back into the detector or film [1].

Higher wavelengths tend to be scattered less by tissues than lower wavelengths, and therefore, ICG is superior for deeper choroidal lesions. Conversely, lower wavelengths have greater resolution so that anterior retinal lesions are better visualized by fluorescein than with ICG.

20.2.1 Technique and Contraindications of FA

Sodium fluorescein is usually injected as a bolus into the antecubital vein of the elbow or radial vein of the wrist. Usually, 5 mL of 10% fluorescein is used. Sodium fluorescein has a molecular weight of 354 Da. About 80% of sodium fluorescein is bound to plasma proteins; therefore, it leaks profusely out of choriocapillaris and leads to a fluorescein paddle, limiting the visualization of choroidal structures.

Fluorescein angiography is characterized by five phases. Pre-arterial or choroidal flush phase starts 10–12 s after dye injection. The second phase, known as the arterial phase, begins seconds after the pre-arterial phase with simultaneous filling of the entire arterial tree. The third phase is the arteriovenous phase and represents start of flow from the retinal capillaries into the venules. The retinal veins demonstrate a railroad track sign as the vessel walls show early staining. The fourth phase is the venous phase, occurring 30–35 s postinjection, and is characterized by complete venous filling, including a recirculation phase after venous drainage. The fifth phase is the late or recirculation phase in which second and third passes of dye occur and hyperfluorescence is greater in the venules than in the arterioles.

Though allergy to this dye is rare, severe cases of anaphylaxis have occurred. Some patients develop hives, and in these cases, it is best not to use fluorescein again. More commonly, patients develop nausea from the injection. This is not a true allergy and slowing the infusion rate can decrease the recurrence of this event. The sodium in the fluorophore can cause worsening of heart failure or hypertension in patients with severe renal insufficiency, so care should be used in these individuals. However, there is no sufficient information precluding the use of FA in patients with cardiovascular or renal disease, including those on dialysis. Fluorescein angiography should probably not be done during pregnancy, especially in the first trimester.

20.2.2 Technique and Contraindications of ICGA

Indocyanine green angiography utilizes a water-soluble tricarbocyanine dye that is 98% bound to plasma proteins confined within blood vessels. Therefore, it leaks slowly through the fenestrations of the choriocapillaris. This feature, together with the long-wavelength of light used in ICGA, allows for better visualization of deeper choroidal vasculature. Indocyanine green has a molecular weight of 775 Da. Usually, 25 mg of the dye in 5 mL is injected either immediately after fluorescein injection or as a mixture of both fluorescein and ICG. This dye fluoresces in the infrared frequencies, allowing visualization through retinal and thin subretinal hemorrhages as well as lipid and pigment to better image the choroid.

Normal ICGA phases include early phase (<3 min), midphase (3–15 min), and late phase (15–60 min). The early phase is characterized by the filling of the retinal arteries and choriocapillaris, followed by choroidal veins. Towards the end of the early phase, these vessels start to fade. In the midphase, there is continued fading of choroidal and retinal vessels. The late phase is characterized by staining of extrachoroidal tissue so that the choroidal tissue becomes relatively hypofluorescent.

There is iodine in ICG, so patients who are truly allergic to iodine should not undergo ICGA. True iodine allergy is rare. Individuals with seafood allergy most often have an allergy to proteins in the seafood and not to iodine [2]. Indocyanine green is eliminated mainly through the liver. Therefore, ICGA is not recommended in patients with severe liver disease. Indocyanine green angiography is not cleared for use in pregnancy, similar to FA.

20.3 Recent Definitions on Widefield and Ultra-widefield Imaging

The conventional fundus photographs provide view of the posterior pole within the major vascular arcades and slightly beyond, which corresponds to a viewing angle of 50°. It is possible to construct montage or composite color fundus photographs, which provide an extended field of view. The terms widefield (WF) and ultra-widefield (UWF) imaging were frequently used without a clear agreement on the definitions of these terms. Recently, a consensus group of retinal imaging experts (International Widefield Imaging Study) formalized a definition of the terms based on anatomic landmarks [3]. Based on their consensus, WF images were defined as a single-capture image, centered on the fovea, which captures retinal anatomic features beyond the posterior pole but *posterior* to the vortex vein ampullae in all four quadrants. Ultra-widefield was defined as a single-capture image, centered on the fovea, which captures retinal anatomic features *anterior* to the vortex vein ampullae in all four quadrants. Widefield images provide a 60–100° field of view and UWF images about 110–220°. There is currently no imaging modality available for panretinal fundus imaging covering the entire fundus to the ora serrata. Current studies with UWF imaging have suggested important clinical applications for numerous retinal diseases including diabetic retinopathy, retinal vein occlusion, pediatric vitreoretinal disorders, uveitis, and posterior segment tumors as well as in telemedicine applications. The ability to capture large fundus tumors in a single shot without the need for composite imaging and inherent technical difficulties and problems is a major advance from the ocular oncology perspective. Many devices, including Zeiss Clarus 700 (133°), RetCam (130°), Optos (200°), and Heidelberg Spectralis (110°) allow for UWF color imaging and FA. With the exception of RetCam, these devices also possess software for fundus autofluorescence and ICGA imaging.

20.4 Anterior Segment Tumors

20.4.1 Iris Tumors

The three most common anterior segment tumors include iris nevus (42%), iris pigment epithelial cyst (19%), and iris melanomas (17%) [4]. These three lesions comprise 78% of all iris tumors. There are several other tumors and simulating conditions that can occur in the iris including vascular, metastatic, epithelial, and myogenic tumors; granulomas; and iris stromal cysts [4]. Tumors and granulomas of the iris tend to have blood vessels that can be visualized by FA, together with any leakage (Fig. 20.1). Melanomas of the iris usually demonstrate intrinsic vascularity and leakage on FA (Fig. 20.1) [5–7]. The presence of intrinsic vessels +/− feeder vessels supports the diagnosis of iris melanoma, while the absence of these findings does not definitively exclude melanoma [5–7]. However, angiographic silence characterized by the normal appearance of iris vessels with the absence of feeder vessels, intrinsic vessels, or leakage usually indicates iris nevi rather than iris melanomas (Fig. 20.2) [4]. Therefore, FA does not reliably distinguish between benign and malignant iris lesions. Furthermore, FA holds significant utility in differentiating solid lesions from cysts since cysts typically exhibit lack of vascularization.

20.4.2 Vascular Anomalies of the Iris

Vascular anomalies of the iris are rare. They are classified into five distinct clinical entities based on their clinicopathologic features: racemose hemangioma or iris arteriovenous malformation (AVM), capillary hemangioma, cavernous hemangioma, microhemangiomatosis, and iris varix [8–11]. Iris capillary and cavernous hemangiomas can be associated with diffuse neonatal hemangiomatosis and cutaneous hemangiomas, including periorbital ones.

Microhemangiomatosis is associated with myotonic dystrophy and diabetes mellitus. Iris hemangiomas, including cavernous hemangioma, varix, and microhemangiomatosis, may cause spontaneous hyphema. Some types of iris hemangioma, including racemose hemangioma and microhemangiomatosis, are clearly documented on FA. For iris lesions, ICGA is similar to FA.

Iris AVM is the most common vascular tumor of the iris and can be subdivided into simple (single tortuous vessel) and complex (multiple convoluted vessel involvement). Fluorescein angiography of iris AVM shows uniform hyperfluorescence in the early phases and rapid transit in the affected iris vessels with no leakage in the late phase [11]. In between the AVM vessels are areas of non-perfusion of the iris. With FA, microhemangiomatosis is usually located on the pupillary margin and is hyperfluorescent with leakage of dye into the aqueous humor [10]. Iris cavernous hemangioma appears as a hypofluorescent mass without prominent feeder vessels or intrinsic vasculature throughout all phases of FA. Iris varix, especially those that have undergone thrombosis, may remain entirely hypofluorescent on FA [9].

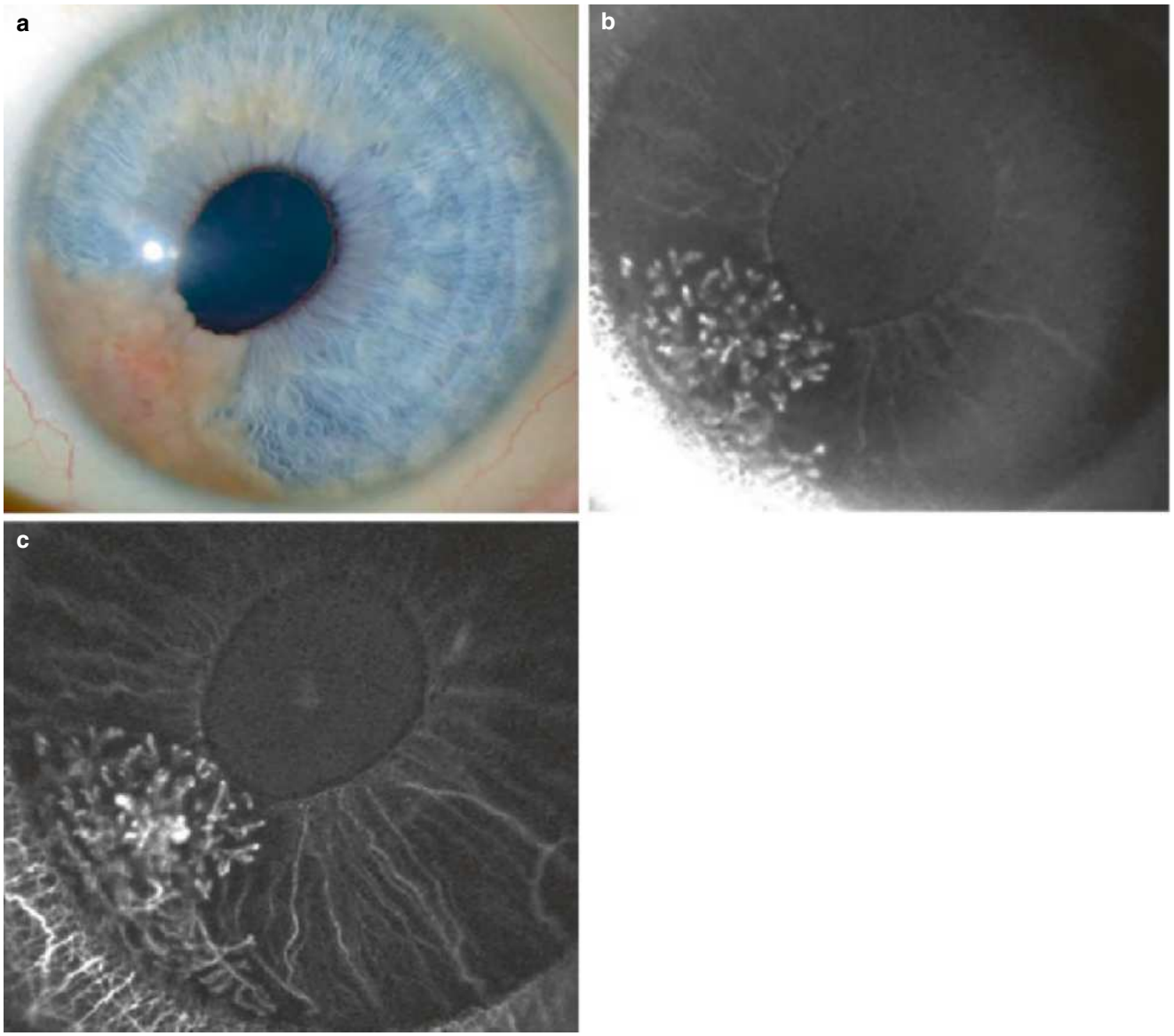

Fig. 20.1 Iris melanoma (**a**). Fluorescein (**b**) and ICG angiography (**c**) showing the intrinsic vascularity of the iris melanoma

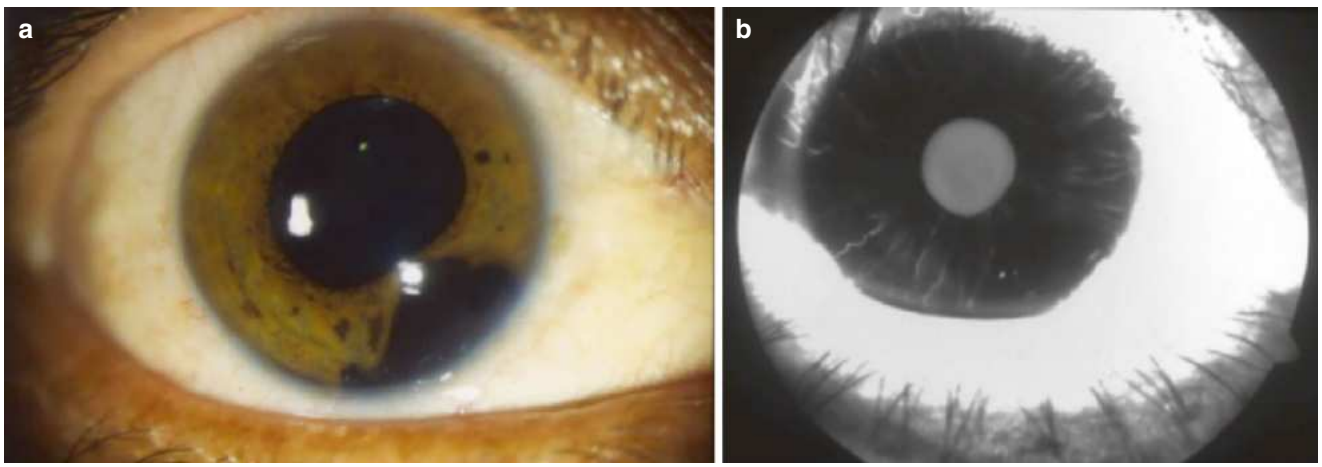

Fig. 20.2 Deeply pigmented iris melanocytoma (**a**). Fluorescein angiogram shows a predominantly hypofluorescent lesion with absence of feeder/intrinsic vessels or leakage (angiographic silence) in contrast to the iris melanoma depicted in Fig. 20.1 (**b**)

20.5 Retinal Tumors

In general, ICGA is not needed for retinal tumors since these are usually well-visualized by FA. Some exophytic retinal tumors that are masked by the overlying retina might be better visualized with ICGA. Table 20.1 lists the FA and ICGA features of retinal and choroidal tumors mentioned in this chapter. Retinal tumors covered in this section include retinoblastoma, retinal vascular tumors, retinal astrocytic hamartoma, and retinal pigment epithelial tumors.

20.5.1 Retinoblastoma

Fluorescein angiography shows retinoblastomas to be vascular, with rapid filling and late hyperfluorescence (Figs. 20.3 and 20.4) [8, 12]. During the vascular filling phase, the feeding arteries fill rapidly, and fine capillaries are seen in the superficial portions of the tumor. These vessels leak profusely in the later phases of FA. Leakage into the vitreous and subretinal space is seen in more advanced tumors. Large tumors show dilated and tortuous arterioles and draining veins. After successful treatment of the tumor, the blood supply is diminished or absent, and the lesion is more hypofluorescent [13]. Spontaneously arrested or regressed retinoblastomas also show variable degrees of hyperfluorescence even though they are clinically inactive.

20.5.2 Retinal Vascular Tumors

Retinal vascular tumors include retinal hemangioblastoma, retinal cavernous hemangioma, retinal arteriovenous malformation or racemose hemangioma, and retinal vasoproliferative tumor.

20.5.2.1 Retinal Hemangioblastoma (Retinal Capillary Hemangioma)

There are three types of retinal hemangioblastoma including papillary, exophytic, and endophytic tumors. Exophytic tumors grow into the subretinal space while endophytic tumors extend into the vitreous cavity[14, 15].

- Endophytic hemangioblastoma can usually be diagnosed based on clinical findings, especially if the tumor is not papillary. Endophytic hemangioblastoma has feeder and draining vessels. Fluorescein angiography is helpful in distinguishing the artery from the vein (Fig. 20.5). This determination is important if there is consideration of laser photocoagulation or even photodynamic therapy of the hemangioblastoma. By identifying the feeding artery, which would have shown fluorescence earlier than the tumor in FA, laser photocoagulation is first applied to the artery to slow flow to the tumor, allowing better uptake of laser energy by the vasculature of the tumor. In addition, high flow also inhibits the formation of occlusion by platelets or white cells in the vascular bed. Therefore, decreasing flow within the tumor also helps the formation of vascular occlusive events, contributing to tumor regression.
- Exophytic hemangioblastoma of the retina is less common than endophytic hemangioblastoma and papillary hemangioblastoma. The dilated feeding and draining vessels can be seen diving through the retina into the tumor, and FA can delineate these vessels. In these cases, as well as in exophytic papillary tumors, ICGA can reveal

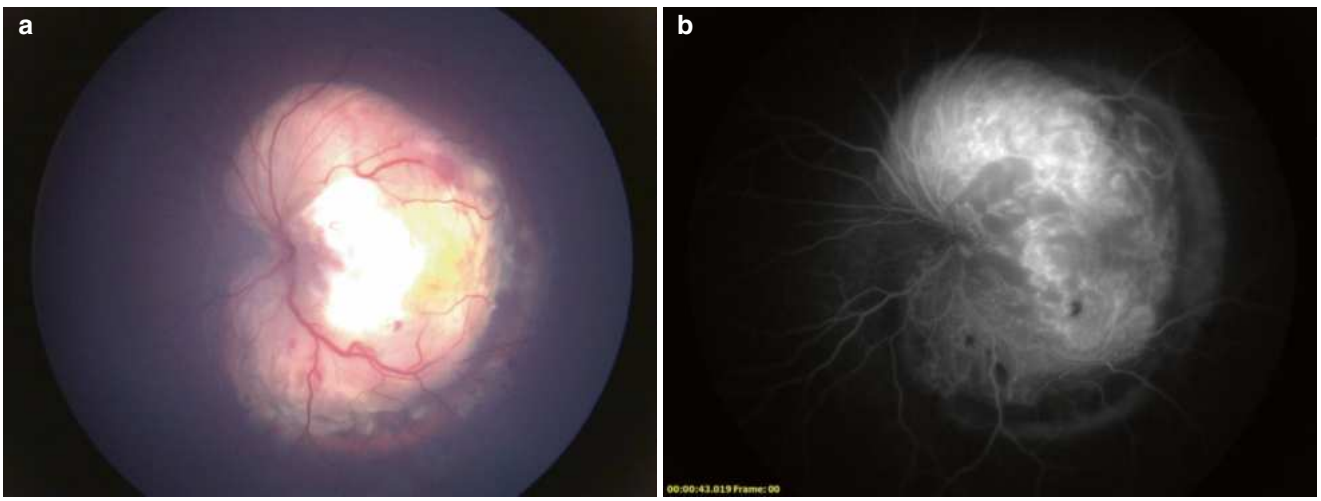

Fig. 20.3 RetCam color fundus photograph demonstrates group B retinoblastoma (**a**). RetCam fluorescein angiogram shows intense hyperfluorescence in the tumor in the early venous phase (**b**). The cuff of subretinal fluid surrounding the tumor appears hyperfluorescent due to the pooling of dye in the subretinal space. Few specks of retinal hemorrhage overlying the tumor manifest as hypofluorescent spots due to blockage of fluorescence

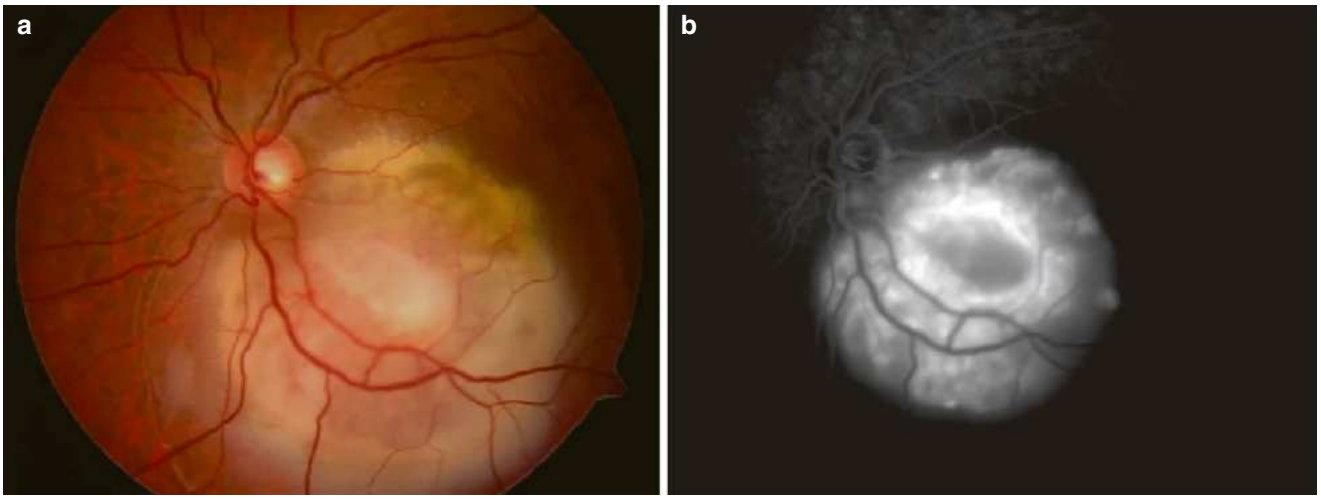

Fig. 20.4 Retinoblastoma that has undergone intravenous chemotherapy in the left eye (**a**). Fluorescein angiography still shows intense hyperfluorescence of the lesion in the late phase (**b**)

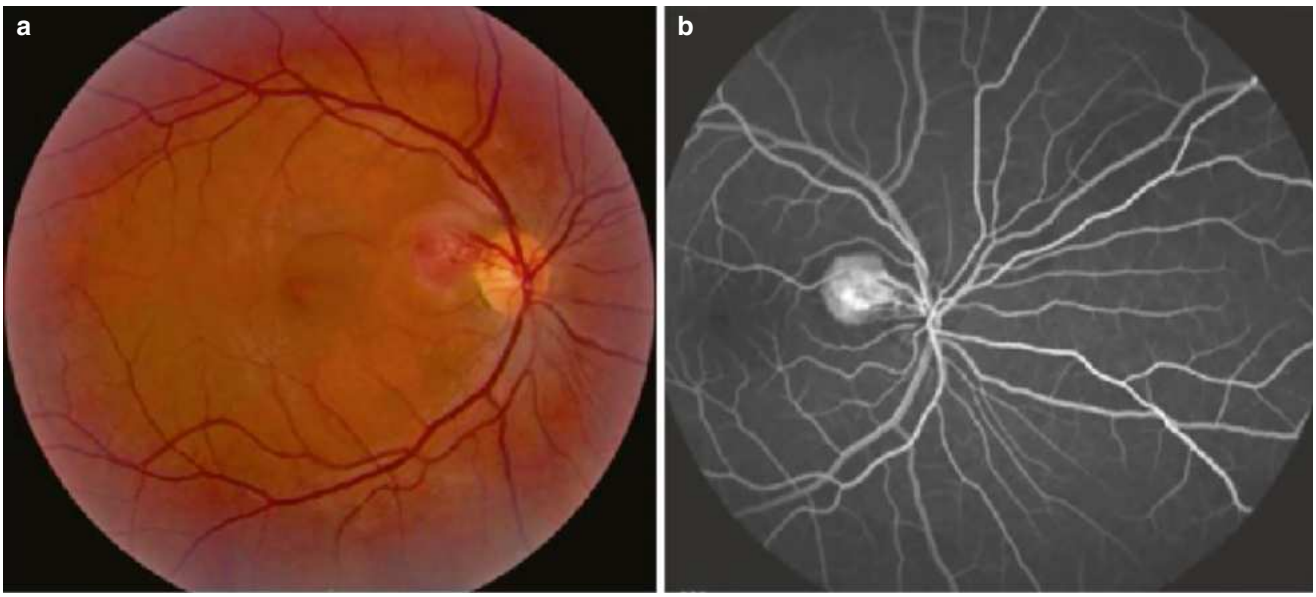

Fig. 20.5 Color fundus photograph of a peripapillary exophytic hemangioblastoma (**a**). Venous phase FA shows the feeding arterioles and the large draining vein (**b**). Late-phase FA shows leakage from the hemangioblastoma (**c**). Optical coherence tomography demonstrates that the tumor is exophytic (**d**)

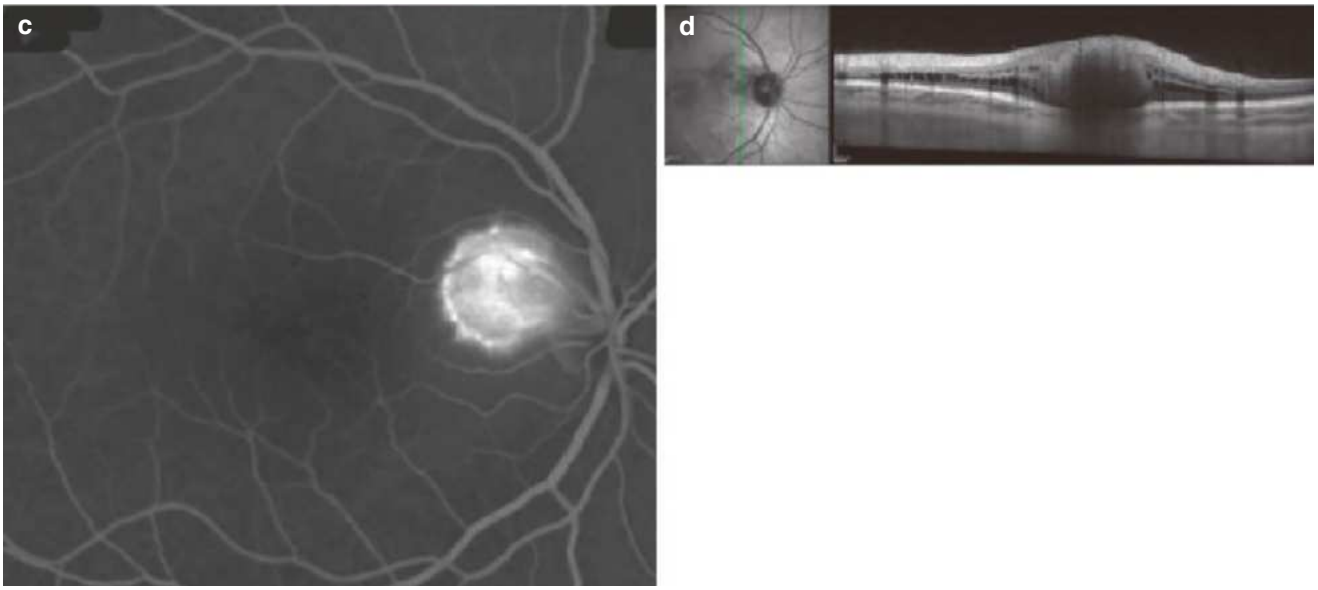

Fig. 20.5 (continued)

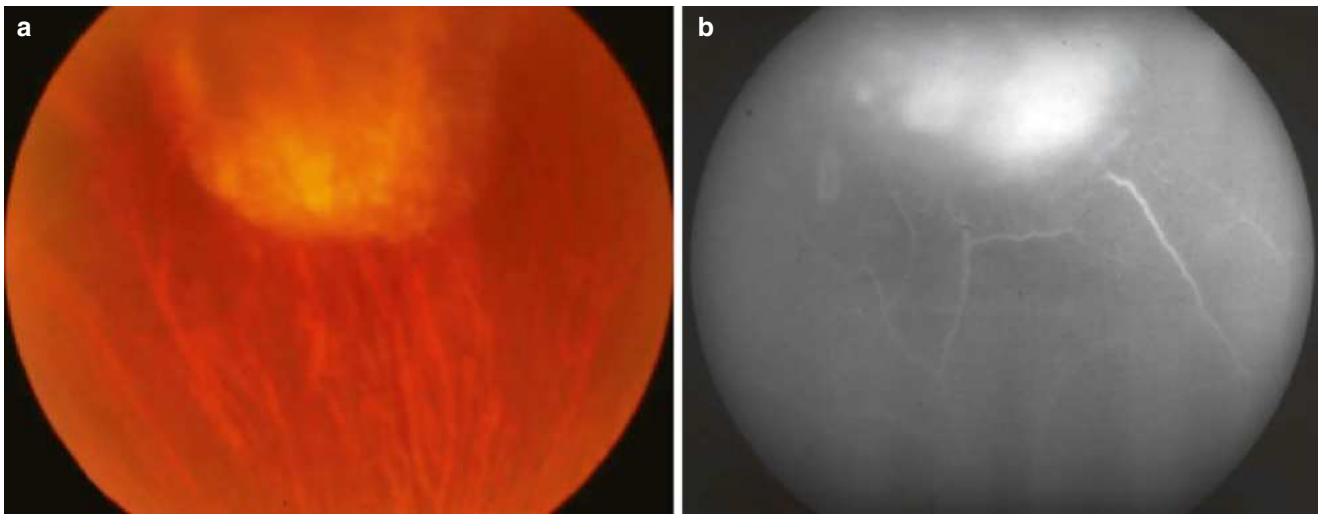

Fig. 20.6 Primary retinal vasoproliferative tumor located superiorly (**a**). Late-phase FA shows hyperfluorescence of the tumor. The feeding and draining vessels seem to be of normal caliber (**b**)

the capillaries under the retina. This is probably the only time that ICGA is useful in diagnosing retinal tumors.

- Papillary hemangioblastoma can be both endophytic and exophytic. Endophytic hemangioblastoma is relatively easy to diagnose. Fluorescein angiography will show the capillaries within the tumor as well as the feeding and draining vessels. Exophytic papillary tumor is harder to diagnose because the tumor is usually not directly visible (Fig. 20.5). Fluorescein angiography may show dilated vessels entering into the disc or at the edge of the tumor. With exophytic tumors, ICGA demonstrates leakage from the deeper aspects of the optic nerve or surrounding retina.

20.5.2.2 Retinal Vasoproliferative Tumor

Retinal vasoproliferative tumor is a benign reactive vascular tumor. It is idiopathic in about 75% of the cases and can be caused by intermediate uveitis, toxoplasmosis, retinitis pigmentosa, Coats' disease, intraocular surgery, and other causes in the remaining 25% [14]. The tumor usually occurs in the inferotemporal peripheral fundus and has a pink or yellow color in most cases. It may be associated with retinal exudation and hemorrhage (Fig. 20.6). Fluorescein angiography shows rapid filling of the tumor in the arterial phase through a nondilated or mildly dilated retinal feeder arteriole [16, 17]. A capillary network may appear on the tumor sur-

face. In the venous phase, diffuse leakage and staining of the mass and subretinal fluid are usually demonstrated (Fig. 20.6). As opposed to retinal hemangioblastoma, this benign reactive vascular tumor does not have large, dilated draining and feeding vessels. The filling with fluorescein is not as rapid as that seen with retinal hemangioblastoma.

20.5.2.3 Retinal Cavernous Hemangioma

Retinal cavernous hemangioma can occur as an isolated lesion or as part of a syndrome with skin and central nervous system manifestations. The lesion consists of blood-filled saccular spaces in the inner retina, clinically resembling a bunch of grapes. The lesion usually occurs in the posterior pole and near the optic nerve. There is no retinal detachment or exudation. Epiretinal membrane formation and vitreous hemorrhage may be seen. Fluorescein angiography demonstrates the saccular spaces, which are hyperfluorescent superiorly and hypofluorescent inferiorly, because of sedimentation of red blood cells in the lower part of the lesion called the fluorescein cap sign (Fig. 20.7) [18]. Usually, there is no leakage.

20.5.2.4 Retinal Racemose Hemangioma (Retinal Arteriovenous Malformation)

Retinal racemose hemangioma is usually associated with similar changes in the midbrain (Wyburn-Mason syndrome). On ophthalmoscopy, dilated and tortuous blood vessels communicating with each other are seen. There is usually no retinal exudation or detachment. The vessels usually become apparent during the arteriovenous phase on FA and do not leak [19]. Delayed emptying of the vessels is seen in the late phase. In long-standing cases, minimal focal leakage may be observed.

20.5.3 Retinal Astrocytic Hamartoma

Retinal astrocytic hamartoma (RAH) can occur as an isolated lesion or can be seen in patients with tuberous sclerosis. Isolated RAHs tend to be unilateral and unifocal, whereas those associated with tuberous sclerosis tend to be bilateral and multiple and are usually diagnosed earlier than the isolated ones. The tumor can be translucent or calcified. Retinal astrocytic hamartoma is relatively hypofluorescent in the arterial phase of the FA in most cases. Tortuous or corkscrew retinal blood vessels may be seen in and around the tumor. In the venous phase, a network of fine blood vessels typically becomes apparent in the superficial portion of the tumor with fairly intense late staining from leakage (Fig. 20.8) [20]. There is limited data on the ICGA characteristics of RAH.

20.5.4 Retinal Pigment Epithelial Tumors

Retinal pigment epithelial tumors include simple hamartoma of the retinal pigment epithelium (RPE), congenital hypertrophy of the RPE (CHRPE), combined hamartoma of the retina and RPE, and RPE adenoma/adenocarcinoma. Simple

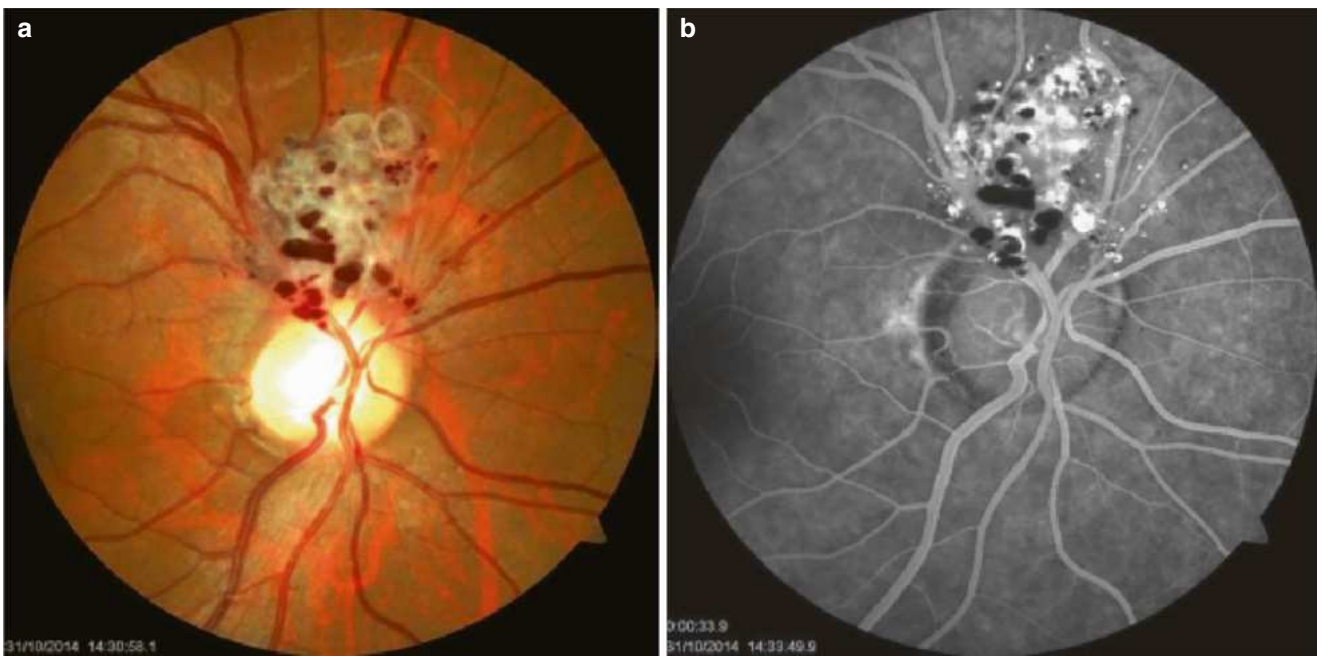

Fig. 20.7 Retinal cavernous hemangioma located superior to the optic disc (**a**). Fluorescein angiography shows the typical saccular spaces in the cavernous hemangioma with fluorescein cap sign (hyperfluorescent upper and hypofluorescent lower portions) (**b**). (Courtesy of Dr. Mehmet Teke)

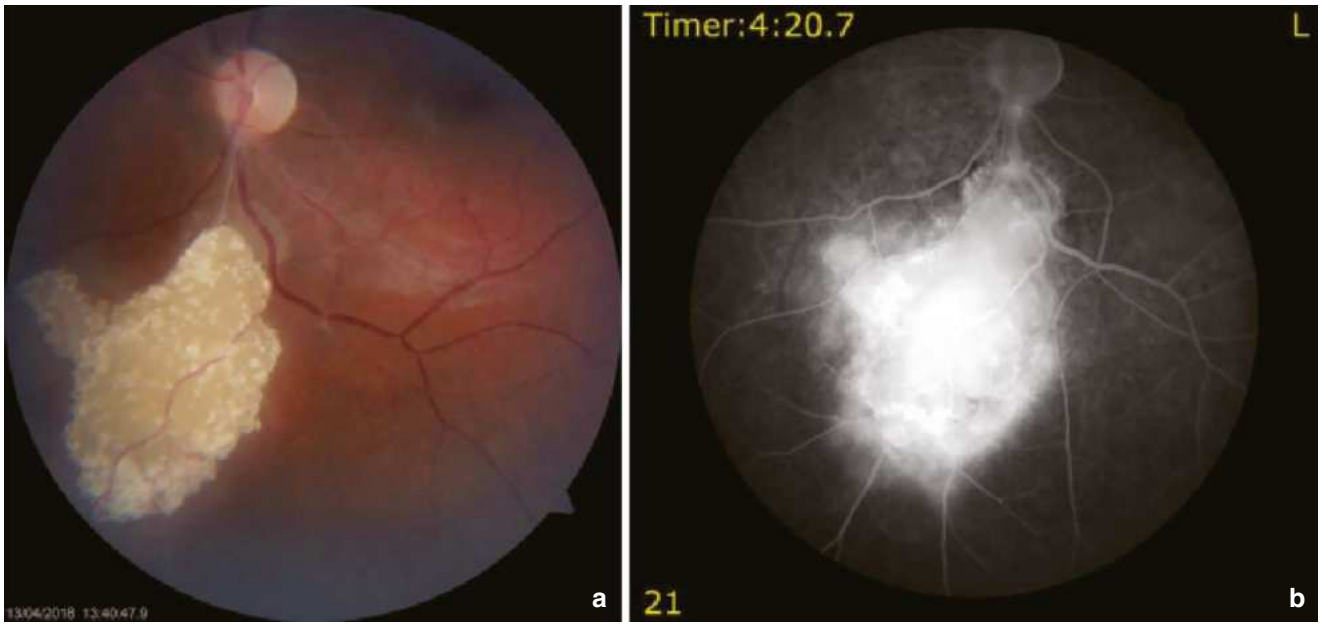

Fig. 20.8 Calcified retinal astrocytic hamartoma in the left eye (**a**). Fluorescein angiography shows intense staining and leakage from the lesion in the late phase (**b**)

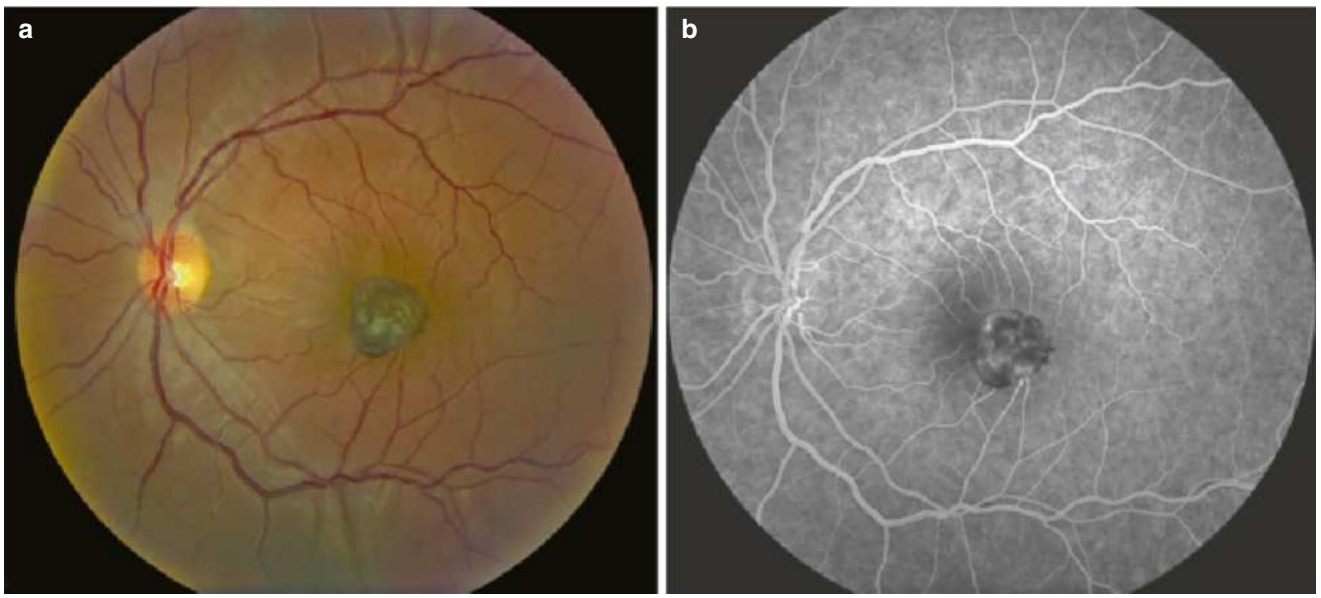

Fig. 20.9 Simple hamartoma of the retinal pigment epithelium. Notice the jet-black color (**a**). Fluorescein angiogram highlights the feeding and draining of retinal vessels (**b**)

hamartoma of the RPE and RPE adenoma/adenocarcinoma tend to be pigmented tumors. Congenital hypertrophy of the RPE is typically a pigmented flat lesion with a halo around its margins and lacunae within the lesion. It usually occurs as a unifocal and isolated lesion. In congenital grouped pigmentation of the retina or bear tracks, multiple CHRPE lesions can be seen. This multifocal variant may be associated with familial adenomatous polyposis and Gardner's syndrome. Combined hamartoma of the retina and RPE appears as a gray-white mass situated in the juxtapapillary region. It occurs as an isolated lesion or may be associated with neurofibromatosis type 2 (NF-2) [21].

Simple hamartoma of RPE and RPE adenoma/ adenocarcinoma are located anterior to Bruch's membrane and have dilated feeding and draining retinal vessels. These tumors are relatively hypofluorescent in the early phases but show leakage in the late phase of FA. Indocyanine green angiography shows the internal tumor vascularity (Fig. 20.9) [22].

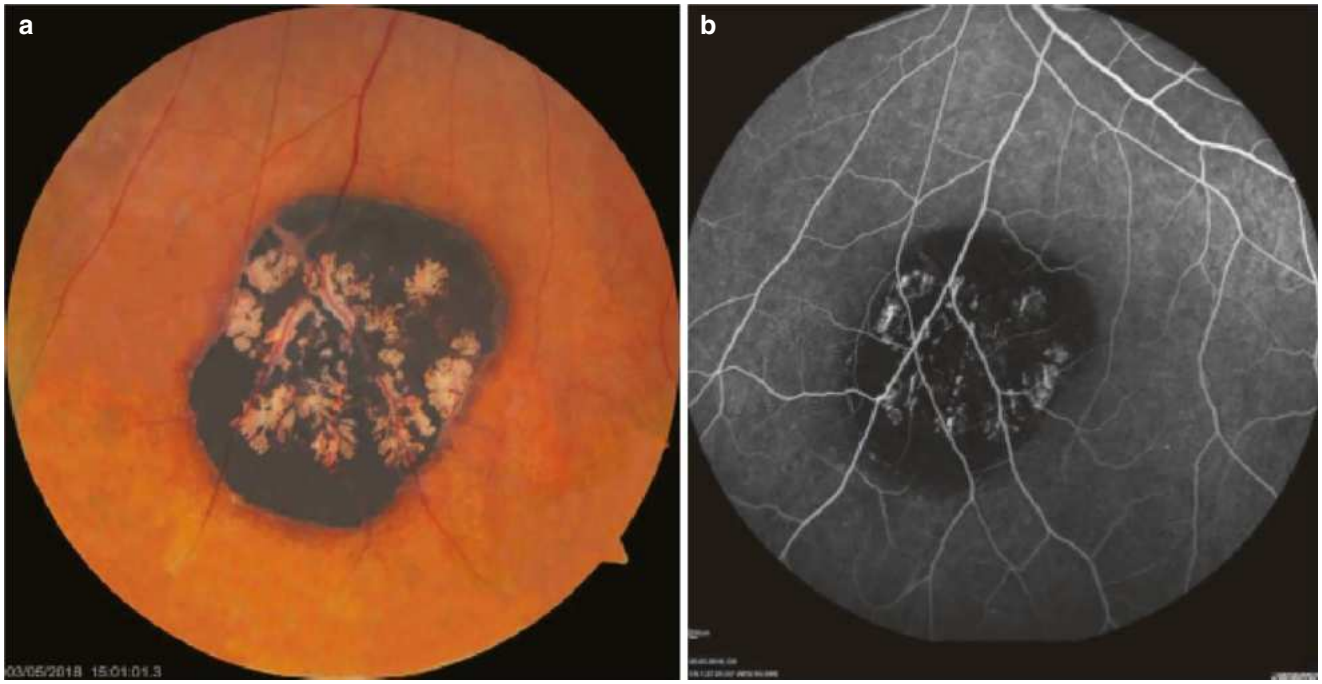

Fig. 20.10 Congenital hypertrophy of the retinal pigment epithelium (**a**). The lesion is hypofluorescent on all phases of FA, and there is early and late hyperfluorescence from pigment epithelial atrophy (window defect) in the lacunae (**b**)

Congenital hypertrophy of the RPE demonstrates a fairly uniform hypofluorescence pattern with increased pigment in the lesion blocking the dye on FA (Fig. 20.10). Halos and lacunae of depigmentation appear as window defects. Indocyanine green angiography shows similar findings with choroidal vascular patterns visible through the larger lacunae [23]. Combined hamartoma of the retina and RPE shows early hypofluorescence in the arterial phase with hyperfluorescence becoming visible in the early venous phase and subsequent blotchy hyperfluorescence in the late phase of FA.

20.6 Choroidal Tumors

The tumors covered in this section include choroidal nevus, choroidal melanoma, melanocytoma, choroidal hemangioma, choroidal osteoma, choroidal granuloma, choroidal metastatic tumors, choroidal lymphoma, and vitreoretinal lymphoma. Vitreoretinal lymphoma, although technically a retinal tumor, is discussed with choroidal lymphoma to point out differences between the two entities.

20.6.1 Choroidal Nevus

Choroidal nevus is the most common benign intraocular tumor in adults and children. Fluorescein angiography is not a routine test for small asymptomatic choroidal nevi if the diagnosis can be established ophthalmoscopically. Fluorescein angiographic features of a choroidal nevus depend mainly on three factors: the degree of pigmentation within the tumor, its location within the choroid, and the alterations in the overlying RPE [8, 24–26]. Deeply pigmented choroidal nevi tend to be relatively hypofluorescent whereas those that are less pigmented tend to be isofluorescent (Fig. 20.11). A deep nevus, confined to the outer choroid and sparing the choriocapillaris, gives a relatively normal fluorescein pattern because the fluorescein enters the patent choriocapillaris. If the nevus is thicker and compresses or replaces the choriocapillaris, FA may demonstrate relative hypofluorescence because there is less fluorescein in the choroidal vessels over the tumor. Late staining from overlying drusen can lead to hyperfluorescence. Fluorescein angiography shows that areas of orange pigment remain hypofluorescent throughout the study. The hypofluorescence of orange pigment appears to be due to the blocking of choroidal fluorescence transmitted through the melanocytic choroidal lesion.

Choroidal nevi rarely display choroidal neovascularization, retinal pigment epithelial detachment (PED), or subretinal fluid over the lesion. The occurrence of a choroidal neovascular membrane can be suspected based on the ophthalmoscopic presence of subretinal hemorrhage or subretinal fluid over the lesion. Fluorescein angiography in these cases usually reveals a choroidal neovascular membrane that

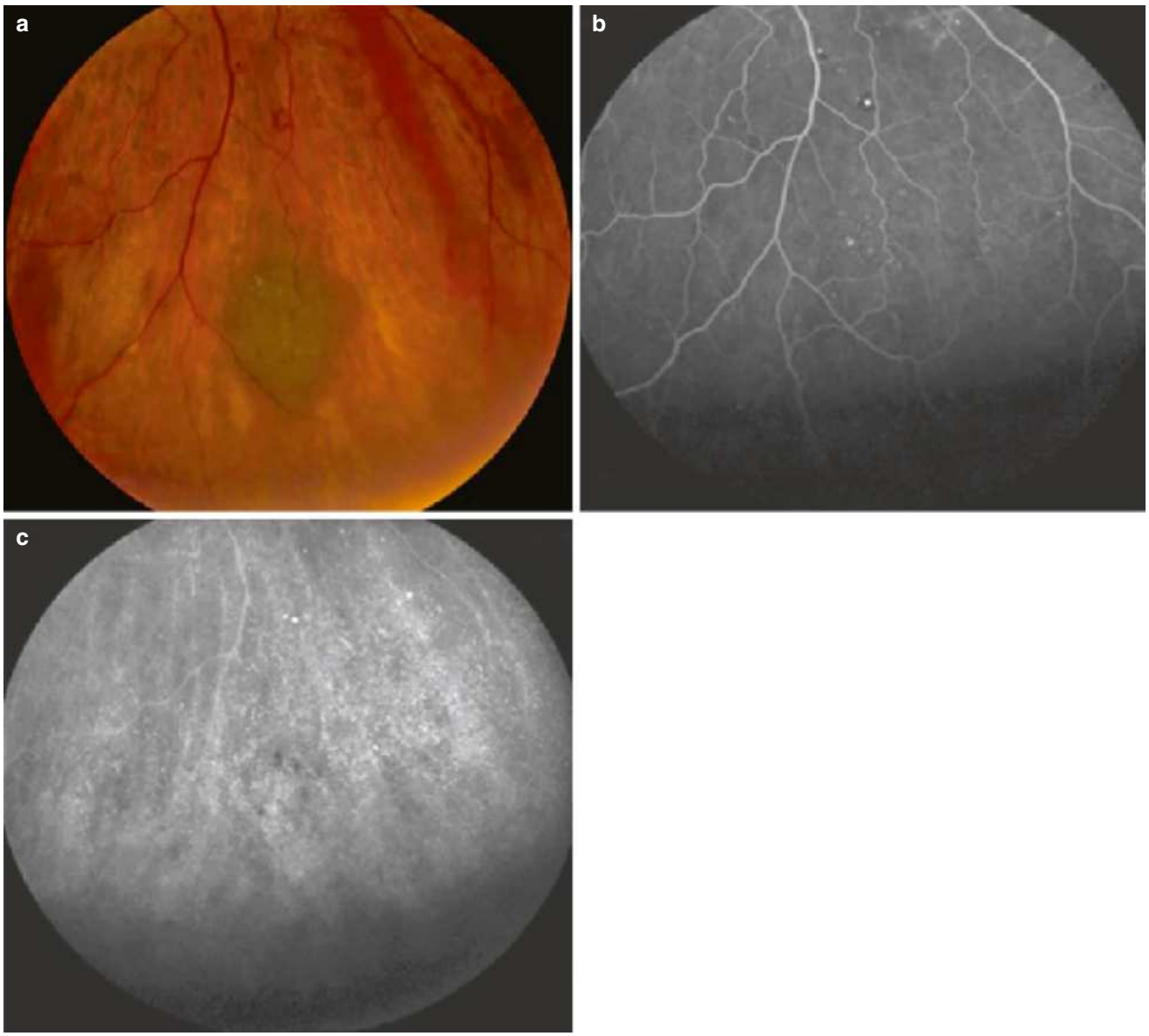

Fig. 20.11 Choroidal nevus with overlying drusen in a patient that has nonproliferative diabetic retinopathy (**a**). Fluorescein (**b**) and ICG angiography (**c**) show isofluorescence of the lesion with only some staining of the drusen

appears brightly in the early frames of the study and leaks progressively by the late frames. Retinal pigment epithelial detachment usually presents as late hyperfluorescence from the pooling of the dye under the PED. In cases with subretinal fluid, RPE hyperfluorescent leakage sites can be seen in the early frames of the study and gradually increase in prominence as the study continues. Fluorescein usually leaks into an ophthalmoscopically evident localized blister of subretinal fluid.

On ICGA, most pigmented choroidal nevi are hypofluorescent. A nonpigmented choroidal nevus demonstrates isofluorescence. However, some nonpigmented nevi are still hypofluorescent because of the compression of the choroidal vessels by the choroidal mass [26]. Choroidal nevi may appear to be larger on ICGA than observed on ophthalmoscopy and FA [27].

20.6.2 Choroidal Melanoma

Choroidal melanoma is the most common primary malignant intraocular tumor in adults. Risk factors for the development of choroidal melanoma include Caucasian race and the presence of ocular melanocytosis. BAP 1 gene mutations are important in the final development of choroidal melanoma. In most cases, FA does not provide findings that are pathog-

nomonic of choroidal melanoma. The FA findings can be described as compatible or incompatible with the diagnosis of choroidal melanoma [8]. Fluorescein angiographic patterns of choroidal melanoma usually reflect the degree of pigmentation of the tumor and its effect on adjacent ocular structures, particularly the RPE. A small choroidal melanoma with an intact overlying RPE can demonstrate no appreciable change in FA [8, 28].

For most choroidal melanomas, FA in the arterial or early venous phase usually shows hypofluorescence with mottled hyperfluorescence [29–32]. This mottled hyperfluorescence is due to several ill-defined, large-caliber intralesional blood vessels that usually become identifiable against the hypofluorescent background through atrophy of the overlying RPE. As the study continues, the large intralesional blood vessels leak progressively, so that the surface of the lesion commonly appears hyperfluorescent in the late frames. Lipofuscin and/or pigment clumps within the tumor appear intensely hypofluorescent throughout the entire study because of blockage of the underlying choroidal and tumor vascular fluorescence. A deeply pigmented choroidal melanoma appears hypofluorescent throughout the entire FA. If there is associated serous retinal detachment, fluorescein can also accumulate in the surrounding and overlying subretinal fluid by the late frames, leading to hyperfluorescence. In amelanotic choroidal melanoma, the early frames of FA show less lesional hypofluorescence and more prominent intralesional blood vessels. The remainder of FA is similar to that seen in the more typical pigmented melanoma.

A proportion of the melanomas can grow through the overlying Bruch's membrane, giving the lesion a mushroom shape in cross-section. In most cases of mushroom-shaped melanoma, the portion of the tumor that has broken through Bruch's membrane appears to be less darkly pigmented compared to the base of the tumor [29, 32]. Many large-caliber intralesional blood vessels can often be observed ophthalmoscopically within the apical portion of the mass (Fig. 20.12). These correspond mostly with the tumor veins that are congested in response to the constricting effect of the intact portion of Bruch's membrane. The simultaneous fluorescence of retinal and choroidal vessels leads to a double circulation pattern, which is a characteristic of melanomas that have broken through Bruch's membrane [33, 34]. Fluorescein angiography in such cases shows progressive hyperfluorescence of the apical blood vessels of the lesion, starting usually in the early venous phase with intense staining in the late phase.

Some choroidal melanomas invade the overlying sensory retina. Areas of tumor invasion of the overlying sensory retina are relatively hypofluorescent throughout the entire FA [34]. The retinal blood vessels at the margins of the melanoma with retinal invasion are often abnormal and leaky, as might be expected on the basis of the associated retinal invasion. Choroidal neovascularization over a melanoma can occur but is rare [35].

On ICGA, most choroidal melanomas remain hypofluorescent/isofluorescent with respect to the surrounding tissues during the entire FA. This is because pigmented choroidal melanoma blocks ICG fluorescence because of the absorption of the near-infrared light by the melanin containing lesion (Fig. 20.13). Some large choroidal melanomas may show moderate hyperfluorescence in the late phase of ICGA. Choroidal melanomas similar to choroidal nevi may appear to be larger on ICGA than observed on ophthalmoscopy and FA. Microvascularization patterns can be imaged by ICGA using a confocal scanning laser ophthalmoscope. On ICGA, the presence of arcs, loops, cross-links between parallel vessels, irregular or tortuous vessels, abnormal branching patterns, and networks collectively classified as complex microvascular patterns is considered significant for intrinsic tumor vessels [36, 37]. Straight vessels, parallel vessels, and vascular silence are classified as noncomplex vascular patterns and can also be observed in choroidal nevi. The presence of complex microvascular patterns has been found to be a predictor of growth and metastasis in choroidal melanocytic lesions [38]. The double circulation pattern consisting of internal tumor vessels and normal vascularity of the overlying retina is more evident in ICGA. Indocyanine green angiography can also assist in visualizing the typical pattern of choroidal blood vessels in the tumor when there is overlying blood [1]. Prominent early choroidal filling is a more typical feature of circumscribed choroidal hemangioma [39].

20.6.3 Melanocytoma

Melanocytoma or magnocellular nevus is considered as a variant of uveal nevus and is, therefore, a benign lesion. It can be found anywhere in the uveal tract but more commonly on the optic disc [40]. As such, this tumor has sometimes been classified under retinal and optic disc tumors in the earlier literature. Melanocytoma is seen in white and black races, unlike uveal melanoma, which occurs predominantly in Caucasians. The tumor appears as a black tumor, usually occurring on the inferior or inferotemporal portion of the optic nerve. About half of the optic disc melanocytomas have a choroidal component. On FA, the melanocytoma is usually hypofluorescent throughout the study (Fig. 20.14) [40]. The choroidal component may show slight hyperfluorescence due to overlying RPE changes. Growth can be documented in about 30% of cases, and malignant transformation can occur, although this is rare. Fluorescein angiography usually shows prominent vascularity and leakage in melanocytoma

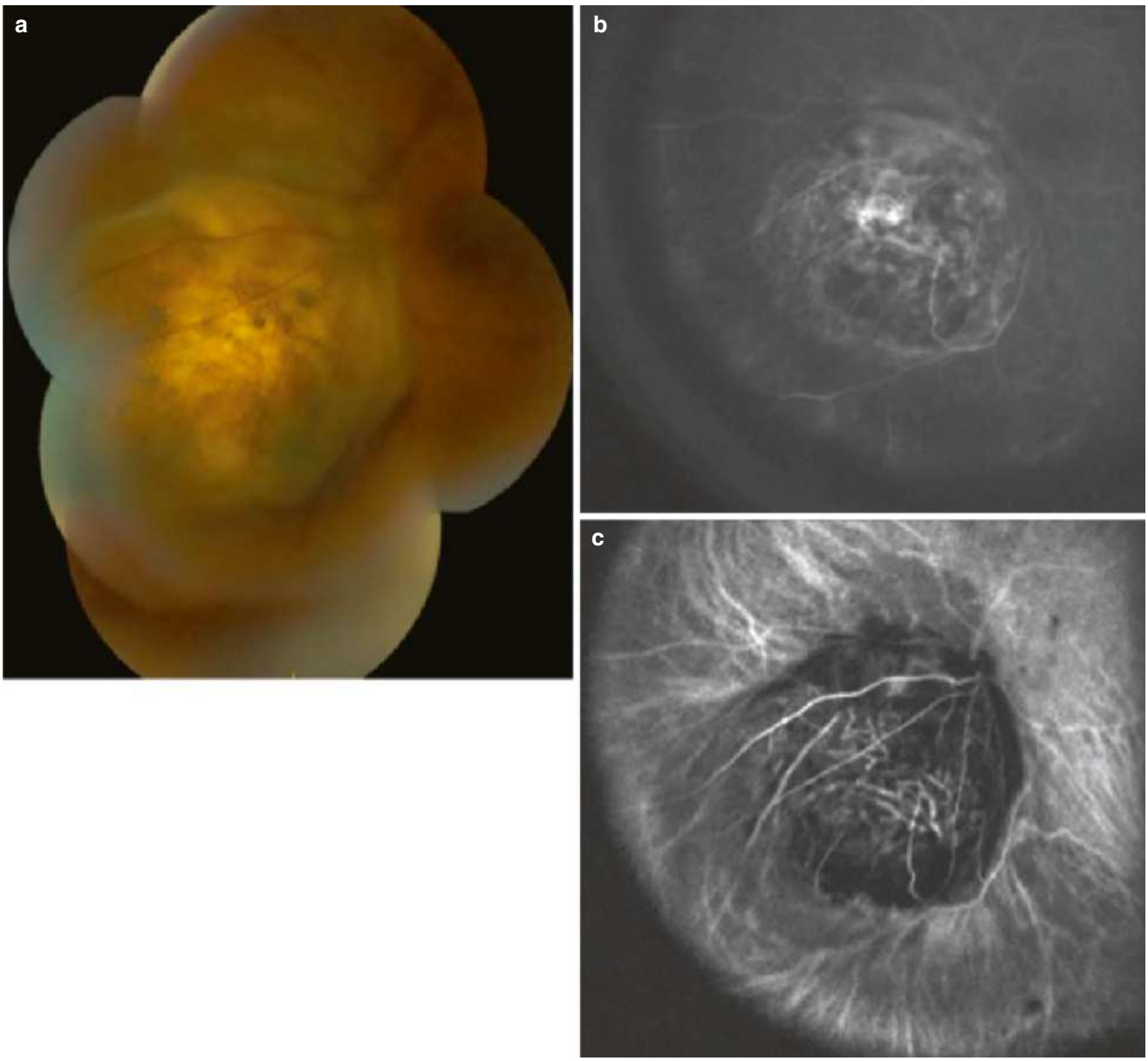

Fig. 20.12 Amelanotic mushroom-shaped peripapillary choroidal melanoma (**a**). Fluorescein (**b**) and ICG angiography (**c**) showing internal vascularity in the relatively hypofluorescent tumor background. The internal tumor vessels together with the overlying retinal vasculature give rise to the so-called double-circulation pattern

cases that have undergone malignant transformation into melanoma.

20.6.4 Choroidal Hemangioma

Choroidal hemangioma is a benign abnormal collection of blood vessels in the choroid, which is better documented on ICGA than FA. It can be found in either a discrete, circumscribed form or a diffuse form associated with Sturge-Weber syndrome. Circumscribed choroidal hemangioma is usually seen in middle-aged adults and occurs unilaterally. The tumor appears as a reddish-orange mass posterior to the equator. In Sturge-Weber syndrome, there can be discrete hemangiomatous tumefactions overlying the diffuse tumor. Fluorescein angiography of circumscribed choroidal hemangioma typically shows early irregular hyperfluorescence of the choroidal vessels during the choroidal phase prior to the filling of the retinal arterioles. Subsequently, the fluorescence increases and develops a more confluent pattern during the arteriovenous phase of FA. The later phases display the accumulation of dye in multiple cavities in the outer retina [41]. This typical angiographic appearance is characteristic of choroidal hemangioma but not pathognomonic for this

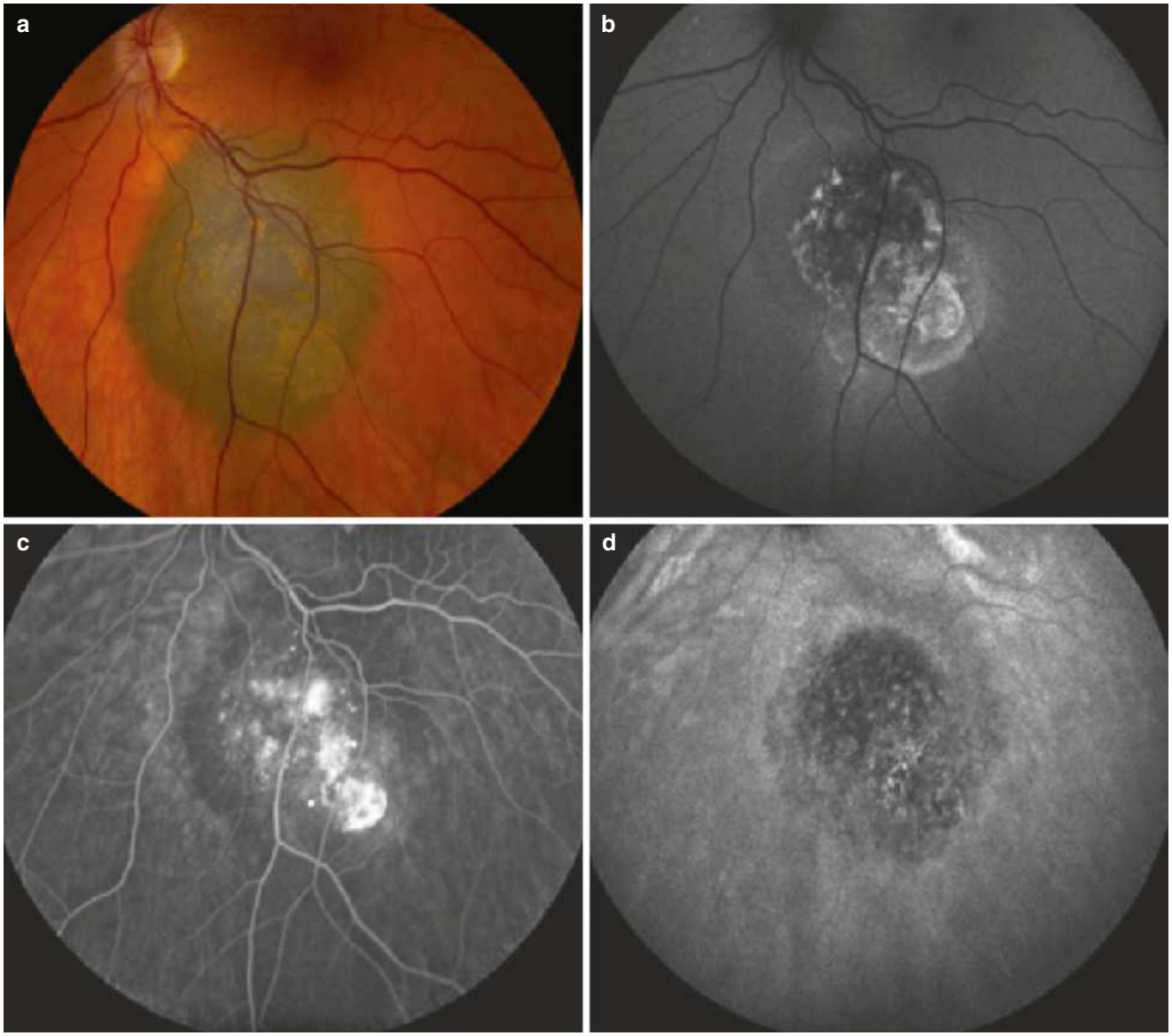

Fig. 20.13 Symptomatic small posterior choroidal melanoma with orange pigment and subretinal fluid (**a**). Fundus autofluorescence shows hyperautofluorescence from subretinal fluid (leakage) and the orange pigment overlying the tumor (**b**). The late-stage angiogram shows focal spots of leakage by FA (**c**) and also from ICGA (**d**)

tumor because other choroidal disorders have been noted to have a similar appearance, especially in the choroidal phase [39]. Fluorescein angiography is often useful in making the diagnosis of choroidal hemangioma; however, ICGA is superior in documenting this tumor (Fig. 20.15).

Indocyanine green angiography of choroidal hemangioma shows a well-defined area of early, intense, and fairly even hyperfluorescence with a late rapid loss of fluorescence (i.e., "washout phenomenon") after 1 min. The tumor usually demonstrates moderate hyperfluorescence in the mid-phase followed by isofluorescence or hypofluorescence in the late phase with staining of tissue surrounding the vascular tumor. The washout phenomenon is attributed to high-flow tumor vessels with lower resistance that allow emptying of the dye sooner than the surrounding normal choroidal vessels. On ICGA, the intrinsic vessels of the choroidal hemangioma are observed in the majority of patients; hyperfluorescent peripheral rim and the late multifocal spots of dye accumulation without leakage are seen in about 50% of the tumors [39, 41]. Compared to choroidal hemangioma, most other choroidal tumors are hypofluorescent compared with the normal choroid.

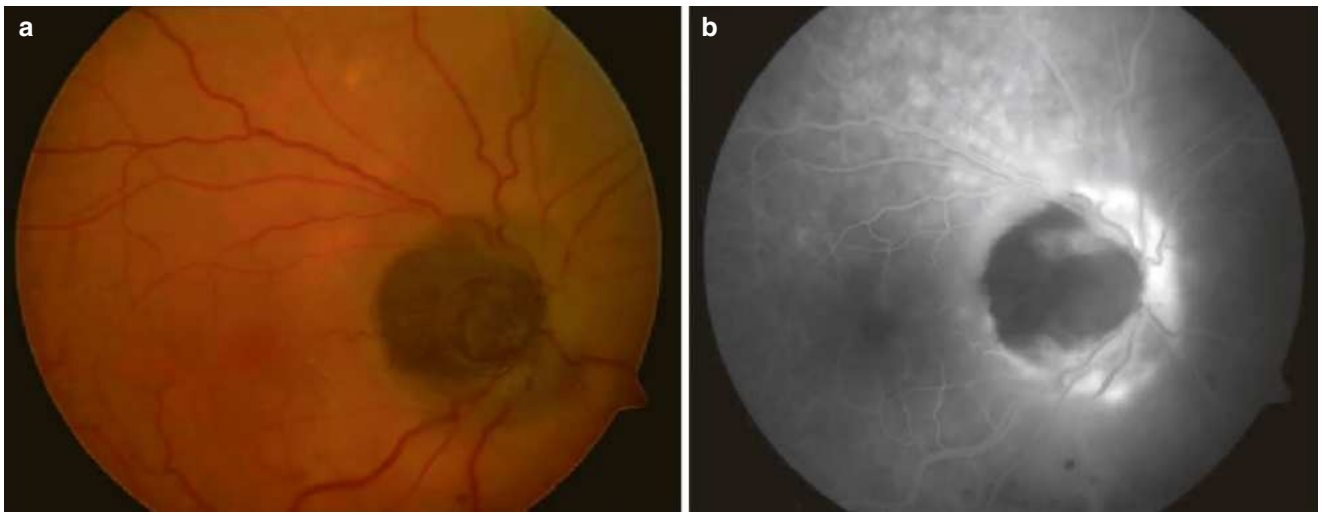

Fig. 20.14 Melanocytoma occupying almost the entire aspect of the optic disc in the right eye. Note the dark brown color and choroidal component extending nasal to the optic disc (**a**). Late phase FA shows marked hypofluorescence in the main tumor body with some hyperfluorescent areas. The choroidal component nasal to the disc shows hyperfluorescence as well (**b**)

20.6.5 Choroidal Osteoma

Choroidal osteoma is a tumor composed of mature bone in various stages of calcification [42]. The tumor is usually unilateral and more common in young females. Choroidal osteoma has a juxtapapillary location in many cases, and macular involvement is usually seen. Growth is observed in 50% of the cases and vision loss may occur eventually. Although choroidal osteoma is a benign tumor, the visual outcome is poor; with more than 50% of patients losing vision >3 Snellen lines of acuity and 50% losing vision to <20/200 at the end of 10 years [42].

Fluorescein angiography of choroidal osteoma typically shows early patchy hyperfluorescence with late diffuse intense staining [42, 43]. The fluorescein flows through the Haversian canals of the bone and due to the bony nature of the tumor, the fluorescein dye is slow to penetrate the mass leading to early patchy hyperfluorescence. The dye also has difficulty exiting the tumor, and thus, the typical fluorescein pattern of choroidal osteoma is slow uptake of fluorescein early on during FA and persistent late hyperfluorescence. The early hyperfluorescence of the capillary network inside the bony tumor corresponds to the yellow-white areas of the tumor (Fig. 20.16).

Choroidal osteoma may be complicated by the occurrence of a choroidal neovascular membrane in 30% of the cases. The presence of choroidal neovascularization has a lace-like pattern of early hyperfluorescence with early leakage of dye followed by late staining of the surrounding tissues. Meanwhile, subretinal hemorrhage or clumps of pigment at the level of RPE are visible as areas of persistent hypofluorescence. Indocyanine green angiography of choroidal osteoma shows hypofluorescence in the early frames. During the mid and late phases, the tumor shows focal areas of isofluorescence that gradually become confluent in later frames (Fig. 20.16) [44].

20.6.6 Choroidal Granuloma

Choroidal granuloma can be idiopathic or can occur as an uncommon ocular manifestation of inflammatory diseases such as sarcoidosis, tuberculosis, and secondary syphilis. On FA, the granulomas show early choroidal hypofluorescence from blockage of the choroidal vessels, followed by late hyperfluorescence due to subretinal fluorescein staining and leakage [45]. There can be a chorioretinal anastomosis, which is rare in other choroidal tumors. Indocyanine green angiography is not typically performed, because it does not add significantly to the findings than elucidated by FA.

A secondary choroidal neovascular membrane can occur, in which case there can be lacy hyperfluorescence, sometimes better seen with ICGA. The choroidal neovascular membrane demonstrates late leakage, and there may be areas of hypofluorescence if there is subretinal blood.

Solitary choroidal granuloma, unassociated with any systemic disease and uveitis, was first described by Hong et al. and called unifocal helioid choroiditis [46]. Later, Shields et al. renamed the condition as solitary idiopathic choroiditis [47]. Recent observations, using multimodal imaging including swept-source optical coherence tomography (SS-OCT), revealed that these lesions usually start in the sclera, producing secondary effects on the choroid. Therefore, a new name, focal scleral nodule, was proposed to describe this condition (Fig. 20.17) [48].

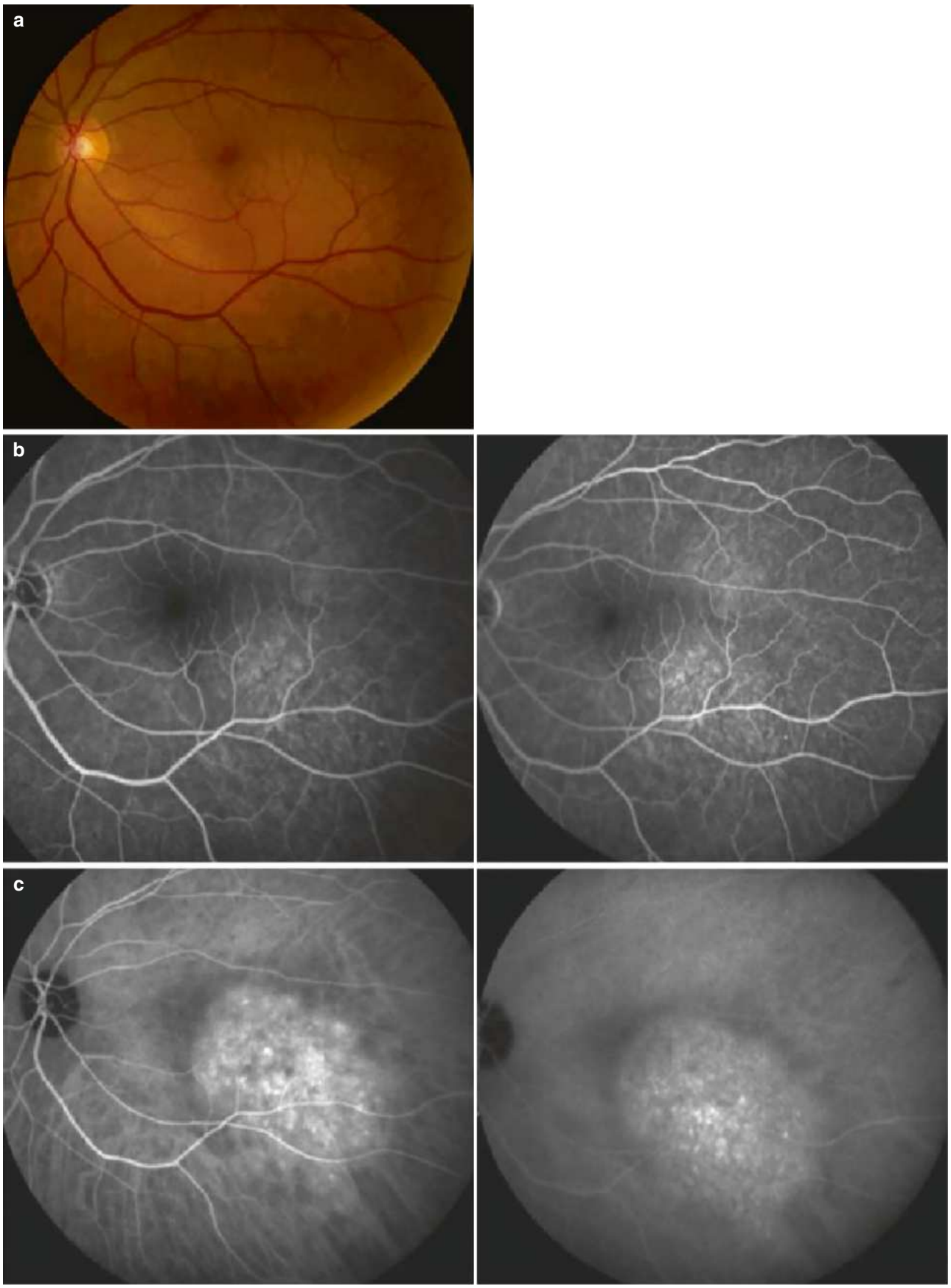

Fig. 20.15 Asymptomatic choroidal hemangioma (**a**). Fluorescein (**b** left) and ICG angiography (**c** left) in the early venous phase showing hyperfluorescence in both modalities. In the late phase, there is actually less fluorescence on ICGA (**c** right) compared to FA (**b** right)

Fig. 20.16 Choroidal osteoma that was partially treated with photodynamic therapy (**a**). Indocyanine green angiography early (**b**) and late phase (**c**). Note the small penetrating vessels through the bone in the inferior aspect of the tumor

20.6.6.1 Choroidal Metastatic Tumors

Breast, lung, gastrointestinal, and prostate cancers comprise the majority of choroidal metastatic tumors. Choroidal metastases tend to affect the posterior pole. They are usually amelanotic and often associated with exudative retinal detachment leading to metamorphopsia and vision loss, which are the most common ocular symptoms. Choroidal metastases from carcinoid tumors, thyroid, and renal carcinomas may have a more pigmented or orange color. The choroid, ciliary body, and iris are the most common sites of ocular metastases, probably due to their rich vascular supply. Metastatic tumors of the optic nerve and retina are much less common.

In contrast to choroidal hemangioma and melanoma, metastatic carcinoma is usually hypofluorescent in the arterial and early venous phases and shows progressive hyperfluorescence in the subsequent phases [49–51]. Pinpoint foci of hyperfluorescence appear over the tumor in the late phase of the study. This appearance is typical of choroidal metastatic lesions and is attributed to microcystic RPE degeneration. These pinpoint foci of hyperfluorescence may enlarge to form globular areas of hyperfluorescence over the tumor. The late angiograms also demonstrate marked hypofluorescence of the brown pigment clumping on the tumor surface, similar to the pattern seen with the orange pigment over melanotic choroidal melanomas (leopard spot or skin appear-

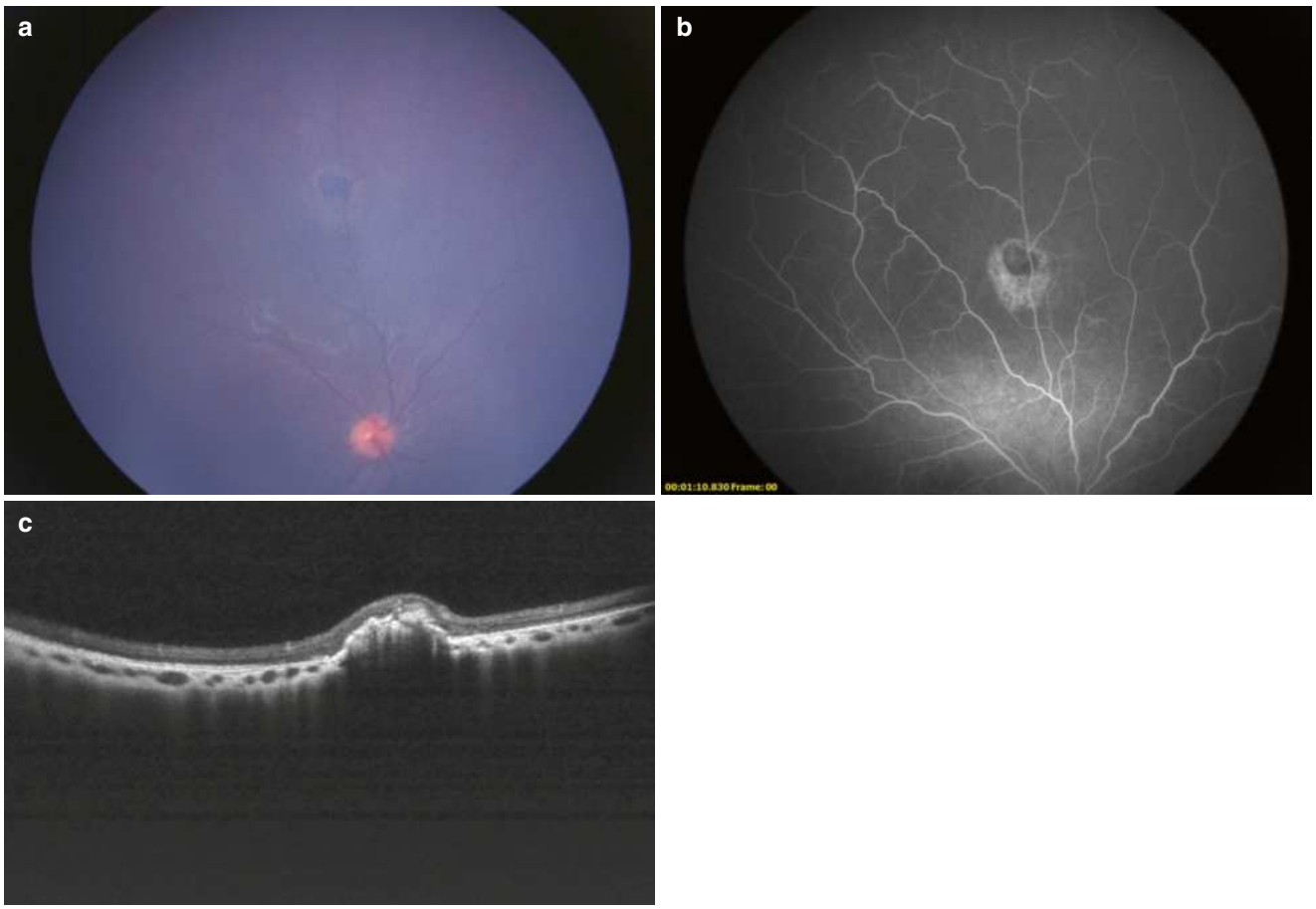

Fig. 20.17 RetCam fundus photograph shows superiorly located focal scleral nodule (**a**). RetCam fluorescein angiogram shows window defects peripherally and blocked fluorescence centrally (**b**). Spectral domain optical coherence tomography shows an essentially scleral lesion producing compressive effects on the overlying choroid (**c**)

ance). There may be moderate late hyperfluorescence of the serous subretinal fluid overlying and adjacent to the metastatic tumor.

Diffuse and multifocal hypo- and hyperfluorescence occur as a result of the damaging effects of the choroidal tumor on the overlying RPE. The large-caliber vessels and double circulation pattern often seen with choroidal melanomas and the late multiloculated diffuse staining pattern usually observed with choroidal hemangiomas are rarely present in the FA of choroidal metastases (Fig. 20.18).

Indocyanine green angiography is rarely of significant help in diagnosing uveal metastatic lesions. Choroidal metastases usually show homogeneous hypofluorescence in comparison with the surrounding choroid, as if the tumor were acting as a relative filter of the fluorescence of the underlying choroid. This filtering effect extends for the entire base of the metastasis and stops abruptly at the margin of the tumor, helping to define the precise margins of the tumor. Indocyanine green angiography may reveal subtle occult lesions separate from the symptomatic lesion manifesting as hypofluorescent areas of the choroid. In thick choroidal metastatic lesions, intrinsic tumor vessels might be visible on ICGA (Fig. 20.19).

20.6.6.2 Choroidal Lymphoma and Vitreoretinal Lymphoma

It is important to distinguish the different forms of intraocular lymphoma. Choroidal lymphoma tends to be a low-grade B-cell lymphoma, while vitreoretinal lymphoma is a form of diffuse large B-cell lymphoma in 95% of cases. In the remaining 5% of cases, vitreoretinal lymphoma consists of T-cell lymphoma. Both types of vitreoretinal lymphoma are much more aggressive than choroidal lymphomas. Vitreoretinal lymphoma represents a variant of primary central nervous lymphoma. As a rule, choroidal lymphoma does not extend anterior to Bruch's membrane and vitreoretinal lymphoma does not extend posterior to Bruch's membrane. Vitreoretinal lymphoma may involve

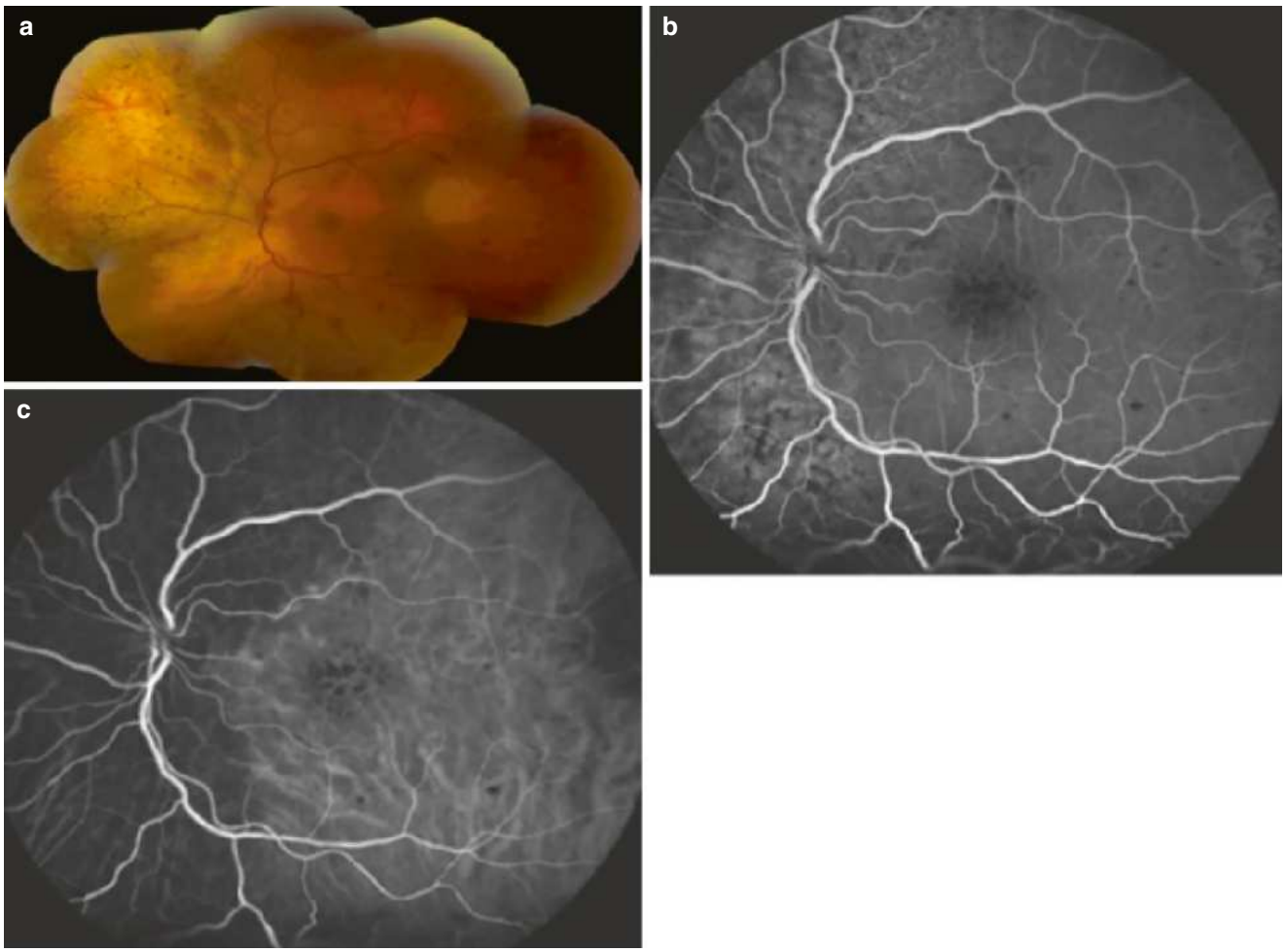

Fig. 20.18 Breast metastases with leopard spotting (**a**). The fluorescein angiogram accentuates the location of the leopard spots as hypofluorescent areas (**b**). Indocyanine green angiography shows an infiltrative process that has segmentally abolished the inner choroidal vessels (**c**)

only the vitreous, retina, or both. Some cases involve only the subretinal pigment epithelial space while others present with full-thickness retinal involvement. Such cases have to be distinguished from severe infectious retinitis. Central nervous system lymphoma develops in 80–90% of patients who initially present with vitreoretinal lymphoma, whereas only 20% of patients with central nervous system lymphoma have vitreoretinal lymphoma. This is because many patients with central nervous system lymphoma die before ocular involvement occurs or is clinically detected. For this reason, some consider systemic therapy to be indicated even for patients who have only vitreoretinal lymphoma at initial staging.

Fluorescein angiography in the majority of cases of diffuse large B-cell vitreoretinal lymphoma does not usually show macular edema, even in the presence of dense lymphomatous infiltrates. In about 15% of cases, there is leakage from the retinal vessels [52, 53]. Another common finding in vitreoretinal lymphoma is the accumulation of cells under the RPE. These cells can form small aggregates or very large clumps. These lymphomatous deposits block fluorescence, giving a leopard spot appearance in the early phase of FA (Fig. 20.20). In the late phase, there is leakage with hyperfluorescence.

Choroidal lymphoma shows FA and ICGA features similar to choroidal metastasis. Choroidal lymphoma can present as initial hypofluorescent spots in the choroid by both FA and ICGA (Fig. 20.21). These can remain hypofluorescent, especially on FA, but occasionally, some lesions become hyperfluorescent on ICGA. A minority of choroidal lymphomas may demonstrate blotchy hyperfluorescence in the late venous and late phases of FA. A leopard spot appearance also occurs in choroidal lymphoma, as with choroidal metastases. In addition, choroidal lymphoma causes choroidal folds, which would appear as alternating areas of hyper- and hypofluorescence.

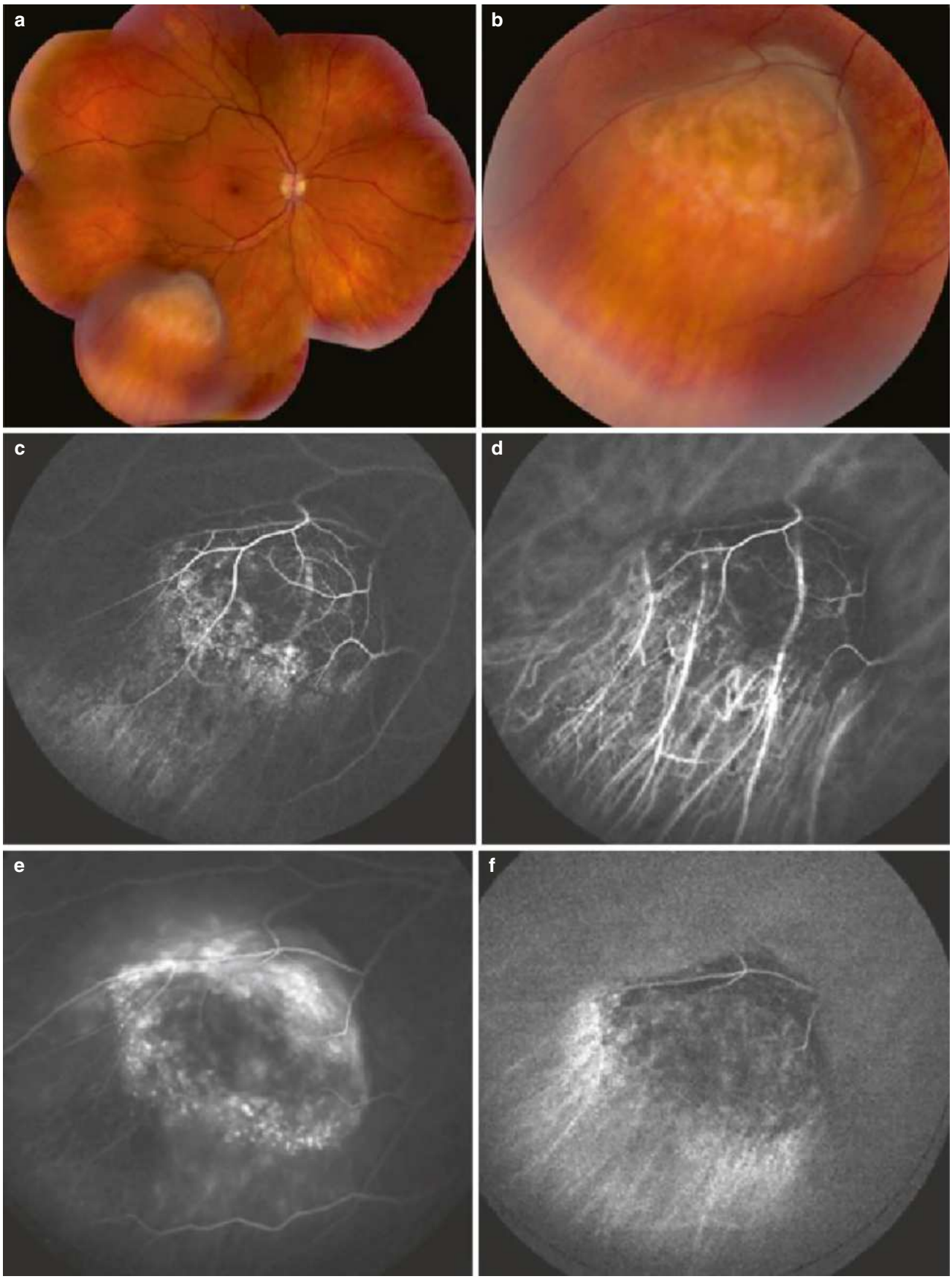

Fig. 20.19 Metastatic neuroendocrine tumor (**a**, **b**). Fluorescein (**c**) and ICG (**d**) angiography venous phases show a few intrinsic small vessels. In the late phase of FA (**e**) and ICGA (**f**), there are a few mild punctate leakages

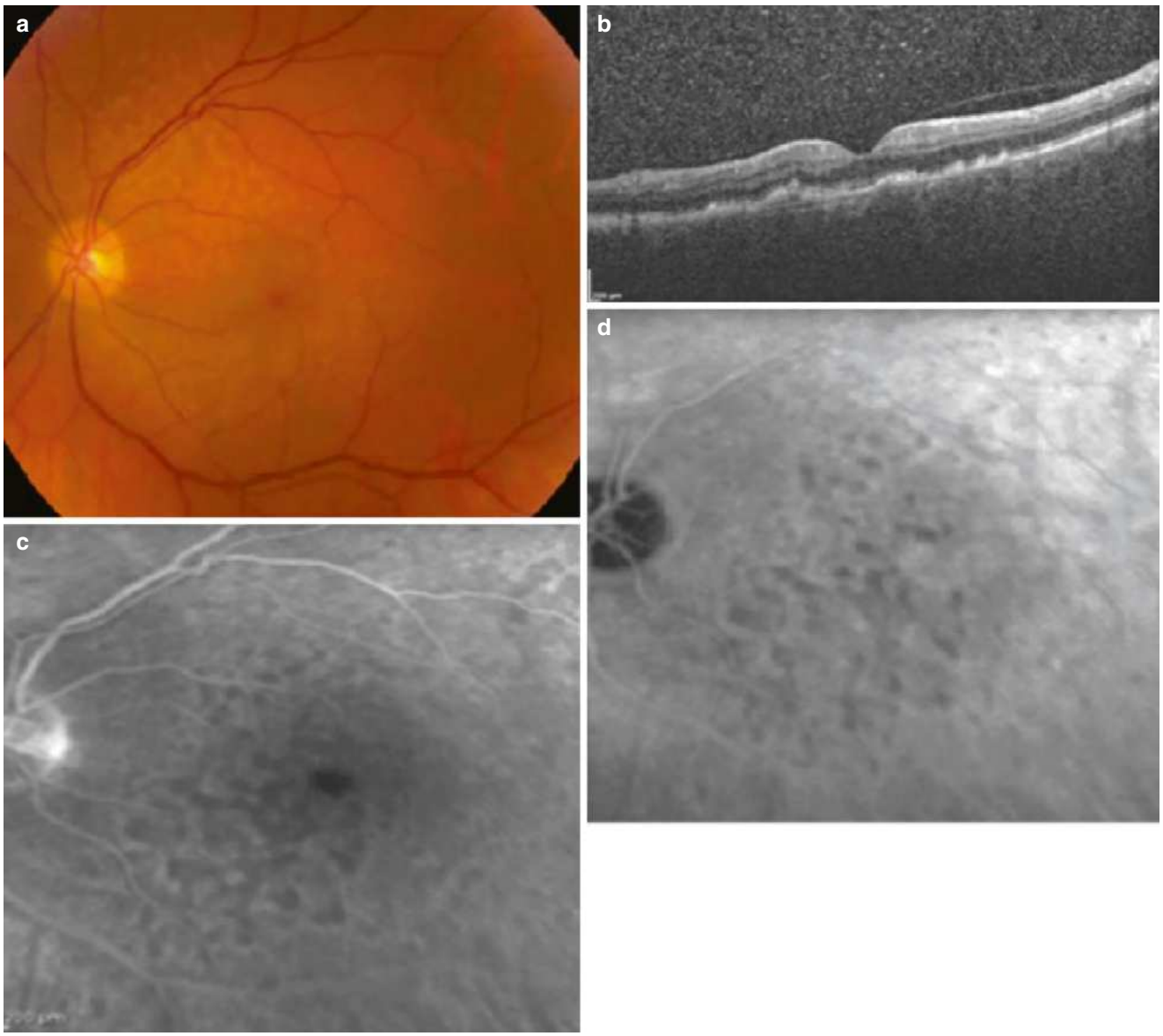

Fig. 20.20 Fundus photograph of a case of primary vitreoretinal lymphoma showing whitish subretinal pigment epithelial deposits of the lymphoma (**a**). This is confirmed by optical coherence tomography (**b**). Fluorescein (**c**) and ICG (**d**) angiographies show hypofluorescent spots because of blockage by the subretinal deposits

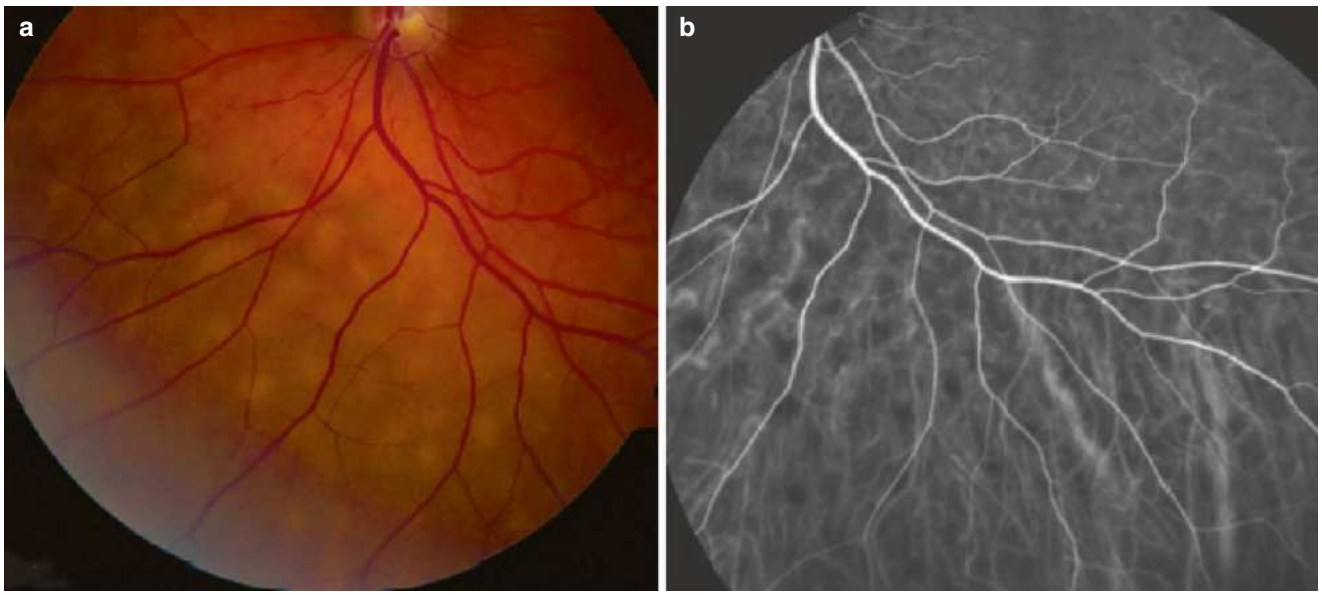

Fig. 20.21 Fundus photograph of an eye with choroidal lymphoma demonstrating focal choroidal infiltrates in the mid-periphery (**a**). Indocyanine green angiography demonstrating areas of hypofluorescence corresponding to focal choroidal infiltrates (**b**)

20.7 Simulating Conditions Causing Diagnostic Confusion with Retinal and Choroidal Tumors

Conditions causing diagnostic confusion with retinal and choroidal tumors include Coats' disease, persistent hyperplastic primary vitreous (PHPV), familial exudative vitreoretinopathy (FEVR), scleritis, peripheral exudative hemorrhagic chorioretinopathy (PEHCR), central serous chorioretinopathy (CSCR), polypoidal choroidal vasculopathy (PCV), uveal effusion syndrome, and paraneoplastic disorders.

20.7.1 Coats' Disease

Coats' disease is usually seen as a unilateral condition, more commonly in young males. The typical fluorescein angiographic findings in Coats' disease include telangiectatic vessels (light-bulb telangiectasia), microaneurysms, hard exudates, exudative retinal detachment, and peripheral retinal avascularity. The most common location of these vessels is in the temporal retina, followed by the inferior retina. Retinal macrocysts, retinal vasoproliferative tumors, and retinal neovascularization can also be seen. On FA, the telangiectatic vessels display early hyperfluorescence and persistent fluorescein leakage while exudation shows hypofluorescence [54, 55]. Microvascular involvement is reflected by areas of diffuse loss of the capillary bed or areas of complete capillary non-perfusion (Figs. 20.22 and 20.23).

20.7.2 Persistent Hyperplastic Primary Vitreous

Persistent hyperplastic primary vitreous, also known as persistent fetal vasculature (PFV), usually involves only one eye. Anterior PHPV represents prominent persistent tunica vasculosa lentis attaching to the lens and iris. In posterior PHPV, remnants of the hyaloid artery are present extending from the optic disc to the posterior lens capsule (Fig. 20.24). This canal contracts over time because of fibrosis. This can cause tractional retinal detachment in severe cases. In milder cases, the posterior lens capsule contracts, causing a cataract. There can also be persistence of the iris vasculature and vascularity over the ciliary body [56].

Fluorescein angiography can show leakage from the vessels under traction in the retina. Anterior segment FA can demonstrate the persistent vasculature and leakage from it. In dense cataracts, there can still be evidence of the vascularity behind the lens.

20.7.3 Familial Exudative Vitreoretinopathy

Familial exudative vitreoretinopathy can show similar leakage from the retinal vessels on the tractionally detached retina (Fig. 20.25) [55]. In milder cases, there can be evidence of peripheral avascularity. FEVR and retinopathy of prematurity demonstrate similar clinical features; however, patients with FEVR usually have normal gestational age and birth

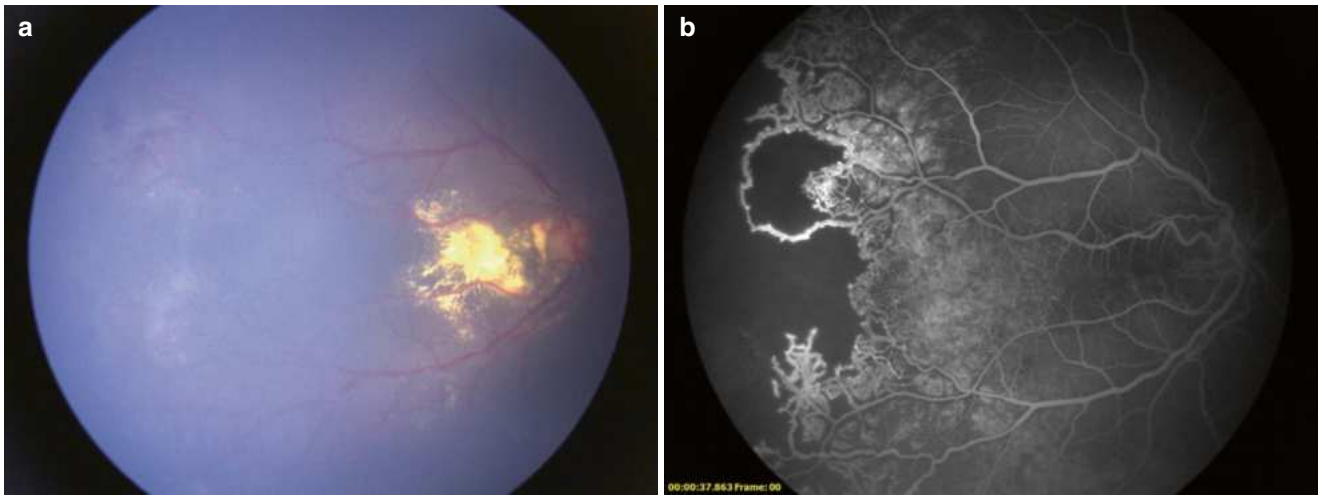

Fig. 20.22 RetCam fundus photograph (**a**) and fluorescein angiogram (**b**) of an eye with Coats' disease. Color photograph shows extensive macular exudation and temporal peripheral retinal non-perfusion. Fluorescein angiography demonstrates light-bulb telangiectasia, microaneurysms, dilated vessels, and peripheral non-perfusion

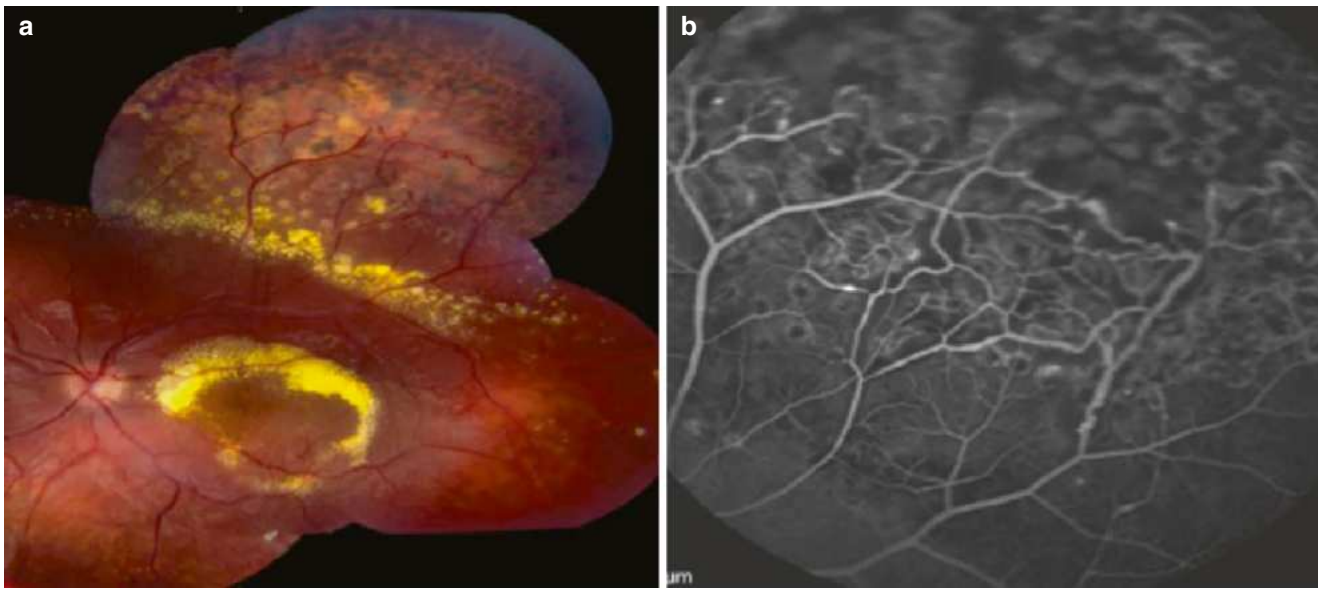

Fig. 20.23 Fundus photograph shows partially treated Coats' disease (**a**). Fluorescein angiography demonstrates telangiectatic vessels in the peripheral retina (**b**)

weights and have not been exposed to O_2 therapy. Similar findings can be seen in incontinentia pigmenti.

20.7.4 Scleritis

Scleritis is included in the differential diagnosis of patients with choroidal masses. Patients with scleritis usually have pain. There is thickening of the sclera in scleritis leading to decreased outflow from the choroid. Fluorescein angiography can show the presence of choroidal folds, as discussed in the section on choroidal lymphoma. In addition, with chronicity, leopard spotting occurs, as well as leakage from the choroid. There can also be leakage from the disc if the scleritis is near the posterior pole.

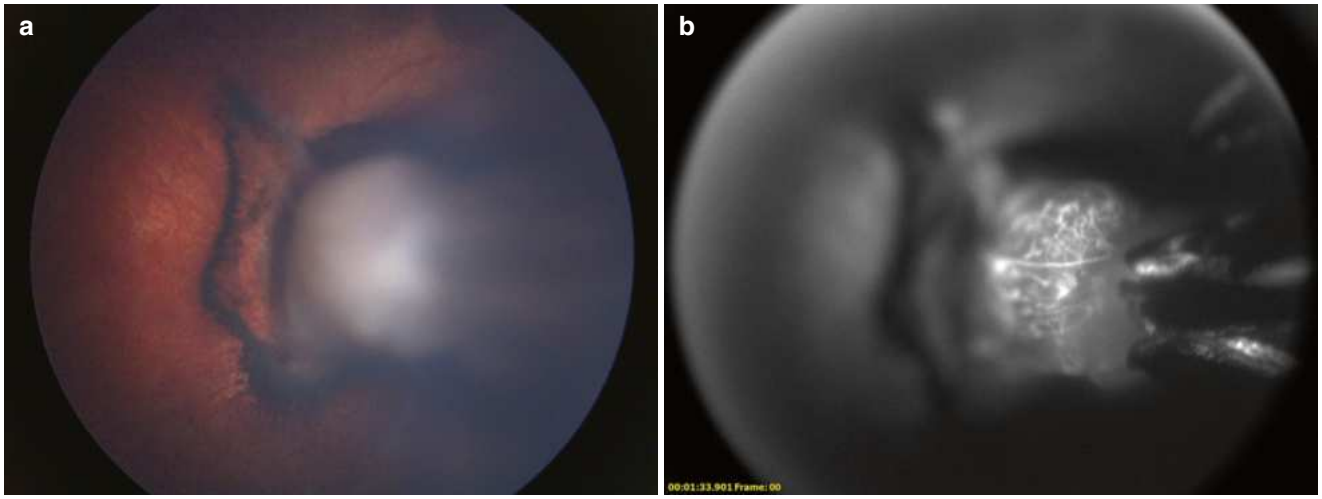

Fig. 20.24 RetCam fundus photograph (**a**) and fluorescein angiogram (**b**) of an eye with persistent hyperplastic primary vitreous. Color photograph shows the remnants of the tunica vasculosa lentis obscuring the optic disc. Fluorescein angiography demonstrates increased hyperfluorescence over the optic disc as well dragged ciliary processes more anteriorly demonstrating central core hyperfluorescence

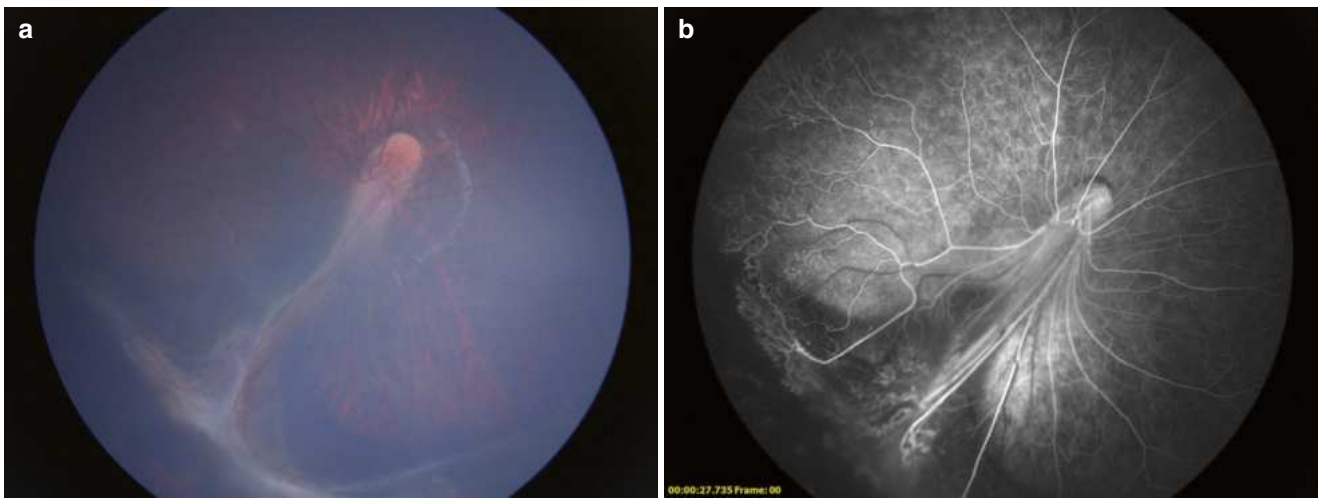

Fig. 20.25 RetCam fundus photograph (**a**) and fluorescein angiogram (**b**) of an eye with familial exudative vitreoretinopathy. Color photograph shows the falciform fold extending from the optic disc to the retinal periphery. Fluorescein angiography demonstrates peripheral retinal non-perfusion, telangiectatic vessels, and hyperfluorescence of the falciform fold

20.7.5 Peripheral Exudative Hemorrhagic Chorioretinopathy (PEHCR)

Peripheral exudative hemorrhagic chorioretinopathy (aka extramacular age-related macular degeneration) lesions are often mistaken for peripheral choroidal melanoma. PEHCR is an uncommon degenerative process of the retina with PED, subretinal and sub-RPE hemorrhage or exudates, and/or fibrotic exudative mass lesions outside of the macula [57]. On FA, PEHCR lesions are usually hypofluorescent in the early frames and continue to show hypofluorescence or isofluorescence with sharply demarcated edges in the late frames (Fig. 20.26). This appearance is mostly due to subretinal and sub-RPE hemorrhage. The overlying retinal vessels can show hyperfluorescence. Optical coherence tomography can confirm the presence of hemorrhagic PED [58]. The observation of hemorrhagic PED on OCT strongly supports the diagnosis of PEHCR against choroidal melanoma. Peripheral choroidal melanoma usually shows some extent of hyperfluorescence based on the RPE changes present on FA. Further, ciliary body involvement can also be seen in UWF imaging, ultrasound biomicroscopy, and transillumination. Peripheral exudative hemorrhagic chorioretinopathy lesions, in contrast to peripheral choroidal melanomas, never cross the ora serrata.

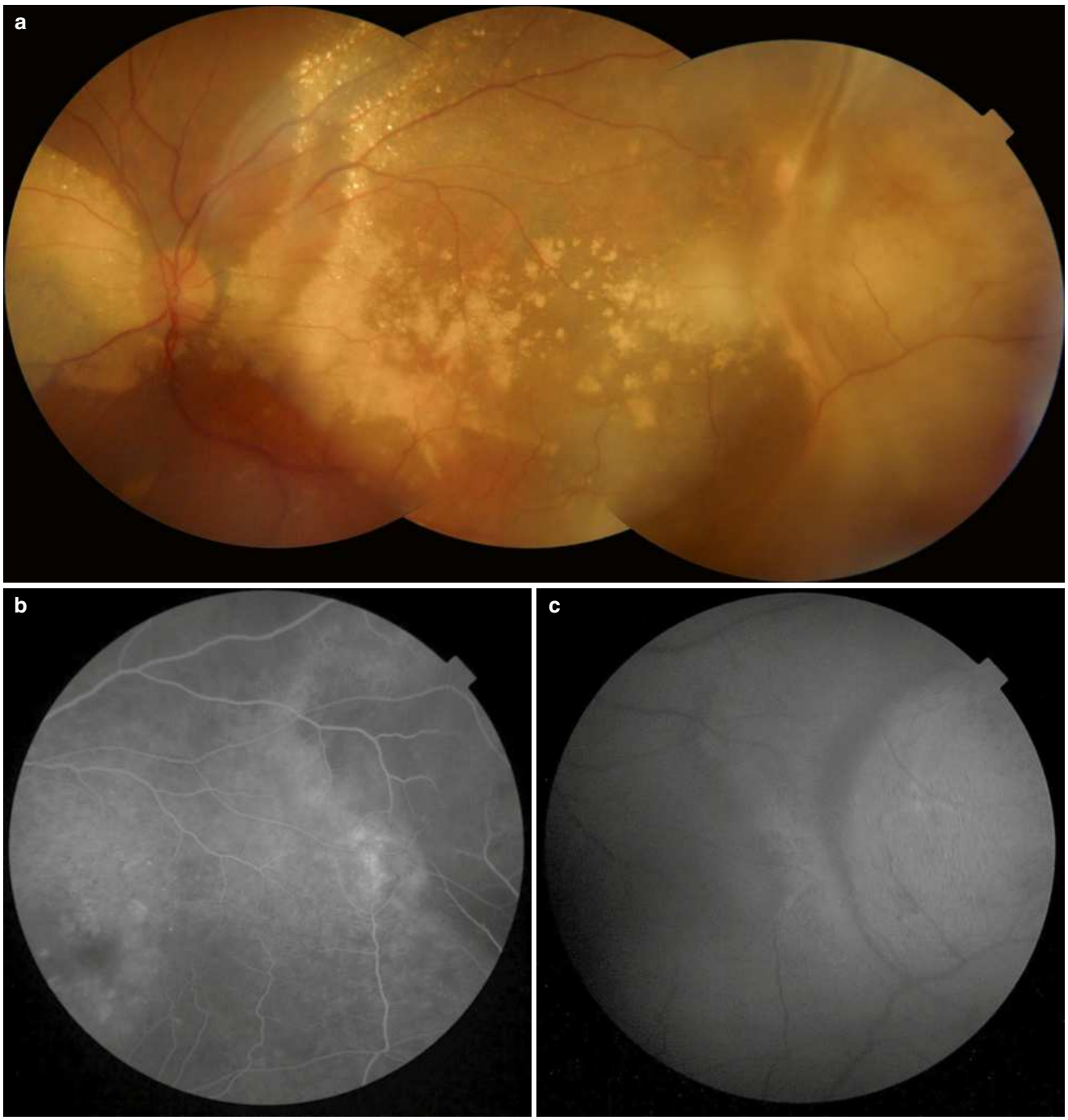

Fig. 20.26 Composite color fundus photograph shows temporally located PEHCR lesion and extensive hard exudates in the posterior pole (**a**). Fluorescein angiogram demonstrates isofluorescence in the lesion in the mid-phase (**b**). Fundus autofluorescence imaging shows PEHCR as an isoautofluorescent lesion (**c**)

20.7.6 Central Serous Chorioretinopathy

Central serous chorioretinopathy (CSCR) may cause diagnostic confusion with amelanotic lesions, especially choroidal hemangioma. Central serous chorioretinopathy has been historically diagnosed using FA; however, the availability of ICGA has increased our understanding of this disease. On FA, CSCR typically appears as one or several hyperfluorescent leaks at the level of the RPE. The fluorescein dye can have a "smokestack" appearance or can spread symmetrically, slowly staining the subretinal detachment area evenly. There is no retinal staining beyond the edges of the detachment.

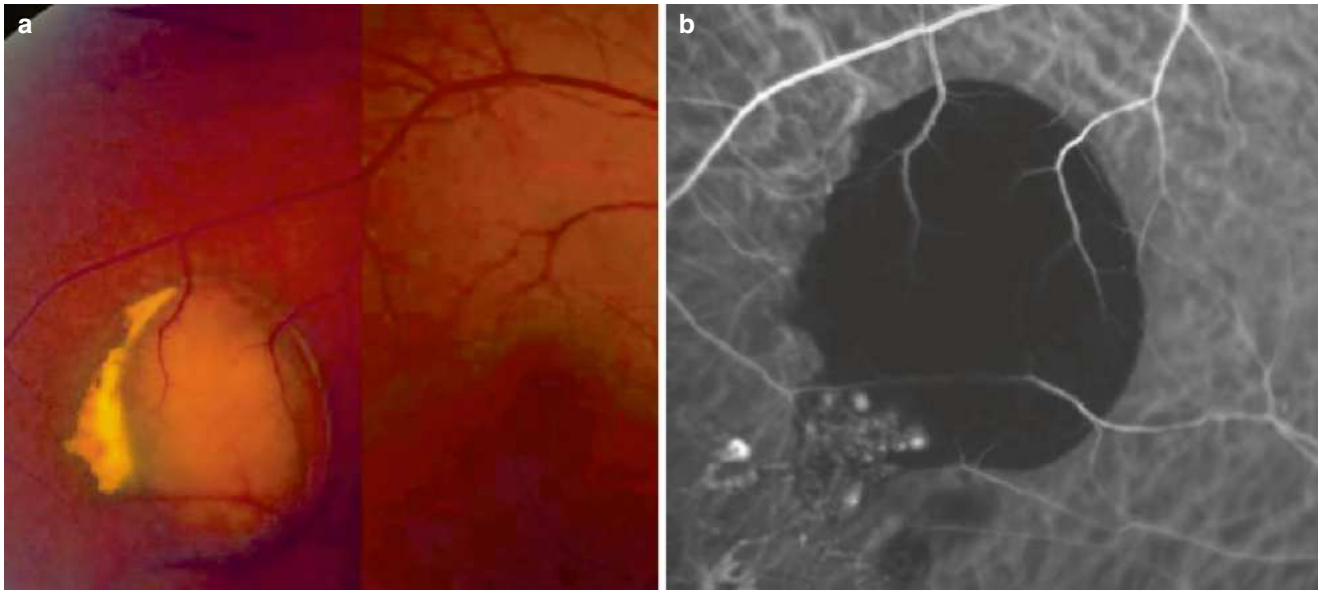

Fig. 20.27 The patient presented with this elevated subretinal lesion temporal to the macula with associated exudate (**a**). Indocyanine green angiography revealed characteristic hyperfluorescent "polyps," helping to make the diagnosis of polypoidal choroidal vasculopathy (**b**)

On ICGA, CSCR is displayed as localized vascular hyperpermeability of the choroid best visualized in the mid-phase of the angiogram. The leaked dye disperses into the deeper layers of the choroid, producing a characteristic hyperfluorescent patch in the choroid that enlarges away from the center during the later stages of ICGA [59]. In comparison to tumors, there are very small areas of leakage, and the fellow eye could have evidence of staining. In addition, enhanced depth imaging optical coherence tomography (EDI-OCT) and SS-OCT help in determining the status of the choroid in the areas that are involved. The underlying choroid is thick but not infiltrated. Central serous chorioretinopathy is now considered part of the pachychoroid disease spectrum.

20.7.7 Polypoidal Choroidal Vasculopathy (PCV)

Indocyanine green angiography is the standard of diagnosis of PCV. On ICGA, the branching vascular network (BVN) of PCV, which is essentially a choroidal neovascular membrane, is easily identified. The polyps present as focal hyperfluorescent outpouches or spots arising from the BVN and usually become apparent in the first 6 min of ICGA (Fig. 20.27) The late phase of ICGA shows a reversal in the pattern of fluorescence so that the area surrounding the lesion becomes hyperfluorescent and the center of the lesion is hypofluorescent [60].

Polypoidal choroidal vasculopathy lesions usually present as occult choroidal neovascularization on FA. Hyperfluorescent nodules, blocked fluorescence, and PEDs are some FA features that may be predictive of PCV.

20.7.8 Uveal Effusion Syndrome

In this syndrome, there appears to be a thickening of the sclera, causing decreased outflow from the choroid [61]. Again, leopard spotting is noted because of chronic leakage similar to patients with scleritis, choroidal lymphoma, and choroidal metastasis. Leopard spotting is due to RPE alterations with RPE clumps revealing hypofluorescence and RPE atrophy leading to window defects or hyperfluorescence (Fig. 20.28).

20.7.9 Paraneoplastic Disorders

There are several paraneoplastic disorders that involve the retina or choroid:

1. Carcinoma-associated retinopathy is the most common. There may be disc pallor or atrophy, attenuation of the retinal vessels, occasionally bone-spicule pigmentation, and cystoid macular edema; otherwise, the fundus is nondescript. Fluorescein angiography does not help much in making the diagnosis.
2. Acute exudative polymorphous paraneoplastic vitelliform maculopathy (AEPPVM) has been reported in cases with cutaneous melanoma, choroidal melanoma, breast

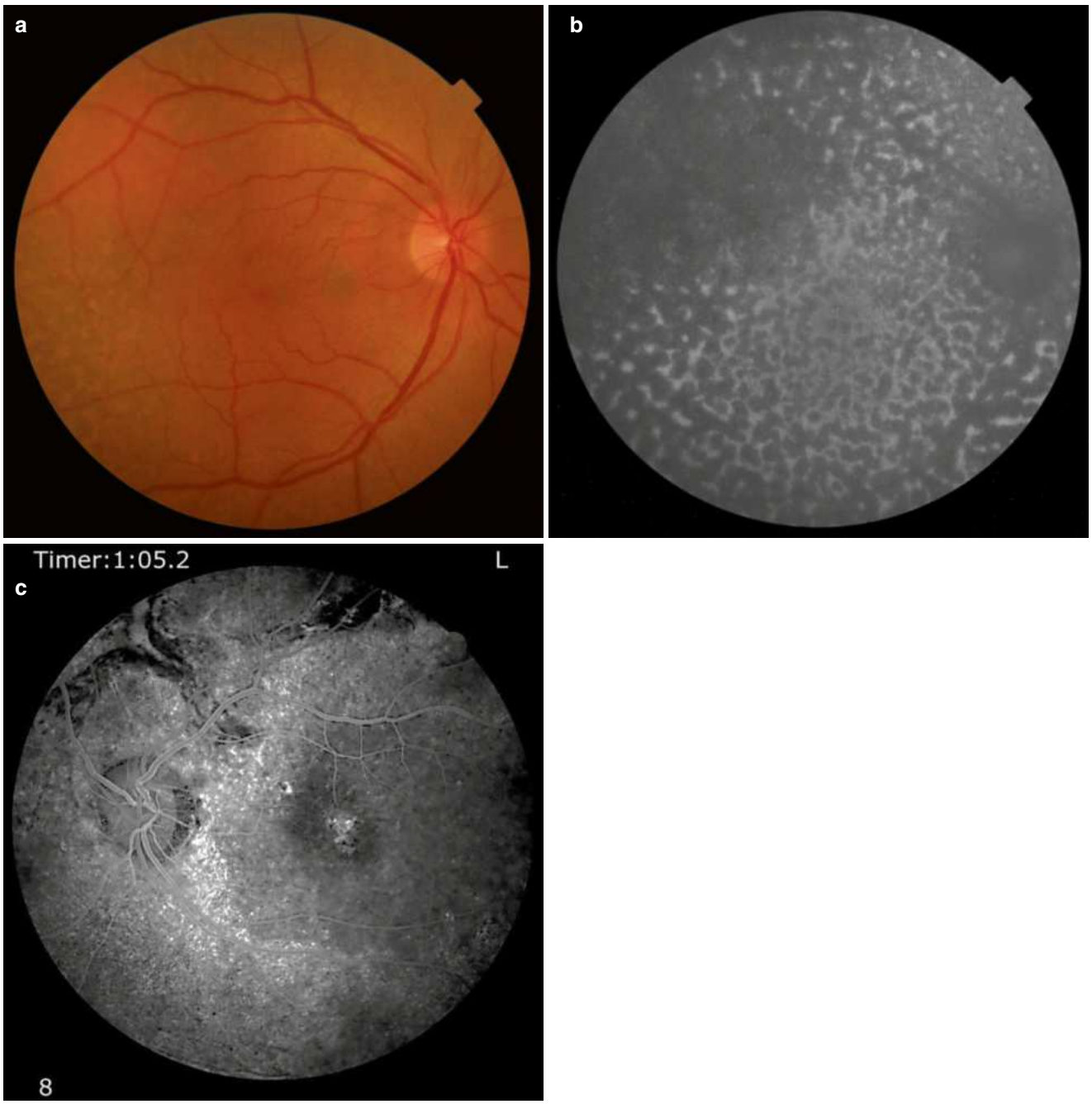

Fig. 20.28 Color fundus photograph shows leopard spotting in uveal effusion syndrome (**a**). Fundus autofluorescence imaging reveals hyper and hypoautofluorescent areas corresponding respectively to RPE clumping and atrophy (**b**). Fluorescein angiogram from another patient showing hyper and hypofluorescent spots corresponding respectively to RPE atrophy and clumping. Superiorly areas of fibrosis and dense hyperpigmentation appear as hyper and hypofluorescent areas respectively (**c**). The leopard pattern is reverse on FA and hyperfluorescent spots on FA correspond to hypoautofluorescence on autofluorescence imaging

cancer, pulmonary adenocarcinoma, and multiple myeloma. Fluorescein angiography in these cases shows initial blockage by the vitelliform material, followed by slow staining in the late phase [62]. Indocyanine green angiography does not add any further information. Acute exudative polymorphous paraneoplastic vitelliform maculopathy is best detected on OCT as shallow retinal detachments with underlying vitelliform material sometimes associated with outer retinal damage.

3. Bilateral diffuse uveal melanocytic proliferation (BDUMP) is associated most commonly with small-cell lung cancers and gynecologic cancers. It can occur unilaterally, hence the acronym DUMP [63]. Diffuse uveal melanocytic proliferation has been associated with

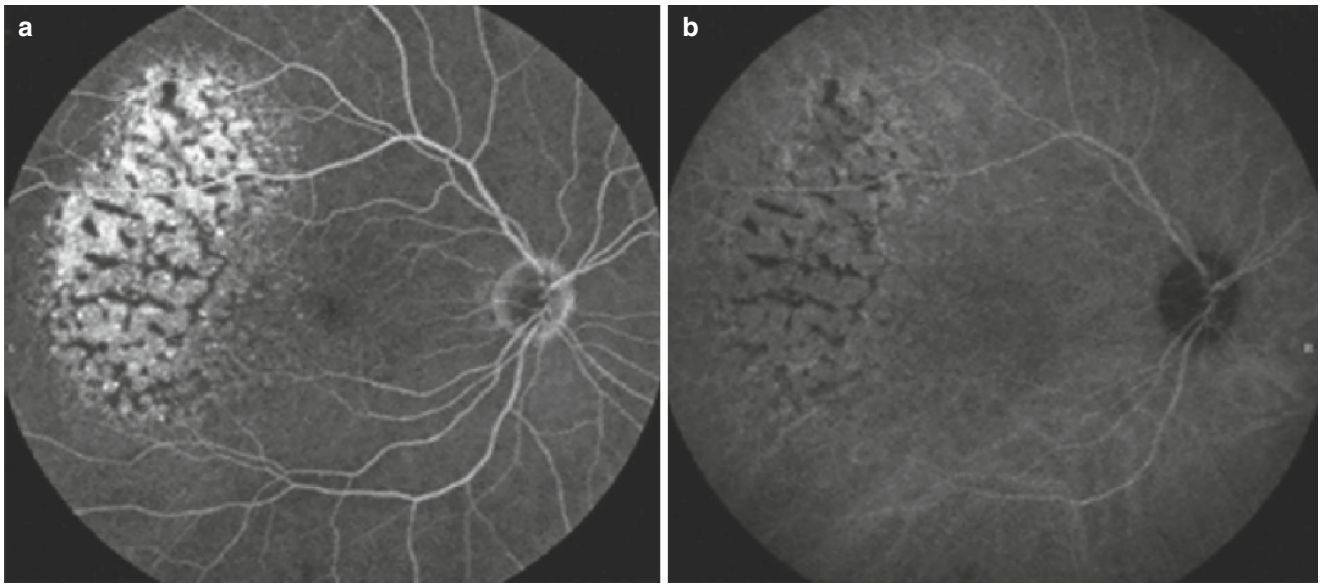

Fig. 20.29 Bilateral diffuse uveal melanocytic proliferation in the right eye. Fluorescein (**a**) and ICG angiograms (**b**) showing the blockage by the orange pigment and the intervening window defects

a factor termed CMEP factor (cultured melanocyte elongation and proliferation factor), which is present in the IgG fraction of serum. Fluorescein and ICG angiographies show a reticular pattern of staining where the RPE has atrophied secondary to the loss of the choriocapillaris resulting from infiltration of the uvea by the proliferating melanocytes (Fig. 20.29). There is also hypofluorescence from the areas of orange lipofuscin accumulations.

20.8 Radiation Retinopathy

Radiation retinopathy can develop after both brachytherapy of intraocular tumors and teletherapy of intraocular, periorbital, and paranasal tumors. The primary lesion in radiation retinopathy is vascular endothelial damage leading to vascular occlusion. Radiation retinopathy can sometimes occur together with radiation papillopathy. Radiation retinopathy runs a course similar to diabetic retinopathy and can be classified as nonproliferative or proliferative. Fluorescein angiography is helpful in quantitating the amount of ischemia in the peripheral retina, documenting retinal/disc neovascularization as well as showing the amount of capillary dropout, microvascular changes, and leakage from the macula (Fig. 20.30). Using FA, radiation-related macular edema is classified into focal, diffuse, and mixed types based on the pattern of dye leakage [64]. Fluorescein angiography is especially useful for ruling out ischemic maculopathy, in which case, little benefit might be anticipated from treatment. Optical coherence tomography has the advantages of providing quantitative measurement of macular edema and determining treatment response, but the determination of where to treat with laser photocoagulation is best done with wide-field FA. Indocyanine green angiography can demonstrate areas of choroidal hypoperfusion; however, this method of angiography is not routinely used in the evaluation of radiation retinopathy.

Optical coherence tomography angiography is currently the most important non-invasive tool in the evaluation of radiation maculopathy in eyes with choroidal melanoma as well as other tumors [65]. Using OCTA, Shields et al. found a decrease in capillary density of superficial and deep capillary plexuses and enlargement of the foveal avascular zone (FAZ) after plaque radiotherapy of choroidal melanoma [66]. Matet and associates reported that younger age, ellipsoid zone (EZ) disruption, larger FAZ, and lower superficial and deep capillary plexus density were associated with poor vision after proton beam irradiation of uveal melanoma [67]. Ellipsoid zone disruption, indicating photoreceptor damage, was associated with worse visual outcomes after irradiation and can result from long-standing macular edema [67]. These studies show that both plaque radiotherapy and proton beam irradiation have similar effects on retinal microvasculature, including enlargement of FAZ and a decrease in both superficial and deep retinal capillary plexus density [65–67]. Fluorescein angiography still holds an important place for the evaluation of radiation retinopathy because, in most cases, it provides a wider field of view compared to OCTA [68].

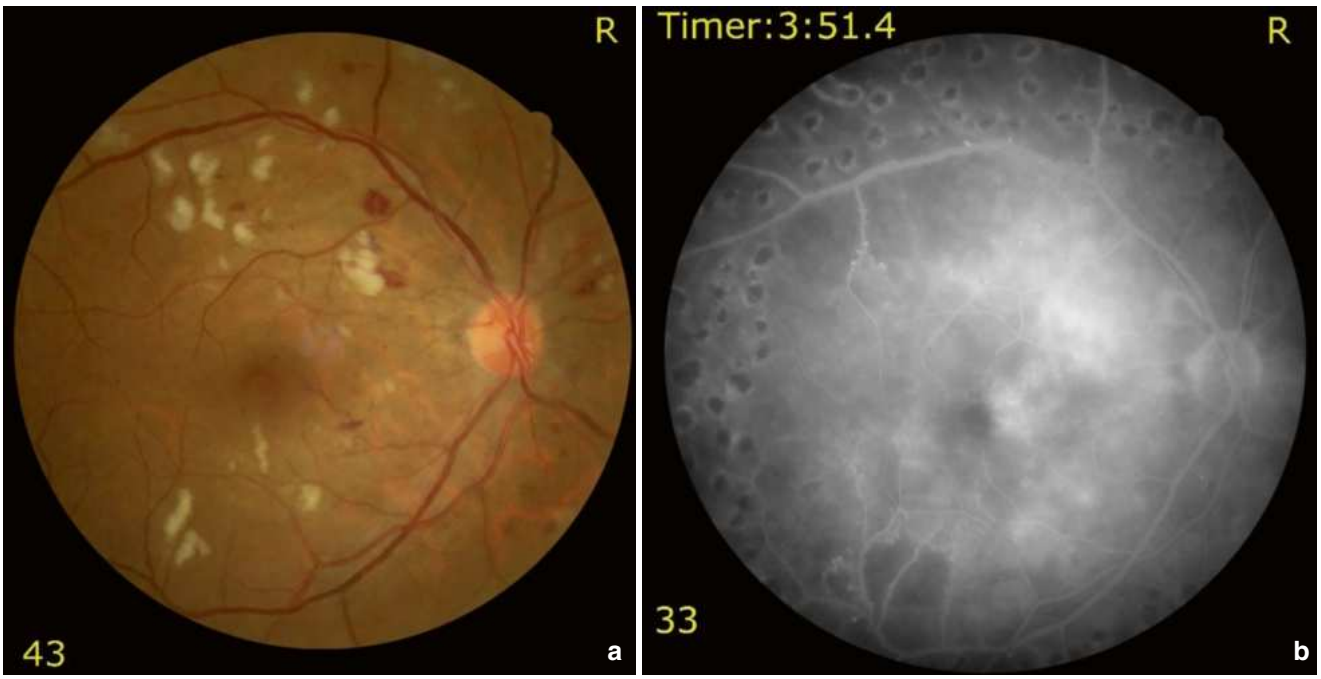

Fig. 20.30 Radiation retinopathy developing after external beam radiotherapy for lacrimal gland adenoid cystic carcinoma. Color fundus photograph shows numerous cotton-wool spots and retinal hemorrhages at the posterior pole and equator (**a**). Late-phase fluorescein angiogram of the same patient shows laser photocoagulation spots, retinal microaneurysms, areas of non-perfusion, and macular edema (**b**). Laser photocoagulation spots display hypofluorescence centrally due to pigment clumping and window defect peripherally due to RPE loss

References

1. Dzurinko VL, Gurwood AS, Price JR. Intravenous and indocyanine green angiography. Optometry. 2004;75:743–55.
2. Wykoff CC, Flynn HW Jr, Han DP. Allergy to povidone-iodine and cephalosporins: the clinical dilemma in ophthalmic use. Am J Ophthalmol. 2011;151:4–6.
3. Patel SN, Shi A, Wibbelsman TD, Klufas MA. Ultra-widefield retinal imaging: an update on recent advances. Ther Adv Ophthalmol. 2020;12:1–12.
4. Shields CL, Kancherla S, Patel J, et al. Clinical survey of 3680 iris tumors based on patient age at presentation. Ophthalmology. 2012;119:407–14.
5. Dart JK, Marsh RJ, Garner A, et al. Fluorescein angiography of anterior uveal melanocytic tumours. Br J Ophthalmol. 1988;72:326–37.
6. Singaravelu J, Melendez-Moreno A, Wrenn J, Singh AD. Angiographic features of iris melanocytic tumors: nevus versus melanoma. Ocul Oncol Pathol. 2023;9:9–16.
7. Bandello F, Brancato R, Lattanzio R, et al. Biomicroscopy and fluorescein angiography of pigmented iris tumors. A retrospective study on 44 cases. Int Ophthalmol. 1994;18:61–70.
8. Bowen RC, Raval V, Soto H, Singh AD. Intraocular tumors: angiographic patterns. Asia Pac J Ophthalmol (Phila). 2020;9:449–60.
9. Broaddus E, Lystad LD, Schonfield L, et al. Iris varix: report of a case and review of iris vascular anomalies. Surv Ophthalmol. 2009;54:118–27.
10. Shields JA, Bianciotto C, Kligman BE, et al. Vascular tumors of the iris in 45 patients: the 2009 Helen Keller lecture. Arch Ophthalmol. 2010;128:1107–13.
11. Shields JA, Streicher TF, Spirkova JH, Shields CL. Arteriovenous malformation of the iris in 14 cases. Arch Ophthalmol. 2006;124:370–5.
12. Gündüz AK, Tetik D. Follow-up of retinoblastoma using RetCam fluorescein angiography and correlation with clinical findings. Eur J Ophthalmol. 2023;33:2290-302.
13. Bianciotto C, Shields CL, Iturralde JC, et al. Fluorescein angiographic findings after intra-arterial chemotherapy for retinoblastoma. Ophthalmology. 2012;119:843–9.
14. Heimann H, Jmor F, Damato B. Imaging of retinal and choroidal vascular tumours. Eye. 2013;27:208–16.
15. Agarwal A, Kumari N, Singh R. Intravitreal bevacizumab and feeder vessel laser treatment for a posteriorly located retinal capillary hemangioma. Int Ophthalmol. 2016;36:747–50.
16. Shields CL, Kaliki S, Al-Dahmash S, et al. Retinal vasoproliferative tumors: comparative clinical features of primary vs secondary tumors in 334 cases. JAMA Ophthalmol. 2013;131:328–34.
17. Shields JA, Decker WL, Sanborn GE, et al. Presumed acquired retinal hemangiomas. Ophthalmology. 1983;90:1292–300.
18. Drummond JW, Hall DL, Steen WH, et al. Cavernous hemangioma of the optic disc. Ann Ophthalmol. 1980;12:1017–8.
19. Materin MA, Shields CL, Marr BP, et al. Retinal racemose hemangioma. Retina. 2005;25:936–7.
20. Mennel S, Meyer CH, Eggarter F, et al. Autofluorescence and angiographic findings of retinal astrocytic hamartomas in tuberous sclerosis. Ophthalmologica. 2005;219:350–6.
21. Shields JA, Shields CL. Tumors and related lesions of the pigment epithelium. In: Shields JA, Shields CL, editors. Intraocular tumors: an atlas and textbook. Philadelphia: Lippincott, Williams and Wilkins; 2008. p. 432–79.
22. Shields CL, Shields JA, Marr BP, et al. Congenital simple hamartoma of the retinal pigment epithelium: a study of five cases. Ophthalmology. 2003;110:1005–11.
23. Shields CL, Mashayekhi A, Ho T, et al. Solitary congenital hypertrophy of the retinal pigment epithelium: clinical features

and frequency of enlargement in 330 patients. Ophthalmology. 2003;110:1968–76.
24. Arevalo JF, Shields CL, Shields JA, et al. Angiography of retinal and choroidal tumors. In: Arevalo JF, editor. Retinal angiography and optical coherence tomography. New York: Springer; 2009. p. 179–98.
25. Gass JD. Fluorescein angiography. An aid in the differential diagnosis of intraocular tumors. Int Ophthalmol Clin. 1972;12:85–120.
26. Gunduz K, Pulido JS, Pulido JE, et al. Correlation of fundus autofluorescence with fluorescein and indocyanine green angiography in choroidal melanocytic lesions. Retina. 2008;28:1257–64.
27. Zografos L, Uffer S, Coscas G. Tumors of the choroid and retinal pigment epithelium. In: Coscas G, Coscas F, Zourdani A, editors. Atlas of indocyanine green angiography. Paris: Elsevier; 2015. p. 345–83.
28. Shields JA, Annesley WH Jr, Totino JA. Nonfluorescent malignant melanoma of the choroid diagnosed with the radioactive phosphorus uptake test. Am J Ophthalmol. 1975;79:634–40.
29. Flindall RJ, Gass JD. A histopathologic fluorescein angiographic correlative study of malignant melanomas of the choroid. Can J Ophthalmol. 1971;6:258–67.
30. Hayreh SS. Choroidal melanomata. Fluorescence angiographic and histopathological study. Br J Ophthalmol. 1970;54:145–60.
31. Pettit TH, Barton A, Foos RY, et al. Fluorescein angiography of choroidal melanomas. Arch Ophthalmol. 1970;83:27–38.
32. Shields JA, Shields CL, editors. Intraocular tumors: a text and atlas. Philadelphia: WB Saunders; 1992. p. 137–69.
33. Cantrill HL, Cameron JD, Ramsey RC, et al. Retinal vascular changes in malignant melanoma of the choroid. Am J Ophthalmol. 1984;97:411–8.
34. Augsburger JJ, Golden MI, Shields JA. Fluorescein angiography of choroidal malignant melanomas with retinal invasion. Retina. 1984;4:232–41.
35. Keunen JE, Hooymans JM, Ulbig MW, et al. Retinal neovascularization in choroidal melanoma without retinal ischemia. Retina. 2002;22:371–4.
36. Mueller AJ, Freeman WR, Schaller UC, et al. Complex microcirculation patterns detected by confocal indocyanine green angiography predict time to growth of small choroidal melanocytic tumors: MuSIC report II. Ophthalmology. 2002;109:2207–14.
37. Mueller AJ, Bartch DU, Folberg R, et al. Imaging the microvasculature of choroidal melanoma with confocal indocyanine green scanning laser ophthalmoscopy. Arch Ophthalmol. 1998;116:31–9.
38. Rummelt V, Folberg R, Rummelt C, et al. Microcirculation architecture of melanocytic nevi and malignant melanomas of the ciliary body and choroid. Ophthalmology. 1994;101:718–27.
39. Shields CL, Shields JA, De Potter P. Patterns of indocyanine green videoangiography of choroidal tumours. Br J Ophthalmol. 1995;79:237–45.
40. Shields JA, Demirci H, Mashayekhi A, et al. Melanocytoma of optic disc in 115 cases: the 2004 Samuel Johnson Memorial Lecture, part 1. Ophthalmology. 2004;111:1739–46.
41. Witschel H, Font RL. Hemangioma of the choroid. A clinicopathologic study of 71 cases and a review of the literature. Surv Ophthalmol. 1976;20:415–31.
42. Shields CL, Sun H, Demirci H, et al. Factors predictive of tumor growth, tumor decalcification, choroidal neovascularization, and visual outcome in 74 eyes with choroidal osteoma. Arch Ophthalmol. 2005;123:1658–66.
43. Gass JD. New observations concerning choroidal osteomas. Int Ophthalmol. 1979;1:71–84.
44. Shields CL, Brown GC, Sharma S, et al. Choroidal osteoma. In: Ryan S, Schachat A, Wilkinson C, et al., editors. Retina. 4th ed. Philadelphia: Elsevier Mosby; 2006. p. 819–28.
45. Desai UR, Tawansy KA, Joondeph BC, et al. Choroidal granulomas in systemic sarcoidosis. Retina. 2001;21:40–7.
46. Hong PH, Jampol LM, Dodwell DG, Hrisomalos NF, Lyon AT. Unifocal helioid choroiditis. Arch Ophthalmol. 1997;115:1007–13.
47. Shields JA, Shields CL, Demirci H, Hanovar S. Solitary idiopathic choroiditis. The Richard B. Weaver Lecture. Arch Ophthalmol. 2002;120:311–9.
48. Fung AT, Waldstein SM, Gal-Or O, et al. Focal scleral nodule. A new name for solitary idiopathic choroiditis and unifocal helioid choroiditis. Ophthalmology. 2020;127:1567–77.
49. Davis DL, Robertson DM. Fluorescein angiography of metastatic choroidal tumors. Arch Ophthalmol. 1973;89:97–9.
50. Arepalli S, Kaliki S, Shields CL. Choroidal metastases: origin, features, and therapy. Indian J Ophthalmol. 2015;63:122–7.
51. Natesh S, Chin KJ, Finger PT. Choroidal metastases fundus autofluorescence imaging: correlation to clinical, OCT, and fluorescein angiographic findings. Ophthalmic Surg Lasers Imaging. 2010;41:406–12.
52. Chan CC, Rubenstein JL, Coupland SE, et al. Primary vitreoretinal lymphoma: a report from an International Primary Central Nervous System Lymphoma Collaborative Group symposium. Oncologist. 2011;16:1589–99.
53. Gunduz K, Pulido JS, McCannel CA, et al. Ocular manifestations and treatment of central nervous system lymphomas. Neurosurg Focus. 2006;21:E9.
54. Ghorbanian S, Jaulim A, Chatziralli IP. Diagnosis and treatment of coats' disease: a review of the literature. Ophthalmologica. 2012;227:175–82.
55. Gündüz AK, Mirzayev I, Tetik D. Wide-field fundus imaging and fluorescein angiography findings in various pseudoretinoblastoma conditions. J Pediatr Ophthalmol Strabismus. 2023;60:60–74.
56. Goldberg MF. Persistent fetal vasculature (PFV): an integrated interpretation of signs and symptoms associated with persistent hyperplastic primary vitreous (PHPV). LIV Edward Jackson Memorial Lecture. Am J Ophthalmol. 1997;124:587–626.
57. Shields CL, Salazar PF, Mashayekhi A, Shields JA. Peripheral exudative hemorrhagic chorioretinopathy simulating choroidal melanoma in 173 eyes. Ophthalmology. 2009;116(3):529–35.
58. Sodhi GS, Singh N, Wrenn J, Singh AD. Peripheral hemorrhagic chorioretinopathy: differentiating features from choroidal melanoma. Ocul Oncol Pathol. 2023;9:1–8.
59. Piccolino FC, Borgia L. Central serous chorioretinopathy and indocyanine angiography. Retina. 1994;14:231–42.
60. Ciardella AP, Donsoff IM, Huang SJ, et al. Polypoidal choroidal vasculopathy. Surv Ophthalmol. 2004;49:25–37.
61. Elagouz M, Stanescu-Segall D, Jackson TL. Uveal effusion syndrome. Surv Ophthalmol. 2010;55(2):134–45.
62. Gündüz K, Çöndü G, Shields CL. Acute exudative polymorphous paraneoplastic vitelliform maculopathy managed with intravitreal aflibercept. Ophthalmic Surg Lasers Imaging Retina. 2017;48:844–50.
63. Reddy S, Finger PT. Unilateral diffuse uveal melanocytic proliferation (DUMP). Br J Ophthalmol. 2007;91:1726–7.
64. Gündüz K, Shields CL. Radiation retinopathy and papillopathy. In: Yanoff M, Duker J, editors. Ophthalmology. 6th ed. Philadelphia: Elsevier; 2023. p. 522–6.
65. Veverka KK, AbouChelade JE, Iezzi R Jr, et al. Noninvasive grading of radiation retinopathy: the use of optical coherence tomography angiography. Retina. 2015;35:2400–10.

66. Shields CL, Say EA, Samara WA, et al. Optical coherence tomography angiography of the macula after plaque radiotherapy of choroidal melanoma: comparison of irradiated versus nonirradiated eyes in 65 patients. Retina. 2016;36:1493–505.
67. Matet A, Daruich A, Zografos L. Radiation maculopathy after proton beam therapy for uveal melanoma: optical coherence tomography angiography alterations influencing visual acuity. Invest Ophthalmol Vis Sci. 2017;58:3851–61.
68. Finger PT, Kurli M. Laser photocoagulation for radiation retinopathy after ophthalmic plaque radiation therapy. Br J Ophthalmol. 2005;89:730–8.

Diagnostic Techniques: OCT

21

Rubens N. Belfort, Aluisio Rosa Gameiro Filho, and Arun D. Singh

21.1 Introduction

Optical coherence tomography (OCT) is a powerful imaging technique that provides cross-sectional imaging of tissues [1]. Among several implementations of OCT, spectral-domain OCT (SD-OCT) provides high-resolution, high-sensitivity, and high-speed imaging. Such implementations enable visualization of the microstructures of the human eye by noninvasive and noncontact equipment. The high sensitivity of OCT detection enables imaging of structures with very low optical scattering, such as the retina. The high axial and lateral resolution enables the precise morphological investigation of various pathological conditions.

21.2 Enhanced Depth Imaging

Recently, Spaide and associates have described enhanced depth imaging (EDI), a simple method using commercially available OCT devices to image the choroid [2]. In an exploratory study, Torres et al. described the intrinsic optical characteristics of choroidal tumors imaged with the EDI OCT technique and correlated tumor measurements with ultrasonography [3]. In their study, all the tumors that were too small (<1.0 mm in thickness) to be adequately identified by ultrasonography (such as choroidal nevi) were adequately imaged and objectively measurable by EDI OCT techniques. On the other hand, tumors that were >1.0 mm in height and/or >9.0 mm in diameter were not suitable to be measured by EDI OCT. Consequently, they suggested that EDI OCT and ultrasound may be considered complementary techniques for tumor thickness measurement [3].

21.3 Swept-Source OCT (SS-OCT)

Choroidal imaging has been improved by innovations in technology that use a laser source across a range of wavelengths [4]. The swept laser light source sequentially emits various frequencies, increasing the signal quality from deep tissues such as choroid [5]. Characteristics of choroidal nevi imaged by SS-OCT include visualization of intralesional details such as vessels, cavities, and granularity [6]. Nevertheless, similar to EDI OCT [3], image quality is superior for choroidal lesions that are small, closer to the fovea, and with lighter choroidal pigmentation [6, 7].

21.4 Optical Coherence Tomography Angiography

Optical coherence tomography angiography (OCTA) is a new noninvasive technique that allows three-dimensional mapping of the retina and choroidal microvasculature [8]. The rapid acquisition time, the avoidance of intravenous dye, and the ability to identify capillary abnormalities without being obscured by leakage or staining are some of the advantages over FA. Another advantage is the ability of OCTA to clearly distinguish between the superficial capillary plexus (SCP) and deep capillary plexus (DCP), which is not possible in FA, and this can influence clinical care [9, 10]. Technological advancements have made it possible to correlate pathologic vascular lesions with the structural changes seen on OCT angiography both for anterior segment and posterior segment tumors.

R. N. Belfort (✉) · A. R. Gameiro Filho
Department of Ophthalmology and Visual Sciences, Escola Paulista de Medicina—Federal University of São Paulo, São Paulo, Brazil
e-mail: rubens@belfort.med.br

A. D. Singh
Department of Ophthalmic Oncology, Cole Eye Institute, Cleveland Clinic, Cleveland, OH, USA
e-mail: singha@ccf.org

© The Author(s), under exclusive license to Springer Nature Switzerland AG 2025

A. D. Singh, B. E. Damato (eds.), *Clinical Ophthalmic Oncology*, https://doi.org/10.1007/978-3-031-75907-9_21

21.5 Conjunctival and Corneal Tumors

OCT can provide valuable diagnostic information when assessing tumors of the cornea and conjunctiva.

Conjunctival nevus is one of the most common benign tumors of the ocular surface. On histopathology, a nevus typically consists of nests of melanocytic cells that are present in the junctional and subepithelial regions of the conjunctiva. Conjunctival inclusion cysts are characteristic of nevi and are usually visible clinically. Anterior segment OCT enables high-quality imaging of conjunctival nevi, revealing all margins and providing information on the presence of the typical intralesional cysts (Fig. 21.1). OCT allows identification of the tumor margins and additional features, which include conjunctival thickening. One of the main disadvantages of OCT is the optical shadowing of deeper structures from pigment in conjunctival nevi [11].

In contrast, primary acquired melanosis (PAM) is characterized by basal epithelial hyper-reflective band with a normal overlying epithelium and no cysts [12]. The OCT findings have been shown to correlate well with clinical and histopathologic features of conjunctival and corneal PAM (Fig. 21.2) [12].

Conjunctival melanoma appears as a hyper-reflective, thickened epithelium with the extension of hyper-reflectivity into the subepithelial layer and significant optical shadowing, which may obscure the underlying tissue [13].

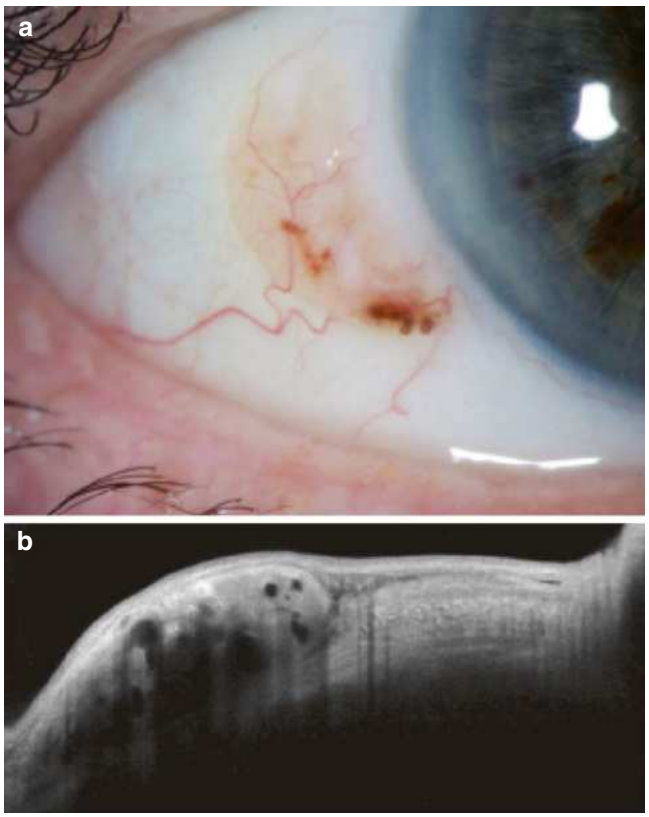

Fig. 21.1 Conjunctival nevus. Clinical appearance (**a**). Anterior segment OCT confirms the presence of an intralesional cyst (**b**)

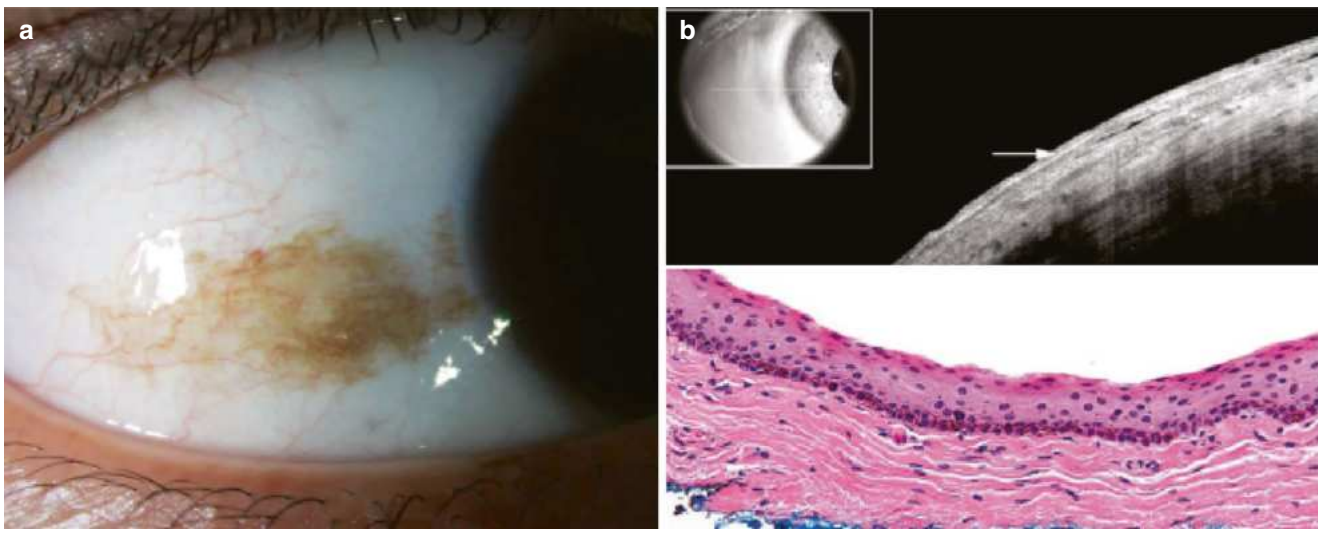

Fig. 21.2 Primary acquired melanosis. Clinical appearance (**a**). Note the basal epithelial hyper-reflective band of approximately 20 μm thickness (**b**, above, arrow) and the corresponding melanocytic hyperpigmentation that is restricted to the basal layer (**b**, below, HE. ×200). (Reprinted from Alzahrani et al. [12]. With permission from Karger Publishers. Copyright © 2015, © 2015 S. Karger AG, Basel)

Table 21.1 Conjunctival melanocytic lesions: anterior segment OCT features

Diagnosis	Epithelial hyper-reflective band	Stroma	Shadowing	Cyst
PAM	+++	Normal	+/−	Absent
Nevus	++	Normal/abnormal	++	Present
Melanoma	+	Abnormal	+++	Absent

Adapted from Alzahrani et al. [12]. With permission from Karger Publishers. Copyright © 2015, © 2015 S. Karger AG, Basel

Characteristically, cysts are absent [14]. Comparative OCT findings of conjunctival and corneal melanocytic lesions are summarized in Table 21.1.

Ocular surface squamous neoplasia can involve the conjunctiva, the cornea, or both and comprise a spectrum of neoplasia ranging from intraepithelial neoplasia to invasive squamous cell carcinoma. A small pilot study involving the uterine cervix demonstrated the ability of OCT to distinguish abnormal epithelium from normal epithelium [15]. Kieval et al. investigated the use of an ultrahigh-resolution OCT as an adjuvant diagnostic tool in distinguishing ocular surface squamous neoplasia from pterygia (Fig. 21.3) [16]. Preoperative ultrahigh-resolution OCT images demonstrate similarities to the histopathologic specimens. Both optical and pathologic specimens show a thickened layer of epithelium, often with an abrupt transition from normal to neoplastic tissue in the eyes with squamous cell carcinoma. Differences in the measured epithelial thickness on ultrahigh-resolution OCT between squamous cell carcinoma and pterygia are statistically significant. More recently, OCT-A of the anterior segment is also under investigation (Fig. 21.4). Binotti et al. [17] published a retrospective case-control study that showed peri-lesional vessel depth and diameter were significantly increased in malignant lesions and could represent feeder vessels seen during slit-lamp examination. They proposed that these findings—which can be easily assessed with OCT-A—could be used as potential parameters, with high sensitivity and specificity, to help distinguish malign and benign lesions.

Liu [18] used OCTA-A to evaluate patients with OSSN, we noticed a higher vessel area density (VAD) within the tuner, followed by adjacent sub-epithelial tissue and the tissue directly under the tumor. The vessels in the tumor were similar to the sea fan-shaped vessels seen on indocyanine green (ICG). Also, OCTA-A was able to demonstrate vessel enface and blood flow on corneal lesions that were not visualized clinically.

Limitations of OCT-A include the fact that this exam cannot access vascular leakage or evaluate the direction of the blood flow. Also, protection artifacts and the fact that manual measurements of vessel depth and diameter could carry some degree of subjectivity (ideally, automated software for the anterior segment should be implemented) can lead to some errors in interpretation.

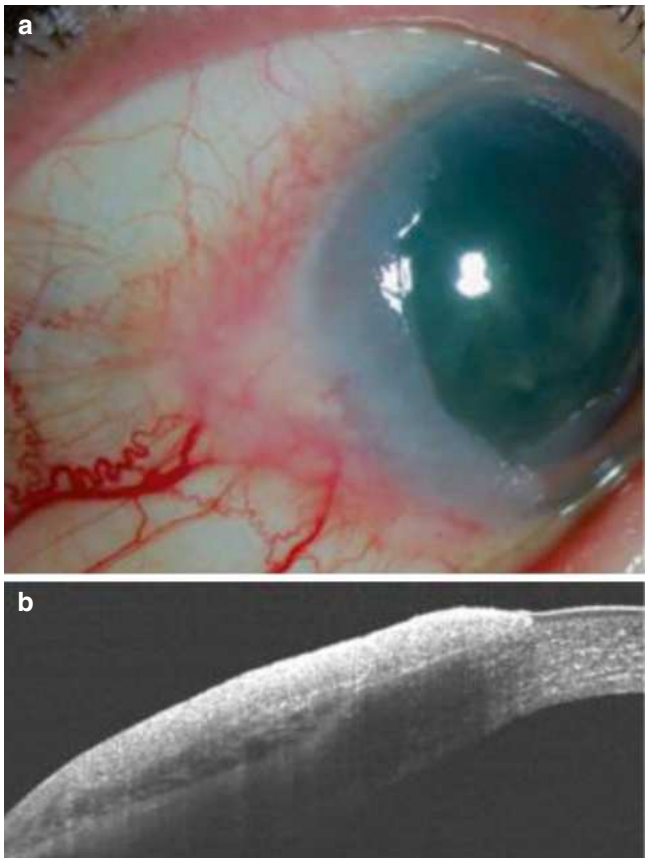

Fig. 21.3 Ocular surface squamous neoplasia of the conjunctiva and cornea. Clinical appearance (**a**). Anterior segment OCT shows a thickened hyper-reflective epithelium with an abrupt transition from normal to neoplastic tissue (**b**)

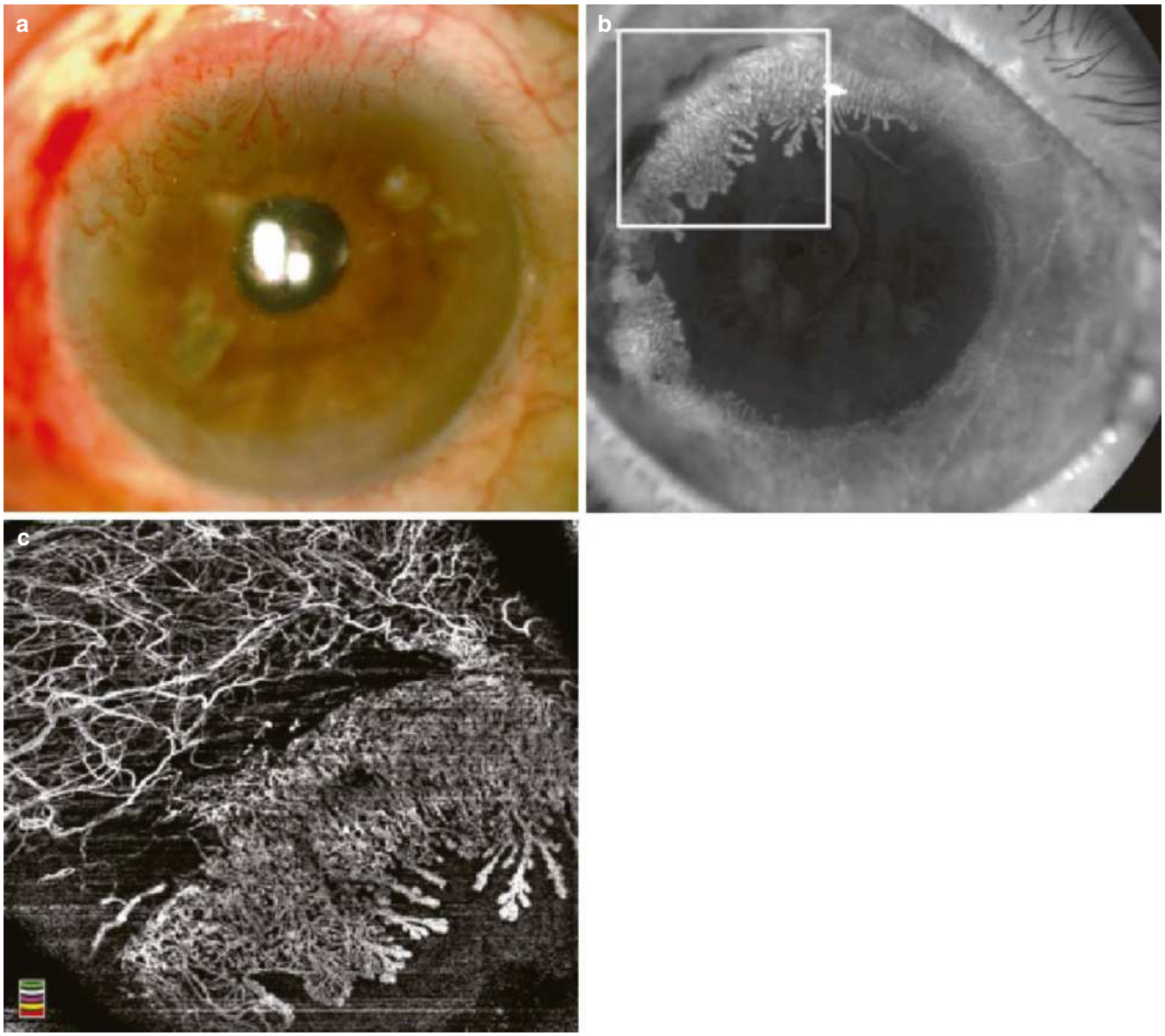

Fig. 21.4 Anterior segment OCTA. Squamous conjunctival neoplasia affecting the superior left limbus (**a**), anterior segment fluorescein angiography showing a vascular pattern within the neoplastic area (**b**). Corresponding view of the specified area (rectangle) with anterior segment OCTA. OCTA shows normal vessels on superior part and the neoplastic vessels inferiorly (**c**)

21.6 Scleral Lesions

Depending upon the thickness, pigmentation, and internal composition, scleral lesions can be partially visualized by OCT (Fig. 21.5).

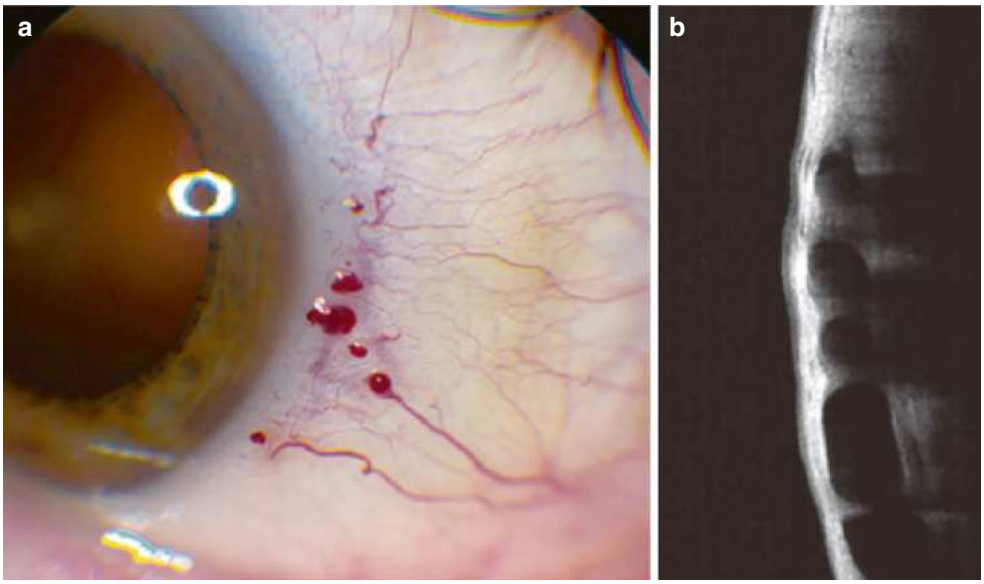

Fig. 21.5 Scleral vascular anomaly. Clinical appearance (**a**). Anterior segment OCT showing partial view of several intrascleral clear spaces (**b**)

21.7 Anterior Uveal Tumors

Imaging technologies of the anterior segment provide useful information on tumor size, shape, internal features, and extension. Given that some of these conditions, such as iris melanoma, can threaten vision and life, a precise and complete image of the lesion is highly relevant.

Few clinical studies have compared OCT with UBM in the evaluation of ciliary body and iris tumors (Fig. 21.6). Siahmed et al. described the use of UBM and AS-OCT for imaging 61 cases of iris tumors, observing that only UBM provided a precise measurement and regular surveillance capabilities compared [19]. Pavlin et al. published a series of patients with iris and ciliary body tumors that were evaluated with both UBM and OCT [20]. They observed that OCT was able to visualize the margins of only small hypopigmented tumors, whereas UBM had a superior ability to penetrate larger, highly pigmented tumors and those located in the ciliary body (Fig. 21.7). Bianciotto and coworkers also reported UBM as a superior method for imaging of anterior segment tumors, such as ciliary body and iris melanoma [21].

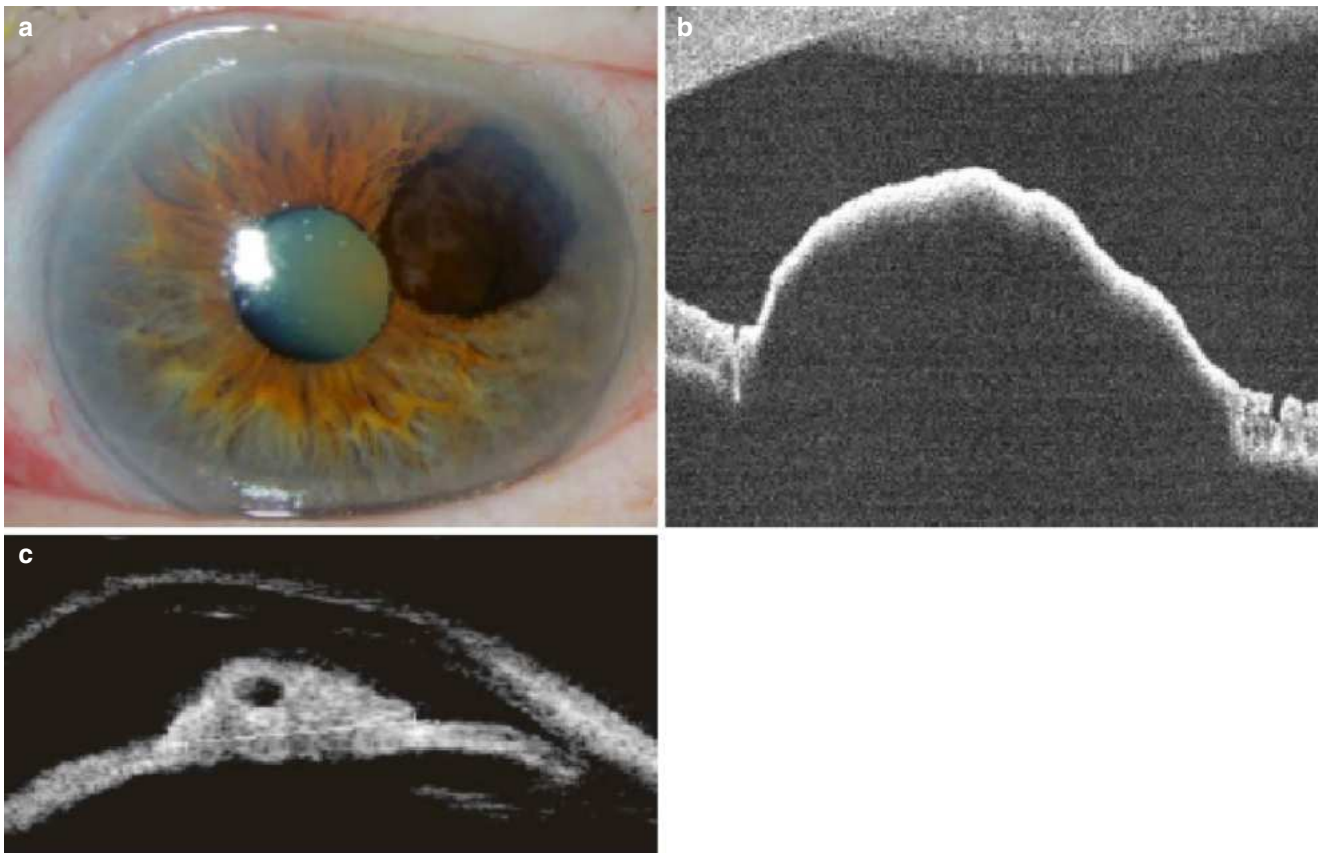

Fig. 21.6 Pigmented iris melanoma. Clinical appearance (**a**). Anterior segment OCT shows hyper-reflectivity with shadowing and obscuration of the posterior margin (**b**). Ultrasound biomicroscopy revealed isolated iris involvement (**c**)

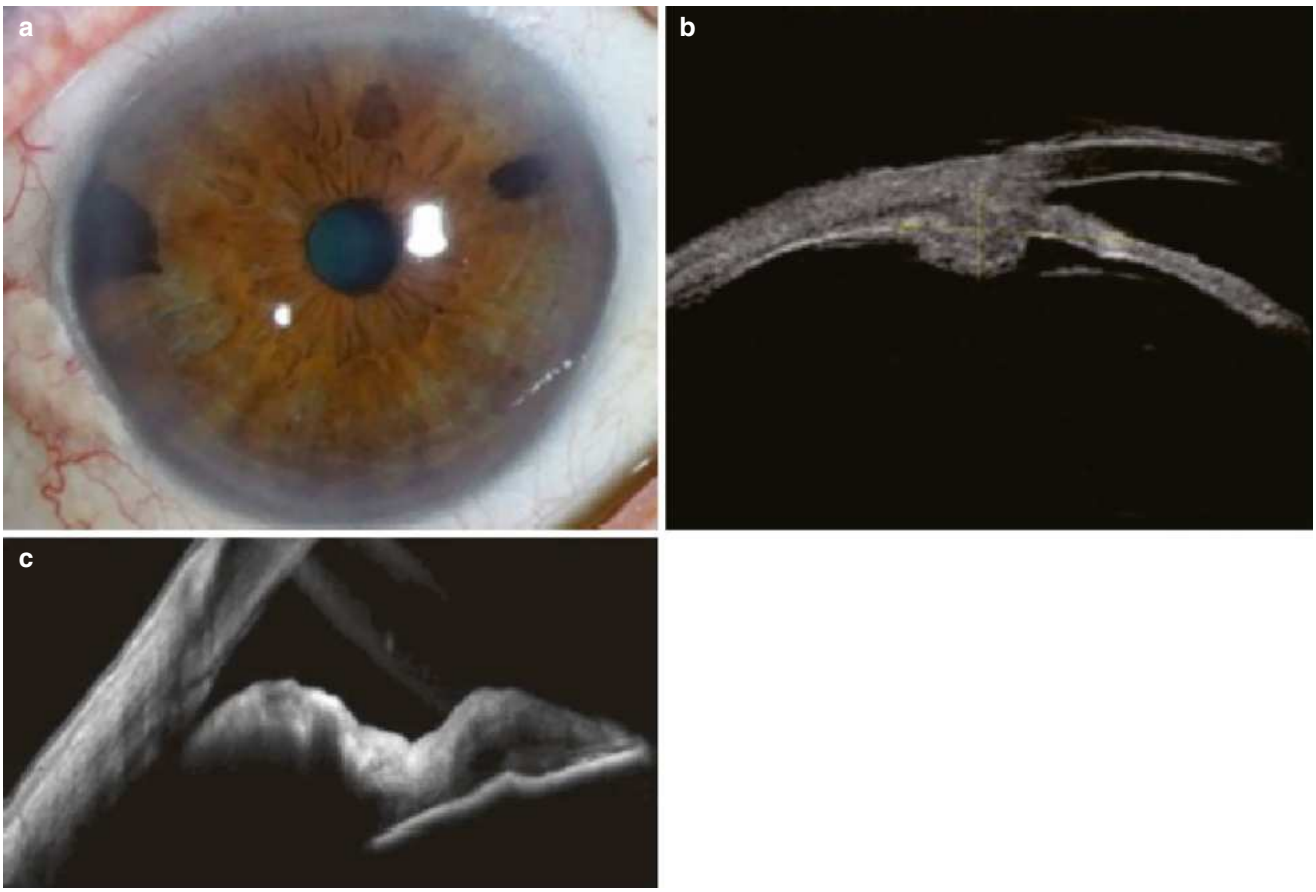

Fig. 21.7 Iridociliary melanocytic tumor. Clinical appearance (**a**). Anterior segment OCT shows hyper-reflectivity with shadowing and poor visualization of the ciliary body (**b**). Ultrasound biomicroscopy reveals ciliary body involvement (**c**)

21.8 Intraocular Tumors

21.8.1 Retinal Pigment Epithelial Tumors

On OCT, the typical appearance of congenital hypertrophy of the retinal pigment epithelium (CHRPE) is a flat lesion, usually with a thick RPE layer [22] (Fig. 21.8). Fung et al. [23] described enhanced depth imaging OCT (EDI-OCT) findings of patients with CHRPE: they noted a thickened RPE in 89% of the patients, with the overlying retina showing marked photoreceptor loss immediately at the site of the CHRPE. Subretinal cleft was seen in 33% of the lesions, and it was speculated to represent a thinned excavated posterior retina with photoreceptor atrophy, leaving an empty space. The underlying choroid was normal in all cases of the study. One limitation of the OCT used for these tumors is the usual peripheral location, which makes obtaining a good image challenging.

Congenital simple hamartoma of the RPE is a rare, pigmented hamartoma, typically located on the parafoveal region. On OCT, an elevation of the inner retina, with marked shadowing, no adjacent retinal tissue disturbance, and a normal underlying choroid can be noticed [22].

Combined hamartoma of the retina and RPE is an elevated grey massif on the retina, blending imperceptibly with the surrounding retina and RPE without retinal detachment or vitreous inflammation. Spectral-domain OCT reveals an elevated hyper-reflective mass in the retina with mild attenuation of the retinal pigment epithelium and photoreceptor inner/outer segment junction, which may be accompanied by a hyper-reflective epiretinal membrane [24–26]. EDI-OCT shows vitreoretinal traction in the inner or full-thickness retina, leading to patterns of sawtooth and/or full-thickness retinal folds [27].

Retinal pigment adenoma/adenocarcinoma is another rare intraocular tumor, classically presenting as a black full-thickness retinal mass. On EDI-OCT, it appears with a "rugged" ocular surface, with full-thickness retinal tumor and dense posterior optical shadowing. Remote macular findings such as epiretinal membrane, edema, and macular holes can be seen [22].

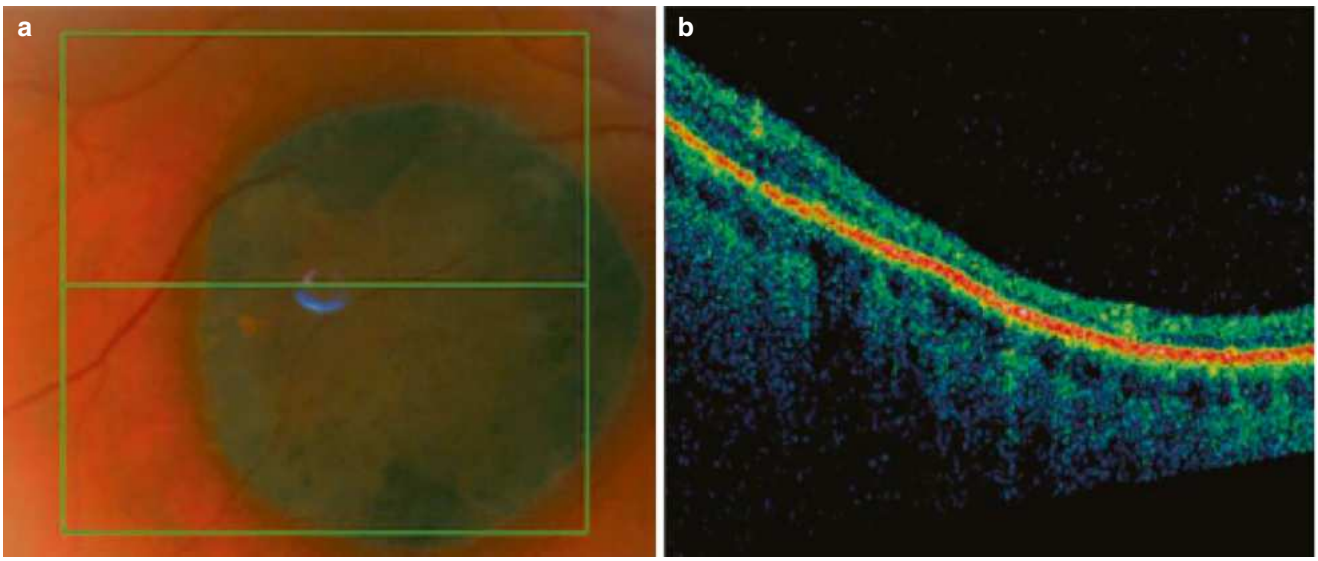

Fig. 21.8 A typical fundus appearance of congenital hypertrophy of the retinal pigment epithelium (RPE) (**a**) is of thickened RPE layer by OCT (**b**)

21.9 Retinal Tumors

21.9.1 Retinal Astrocytic Hamartoma

Retinal astrocytic hamartoma (astrocytoma) is a vascularized, benign, glial tumor of the retina. SD-OCT shows a thickened inner retina with an epiretinal membrane, some disorganization of the inner and outer retinal layers, and an intact RPE underlying the tumor. Intraretinal fluid and multiple ovoid hypolucencies within the tumor stroma are also commonly observed (Fig. 21.9) [28–30]. A SD-OCT based classification of retinal astrocytic was proposed, in which RAH can be divided into four types: Type 1, in which the lesion is flat, and there is no clinical evidence of retinal traction; Type 2, showing a slightly elevated (height <500 μm), with clinical evidence of retinal traction; Type 3, showing an elevated retinal mass (>500 μm), with inner retinal calcification and clinical evidence of mulberry like-calcification; and Type 4, with an elevated retinal mass (>500 μm), optically empty cavity, and clinical evidence of smooth noncalcified inner retinal mass. (Fig. 21.10) [31] The OCT-A reveals a dense vascular network within the tumor [32].

21.9.2 Retinoblastoma

Handheld optical coherence tomography (OCT) has been evaluated in children with retinoblastoma as a tool for guiding management. OCT can be used to evaluate treated scars and foveal health and to detect small new tumors in the posterior pole. The tumor appears as a sphere located in the inner retinal layers (Fig. 21.11). Other findings on OCT include intratumor cavities, intratumor calcification, subretinal seeds, epiretinal vitreous seeds, photoreceptor loss in areas of chronic subretinal fluid, traction retinal detachment, retinal edema, and epiretinal membrane [22]. Soliman et al. evaluated 63 eyes of 44 children with retinoblastoma and found that in 94% of cases, OCT influenced treatment decisions (58%), diagnosis (16%), and follow-up (26%). Optical coherence tomography altered management in 15% of all OCT sessions [33].

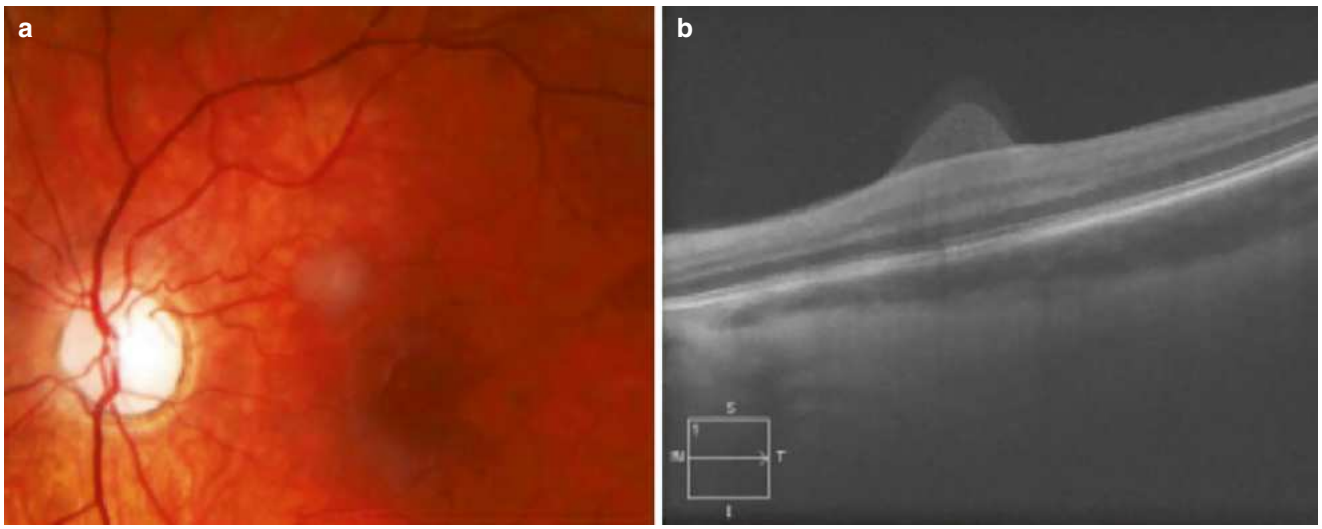

Fig. 21.9 Retinal astrocytic hamartoma. Clinical appearance (**a**). Note thickened inner retina with disorganization of the inner and outer retinal layers (**b**)

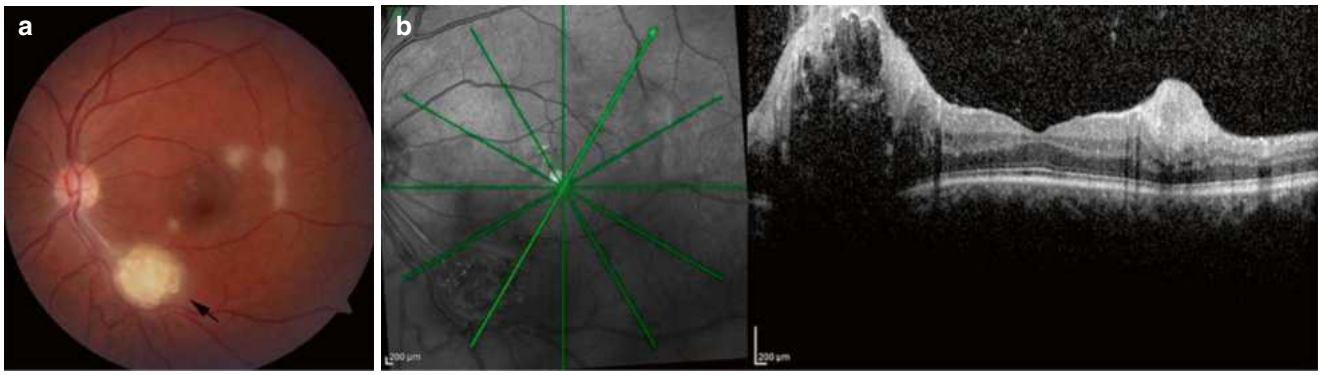

Fig. 21.10 Patient with multiple retinal astrocytic hamartomas (RAH). Clinical appearance (**a**). OCT scans (**b**) showing a type 3 and a type 2 RAH according to the SD-OCT classification

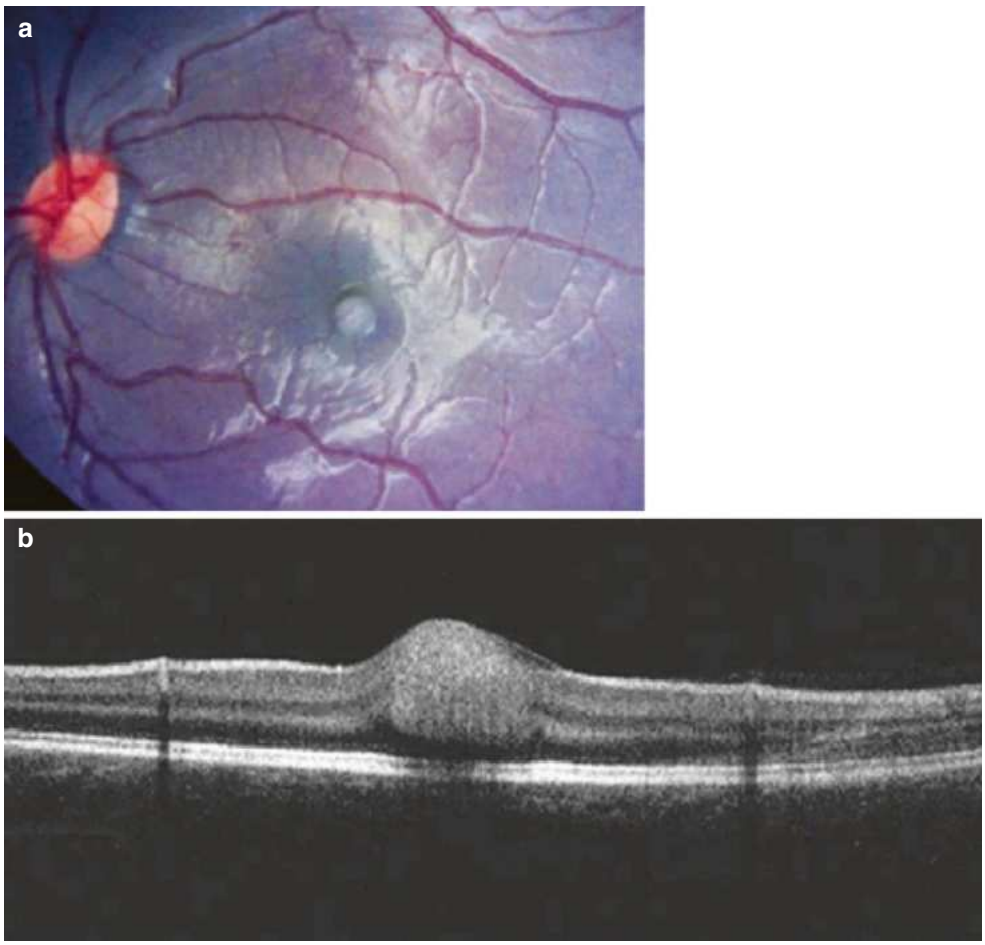

Fig. 21.11 Retinoblastoma. A 15-month-old child with family history of retinoblastoma on screening examination is noted to have bilateral macular lesions. On fundus examination, the tumor is barely detectable (**a**). By OCT, the tumor appears as a sphere located in the inner retinal layers (**b**). (Reprinted from Palazzi et al. [60]. With permission from Creative Commons License 4.0: https://creativecommons.org/licenses/by/4.0/deed.en)

21.10 Primary Vitreoretinal Lymphoma

Primary vitreoretinal lymphoma (PVRL), a subset of primary central nervous system lymphoma (PCNSL), is a high-grade malignant tumor that shows various chorioretinal findings. OCT has been used to identify subretinal lymphoma deposits. Mapelli and associates found small retinal pigmented epithelial detachments (PEDs) in 77% and large PEDs in 36% of patients with PVRL [34]. Barry and Morfield's colleagues evaluated OCTs from biopsy-proven vitreoretinal lymphoma and found hyper-reflective subretinal infiltrates (17/32), hyper-reflective infiltration in inner retinal layers (6/32), retinal pigment epithelial undulation (5/32), clumps of vitreous cells (5/32), and sub-RPE deposits (3/32) (Fig. 21.12). They proposed that the hyper-reflective subretinal infiltrates have an appearance that is unique to PVRL [35].

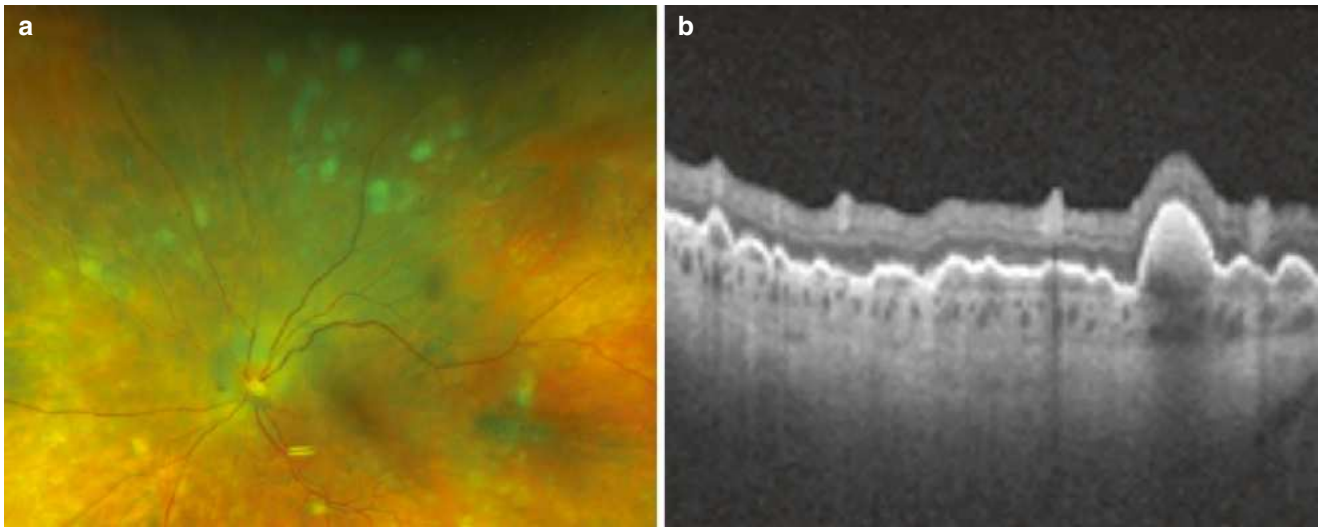

Fig. 21.12 Primary vitreoretinal lymphoma. Clinical appearance (**a**). OCT findings include hyper-reflective retinal infiltrates, retinal pigment epithelium undulations, and sub-RPE deposits (**b**)

21.11 Retinal Cavernous Hemangioma

Cavernous hemangioma is a benign retinal vascular tumor that appears as a dark-red, saccular aneurysm. It is often associated with vitreous hemorrhage, preretinal fibrosis, and vascular occlusion. Descriptions of retinal cavernous hemangioma on OCT mention a disorganized epiretinal membrane with cystic spaces within inner and outer retinal layers, these spaces representing the saccular aneurysms (Fig. 21.13) [24, 36]. OCTA reveals rarefaction of retinal vessels overlying the tumor and the absence of a flow signal at the superficial and deep plexi [36].

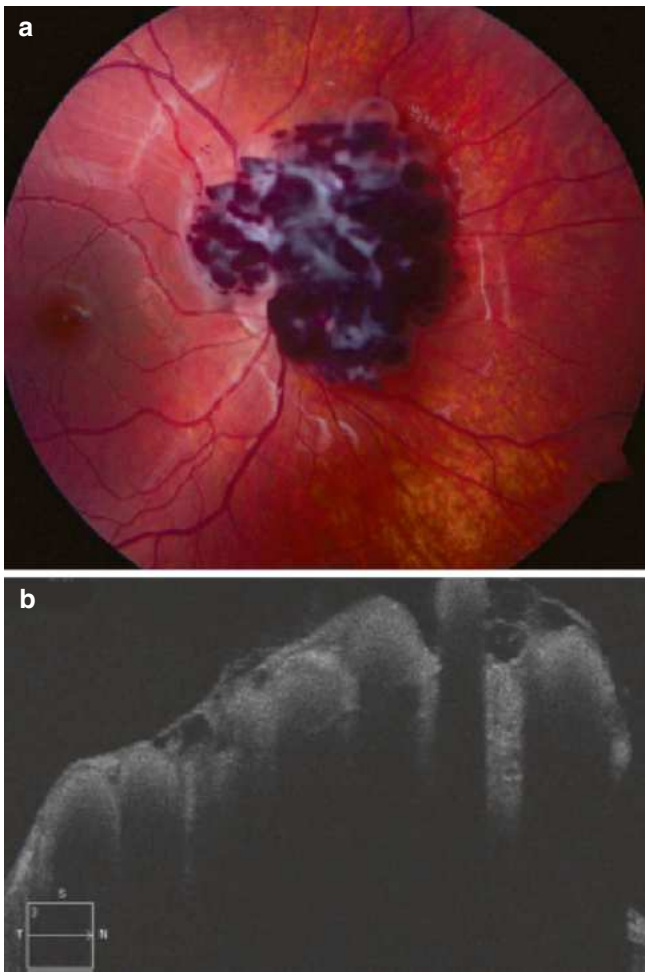

Fig. 21.13 Retina cavernous hemangioma. Clinical appearance (**a**). Epiretinal membrane bridging across multiple cystic spaces within inner and outer retinal layers (**b**)

21.12 Retinal Capillary Hemangioma

Retinal hemangioblastoma (capillary hemangioma) is an orange circumscribed vascular lesion with a dilated feeding artery and draining vein. They can be associated with von Hippel-Lindau disease. OCT evaluation of these lesions shows a hyper-reflective lesion with little inner tumor detail, but macular evaluation by OCT is useful for detecting associated macular edema, epiretinal membranes, and subretinal fluid (Fig. 21.14) [38]. When OCTA was compared to fluorescein angiography, OCTA was able to identify tiny tumors but only those closer to the posterior pole. Both FA and OCTA could identify the intrinsic vasculature and feeder vessel in juxtapapillary tumors and small tumors not identified on ophthalmoscopic examination. However, the tumors and their feeding and draining vessels were better defined by OCTA than by FA. OCTA failed to image the peripheral tumors [39].

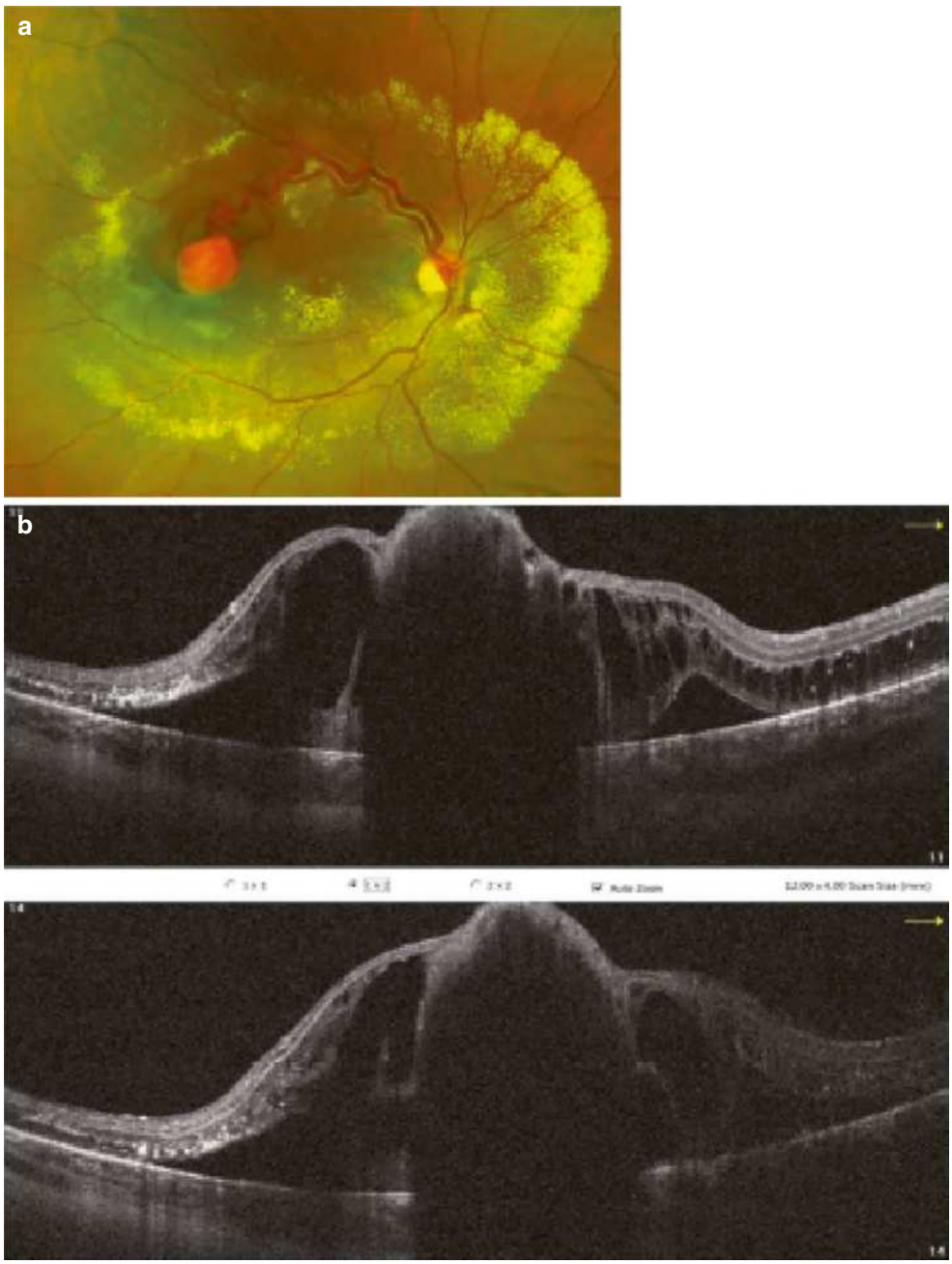

Fig. 21.14 Retinal capillary hemangioma. Clinical appearance (**a**). OCT evaluation shows a round hyper-reflective lesion with little inner tumor details (**b**). Macular evaluation by OCT is useful to detect associated macular edema, epiretinal membrane, and subretinal fluid (**c**)

c

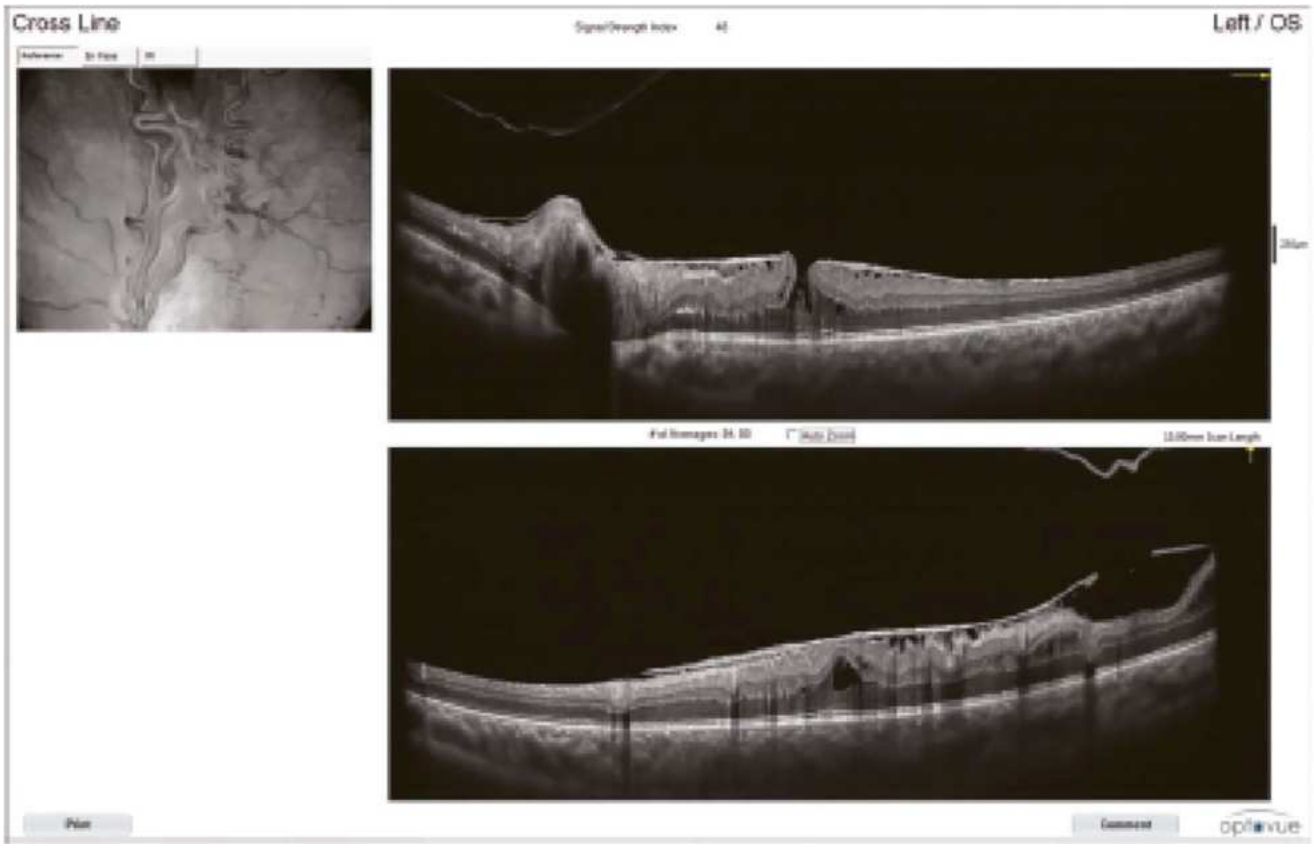

Fig. 21.14 (continued)

21.13 Retinal Vasoproliferative Tumor

Vasoproliferative tumor of the retina is usually a unilateral, yellow-red, retinal lesion usually located in the inferotemporal periphery with a minimally dilated or non-dilated feeding artery and draining vein, in contrast to hemangioblastoma. The peripheral tumor location makes it difficult to image with OCT. Disorganization of the inner retinal layer and posterior shadowing are features of vasoproliferative tumors on OCT [38]. Vision loss is usually due to epiretinal membrane or exudative macular detachment, and OCT is useful for identifying these changes.

21.14 Wyburn-Mason Syndrome

Wyburn-Mason syndrome, or *racemose angioma*, is a non-hereditary arteriovenous malformation of the eye and brain, typically involving the optic disc or retina and the midbrain. Ocular manifestations are unilateral and congenital but may progress somewhat during childhood. The typical lesion consists of markedly dilated and tortuous vessels that shunt blood flow directly from arteries to veins; these vessels do not leak fluid. On OCT, dilated intraretinal vascular channels are observed (Fig. 21.15). Vision ranges from normal to markedly reduced in the involved eye. Intraocular hemorrhage and secondary neovascular glaucoma are possible complications. No treatment is indicated for primary lesions.

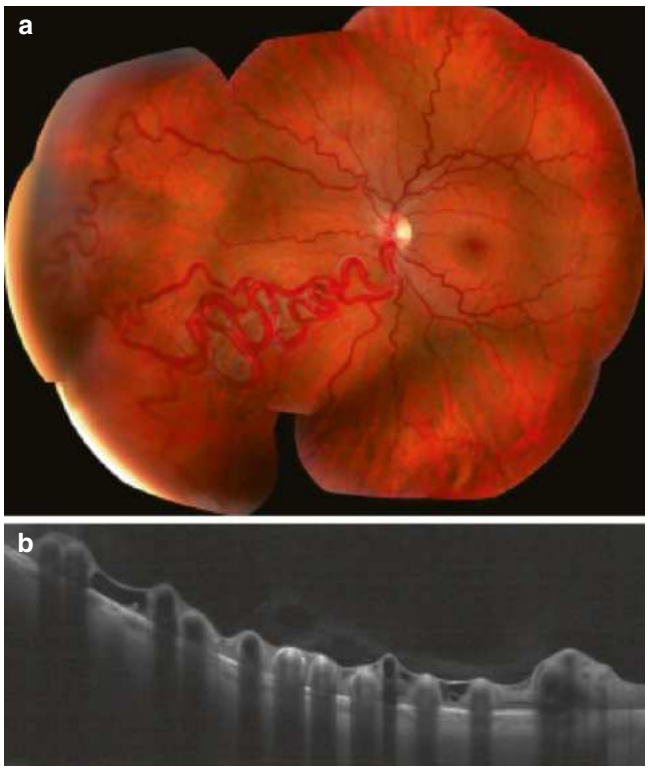

Fig. 21.15 Wyburn-Mason syndrome. Clinical appearance of a typical lesion consisting of markedly dilated and tortuous vessels (**a**). On OCT, dilated intraretinal vascular channels are observed (**b**)

21.15 Optic Disc Melanocytoma

Melanocytoma of the optic nerve head is a benign melanocytic tumor that usually occurs in the inferotemporal area of the optic nerve head. OCT reveals a dome-shaped lesion with a gradual slope at the tumor margin. Areas of irregular hyper-reflectivity are observed in the melanocytoma but with little internal detail of the tumor (Fig. 21.16) [40]. Nevertheless, OCT can help delineate the tumor margins [41]. Two categories of OCT findings in optic disc melanocytoma have been identified: (a) type 1, hyperreflective lesion with disorganized overlying retina and a posterior hyporeflective shadow and (b) the less common, type 2 lesion overlaid by a relatively well-organized retina without a posterior hyporeflective shadow [42].

Fig. 21.16 Optic disc melanocytoma. Clinical appearance (**a**). On OCT, the lesion extends into the superficial retinal layers (**b**) with total shadowing of deeper structures due to intense pigmentation

21.16 Choroidal Tumors

Choroidal imaging has been improved by innovations in technology that use a laser source across a range of wavelengths [4]. The swept laser light source sequentially emits various frequencies, increasing the signal quality from deep tissues such as the choroid [5]. Nevertheless, as with EDI OCT [3], image quality is superior with choroidal lesions that are small, close to the fovea, and with less choroidal pigmentation [6, 7].

21.17 Choroidal Nevus

OCT is able to detect retinal and anterior choroidal changes that include retinal thinning, retinal edema, subretinal fluid, RPE detachment, and drusen. Enhanced depth imaging (EDI) OCT shows a dome-shaped lesion replacing normal choroid (Fig. 21.17) [3, 43]. OCT evaluation is more sensitive than clinical examination in detecting retinal edema, subretinal fluid, retinal thinning, and RPE detachment. Also,

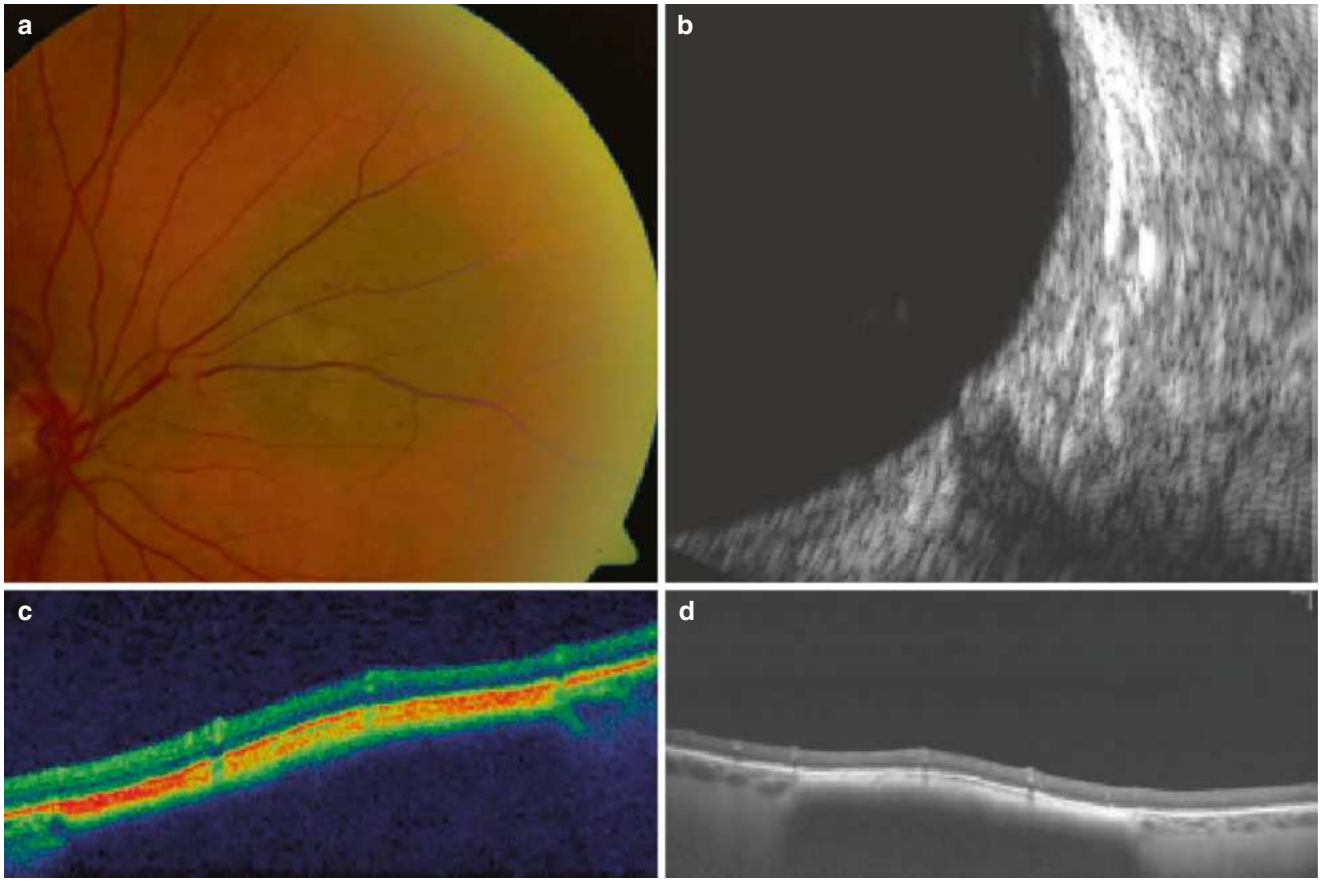

Fig. 21.17 Choroidal nevus. Fundus appearance (**a**). B-scan ultrasound is unable to detect the lesion (**b**). Spectral-domain OCT (Topcon-1000). The lesion appears as a sharply highly reflective band at the Bruch's/RPE/choriocapillaris layer (**c**). Spectral-domain OCT EDI technique (inverted). The lesion is well distinguished from surrounding normal choroid as highly reflective band with posterior shadowing. A thin hyporeflective line separates the RPE and the anterior tumor surface (**d**). (Reprinted from Torres et al. [3]. With permission from Elsevier)

it helps to detect photoreceptor loss and to characterize retinal edema (i.e., cystoid versus non-cystoid). Drusen that are clinically visible is evidenced by OCT as small dome-shaped elevations at the level of Bruch's membrane. Characteristics of choroidal nevi imaged by SS-OCT include vessels, cavities, and granularity (Fig. 21.18) [6]. OCT angiography has demonstrated neovascular membranes associated with choroidal nevus [44].

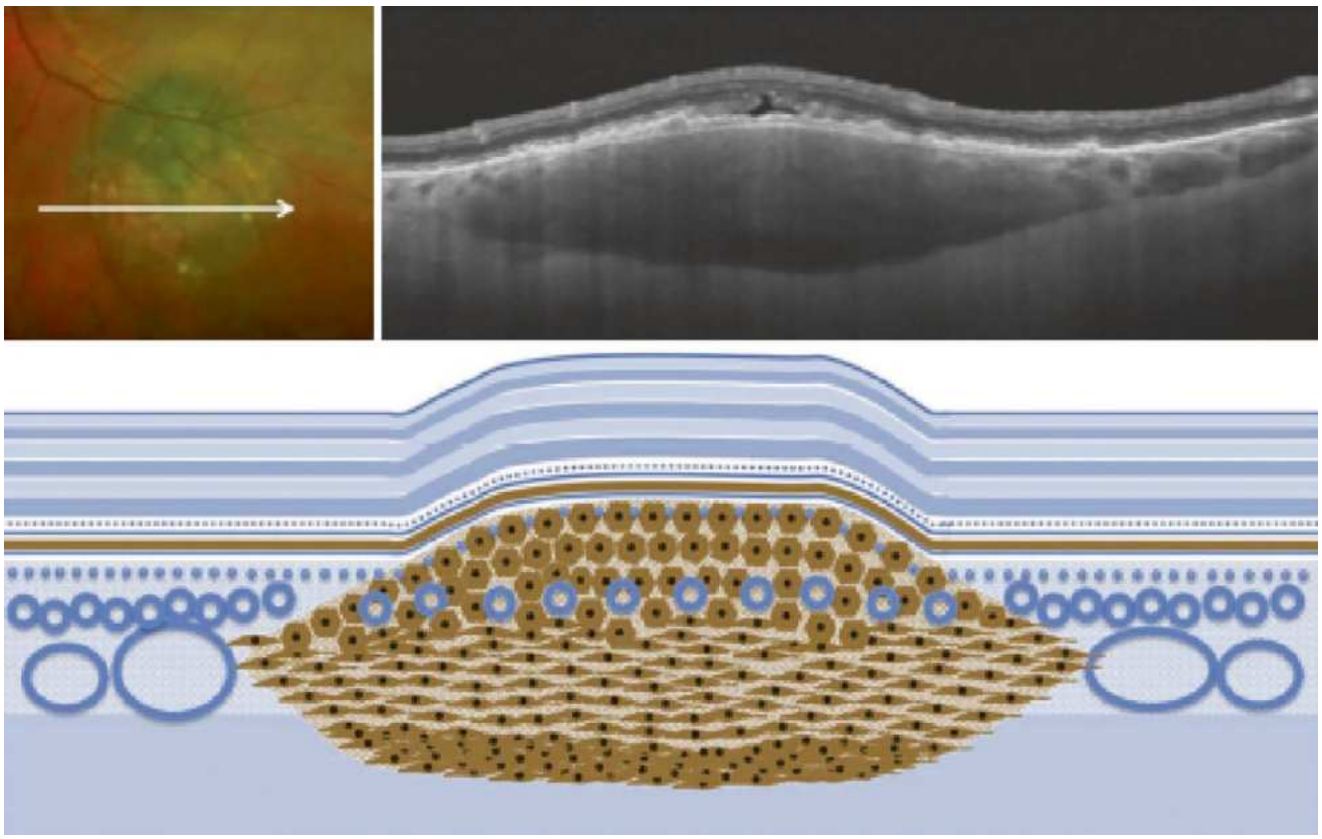

Fig. 21.18 Choroidal nevus imaged with swept-source optical coherence tomography (SS-OCT). (Top left) Color fundus photograph of amelanotic and melanocytic nevus. (Top right) SS-OCT image of choroidal nevus with an almond configuration demonstrating intralesional vessels, distended bordering vessels, and gradation of reflectivity from inner to outer portion of nevus, perhaps representing distribution of different cell types. Note relative gradient of hyperreflectivity as the nevus transitions to sclera, possibly a result of the densely packed spindle cells. (Bottom) Diagrammatic schema illustrating histopathologic characteristics of a representative choroidal nevus that are found on SS-OCT. (Reprinted from Francis et al. [6]. With permission from Elsevier)

21.18 Choroidal Melanoma

Uveal melanoma is the most common primary intraocular malignant tumor. About 85% of these tumors develop in the choroid. They often present as a pigmented, elevated choroidal mass. In medium- to large-sized melanomas, OCT analysis is limited to superficial changes in the retina and anterior surface of the tumor. Subretinal fluid helps to differentiate small melanomas from nevi and is detectable by OCT in almost all cases (Fig. 21.19) [45]. Sayanagi and coworkers used 3D spectral-domain OCT and found a significantly higher prevalence of subretinal fluid (91% versus 14%), retinal edema (61% versus 14%), and subretinal deposits (61% versus 11%) in choroidal melanoma compared with nevi [46]. A limitation of OCT for choroidal melanoma lies in its inability to image past the anterior choroidal surface [47]. The reflectivity of the anterior choroid in melanoma is variable even with spectral-domain OCT. [48] Even with EDI OCT, both nevus and melanoma demonstrate a highly reflective band within the choriocapillaris layer with posterior shadowing (Fig. 21.20) [3]. OCTA provides additional details of the intrinsic microvasculature of the tumor [49]. Reduction of the vessels and flow areas can be observed after brachytherapy [50].

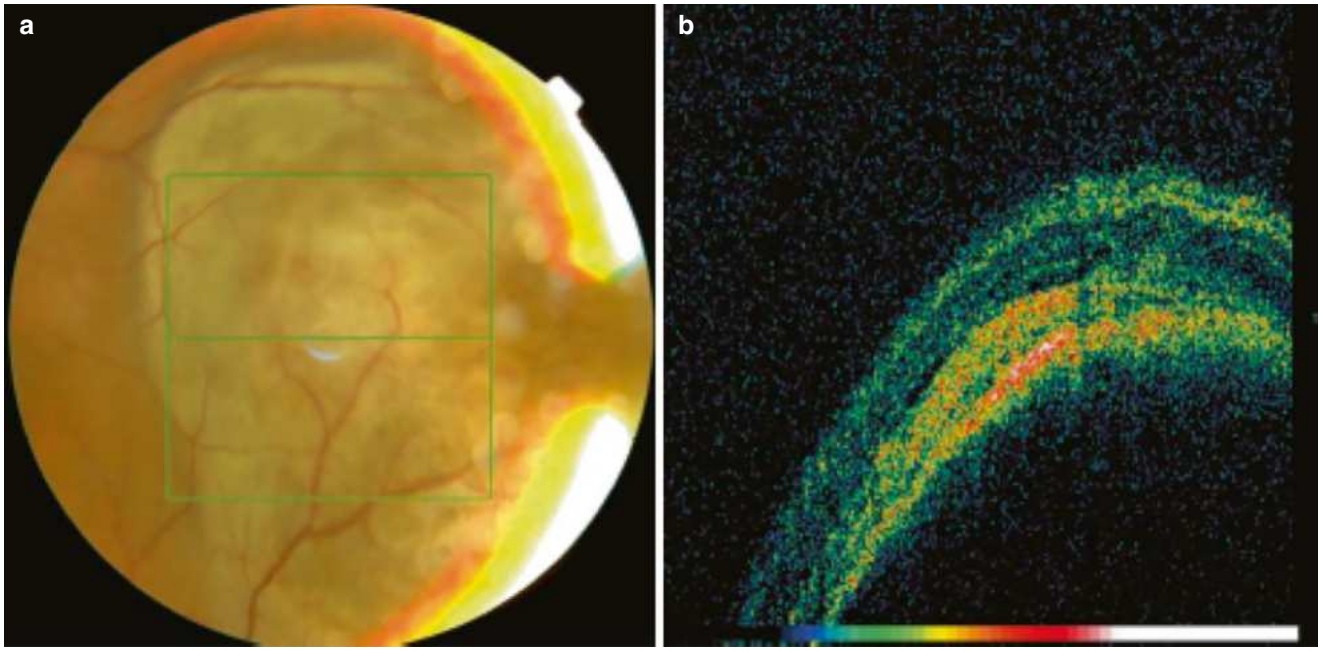

Fig. 21.19 Choroidal melanoma. Fundus appearance (**a**). OCT image notes irregularity of retinal pigment epithelium, subretinal fluid, intraretinal edema, and cyst (**b**). (Reprinted from Sayanagi et al. [46]. With permission from Sage Publications Ltd.)

21.19 Choroidal Osteoma

Choroidal osteoma is an osseous tumor occurring most commonly in young females. The tumor is located in the juxtapapillary region or macula and presents an orange-yellow color when calcified and a white tumor when decalcified. Complications of choroidal osteoma that cause vision loss are related to the tumor decalcification and include neovascular membranes and retinal changes (subretinal fluid or photoreceptor loss), both identifiable by OCT imaging. Shields and coworkers reported on the OCT features of choroidal osteoma that included heterogeneity that depended upon the amount of tumor calcification. Calcified portions of the tumor reveal mostly intact inner and outer retinal layers, a distinct RPE, and mild transmission of light. In contrast, decalcified portions of the tumor reveal intact inner retinal layers, thinned outer retinal layers, an indistinct RPE, and marked light transmission into the tumor (Fig. 21.21) [51]. The anterior tumor surface is either iso- or hyper-reflective if calcified but is mostly hyper-reflective when decalcified [52]. Enhanced depth imaging optical coherence tomography reveals characteristic dome-shaped or undulating surfaces with unique intrinsic features of lamellar lines, tubules, and speckled regions [53].

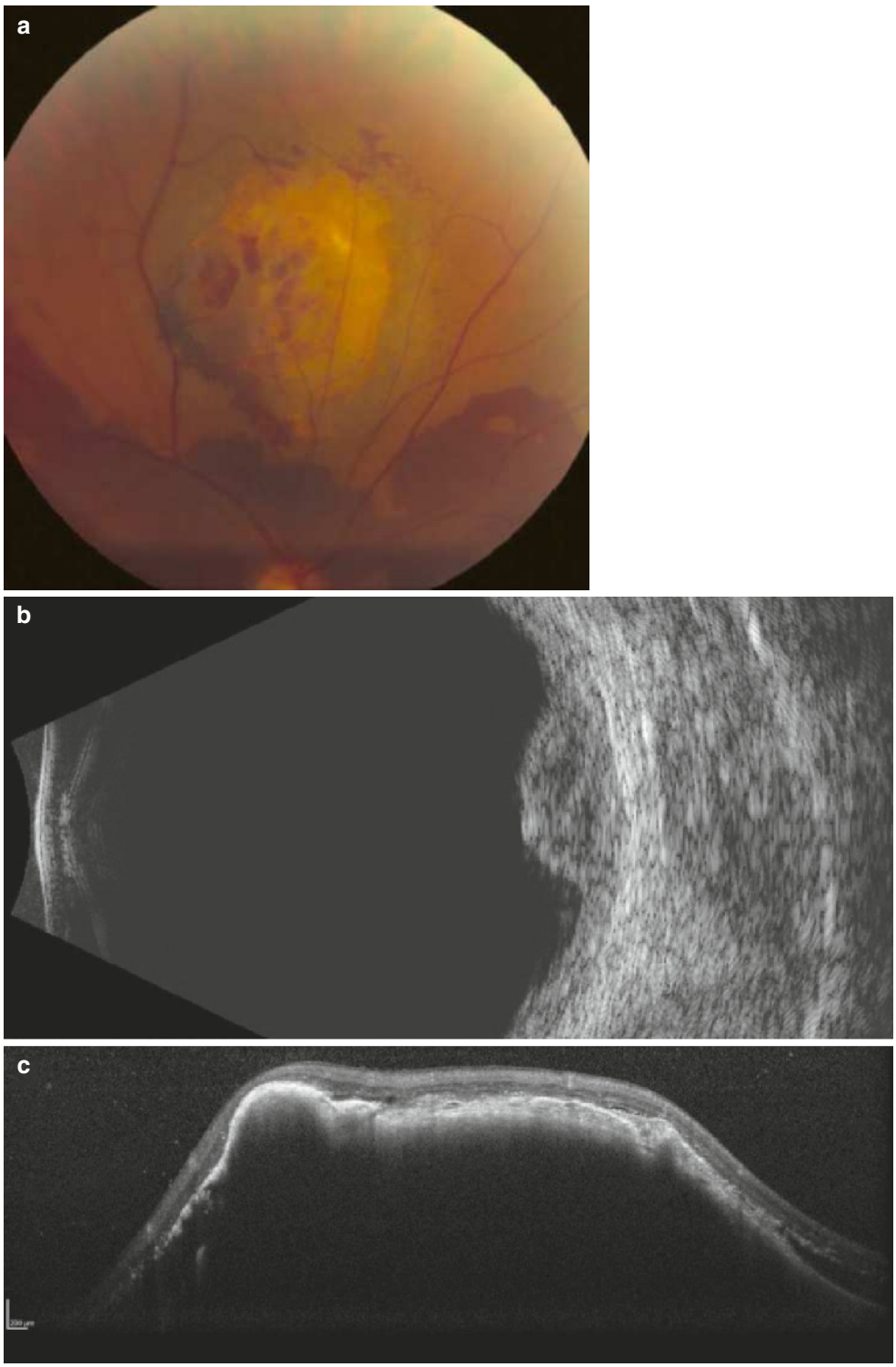

Fig. 21.20 Choroidal melanoma. Color fundus photograph shows a choroidal melanocytic tumor associated with subretinal hemorrhage (**a**). B-scan ultrasound shows a slightly irregular dome-shaped mass with medium to low internal reflectivity (**b**). SD-OCT EDI Technique: the image is of poor quality due to artifacts caused by lesion thickness (**c**). (Reprinted from Torres et al. [3]. With permission from Elsevier)

Fig. 21.21 Choroidal osteoma. Fundus appearance (**a**). OCT image reveals heterogeneous internal structure (**b**)

21.20 Choroidal Metastasis

On OCT, choroidal metastases demonstrate a "lumpy-bumpy" anterior surface, overlying subretinal fluid. OCT imaging of choroidal lesions is limited to retinal changes and anterior choroid evaluation. Retinal changes include retinal edema, intraretinal cysts, thickening, and detachment of the RPE. Arevalo and colleagues found highly reflective points within neurosensory detachment in 14% of cases and concluded that these points "may correspond to retinal compromise by cancer cells or macrophages containing lipofuscin and melanin granules" [54]. EDI-OCT shows outer retinal layer disruption with preservation of inner retinal layers [55] and choriocapillaris thinning (Fig. 21.22) [56].

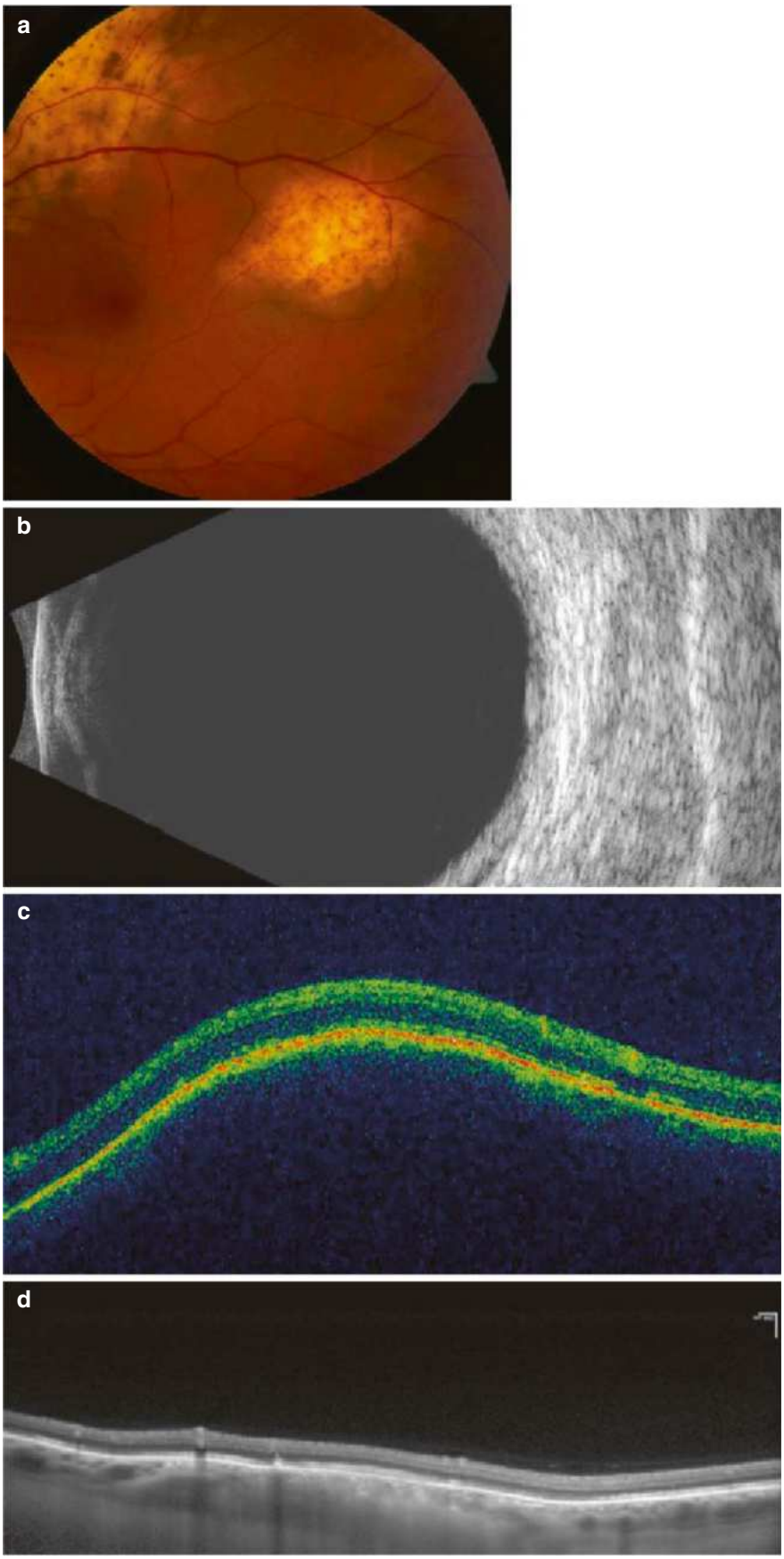

Fig. 21.22 Choroidal metastasis. Color fundus photograph shows an amelanotic tumor with overlying RPE changes (**a**). B-scan ultrasound depicts slight nonspecific choroidal thickening (**b**). SD-OCT (Topcon-1000): elevation of the retina/choroid complex (**c**). SD-OCT EDI technique (inverted): choriocapillaris layer is identified as normal. In the large vessels and suprachoroidal space, a low/medium reflective signal is observed (**d**). The inner limit of the sclera is also identifiable permitting measurement of tumor thickness. (Reprinted from Torres et al. [3]. With permission from Elsevier)

21.21 Choroidal Hemangioma

Circumscribed choroidal hemangioma is usually orange-colored, round, and located at the posterior pole. It usually exhibits overlying retinal edema, subretinal fluid, and RPE alterations [38]. Ramasubramanian and colleagues described OCT findings in circumscribed choroidal hemangioma and found subretinal fluid (19%), retinal edema (42%), retinal schisis (12%), macular edema (24%), and localized photoreceptor loss (35%) [40]. Retinal changes are secondary to tumor leakage. OCT shows preserved photoreceptors and normal retinal thickness if the leakage is acute and degenerated photoreceptors, retinoschisis, and intraretinal edema if the leakage is chronic [38]. EDI-OCT depicts a smooth, gently sloping choroidal mass with expansion of medium- and large-sized choroidal vessels with normal appearance of the choriocapillaris (Fig. 21.23) [57, 58]. OCTA at the level of large choroidal vessels shows various vascular patterns [59].

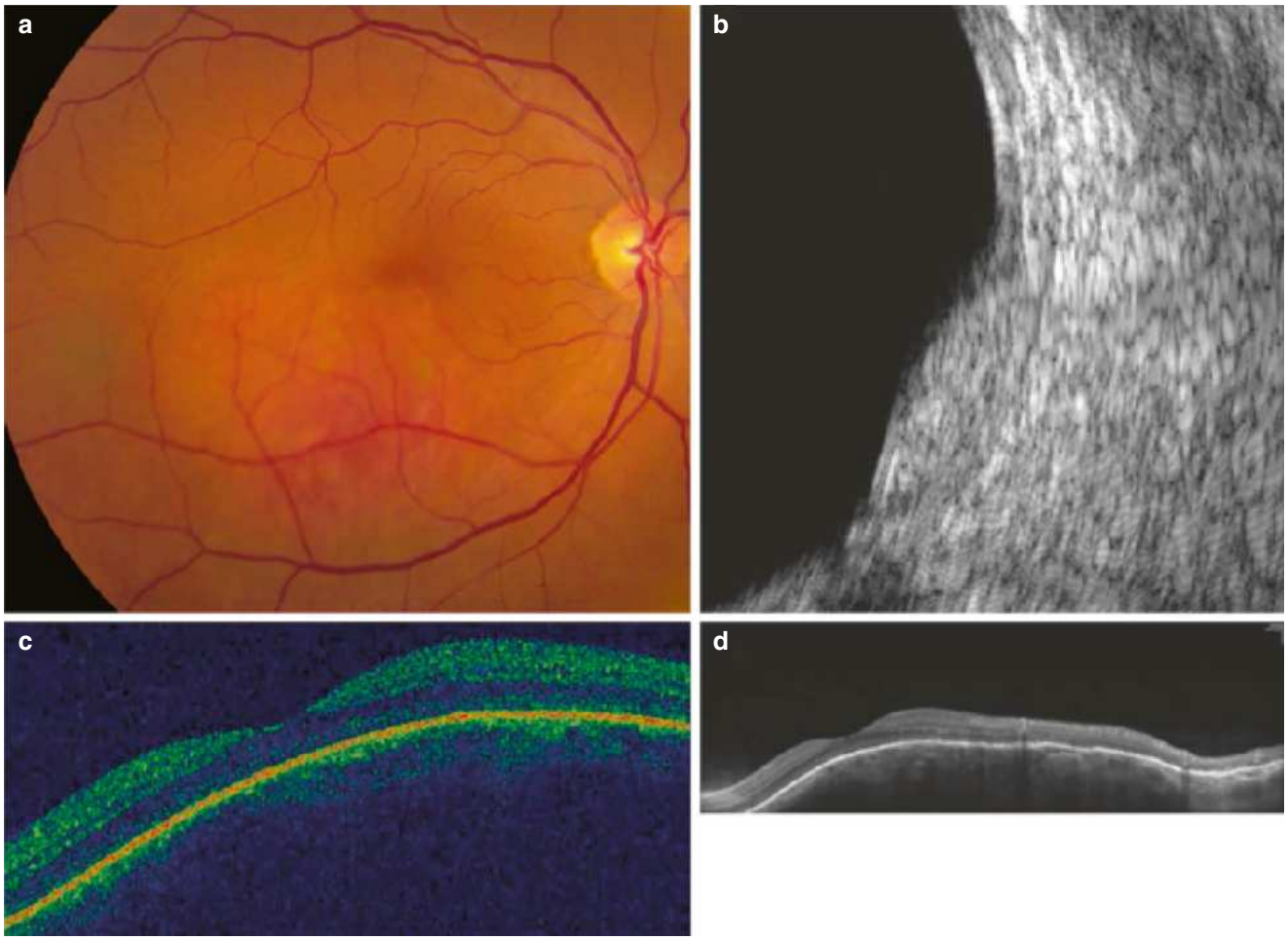

Fig. 21.23 Circumscribed choroidal hemangioma. Fundus appearance (**a**). B-scan ultrasound shows a domeshaped solid lesion, with high and homogenous reflectivity (**b**). Spectral-domain OCT (Topcon1000). There is elevation of retina/choroid complex with nonspecific signals from the underlying choroid (**c**). Spectral-domain OCT EDI technique (inverted). Note a low to medium reflective signal from the lesion. Small and large spaces (possibly vascular) are also identified within the tumor (**d**). (Reprinted from Torres et al. [3]. With permission from Elsevier)

21.22 Conclusions

OCT enables the identification of conjunctival tumor margins, alterations of the overlying epithelium, and recognition of secondary features, such as conjunctival cysts. OCT is also a useful tool for the evaluation of small iris tumors. It enables the identification of tumor margins and tumor surfaces. In cases of posterior iris and ciliary body tumors, OCT tends to be inferior to UBM. With posterior segment tumors, OCT provides useful diagnostic clues and demonstrates spontaneous and iatrogenic pathology in the RPE and retina. Novel developments in OCT technology, such as EDI OCT and OCTA, are enabling better visualization of the composition and intrinsic vascular patterns of retinal and choroidal tumors.

References

1. Huang D, Swanson EA, Lin CP, et al. Optical coherence tomography. Science. 1991;254(5035):1178–81.
2. Spaide RF, Koizumi H, Pozzoni MC. Enhanced depth imaging spectral-domain optical coherence tomography. Am J Ophthalmol. 2008;146(4):496–500.
3. Torres VL, Brugnoni N, Kaiser PK, et al. Optical coherence tomography enhanced depth imaging of choroidal tumors. Am J Ophthalmol. 2011;151(4):586–93.e2.
4. Mrejen S, Spaide RF. Optical coherence tomography: imaging of the choroid and beyond. Surv Ophthalmol. 2013;58(5):387–429.
5. Adhi M, Duker JS. Optical coherence tomography—current and future applications. Curr Opin Ophthalmol. 2013;24(3):213–21.
6. Francis JH, Pang CE, Abramson DH, et al. Swept-source optical coherence tomography features of choroidal nevi. Am J Ophthalmol. 2015;159(1):169–76.e1.
7. Ung C, Lains I, Silverman RF, et al. Evaluation of choroidal lesions with swept-source optical coherence tomography. Br J Ophthalmol. 2018;103:88.
8. JiaY TO, Tokayer J, et al. Split-spectrum amplitude-decorrelation angiography with optical coherence tomography. Opt Express. 2012;20(4):4710–25.
9. de Carlo TE, Romano A, Waheed NK, et al. A review of optical coherence tomography angiography (OCTA). Int J Retina Vitreous. 2015;1:5.
10. Kashani AH, Chen CL, Gahm JK, et al. Optical coherence tomography angiography: a comprehensive review of current methods and clinical applications. Prog Retin Eye Res. 2017;60:66–100.
11. Razzaq L, Emmanouilidis-van der Spek K, Luyten GP, et al. Anterior segment imaging for iris melanocytic tumors. Eur J Ophthalmol. 2011;21(5):608–14.
12. Alzahrani YA, Kumar S, Abdul Aziz H, et al. Primary acquired melanosis: clinical, histopathologic and optical coherence tomographic correlation. Ocul Oncol Pathol. 2016;2(3):123–7.
13. Shousha MA, Karp CL, Canto AP, et al. Diagnosis of ocular surface lesions using ultra-high-resolution optical coherence tomography. Ophthalmology. 2013;120(5):883–91.
14. Nanji AA, Sayyad FE, Galor A, et al. High-resolution optical coherence tomography as an adjunctive tool in the diagnosis of corneal and conjunctival pathology. Ocul Surf. 2015;13(3):226–35.
15. Gallwas JK, Turk L, Stepp H, et al. Optical coherence tomography for the diagnosis of cervical intraepithelial neoplasia. Lasers Surg Med. 2011;43(3):206–12.
16. Kieval JZ, Karp CL, Abou Shousha M, et al. Ultra-high resolution optical coherence tomography for differentiation of ocular surface squamous neoplasia and pterygia. Ophthalmology. 2012;119(3):481–6.
17. Binotti WW, Mills H, Nosé RM, et al. Anterior segment optical coherence tomography angiography in the assessment of ocular surface lesions. Ocul Surf. 2021;22:86–93.
18. Liu Z, Karp CL, Galor A. Role of optical coherence tomography angiography in the characterization of vascular network patterns of ocular surface squamous neoplasia. Ocul Surf. 2020;18(4):926–35.
19. Siahmed K, Berges O, Desjardins L, et al. Anterior segment tumor imaging: advantages of ultrasound (10, 20 and 50 MHz) and optical coherence tomography. J Fr Ophtalmol. 2004;27(2):169–73.
20. Pavlin CJ, Vasquez LM, Lee R, et al. Anterior segment optical coherence tomography and ultrasound biomicroscopy in the imaging of anterior segment tumors. Am J Ophthalmol. 2009;147(2):214–9.e2.
21. Bianciotto C, Shields CL, Guzman JM, et al. Assessment of anterior segment tumors with ultrasound biomicroscopy versus anterior segment optical coherence tomography in 200 cases. Ophthalmology. 2011;118(7):1297–302.
22. Shields CL, Manalac J, Das C, Saktanasate J, Shields JA. Review of spectral domain-enhanced depth imaging optical coherence tomography of tumors of the retina and retinal pigment epithelium in children and adults. Indian J Ophthalmol. 2015;63(2):128–32.
23. Fung AT, Pellegrini M, Shields CL. Congenital hypertrophy of the retinal pigment epithelium: enhanced-depth imaging optical coherence tomography in 18 cases. Ophthalmology. 2014;121:251–6.
24. Shields CL, Mashayekhi A, Dai VV, et al. Optical coherence tomographic findings of combined hamartoma of the retina and retinal pigment epithelium in 11 patients. Arch Ophthalmol. 2005;123(12):1746–50.
25. Brue C, Saitta A, Nicolai M, et al. Epiretinal membrane surgery for combined hamartoma of the retina and retinal pigment epithelium: role of multimodal analysis. Clin Ophthalmol. 2013;7:179–84.
26. Huot CS, Desai KB, Shah VA. Spectral domain optical coherence tomography of combined hamartoma of the retina and retinal pigment epithelium. Ophthalmic Surg Lasers Imaging. 2009;40(3):322–4.
27. Arepalli S, Pellegrini M, Ferenczy SR, Shields CL. Combined hamartoma of the retina and retinal pigment epithelium: findings on enhanced depth imaging optical coherence tomography in eight eyes. Retina. 2014;34(11):2202–7.
28. Kimoto K, Kishi D, Kono H, et al. Diagnosis of an isolated retinal astrocytic hamartoma aided by optical coherence tomography. Acta Ophthalmol. 2008;86(8):921–2.
29. Say EA, Shah SU, Ferenczy S, et al. Optical coherence tomography of retinal and choroidal tumors. J Ophthalmol. 2012;2012:385058.
30. Semenova E, Veronese C, Ciardella A, et al. Multimodality imaging of retinal astrocytoma. Eur J Ophthalmol. 2015;25(6):559–64.
31. Pichi F, Massaro D, Serafino M, et al. Retinal astrocytic hamartoma: optical coherence tomography classification and correlation with tuberous sclerosis complex. Retina. 2016;36(6):1199–208.
32. Despreaux R, Mrejen S, Quentel G, et al. En face optical coherence tomography (Oct) and Oct angiography findings in retinal astrocytic hamartomas. Retin Cases Brief Rep. 2017;11(4):373–9.
33. Soliman SE, VandenHoven C, MacKeen LD, et al. Optical coherence tomography-guided decisions in retinoblastoma management. Ophthalmology. 2017;124(6):859–72.
34. Mapelli C, Invernizzi A, Barteselli G, et al. Multimodal imaging of vitreoretinal lymphoma. Ophthalmologica. 2016;236(3):166–74.

35. Barry RJ, Tasiopoulou A, Murray PI, et al. Characteristic optical coherence tomography findings in patients with primary vitreoretinal lymphoma: a novel aid to early diagnosis. Br J Ophthalmol. 2018;102:1362.
36. Andrade RE, Farah ME, Costa RA, et al. Optical coherence tomography findings in macular cavernous haemangioma. Acta Ophthalmol Scand. 2005;83(2):267–9.
37. Cennamo G, Amoroso F, Solari D, Alfieri M, de Crecchio G. Optical coherence tomography angiography in retinal cavernous hemangioma. Int J Ophthalmol. 2017;10(12):1945–1946. https://doi.org/10.18240/ijo.2017.12.27. PMID: 29259920; PMCID: PMC5733529
38. Shields CL, Shields JA. Intraocular tumors: an atlas and textbook. Philadelphia: Lippincott Williams & Wilkins; 2008.
39. Sagar P, Rajesh R, Shanmugam M, et al. Comparison of optical coherence tomography angiography and fundus fluorescein angiography features of retinal capillary hemangioblastoma. Indian J Ophthalmol. 2018;66(6):872–6.
40. Ramasubramanian A, Shields CL, Harmon SA, et al. Autofluorescence of choroidal hemangioma in 34 consecutive eyes. Retina. 2010;30(1):16–22.
41. Sutter C, Jean-Charles A, Merle H. [Clinical and paraclinical course of melanocytoma of the optic disk. Contribution of spectral- and time-domain OCT in the study of 10 patients]. J Fr Ophtalmol. 2011;34(9):615–23.
42. Apinyawasisuk S, McCannel T, Arnold AC. Clinical and spectral-domain optical coherence tomography appearance of optic disc melanocytoma: a new classification and differentiation from pigmented choroidal lesions. Ocul Oncol Pathol. 2017;3(2):142–8.
43. Shah SU, Kaliki S, Shields CL, et al. Enhanced depth imaging optical coherence tomography of choroidal nevus in 104 cases. Ophthalmology. 2012;119(5):1066–72.
44. Hanhart J, Brosh K, Weill Y, et al. Choroidal nevusassociated neovascular membrane demonstrated by OCT angiography. Case Rep Ophthalmol. 2017;8(1):104–7.
45. Muscat S, Parks S, Kemp E, et al. Secondary retinal changes associated with choroidal naevi and melanomas documented by optical coherence tomography. Br J Ophthalmol. 2004;88(1):120–4.
46. Sayanagi K, Pelayes DE, Kaiser PK, et al. 3D spectral domain optical coherence tomography findings in choroidal tumors. Eur J Ophthalmol. 2011;21(3):271–5.
47. Shields CL, Kaliki S, Rojanaporn D, et al. Enhanced depth imaging optical coherence tomography of small choroidal melanoma: comparison with choroidal nevus. Arch Ophthalmol. 2012;130(7):850–6.
48. Singh AD, Belfort RN, Sayanagi K, et al. Fourier domain optical coherence tomographic and auto-fluorescence findings in indeterminate choroidal melanocytic lesions. Br J Ophthalmol. 2010;94(4):474–8.
49. Pellegrini M, Corvi F, Invernizzi A, et al. Swept-source optical coherence tomography angiography in choroidal melanoma: an analysis of 22 consecutive cases. Retina. 2018;39:1510.
50. Cennamo G, Rossi C, Breve MA, et al. Evaluation of vascular changes with optical coherence tomography angiography after ruthenium-106 brachytherapy of circumscribed choroidal hemangioma. Eye (Lond). 2018;32:1401.
51. Shields CL, Perez B, Materin MA, et al. Optical coherence tomography of choroidal osteoma in 22 cases: evidence for photoreceptor atrophy over the decalcified portion of the tumor. Ophthalmology. 2007;114(12):e53–8.
52. Shields CL, Mashayekhi A, Materin MA, et al. Optical coherence tomography of choroidal nevus in 120 patients. Retina. 2005;25(3):243–52.
53. Shields CL, Arepalli S, Atalay HT, et al. Choroidal osteoma shows bone lamella and vascular channels on enhanced depth imaging optical coherence tomography in 15 eyes. Retina. 2015;35(4):750–7.
54. Arevalo JF, Fernandez CF, Garcia RA. Optical coherence tomography characteristics of choroidal metastasis. Ophthalmology. 2005;112(9):1612–9.
55. Al-Dahmash SA, Shields CL, Kaliki S, et al. Enhanced depth imaging optical coherence tomography of choroidal metastasis in 14 eyes. Retina. 2014;34(8):1588–93.
56. Demirci H, Cullen A, Sundstrom JM. Enhanced depth imaging optical coherence tomography of choroidal metastasis. Retina. 2014;34(7):1354–9.
57. Rojanaporn D, Kaliki S, Ferenczy SR, et al. Enhanced depth imaging optical coherence tomography of circumscribed choroidal hemangioma in 10 consecutive cases. Middle East Afr J Ophthalmol. 2015;22(2):192–7.
58. Ozkurt ZG, Slimani N, Demirci H. Evaluation of choroidal hemangioma and treatment with photodynamic therapy by using enhanced depth imaging optical coherence tomography. Ophthalmic Surg Lasers Imaging Retina. 2018;49(3):171–8.
59. Konana VK, Shanmugam PM, Ramanjulu R, et al. Optical coherence tomography angiography features of choroidal hemangioma. Indian J Ophthalmol. 2018;66(4):581–3.
60. Palazzi MA, Abreu HFH, Freitas ACLH, et al. Optical coherence tomography in the evaluation of macular retinoblastoma. Rev Bras Oftalmol. 2015;74:275–8.

Diagnostic Techniques: Autofluorescence

22

R. Chris Bowen, Edoardo Midena, Raffaele Parrozzani, and Giulia Midena

22.1 Introduction

What is fundus autofluorescence (FAF)? Fundus autofluorescence is an in vivo imaging method that allows for noninvasive metabolic topographic mapping of naturally or pathologically occurring intrinsic bis-retinoid fluorophores of the ocular fundus. Most bis-retinoid fluorophores accumulate within lysosomal storage bodies in post-mitotic retinal pigment epithelial (RPE) cells known as lipofuscin. Other bis-retinoid fluorophores can occur in the outer retina and subretinal space in various disease states. Consequently, most FAF signals originate at the level of the RPE/photoreceptor complex [1]. Since choroidal tumors can cause metabolic dysfunction of RPE cells, the accumulation of bis-retinoid fluorophores can result in orange appearing deposits overlying a choroidal tumor.

The creation of a fundus autofluorescence image is obtained in a similar method as fluorescein angiography (FA) and indocyanine green angiography (ICG), where the molecules within the ocular fundus are excited and glow by excitation of light within a specific wavelength range. The major difference is that FAF is based on the excitation of endogenous molecules, while FA and ICG are excitation of intravenously injected exogenous molecules [1].

R. C. Bowen
Department of Ophthalmology, Northwestern University, Chicago, IL, USA

E. Midena (✉)
Department of Ophthalmology, University of Padova, Padova, Italy

IRCCS—Fondazione Bietti, Rome, Italy
e-mail: edoardo.midena@unipd.it

R. Parrozzani
Department of Ophthalmology, University of Padova, Padova, Italy
e-mail: raffaele.parrozzani@unipd.it

G. Midena
IRCCS—Fondazione Bietti, Rome, Italy
e-mail: giulia.midena@fondazionebietti.it

22.2 The Basics of Fundus Autofluorescence and Orange Pigment on Choroidal Tumors

Why are the fovea, parafovea, blood vessels, and optic nerve head hypo-autofluorescent? The answer is blocking or lack of autofluorescent materials in these structures. To explain, the outer photoreceptor segment contains photopigment, which acts as a filter of excitation light. The fovea and parafovea have reduced FAF signal as a result of the increased melanin optical density from high photopigment concentration, causing blocking of fluorophores. Hemoglobin within the retinal blood vessels physically blocks both the excitation light and emitting light and consequently hypo-autofluorescent. The optic nerve head is hypo-autofluorescent due to a lack of RPE/lipofuscin (absence of autofluorescent material). As of note, advanced cataracts can absorb the emitting light and cause pseudofluorescence at or near the optic nerve head [1].

In the normal aging process, lipofuscin gradually accumulates in the cytoplasm of RPE cells. This occurs as vitamin A aldehyde (retinaldehyde) with phosphatidylethanolamine in the photoreceptor outer segment undergoes a nonenzymatic reaction. 11-cis-retinal is converted to all-trans-retinal in the visual cycle, resulting in by-products of more than 20 different bis-retinoid fluorophores (A2E is the most well-known but is only one of these compounds), which can then be phagocytosed by the RPE cells and processed via lysosomes. Consequently, conditions that impair the chemical reduction and removal of retinaldehyde result in increased bis-retinoid fluorophore formation. In conditions that prevent phagocytosis of the outer segments (subretinal fluid, RPE dysfunction), the subretinal bis-retinoid fluorophores will accumulate in the subretinal space [1].

Lipofuscin is normally a yellow-gray-tan color on exam but when seen overlying a choroidal melanocytic tumor (such as a choroidal nevus or melanoma), because of the dark melanocytic infiltrated choroid background, lipofuscin

© The Author(s), under exclusive license to Springer Nature Switzerland AG 2025

A. D. Singh, B. E. Damato (eds.), *Clinical Ophthalmic Oncology*, https://doi.org/10.1007/978-3-031-75907-9_22

appears as an orange color. Some authors have suggested that the orange pigment seen overlying choroidal tumors are macrophages containing lipofuscin in the subretinal space [1]. However, Garcia et al. analyzed two enucleated eyes of patients with choroidal melanoma and showed that the orange pigment overlying the melanoma corresponded to proliferating RPE cells containing intracellular lipofuscin and melanolipofuscin granules, and not subretinal macrophage containing lipofuscin [2]. Regardless, I hypothesize that choroidal tumor infiltration causes metabolic disruption of normal RPE activity, causing poor phagocytoses and lysozyme processing, resulting in accumulation of bis-retinoid fluorophore deposits in the subretinal space and increased intracellular deposits within overlying tumor RPE cells.

22.3 The Origin of Autofluorescence

The retinal pigment epithelium (RPE) digests the tips of the outer photoreceptor segments by phagocytosis on a daily basis [3]. The digestion process is physiologically efficient, but a tiny fraction of this material cannot be degraded and accumulates in RPE lysosomes with increasing age. This undigested fraction is called lipofuscin (LF). LF exhibits a characteristic autofluorescence (AF) (fluorophore) when excited in ultraviolet (UV) or blue light. Above the age of 70, as much as 20% of the free cytoplasmic space of the RPE cells is occupied by LF granules but also by melanolipofuscin granules (MLF), a compound product of LF and melanin [4]. Also, MLF acts as a fluorophore, needing specific wavelengths of excitation and cutoff filters for emitting light (different from LF) to obtain the MLF-related emission peak [5]. MLF is present in RPE in physiologic conditions but increases in different pathologic conditions together with LF. Almost all disorders causing RPE changes by direct or indirect involvement, as well as any disease affecting RPE metabolism, may alter fundus AF by changing the amount of RPE-related fluorophores [5].

22.4 Types of Autofluorescence

22.4.1 Short-Wavelength AF

Short-wavelength AF (SW-AF), also called standard AF, mainly indicates the amount and the topographic distribution of LF deposits in the RPE [3–5]. Ex vivo studies have shown that the amount of RPE LF increases gradually from the fovea to a maximum of about 10° from the fovea and then decreases toward the periphery [6]. The topographic distribution of fundus AF, measured with an excitation at 550 nm, confirmed in vivo, reveals that SW-AF is maximal at an eccentricity of 7–13°, where AF is 1.7 times greater than in the fovea (Fig. 22.1a) [7]. Fundus SW-AF is also not symmetrically distributed around the fovea and is maximal about 12° temporally and superiorly and lower inferiorly and nasally, roughly matching the distribution of rod photoreceptors [3].

Despite extensive research, the composition of LF is still not completely known. RPE LF is proposed to contain highly

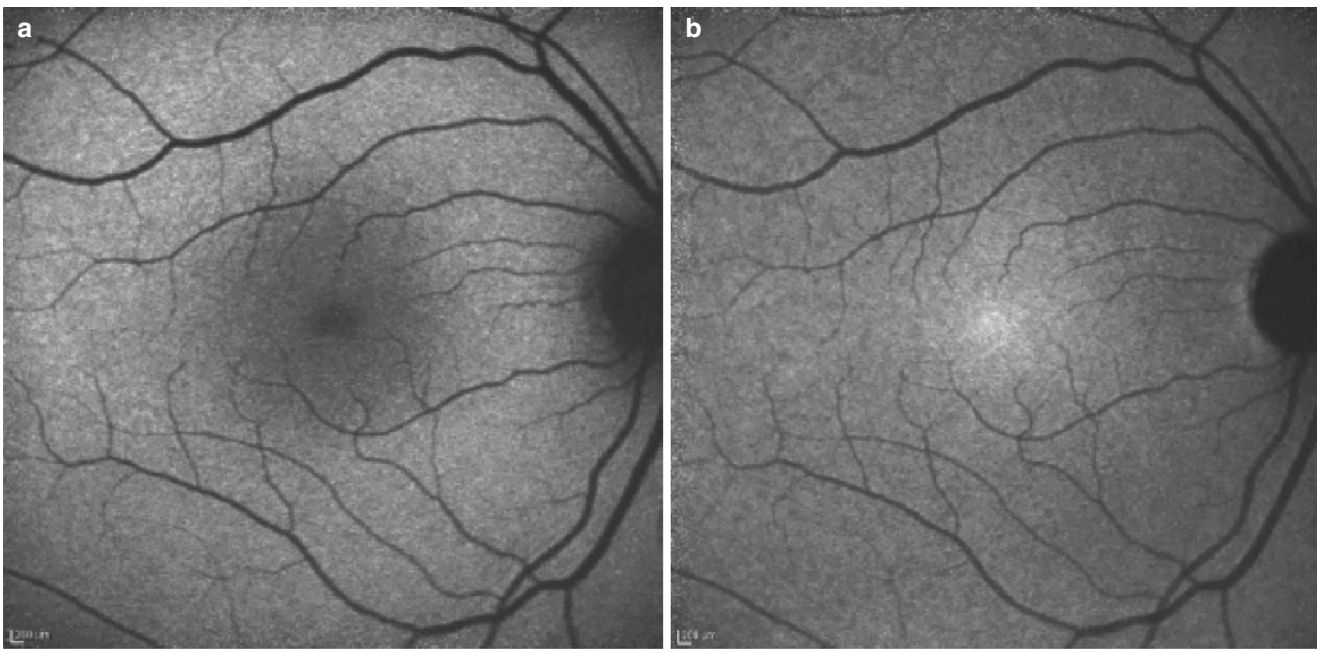

Fig. 22.1 Normal SW- (**a**) and NIR-AF (**b**) macular patterns

modified, undegradable remnants of phagocytosed photoreceptor outer segments (e.g., retinoids and carotenoids), and the best-characterized fluorescent component of RPE LF is the Schiff base *N*-retinyl-*N*-retinylidene ethanolamine (A2E), a degradation product of retinal photoreceptors [3]. The emission spectra of SW-AF are broad and maximal in the 600–640 nm region of the spectrum, shifting slightly toward longer wavelengths with increasing excitation wavelength. This "red shift" occurs for excitation at the long-wavelength end of the absorption spectrum for some fluorophores in viscous or polar environments [3]. This red shift may explain the variability of emission spectra reported in the literature; with excitation wavelength ranging from 364 to 580 nm, the emission peak varies between 590 and 660 nm. The excitation spectra have their maxima between 490 and 530 nm. In contrast to the spectra measured in extrafoveal areas (usually 7° temporal to the fovea), the foveal spectra are attenuated. This is because of the lower amount of LF in the foveal area and also because of the absorption of the excitation light by macular pigments [3].

Other fluorophores may theoretically influence SW-AF, mainly in young patients because of the low amount of LF deposits in the RPE of these individuals [8, 9]. Therefore, secondary fluorophores emitting in the 500–540 nm spectral range are under investigation. The macular pigment itself, flavins, collagen, microglia, and hyaluronic acid in the vitreous have specific AF characteristics, similar to those described for LF, although weaker than LF itself. Finally, AF contributions from the choroid and sclera have been estimated in patients with geographic atrophy to be 6–15% of the total fundus SW-AF, for dark- and light-pigmented subjects, respectively [3].

22.5 Near-Infrared AF

Near-infrared AF (NIR-AF), which uses the same excitation light and cutoff filters employed for indocyanine green angiography (ICG), was originally described as pseudofluorescence, commonly detected prior to standard ICG angiography [10].

Because different fluorophores are present within the retina and RPE, a specific selection of the wavelength for AF excitation (and the wavelength of the cutoff filter for emitting light) could provide additional possibilities (theoretically a wide range of possibilities) to analyze specific RPE substances [3, 5]. NIR-AF was first reported in 2006 and has been applied in several recently published studies on age-related macular degeneration. As the intensity of emitted AF is about 60–100 times lower compared to that of SW-AF, imaging of NIR-AF is usually obtained using a confocal scanning laser ophthalmoscope [3]. Diode laser light (787 nm) is used to excite NIR-AF, whereas a band-pass filter with a cutoff at 800 nm is inserted in front of the detector. Because of the lower intensity, images are averaged to obtain the final image. Optimal imaging is obtained with dilated pupils.

Physiologic NIR-AF is characterized by the dark appearance of optic discs and retinal vessels [5]. The NIR-AF signal is maximal at the posterior pole, with a peak at the fovea and a marked decline toward the peripheral regions (Fig. 22.1b) [3]. The major fluorophores contributing to NIR-AF are most likely melanin and its related compounds (melanolipofuscin (MLF), melanolysosomes, and oxidized melanin) [3, 5]. The notion that the NIR-AF signal derives from melanin is based on the following evidence: the NIR-AF distribution corresponds to that of RPE melanin; the severely reduced signal of NIR-AF in areas of RPE loss indicates that the major source of NIR-AF is the RPE; and the marked increase of NIR-AF in flat choroidal nevi [11]. Melanin AF is increased by oxidation. MLF (melanin with a cortex of LF) and melanolysosomes (melanin with a cortex of enzyme-reactive material) accumulate with age (and RPE disease) and represent melanin in the process of repair, modification, or degradation [11]. The AF of melanin, oxidized melanin, and compound granules containing melanin contribute to the NIR-AF signal. An increase in NIR-AF could be caused by melanogenesis, the formation of melanolysosomes, or MLF, or altered characteristics of melanin in the disease process [3, 11]. The possible contribution of other fluorophores to the NIR-AF signal is under investigation [11]. Although the possibility that LF contributes to NIR-AF signal cannot be ruled out, this is unlikely because of the different AF distributions observed in normal subjects and in patients with a variety of retinal diseases. Possible fluorophores include collagen, elastin, and porphyrin [3, 11].

22.6 Choroidal Melanocytic Tumors

AF patterns in small, medium, and large choroidal melanomas share common characteristics, such as a homogeneous increased AF signal and a confluent plaque-like configuration [3]. As long ago as 1976, Shields et al. demonstrated that LF accumulates in RPE cells and macrophages overlying choroidal melanomas [12]. This phenomenon is clinically evident by biomicroscopy, described as "orange pigment" over the lesions. However, depending on whether the tumor is melanotic or amelanotic, the color may vary from orange to brown, respectively. Various authors have reported that the presence of orange pigment over small indeterminate choroidal-pigmented lesions is a specific risk factor for malignancy [13, 14]. The exact mechanism by which choroidal melanoma induces lipofuscinogenesis remains unclear. Font et al. reported that sheets of proliferated RPE cells and clusters of pigment-laden macrophages are present under the

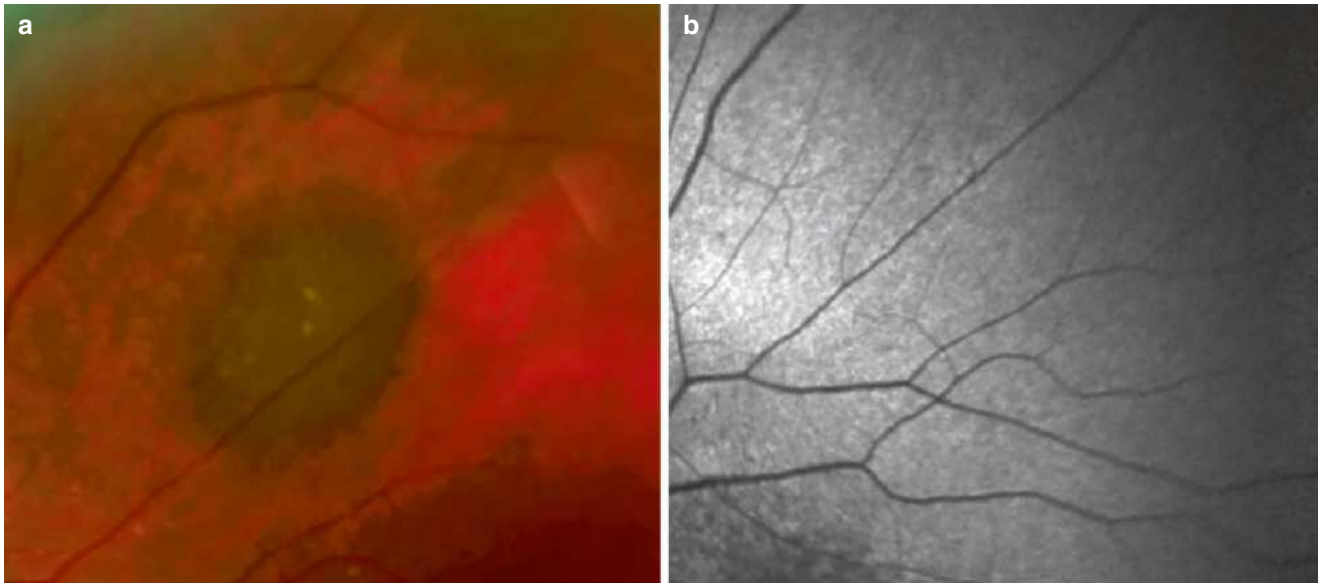

Fig. 22.2 Choroidal nevus (**a**) (fundus appearance) showing a normal pattern of background fundus SW-AF (**b**). Note absence of hyper- or hypofluorescence despite the presence of drusen over the lesion

degenerated neurosensory retina, corresponding to the position of the clinically observed orange pigment [14]. Histochemical analysis indicates that the orange pigment of tumors stains positive for PAS, Sudan Black B, and long Ziehl-Neelsen reduces silver salts with the Fontana-Masson method, bleaches partially with potassium permanganate, and is acid-fast and oil red O positive in paraffin sections. It also exhibits a golden yellow AF when examined using UV light or a fluorescence microscope, confirming that this pigment is in fact LF [3].

22.6.1 Choroidal Nevus

SW-AF imaging of choroidal nevus usually shows a normal pattern of background fundus AF, with no areas of increased or decreased AF signal (Fig. 22.2). In a minority of cases, nevi may also reveal areas of mild decreased or increased SW-AF signal (Fig. 22.3) [3]. Drusen, commonly overlying choroidal nevi, when large or coalescent, may appear as areas of localized increased SW-AF (Fig. 22.4). These must be distinguished from LF accumulation occurring in choroidal melanomas and small indeterminate choroidal-pigmented lesions with risk factors for growth [3]. Shields et al. reported that choroidal nevi can show faint intrinsic AF [15]. Nevertheless, overlying RPE alterations (quite common in choroidal nevi) may show different AF patterns, ranging from normal (Fig. 22.2) to mild or dark hypo-AF due to RPE atrophy (Fig. 22.3) to bright hyper-AF (Fig. 22.4). Common causes of increased SW-AF in nevi include hyperpigmentation, and fibrous metaplasia (probably because they also cause LF accumulation in the overlying RPE). Drusen by themselves are usually not correlated with notable FAF changes, but increased FAF signal adjacent to drusen has been noted to correspond to focal hyperpigmentation and pigment figures on biomicroscopy, attributed to melanolipofuscin or changes in the metabolic activity of the RPE. However, some drusen will have a decreased FAF signal, which is postulated to be due to degenerated RPE [1].

Edoardo Midena and colleagues investigated SW-AF in 30 choroidal-pigmented lesions, analyzing the role of this technique in the diagnosis and characterization of these lesions (unpublished data). In this study, AF imaging was performed using a confocal system (Heidelberg Retinal Angiograph, HRA 2; Heidelberg Engineering, Heidelberg, Germany). SW-AF images were recorded at 488 nm wavelength using a barrier filter for the detection of emitted light above 500 nm (SW-AF). At SW-AF, choroidal nevi showed a normal pattern of background AF with no corresponding areas of hyperfluorescence or hypo-AF over the nevi in 50% of the cases. In the remaining 50% of cases, the lesion showed mild hypo-AF (in 25%) or hyper-AF (in 25%), with faint localized hyper-AF small areas in all cases. Nevi with normal background fundus AF were flat, while nevi with a different pattern of fundus fluorescence were elevated with drusen or LF.

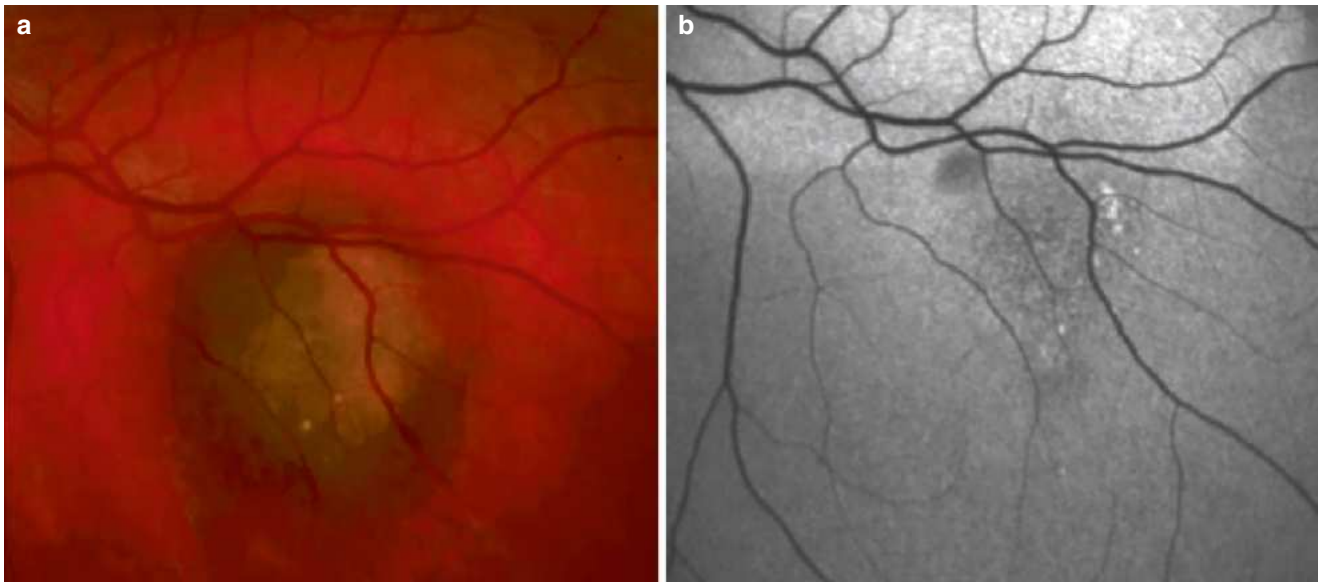

Fig. 22.3 Choroidal nevus (**a**) (fundus appearance) showing mild hypo-AF with bright hyper-AF spots in SW-AF (**b**)

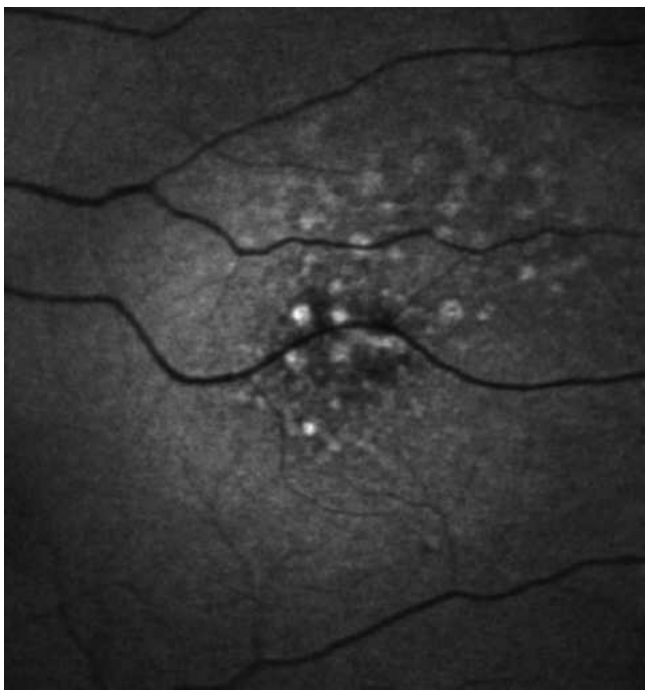

Fig. 22.4 Choroidal nevus showing mild hyper-AF with bright hyper-AF spots in SW-AF, corresponding to overlying areas with or adjacent to drusen

22.7 Indeterminate Choroidal Melanocytic Tumor (Small Choroidal Melanoma)

Materin et al. investigated small choroidal melanomas by SW-AF, reporting that all tumors with orange pigment had an increased AF signal, although of different intensities, and the majority of lesions showed diffuse mild increased SW-AF [16]. Subretinal fluid associated with choroidal melanoma showed an increased SW-AF signal in 60% of the cases.

Gunduz et al. reviewed the SW-AF characteristics of a variety of choroidal melanocytic lesions [17]. The AF patterns of these lesions were classified as patchy or diffuse. The patchy pattern was defined as the presence of distinct areas of increased AF between areas of normal AF. The diffuse pattern was characterized by the presence of increased AF with indistinct borders over most of the lesion in the absence of such intervening areas. Choroidal melanomas presented with either a diffuse or patchy pattern, whereas choroidal nevi demonstrated only a patchy pattern (Figs. 22.5, 22.6, and 22.7). The diffuse AF pattern was more often associated with larger choroidal melanomas, as well as with early venous and late hyperfluorescence on fluorescein angiography (Fig. 22.6) [17]. Because of the limited depth of field of

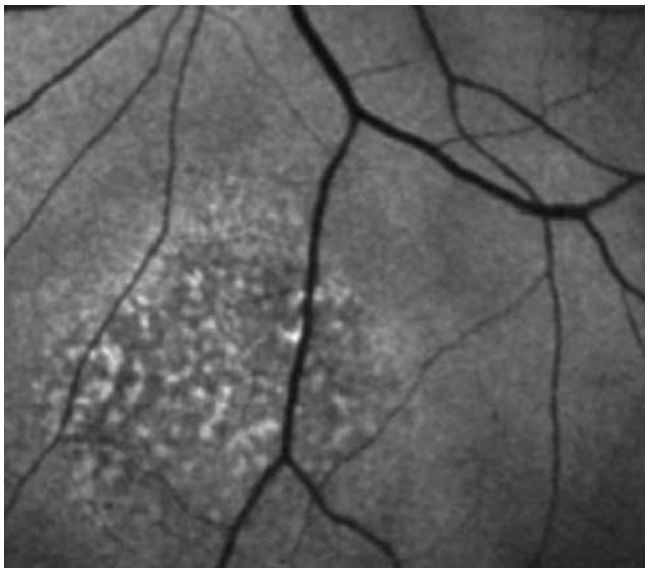

Fig. 22.5 Patchy SW-AF pattern in indeterminate choroidal melanocytic lesion. This pattern is more frequently observed among nevi

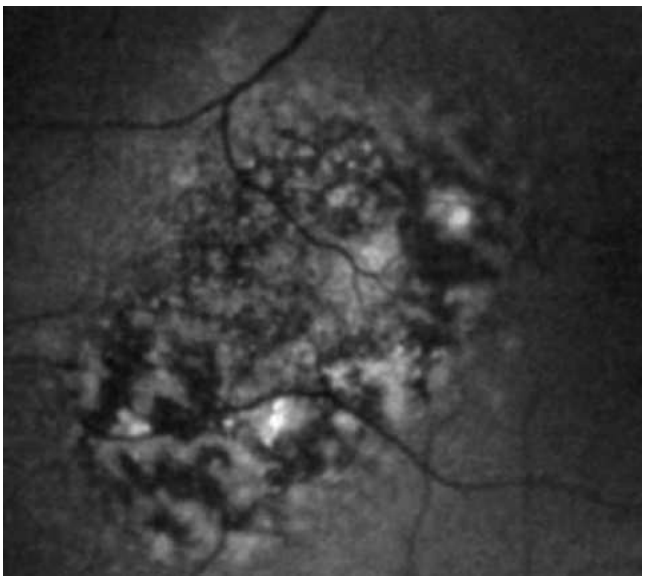

Fig. 22.6 Diffuse SW-AF pattern in an indeterminate choroidal melanocytic lesion. This pattern is more frequently observed in melanomas compared to nevi

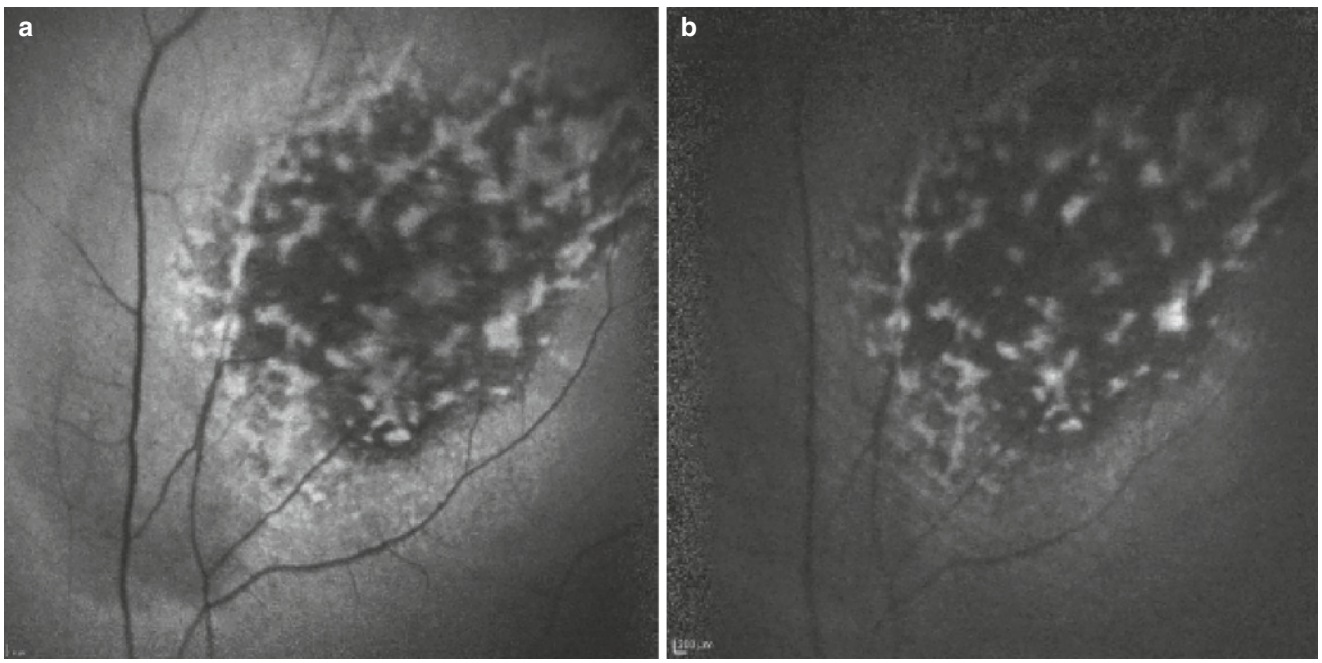

Fig. 22.7 Patchy SW-AF (**a**) and NIR (**b**) pattern in a small choroidal melanoma. This pattern, resembling a leopard coat, is more frequently observed among small melanomas or indeterminate choroidal melanocytic lesions with multiple risk factors for growth

confocal scanning laser ophthalmoscopy, AF from other planes could not be detected. Increased retinal thickness, intraretinal edema, and the presence of subretinal fluid may also affect the AF signal. Nevertheless, the same authors reported a total or partial correlation between AF and the foci of LF and hyperpigmentation in about 90% of the cases [17]. AF pattern can also detect lipofuscin scattered within subretinal fluid that is overlying and surrounding small melanomas (Fig. 22.8).

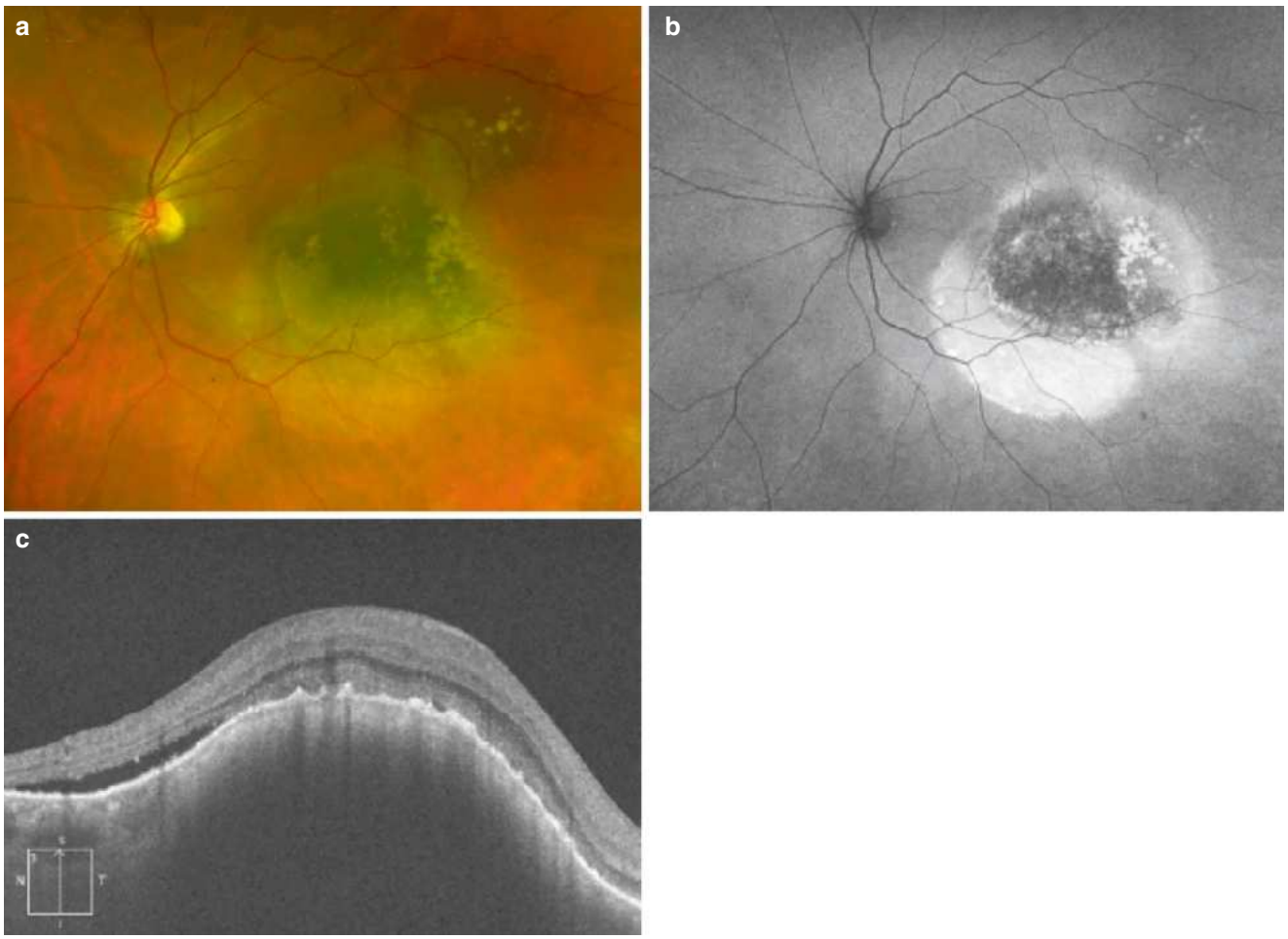

Fig. 22.8 Fundus photograph of a small choroidal melanoma (**a**). Note surface orange pigment and shallow subretinal fluid. With AF (**b**) using green laser source (532 nm, Optos system), the lipofuscin on the surface of the lesion and subretinal fluid becomes very evident. The presence of SRF and lipofuscin correlates with OCT findings (**c**)

22.8 Choroidal Melanoma

Gunduz et al. reported that nearly 90% of choroidal melanomas show at least one focus of increased SW-AF, corresponding to the location of LF or hyperpigmentation of the lesion [17]. Moreover, in 75% of amelanotic choroidal melanomas, increased SW-AF was observed in areas of hyperpigmentation. Medium and large choroidal melanomas also appear to have increased SW-AF. Superficial fibrosis and subretinal fluid have been reported to have an increased SW-AF also in large tumors. However, in highly elevated tumors, artifacts related to the technique may limit the analysis [17]. More recently, Cennamo et al. reported that most choroidal melanomas are surrounded by confluent hyper-AF, whereas most nevi are not characterized by intrinsic hyper-AF [18].

It has been suggested that longer and deeper wavelengths, such as NIR, could provide more information about the pigment composition of choroidal melanocytic lesions [5]. With NIR-AF, the melanin distribution can be explored as oxi-

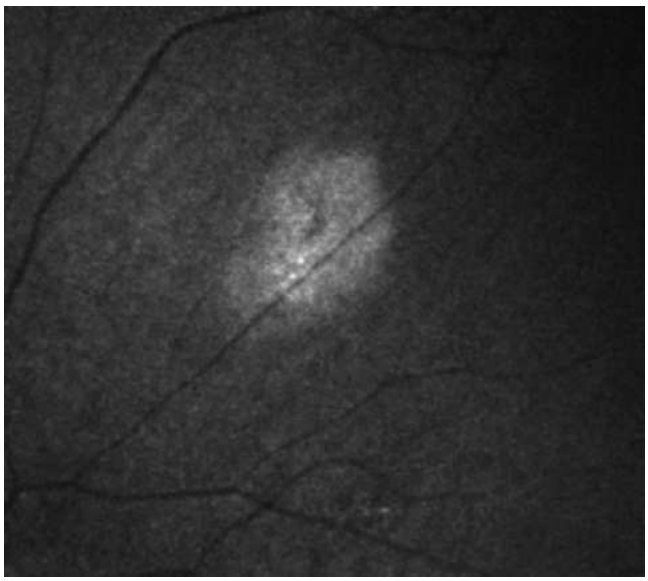

Fig. 22.9 NIR-AF of the same lesion reported in Fig. 22.2. Note the marked hyper-AF of this lesion in the NIR-AF despite the normal pattern of background fundus in SW-AF

dized melanin or compounds closely associated with melanin. Edoardo Midena and colleagues investigated SW-AF and NIR-AF in 30 choroidal-pigmented lesions, analyzing the role of these techniques in the diagnosis and characterization of these lesions (unpublished data). In this study, AF imaging was performed using a confocal system (Heidelberg Retinal Angiograph, HRA 2; Heidelberg Engineering, Heidelberg, Germany). The NIR-AF images were recorded at 780 nm with a barrier filter at 820 nm. Using NIR-AF, flat nevi appeared as bright hyper-AF areas (Fig. 22.9). Elevated nevi with mild hyper-AF or hypo-AF in SW-AF were hypo-AF in NIR-AF. Edoardo Midena and colleagues analyzed NIR-AF vs. SW-AF in choroidal-pigmented lesions, at NIR-AF imaging, choroidal melanomas showed hypo- and hyper-AF areas in all cases, with a hyper-AF halo in 62%, due to retinal detachment around the tumor. The hyper-AF areas at NIR-AF corresponded to the pigmented areas of the tumor. Comparing SW-AF and NIR-AF images of choroidal melanomas, they were unable to detect significant differences (Fig. 22.10).

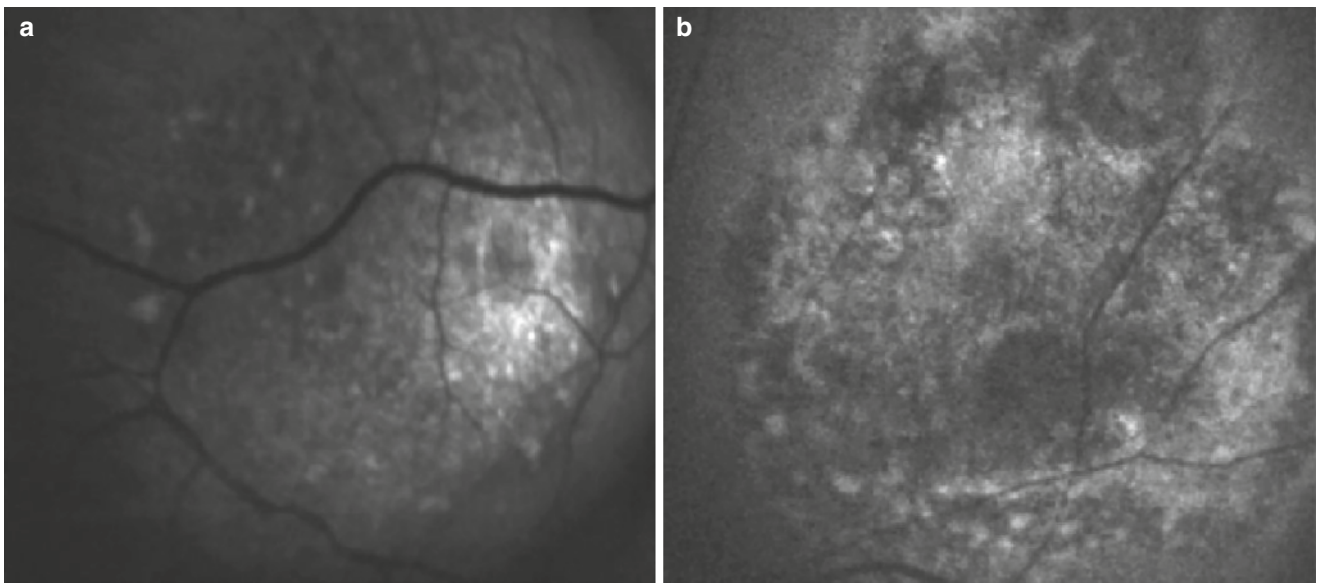

Fig. 22.10 SW-AF (**a**, **b**) and NIR-AF (**c**, **d**) of two choroidal melanomas. Comparing SW-AF and NIR-AF of these lesions, only small and nonsignificant differences in AF patterns are present

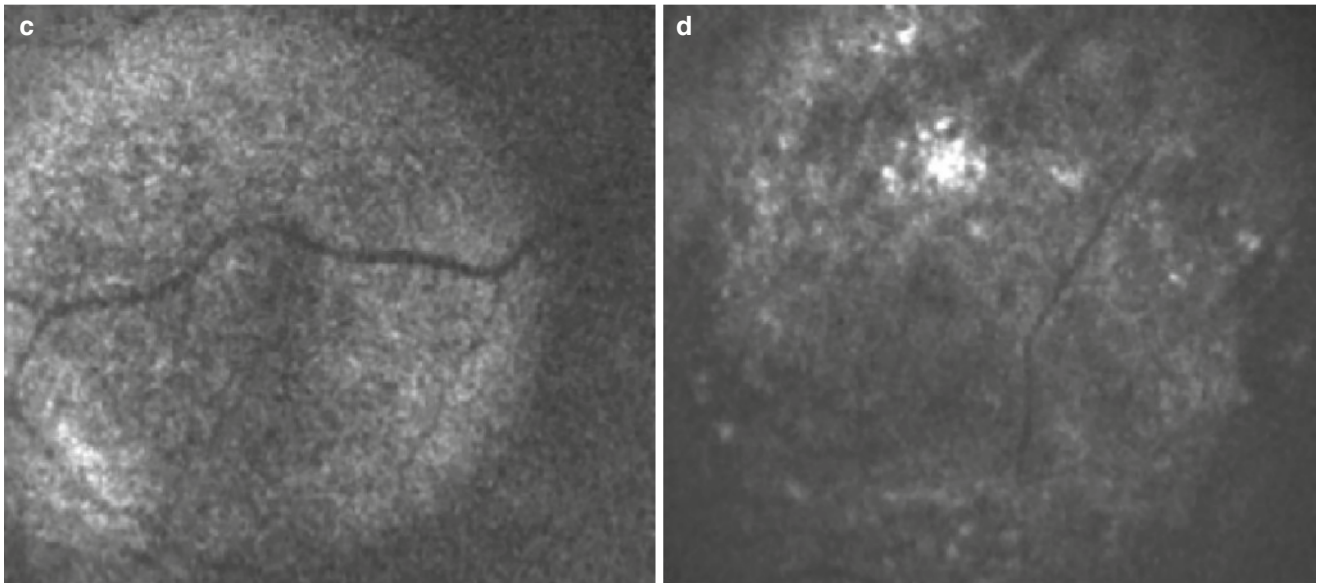

Fig. 22.10 (continued)

22.9 Choroidal Hemangioma

Shields et al. described the intrinsic SW-AF properties of choroidal hemangioma (CH) and the extrinsic features in the overlying retinal/RPE alterations [19, 20]. They reported that both circumscribed and diffuse CH (untreated) showed general intrinsic iso-SW-AF or hypo-SW-AF (Figs. 22.11 and 22.12) [19, 20]. In contrast, treated choroidal hemangioma appeared more hypo-SW-AF. The intrinsic AF pattern did not correlate with tumor location, size, or thickness. The extrinsic SW-AF features of choroidal hemangioma were more dramatic. The most brilliant hyper-SW-AF was from overlying orange pigment notable in some eyes. Other extrinsic findings of RPE hyperplasia, RPE atrophy, and RPE fibrous metaplasia generally were seen as hypo-SW-AF in both circumscribed and diffuse CH. Retinal pigment epithelium atrophy (found in 25% of untreated circumscribed CH and 87% of treated circumscribed CH) appeared moderately to markedly hypo-AF in SW. Retinal pigment epithelium hyperplasia, commonly found in treated choroidal hemangioma, appeared moderately to markedly hypo-AF in SW. The intrinsic and extrinsic AF patterns were most often altered after therapy. Most tumors showed intrinsic hypo-AF after therapy, and most showed extrinsic hypo-AF from RPE hyperplasia or atrophy. Moreover, subretinal fluid showed varying SW-AF patterns depending on the chronicity. Fresh subretinal fluid with intact RPE appeared moderately hyper-AF, whereas chronic subretinal fluid with RPE hyperplasia and atrophy showed moderate to marked hypo-AF in SW mode [19]. Edoardo Midena and colleagues noted that in their cohort of patients, circumscribed or diffuse hemangioma shows a specific NIR-AF pattern, usually depending on RPE status overlying the lesions and commonly characterized by hypo-NIR-AF with bright hyper-NIR-AF spots.

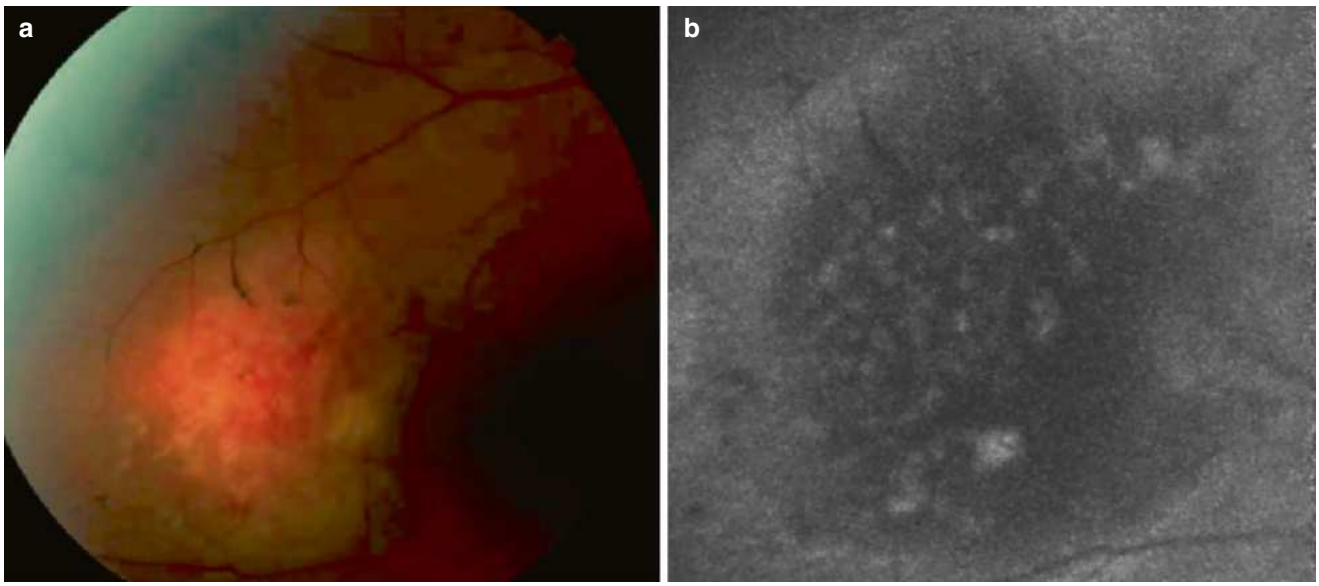

Fig. 22.11 Choroidal hemangioma. Fundus appearance (**a**). Hypo-AF area with hyper-AF spots in a case of untreated circumscribed choroidal hemangioma (SW-AF) (**b**)

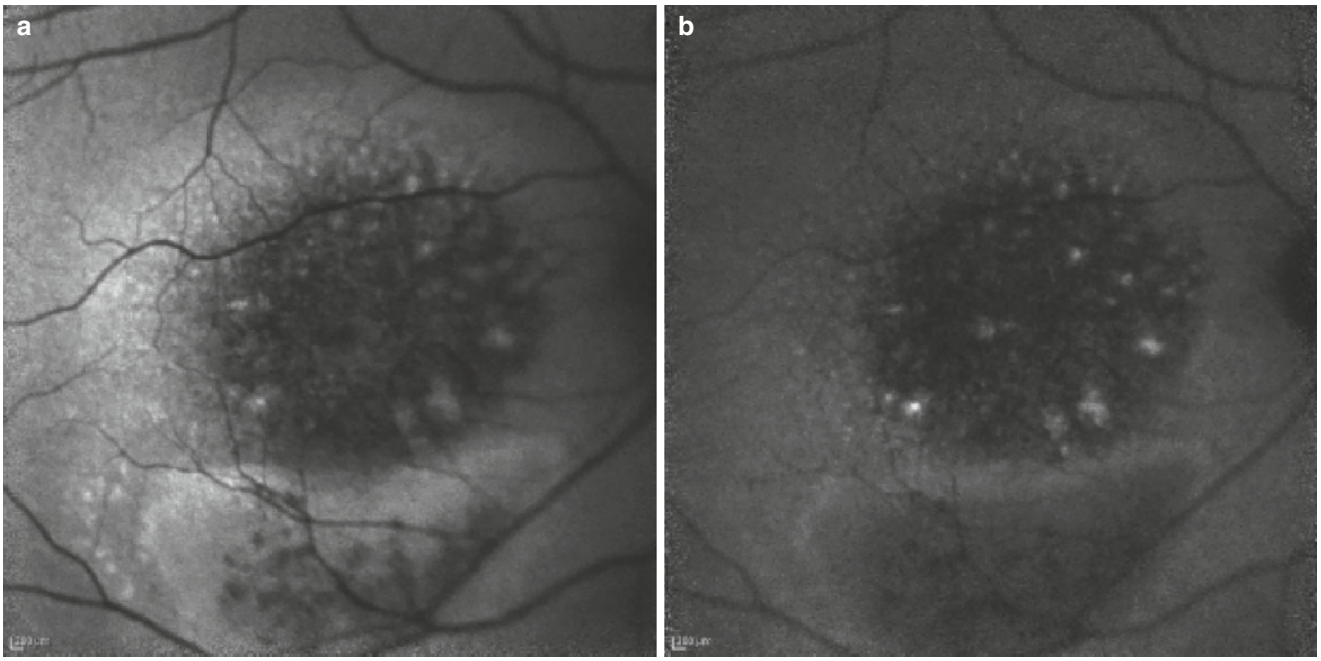

Fig. 22.12 Choroidal hemangioma. The SW-AF (**a**) is characterized by a hypo-AF area with hyper-AF spots. Please note the hyper-AF area under the lesion is related to the presence of serous retinal detachment. The NIR-AF (**b**) is characterized by similar AF characteristics over the lesion and by a diffuse hypo-AF halo with hyper-AF margins in the area corresponding to the serous retinal detachment

22.10 Choroidal Metastasis

Limited data are reported on SW-AF of choroidal metastatic lesions. Collet et al. reported on 15 metastatic tumors in 14 eyes of 11 consecutive patients, concluding that amelanotic choroidal metastases with hyperpigmented foci are associated with increased SW-AF in most of the cases and that subretinal fluid overlying choroidal metastasis may cause increases in SW-AF as well [21]. Ishida et al. reported two cases of metastatic choroidal tumors, concluding that the AF pattern of these cases was approximately the reverse picture of the fluorescein angiography pattern [22]. Natesh et al.

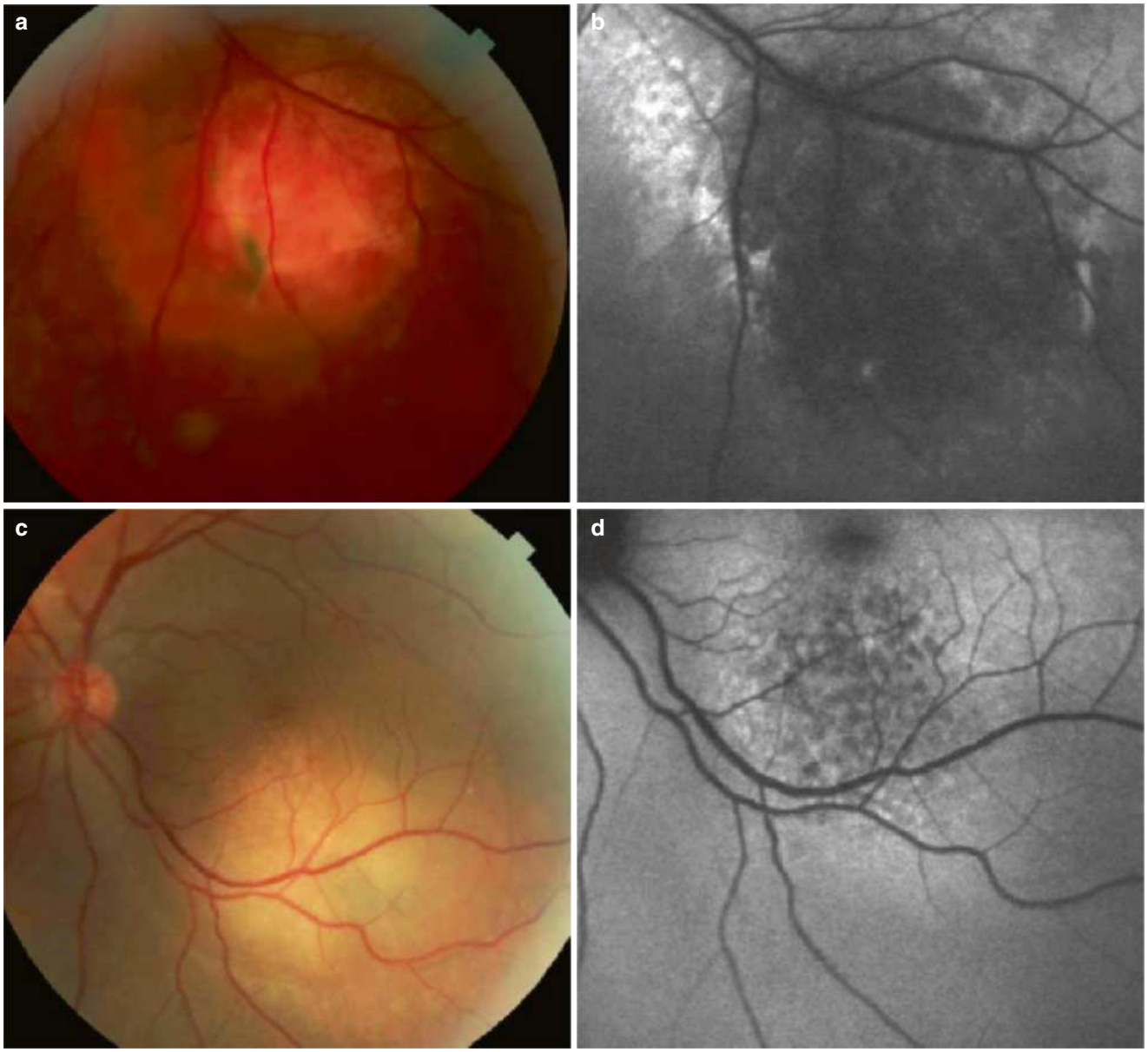

Fig. 22.13 Choroidal metastases. Fundus appearance (**a**, **c**) and SW-AF imaging (**b**, **d**). These lesions are characterized by intrinsic hypo-AF with hyper-AF spots and hyper-AF halo (SW-AF)

investigated the correlation between SW-AF imaging and clinical, OCT, and fluorescein angiographic findings in ten choroidal metastases, concluding that hyper-AF in SW-AF mode correlates with focal hyperpigmentation, subretinal fluid, and advancing tumor edges. Moreover, SW-AF appears to better define surface characteristics and tumor margins compared to standard biomicroscopy [23]. Edoardo Midena and colleagues noted that in their experience, SW-AF of choroidal metastasis is usually characterized by hypo-AF with hyper-AF spots and hyper-AF halo (Fig. 22.13). Edoardo Midena and colleagues noted that in their cohort of patients, NIR-AF of choroidal metastases is extremely variable. Therefore, AF needs to be investigated in a larger series before it can be included in the diagnostic process.

22.11 Congenital Hypertrophy of the Retinal Pigment Epithelium

Shields et al. performed SW-AF on 13 consecutive eyes with congenital hypertrophy of the retinal pigment epithelium (CHRPE), reporting that CHRPE showed hypo-AF in all

cases [24]. Compared to the central portion of CHRPE, the margins showed iso-AF (n = 8) or trace hyper-AF (n = 5). There were eight lesions with intralesional lacunae, and this feature generally showed trace to moderate hyper-AF (n = 6). A nonpigmented halo was present around six lesions, showing trace hyper-AF (n = 3). A pigmented halo surrounded eight lesions, usually showing iso-AF (n = 6). The authors concluded that CHRPE shows striking hypo-AF, and this correlates with known histopathologic evidence of lack of LF in the retinal pigment epithelium of CHRPE.

22.12 Neurofibromatosis Type 1 (NF1)

While not formally considered an autofluorescence modality, near-infrared reflectance imaging appears to be a new noninvasive alternative to indocyanine green angiography for the detection of choroidal involvement related to neurofibromatosis type-1 (NF1) [25–27]. The first research regarding the frequency of choroidal abnormalities in NF1 observed with confocal scanning laser ophthalmoscope (SLO) was conducted by Yasunari and colleagues [25]. They evaluated 33 eyes of 17 adult patients affected by NF1 and 76 eyes of 39 age-matched controls. Their results suggest a clear relationship between hypofluorescent regions seen on indocyanine green angiograms of patients and bright patchy areas noted under infrared light examination (Fig. 22.14), although choroid appears normal under conventional ophthalmoscopic examination and fluorescein fundus angiography. In a more recent cross-sectional study, 190 eyes of 95 white patients diagnosed with NF1, including 21 NF1 pediatric patients under 12 years old, were examined [26]. The authors demonstrated that choroidal abnormalities were detectable by neari-nfrared reflectance imaging in 82% of the NF1 patients and in 71% of the NF1 pediatric patients. With a cutoff value of 1.5 choroidal lesions, they also determined that the sensitivity and specificity of this method were 83% and 96%, respectively. Also, Parrozzani and colleagues evaluated a large sample of 140 pediatric patients diagnosed with NF1 and 59 pediatric patients suspected of NF1 [27]. Because children can benefit greatly from the early diagnosis of NF1, they have extended these findings to show that the feasibility rate of near-infrared reflectance image acquisition was 82%, which is slightly inferior compared with the detection of Lisch nodules (87%).

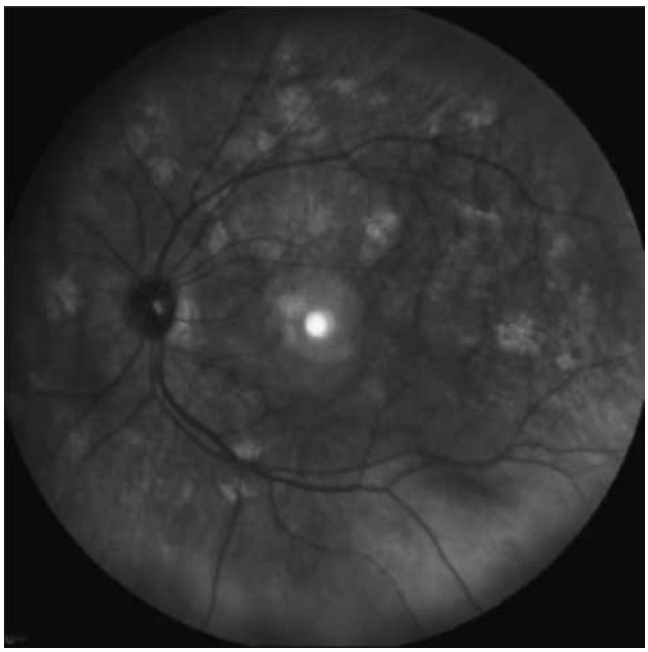

Fig. 22.14 Near-infrared reflectance imaging of a 5-year-old boy with NF1 showing NF1-related choroidal abnormalities in his left eye (bright patchy areas)

22.13 Vitreoretinal Lymphoma

Fundus autofluorescence is helpful in the diagnosis and monitoring of the progression of vitreoretinal lymphoma [28]. Active lesions appear as hyper-AF lesions as compared with inactive (atrophic) lesions that appear as hypo-AF (Fig. 22.15). In general, hyper-AF lesions correspond with hypofluorescent appearance on the fluorescein angiogram [29]. The hyper-AF is explained on the basis of RPE and photoreceptor disruption by the sub-RPE lymphoma infiltrates [30]. After treatment, as active lesions become inactive (atrophic), the AF pattern correspondingly changes from that of hyper-AF to hypo-AF [31].

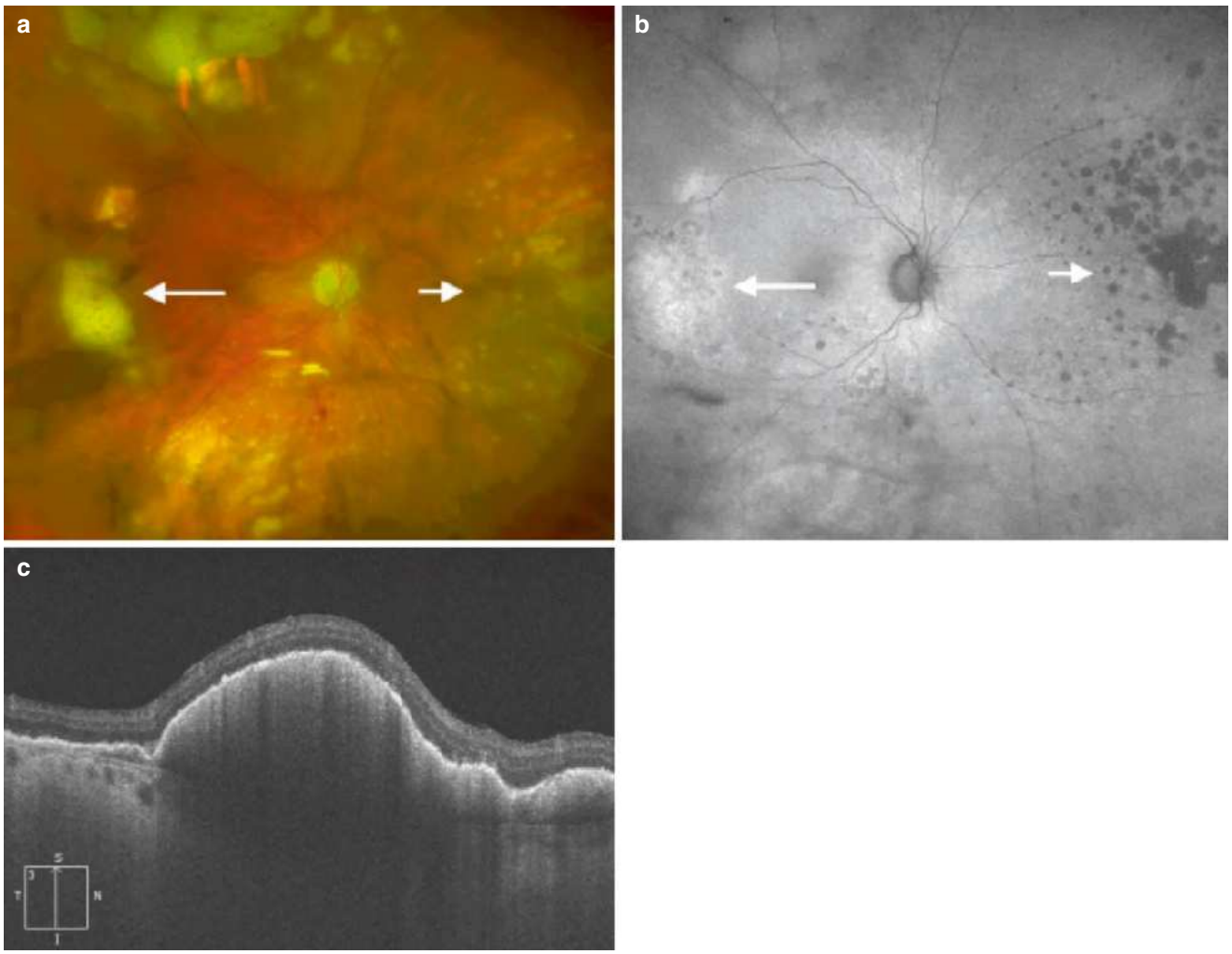

Fig. 22.15 Fundus photograph of vitreoretinal lymphoma (**a**). Note active lesion (large arrow) and inactive atrophic lesions (small arrow). With AF using green laser source (532 nm, Optos system), the active lesion appears hyper-AF (large arrow) as compared with inactive (atrophic) lesions that appear hypo-AF (**b**) (small arrow). The hyper-AF is explained on the basis of RPE and photoreceptor disruption by the sub-RPE lymphoma infiltrates (**c**)

22.14 Conclusions

AF is a noninvasive, valuable diagnostic tool for assessing intraocular tumors, mainly revealing the effects of these lesions on the overlying retinal pigment epithelium [32]. SW-AF is the most commonly used form of AF, useful in detecting specific neuroretinal and RPE changes related to different choroidal tumors (Table 22.1). NIR-AF may also provide specific information on intrinsic pigments that compose and characterize benign and malignant, congenital, and acquired chorioretinal lesions. LF, melanin, and MLF play the leading role in the different AF patterns of chorioretinal tumors, but other pigments (such as porphyrin) may influence AF imaging of these lesions. Some findings are strongly characteristic of specific lesions, mainly the bright hyper-AF overlying choroidal melanoma and the dark hypo-AF of congenital hypertrophy of the RPE. Moreover, SW-AF enhances the visualization of orange pigment located over small indeterminate choroidal-pigmented tumors, allowing better stratification of the risk of growth of these lesions. The use of AF may contribute to the diagnosis and characterization of choroidal tumors.

Table 22.1 SW-AF characteristics in different choroidal tumors

Lesion type	SW-AF characteristics
Choroidal nevus	Hypo-AF: RPE atrophy Hyper-AF: Orange pigment, subretinal fluid, drusen Iso-AF: No changes in the background AF correspondent to normal, drusen RPE and neuroretinal aspect on OCT
Indeterminate choroidal melanocytic tumors and small choroidal melanoma	Hypo-AF: RPE atrophy Hyper-AF: Orange pigment, subretinal fluid, RPE detachment, +/− drusen
Circumscribed choroidal hemangioma	General intrinsic iso-AF or hypo-AF Hypo-AF: RPE atrophy Hyper-AF: Subretinal fluid, lipofuscin accumulation
Choroidal metastasis	Hypo-AF: RPE atrophy Hyper-AF: Subretinal fluid, lipofuscin accumulation, focal pigmentation
CHRPE	Hypo-AF: Intense hypo-AF in CHRPE area and lacunae Hyper-AF: Margins Iso-AF: Some lacunae
Vitreoretinal lymphoma	Hyper-AF: Active lesions Hypo-AF: Inactive (atrophic) lesions

Based on data from Ref. [32]
CHRPE congenital hypertrophy of the retinal pigment epithelium, *SW* short-wavelength, *AF* autofluorescence, *RPE* retinal pigment epithelium, *OCT* optical coherence tomography

Acknowledgments The contribution of the IRCCS Fondazione Bietti to this paper was supported by the Ministry of Health and Fondazione Roma. The authors have no relevant financial disclosures to report. Each author has equally contributed to the study, and they present the same rights to its intellectual properties.

References

1. Schmitz-Valckenberg S, Pfau M, Fleckenstein M, Staurenghi G, Sparrow JR, Bindewald-Wittich A, Spaide RF, Wolf S, Sadda SR, Holz FG. Fundus autofluorescence imaging. Prog Retin Eye Res. 2021;81:100893. https://doi.org/10.1016/j.preteyeres.2020.100893. Epub 2020 Aug 3. PMID: 32758681.
2. Garcia MD, Salomao DR, Marmorstein AD, Pulido JS. Histopathologic findings in the areas of Orange pigment overlying choroidal melanomas. Transl Vis Sci Technol. 2016;5(3):4. https://doi.org/10.1167/tvst.5.3.4. PMID: 27190699; PMCID: PMC4867953.
3. Lois N, Forrester JV. Fundus autofluorescence. Philadelphia: Lippincott Williams & Wilkins; 2009.
4. Feeney-Burns L, Hilderbrand ES, Eldridge S. Aging human RPE: morphometric analysis of macular, equatorial, and peripheral cells. Invest Ophthalmol Vis Sci. 1984;25(2):195–200.
5. Pilotto E, Vujosevic S, Melis R, et al. Short wavelength fundus autofluorescence versus near-infrared fundus autofluorescence, with microperimetric correspondence, in patients with geographic atrophy due to age-related macular degeneration. Br J Ophthalmol. 2011;95(8):1140–4.
6. Weiter JJ, Delori FC, Wing GL, et al. Retinal pigment epithelial lipofuscin and melanin and choroidal melanin in human eyes. Invest Ophthalmol Vis Sci. 1986;27(2):145–52.
7. Delori FC, Goger DG, Keilhauer C, et al. Bimodal spatial distribution of macular pigment: evidence of a gender relationship. J Opt Soc Am A Opt Image Sci Vis. 2006;23(3):521–38.
8. Frandsen JE, Llop S, Digre KB, et al. Quantification of macular carotenoids using autofluorescence imaging in patients with photosensitive migraine and benign essential blepharospasm. Arch Ophthalmol. 2012;130(2):259–60.
9. Monici M. Cell and tissue autofluorescence research and diagnostic applications. Biotechnol Annu Rev. 2005;11:227–56.
10. Piccolino FC, Borgia L, Zinicola E, et al. Pre-injection fluorescence in indocyanine green angiography. Ophthalmology. 1996;103(11):1837–45.
11. Keilhauer CN, Delori FC. Near-infrared autofluorescence imaging of the fundus: visualization of ocular melanin. Invest Ophthalmol Vis Sci. 2006;47(8):3556–64.
12. Shields JA, Rodrigues MM, Sarin LK, et al. Lipofuscin pigment over benign and malignant choroidal tumors. Trans Sect Ophthalmol Am Acad Ophthalmol Otolaryngol. 1976;81(5):871–81.
13. Singh AD, Schachat AP, Diener-West M, et al. Small choroidal melanoma. Ophthalmology. 2008;115(12):2319–e3.
14. COMS Report No. 5. The Collaborative Ocular Melanoma Study Group. Factors predictive of growth and treatment of small choroidal melanoma. Arch Ophthalmol. 1997;115:1537–44.
15. Shields CL, Pirondini C, Bianciotto C, et al. Autofluorescence of choroidal nevus in 64 cases. Retina. 2008;28(8):1035–43.
16. Materin MA, Raducu R, Bianciotto C, et al. Fundus autofluorescence and optical coherence tomography findings in choroidal melanocytic lesions. Middle East Afr J Ophthalmol. 2010;17(3):201–6.
17. Gunduz K, Pulido JS, Ezzat K, et al. Review of fundus autofluorescence in choroidal melanocytic lesions. Eye. 2009;23:497–503.
18. Cennamo G, Romano MR, Velotti N, et al. Fundus autofluorescence of choroidal nevi and melanoma. Acta Ophthalmol. 2018;96:e102–4.
19. Ramasubramanian A, Shields CL, Harmon SA, et al. Autofluorescence of choroidal hemangioma in 34 consecutive eyes. Retina. 2010;30(1):16–22.
20. Almeida A, Kaliki S, Shields CL. Autofluorescence of intraocular tumours. Curr Opin Ophthalmol. 2013;24(3):222–32.
21. Collet LC, Pulido JS, Gunduz K, et al. Fundus autofluorescence in choroidal metastatic lesions: a pilot study. Retina. 2008;28(9):1251–6.
22. Ishida T, Ohno-Matsui K, Kaneko Y, et al. Autofluorescence of metastatic choroidal tumor. Int Ophthalmol. 2009;29(4):309–13.
23. Natesh S, Chin KJ, Finger PT. Choroidal metastases fundus autofluorescence imaging: correlation to clinical, OCT, and fluorescein angiographic findings. Ophthalmic Surg Lasers Imaging. 2010;41(4):406–12.

24. Shields CL, Pirondini C, Bianciotto C, et al. Autofluorescence of congenital hypertrophy of the retinal pigment epithelium. Retina. 2007;27(8):1097–100.
25. Yasunari T, Shiraki K, Hattori H, et al. Frequency of choroidal abnormalities in neurofibromatosis type 1. Lancet. 2000;356:988–92.
26. Viola F, Villani E, Natacci F, et al. Choroidal abnormalities detected by near-infrared reflectance imaging as a new diagnostic criterion for neurofibromatosis 1. Ophthalmology. 2012;119:369–75.
27. Parrozzani R, Clementi M, Frizziero L, et al. In vivo detection of choroidal abnormalities related to NF1: feasibility and comparison with standard NIH diagnostic criteria in pediatric patients. Invest Ophthalmol Vis Sci. 2015;56(10):6036–42.
28. Ishida T, Ohno-Matsui K, Kaneko Y, et al. Fundus autofluorescence patterns in eyes with primary intraocular lymphoma. Retina. 2010;30(1):23–32.
29. Casady M, Faia L, Nazemzadeh M, et al. Fundus autofluorescence patterns in primary intraocular lymphoma. Retina. 2014;34(2):366–72.
30. Egawa M, Mitamura Y, Hayashi Y, et al. Spectral-domain optical coherence tomographic and fundus autofluorescence findings in eyes with primary intraocula lymphoma. Clin Ophthalmol. 2014;8:335–41.
31. Egawa M, Mitamura Y, Hayashi Y, et al. Changes of fundus autofluorescence and spectral-domain optical coherence tomographic findings after treatment of primary intraocular lymphoma. J Ophthalmic Inflamm Infect. 2014;4(1):7.
32. Kaur G, Anthony SA. Multimodal imaging of suspicious choroidal neoplasms in a primary eye-care clinic. Clin Exp Optom. 2017;100:549–62.

Diagnostic Techniques: Ultrasonography

23

Brandy H. Lorek and Arun D. Singh

23.1 Introduction

Ophthalmic ultrasonography is essential for documentation, measurement, and differentiation of intraocular tumors. It is a safe, noninvasive diagnostic technique that provides instant images for interpretation. This chapter provides a description of the instrumentation and special techniques necessary for the evaluation of intraocular tumors. Additionally, ultrasonographic findings of common intraocular lesions, including iris and ciliary body melanoma, choroidal melanoma, choroidal hemangioma, choroidal metastases, disciform lesions, and retinoblastoma are included.

23.2 Basic Physics

Ultrasound is an acoustic wave with a frequency above the audible range (20 kHz). When ultrasound waves encounter an interface with unequal acoustic impedance, echoes are generated. Modern ultrasound machines produce, detect, process, and amplify the returning echoes. A piezoelectric crystal is used to generate a mechanical short acoustic pulse that acts as a transducer to convert electric energy into ultrasound. When the probe receives the reflected echoes, they are converted back into an electrical signal and processed. Each ultrasound receiver is designed slightly differently, and thus, the images produced must be evaluated based on the model and calibration needed for each machine and probe combination. The parameters for processing usually include amplification, compensation, compression, demodulation, and rejection. A variety of amplification curves are preset on most ultrasound machines; however, it is essential that they are also adjusted manually by the examiner. The adjustment of this relative amplification is measured in decibels (dB) and referred to as the gain.

The physical laws of acoustic energy are dependent on reflection, refraction, and absorption [1]. The strength of the echo returning to the probe is largely dependent on the angle of incidence. The sound beam with an angle of incidence of 90°, i.e., perpendicular to the structures being examined, is necessary to accurately assess these structures based on the intensity of the echoes. If the sound beam is misdirected at an oblique angle, the resulting signal is weaker than it should be due to the reflection of some of the sound beams away from the probe. Differences in the shape and size of the acoustic interface can also result in scattering of the sound beams. Additionally, irregular surfaces can lead to scattering of reflected echoes, resulting in a significant loss of echo strength.

Ophthalmic ultrasound machines currently use frequencies ranging from 8 to 80 MHz. These frequencies are higher than those most commonly used in other fields of diagnostic ultrasound, which are in the range of 2–6 MHz. In order to evaluate small ocular structures, a high-frequency device with a directly proportional high resolution is essential. The superficial location of the eye and its primarily aqueous composition allows the use of high frequencies [2]. The limitations of physics make it difficult to assemble array elements with the necessary half-wavelength spacing, therefore necessitating the use of mechanical scanning by single-element focused transducers [3]. However, movement of the eye and positioning of the transducer allow the sound beam in ophthalmic devices to reach all areas of the eye in a close-to-optimal perpendicular orientation.

B. H. Lorek (✉) · A. D. Singh
Department of Ophthalmic Oncology, Cole Eye Institute, Cleveland Clinic, Cleveland, OH, USA
e-mail: lorekb@ccf.org; singha@ccf.org

© The Author(s), under exclusive license to Springer Nature Switzerland AG 2025

A. D. Singh, B. E. Damato (eds.), *Clinical Ophthalmic Oncology*, https://doi.org/10.1007/978-3-031-75907-9_23

23.3 Instrumentation

23.3.1 Diagnostic A-Scan

A-scan is echo strength over time displayed in one dimension. Spikes in the vertical orientation correspond to echo intensity and are displayed along the horizontal axis as a function of time. Standardized A-scan was developed by Ossoinig as a special diagnostic instrument for the differentiation of ocular structures [4, 5]. The A-scan probe has an operating frequency of 8 MHz and an S-shaped amplification curve for post-processing [6]. The S-shaped curve is beneficial in the differentiation of tissues with acoustic impedances that are close to one another. It provides the benefit of the wide range of logarithmic amplification and the high sensitivity of linear amplification. Standardized A-scan has a standardized decibel setting, referred to as tissue sensitivity. At the tissue sensitivity setting, a standardized A-scan is designed to display an echo spike for the retina that is 100% on the echo intensity scale when the sound beam is directed perpendicular to the retina (Fig. 23.1). All ocular structures that are equal to or denser than retina will also produce 100% echo spikes. Intraocular structures that are lower in density than the retina, including the diffuse vitreous hemorrhage and thin vitreous membranes, will produce echoes of less than 100% intensity. The varying reflectivity of the A-scan spike at tissue sensitivity also allows intraocular and orbital tumor structures to be evaluated and differentiated. In combination with a B-scan, a diagnostic A-scan is essential in the differentiation of intraocular tumors.

23.3.2 B-Scan

The foundation for diagnostic ultrasound in ophthalmology is based on B-scan images. Contact B-scan displays the shape, location, and extension of structures by using horizontal and vertical orientation in two dimensions. The strength of the echo is determined by the brightness of dots on the screen representing each echo. Logarithmic or S-shaped amplification curves are most commonly used at a frequency range of 10 MHz [7].

The two-dimensional, high-resolution images provide an accurate representation of ocular structures [8, 9]. Three basic B-scan probe orientations are used in ophthalmic ultrasonography: axial, longitudinal, and transverse (Figs. 23.2, 23.3, and 23.4) [10]. B-scan evaluation is a dynamic process requiring sweeping motions of the probe and specific attention to the mobility of echoes. The evaluation of static B-scan images in isolation can lead to misinterpretation [10].

23.3.3 Ultrasound Biomicroscopy (UBM)

UBM utilizes frequencies from 35 to 80 MHz for the acoustic evaluation of the anterior segment of the eye [11]. UBM can be of paramount importance when examining an eye with a lesion that is too far anterior to be imaged with a transscleral B-scan. Lesions of the conjunctiva, iris, ciliary body, and pars plana regions are best imaged with UBM. A typical high-resolution 50 MHz UBM probe has a penetration depth

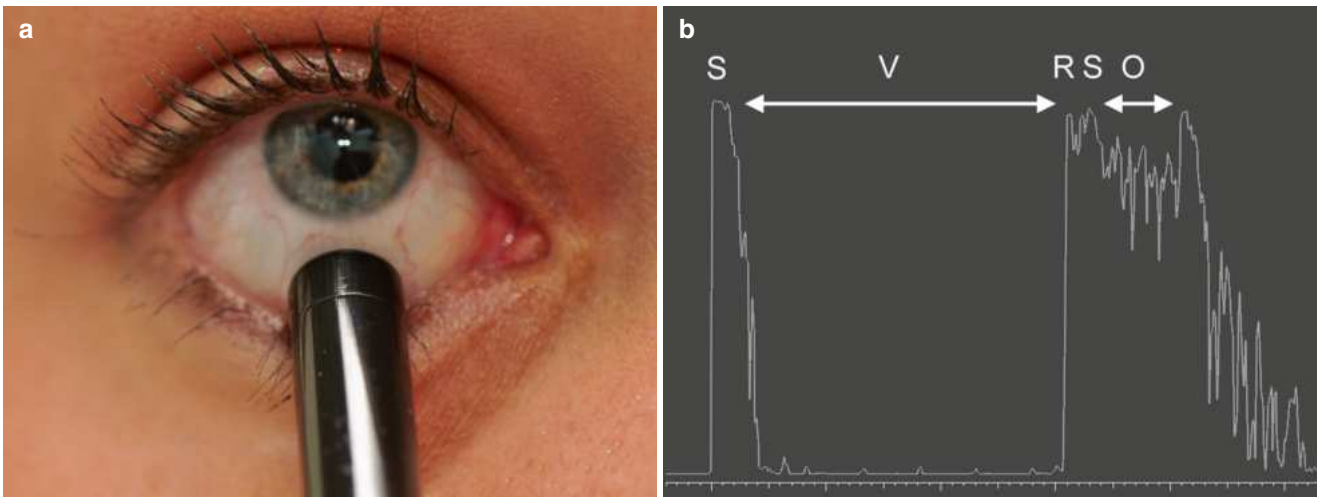

Fig. 23.1 Diagnostic A-scan. A-scan probe tip placed near the limbus with a sound beam directed at 12 o'clock posterior to the equator (**a**). Resulting A-scan image shows a linear display with echo spikes representing each tissue interface (**b**, *V* vitreous, *R* retina, *S* sclera, *O* orbital tissue). [Reprinted from Ophthalmic Ultrasonography: Clinical Methods: A- and B-scans. Hayden BC, Singh AD. Elsevier, London, 2011. With permission from Elsevier]

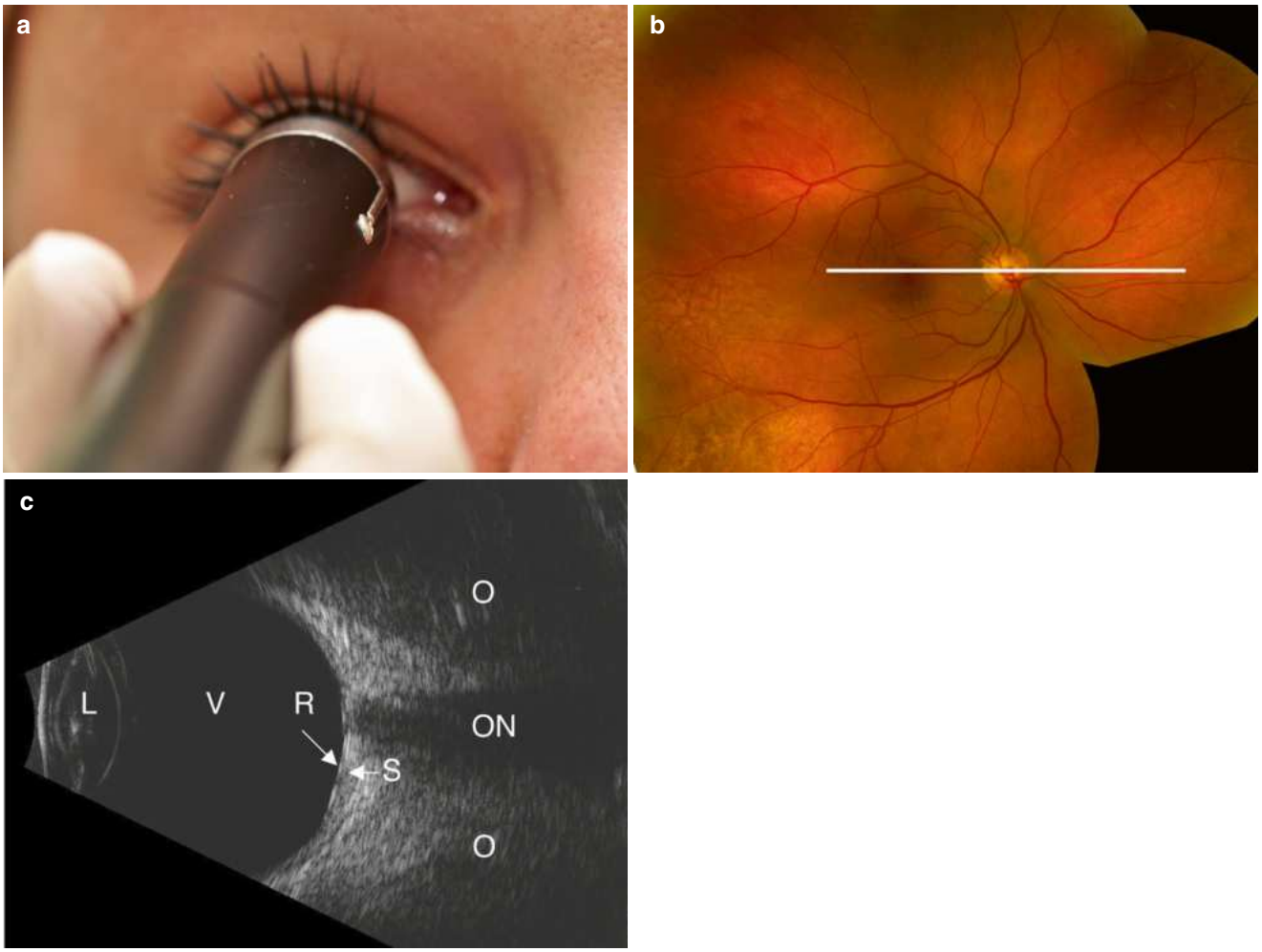

Fig. 23.2 Axial probe position. B-scan probe tip placed directly over the cornea (**a**). Corresponding ultrasonographed fundus (**b**, line). Resulting B-scan image showing the centered crystalline lens and optic nerve (**c**, *L* lens, *V* vitreous, *R* retina, *S* sclera, *ON* optic nerve, *O* orbital tissue). [Reprinted from Hayden BC, Kelley L, Singh AD. Ophthalmic Ultrasonography: Theoretic and Practical Considerations. Ultrasound Clinics 2008; 3(2): 179–183. With permission from Elsevier]

of approximately 5 mm and a resolution of 37 μm. During a UBM examination, the probe is placed directly over the anterior ocular structures to be imaged, not transocularly, as in contact B-scan. Additionally, a fluid immersion technique is necessary to provide the standoff distance required to view the anterior structures (Fig. 23.5). Similar to B-scans, axial, radial (longitudinal), and transverse scans are used to best document anterior lesions. The radial scan is best suited to access the anterior to posterior extent of mass lesions of the iris and ciliary body (Fig. 23.6).

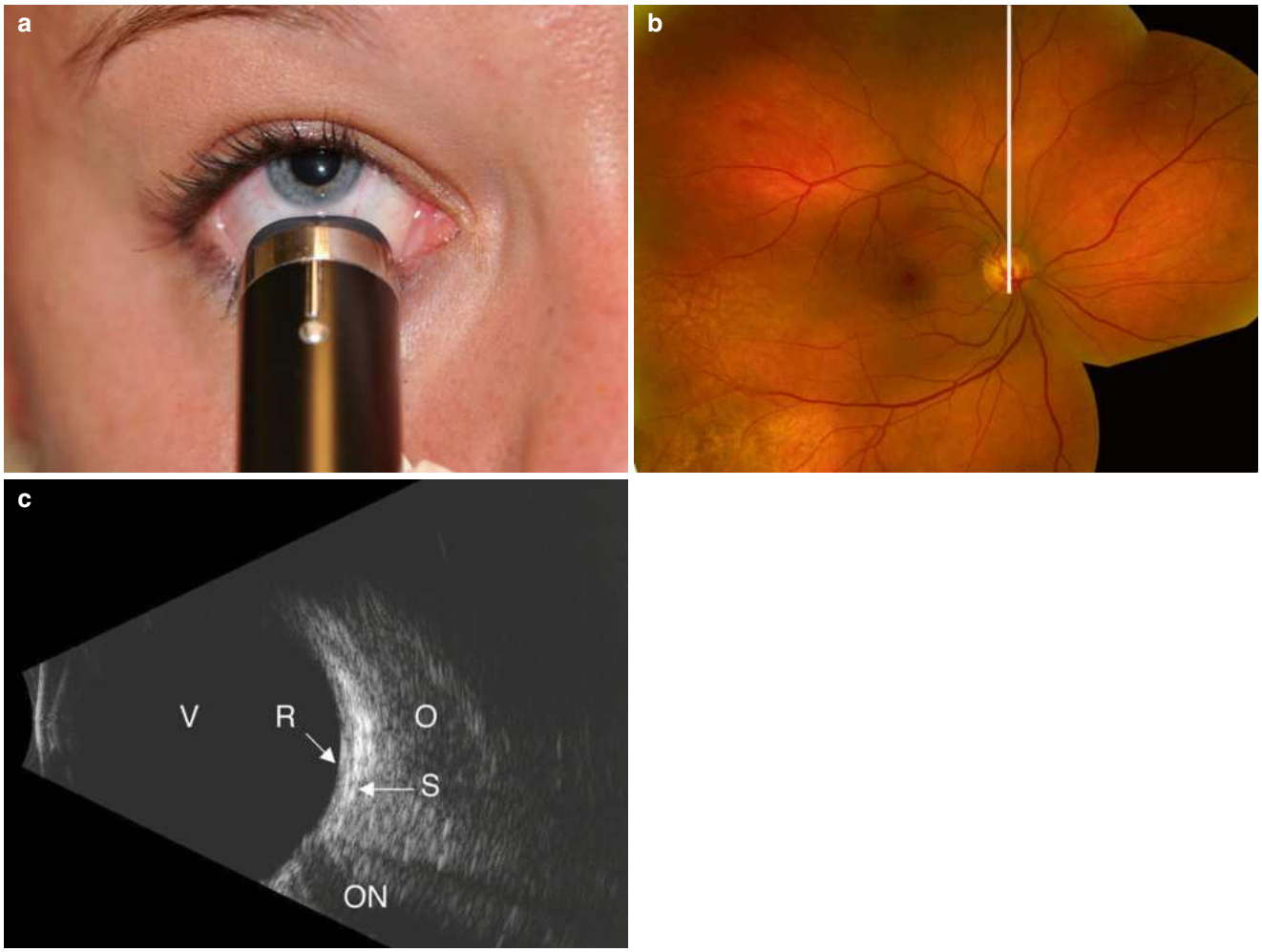

Fig. 23.3 Longitudinal B-scan position. B-scan probe tip placed on the conjunctiva near the limbus with the marker pointed superiorly (**a**). Corresponding ultrasonographed fundus (**b**, line). Resulting B-scan image showing a radial plane superiorly (**c**, *V* vitreous, *R* retina, *S* sclera, *ON* optic nerve, *O* orbital tissue). [Reprinted from Hayden BC, Kelley L, Singh AD. Ophthalmic Ultrasonography: Theoretic and Practical Considerations. Ultrasound Clinics 2008; 3(2): 179–183. With permission from Elsevier]

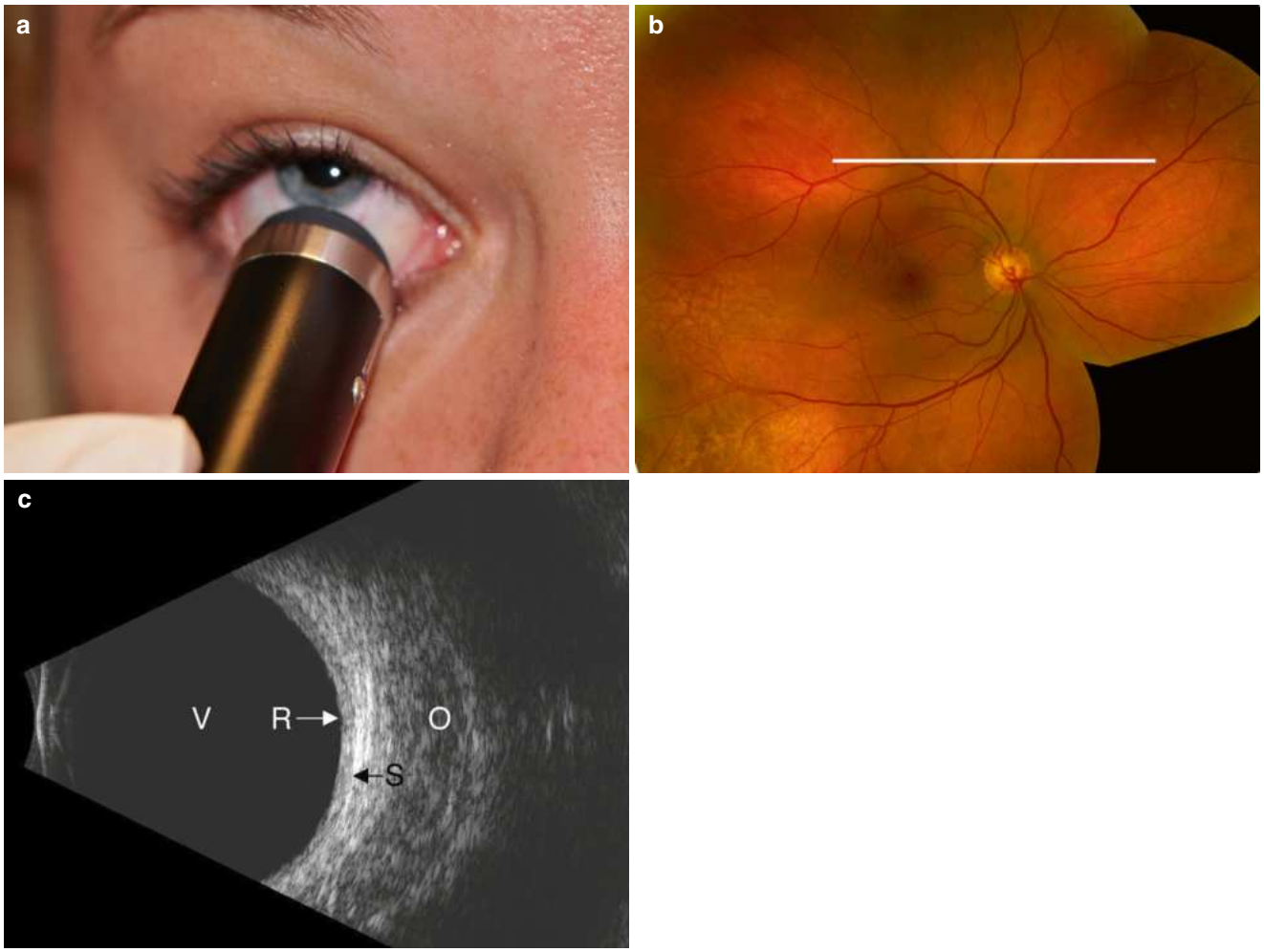

Fig. 23.4 Transverse B-scan position. B-scan probe tip placed on the conjunctiva near the limbus (**a**). Corresponding ultrasonographed fundus (**b**, line). Resulting B-scan image showing the superior quadrant (**c**, *V* vitreous, *R* retina, *S* sclera, *ON* optic nerve, *O* orbital tissue). [Reprinted from Hayden BC, Kelley L, Singh AD. Ophthalmic Ultrasonography: Theoretic and Practical Considerations. Ultrasound Clinics 2008; 3(2): 179–183. With permission from Elsevier]

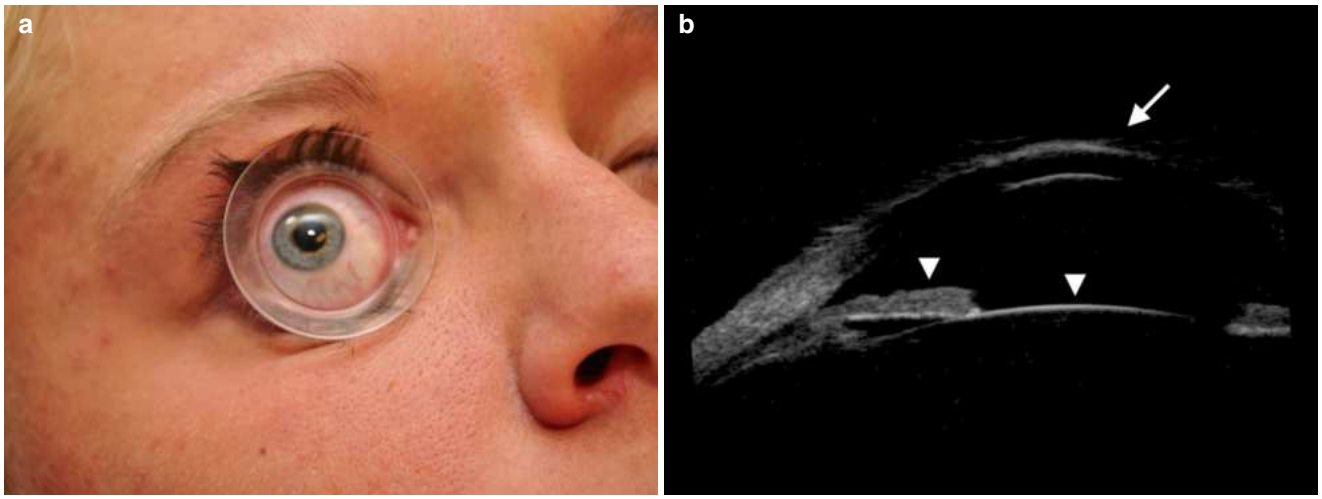

Fig. 23.5 UBM. UBM immersion shell designed to hold the eyelids open and provide a reservoir for the coupling agent (**a**). Resulting B-scan image showing the cornea at the top of the screen, close to the probe tip (arrow), and the anterior portion of the crystalline lens and iris are at the bottom of the screen (arrowheads, **b**)

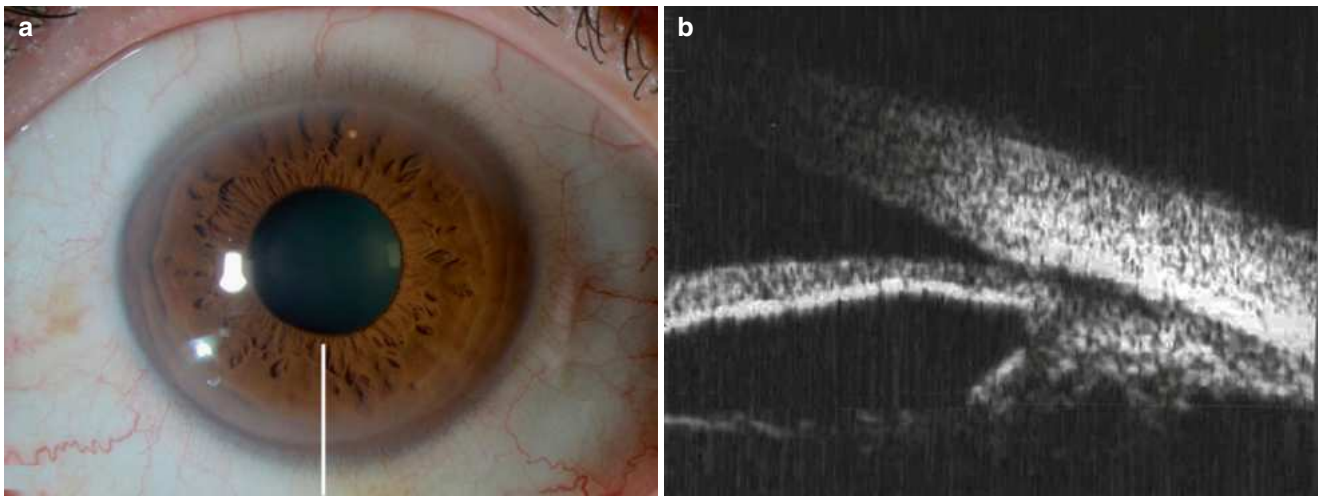

Fig. 23.6 Radial (longitudinal) scan. Slit lamp photography of the anterior segment of the eye showing the plane of a radial scan (**a**). Corresponding UBM image showing the cornea and the central iris on the left side of the display, and the limbus, ciliary body and sclera on the right (**b**). [Reprinted from: Ophthalmic Ultrasonography: Clinical Methods: Ultrasound Biomicroscopy. Hayden BC, Singh AD. Elsevier, London, 2011. With permission from Elsevier]

23.4 Methods for Differentiation of Intraocular Tumors

Standardized echography refers to the combined use of contact B-scan and standardized A-scan. It provides a reliable method to evaluate ocular lesions based on the topographic, quantitative, and kinetic properties of the echo intensities and patterns [5, 12–14]. Topographic, quantitative, and kinetic features of many intraocular tumors are well established in the literature [15–17]. B-scan and UBM examination yield topographic information, including shape, size, and location, as well as vascularity, a kinetic feature.

Table 23.1 Diagnostic features for assessing intraocular lesions

Topographic	Quantitative	Kinetic
Location	Reflectivity	Mobility
Shape	Internal structure	Vascularity
Extent	Sound attenuation	Convection movement

Diagnostic A-scan examination yields quantitative information, including structure and reflectivity and, in some instances, vascularity. Utilizing these combined techniques (standardized echography), malignant intraocular tumors can be differentiated from benign lesions whose appearance on visual examination may be similar (Table 23.1).

23.4.1 Topographic Ultrasonography

Topographic evaluation includes the determination of the location, shape, and extension of the lesion. A transverse B-scan of the lesion should be performed first to display the lateral extent of the lesion and the gross shape. A transverse scan, utilizing a sweeping motion through the solid intraocular mass, is important in order to determine the maximal height and lateral basal dimensions (Fig. 23.7) [15, 16]. A longitudinal B-scan is then performed to evaluate the anterior to posterior topographic features of the lesion. This scan displays the shape and anterior to posterior extent of the lesion. The probe does not need to be shifted dramatically as required during the transverse scan. However, subtle shifts around the clock hour of interest will aid in the identification of the maximal dimensions of a solid intraocular lesion. Axial scans are not usually necessary in the evaluation of topographic features. However, in very posterior lesions, the relationship between the optic nerve and the maximal height can be assessed with axial scans. The measurements obtained should be rounded up to the nearest tenth of a millimeter for the height and rounded up to the nearest one-half millimeter for the base (Table 23.2).

23.4.2 Quantitative Ultrasonography

Quantitative ultrasonography utilizing diagnostic A-scan can determine reflectivity, internal structure, and sound attenuation.

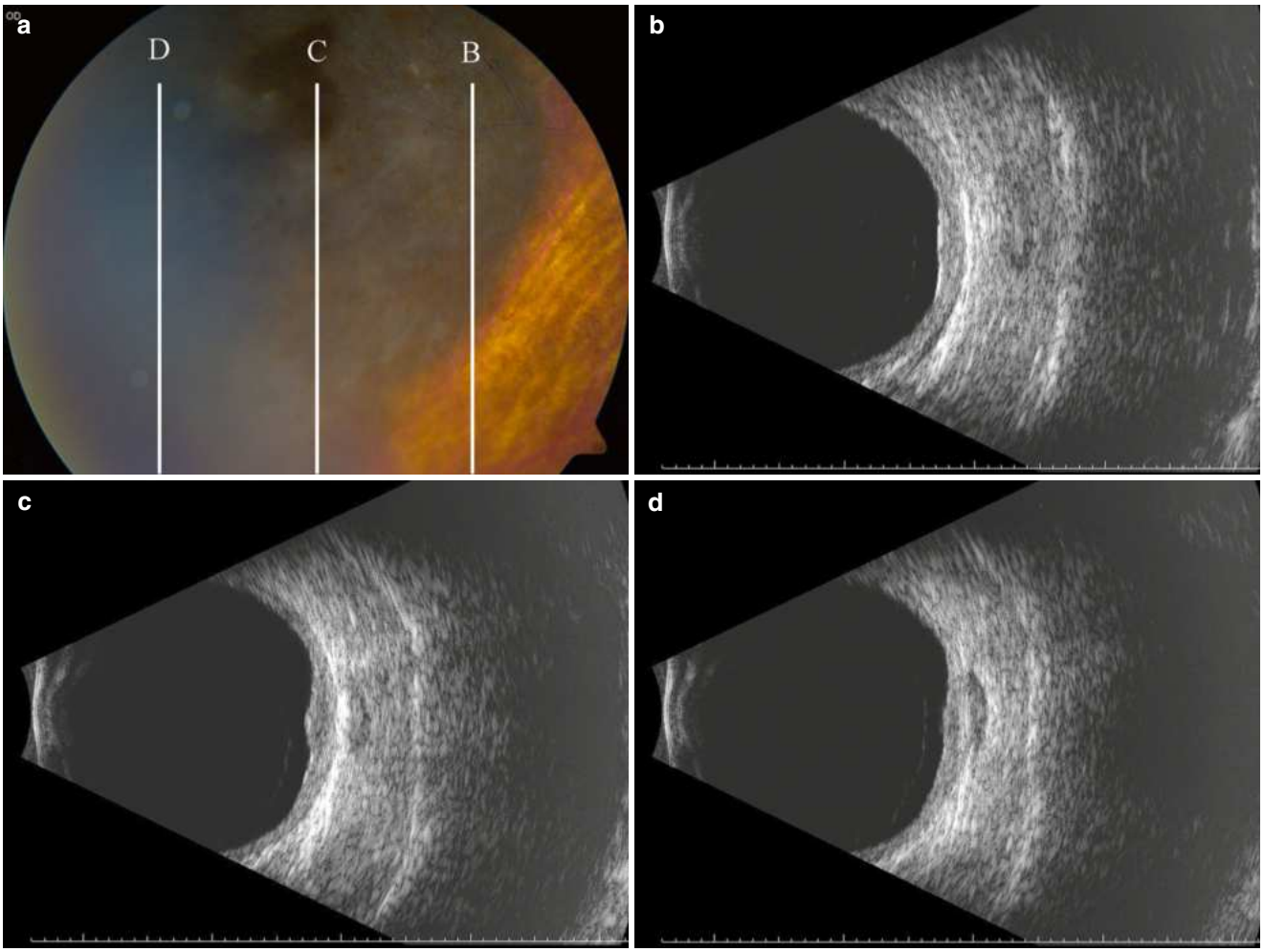

Fig. 23.7 Topographic ultrasonography. Transverse B-scan of a solid intraocular mass at 8:30 posterior to the equator. Fundus photograph (**a**). Lines represent ultrasonographed fundus as shown in Fig. 23.12b–d). Resulting B-scan image shows a dome-shaped elevated fundus lesion (**b**). Slight shifting of the probe anteriorly centers the sound beam on the thickest portion of the mass lesion (**c**). Continued shifting of the probe assesses the peripheral aspect of the mass lesion (**d**). (Arrows = mass lesion, Arrowhead = cross-section of lateral rectus). [Reprinted from Ophthalmic Ultrasonography: Clinical Methods: Ultrasound Biomicroscopy. Hayden BC, Singh AD. Elsevier, London, 2011. With permission from Elsevier]

Table 23.2 Measurement of fundus lesions

Dimension	Lesion location	Scan type	Units
Apical height	Posterior to the equator	Longitudinal and transverse[a]	Round up to the nearest 0.1 mm
Apical height	Anterior to the equator	Longitudinal[a]	Round up to the nearest 0.1 mm
Base-anterior to posterior	Anterior and posterior to the equator	Longitudinal[a]	Round up to the nearest 0.5 mm
Base-lateral	Anterior and posterior to the equator	Transverse[a]	Round up to the nearest 0.5 mm

[a] Axial scans may be obtained instead of the indicated scans when the lesion is on the peripapillary margin or wrapping around the optic disc

23.4.2.1 Reflectivity

The height of the spike on the A-scan corresponds to grades of reflectivity. The reflectivity of a lesion can only be graded when both the A-scan probe is calibrated for tissue sensitivity and the sound beam is directed perpendicular to the lesion (Fig. 23.8). Evaluating the reflectivity of a lesion from the contact B-scan signal intensity echoes is only an estimate of reflectivity and should not be relied upon.

23.4.2.2 Internal Structure

Quantitative ultrasonography can further assess the internal structure that reflects the histologic composition [18]. Homogenous tissue architecture within the lesion results in

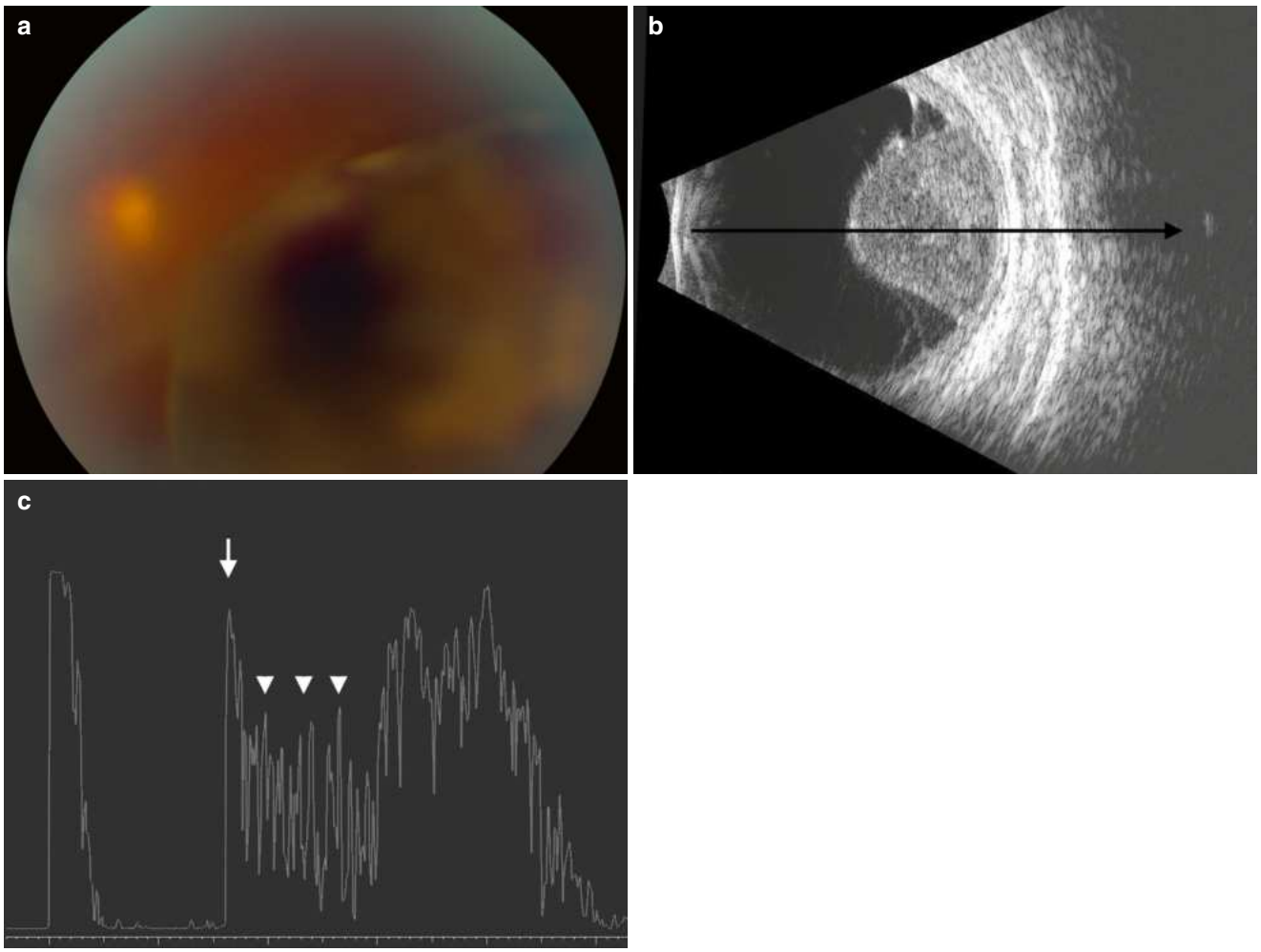

Fig. 23.8 Quantitative ultrasonography (reflectivity). Fundus photo showing choroidal melanoma with vitreous hemorrhage (**a**). Corresponding B-scan (**b**). Arrow represents the path of the sound beam used to generate the A-scan. Diagnostic A-scan of the solid fundus mass shows high reflectivity of the retina (**c**, arrow) and low to medium internal reflectivity of the mass lesion (**c**, arrowheads). [Reprinted from: Ophthalmic Ultrasonography: Clinical Methods: Ultrasound Biomicroscopy. Hayden BC, Singh AD. Elsevier, London, 2011. With permission from Elsevier]

little variation in the height and length of the spikes on the A-scan, whereas a heterogeneous tissue architecture results in marked variation.

23.4.2.3 Sound Attenuation

The last component of quantitative ultrasonography is sound attenuation or acoustic shadowing. It can be caused by many different echo-dense structures, including calcified lesions, foreign bodies, and bone (Fig. 23.9). Sound attenuation from or within a lesion can be detected on both contact B-scan and diagnostic A-scan. It is delineated by a marked, progressive decrease in the strength of the echoes within or behind the lesion. On the B-scan, this results in a reduction of the intensity of echoes or a complete lack of echoes behind the lesion, termed shadowing. On the A-scan, a linear decrease in the height of the spikes is evaluated as an angular measurement (angle kappa) [5]. Angle kappa is directly proportional to the amount of sound attenuation; the greater the attenuation of sound, the greater the angle kappa. Large choroidal melanomas often present with a positive angle kappa (Fig. 23.10).

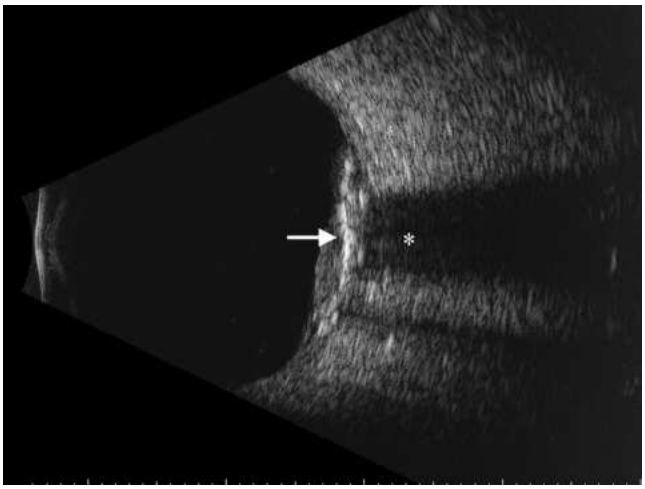

Fig. 23.9 Quantitative ultrasonography (sound attenuation, B scan). Transverse B-scan shows an irregularly shaped fundus lesion with highly reflective areas (arrow), causing shadowing of the orbital structures (asterisk). [Reprinted from: Ophthalmic Ultrasonography: Clinical Methods: Ultrasound Biomicroscopy. Hayden BC, Singh AD. Elsevier, London, 2011. With permission from Elsevier]

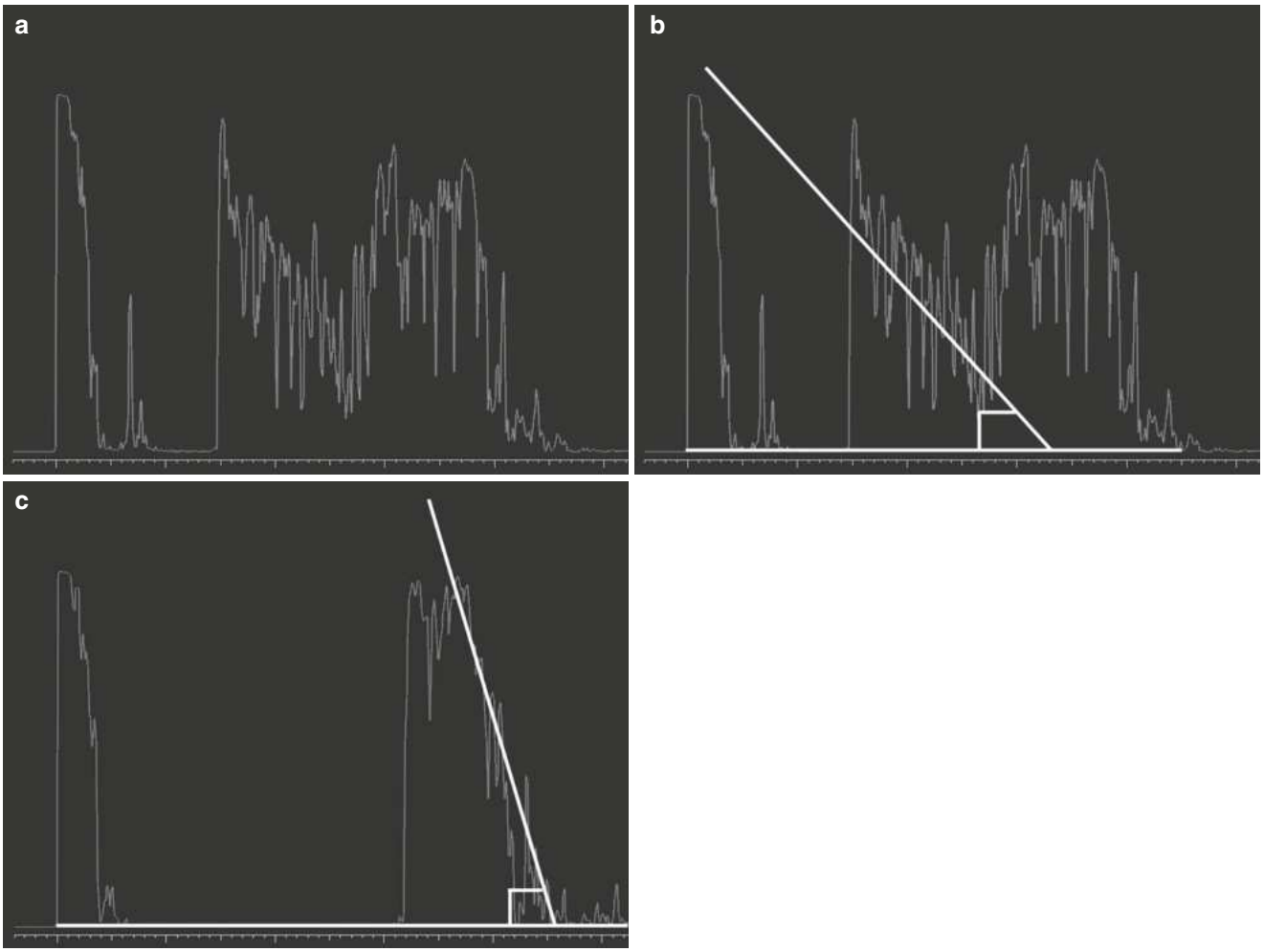

Fig. 23.10 Quantitative ultrasonography (sound attenuation, A-scan, angle Kappa). Progressive decrease in the height of the spikes can be depicted as an angular measurement (**a**, **b**). Angle kappa is proportional to the extent of sound attenuation, greater the attenuation of sound, larger the angle kappa (**b**, **c**). [Reprinted from: Ophthalmic Ultrasonography: Clinical Methods: Ultrasound Biomicroscopy. Hayden BC, Singh AD. Elsevier, London, 2011. With permission from Elsevier]

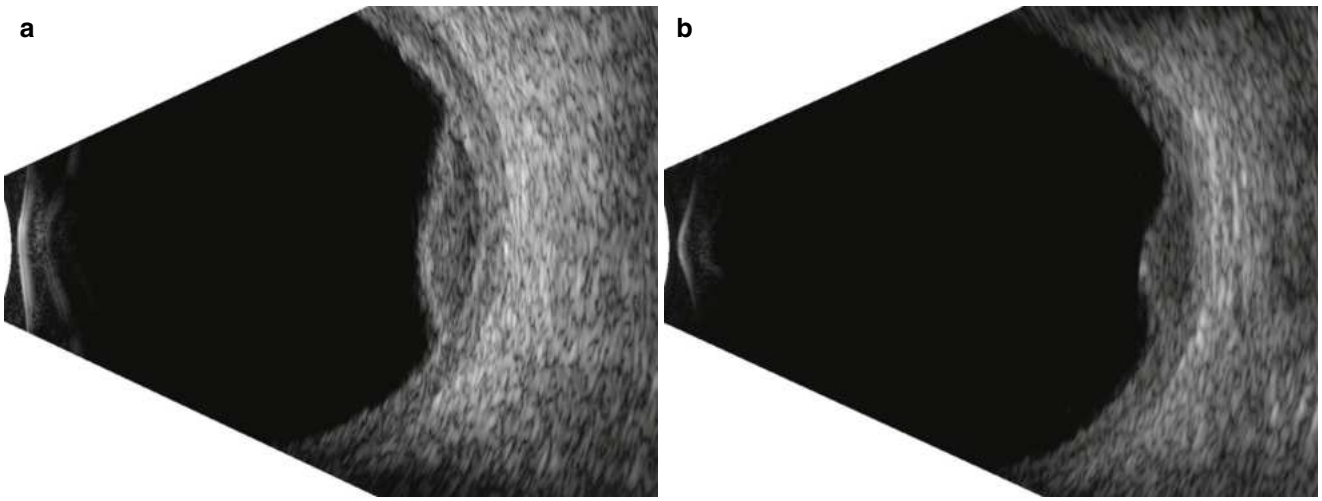

Fig. 23.11 Differentiation of a choroidal melanoma from a hemorrhagic choroidal detachment. Transverse B-scan demonstrating a dome-shaped choroidal melanoma (**a**) and hemorrhagic choroidal detachment (**b**). B-scan ultrasonography alone cannot differentiate between these two small choroidal lesions

23.4.3 Kinetic Ultrasonography

Ocular lesions can be further defined in near real-time by dynamically observing and documenting mobility, vascularity, and convection movement.

23.4.3.1 Mobility

The mobility of a lesion is most easily evaluated with a B-scan. It is determined by the movement of a membrane or opacity following a change in gaze. Depending on the location of the intraocular lesion, either a transverse or a longitudinal B-scan is performed, and the patient is instructed to move their eyes. Truly solid intraocular lesions will not exhibit any subretinal or subchoroidal movement. Assessing the mobility of presumed solid intraocular lesions is often essential to differentiate choroidal melanoma from hemorrhagic choroidal detachment (Fig. 23.11).

23.4.3.2 Vascularity

Vascularity is the detection of blood flow within an ocular lesion and can be detected by both A-scan and B-scan. It is defined as fast, low-amplitude flickering consistent with blood flow. The probe and gaze are held stationary, while the internal echo flickering is observed over time. The intensity of the echo flickering is documented as mild, moderate, or marked, corresponding to grades of vascularity.

23.4.3.3 Convection

Convection movement is the slow, continuous movement of intraocular contents that occurs secondary to convection currents, best detected with a B-scan while holding both the probe and the eye fixed. The moving echoes most often represent blood, layered inflammatory cells, or cholesterol debris. This slow movement is most often seen in eyes with long-standing vitreous hemorrhage that has settled beneath a tight funnel-shaped retinal detachment. Solid intraocular mass lesions can be differentiated from layered debris with specific attention to this minor movement (Fig. 23.12).

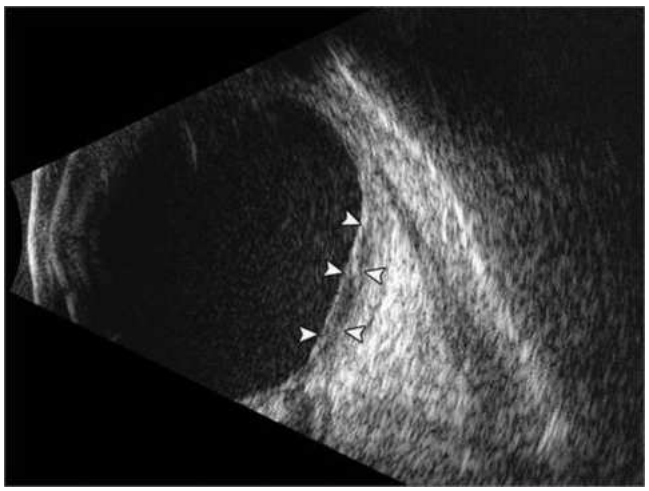

Fig. 23.12 Layered vitreous hemorrhage mimicking a choroidal lesion. Longitudinal B-scan showing a pseudomembranous surface and dense opacities at the posterior fundus. Dynamic eye movements are necessary to clearly differentiate this layered vitreous hemorrhage from a solid mass lesion

23.5 Differentiation of Anterior Segment Tumors

23.5.1 Iridociliary Pigment Epithelial Cyst (IPE Cyst)

IPE cysts frequently appear as anterior bulging of the iris stroma, most commonly near the iris root [19]. On UBM, the lesions are round to oval in shape and bow the iris forward while conforming to the structures of the posterior segment. IPE cysts demonstrate a thin wall with echolucent internal reflectivity, differentiating them from mass lesions of the iris (Fig. 23.13). Eyes presenting with a single large cyst are frequently found to have additional small cysts when other quadrants are explored. It is also important to note that IPE cysts may be present adjacent to solid lesions of the iris and ciliary body. Thus, it is essential to thoroughly examine all surrounding structures.

23.5.2 Iris and Ciliary Body Melanoma

Melanomas of the iris and ciliary body can vary in pigmentation, size, and patterns of growth. They can present as circumscribed or diffuse lesions, and iris melanoma has a predilection for the inferior half of the iris (Fig. 23.14). Due to their anterior location, UBM is the preferred modality of ultrasonographic examination. Circumscribed lesions on UBM usually appear as dome-shaped or lobulated. Diffuse iris and ciliary body lesions are irregular in shape and can span from a few clock hours to 360° [20, 21]. Careful examination with UBM of all tumor margins, including the ciliary body, is necessary to rule out ring patterns and ciliary body involvement not readily seen clinically. Likewise, the posterior borders of a ciliary body melanoma should be examined to rule out further posterior extension (Fig. 23.15). When the posterior boundary of the ciliary body lesion cannot be imaged with UBM, a posterior B-scan examination should be performed. Both circumscribed and diffuse lesions are mainly regular in structure and echo-dense with no sound attenuation. Iris and ciliary body melanomas are usually too shallow to be evaluated with a diagnostic A-scan or assessed for vascularity.

23.5.3 Ciliary Body Melanocytoma

Uveal melanocytoma is a benign, darkly pigmented, circumscribed mass with minimal elevation involving the uveal tract or optic disc. When present in the ciliary body, these lesions can be confused with melanomas. On both UBM and B-scan, these lesions appear as a dome-shaped solid mass with a regular structure, very echo-dense reflectivity, and marked sound attenuation (Fig. 23.16). The tightly packed, heavily pigmented structure of an iridociliary melanocytoma is responsible for the sound attenuation, often leading to shadowing of the internal portions of the lesion on UBM. This finding is rare in UBM evaluation of melanoma and, therefore, may be helpful in diagnosis.

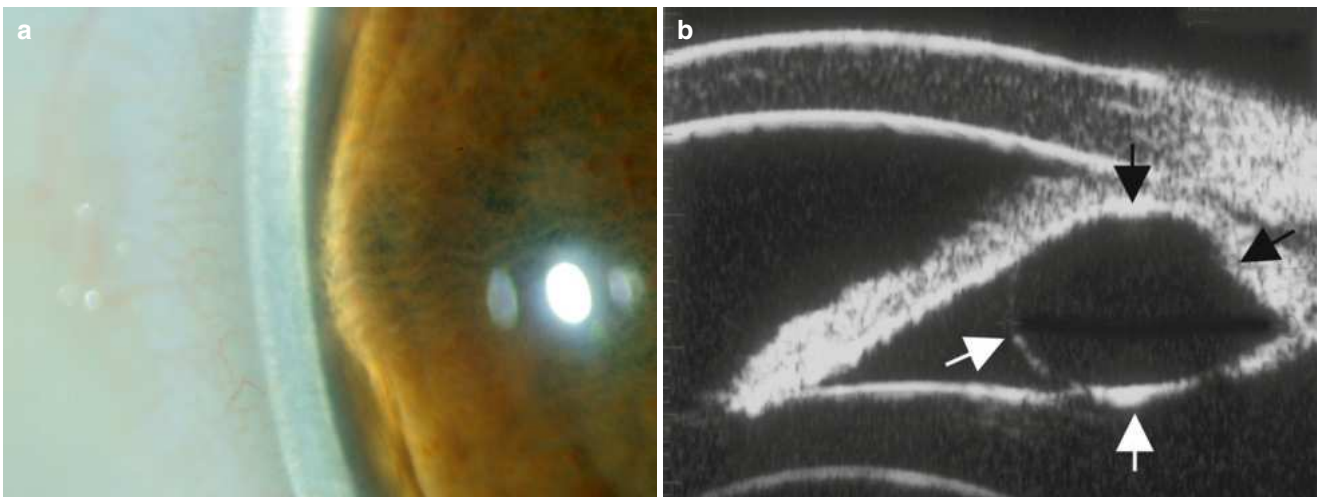

Fig. 23.13 Iridociliary pigment epithelial cyst. Anterior segment photogrph with a slit beam (**a**). Note anterior bulging of the iris. UBM revealed echolucent thin-walled cyst (**b**, arrows). [Reprinted from Rockwood EJ, Sharma S, Hayden Singh AD. Ophthalmic Ultrasonography: Glaucoma. Ultrasound Clinics 2008; 3(2): 207–215. With permission from Elsevier]

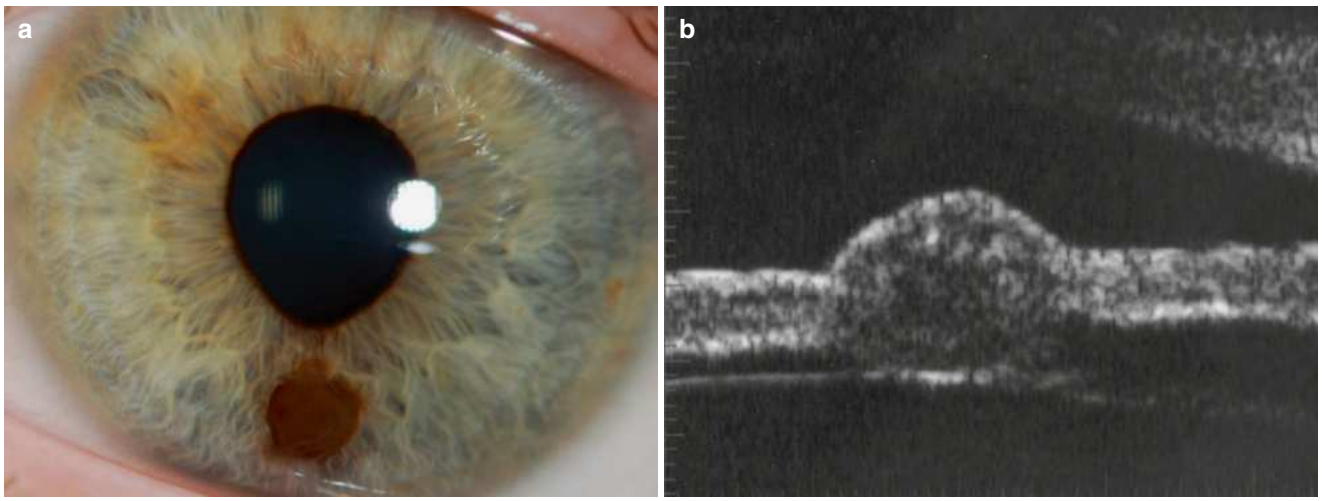

Fig. 23.14 Iris melanoma. Clinical photograph demonstrating pigmented iris lesion (**a**). UBM revealed isolated iris involvement (**b**). [Reprinted from Hood CT, Schoenfield LR, Torres V, Singh AD. Iris Melanoma. Ophthalmology: Journal of the American Academy of Ophthalmology 2011;118(1):221–222. With permission from Elsevier]

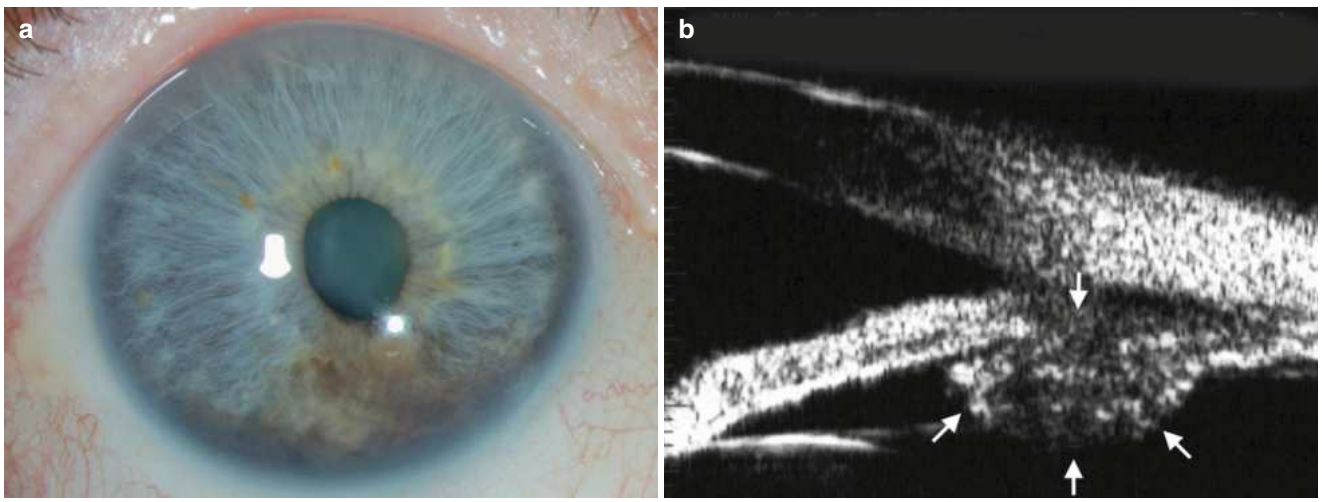

Fig. 23.15 Radial (Longitudinal) scan for the evaluation of a mass lesion of the peripheral iris and ciliary body. Slit lamp photograph showing iris melanoma (**a**). UBM inferiorly reveals a mass in the peripheral iris and ciliary body (**b**). [Reprinted from Ophthalmic Ultrasonography: Clinical Methods: UBM. Hayden BC, Singh AD. Elsevier, London, 2011. With permission from Elsevier]

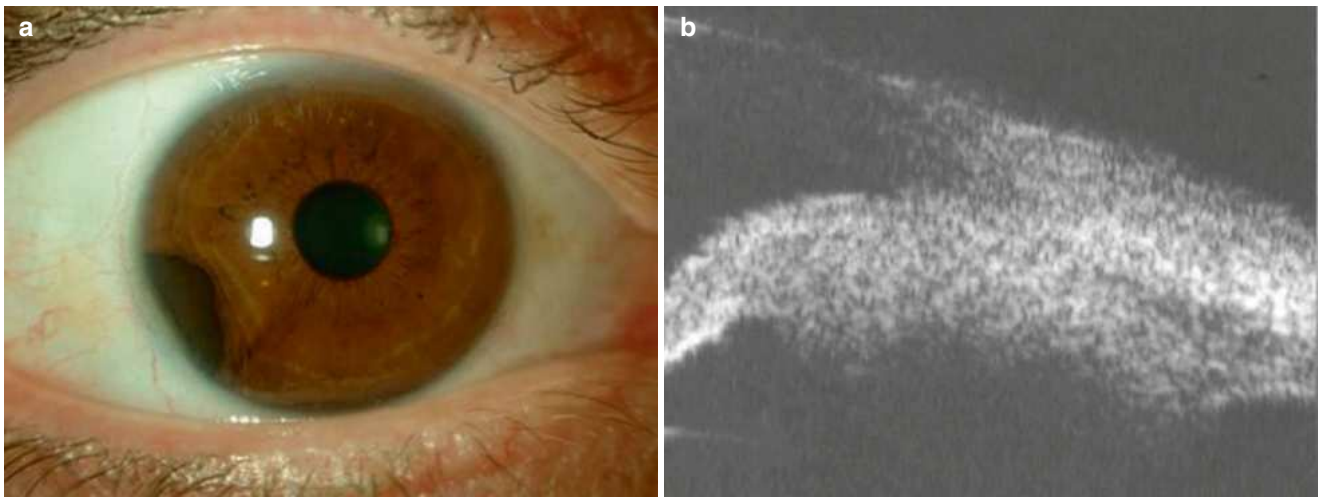

Fig. 23.16 Ciliary body melanocytoma. Slit lamp photograph demonstrating pigmented peripheral iris mass (**a**). UBM showing a dense ciliary body mass with sound attenuation (**b**). [Reprinted from Ophthalmic Ultrasonography: Intraocular Tumors. Turell, ME, Hayden BC, Schoenfield L, Singh AD. Elsevier, London, 2011. With permission from Elsevier]

23.6 Differentiation of Retinal Tumors

23.6.1 Retinoblastoma

23.6.1.1 Topographic

Ophthalmic ultrasonography plays an integral role in the differentiation of retinoblastoma from other causes of leukocoria, particularly in the presence of an extensive retinal detachment. Retinoblastoma can be unilateral or bilateral and varies somewhat in appearance based on the stage at presentation. On B-scan examination, retinoblastoma appears most commonly as an irregularly surfaced, round, or dome-shaped lesion. Mildly elevated and diffuse lesions have been reported in the literature but are rare [22, 23]. Most cases of retinoblastoma exhibit marked internal calcification that is readily detected with a B-scan if examined at a low to medium gain. At these gain settings, internal calcification of the lesion remains very highly reflective, and causes marked shadowing of the intraocular and orbital structures behind the lesion (Fig. 23.17). B-scan may also reveal associated retinal detachment and vitreous opacities frequently indicative of vitreous seeding. Extraocular extension of retinoblastoma most often involves the retrobulbar optic nerve. B-scan ultrasonography is helpful in the gross determination of enlargement of the nerve; however, shadowing from calcification often limits its diagnostic use.

23.6.1.2 Quantitative and Kinetic

The structure and reflectivity profiles in retinoblastoma vary greatly depending on the degree of internal calcification. Lesions with little or no calcification have a regular structure and low to medium reflectivity, whereas highly calcified lesions are irregularly structured with mainly medium to high reflectivity with marked acoustic shadowing. Due to the lack of intrinsic vessel formation within retinoblastoma, acoustic vascularity is absent.

23.6.2 Persistent Fetal Vasculature (PFV)

PFV, formally known as persistent hyperplastic primary vitreous (PHPV), is a unilateral condition that is usually associated with microphthalmos or shallow anterior chamber. On the B-scan, a taut, nonmobile vitreous band, persistent hyaloid remnant, is detected connecting the optic nerve to the posterior lens capsule (Fig. 23.18). Often, the vitreous band is very thin, and it cannot be imaged in its entirety. In some cases, the band is very thick and resembles a closed total retinal detachment. For these reasons, it is necessary to examine the eye at both a high gain to delineate the thin membranes and a low gain to rule out retinal detachment. On diagnostic A-scan, the band will exhibit an initial spike that is not 100% of the tissue sensitivity, further excluding retinal detachment.

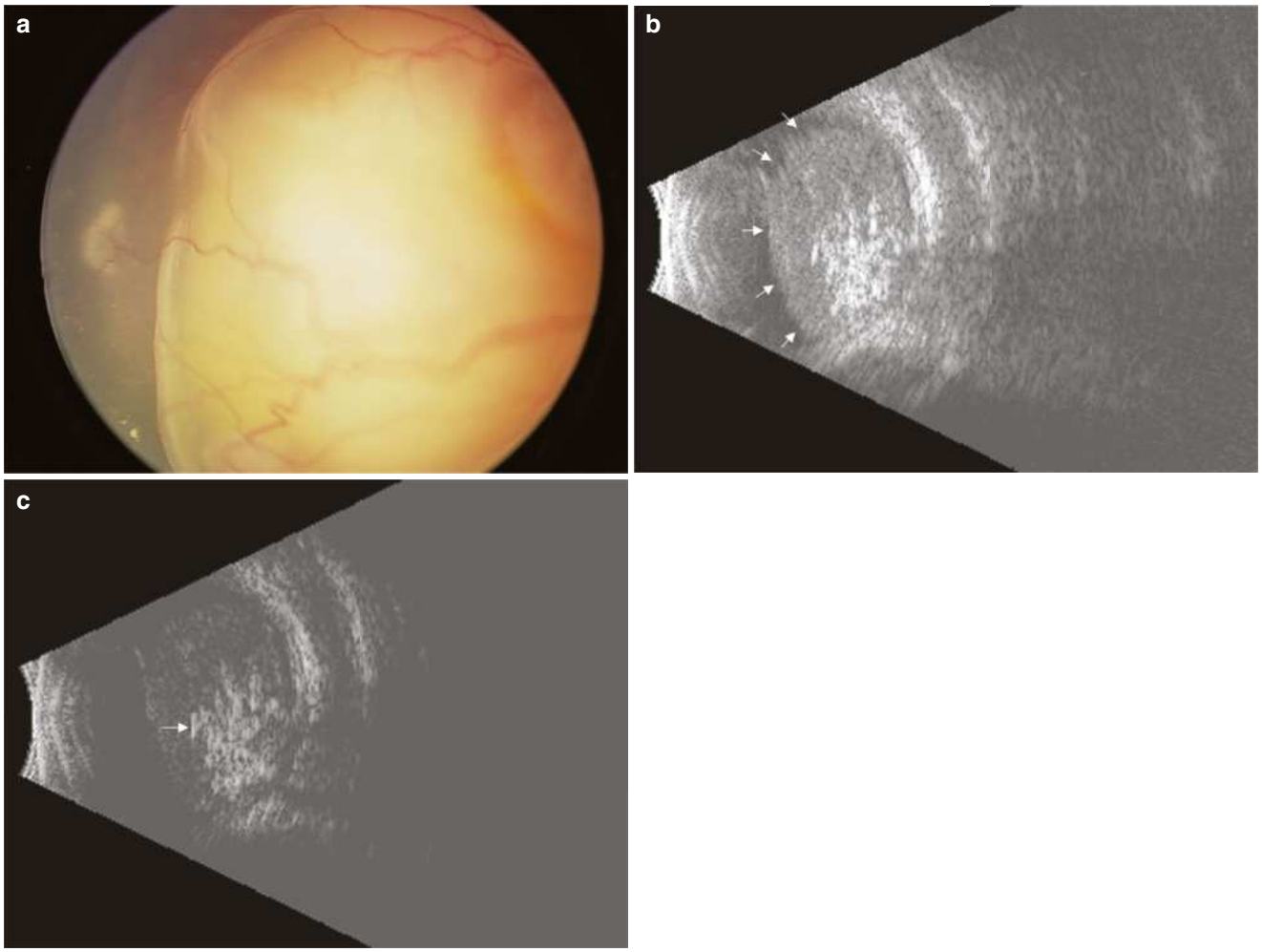

Fig. 23.17 Classic presentation of retinoblastoma. Retinoblastoma with calcification. Fundus photograph (**a**). Transverse B-scans demonstrates a large, dome-shaped lesion with marked internal calcification. High gain showing the lesional boundaries (**b**, arrows). Low gain showing the internal calcification causing shadowing of the orbit (**c**, arrow). [Reprinted from Fu EX, Hayden BC, Singh AD. Intraocular tumors. Ultrasound Clinics 2008; 3(2): 229–244. With permission from Elsevier]

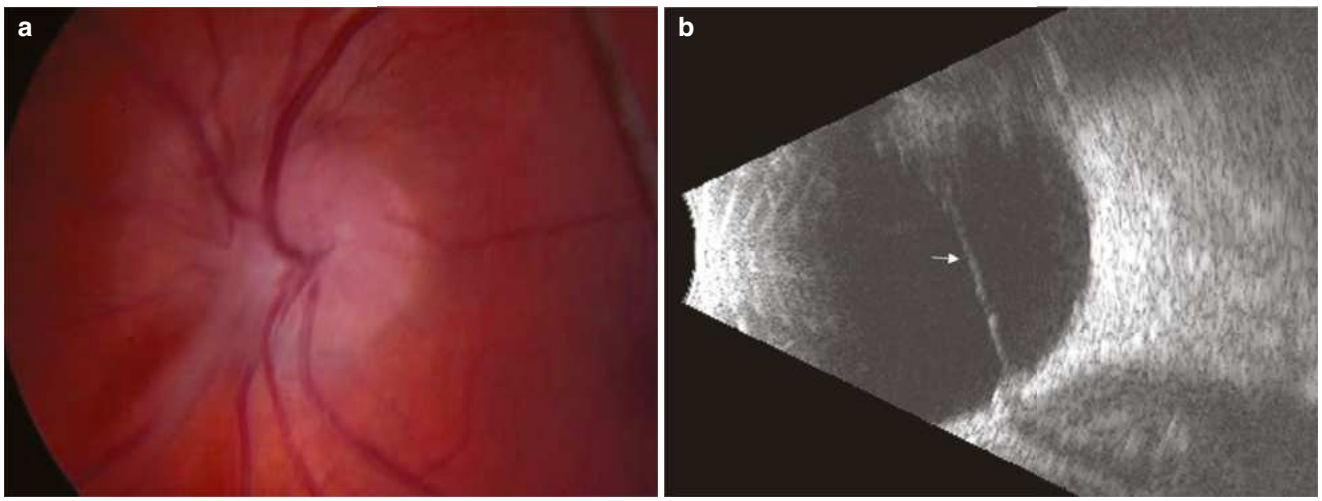

Fig. 23.18 Persistent fetal vasculature (PFV). Fundus photograph (**a**). Longitudinal B-scan demonstrates taunt, thickened vitreous band adherent to the slightly elevated optic disc (**b**, arrow). [Reprinted from Fu EX, Hayden BC, Singh AD. Intraocular tumors. Ultrasound Clinics 2008; 3(2): 229–244. With permission from Elsevier]

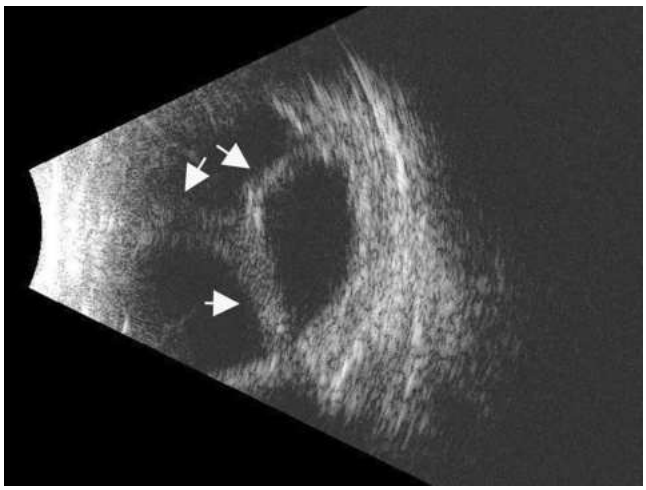

Fig. 23.19 ROP (Retinopathy of Prematurity). Retinopathy of prematurity. Longitudinal B-scan demonstrates a highly reflective, closed funnel-shaped retinal detachment (arrows) inserting into the disc. [Reprinted from Fu EX, Hayden BC, Singh AD. Intraocular tumors. Ultrasound Clinics 2008; 3(2): 229–244. With permission from Elsevier]

23.6.3 Retinopathy of Prematurity (ROP)

ROP occurs in a setting of low birth weight and exposure to supplemental oxygen in the neonatal period due to premature birth. In contrast to eyes with retinoblastoma, which are usually of normal axial eye length and unilateral or bilateral, eyes with ROP have shorter axial length than normal, and presentation is typically bilateral. On the B-scan, advanced ROP appears as a highly reflective, nonmobile, thick, closed funnel-shaped retinal detachment inserted into the disc (Fig. 23.19). Diagnostic A-scan shows an initial spike that is 100% of the tissue sensitivity, confirming retinal detachment.

23.6.4 Coats' Disease

Coats' disease is a retinal vascular disorder that is usually unilateral and most commonly diagnosed in young males between 4 and 10 years of age [24]. On B-scan, Coats' disease usually appears as a poorly defined fundus lesion with focal areas of high reflectivity (Fig. 23.20). In advanced

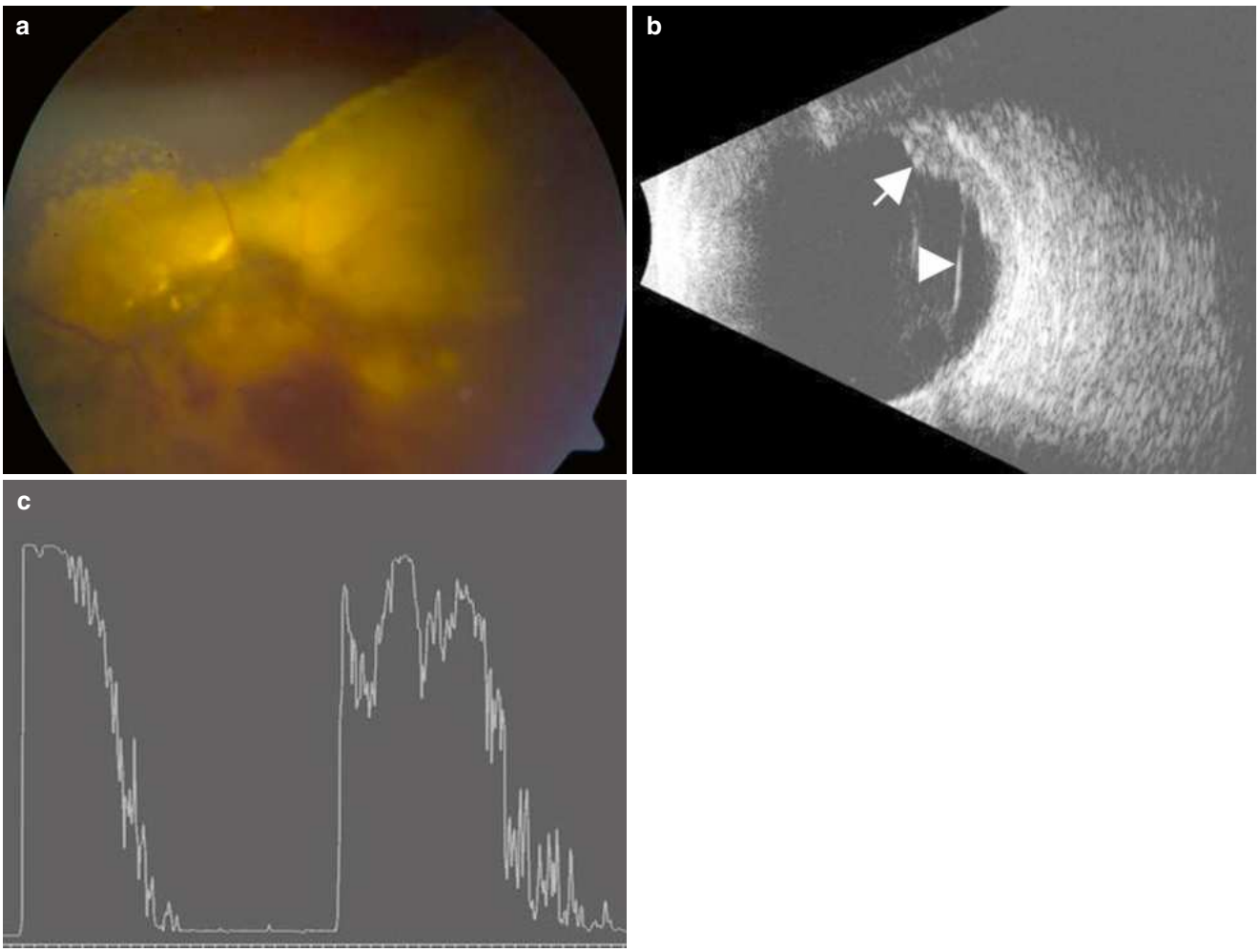

Fig. 23.20 Coats's disease. Clinical photograph showing lipid exudation (**a**). B-scan demonstrating exudative retinal detachment (**b**, arrow) and vitreous band (**b**, arrowhead) and A-scan with high internal reflectivity (**c**). [Reprinted from: Ophthalmic Ultrasonography: Intraocular Tumors. Turell, ME, Hayden BC, Schoenfield L, Singh AD. Elsevier, London, 2011. With permission form Elsevier]

cases, total retinal detachment is also observed. Diagnostic A-scan evaluation most commonly shows a solid mass with regular to slightly irregular structure, mainly high reflectivity, and absent internal vascularity. Ultrasonography is often most helpful in the differentiation of Coats' disease from retinoblastoma. On B-scan examination at a low gain, highly reflective calcium deposits (retinoblastoma) display shadowing, whereas medium to highly reflective cholesterol deposits (Coats' disease) do not exhibit acoustic shadowing.

23.7 Differentiation of Choroidal Tumors

23.7.1 Choroidal Nevus

Choroidal nevi are usually less than 1.0 mm in height and have a greatest basal dimension of less than 5.0 mm [25]. Often, choroidal nevi are too flat to be well evaluated with ultrasonography. On the B-scan, they appear only as focal elevations of the choroid with sloping basal margins that are difficult to delineate. Most lesions under 0.8 mm cannot be evaluated with a diagnostic A-scan. Lesions with sufficient apical height appear as regularly structured, highly reflective, and avascular (Fig. 23.21).

23.7.2 Choroidal Melanoma

23.7.2.1 Topographic

Choroidal melanoma is solid and most commonly collar button, dome, or lobulated in shape. Although unusual, choroidal melanoma can present in a diffuse pattern or as a ring lesion. They have no predilection for lateral or radial locations in the eye and can be detected at all clock hours both

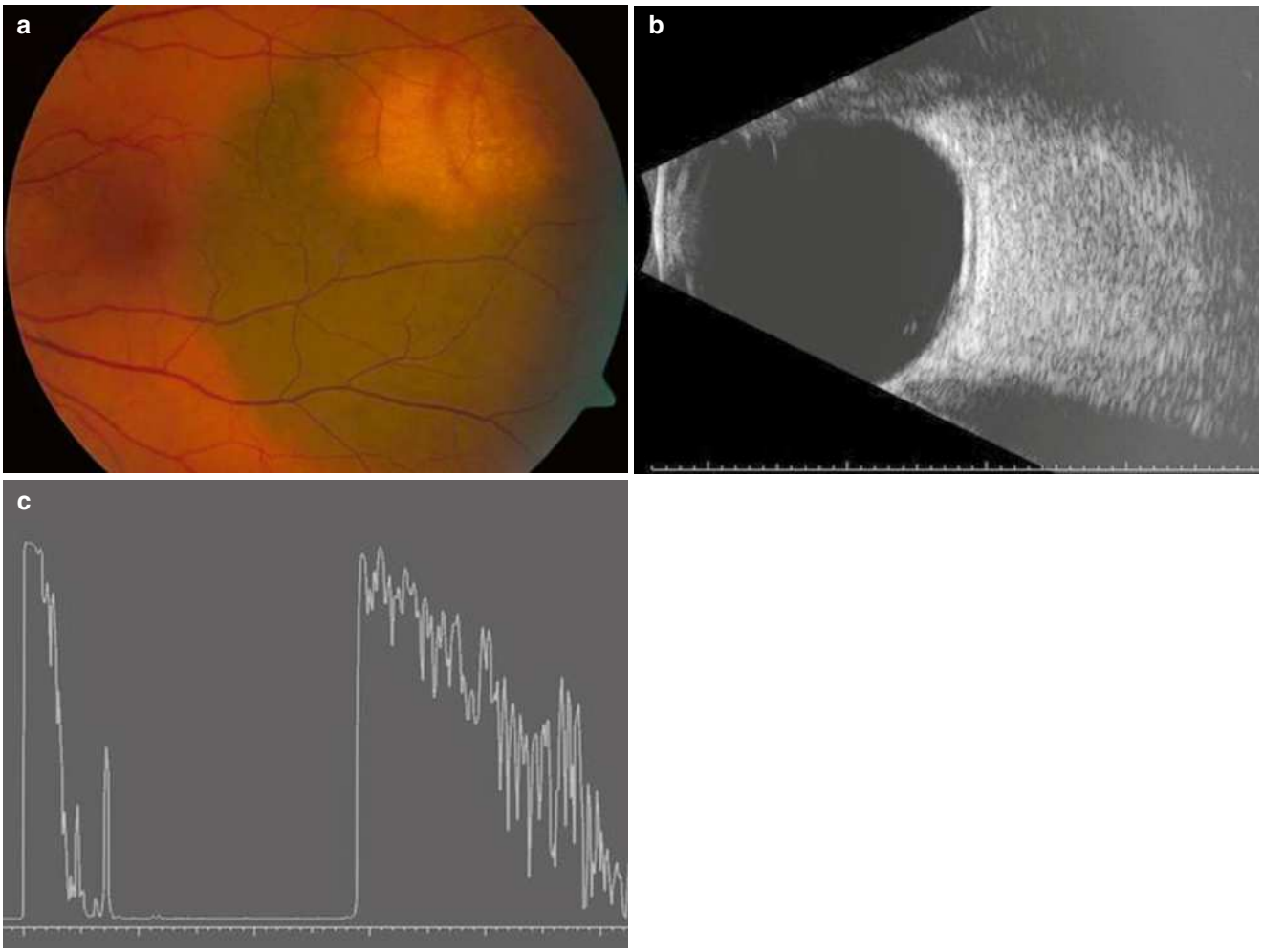

Fig. 23.21 Choroidal nevus. Clinical photograph showing partially amelanotic nevus with overlying drusen. Note absence of orange pigmentation or subretinal fluid (**a**). B-scan demonstrating that nevus is less than 1 mm in height (**b**). A-scan with high internal reflectivity (**c**). [Reprinted from: Ophthalmic Ultrasonography: Intraocular Tumors. Turell, ME, Hayden BC, Schoenfield L, Singh AD. Elsevier, London, 2011. With permission form Elsevier]

anterior and posterior to the equator. Determination of the apical height of the tumor from both a B-scan and diagnostic A-scan is essential in the diagnosis, categorization, and treatment of choroidal melanoma [15, 16]. When determining the height of choroidal melanoma, the measurement is most reproducible when it is obtained by placing the first caliper on the leading anterior edge of the retina and the second caliper on the leading edge of the inner sclera. Measuring to the inner sclera is preferred to measuring to the outer sclera to minimize measuring errors due to scleral inflammation following radiation plaque treatment (Fig. 23.22). The maximal height obtained should be rounded up to the nearest tenth of a millimeter for documentation (Table 23.2). In many cases, diagnostic A-scan is the most accurate method to obtain apical height. As long as the sound beam is directed perpendicular to the most elevated portion of the lesion, the inner scleral spike is easily identified. Obtaining the measurement with a diagnostic A-scan is particularly helpful in the measurement of treated choroidal melanoma, where the lesion becomes highly reflective, and the inner sclera is difficult to delineate on the B-scan. Diagnostic A-scan can also identify the thickening of the retina and subretinal fluid at the apex of the lesion, which appears as high double peaks at the tumor surface (Fig. 23.23). In most cases, both the choroidal melanoma and its overlying shallow retinal irregularity should be included in the apical measurement. In cases where there is a large exudative retinal detachment, the measurement should be taken only to the tumor surface (Fig. 23.24). B-scan ultrasonography, utilizing both transverse and longitudinal scans, is the preferred method to obtain apical height for small lesions (<1.5 mm) and is necessary to obtain basal dimensions. The maximal basal dimensions obtained should be

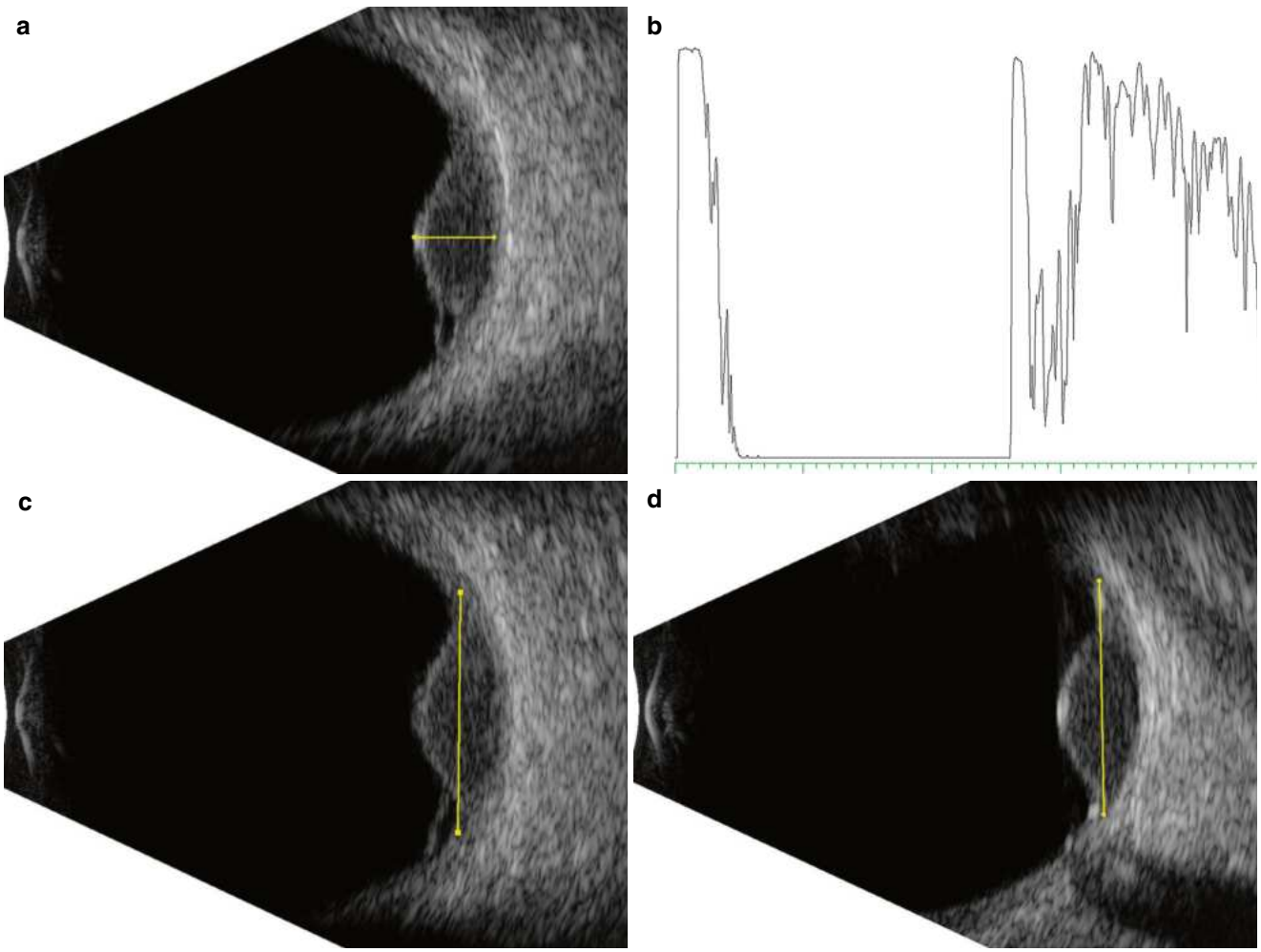

Fig. 23.22 Measurement of choroidal melanoma. Transverse B-scan of a dome-shaped melanoma shows the calipers properly positioned on the leading edge of the retina at the lesion apex and at the inner sclera (**a**) and corresponding diagnostic A-scan (**b**). Transverse B-scan with the calipers showing the lateral extent of the lesion (**c**). Longitudinal B-scan with calipers showing the anterior to posterior extent of the lesion (**d**)

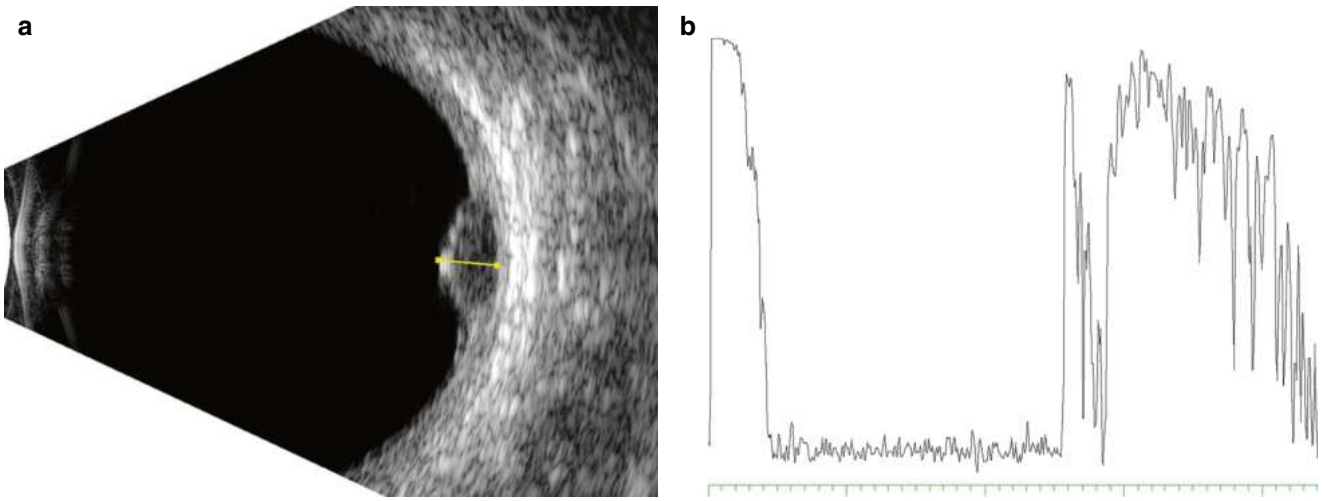

Fig. 23.23 Subretinal fluid at the apex of a choroidal melanoma. Transverse B-scan showing a dome-shaped choroidal melanoma (**a**) and corresponding diagnostic A-scan showing a double peak (arrows) at the apex (**b**)

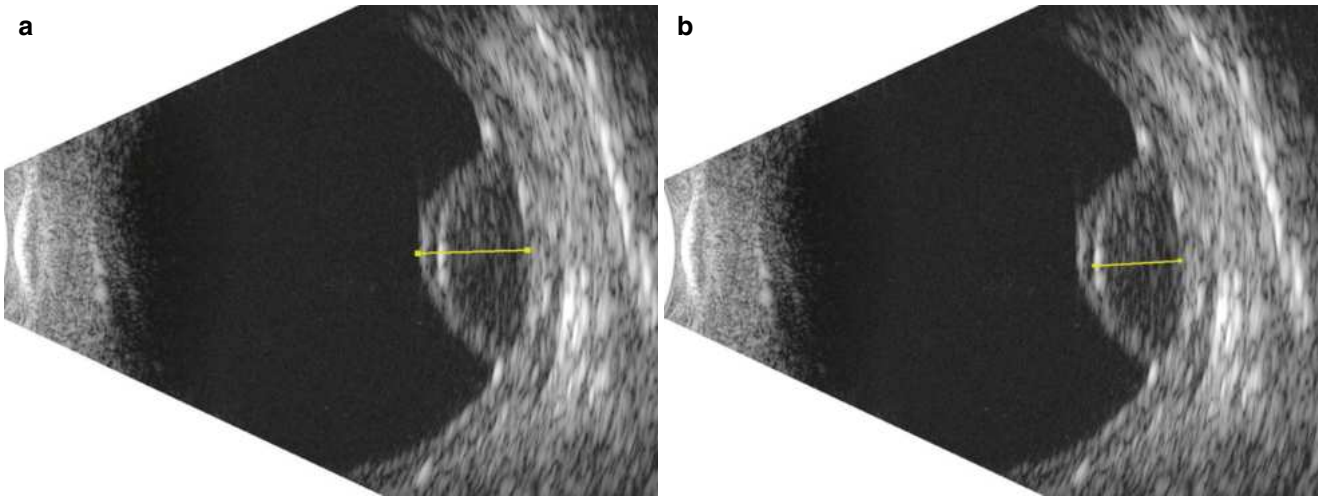

Fig. 23.24 Measuring the height of a choroidal melanoma in the presence of an overlying retinal detachment. Transverse B-scan showing a very shallow overlying retinal detachment. Note tumor height measured including (**a**) and excluding (**b**) the retinal detachment

rounded up to the nearest one-half of a millimeter for documentation. In some cases, the clear delineation of basal boundaries is difficult to identify on a B-scan, and in such cases, clinical correlation is essential.

23.7.2.2 Quantitative and Kinetic

Due to its homogeneous cell structure, choroidal melanoma is usually regularly structured, low reflective, and a moderate to markedly vascular lesion [18, 26]. However, unlike dome or lobulated-shaped lesions, collar button-shaped melanoma is the result of the tumor breaking through Bruch's membrane; therefore, they can differ somewhat in quantitative features. The anterior portion often has higher reflectivity and varying degrees of vascularity (Fig. 23.25), while at the tumor base, reflectivity is low and, in some cases echolucent, known as acoustic hollowing [27]. Moderate to marked vascularity within a choroidal melanoma is usually evident on B-scan ultrasonography, demonstrated dynamically as tiny flickering echo intensity variations within the lesion.

23.7.2.3 Special Cases

Associated Hemorrhage

Vitreous hemorrhage, subretinal hemorrhage, and intratumoral hemorrhage can occur in choroidal melanoma, making standardized echography challenging. Dense vitreous hemorrhage and subretinal hemorrhage can mask an underlying choroidal melanoma. In order to correctly image the tumor surface and borders, it is essential to lower B-scan gain because choroidal melanoma is almost always denser than

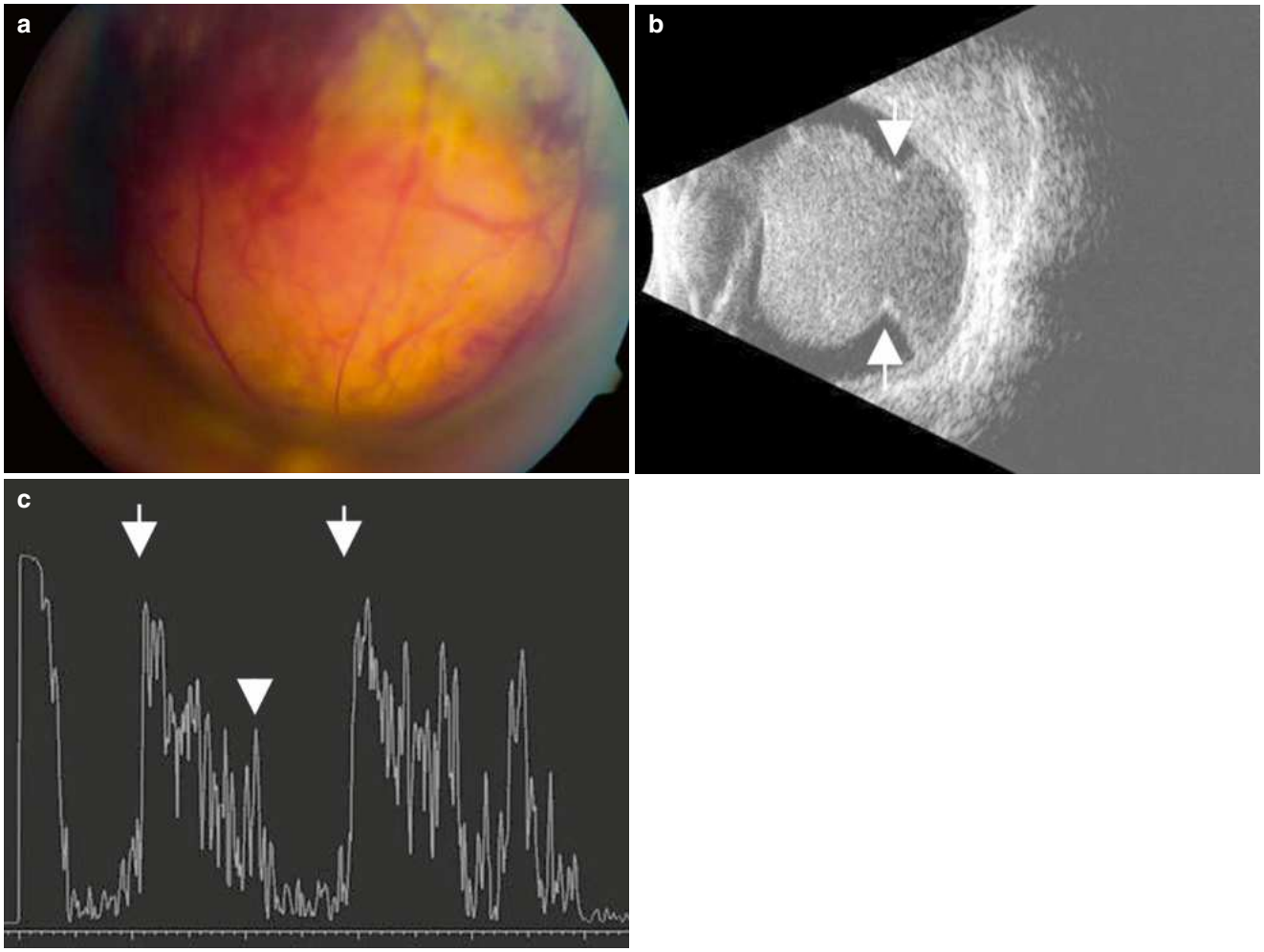

Fig. 23.25 Choroidal melanoma. Clinical photograph showing large, partially amelanotic dome-shaped choroidal mass (**a**). B-scan reveals a large mushroom-shaped choroidal mass that has broken through Bruch's membrane (arrows), touching the posterior surface of the lens (**b**). A-scan demonstrates internal reflectivity (arrows) with medium to high reflectivity in the anterior portion and low reflectivity beneath Bruch's membrane (arrowhead) in the posterior portion of the lesion (**c**). [Reprinted from Ophthalmic Ultrasonography: Intraocular Tumors. Turell, ME, Hayden BC, Schoenfield L, Singh AD. Elsevier, London, 2011. With permission from Elsevier]

layered vitreous hemorrhage and subretinal hemorrhage. Intratumoral hemorrhage can change the quantitative properties of choroidal melanoma by disrupting the typical homogenous structure. Instead of appearing regular in structure, low reflective, and vascular, these tumors are frequently irregular in structure, with reflectivity ranging from low to high, and intrinsic pulsations indicative of vascularity may be absent.

Extraocular Extension

Extraocular extension of choroidal melanoma appears as an echolucent nodule adjacent to the sclera at the tumor base (Fig. 23.26). The low reflectivity of the extraocular component compared to the intraocular component is due to sound attenuation from the sclera. High-resolution examination of the posterior segment frequently reveals slight excavation of the inner sclera at the tumor base or the suggestion of a tiny break in the sclera representing a transocular vessel.

Episcleral Brachytherapy

Intraoperatively, ultrasonography can aid in the precise radioactive episcleral plaque placement. The iodine-125 plaque, used in the Collaborative Ocular Melanoma Study (COMS), produces distinct hyper- and hyporeflective patterns on B-scan, clearly delineating the plaque edges and causing shadowing of orbital structures posteriorly (Fig. 23.27) [28, 29]. Proper utilization of ultrasound for the confirmation of plaque placement intraoperatively has been shown to reduce the risk of early local recurrence of choroidal melanoma [30].

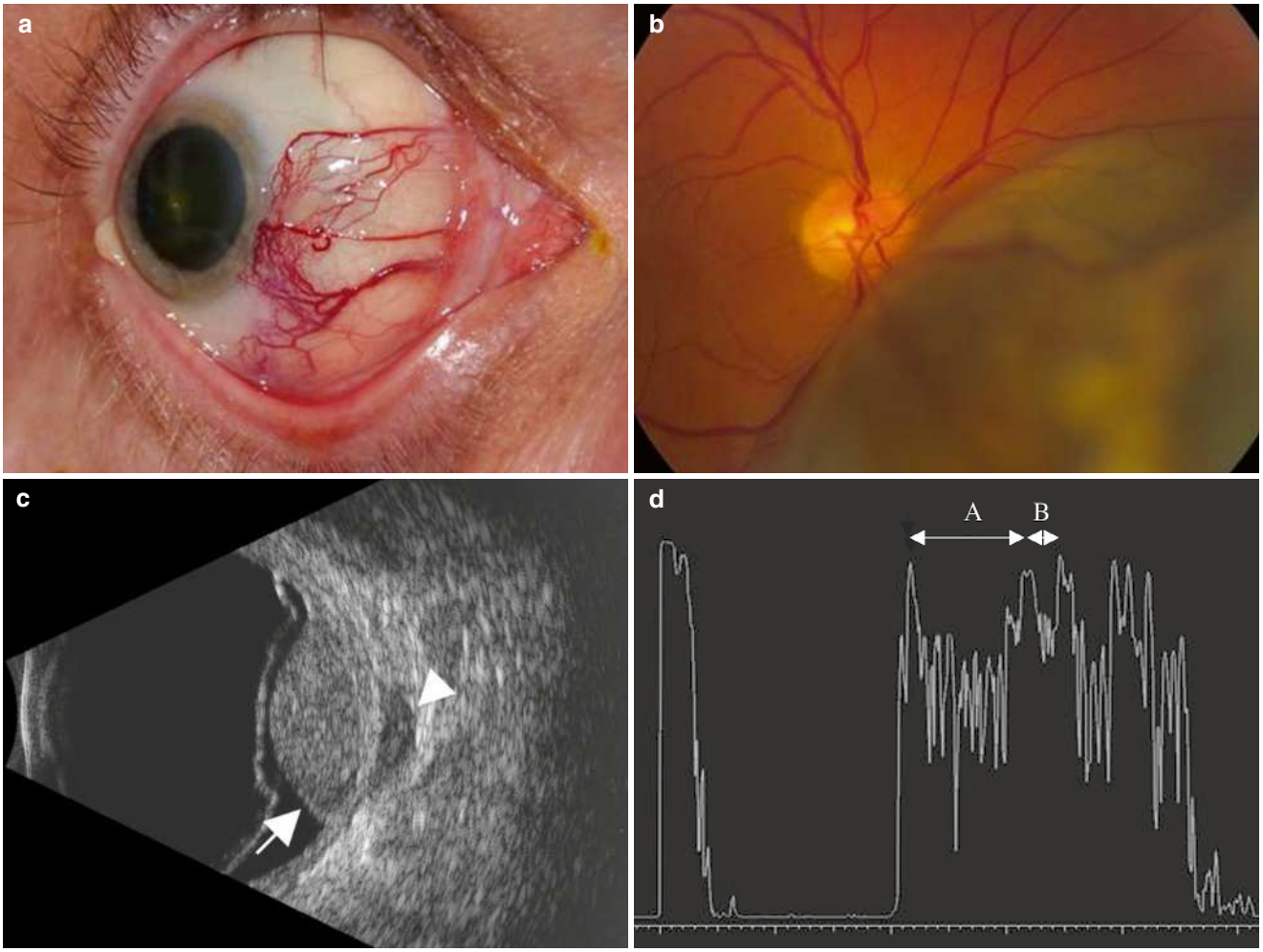

Fig. 23.26 Choroidal melanoma with extrascleral extension. Slit lamp photograph with sentinel vessels (**a**). Fundus photograph showing a large choroidal mass (**b**). B-scan demonstrating dome-shaped choroidal mass (arrow) with extrascleral extension (arrowhead) (**c**). A-scan shows medium to high internal reflectivity of the choroidal lesion (arrows—**a**) and high internal reflectivity of the extraocular extension (arrows—**b**) (**d**). [Reprinted from Ophthalmic Ultrasonography: Intraocular Tumors. Turell, ME, Hayden BC, Schoenfield L, Singh AD. Elsevier, London, 2011. With permission from Elsevier]

Postoperatively, serial examination with standardized echography following radiation plaque treatment of choroidal melanoma is essential for the precise measurement of decreasing tumor apical height. In addition to topographic changes, marked changes in the quantitative and kinetic properties of the treated lesions also occur. The internal structure often becomes irregular, the reflectivity higher, and the vascularity absent.

23.7.3 Choroidal Hemangioma

23.7.3.1 Topographic

Circumscribed hemangioma is a dome-shaped lesion with smooth sloping edges and usually measures less than 6.0 mm in apical height [31]. On the B-scan, dimensions can be difficult to delineate due to the hyperreflectivity of the lesion and sloping base (Fig. 23.28). A diagnostic A-scan is recom-

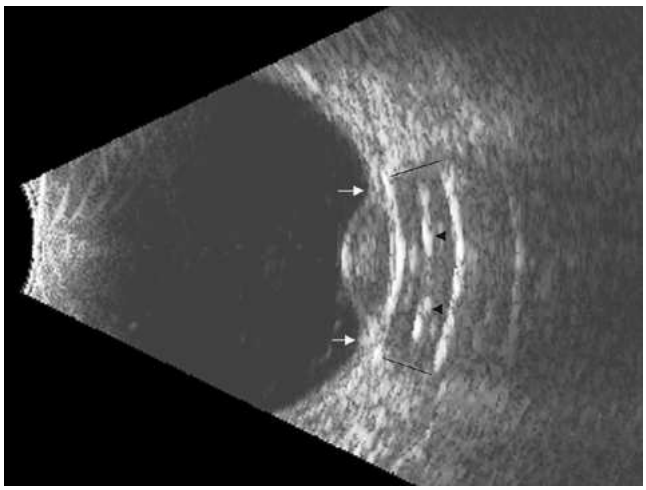

Fig. 23.27 Placement of iodine-125 radiation plaque. Transverse B-scan demonstrates a dome-shaped intraocular lesion with a concave radiation plaque behind the lesion and adjacent to the sclera. The highly reflective linear points within the plaque correspond to the I-125 seeds (arrow heads). Note that the margins of the tumor (arrows) are well within the margins of the plaque (lines). [Reprinted from Fu EX, Hayden BC, Singh AD. Intraocular tumors. Ultrasound Clinics 2008; 3(2): 229–244. With permission from Elsevier]

mended to determine the maximal apical height and ophthalmoscopy to estimate the basal dimensions. Diffuse choroidal hemangioma (in association with Sturge-Weber syndrome) appears as a diffuse thickening in all quadrants of the choroid, posterior to the equator, with maximal elevation, usually in the macula.

23.7.3.2 Quantitative and Kinetic

Choroidal hemangioma is regularly structured and highly reflective on standardized echography. Although these lesions are composed of a network of fine lacy vessels, on ultrasonographic examination, vascularity is not detected, perhaps due to nonpulsatile blood flow. These quantitative and kinetic features are markedly different from the low reflective and vascular properties of choroidal melanoma (Table 23.3).

23.7.4 Choroidal Metastasis

23.7.4.1 Topographic

Choroidal metastasis is usually flat or dome-shaped with a smooth or irregular surface and is most frequently present in the posterior pole (Fig. 23.29). They can be focal, multifocal, or diffuse lesions occurring unilaterally or bilaterally. Extensive associated retinal detachment is frequently detected. If diffuse infiltrative metastasis to the choroid is suspected, an axial B-scan examination is recommended to delineate peripapillary involvement and orbital extension.

23.7.4.2 Quantitative and Kinetic

On diagnostic A-scan, the internal structure is usually slightly irregular and most commonly medium to highly reflective. However, irregular metastatic lesions of the choroid can present with reflectivity ranging from low to high. Vascularity is usually absent or very minimal within the lesion, yet the surrounding choroid appears to have a marked increase in vascularity.

23.7.5 Hemorrhagic Disciform Lesion

Subretinal hemorrhage or disciform lesions from age-related macular degeneration (AMD) can resemble choroidal melanoma. Solidified subretinal and intrachoroidal hemorrhage is usually irregularly shaped with poorly defined margins but can appear smooth and dome-shaped (Fig. 23.30). Due to the heterogeneous internal structure, most disciform lesions are irregularly structured and are medium to highly reflective and thus can be differentiated from choroidal melanoma. However, over time, subretinal hemorrhage can become organized, with choroidal excavation becoming regularly structured and low to medium reflectivity, mimicking choroidal melanoma. The complete absence of internal vascularity is the distinguishing kinetic feature of AMD lesions, differentiating them from highly vascular choroidal melanoma.

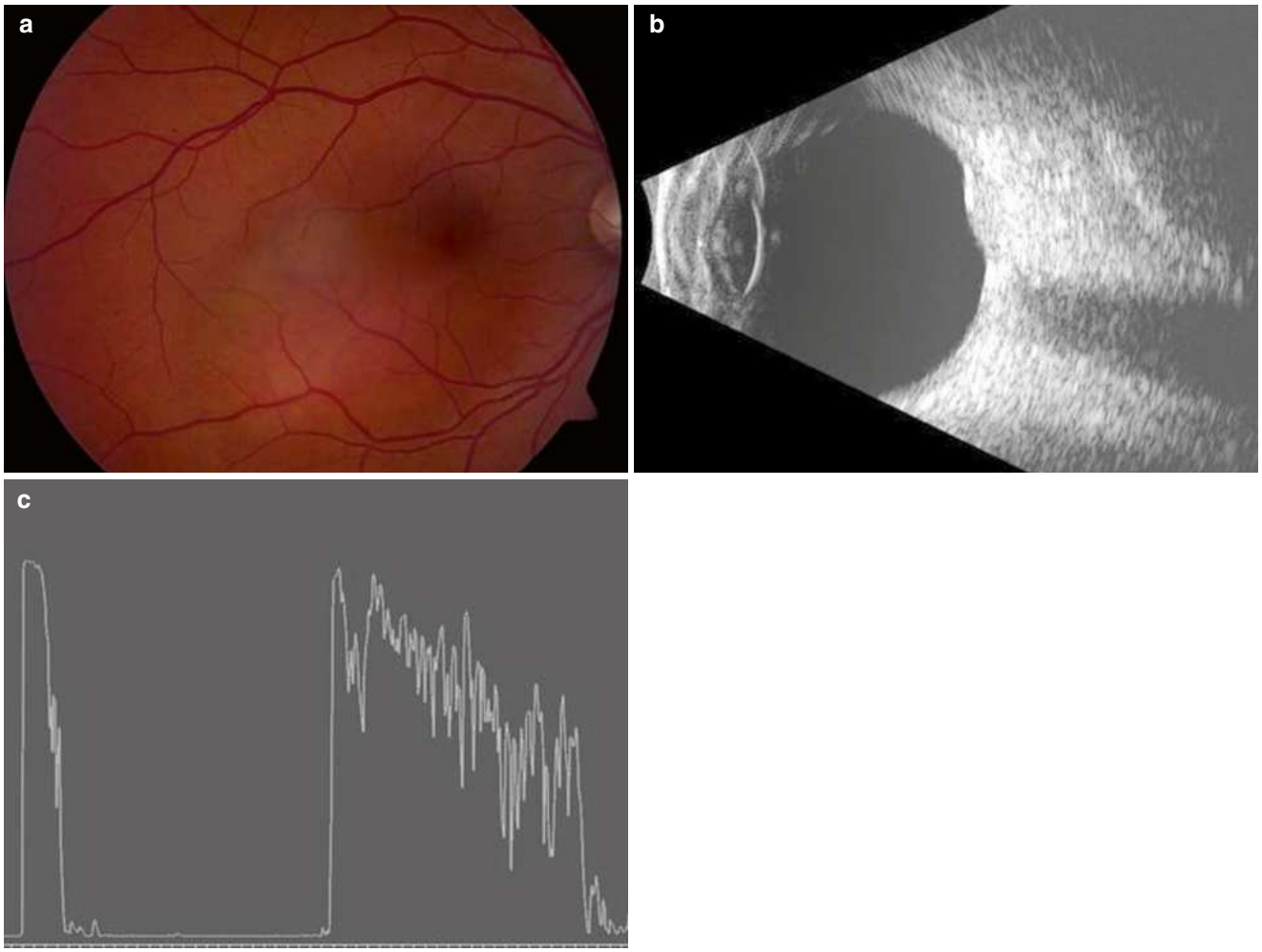

Fig. 23.28 Circumscribed choroidal hemangioma. Clinical photograph with elevated choroidal mass with indistinct borders (**a**), Axial B-scan showing dome-shaped mass (**b**), A-scan with high internal reflectivity (**c**). [Reprinted from Ophthalmic Ultrasonography: Intraocular Tumors. Turell, ME, Hayden BC, Schoenfield L, Singh AD. Elsevier, London, 2011. With permission from Elsevier]

Table 23.3 Differential diagnosis of choroidal melanoma

Condition	Shape	Reflectivity	Attenuation	Vascularity	Specific features
Choroidal melanoma	Collar button/dome/lobulated	Low–medium	High	High	Regular internal structure
					Acoustic hollowness
					Choroidal excavation
Choroidal nevus	Flat/dome	Medium–high	High	No	Height less than 2 mm
Choroidal hemangioma	Dome	High	No	No	Regular internal structure
Choroidal metastasis	Placoid/irregular/multiple	Medium–high	Low	No	Multiple lesions
ARMD with hemorrhage	Dome/irregular	High	No	No	Irregular internal structure

ARMD age-related macular degeneration
[Adapted from Turell, ME, Hayden BC, Schoenfield L, Singh AD. Intraocular Tumors. Ophthalmic Ultrasonography. Hayden BC, Singh AD (Eds). Elsevier, London, 2011. With permission from Elsevier]

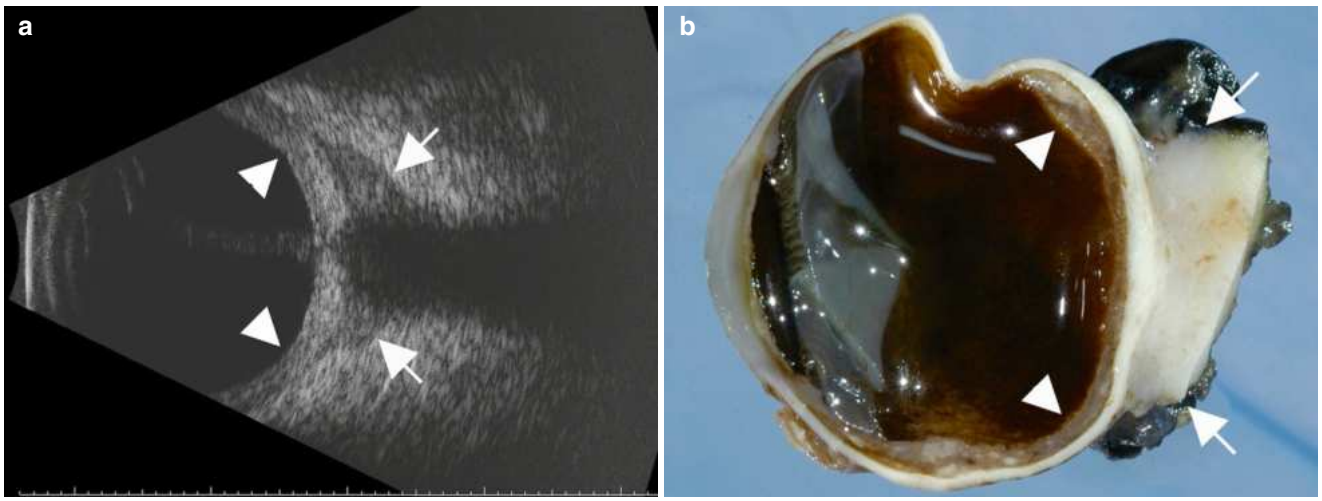

Fig. 23.29 Choroidal metastasis. B-scan demonstrating a total retinal detachment, diffuse choroidal thickening (arrowheads), and extraocular extension (arrows) near the retrobulbar optic nerve (**a**). Gross photograph of the opened globe showing chalky white tumor deposits involving most of the choroid (arrowheads) and tumor extending outside of globe (arrows **b**, 2× magnification. Hematoxylin and eosin stain). [Reprinted from Ophthalmic Ultrasonography: Intraocular Tumors. Turell, ME, Hayden BC, Schoenfield L, Singh AD. Elsevier, London, 2011. With permission from Elsevier]

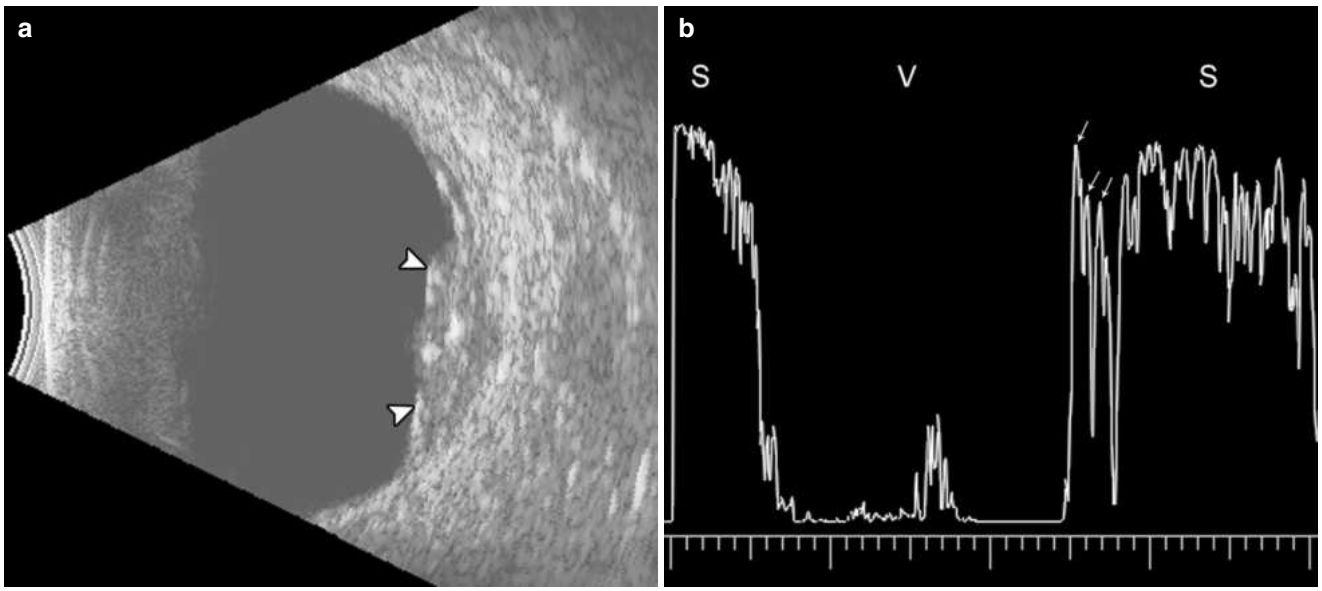

Fig. 23.30 Disciform lesion. B-scan shows a mildly elevated lesion in the macular region, arrowheads). (**a**) scan shows multiple highly reflective peaks (arrows) corresponding to the lesion [(**b**) *S* sclera, *V* vitreous]. [Reprinted from Sharma S, Ventura ACM, Waheed N. Ophthalmic Ultrasonography: Vitreoretinal Disorders. Ultrasound Clinics 2008; 3(2): 217–228. With permission from Elsevier]

References

1. Lizzi FL, Feleppa EJ. Practical physics and electronics of ultrasound. Int Ophthalmol Clin. 1979;19(4):35–63.
2. Fledelius HC. Ultrasound in ophthalmology. Ultrasound Med Biol. 1997;23(3):365–75.
3. Lizzi FL, Coleman DJ. History of ophthalmic ultrasound. J Ultrasound Med. 2004;23(10):1255–66.
4. Ossoinig KC. Quantitative echography—the basis of tissue differentiation. J Clin Ultrasound. 1974;2(1):33–46.
5. Ossoinig KC. Standardized echography: basic principles, clinical applications, and results. Int Ophthalmol Clin. 1979;19(4):127–210.
6. Bryne S. A-scan axial eye length measurements—a handbook for IOL calculations. Mars Hill: Grove Park Publishers; 1995.
7. Byrne S, Green R. Ultrasound of the eye and orbit. 2nd ed. St. Louis: Mosby; 2002.
8. Bronson NR. Development of a simple B-scan ultrasonoscope. Trans Am Ophthalmol Soc. 1972;70:365–408.
9. Feibel RM. Diagnostic ultrasonography. Int Ophthalmol Clin. 1978;18(1):167–78.
10. Fisher YL. Contact B-scan ultrasonography: a practical approach. Int Ophthalmol Clin. 1979;19(4):103–25.
11. Pavlin CJ, Harasiewicz K, Sherar MD, Foster FS. Clinical use of ultrasound biomicroscopy. Ophthalmology. 1991;98(3):287–95.
12. Ossoinig KC. Ruling out posterior segment lesions with echography. Int Ophthalmol Clin. 1978;18(2):117–20.
13. Byrne SF. Standardized echography. Part I: A-scan examination procedures. Int Ophthalmol Clin. 1979;19(4):267–81.
14. Byrne SF. Standardized echography in the differentiation of orbital lesions. Surv Ophthalmol. 1984;29(3):226–8.
15. Echography (ultrasound) procedures for the Collaborative Ocular Melanoma Study (COMS), Report No. 12, Part II. J Ophthal Nurs Technol. 1999;18(5):219–32.
16. Echography (ultrasound) procedures for the Collaborative Ocular Melanoma Study (COMS), Report No. 12, Part I. J Ophthal Nurs Technol. 1999;18(4):143–9.
17. The COMS randomized trial of iodine 125 brachytherapy for choroidal melanoma: IV. Local treatment failure and enucleation in the first 5 years after brachytherapy. COMS Report No. 19. [erratum appears in Ophthalmology. 2004;111(8):1514]. Ophthalmology. 2002;109(12):2197–206.
18. Green R, Byrne S. Diagnostic ophthalmic ultrasound. In: Ryan S, editor. Retina. 3rd ed. St. Louis: Mosby; 2001. p. 240.
19. Lois N, Sheilds CL, Sheilds JA, Mercado G. Primary cysts of the iris pigment epithelium. Clinical features and natural course in 234 patients. Ophthalmology. 1998;105(10):1879–85.
20. Brown D, Boniuk M, Font RL. Diffuse malignant melanoma of iris with metastases. Surv Ophthalmol. 1990;34(5):357–64.
21. Char DH, Crawford JB, Gonzales J, et al. Iris melanoma with increased intraocular pressure. Differentiation of focal solitary tumors from diffuse or multiple tumors. Arch Ophthalmol. 1989;107(4):548–51.
22. Shields CL, Shields JA, Shah P. Retinoblastoma in older children. Ophthalmology. 1991;98:395–9.
23. All-Ericsson C, Economou MA, Landau I, et al. Uveitis masquerade syndromes: diffuse retinoblastoma in an older child. Acta Ophthalmol Scand. 2007;85:569–70.
24. Ridley ME, Shields JA, Brown GC, et al. Coats' disease. Evaluation of management. Ophthalmology. 1982;89:1381–7.
25. Factors predictive of growth and treatment of small choroidal melanoma: COMS Report No. 5. The Collaborative Ocular Melanoma Study Group. Arch Ophthalmol. 1997;115(12):1537–44.
26. Fuller DG, Snyder WB, Hutton WL, et al. Ultrasonographic features of choroidal malignant melanomas. Arch Ophthalmol. 1979;97(8):1465–72.
27. Goldberg MF, Hodes BL. Ultrasonographic diagnosis of choroidal malignant melanoma. Surv Ophthalmol. 1977;22(1):29–40.
28. Collaborative Ocular Melanoma Study Group. The COMS randomized trial of iodine 125 brachytherapy for choroidal melanoma. III. Initial mortality findings. COMS Report No. 18. Arch Ophthalmol. 2001;119:969–82.
29. Collaborative Ocular Melanoma Study Group. The COMS randomized trial of iodine 125 brachytherapy for choroidal melanoma. Local treatment failure and enucleation in the first 5 years after brachytherapy. COMS Report No. 19. Ophthalmology. 2002;198:2197–206.
30. Aziz HA, Al Zahrani YA, Bena J, Lorek B, Wilkinson A, Suh J, Singh AD. Episcleral brachytherapy of uveal melanoma: role of intraoperative echographic confirmation. Br J Ophthalmol. 2017;101:747–51.
31. Witschel H, Font R. Hemangioma of the choroid. A clinicopathologic study of 71 cases and a review of the literature. Surv Ophthalmol. 1976;20(6):415–31.

Diagnostic Techniques: FNAB

24

Hassan A. Aziz, David Pelayes, Charles V. Biscotti, and Arun D. Singh

24.1 Introduction

Fine-needle aspiration biopsy (FNAB) of tumors has a long history [1–6]. The first intraocular biopsy was performed by Hirschberg in 1868 [7–13]. Since the publication of a major report by Jakobiec in 1979, FNAB has been increasingly used in the evaluation of ophthalmic tumors [14] (Box 24.1).

Box 24.1 Intraocular Biopsy

- Biopsy is useful for diagnosis and prognostication.
- Techniques include FNAB, vitrectomy-assisted aspiration biopsy, incisional biopsy, and excisional biopsy.
- The technique depends on tumor size, location, and suspected diagnosis.
- Successful biopsy requires adequate handling of the specimen.
- Close collaboration with the pathologist and/or cytologist is essential.
- Aspiration biopsy is essentially contraindicated if retinoblastoma is a possibility.

Multiple reports determine the safety and reliability of ophthalmic FNAB in diagnosing or managing intraocular tumors (Table 24.1) [15–27]. Six of the papers report on the utility of FNAB for all solid intraocular tumors [15, 18–22], while the more recent publications focus on the genetic type of uveal melanoma [23–27].

H. A. Aziz
Clemenceau Medical Center, Dubai, UAE
e-mail: hassanabdulaziz@cmc.com.lb

D. Pelayes (✉)
Department of Ophthalmology, Buenos Aires University, Maimonides University, FASTA University, Buenos Aires, Argentina

C. V. Biscotti
Department of Anatomic Pathology, Cole Eye Institute, Cleveland Clinic, Cleveland, OH, USA

A. D. Singh
Department of Ophthalmic Oncology, Cole Eye Institute, Cleveland Clinic, Cleveland, OH, USA
e-mail: singha@ccf.org

© The Author(s), under exclusive license to Springer Nature Switzerland AG 2025

A. D. Singh, B. E. Damato (eds.), *Clinical Ophthalmic Oncology*, https://doi.org/10.1007/978-3-031-75907-9_24

Table 24.1 A summary of large published reports examining the role of ocular FNAB

Author	Year	Number of cases	Histology/ cytology correlation (%)	Genetic correlation (%)	Lesion type(s)
Augsburger	1985	71	94	N/A	Melanoma/rule out melanoma (44), metastasis (4), RB/rule out RB (18), ME/ rule out ME (2), rule out sarcoma (2), rule out leukemia (1)
Char	1989	29	89	N/A	Melanoma
Shields	1993	140	95	N/A	Melanoma (54), metastasis (28), melanocytoma (4), lymphoma (4), leukemia (3) RB (3), ME (2), benign/inflammatory (42)
Davila	1998	17[b]	83	N/A	Melanoma (5), suspicious for melanoma (2), lymphoma (5), suspicious for lymphoma (2), metastasis (2), RB (1)
Eide	1999	80	N/A	N/A	Melanoma (52), metastasis (6), RB (2), leukemia (1), lymphoma (3), benign lesions (16)
Faulkner-Jones	2005	33	83	N/A	Melanoma (26), metastasis (4), lymphoma (1), hemangioma (1), choroidal detachment (1)
Shields	2006	100	N/A	N/A	Melanoma (47), metastasis (20), melanocytoma (3), IPEA (1), lymphoma (1), leukemia (1), ME (3), RB (1), vascular tumor (1), conjunctival SCC (1), iris stromal cyst (10), inflammatory (9)
Char	2006	16	69[a]	N/A	Melanoma
Shields	2007	140	N/A	86	Melanoma
Correa	2014	159	78.1	99	Melanoma
Sellam	2016	217	N/A	77.9	Melanoma
Singh	2016	150	92	85	Melanoma
Shields	2017	1059	N/A	96	Melanoma

We have included reports involving multiple patients presenting with solid intraocular tumors. Case reports were excluded
IPEA iris pigment epithelial adenoma, *ME* medulloepithelioma, *RB* retinoblastoma, *SCC* squamous cell carcinoma
[a] Cyto-clinical correlation
[b] Includes vitreous, anterior chamber, and FNA samples

24.2 Surgical Technique

The technique and instrumentation for FNAB vary depending upon (1) the involved tissue (aqueous, iris, ciliary body, choroid, retina, subretinal space, vitreous) [28, 29]; (2) suspected tumor diagnosis, size, and location; (3) associated retinal detachment; and (4) clarity of the media (Fig. 24.1) [30–38].

Most frequently used needles for ophthalmic FNAB are of 25–30 gauge (Fig. 24.2) [38, 39]. The likelihood of insufficient samples may be lower with a 22-gauge needle [22] and higher with a 30-gauge needle [40]. Some authors have recommended bending the needle tip to 90° and entering the tumor tangentially rather than radially [36]. A prototype needle with a short bevel and millimeter graduations has also become available, and a second generation of the same improved prototype allows its use with vitrectomy (Fig. 24.7) [41, 42].

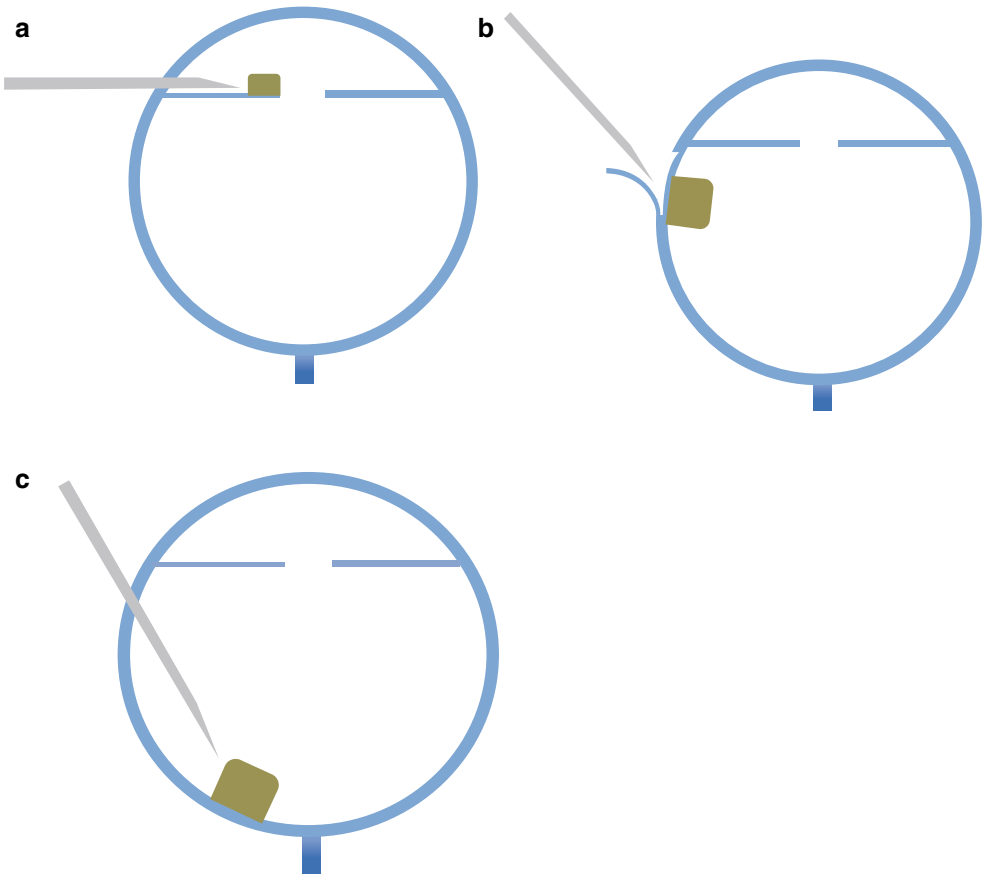

Fig. 24.1 Schematic representation of approaches for fine-needle aspiration biopsy. For iris tumors, the needle bevel is up, the needle is parallel to the iris plane, and the needle is not going across the pupil (**a**). Transscleral FNAB of an anterior choroidal tumor. Note that the needle is inserted toward the center of the tumor under a partial thickness scleral flap (**b**). Transvitreal approach for biopsy of a posterior choroidal tumor (**c**). The entry point is 4 mm behind the limbus in the anteroposterior meridian of the tumor. (Reprinted from Singh et al. [38]. With permission from Karger Publishers. Copyright © 2011, Karger Publishers)

Fig. 24.2 A short 25-gauge needle attached to a short tube is inserted through the scleral bed into the tumor and aspiration is performed (**a**). The aspirate sample is placed in a preservative solution, such as CytoLyt®, and the needle is rinsed to optimize cell yield (**b**). A 25-gauge needle with a calibrated tip (**c**). (Reprinted from Singh et al. [38]. With permission from Karger Publishers. Copyright © 2011, Karger Publishers)

24.3 Iris Tumors

In the case of iris tumors, entry is through the anterior chamber (Fig. 24.1) [41]. A 26–30 gauge needle is swept over the surface of the lesion, aspirating about 0.5 mL of the aqueous humor [41]. Direct insertion of the needle into the tumor may increase the cellular yield [21]. Complications such as persistent hyphema, prolonged hypotony, lens damage, and endophthalmitis are rare (<1%) [21].

24.4 Ciliary Body and Pre-equatorial Tumors

Tumors located in the ciliary body or anterior choroid are approached transsclerally (Fig. 24.1). A 3-mm square scleral flap to a depth of approximately 80% is fashioned. A short 25-gauge needle attached to short tubing is inserted through the scleral bed.

24.5 Post-equatorial Tumors

Posterior choroidal tumors are most accessible by a transvitreal approach (Fig. 24.1). A 25-gauge valved cannula is inserted using a standard technique, 3.5–4 mm posterior to the limbus [42]. A 25–30 gauge needle attached to a 5 mL syringe by a short tubing is introduced into the mid-vitreous cavity through the cannula. The meridian of insertion is selected according to the location of the tumor. The needle can be guided into the tumor either under indirect ophthalmoscopic control or using the operating microscope, depending on the surgeon's preference [36]. Ultrasonic guidance is rarely used in the presence of clear media [14]. The needle tip is inserted into the tumor, avoiding major blood vessels. Gentle aspiration is performed by pulling the plunger of the syringe. Once the suction force has balanced out, the needle is withdrawn along the path of insertion [36]. Hemorrhage is controlled by applying pressure at the entry site by a cotton-tipped applicator [22, 34, 36, 40]. If the globe softens, a balanced salt solution can be injected into the vitreous cavity.

24.6 Vitrectomy-Assisted Aspiration Biopsy

With the advent of small-gauge vitrectomy systems, vitrectomy-assisted aspiration biopsy has been utilized for sampling intraocular tumors. A 25- or 27-gauge vitreous cutter can be used to biopsy both anterior chamber and posterior segment tumors (Chap. 25).

24.7 Sample Handling

Close collaboration with the cytopathologist is of paramount importance in handling aspiration samples from intraocular tumors. All the material is placed in a transport medium such as Cytolyt® solution for ThinPrep processing (Fig. 24.2) [43]. The sample in Cytolyt® is then subjected to one or more centrifugation and concentration steps (Fig. 24.3) [43]. The pellet obtained is resuspended in a cell preservative solution, PreservCyt®, for automated processing. The ThinPrep® processor mixes the sample and then, using a gentle vacuum, collects cells on a filter in a monolayer. This filter is then inverted, and its cellular contents are transferred to a microscope slide**.** This method optimizes cell yield and preservation and standardizes slide preparation for interpretation in this setting of limited material. If abundant aspirate material is obtained, a paraffin-embedded cell block can be processed. While we rarely perform immunostains on preparations other than a cell block, some authors have reported successful immunohistochemical analyses on thin-layer cytology preparations [20, 37, 44].

24.7.1 Indications

The indications for aspiration biopsy may be considered diagnostic, prognostic, and investigational [45]. One of the major indications for ophthalmic aspiration biopsy is to establish a diagnosis when clinical examination and ancillary tests are inconclusive [22, 37, 44, 46]. Potential scenar-

Fig. 24.3 Automated ThinPrep® processing. The ThinPrep® filter rotates in the sample, separating cellular material from background debris. A vacuum collects cells on the exterior surface of the filter membrane. The filter is then inverted and gently pressed against the ThinPrep® slide. Surface tension and air pressure cause the cells to adhere to the slide, resulting in an even distribution of cells in a central circular region of a slide. (Reprinted from Brainard and Biscotti [45]. With permission from Karger Publishers. Copyright © 2011, Karger Publishers)

ios include atypical clinical presentation, dense media opacity, possible uveal metastasis without a known primary tumor, and patients requesting histopathologic confirmation before undergoing recommended therapy such as enucleation [36]. Recently, with improved genetic testing of uveal melanoma, aspiration biopsy has been incorporated into routine clinical practice for prognostication in many centers.

24.7.2 Melanoma: Prognostic

Significant progress has been made in evaluating the role of tumor histopathology, cytogenetics, and gene expression patterns in predicting the metastatic potential of uveal melanoma [47]. Therefore, it has become increasingly common to perform biopsy for prognostic purposes. Fluorescence in situ hybridization (FISH), single-nucleotide polymorphism (SNP) array, multiplex ligation-dependent probe amplification (MLPA), next-generation sequencing, and gene expression profiling (GEP) are frequently employed to assess metastatic risk [47].

24.7.3 Amelanotic Uveal Tumor (Primary Versus Metastasis)

Shields and associates have reported on the diagnostic success of intraocular FNAB in 140 patients with intraocular malignancies such as uveal melanoma, uveal metastasis, lymphoma, and leukemia (Fig. 24.4) [22, 47]. A histologic correlation was available in 57 of the cases, with histology-cytology diagnostic concordance in 54 of 57 (95%) cases. Augsburger and colleagues examined 71 ophthalmic FNA samples [15]. The histologic correlation was available for nine of those, and the cytologic diagnoses were confirmed in eight out of nine cases. In addition, all 11 aspirates done to confirm benign conditions were read as benign [15]. Cases of unsuspected uveal inflammation or infection simulating an amelanotic uveal tumor can also be identified by diagnostic FNAB [48, 49].

24.7.4 Nevus Versus Melanoma (Indeterminate Melanocytic Lesions)

Since cell yield varies directly with lesion size, adequacy is more of an issue in this setting, as evidenced by a 35% failure rate in one study of small melanocytic choroidal tumors [50]. Further, cytologists struggle to distinguish between spindle cell nevus and spindle cell melanoma [51]. Therefore, in such cases, cytologists should look for epithelioid cells, which usually have malignant nuclear features, including nuclear pleomorphism and prominent nucleoli [17, 51]. However, the absence of cellular features of malignancy should not be regarded as definitive evidence of a benign nevus [17, 22].

Given that cellular yield is lower with smaller tumors [25, 46, 52] and because even an expert cytopathologist may not be able to unequivocally distinguish a nevus from melanoma [37], the authors feel that such indeterminate melanocytic lesions (large nevus vs. small melanoma) should not be routinely subjected to diagnostic FNAB [47].

24.7.5 Melanoma: Diagnostic

A number of studies have shown that FNAB has a diagnostic accuracy rate of over 90% (Fig. 24.5) [18, 22, 37, 44, 53, 54]. Char observed FNAB to be accurate in both the diagnosis and cytologic typing of uveal melanomas [17]. Shields et al. have also reported similar results, with 26 of 27 (96%) melanomas diagnosed on FNAB being subsequently confirmed on enucleation [22].

Regardless of the differential diagnosis, cytologists must interpret the cellular features within the clinical context. This emphasizes the importance of good communication between cytologists and ophthalmologists. A stepwise diagnostic approach for uveal melanoma has proved useful [54]. Cytologists should first look for spindle cell morphology, observed in 98% of cases (Fig. 24.6b) [55]. The spindle melanoma cell is the most helpful diagnostic criterion in the differential diagnosis with metastasis because the vast majority of uveal metastases are carcinomas, mostly from the breast and lung [56]. These tumors have an epithelioid appearance and cohesive cell clusters. Spindle cell carcinomatous metastases occur rarely [57] (Fig. 24.7).

Cytoplasmic melanin pigment is the second important diagnostic feature, observed in 80% of uveal melanoma cases [55]. Melanin has a finely granular cytoplasmic distribution that can be focal and inconspicuous (Fig. 24.6a). Immunohistochemistry for epithelial markers, including cytokeratins, neuroendocrine markers, and melanoma markers such as S100 and HMB45, can be helpful, especially in cases of amelanotic epithelioid cell melanoma (Fig. 24.6c) [20, 54].

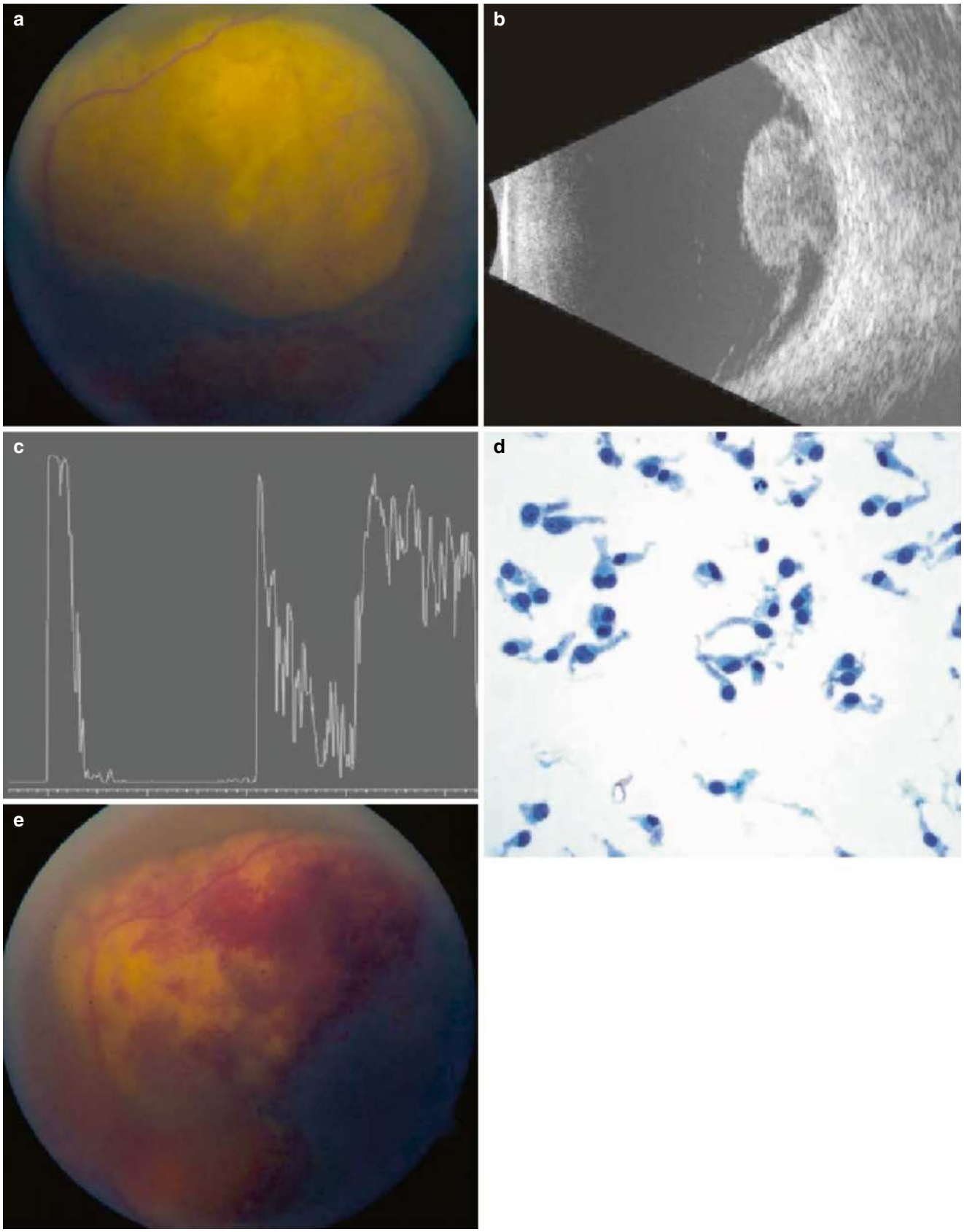

Fig. 24.4 Fundus photograph depicting a completely amelanotic tumor (**a**). B-scan ultrasonography demonstrated a collar-button-shaped tumor (**b**). A-scan ultrasonography showed low to medium internal reflectivity (**c**). Fine-needle aspiration biopsy revealed spindle cells lacking melanin, consistent with the clinical impression of amelanotic choroidal melanoma (**d**). A localized preretinal hemorrhage is seen overlying the needle biopsy site, which generally clears in several weeks (**e**)

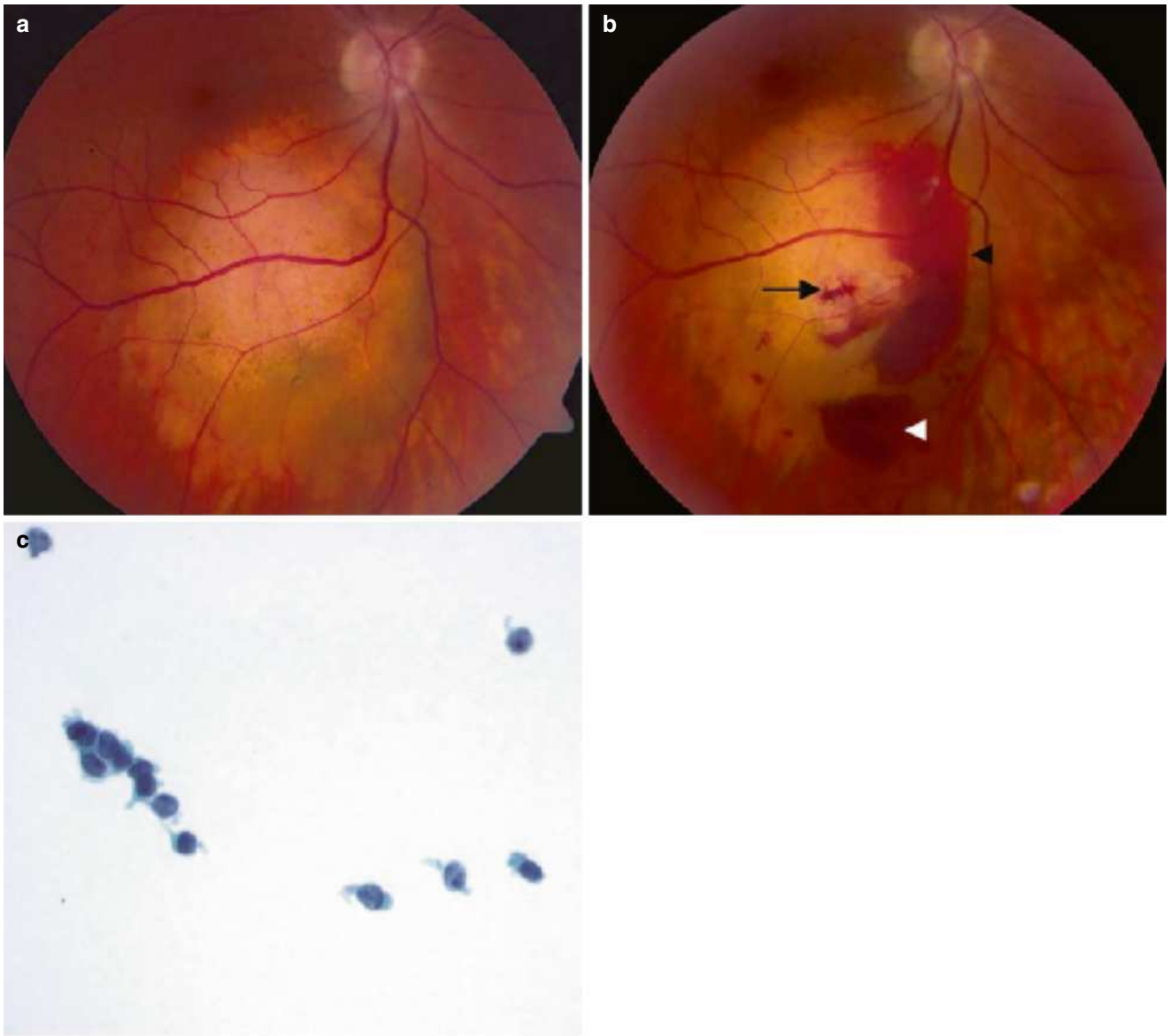

Fig. 24.5 A 42-year-old woman was evaluated for a partially amelanotic choroidal mass OD (**a**). Her past medical history was noncontributory. Systemic evaluation, including CT scans of the chest, abdomen, and pelvis and mammography, were negative. As the possibility of choroidal metastasis could not be completely excluded by clinical examination, a diagnostic transvitreal FNAB was performed (**b**). Note the biopsy site [arrow] and localized subretinal hemorrhage [black arrowhead] and the pocket of preretinal hemorrhage [white arrowhead]). FNAB showed the mass to be choroidal melanoma (**c**). (Reprinted from Biscotti and Singh [56]. With permission from Karger Publishers. Copyright © 2011, Karger Publishers)

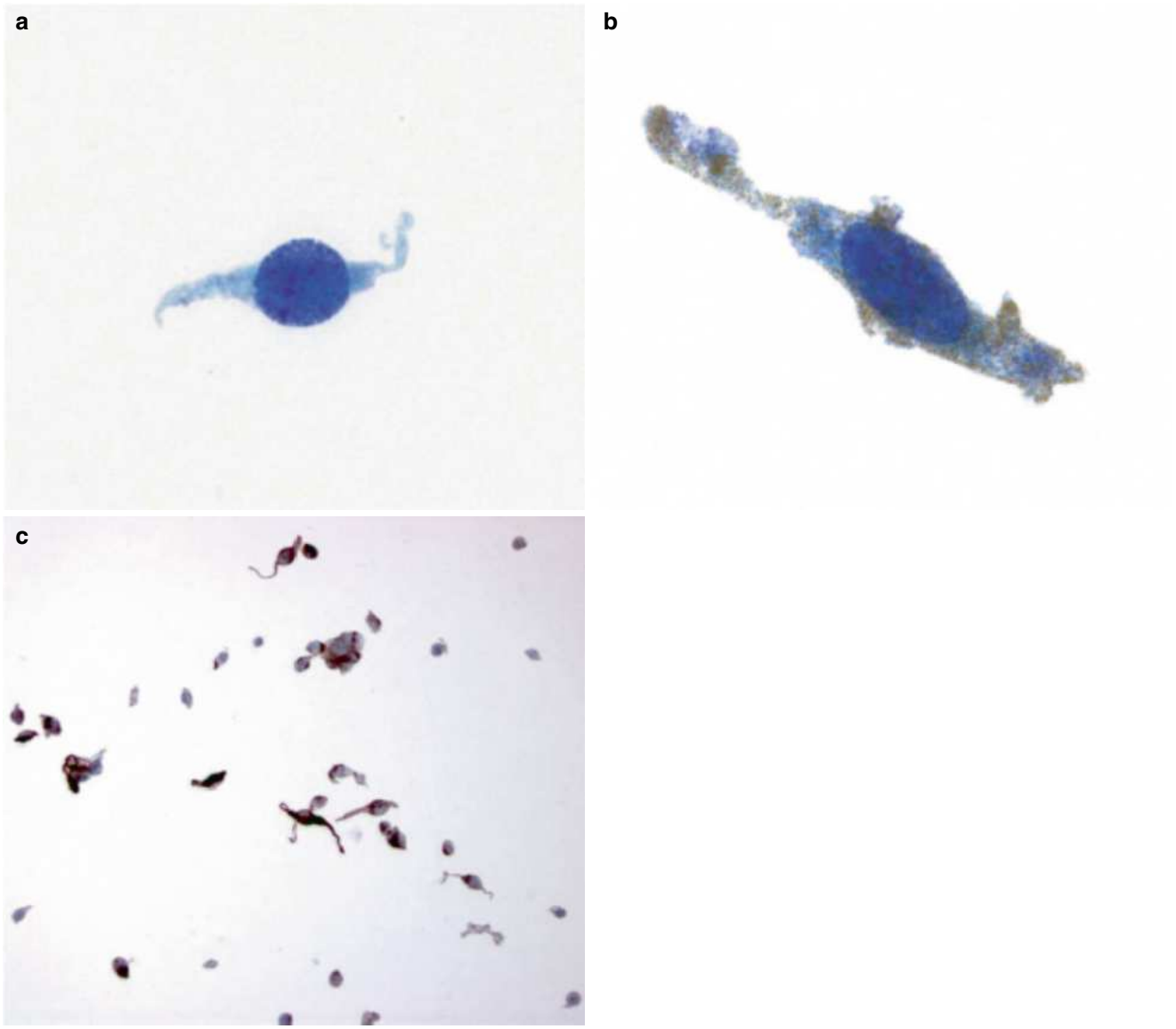

Fig. 24.6 Presence of spindle cells and melanin are helpful cytologic diagnostic features. A spindle cell without melanin (**a**). A uveal melanoma cell with melanin (**b**). Though rarely needed, immunohistochemical stains for melanoma markers, such as HMB45 illustrated here, can help identify amelanotic melanoma cells (**c**). (Reprinted from Biscotti and Singh [56]. With permission from Karger Publishers. Copyright © 2011, Karger Publishers)

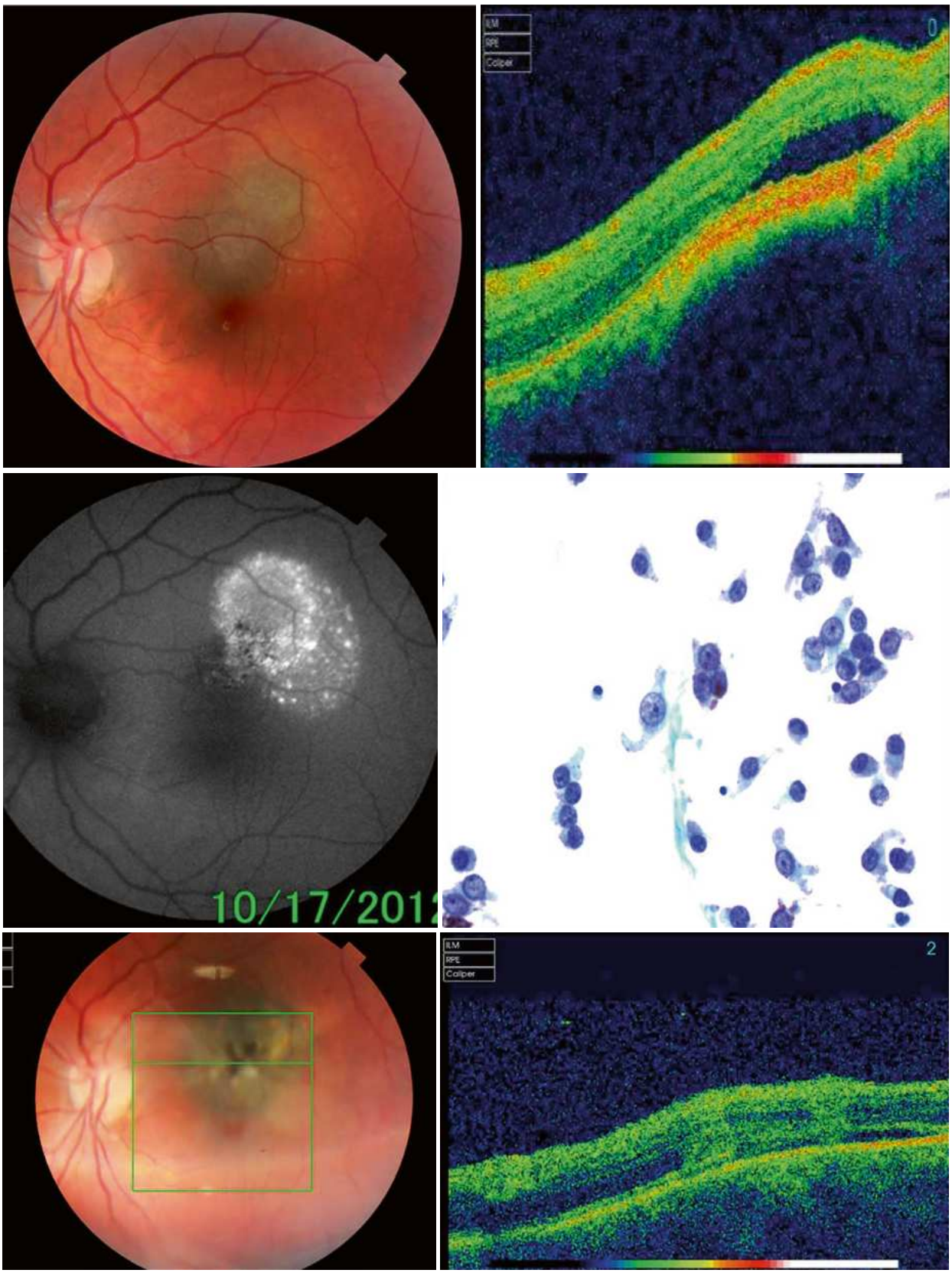

Fig. 24.7 A 14-year-old girl was evaluated for a small melanotic choroidal mass left eye (**a**) After a 5-year follow-up of the lesion, visual acuity began to decrease to 20/100, and growth and presence of subretinal fluid were detected. The ultrasound could not determine echogenicity due to the thin thickness of the lesion: 2.1 × 1.7 × 1.9 mm. Fine-needle aspiration biopsy indicated a transvitreous pathway with vitrectomy. Cytology confirmed choroidal melanoma, HMB45 positive. After 8 weeks, the OCT shows the foveal area in good condition, the retina applied, and no subretinal fluid. (**a**) Fundus SPCT (Small Pigment Choroidal Tumor). (**b**) OCT Subretial Fluid. (**c**) Autofluorescence SRF and Pigment Alteration. (**d**) Cytology. (**e**) Post FNAB Fundus Pospt Op. (**f**) OCT Macula Attach and FNAB`s Area in good condition

24.8 Intraocular Lymphoma

Vitrectomy is required to diagnose vitreoretinal lymphoma as it predominantly manifests as lymphocytic infiltration of the vitreous [58]. Cellular assessment is often done in conjunction with ancillary studies, such as immunohistochemistry or flow cytometry [59–61]. The technique of diagnostic vitrectomy is discussed elsewhere.

24.9 Retinoblastoma and Other Retinal Tumors

Aspiration biopsy in cases of retinoblastoma or suspected retinoblastoma is considered to be a relative contraindication because the risk of seeding of the tumor outside the eye is of particular concern [22, 37, 62, 63]. FNAB is recommended only in highly selected cases of retinal tumors where there is a true diagnostic dilemma after all possible clinical investigations, including an opinion by an expert ophthalmic oncologist, have been obtained [63, 64]. Even so, the FNAB should be done by a modified technique, wherein the needle is passed parallel to the visual axis through the peripheral cornea, anterior chamber, peripheral iris, zonules (avoiding the lens), and into the suspicious area [22]. Tripe freeze-thaw cryotherapy to the needle entry site, similar to the method of intravitreal chemotherapy injection, may also be considered [65].

24.10 Orbital Tumors

The role of orbital FNAB, particularly for lacrimal gland tumors, lymphoproliferative tumors, and metastatic lesions of the orbit, is discussed elsewhere [66].

24.11 Complications

24.11.1 False-Negative Biopsy

Limited cellularity can compromise the diagnostic potential of ophthalmic aspirate samples [16, 67]. In our series of 30 unpublished cases, four cases had limited cellularity. One patient, whose biopsy was read as "negative," subsequently underwent an incisional biopsy, which revealed a uveal schwannoma [68]. Augsburger, in his case series, reported two false negatives out of five total negative reports [15].

A negative cytologic diagnosis of malignancy should not be considered unequivocal proof that an intraocular malignancy does not exist [15]. Others have also echoed similar views regarding the unreliability of negative diagnoses [37, 46]. Care must be given to important practical considerations to reduce the likelihood of a negative biopsy (Table 24.2).

Table 24.2 Practical considerations to reduce likelihood of a nondiagnostic ocular fine-needle aspiration biopsy

Factors	Guidance
Tumor size	Avoid small tumors (less than 2.5 mm in height)
Needle size	Avoid thinner needle (such as 30-gauge)
Aspiration	Avoid plunger retraction once aspiration has been completed
Sample	Avoid dry smears. Rinse the needle into a transport medium flushing the contents of the needle and syringe several times
Experience	Practice on enucleated globes to familiarize with the techniques
Personnel	Experienced cytopathologist is essential

Reprinted from Singh et al. [38]. With permission from Karger Publishers. Copyright © 2011, Karger Publishers

24.11.2 False-Positive Biopsy

Overall concordance between histologic findings and cytologic diagnosis (in experienced centers) may be as high as 95% [15, 38, 53]. In particular, uveal melanocytoma can pose a diagnostic challenge [15, 20].

24.11.3 Needle Tract Seeding

The risk of tumor seeding is low but cannot be overlooked, as it can increase morbidity and mortality. Tumor seeding has been reported after both FNAB and vitrectomy-assisted aspiration biopsy of uveal melanoma [69–71]. A number of approaches have been utilized to decrease the chances of tumor seeding after tumor biopsy, such as the use of small-gauge needles, release of negative pressure before withdrawing the needle, and cryotherapy at the scleral entry site [38]. Singh et al. reported on the use of a valved cannula to access the vitreous cavity, therefore theoretically minimizing the risk of needle tract seeding. Cytopathological analysis has revealed the presence of melanoma and atypical cells in 16/20 cannulas (Fig. 24.8) [42]. Thus, the use of a valved cannula may protect against tumor seeding by trapping tumor cells within the cannula rather than in the sclera tract or pars plana.

24.11.4 Hemorrhage

The most frequent complications are localized subretinal and vitreous hemorrhage at the biopsy site [72]. The hemorrhage

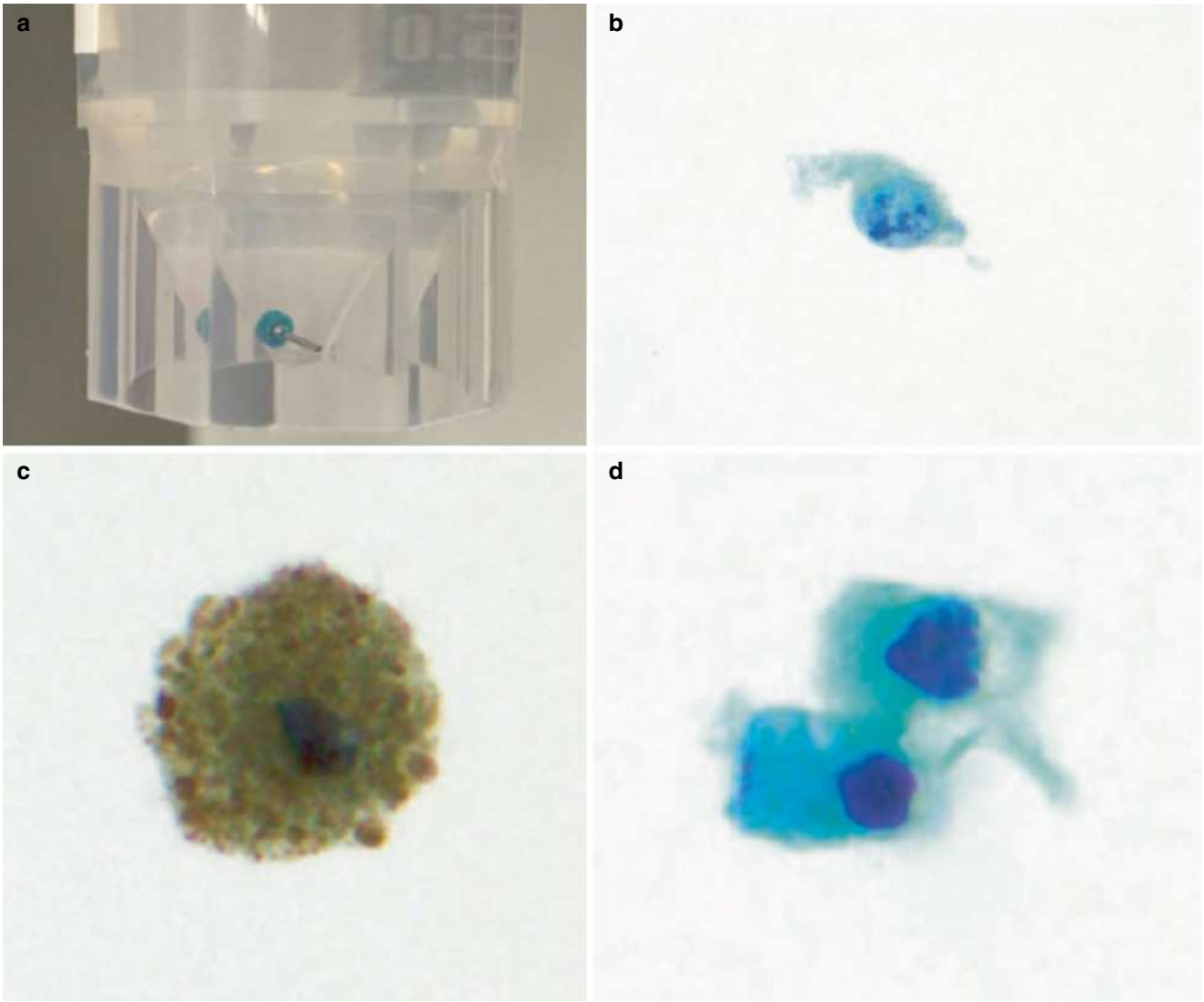

Fig. 24.8 Cells retrieved from the 25G cannula placed in a Cytolyt® solution after ThinPrep processing (Hologic Inc., Marlborough, MA) (**a**). Spindle-shaped melanoma cells with a nucleus containing coarse chromatin and prominent nucleolus (**b**, Papanicolou; original magnification 40×). Coarse melanin granules are typically seen in histiocytes (**c**, Papanicolou; original magnification 40×). Occasional samples contained conjunctival columnar cells consistent (**d**, Papanicolou; original magnification 40×)

is controlled by gentle pressure on the globe immediately after the withdrawal of the needle or by raising the infusion pressure. The hemorrhages typically resolve within a few weeks (Fig. 24.9) [38].

24.11.5 Retinal Detachment

The retinal break created when a subretinal tumor is biopsied transvitreally almost never leads to rhegmatogenous retinal detachment. The break is sealed by the blood clot at the biopsy site (Fig. 24.10) [38].

24.11.6 Endophthalmitis

Aspiration biopsy-induced endophthalmitis is extremely rare as biopsy of intraocular tumors is performed under sterile conditions. Only two such cases have been reported [20, 38, 52].

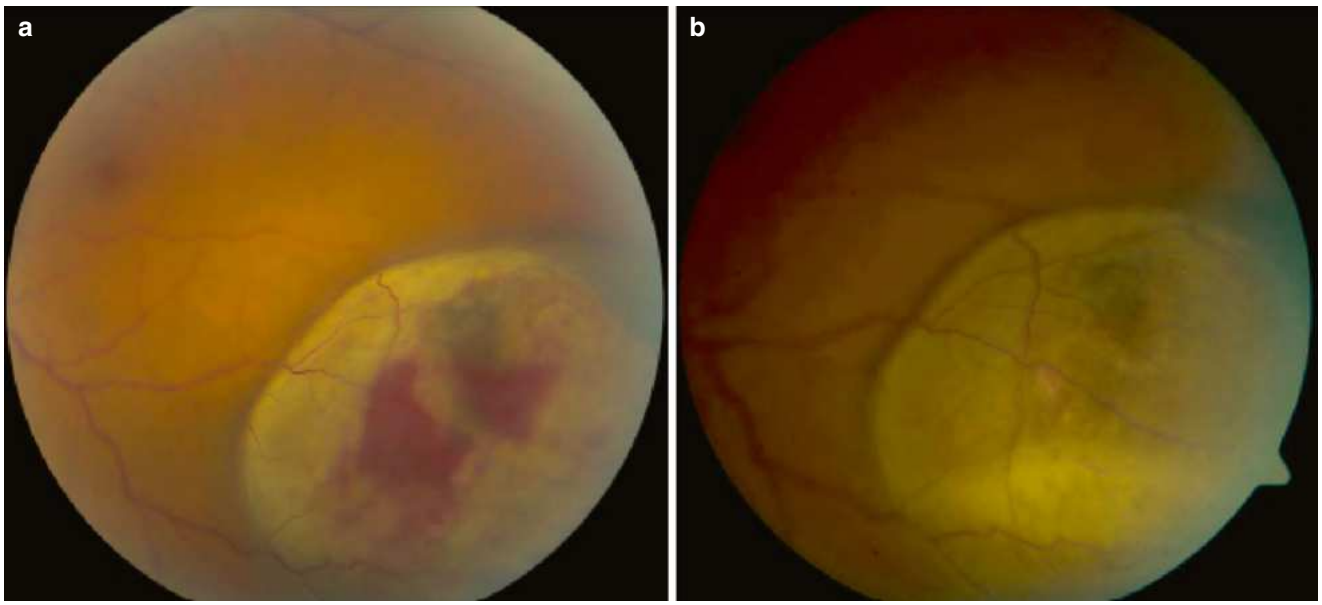

Fig. 24.9 Localized subretinal hemorrhage at the biopsy site, 2 days postoperatively (**a**). Note the total resolution of hemorrhage at 4 weeks (**b**). (Reprinted from Singh et al. [38]. With permission from Karger Publishers. Copyright © 2011, Karger Publishers)

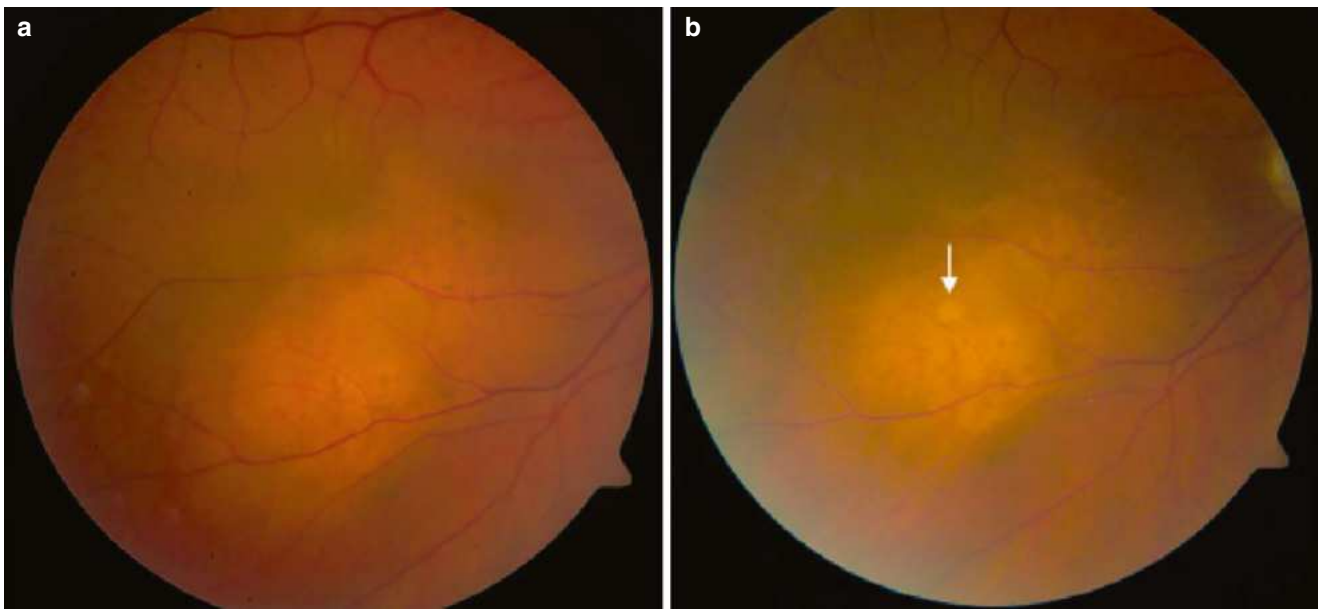

Fig. 24.10 Retinal detachment. Pre-biopsy appearance (**a**). Spontaneous closure of the retinal break created during transvitreal fine needle aspiration biopsy (**b**, arrow). (Reprinted from Singh et al. [38]. With permission from Karger Publishers. Copyright © 2011, Karger Publishers)

24.12 Conclusions

The large majority of intraocular tumors can be diagnosed by clinical examination and ocular imaging studies, which obviate the need for diagnostic ophthalmic biopsy. Overall, the diagnostic accuracy of ophthalmic biopsy is high, but limited cellularity can compromise the diagnostic potential of ocular aspirate samples. Procedures to obtain tumor cells are commonly performed not only to confirm the diagnosis of UM but also to obtain a tissue sample for prognosis, which can help assess the risk of producing patient-specific metastasis. This is currently so, but in the case of lesions less than 3 mm thick, we do not believe in having another way of diagnosis except waiting for the growth of the lesion with the risks involved in such conduct. The assistance of an experienced cytopathologist cannot be overemphasized. With an improved

understanding of genetic prognostic factors of uveal melanoma, ophthalmic aspiration biopsy is gaining popularity for prognostic purposes in combination with eye-conserving treatment of the primary tumor.

References

1. Long SR, Cohen MB. Classics in cytology VII: Kun, Lebert, and early efforts at fine-needle aspiration biopsy. Diagn Cytopathol. 1996;14(2):182–3.
2. Webb AJ. Early microscopy: history of fine needle aspiration (FNA) with particular reference to goitres. Cytopathology. 2001;12(1):1–6.
3. Ansari NA, Derias NW. Fine needle aspiration cytology. J Clin Pathol. 1997;50(7):541–3.
4. Rosa M. Fine-needle aspiration biopsy: a historical overview. Diagn Cytopathol. 2008;36(11):773–5.
5. Frable WJ. Fine-needle aspiration biopsy: a review. Hum Pathol. 1983;14(1):9–28.
6. Hajdu SI, Ehya H. Foundation of diagnostic cytology. Ann Clin Lab Sci. 2008;38(3):296–9.
7. Veasey CA Jr. Intraocular biopsy. Am J Ophthalmol. 1951;34(3):432–4.
8. Long JC, Black WC, Danielson RW. Aspiration biopsy in intraocular tumors. AMA Arch Ophthalmol. 1953;50(3):303–10.
9. Jensen OA, Andersen SR. Late complications of biopsy in intraocular tumors. Acta Ophthalmol. 1959;37:568–75.
10. Takemura T, Tomatsu Y. Studies on malignant melanoma of the choroid. I. Needle biopsy, light microscopy, and electron microscopy. Nippon Ganka Gakkai Zasshi. 1967;71(8):1317–22.
11. Makley TA Jr. Biopsy of intraocular lesions. Am J Ophthalmol. 1967;64(3 Suppl):591–9.
12. Sagiroglu N, Ozgonul T, Muderris S. Diagnostic intraocular cytology. Acta Cytol. 1975;19(1):32–7.
13. Grgic Z, Ljustina-Ivancic N. Cytomorphologic findings in the diagnosis of intraocular lymphocytic tumors (author's transl). Klin Monbl Augenheilkd. 1978;173(3):416–8.
14. Jakobiec FA, Coleman DJ, Chattock A, et al. Ultrasonically guided needle biopsy and cytologic diagnosis of solid intraocular tumors. Ophthalmology. 1979;86(9):1662–81.
15. Augsburger JJ, Shields JA, Folberg R, et al. Fine needle aspiration biopsy in the diagnosis of intraocular cancer. Cytologic-histologic correlations. Ophthalmology. 1985;92(1):39–49.
16. Char DH, Kemlitz AE, Miller T, et al. Iris ring melanoma: fine needle biopsy. Br J Ophthalmol. 2006;90(4):420–2.
17. Char DH, Miller TR, Ljung BM, et al. Fine needle aspiration biopsy in uveal melanoma. Acta Cytol. 1989;33(5):599–605.
18. Davila RM, Miranda MC, Smith ME. Role of cytopathology in the diagnosis of ocular malignancies. Acta Cytol. 1998;42(2):362–6.
19. Eide N, Syrdalen P, Walaas L, et al. Fine needle aspiration biopsy in selecting treatment for inconclusive intraocular disease. Acta Ophthalmol Scand. 1999;77(4):448–52.
20. Faulkner-Jones BE, Foster WJ, Harbour JW, et al. Fine needle aspiration biopsy with adjunct immunohistochemistry in intraocular tumor management. Acta Cytol. 2005;49(3):297–308.
21. Shields CL, Manquez ME, Ehya H, et al. Fine-needle aspiration biopsy of iris tumors in 100 consecutive cases: technique and complications. Ophthalmology. 2006;113(11):2080–6.
22. Shields JA, Shields CL, Ehya H, et al. Fineneedle aspiration biopsy of suspected intraocular tumors. The 1992 Urwick Lecture. Ophthalmology. 1993;100(11):1677–84.
23. Correa ZM, Augsburger JJ. Sufficiency of FNAB aspirates of posterior uveal melanoma for cytologic versus GEP classification in 159 patients, and relative prognostic significance of these classifications. Graefes Arch Clin Exp Ophthalmol. 2014;252(1):131–5.
24. Sellam A, Desjardins L, Barnhill R, et al. Fine needle aspiration biopsy in uveal melanoma: technique, complications, and outcomes. Am J Ophthalmol. 2016;162:28–34.e1.
25. Shields CL, Ganguly A, Materin MA, et al. Chromosome 3 analysis of uveal melanoma using fine-needle aspiration biopsy at the time of plaque radiotherapy in 140 consecutive cases: the Deborah Iverson, MD, Lectureship. Arch Ophthalmol. 2007;125(8):1017–24.
26. Shields CL, Say EAT, Hasanreisoglu M, et al. Personalized prognosis of uveal melanoma based on cytogenetic profile in 1059 patients over an 8-year period: the 2017 Harry S. Gradle Lecture. Ophthalmology. 2017;124(10):1523–31.
27. Singh AD, Medina CA, Singh N, et al. Fine-needle aspiration biopsy of uveal melanoma: outcomes and complications. Br J Ophthalmol. 2016;100(4):456–62.
28. Fastenberg DM, Finger PT, Chess Q, et al. Vitrectomy retinotomy aspiration biopsy of choroidal tumors. Am J Ophthalmol. 1990;110(4):361–5.
29. Arbour JD, Mukai S. Biopsy of the retina and the choroid. Int Ophthalmol Clin. 1999;39(1):213–22.
30. Foulds WS. The uses and limitations of intraocular biopsy. Eye. 1992;6(Pt 1):11–27.
31. Bechrakis NE, Foerster MH, Bornfeld N. Biopsy in indeterminate intraocular tumors. Ophthalmology. 2002;109(2):235–42.
32. Kvanta A, Seregard S, Kopp ED, et al. Choroidal biopsies for intraocular tumors of indeterminate origin. Am J Ophthalmol. 2005;140(6):1002–6.
33. Sen J, Groenewald C, Hiscott PS, et al. Transretinal choroidal tumor biopsy with a 25-gauge vitrector. Ophthalmology. 2006;113(6):1028–31.
34. Char DH. Intraocular biopsy. In: Singh AD, Damato BE, Pe'er J, et al., editors. Clinical ophthalmic oncology. Philadelphia: Saunders-Elsevier; 2007.
35. Green WR. Diagnostic cytopathology of ocular fluid specimens. Ophthalmology. 1984;91(6):726–49.
36. Augsburger JJ, Shields JA. Fine needle aspiration biopsy of solid intraocular tumors: indications, instrumentation and techniques. Ophthalmic Surg. 1984;15(1):34–40.
37. Eide N, Walaas L. Fine-needle aspiration biopsy and other biopsies in suspected intraocular malignant disease: a review. Acta Ophthalmol. 2009;87(6):588–601.
38. Singh AD, Pelayes DE, Brainard JA, et al. History, indications, techniques and limitations. Monogr Clin Cytol. 2012;21:1–9.
39. Pelayes DE, Zarate JO, Biscotti CV, et al. Calibrated needle for ophthalmic fine needle aspiration biopsy. Br J Ophthalmol. 2012;96(8):1147–8.
40. Young TA, Burgess BL, Rao NP, et al. Transscleral fine-needle aspiration biopsy of macular choroidal melanoma. Am J Ophthalmol. 2008;145(2):297–302.
41. Pelayes DE, Zárate JO, Biscotti CV, Singh AD. Calibrated needle for ophthalmic fine needle aspiration biopsy. Br J Ophthalmol. 2012;96(8):1147–8. https://doi.org/10.1136/bjophthalmol-2012-301572.
42. Singh AD, Aziz HA, Pelayes D, Biscotti CV. Twenty-five-gauge cannula-assisted fine-needle aspiration biopsy of choroidal melanoma: cytopathological Analysis. Retina. 2017;37(9):1674–7.
43. Grossniklaus HE. Fine-needle aspiration biopsy of the iris. Arch Ophthalmol. 1992;110(7):969–76.
44. Singh AD, Aziz HA, Pelayes D, et al. Twenty-five-gauge cannula-assisted fine-needle aspiration biopsy of choroidal melanoma: cytopathological analysis. Retina. 2017;37(9):1674–7.
45. Brainard JA, Biscotti CV. Cytological preparation. Monogr Clin Cytol. 2012;21:10–6.

46. Pelayes DE, Zarate JO. Fine needle aspiration biopsy with liquid-based cytology and adjunct immunohistochemistry in intraocular melanocytic tumors. Eur J Ophthalmol. 2010;20(6):1059–65.
47. Augsburger JJ, Correa ZM. Taxonomy of intraocular tumor biopsies. Implications for reporting and comparison of results. IOVS 2012;53:ARVO E-Abstract 3397 2012.
48. Seregard S. To biopsy or not to biopsy? Acta Ophthalmol. 2009;87(6):586–7.
49. Turell ME, Tubbs RR, Biscotti CV, et al. Uveal melanoma: prognostication. Monogr Clin Cytol. 2012;21:55–60.
50. Alzahrani YA, Aziz HA, Shrestha NK, et al. Cryptococcal iridociliary granuloma. Surv Ophthalmol. 2016;61(4):498–501.
51. Bianchi JI, Graue EF, Lopez-Rubio S, et al. Diagnostic and therapeutic challenges. Retina. 2018;38(9):1873–5. https://doi.org/10.1097/IAE.0000000000002190. PMID 29864073.
52. Augsburger JJ, Correa ZM, Schneider S, et al. Diagnostic transvitreal fine-needle aspiration biopsy of small melanocytic choroidal tumors in nevus versus melanoma category. Trans Am Ophthalmol Soc. 2002;100:225–32; discussion 32–4.
53. Ylagan LR. Intraocular pigmented proliferations in the context of cytologic evaluation. Diagn Cytopathol. 2009;37(11):853–64.
54. Cohen VM, Dinakaran S, Parsons MA, et al. Transvitreal fine needle aspiration biopsy: the influence of intraocular lesion size on diagnostic biopsy result. Eye (Lond). 2001;15(Pt 2):143–7.
55. Augsburger JJ. Fine needle aspiration biopsy of suspected metastatic cancers to the posterior uvea. Trans Am Ophthalmol Soc. 1988;86:499–560.
56. Biscotti CV, Singh AD. Uveal melanoma: diagnostic features. Monogr Clin Cytol. 2012;21:44–54.
57. Medina CA, Biscotti CV, Singh N, et al. Diagnostic cytologic features of uveal melanoma. Ophthalmology. 2015;122(8):1580–4.
58. Shields CL, Shields JA, Gross NE, et al. Survey of 520 eyes with uveal metastases. Ophthalmology. 1997;104(8):1265–76.
59. Trichopoulos N, Augsburger JJ. Neuroendocrine tumours metastatic to the uvea: diagnosis by fine needle aspiration biopsy. Graefes Arch Clin Exp Ophthalmol. 2006;244(4):524–8.
60. Char DH, Ljung BM, Deschenes J, et al. Intraocular lymphoma: immunological and cytological analysis. Br J Ophthalmol. 1988;72(12):905–11.
61. Davis JL, Solomon D, Nussenblatt RB, et al. Immunocytochemical staining of vitreous cells. Indications, techniques, and results. Ophthalmology. 1992;99(2):250–6.
62. Davis JL, Viciana AL, Ruiz P. Diagnosis of intraocular lymphoma by flow cytometry. Am J Ophthalmol. 1997;124(3):362–72.
63. Farkas T, Harbour JW, Davila RM. Cytologic diagnosis of intraocular lymphoma in vitreous aspirates. Acta Cytol. 2004;48(4):487–91.
64. Karcioglu ZA. Fine needle aspiration biopsy (FNAB) for retinoblastoma. Retina. 2002;22(6):707–10.
65. Ali MJ, Honavar SG, Vemuganti GK. Ciliary body medulloepithelioma in an adult. Surv Ophthalmol. 2013;58(3):266–72.
66. Singh AD, Soto H, Bellerive C, et al. Reactive retinal astrocytic tumor (focal nodular gliosis): report of the clinical spectrum of 3 cases. Ocul Oncol Pathol. 2017;3(3):235–9.
67. Munier FL, Gaillard MC, Balmer A, et al. Intravitreal chemotherapy for vitreous disease in retinoblastoma revisited: from prohibition to conditional indications. Br J Ophthalmol. 2012;96(8):1078–83.
68. Seregard S, Tani E. Fine needle aspiration cytology in orbital tumors. Monogr Clin Cytol. 2012;21:82–9.
69. Ali MJ, Honavar SG, Vemuganti GK, et al. Fine needle aspiration biopsy of retinal tumors. Monogr Clin Cytol. 2012;21:72–81.
70. Turell ME, Hayden BC, McMahon JT, et al. Uveal schwannoma surgery. Ophthalmology. 2009;116(1):163–e6.
71. Caminal JM, Sanz S, Carreras M, et al. Epibulbar seeding at the site of a transvitreal fine-needle aspiration biopsy. Arch Ophthalmol. 2006;124(4):587–9.
72. Raja V, Russo A, Coupland S, et al. Extraocular seeding of choroidal melanoma after a transretinal biopsy with a 25-gauge vitrector. Retin Cases Brief Rep. 2011;5(3):194–6.
73. Schefler AC, Gologorsky D, Marr BP, et al. Extraocular extension of uveal melanoma after fine-needle aspiration, vitrectomy, and open biopsy. JAMA Ophthalmol. 2013;131(9):1220–4.

Diagnostic Techniques: Other Biopsy Techniques

25

Bertil E. Damato, Armin Afshar, Rumana Hussain, Heinrich Heimann, Carl Groenewald, and Sarah E. Coupland

25.1 Introduction

Biopsy involves the removal of a tissue or fluid sample, laboratory analysis, and interpretation of the results (Box 25.1). The usual objective of a biopsy has been to establish or confirm a diagnosis. For example, biopsy is useful when clinical examination fails to distinguish a choroidal melanoma from a nevus or metastasis. Even when there is a confident clinical diagnosis, a biopsy may be performed to determine the tumor subtype. For example, when a choroidal metastasis is diagnosed in a patient who does not have a history of systemic malignancy, morphological and immunohistochemical examinations of the biopsy may indicate the likely site of the primary tumor so that investigations can be targeted accordingly. Increasingly, uveal melanoma biopsy is being performed to enhance prognostication by integrating histologic and genetic findings with the clinical tumor stage. Recently, liquid biopsy of aqueous fluid or blood has been deployed in patients with retinoblastoma, uveal melanoma, and metastasis. Biopsy is essential in the management of patients with suspected vitreoretinal lymphoma and is discussed elsewhere (Volume 6, Chap. 8: Primary Central Nervous System and Retinal Lymphoma).

B. E. Damato (✉)
Ocular Oncology Service, Moorfields Eye Hospital, London, UK
e-mail: bertil.damato@nhs.net

A. Afshar
Ocular Oncology Service, Departments of Ophthalmology and Radiation Oncology, University of California San Francisco, San Francisco, CA, USA
e-mail: armin.afshar@ucsf.edu

R. Hussain · H. Heimann · C. Groenewald
Liverpool Ocular Oncology Centre, St Paul's Eye Unit, Royal Liverpool University Hospital, Liverpool, UK
e-mail: rumana.hussain@liverpoolft.nhs.uk; heinrich.heimann@rlbuht.nhs.uk; carl.groenewald@rlbuht.nhs.uk

S. E. Coupland
Department of Eye and Vision Science, University of Liverpool, Liverpool, UK
e-mail: s.e.coupland@liv.ac.uk

An intraocular tumor can be analyzed by aspiration, incisional, excisional, and liquid biopsy techniques, depending on its size and location in the eye (Box 25.1). Fine-needle aspiration biopsy and liquid biopsy are described elsewhere (Volume 1, Chap. 24: Diagnostic techniques: FNAB & Volume 7, Chap. 24). Here, we overview aspiration biopsy with a vitreous cutter as well as incisional and excisional biopsy techniques.

Box 25.1 Other Biopsy Techniques

- Techniques include vitreous-cutter biopsy, incision and excision biopsy, and liquid biopsy.
- The biopsy procedure depends on the objectives and tumor location.
- Anticoagulant therapy is a relative contraindication if this treatment cannot be suspended.
- Collaboration with an experienced laboratory team is essential.
- Successful biopsy requires adequate handling of the specimen.

25.2 Vitreous-Cutter Aspiration Biopsy of Tumors

A vitreous cutter can be used to biopsy anterior chamber tumors as well as solid lesions in the posterior segment of the eye [1–6]. It provides larger tissue samples than fine-needle aspiration biopsy, even with hard tissue.

25.2.1 Indications and Contraindications

A diagnostic biopsy is performed if the clinical uncertainty is unacceptable to the treating physician or the patient. With melanocytic tumors of uncertain malignancy, a biopsy may

© The Author(s), under exclusive license to Springer Nature Switzerland AG 2025

A. D. Singh, B. E. Damato (eds.), *Clinical Ophthalmic Oncology*, https://doi.org/10.1007/978-3-031-75907-9_25

be performed as an alternative to long-term surveillance if the patient is concerned that delayed treatment may enhance the risk of metastatic disease. If treatment of a small choroidal melanoma is likely to cause severe visual loss, biopsy may be done to estimate the risk of metastasis more reliably and hence decide whether to treat the tumor immediately or whether to defer treatment until growth is detected. When a choroidal metastasis from an occult systemic malignancy is suspected, a biopsy can be performed in the first instance to plan systemic investigations or else only if extensive systemic investigations have proved inconclusive, whichever approach is likely to be most expeditious.

In patients receiving plaque or proton beam radiotherapy, we perform prognostic biopsy after the radiotherapy, if possible, to minimize any risk of tumor seeding and to avoid any possibility of the treatment being hampered by vitreous hemorrhage [7]. This involves biopsy on the last day of proton beam radiotherapy or about 4 weeks after plaque brachytherapy, once the eye has settled down (Fig. 25.1). This approach is successful with genetic methods such as multiplex ligation-dependent probe amplification (MLPA), microsatellite analysis, and next generation sequencing [8, 9].

The main contraindication to biopsy is anticoagulant therapy if this cannot be stopped a few days before the surgical procedure because of the increased risk of a serious intraocular hemorrhage. If the patient has poor vision in the fellow eye or if the individual is monocular, we may dispense with a biopsy if the patient is able to accept a less certain prognosis. High myopia increases the risk of rhegmatogenous retinal detachment after trans-retinal biopsy, which is therefore avoided, if possible, in patients with this condition.

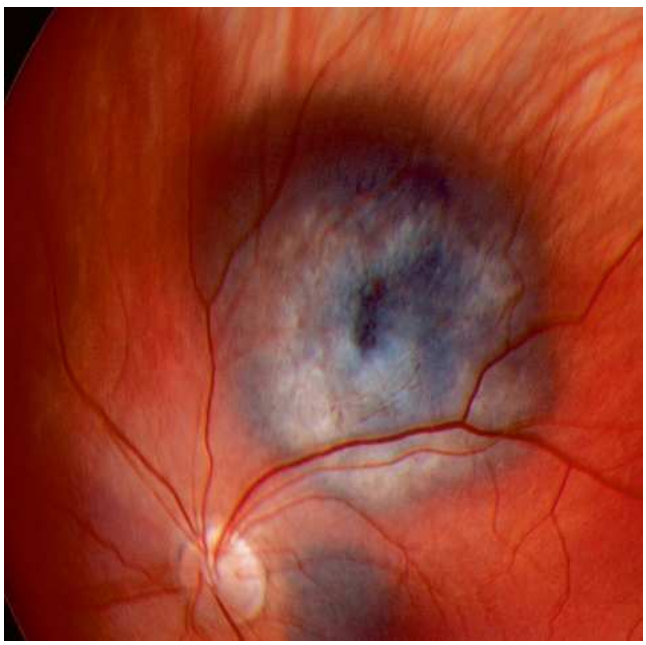

Fig. 25.1 Left fundus of a 61-year-old man with a choroidal melanoma measuring 10.3 mm basally with a thickness of 3.5 mm. The biopsy site is visible as a dark area. The tumor was of spindle-cell type, and multiplex ligation-dependent probe amplification showed no chromosome 3 loss. More than 4.5 years after treatment, the patient was alive and well, with a good tumor response and visual acuity of 20/20 in the treated eye

25.2.2 Surgical Technique

We perform intraocular tumor biopsy with a 25- or 27-gauge vitreous cutter, using a 3-port, sutureless vitrectomy kit. The procedure is usually done under local anesthesia.

The vitreous cutter is passed through the retina, avoiding any large retinal blood vessels. The cutting rate is lowered with maximum suction. If hemorrhage occurs after removing the cutter from the tumor, the intraocular pressure is raised until the bleeding stops. The intraocular pressure is lowered after about a minute. If the hemorrhage recurs, the procedure is repeated. If the tumor is very thin (i.e., less than 2 mm thick), the retinotomy is placed near the tumor margin and the retina is lifted slightly away from the tumor surface by moving the vitreous-cutter sideways toward the tumor center. The vitreous cutter is rotated so that the port faces the center of the tumor before cutting is started. Vitrectomy, endolaser photocoagulation, and internal tamponade are not required. A small amount of vitreous is aspirated, with a high cutting rate, to collect the specimen into a vacutainer tube to which transport medium is then added. Visible tumor fragments are noted before samples are sent for analysis.

With anterior segment tumors, the vitreous cutter is introduced into the anterior chamber through a clear corneal incision, using an anterior chamber maintainer to maintain the intraocular pressure.

25.2.3 Results and Complications

The main complication is the failure to obtain sufficient tissue for both histologic and genetic studies; however, we have modified our surgical and laboratory procedures to optimize the yield, thereby enabling all analyses to be performed, even with small tumors in the large majority of cases. We are of the opinion that the results of all molecular genetic tests should be interpreted within the morphological context. For example, a disomy 3 or a Class 1 result is meaningless without knowing what cells have been assessed since such results could also be obtained from normal tissue (i.e., choroid) or intra-tumoral inflammatory cells, such as macrophages. Limited intravitreal perilesional bleeding is common and resolves spontaneously. Other complications are similar to those of FNAB and include dense vitreous hemorrhage, rhegmatogenous retinal detachment, cataract, and endophthalmitis [10]. Seeding of the tumor into the episclera can

occur but is exceedingly rare, especially if cryotherapy is applied to the sclerotomy sites when the vitrectomy cannulas are removed [11].

25.3 Incisional Biopsy

Incisional biopsy involves the removal of a wedge of tumor tissue. An advantage of this technique over aspiration biopsy is that the tumor sample tends to be larger.

25.3.1 Indications and Contraindications

We perform an incisional biopsy of choroidal melanomas for prognostic purposes if we consider a peripheral tumor to be too thin for trans-scleral FNAB (i.e., <3 mm thick). In such a case, we find that it is easier and safer to obtain a large tumor sample if we can visualize the uvea through a scleral window.

25.3.2 Surgical Technique

The first author's technique is to make a partial-thickness, lamellar scleral flap, which is hinged posteriorly (Fig. 25.2a). This is approximately 8 mm in diameter, both transversely and longitudinally. The radial incisions extend only about two-thirds of the length of the flap to create a pocket in which any blood can collect. The deep scleral incision is made anterior to the midpoint of the tumor, near the hinge of the scleral flap. Essen forceps produce large tumor pellets [12]. These forceps are repeatedly introduced into the tumor until 5–6 tumor pellets have been obtained (Fig. 25.2b, c). The forceps are flushed with BSS into a sterile universal tube in between each introduction to collect the specimens. Bipolar diathermy is applied to any pigment that seeds through the deep sclerotomy (Fig. 25.2d). The superficial scleral flap is glued in place with tissue glue (Fig. 25.2e). Suturing is performed at the discretion of the surgeon on a case-by-case basis (Fig. 25.2f). If the patient is undergoing brachytherapy, the biopsy is performed after removing the plaque template and before inserting radioactive plaque (Fig. 25.2g). Preferably, however, the biopsy is done at the time of plaque removal, when there should be no risk of tumor seeding because all malignant cells have been sterilized by radiation.

25.3.3 Results and Complications

The use of Essen forceps has improved the tissue yield when sampling small, anterior choroidal tumors [13]. Premature perforation of the deep sclera can result in damage to the normal uvea and underlying retina. A buttonhole in the superficial scleral flap or the use of excessive glue can result in damage to the delicate, internal surface of a ruthenium plaque when histoacryl glue is used. Tumor seeding can occur if any hemorrhage is not immediately swabbed away.

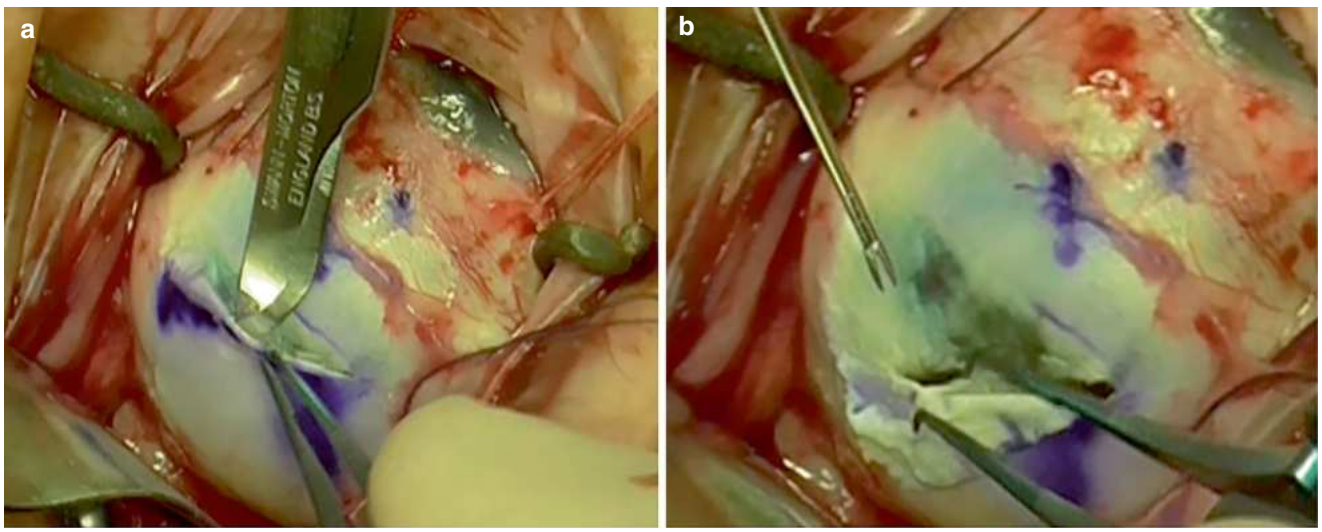

Fig. 25.2 Incisional biopsy technique developed by the first author (BD). A superficial, lamellar scleral flap is created (**a**); a deep scleral incision is made for introduction of Essen forceps into the tumor (**b**); the specimens are collected onto a paper tissue before transferring into a container (**c**); any pigment is treated with bipolar cautery (**d**); the flap is closed with tissue glue (**e**); if necessary, sutures are placed (**f**); the radioactive plaque is inserted (**g**); and the specimen is examined microscopically on arrival at the laboratory (**h**)

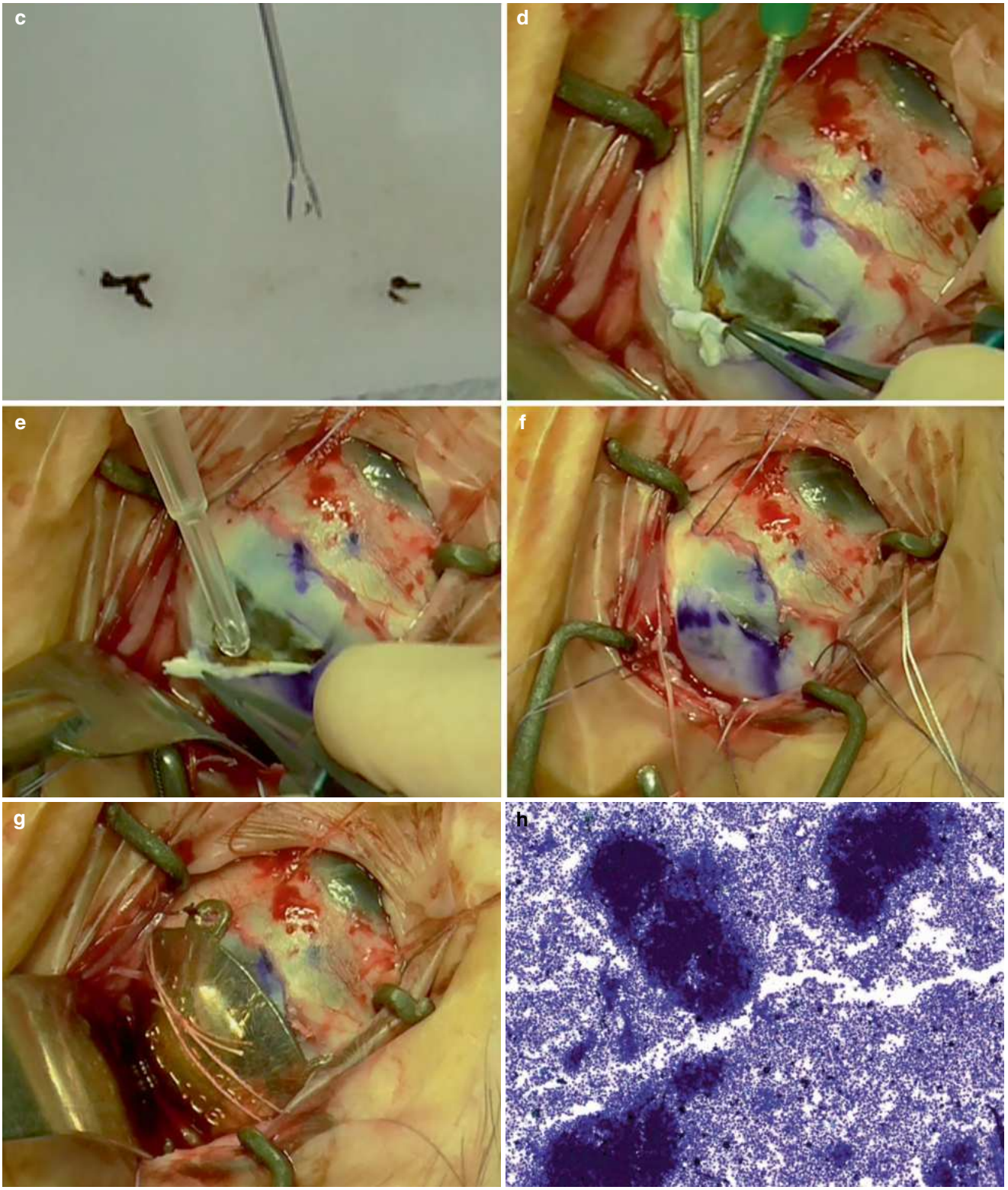

Fig. 25.2 (continued)

25.4 Excisional Biopsy

With excisional biopsy, the entire tumor is surgically removed so that the procedure is therapeutic as well as diagnostic or prognostic. The main difference between excision biopsy and therapeutic resection is in the pre-operative counseling of the patient.

25.4.1 Indications and Contraindications

Excision biopsy is performed when the clinical diagnosis is uncertain, for example, if melanoma cannot reliably be differentiated from lesions such as adenocarcinoma, neurilemmoma, or neurofibroma. Excision biopsy of small ciliary body tumors may be preferred to radiotherapy when aspiration or incisional biopsy is unlikely to produce enough tissue for histologic and genetic studies (Fig. 25.3) [14–16].

25.4.2 Surgical Technique

The surgical techniques are described in Volume 5, Chap. 21 (Uveal Melanoma: Resection Techniques).

25.4.3 Results and Complications

Compared to other biopsy techniques, excision biopsy yields the largest possible tumor sample. The complications of this technique are the same as those of local resection. In the author's experience, orbital recurrence is extremely rare.

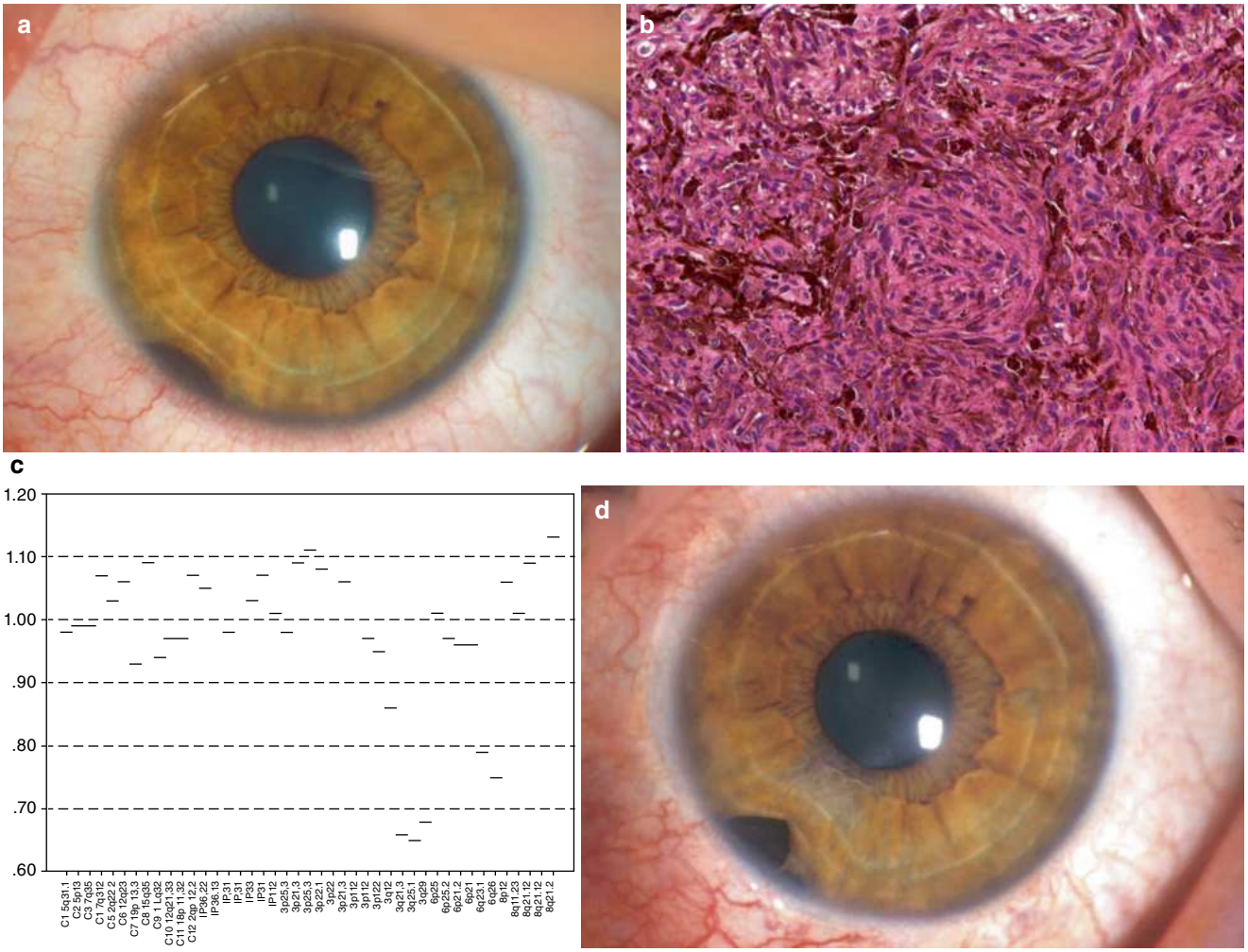

Fig. 25.3 Left eye of a 23-year-old woman, who was referred in 2007 with an infero-nasal ciliary body tumor measuring 4.5 × 3.9 × 2.0 mm (**a**). Excision biopsy showed this to be a melanoma of mixed-cell type (**b**). Fluorescence in situ hybridization suggested disomy 3 and a good prognosis. Multiplex ligation-dependent probe amplification, however, revealed deletions on chromosome 3q, indicating a significant risk of metastasis (**c**). Ocular appearance 2 months postoperatively, when the visual acuity was 20/20 (**d**). (From Damato [14], with permission)

25.5 Liquid Biopsy

25.5.1 Aqueous Humor

With retinoblastoma, it is essential to determine whether the disease is hereditary or non-hereditary. If the patient has only a solitary tumor in one eye and a negative family history, a blood test is performed to establish whether the mutation is constitutional or somatic. The risk of a false-negative blood test is less if the underlying retinoblastoma mutations have been identified by analysis of a tumor sample. Such a specimen can be obtained only after enucleation, because if the eye is conserved, then tumor biopsy would have a high risk of tumor seeding into the orbit. Berry and associates in Los Angeles have found that tumor cell-free DNA can safely be extracted from aqueous humor [17]. In addition to identifying the causative retinoblastoma mutations, this liquid biopsy also reveals secondary genetic abnormalities (i.e., chromosome 6p and/or *MycN* gain) that indicate an increased risk of failed eye-conserving treatment and perhaps an increased risk of metastatic disease (e.g., *BCOR* mutation).

Tumor DNA, RNA, and miRNA have also been successfully extracted from aqueous humor from most eyes with uveal melanomas, especially with larger, anterior tumors with lethal genetic findings, and following brachytherapy [18]. This approach may, therefore, avoid the need for invasive biopsy when estimating the risk of metastasis and planning a schedule for systemic surveillance.

Aqueous *MYD88* L265P analysis is less invasive than a vitreous biopsy and may aid in the diagnosis and monitoring of patients with vitreoretinal lymphoma [19].

25.5.2 Vitreous

Vitreous biopsy is essentially a form of liquid biopsy, although not usually referred to as such. It is essential in patients with suspected vitreoretinal lymphoma, and success rates have improved with advances in surgical techniques and genetic methods such as next-generation sequencing and metagenomic deep sequencing [20–23].

A vitreous biopsy is also useful for identifying malignant cells that have seeded from a uveal melanoma or metastasized from a cutaneous melanoma.

25.5.3 Circulating Blood

Abramson and associates have found that patients with retinoblastoma are more likely to develop metastatic disease if *RB1* DNA detected in blood plasma at presentation persists after the completion of the ocular treatment [24]. This research group has also identified circulating tumor DNA in about 25–30% of patients with uveal melanoma during the first post-operative day after enucleation and 1 or 2 days later after brachytherapy [25]. Increasing levels of circulating tumor DNA (e.g., *GNAS*, *FOXO1*) were found in patients who subsequently developed metastatic disease [25]. Circulating tumor cells and monosomy 3 have been detected in patients with small melanocytic choroidal tumors, especially if these showed clinical features of malignancy, such as lipofuscin and subretinal fluid [26]. This technology may help estimate the risk of metastasis and decide whether to treat such tumors immediately or only if growth is detected. In patients with uveal metastases, liquid biopsy may indicate the site of the primary malignancy and guide treatment [22, 27].

25.6 Laboratory Techniques

25.6.1 Transport

Close collaboration with a specialized ophthalmic laboratory is essential to ensure that the correct transport medium is used and so that the laboratory team can prepare for the arrival of the specimen. Recommended solutions include "soft fixatives" such as CytoLyt and H.O.P.E. Fixation, which enable rapid processing of the samples as cytospins (see below) (Volume 1, Chap. 5: Pathology Specimen: Handling technique) [28].

25.6.2 Laboratory Investigations

If a biopsy is taken for diagnostic purposes, several cytospin slides are prepared for morphological and immunohistochemical staining. One cytospin is stained with May-Grünwald Giemsa (MGG) for cytomorphological assessment, allowing for a targeted immunohistochemical panel. If the biopsy is performed for prognostic purposes in uveal melanoma, the number of cytospin slides is reduced to a minimum to preserve as much material as possible for molecular genetic analyses. The different techniques currently available for molecular genetic analyses in uveal melanoma are described elsewhere (Volume 5, Chap. 10: Uveal Melanoma: Molecular Pathology).

25.7 Discussion

Tumor biopsy requires surgical expertise as well as a highly skilled and well-equipped laboratory team to achieve high success rates without excessive iatrogenic morbidity.

Although we have outlined the main indications and contraindications, much depends on the individual patient's attitudes to diagnostic and/or prognostic uncertainty and concerns about possible complications.

Regarding uveal metastases, the conventional approach is to resort to biopsy only if extensive systemic investigations are inconclusive. We prefer to perform the biopsy in the first instance because immediate biopsy not only expedites diagnosis and treatment but also enables systemic investigations to be selected according to the histologic results. In some cases, laboratory results can help select treatment according to the molecular pathology of the tumor (e.g., HER2 positivity of breast carcinoma metastases and the presence of EGFR mutations in lung carcinoma metastases would result in specific therapeutic regimens being selected for the patients).

Whether to observe melanocytic tumors of uncertain malignancy until growth is observed is controversial because this results in the treatment of some melanomas being delayed by several months or years. It is logistically difficult to evaluate the safety of such procrastination because a randomized clinical trial would require large numbers of patients and many years of follow-up. We have seen a patient with a small choroidal melanoma, which suddenly grew rapidly after enlarging slowly over several years; histologic and genetic analysis after enucleation showed that the older, basal part of the melanoma was of spindle-cell, disomy 3 type, whereas the new, apical region of the tumor was of epithelioid, monosomy 3 type [29]. This patient died of metastatic disease, which might have been prevented if she had been treated without delay. This case also suggests that, although aggressive histology and lethal genetic features indicate the need for urgent treatment, lack of such adverse findings in a "low-grade" melanoma does not necessarily imply that it is safe to leave a melanoma untreated, because malignancy and lethality can increase over time if treatment is deferred [30]. Conversely, only about 50% of small melanocytic choroidal tumors with all TFSOM features (Thickness >2 mm, Fluid under the retina, Symptoms, Orange pigment, Melanoma hollow on ultrasonography) show any growth within 5 years [31]. It would seem reasonable, therefore, to monitor small melanomas closely (i.e., every 4–6 months) and to defer treatment until growth is documented [32]. This approach may enable some patients to retain useful vision for months or years, with some never needing to undergo any treatment at all. However, lethal genetic aberrations are found in a significant proportion of small choroidal melanomas [33]. Ideally, therefore, all small melanomas should be biopsied and analyzed for aberrations of chromosomes 3, 6p and 8q as well as mutations of *BAP1*, *EIF1AX*, and *SF3B1* to estimate the risk of metastatic disease and plan management accordingly (Fig. 25.4). As with any treatment, it is essential to confirm and document the patient's understanding and acceptance of the risks and benefits of deferring treatment if this is the course taken.

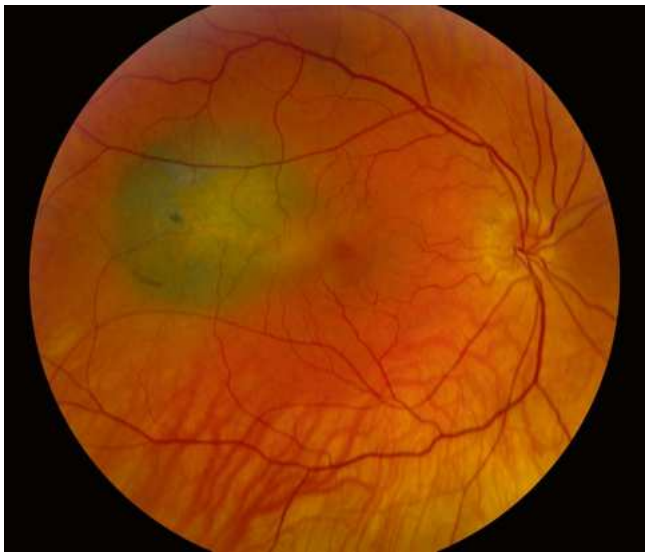

Fig. 25.4 Biopsy to decide between immediate and deferred treatment. A 58-year-old man presented with a choroidal melanoma in the right eye. He initially declined treatment, but when genetic analysis of the tumor with (then experimental) next-generation sequencing showed chromosome 3 loss (confirmed by multiplex ligation-dependent probe amplification), he eventually underwent proton beam radiotherapy

Prognostic biopsy in patients with uveal melanoma is still controversial because some authors believe that there is little scope in predicting metastasis if such disease is usually untreatable; however, recent clinical studies are reporting encouraging results [34, 35]. These raise prospects for clinical trials of systemic adjuvant therapy, which will probably include only patients who have undergone tumor biopsy for metastatic risk stratification by genetic tumor typing. Our impression is that biopsy usually provides results that improve estimates for survival, thereby reassuring patients with a good prognosis and improving their quality of life. Our studies indicate that even patients with a poor prognosis derive psychological benefits from their biopsy because their awareness of their true condition makes them feel empowered to seek expert medical care and to prepare themselves and their families for any eventuality [36]. We have found that the unhappiest patients are those whose biopsy has failed. We, therefore, consider biopsy failure to be a serious complication, which is why we have developed a variety of surgical techniques and laboratory methods to prevent this problem. Some patients initially decline biopsy because they "cannot face facts," only to change their mind subsequently, with regret. For this reason, we have developed protocols for performing the biopsy but not undertaking any analysis unless the patient specifically authorizes such investigation.

Biopsy of small choroidal tumors is challenging and, therefore, more likely to be successful if performed by an

"oncoVR surgeon" having specialist expertise both in retinal surgery and oncology. It is essential for the surgeon to liaise closely with the pathology team to ensure that full use is made of the limited tissue material available. For example, it is important to specify precisely whether the biopsy has been taken for diagnostic or prognostic purposes. This will determine whether the priority is to perform immunohistochemistry or genetic testing.

As mentioned before, estimation of the survival probability in patients with uveal melanoma requires analysis of clinical, histologic, and genetic data [37]. When completing the pathology request form in such cases, it is useful to inform the pathologist of the basal tumor diameter, tumor thickness, presence of ciliary body involvement, and presence of extraocular spread together with the size of any extraocular nodule. A preprinted questionnaire on the pathology request form helps ensure that all these data are provided.

The data resulting from routine biopsy of uveal melanomas are a valuable resource for research. It is, therefore, important to obtain consent from patients prospectively and to provide the pathology team with documented evidence of any such consent.

25.8 Conclusion

The scope of ocular tumor biopsy is increasing thanks to advances in surgical, histologic, and genetic techniques, thereby enhancing opportunities for tumor diagnosis and typing, prognostication, and management planning.

References

1. Petousis V, Finger PT, Milman T. Anterior segment tumor biopsy using an aspiration cutter technique: clinical experience. Am J Ophthalmol. 2011;152(5):771–5.e1.
2. Sen J, Groenewald C, Hiscott PS, Smith PA, Damato BE. Transretinal choroidal tumor biopsy with a 25-gauge vitrector. Ophthalmology. 2006;113(6):1028–31.
3. Hussain RN, Damato B, Heimann H. Choroidal biopsies; a review and optimised approach. Eye (Lond). 2023;37(5):900–6.
4. Finn AP, Materin MA, Mruthyunjaya P. Choroidal tumor biopsy: a review of the current state and a glance into future techniques. Retina. 2018;38(Suppl 1):S79–87.
5. Nagiel A, McCannel CA, Moreno C, McCannel TA. Vitrectomy-assisted biopsy for molecular prognostication of choroidal melanoma 2 mm or less in thickness with a 27-gauge cutter. Retina. 2017;37(7):1377–82.
6. Snyder LL, Daniels AB. Surgical technique, indications, and outcomes of BIOM-assisted transvitreal biopsy for uveal melanoma. Retina. 2022;42(11):2229–35.
7. Hussain RN, Kalirai H, Groenewald C, Kacperek A, Errington RD, Coupland SE, et al. Prognostic biopsy of choroidal melanoma after proton beam radiation therapy. Ophthalmology. 2016;123(10):2264–5.
8. Afshar AR, Damato BE, Stewart JM, Zablotska LB, Roy R, Olshen AB, et al. Next-generation sequencing of uveal melanoma for detection of genetic alterations predicting metastasis. Transl Vis Sci Technol. 2019;8(2):18.
9. Thornton S, Coupland SE, Olohan L, Sibbring JS, Kenny JG, Hertz-Fowler C, et al. Targeted next-generation sequencing of 117 routine clinical samples provides further insights into the molecular landscape of uveal melanoma. Cancers (Basel). 2020;12(4):1039.
10. Grixti A, Angi M, Damato BE, Jmor F, Konstantinidis L, Groenewald C, et al. Vitreoretinal surgery for complications of choroidal tumor biopsy. Ophthalmology. 2014;121(12):2482–8.
11. Raja V, Russo A, Coupland S, Groenewald C, Damato B. Extraocular seeding of choroidal melanoma after a transretinal biopsy with a 25-gauge vitrector. Retin Cases Brief Rep. 2011;5(3):194–6.
12. Akgul H, Otterbach F, Bornfeld N, Jurklies B. Intraocular biopsy using special forceps: a new instrument and refined surgical technique. Br J Ophthalmol. 2011;95(1):79–82.
13. Angi M, Kalirai H, Taktak A, Hussain R, Groenewald C, Damato BE, et al. Prognostic biopsy of choroidal melanoma: an optimised surgical and laboratory approach. Br J Ophthalmol. 2017;101(8):1143–6.
14. Damato EM, Damato B, Sibbring JS, Coupland SE. Ciliary body melanoma with partial deletion of chromosome 3 detected with multiplex ligation-dependent probe amplification. Graefes Arch Clin Exp Ophthalmol. 2008;246(11):1637–40.
15. Tiberti A, Damato B, Hiscott P, Vora J. Iris ectopic thyroid tissue: report of a case. Arch Ophthalmol. 2006;124(10):1497–500.
16. Schalenbourg A, Coupland S, Kacperek A, Damato B. Iridocyclectomy for neovascular glaucoma caused by proton-beam radiotherapy of pigmented ciliary adenocarcinoma. Graefes Arch Clin Exp Ophthalmol. 2008;246(10):1499–501.
17. Berry JL, Pike S, Shah R, Reid MW, Peng CC, Wang Y, et al. Aqueous humor liquid biopsy as a companion diagnostic for retinoblastoma: implications for diagnosis, prognosis and therapeutic options. Five years of progress. Am J Ophthalmol. 2024;263:188–205.
18. Pike SB, Reid MW, Peng CC, Chang C, Xu BY, Gombos DS, et al. Multicentre analysis of nucleic acid quantification using aqueous humour liquid biopsy in uveal melanoma: implications for clinical testing. Can J Ophthalmol. 2023;S0008-4182(23)00342–3. https://doi.org/10.1016/j.jcjo.2023.10.024. Epub ahead of print.
19. Demirci H, Rao RC, Elner VM, Demirci FY, Axenov L, Betz B, et al. Aqueous humor-derived MYD88 L265P mutation analysis in vitreoretinal lymphoma: a potential less invasive method for diagnosis and treatment response assessment. Ophthalmol Retina. 2023;7(2):189–95.
20. Huang RS, Mihalache A, Popovic MM, Cruz-Pimentel M, Pandya BU, Muni RH, et al. Diagnostic methods for primary vitreoretinal lymphoma: a systematic review. Surv Ophthalmol. 2023;69(3):456–64.
21. Bonzheim I, Salmeron-Villalobos J, Susskind D, Szurman P, Gekeler F, Spitzer MS, et al. [Molecular diagnostics for vitreoretinal lymphoma]. Pathologie (Heidelb). 2023;44(Suppl 3):150–4.
22. Kwak JJ, Lee KS, Lee J, Kim YJ, Choi EY, Byeon SH, et al. Next-generation sequencing of vitreoretinal lymphoma by vitreous liquid biopsy: diagnostic potential and genotype/phenotype correlation. Invest Ophthalmol Vis Sci. 2023;64(14):27.
23. Takhar J, Doan T, Gonzales JA. Vitreoretinal lymphoma: a literature review and introduction of a new diagnostic method. Asia Pac J Ophthalmol (Phila). 2021;10(1):93–8.
24. Abramson DH, Robbins MA, Gobin YP, Dunkel IJ, Francis JH. Circulating tumor DNA posttreatment measurements and clinical correlates in retinoblastoma. JAMA Ophthalmol. 2024;142(3):257–61.

25. Francis JH, Barker CA, Brannon AR, Canestraro J, Robbins M, Swartzwelder CE, et al. Detectability of plasma-derived circulating tumor DNA panel in patients undergoing primary treatment for uveal melanoma. Invest Ophthalmol Vis Sci. 2022;63(13):17.
26. Grisanti S, Schindler F, Merz H, Kakkassery V, Sonntag SR, Tura A. Detection of circulating tumor cells in patients with small choroidal melanocytic lesions. Ophthalmology. 2023;130(12):1290–303.
27. Wang VE, Young L, Ali S, Miller VA, Urisman A, Wolfe J, et al. A case of metastatic atypical neuroendocrine tumor with ALK translocation and diffuse brain metastases. Oncologist. 2017;22(7):768–73.
28. Coupland SE. Vitreous biopsy: specimen preparation and interpretation. Monogr Clin Cytol. 2012;21:61–71.
29. Callejo SA, Dopierala J, Coupland SE, Damato B. Sudden growth of a choroidal melanoma and multiplex ligation-dependent probe amplification findings suggesting late transformation to monosomy 3 type. Arch Ophthalmol. 2011;129(7):958–60.
30. Damato BE, Heimann H, Kalirai H, Coupland SE. Age, survival predictors, and metastatic death in patients with choroidal melanoma: tentative evidence of a therapeutic effect on survival. JAMA Ophthalmol. 2014;132(5):605–13.
31. Shields CL, Dalvin LA, Ancona-Lezama D, Yu MD, Di Nicola M, Williams BK Jr, et al. Choroidal nevus imaging features in 3,806 cases and risk factors for transformation into melanoma in 2,355 cases: the 2020 Taylor R. Smith and Victor T. Curtin Lecture. Retina. 2019;39(10):1840–51.
32. Damato B, Eleuteri A, Taktak A, Hussain R, Fili M, Stålhammar G, Heimann H, Coupland SE. Deferral of Treatment for Small Choroidal Melanoma and the Risk of Metastasis: An Investigation Using the Liverpool Uveal Melanoma Prognosticator Online (LUMPO). Cancers (Basel). 2024;16(8):1607. https://doi.org/10.3390/cancers16081607.
33. Damato B, Coupland SE. A reappraisal of the significance of largest basal diameter of posterior uveal melanoma. Eye (Lond). 2009;23(12):2152–60; quiz 61–2.
34. Barbi M, Carvajal RD, Devoe CE. Updates in the management of uveal melanoma. Cancer J. 2024;30(2):92–101.
35. Nathan P, Hassel JC, Rutkowski P, Baurain JF, Butler MO, Schlaak M, et al. Overall survival benefit with tebentafusp in metastatic uveal melanoma. N Engl J Med. 2021;385(13):1196–206.
36. Cook SA, Damato B, Marshall E, Salmon P. Psychological aspects of cytogenetic testing of uveal melanoma: preliminary findings and directions for future research. Eye. 2009;23(3):581–5.
37. Damato B, Eleuteri A, Taktak AF, Coupland SE. Estimating prognosis for survival after treatment of choroidal melanoma. Prog Retin Eye Res. 2011;30(5):285–95.

Index

A
A Cure in Sight (ACIS), 158
Acquired immunodeficiency syndrome (AIDS), 20
Acute exudative polymorphous paraneoplastic vitelliform maculopathy (AEPPVM), 222
Acute GVHD (aGVHD), 186
Acute lymphoblastic leukemia (ALL), 139
Adenomas, 24
Adjuvant chemotherapy, 140
Aerosolized fibers, 18
Aflatoxin, 18
Aflibercept, 34
Age-related macular degeneration (AMD), 100
Alcohol, 18
Alkylating agent busulfan, 140
American Joint Committee on Cancer (AJCC) staging, 87, 88
Anesthesia, 112
Angiogenesis inhibitors, 56
Angiopoietin, 56
Angiostatin, 57
Angle-closure, 175
Anterior chamber-associated immune deviation (ACAID), 73–74
Anterior segment tumors
  iris tumors, 199
  retinal tumors, 201
  retinoblastoma, 201
  vascular anomalies, 199
Anterior uveal tumors, 233
Anti-angiogenic therapy (AAT), 52
Anti-angiogenic therapy (anti-VEGF), 57
Anticancer therapy, 140
Antimetabolites, 138
Antineoplastic agents, 142
Anti-VEGF agents, 131
Apoptosis, 26
Aromatic amines, 18
Arteriovenous malformation (AVM), 199
Aspergillus flavus, 20
Aspiration cytology, 31
ATP-binding cassette (ABC) efflux transporters, 140
Autofluorescence, 254
  choroidal hemangioma, 261
  choroidal melanocytic tumors, 255
  choroidal melanoma, 259, 260
  choroidal metastasis, 263
  choroidal nevus, 256
  near-infrared AF, 255
  neurofibromatosis type 1, 264
  short-wavelength, 254, 255
  small choroidal melanomas, 257
  vitreoretinal lymphoma, 264
Autologous serum eye drops, 192

B
Basal cell carcinoma, 23
B-cell lymphomas, 19
B cells, 73
Belzupacap sarotalocan (Bel-sar), 78
Benign and malignant tumors, 23, 24
Bevacizumab, 59, 128
Bilateral diffuse uveal melanocytic proliferation (BDUMP), 223
Biopsy, 309, 310, 316
Blastomas, 24
Brachytherapy, 109, 121
Bragg peak, 105, 109
BRCA1-associated protein-1 (*BAP1*) gene mapping, 82
Breast cancer, 21
Burkitt's lymphoma, 19, 20

C
Cancer angiogenesis
  angiogenic switch, 52
  angiopoietin, 56
  endogenous, 56–57
  endostatin, 57
  FGF, 56
  metastatic cascade, 54
  metastatic uveal melanoma, 62–64
  MMPs, 56
  non-angiogenic tumor vascularization, 52–53
  pseudovascular channels, 60
  radiation retinopathy, 62
  retinoblastoma, 59
  tumor microenvironment, 53
  tumor vessels, 54
  VEGF, 55, 56
Cancer cells, 17

© The Editor(s) (if applicable) and The Author(s), under exclusive license to Springer Nature Switzerland AG 2025

A. D. Singh, B. E. Damato (eds.), *Clinical Ophthalmic Oncology*, https://doi.org/10.1007/978-3-031-75907-9

Cancer epidemiology
case-control studies, 7
case series, 6
cohort study, 7
confounding, 5
cross-sectional study, 6
differences in mean scores, 5
hazard ratio, 4
incidence, 3
information bias, 6
mortality, 3
odds ratio, 5
pilot study, 7
prevalence, 2
quality-of-life, 4
randomized controlled trials, 7
relative risk, 4
research questions, 1
screening test, 5
selection bias, 5
statistical significance, 5
surrogate endpoints, 3–4
systematic review, 7
time-to-event, 3
Cancer genetics
apoptosis and cell cycle, 82–83
candidate genes, 82
genetic mutations, 81
multi-omics analysis, 83–84
telomeres, 81–82
Cancer staging
AJCC/TNM staging, 87
prognostic relevance, 89
research relevance, 90–91
therapeutic relevance, 89–90
Carbon dioxide laser, 100
Carcinogenic agents, 17–18
Carcinogens, types of, 18
Carcinomas, 24
Case-control studies, 7
Cataracts, 161, 165, 171
Caucasian race, 19
Cause-specific mortality, 3
Cavernous hemangioma, 239
Cell cycle, 137, 138
Cell membrane-bound molecule PD-L1, 76
Cellular differentiation, 30
Cellular pleomorphism, 29–30
Cellular proliferation, 29
Cellular senescence, 27
Cellular therapy, 17
Cemiplimab, 114
Censoring, 11
Central nervous system (CNS), 167
Central serous chorioretinopathy (CSCR), 218, 221
Charged particles, 109
Chemical carcinogens, 18
Chemotherapeutic agents, 139, 144
Chemotherapy, 21, 111
adjuvant chemotherapy, 140
cell cycle, 137
chemotherapy resistance, 140
drug-drug interactions, 140
hematopoietic cell recovery, 138
metastatic uveal melanoma, 141
neoadjuvant chemotherapy, 140
orbital lymphoproliferative disorders, 141
pharmacokinetics, 139
retinoblastoma, 142
RMS, 142
toxicities of, 142–143
Chernobyl nuclear power plant disaster, 19
Childhood glaucoma, 177
Choristomas, 24
Choroidal granuloma, 211
Choroidal hemangioma, 209, 210, 250, 261
Choroidal lymphoma, 214, 215
Choroidal melanoma, 60, 116, 207, 208, 245, 259, 285
Choroidal metastasis, 248, 263, 289
Choroidal metastatic tumors, 213, 214
Choroidal neovascular membranes (CNVM), 100
Choroidal nevus, 206, 243, 244
Choroidal osteoma, 211, 246
Choroidal tumors, 206, 243
Ciliary body melanocytoma, 279
Cilio-choroidal melanoma, 117
Clinical target volume (CTV), 106
Clonorchis, 20
Coats' disease, 218, 283
Cobalt gray equivalents (CGE), 106
Cobalt-60 teletherapy, 104
Collaborative Ocular Melanoma Study (COMS), 165
Conditional mortality, 3
Congenital hypertrophy of the retinal pigment epithelium (CHRPE), 235, 263
Conjunctiva, 189
Conjunctival biopsies, 37
Conjunctival intraepithelial neoplasia, 94
Conjunctival melanoma, 91, 113
Conjunctival tumors, 94, 95
Conjunctivitis, 122
Contact lenses, 192
Convection, 278
Conventional radiation therapy, 108
Coping mechanisms, 153
Cornea, 189
Corticosteroids, 128
Counseling, 112
Cox proportional hazards regression model, 12, 15
Cox regression, 14
Crushed ice and salt (NaCl), 93
Cryotherapy, 111
complications, 96
conjunctival tumors, 95
cooling rate, 94
eyelid tumors, 94, 95
Freeze-Thaw cycle, 94
indications, 94
intraocular tumors, 94
mechanism of tissue injury, 93–94
orbital tumors, 94–95
tissue temperature, 94
Cumulative incidence (CI), 3
Cyberknife® system, 109
Cyclosporine A, 192
Cyclotron, 105
CYP3A, 140
Cytological sampling, 31–32
Cytology handling, 46–48
Cytolyt, 44
Cytotoxic chemotherapy, 137
Cytotoxic T lymphocytes (CTLs), 73

D
Deep learning (DL), 34, 83
Delta-like 4 (DLL4)-Notch signaling pathway, 53
Dendritic cell therapy, 77
Diabetic macular edema (DME), 55
Diets, 21
Differences in risks (RD), 5
DNA and RNA viruses, 19
DNA molecule, 104
DNA sequence, 28
Down's syndrome, 57

E
Electromagnetic/photon radiation, 103
Electromagnetic spectrum, 104
Emitted laser, 97
Endolaser retinopexy, 114
Endophthalmitis, 304
Endophytic hemangioblastoma, 201
Endostatin, 57
Enucleation, 124
Episcleral brachytherapy, 287
Epithelial-mesenchymal transition (EMT), 28
Epithelial-to-mesenchymal (EMT) properties, 52
Eppendorf tube, 43
Epstein-Barr virus (EBV), 19
Evidence-based medicine (EBM), 1
Ewing sarcoma, 139
Excisional biopsy, 313
Exenteration specimens, 46
Exfoliative cytology, 31
Exophytic hemangioblastoma, 201
External beam radiation therapy (EBRT), 88, 121
External beam therapy, 107–108
Extraocular extension, 287
Extraocular muscles, 123
Eye cancer, 151
  communication, 154, 155
  coping mechanisms, 153
  decision-making, 156
  eliciting and addressing patients, 154
  emotions and fears, 152, 153
  family support, 157
  ocular metastasis, 151
  patients' needs, 153, 154
  posttraumatic growth, 157
  psychological support, 156
  retinoblastoma, 152
  self-help, 157
  uveal melanoma, 151
  vitreoretinal lymphoma, 152
Eyelid lesions, 94
Eyelid tumors, 95

F
False-negative biopsy, 303
Familial exudative vitreoretinopathy (FEVR), 218
Fibroblast growth factor (FGF), 52, 56
Fine-needle aspiration biopsy (FNAB)
  amelanotic uveal tumor, 298
  complications, 303, 304
  indications, 297, 298
  orbital tumors, 303
  sample handling, 297
  surgical technique, 294
Fine needle aspiration (FNA) specimens, 44
Fluorescein angiogram, 145
Fluorescein angiography (FA), 125, 197, 198
Fluorescence in situ hybridization (FISH), 298
5-fluorouracil, 139
Fractionation, 106
Fuchs adenoma, 178
Fundus autofluorescence (FAF), 253

G
Gamma Knife radiosurgery, 109
General anesthesia, 95
General toxicities, 142
Genetic mutations, 81
Genetic susceptibility, 21
Glaucoma, 173
  adult, 178, 180
  angle-closure, 175
  childhood, 177
  clinical features, 176
  diagnostic evaluation, 176, 177
  open-angle, 173, 175
  specific entities, 177
  Sturge-Weber syndrome, 177
  treatment, 181, 182
Glutaraldehyde, 44
G-protein coupled receptors (GPCR), 29, 82
Graft-versus-host disease (GVHD), 185
  acute, 186
  cataract surgery, 193
  chronic, 187
  classification, 186
  clinical ophthalmic features, 188
  contact lenses, 192, 193
  diagnostic evaluation, 190
  differential diagnosis, 190
  etiology, 185
  follow-Up, 193
  lacrimal glands, 188
  pathogenesis, 186
  pathophysiology, 194
  prognosis, 194
  treatment, 191
Gray (Gy), 105
Gross target volume (GTV), 106
Group B disease, 142

H
Haematoxylin and Eosin (H&E), 48
Hallmarks of cancer
  emerging hallmarks, 27–28
  evading growth suppressors, 25–26
  genome instability and mutation, 24–25
  immune system, 25
  inducing or accessing vasculature, 26
  invasion-metastasis cascade, 26
  metastatic process, 28
  proliferative signaling, 25
  resisting cell death, 26
  tumor microenvironment, 28–29
Hamartomas, 24

Hazard ratio (HR), 4, 14
Helicobacter pylori (H. Pylori) infection, 20
Hematologic malignancies, 21
Hematopoietic stem cell transplantation (HSCT), 185
Hemorrhage, 303
Hepatitis B and C virus, 19, 20
Heritable gene variants, 81
High-dose chemotherapy, 21
Highly active antiretroviral therapy (HAART), 20
Hippel-Lindau (vHL) protein, 56
Hiroshima and Nagasaki atomic bomb events, 19
Hodgkin lymphoma, 21
Hryniuk model, 139
Human herpesvirus 8, 20
Human leukocyte antigen (HLA) system, 74
Human papilloma virus (HPV), 19, 65
Human T-cell lymphotropic virus type 1 (HTLV-1) infection, 20

I
Immune checkpoint inhibitors, 17
Immune system, 25
Immunohistochemistry, 33–34
Immunological escape, 73–74
Immunosuppression, 21
Immunotherapy, 76–77
Impression cytology, 46–48
In intensity-modulated radiation therapy (IMRT), 108
Incidence density (ID), 3
Incisional biopsy, 311
Incorporating radiotherapy, 111
Indocyanine green angiography, 198
Induced-cataract
  chemotherapy, 167
  radiation, 165
  surgical treatment, 163
Infection control, 117
Infliximab, 21
Information bias, 6
Intensity-modulated radiation therapy (IMRT), 103, 108
Interferon-alpha 2b, 77
Intraocular fine-needle aspiration biopsy (FNAB), 31
Intraocular lesions, 95
Intraocular lymphoma, 303
Intraocular tumors, 94–96
Intravitreal chemotherapy, 142
Intravitreal faricimab, 131
Invasion-metastasis cascade, 26
Ionizing radiation, 19, 124
Ipilimumab, 34, 76
Iridociliary pigment epithelial cyst (IPE cyst), 279
Irinotecan, 142
Iris neovascularization, 123–124
Iris stromal cysts, 178
Iris tumors, 199, 296

J
Juvenile xanthogranuloma, 178

K
Kaplan–Meier method, 12, 15
Kaplan–Meier plot, 3
Kaposi sarcoma (KS), 20
Kaposi sarcoma herpes virus (KSHV), 19, 20
Kaposi's sarcoma, 20
Keratitis, 122
Keratoconjunctivitis sicca, 20
Kinetic ultrasonography, 278
Knudson 2-hit hypothesis, 17

L
Lacrimal glands, 188
Large B-cell lymphoma, 146
Laser beam, 97
Laser delivery systems, 99, 100
Laser photocoagulation, 99–100
Laser therapy, 111
  laser delivery systems, 99
  ophthalmic lasers, 98
  PDT, 100
  photochemical effects, 98
  photomechanical effects, 98
  photothermal effects, 98
  transpupillary thermotherapy, 100
  variables influence, 98
Leukemia, 24, 180
Light microscopy, 33
Linac-based stereotactic radiosurgery, 109
Linear accelerator, 104
Liquid biopsy
  aqueous humor, 314
  circulating blood, 314
  vitreous, 314
Liquid nitrogen, 93
Liver metastases, 30
Liverpool Uveal Melanoma Prognosticator Online (LUMPO), 112
Local tumor control, 118
Lymphomas, 24
Lymphoproliferative disorders, 141

M
Machine learning (ML), 34
Malignant cutaneous melanoma, 145
Malignant transformation, 21
MALT lymphoma, 20
Mapping biopsies, 45
Matrix metalloproteinases (MMPs), 53, 55–57
May-Grünwald Giemsa (MGG), 314
Measure of outcome in ocular disease (MOOD), 4
Median survival, 13
Medulloepithelioma, 167, 178
Meibomian glands, 189
Melanocytoma, 178, 208, 242
Melanoma, 24, 30, 279
Melanoma-specific $CD8^+$ T cells, 74
Melphalan, 142
Metastatic cascade, 54
Metastatic cutaneous melanoma, 62
Metastatic tumors, 180
Metastatic uveal melanoma, 62, 141
Microbiota, 27
Micrometastases, 27
"Micropulse" technology, 99
Mitosis, 137
Mucosa-associated lymphoid tissue (MALT) lymphoma, 20
Multi-drug resistance (MDR), 140

Multimodality therapy, 111
Multi-omics analysis, 83–84
Multiple biopsies, 37
Multiplex ligation-dependent probe amplification (MLPA), 310
Myelodysplastic syndrome, 21, 180

N
Near-infrared AF (NIR-AF), 255
Necrotizing retinal vasculitis, 20
Needed to screen (NNS), 5
Needed to treat (NNT), 5
Neoadjuvant chemotherapy, 114, 140
Neoplasia, 23–24
  aspiration cytology, 31
  cellular differentiation, 30
  cellular pleomorphism, 29–30
  cellular proliferation, 29
  cytological sampling, 31–32
  exfoliative cytology, 31
  immunohistochemistry, 33–34
  light microscopy, 33
  nuclear cytoplasmic ratio, 30
Neovascular age-related macular degeneration (nAMD), 55
Neovascular glaucoma, 123–124, 178
Neurofibromatosis type 1 (NF1), 177, 264
Neuro-ophthalmic disorders, 20
Nevus versus melanoma, 298
Nonmutational epigenetic reprogramming, 28
Novel drug therapies, 192
Nucleotide excision repair pathway (NER), 19

O
Ocular adnexal lymphoma (OAL), 87
Ocular coherence tomography (OCT), 127
Ocular Melanoma Foundation (OMF), 158
Ocular pigments, 99
Ocular side effects, 144
Ocular surface squamous neoplasia (OSSN), 19, 94
Ocular surface tumors, 89
Ocular survival, 11
Ocular toxicities, 143
Odds ratio (OR), 5
Open-angle glaucoma, 173
Ophthalmic lasers, 98
Ophthalmic ultrasonography, 269, 272, 274, 276, 278, 282, 283, 285, 287, 290, 291
  basic physics, 269
  B-scan, 270
  choroidal hemangioma, 288, 289
  choroidal metastasis, 289
  instrumentation, 270
  intraocular tumors, 274
  kinetic ultrasonography, 278
  quantitative ultrasonography, 276, 277
  retinal tumors, 281, 284
  topographic ultrasonography, 275
Opisthorchis, 20
Optic disc melanocytoma, 242
Optical coherence tomography (OCT), 229, 236
  choroidal hemangioma, 250
  choroidal melanoma, 246
  choroidal metastasis, 248
  corneal tumors, 230, 231
  enhanced depth imaging, 229
  intraocular tumors, 235
  primary vitreoretinal lymphoma, 238
  retinal cavernous hemangioma, 239
  swept-source, 229
Optical coherence tomography angiography (OCTA), 197, 229
Orbital lymphoproliferative disorders, 141
Orbital rhabdomyosarcoma, 141
Orbital tumors, 94–95

P
Panretinal laser photocoagulation, 128
Papillary hemangioblastoma, 203
Paraneoplastic disorders, 222, 223
Particle radiation, 103
Pathology request form, 37, 44
Patient-reported outcome measures (PROMs), 157
Pembrolizumab, 114
Peptic ulcer disease, 20
Periocular edema, 96
Periorbital skin, 121–122
Peripheral exudative hemorrhagic chorioretinopathy, 220
Persistent fetal vasculature (PFV), 281, 282
Persistent hyperplastic primary vitreous (PHPV), 218
Pharmacokinetics, 139
Photodisruption, 98
Photodynamic therapy (PDT), 100
Photon, 97
Pigmented choroidal melanocytes, 6
Pilot study, 7
Planning target volume (PTV), 106
Platelet-derived growth factor (PDGF), 52
Polymerase chain reaction (PCR), 34
Polypoidal choroidal vasculopathy (PCV), 218, 222
Population-based surveillance, 11
Posterior choroidal tumors, 297
Post-radiation cataract, 169
Post-transplant lymphoproliferative disorder (PTLD), 19
Posttraumatic growth (PTG), 157
POT1 gene, 82
Primary acquired melanosis (PAM), 230
Primary central nervous system lymphoma (PCNSL), 238
Primary ophthalmic cancers, 141
Primary vitreoretinal lymphoma (PVRL), 238
Prognostic biopsy, 310, 315
Prognostication, 309, 316
Proliferative signaling, 25
Proton beam radiation therapy, 121
Proton beams, 105
Proto-oncogene products, 52
Pulsed laser, 97

Q
Quality-of-life, 4
Quantitative ultrasonography, 275

R
Racemose hemangioma, 204
Radiation-absorbed dose, 105
Radiation-induced cataracts, 125
Radiation-induced dry eye, 122

Radiation-induced optic neuropathy, 131, 132
Radiation-induced retinopathy, 62, 125, 127, 128, 224
Radiation therapy, 21, 165
  brachytherapy, 109
  CGE, 106
  charged particles, 109
  cobalt-60 unit, 104
  conjunctivitis, 122
  conventional radiation therapy, 108
  cyclotron, 105
  electromagnetic/photon radiation, 103
  external beam radiation therapy, 122
  external beam therapy, 107–108
  extraocular muscles, 123
  fractionation, 106
  Gamma Knife radiosurgery, 109
  ionizing and nonionizing effects, 104
  iris neovascularization, 123–124
  keratitis, 122
  lens, 124–125
  linac-based stereotactic radiosurgery, 109
  linear accelerator, 104
  neovascular glaucoma, 123–124
  particle radiation, 103
  periorbital skin, 121–122
  preventive strategies, 129
  radiation retinopathy, 125, 127, 128
  radiation-absorbed dose, 105
  radiation-induced optic neuropathy, 131, 132
  radioactive elements, 104
  RBE, 106
  scleral necrosis, 122, 123
  stereotactic radiosurgery, 109
  target volume, 106
  teletherapy, 104
  3D-CRT, 108
  tissue tolerance, 106–107
  total delivered dose, 106
  toxic tumor syndrome, 131
  treatment delivery, 109
Radioactive elements, 104
Randomized controlled trials, 7
Ranibizumab, 128
Recurrence-free survival, 11
Reese-Ellsworth classification, 88
Relative biological effectiveness (RBE), 105
Relative dose intensity (RDI), 139
Relative mortality, 3
Relative risk (RR), 4
Retinal astrocytic hamartoma (RAH), 204, 236
Retinal cavernous hemangioma, 204
Retinal cryoprobe, 95
Retinal degeneration, 20
Retinal hemangioblastoma, 240
Retinal lymphoma, 167, 168
Retinal pigment epithelium (RPE), 204, 206, 254
Retinal tumors, 236
Retinal vascular tumors, 201
Retinal vasoproliferative tumor, 203
Retinoblastoma, 59, 88–89, 141, 142, 152, 168, 201, 236, 238, 303
Retinopathy of prematurity (ROP), 283
Rhabdomyosarcoma (RMS), 142
Rubeosis iridis, 124

S
Sarcomas, 24
Schistosoma, 20
Sclera-choroidal flap, 38
Scleral necrosis, 122, 123
Scleritis, 219
Secondary glaucoma, 173, 175, 178
"Seed and soil" theory, 27
Selection bias, 5
Senescence-associated secretory phenotype (SASP), 27
Sentinel lymph node (SLN) biopsy, 90
SF3B1 mutations, 82
Shared-decision making (SDM), 156
Short-wavelength AF (SW-AF), 254
Small choroidal melanoma, 100
Small microscopic tumors, 51
Sodium fluorescein, 198
Solid tumors, 28
Specimen containers, 45
Specimen handling technique
  conjunctival biopsies, 37
  cytology handling, 46–48
  enucleation for intraocular tumour, 46
  exenteration specimens, 46
  eyelid skin tumour resections, 45
  fixation of ocular pathology specimens
    FNA samples, 44
    impression cytology plastic rings, 44
    surgical tumour specimens, 43–44
    vitrectomy samples, 44
  fresh sampling, 38
  frozen sections, 37, 38
  frozen tissue handling, 45
  local resections, 45
  mapping biopsies, 45
  multiple biopsies, 37
  orientation of specimens, 37
  pathology request form, 44
  patient's histopathology report, 37
  transporting specimens, 45
Squamous cell carcinoma, 17–18
Standardized echography, 274, 286, 288
Statistical analysis methods, 12
Stereotactic radiosurgery, 109
Stimulated emission, 97
Sturge-Weber syndrome, 177
Subretinal hemorrhage, 114, 289
Surgical tumor excision, 118
  anesthesia, 112
  counseling, 112
  exposure of surgical field, 113
  infection control, 117
  long-term ophthalmic surveillance, 118
  objectives of, 111
  operative field, 113
  post-operative care, 117–118
  pre-operative assessment, 111–112
  pre-operative checks, 113
  pre-operative medications, 112
  prognostication, 112
  surgical outcomes, 118
  systemic investigations, 112
  tumor excision, 113–117
  wound closure, 117

Surrogate endpoints, 3
Survival analysis
  Cox regression, 14
  Kaplan–Meier method, 12
  synthetic dataset, 12
Swept-source OCT (SS-OCT), 229
Synthetic dataset, 12
Systemic chemotherapy, 143
Systemic surveillance, 118

T
T cells, 73, 75
Tebentafusp, 77
Teletherapy, 104
Telomerase reverse transcriptase (*TERT*), 81
Telomerase RNA (*TERC*) genes, 81
Telomeres cap, 81
Telomeric repeat amplification protocol (TRAP) assay, 82
Teratomas, 24
Three-dimensional conformal radiation therapy (3D-CRT), 103, 108
Thrombospondin, 56
Tissue temperature, 94
Tissue tolerance, 106–107
Tobacco, 18
Topical corticosteroids, 122, 191
Topical lubricants, 191
Topical tacrolimus, 192
Topographic ultrasonography, 275
Toxic tumor syndrome, 131
TP53 gene, 82
Transcleral cryotherapy, 95
Transpupillary thermotherapy, 100, 163
Transvitreal incisional biopsy, 32
Tumor-associated cataract, 171
Tumor cells, 24–26, 140
Tumor excision, 113–117
Tumor infiltration, 30
Tumor metastases, 26
Tumor microenvironment, 28–29
Tumor, node, metastasis (TNM) staging system, 87–89, 112
Tumorigenesis, 24, 25, 51
Tumor-infiltrating leukocytes (TIL), 74, 75

U
Ultrasound biomicroscopy (UBM), 271
Ultraviolet light B (UV-B), 19, 65
Ultra-widefield (UWF), 199
Unilateral retinoblastoma, 142
Union Internationale Contre le Cancer (UICC), 87
Urokinase plasminogen activator (uPA), 57
Uveal effusion syndrome, 222
Uveal melanoma (UM), 60–64, 74, 82, 90, 168, 169, 178, 179, 293, 298, 301, 303, 309
  BAP1 gene, 74
  Bel-sar treatment, 78
  dendritic cell therapy, 77
  GNA11 gene, 74
  HLA antigen expression, 74
  immune-related response, 77
  immunotherapy, 76–77
  interferon-alpha 2b, 77
  ipilimumab, 76
  irradiation of tumor, 76
  metastases, 77
  PD-L1, 76
  tebentafusp, 77
  tumor-infiltrating leukocytes, 75
Uveal metastases, 169
Uveitis, 20

V
Vascular anomalies, 199
Vascular endothelial growth factor (VEGF), 26, 55, 99
  expression, 60–62
  receptors, 56
Vascular endothelial growth factor-A (VEGF-A), 52
Vascularity, 278
Vasoproliferative tumor, 241
Verteporfin, 100
Vessel co-option (VCo), 52
Vitrectomy-assisted aspiration biopsy, 297
Vitrectomy samples, 44
Vitreoretinal lymphoma, 152, 264
Vitreous hemorrhage, 286
Vitreous samples, 48
von Hippel Lindau (VHL) disease, 57
von Hippel-Lindau (VHL) protein, 64

W
Widefield, 199
Wound closure, 117
Wyburn-Mason syndrome, 241

X
Xeroderma pigmentosum (XP), 19, 21

Z
Zimmerman hypothesis, 114